

8-2017

# Enantioselective $\gamma$ - and $\delta$ -Borylation of Unsaturated Carbonyl Derivatives: Synthesis, Mechanistic Insights, and Applications.

Gia L. Hoang

University of Nebraska-Lincoln, ghoang2@huskers.unl.edu

Follow this and additional works at: <http://digitalcommons.unl.edu/chemistrydiss>



Part of the [Organic Chemistry Commons](#)

Hoang, Gia L., "Enantioselective  $\gamma$ - and  $\delta$ -Borylation of Unsaturated Carbonyl Derivatives: Synthesis, Mechanistic Insights, and Applications." (2017). *Student Research Projects, Dissertations, and Theses - Chemistry Department*. 83.  
<http://digitalcommons.unl.edu/chemistrydiss/83>

This Article is brought to you for free and open access by the Chemistry, Department of at DigitalCommons@University of Nebraska - Lincoln. It has been accepted for inclusion in Student Research Projects, Dissertations, and Theses - Chemistry Department by an authorized administrator of DigitalCommons@University of Nebraska - Lincoln.

ENANTIOSELECTIVE  $\gamma$ - AND  $\delta$ -BORYLATION OF UNSATURATED CARBONYL  
DERIVATIVES: SYNTHESIS, MECHANISTIC INSIGHTS, AND APPLICATIONS.

by

Gia L. Hoang

A DISSERTATION

Presented to the Faculty of  
The Graduate College at the University of Nebraska  
In Partial Fulfillment of Requirements  
For the Degree of Doctor of Philosophy

Major: Chemistry

Under the Supervision of Professor James M. Takacs

Lincoln, Nebraska

August, 2017

ENANTIOSELECTIVE  $\gamma$ - AND  $\delta$ -BORYLATION OF UNSATURATED CARBONYL  
DERIVATIVES: SYNTHESIS, MECHANISTIC INSIGHTS, AND APPLICATIONS.

Gia L. Hoang, Ph.D.

University of Nebraska, 2017

Advisor: James M. Takacs

Chiral boronic esters are valuable synthetic intermediates widely used in a variety of stereospecific transformations. Transition metal-catalyzed asymmetric hydroboration (CAHB) of alkenes is among the most popular methods for their preparation. Enantioselective hydroboration of activated alkenes (i.e., vinyl arene derivatives or conjugated carbonyl compounds) have been extensively studied by many research groups. We, on the other hand, are interested in enantioselective hydroboration of unactivated alkenes utilizing coordinating functional groups (e.g., carbonyl derivatives) to give functionalized, chiral boronic esters. While conjugate addition and C–H activation methodologies provide efficient alternatives to CAHB for enantioselective  $\beta$ -borylation of carbonyl compounds, direct  $\gamma$ - and  $\delta$ -borylations were essentially unknown prior to our work on CAHB. The  $\gamma$ -borylated products were used for understanding stereochemical aspects of Suzuki–Miyaura cross-coupling reactions resulting in stereoretention and in contrast to similar  $\beta$ -borylated carbonyl derivatives reported in literature. Some other selected transformations were carried out to construct a number of biologically relevant structural motifs, such as lignan precursors, 1,4-amino alcohols,  $\gamma$ -amino acid derivatives, 5-substituted- $\gamma$ -lactone and lactam ring systems. In addition, collaborative experimental and computational studies of the enantioselective desymmetrization via CAHB gain a better understanding of the mechanistic pathways.

## ACKNOWLEDGEMENTS

I would like to first thank my research advisor, Prof. James Takacs for his support, guidance, and kindness throughout my graduate program. I really appreciate the tremendous freedom that he provided in term of designing the projects as well as solving the problems. Thank you for giving me great opportunities to change my life in such a challenging way.

I would like to thank my committee members: Prof. Rajca, Prof. Du, Prof. Zhang, and Prof. Tan for their insight and helpful comments. I also would like to thank Prof. Dussault and Prof. DiMagno for their willingness to write letters of recommendation on my behalf. In addition, I would like to thank my undergraduate research advisor, Prof. James Hagen as well as Prof. James Wood who kindly awarded me a scholarship for outstanding organic chemistry student. Those support, in fact, motivated me a lot in the decision of going to graduate school.

It has been great to work with colleagues in the Takacs group. I would like to give my special thanks to Dr. Sean M. Smith and Dr. Nathan C. Thacker for their guidance when I first joined the group. I also would like to thank past and current group members: Dr. Konstantyn Marichev, Dr. Kazuya Toyama, Andy Geis, Veronika Shoba, Suman Chakrabarty, Ryan Carr, Shuyang Zhang, Andy Bochat and wish the current students best of luck in their future endeavors.

Last but not least, I would like to thank my parents, my wife and my daughter for their support and love throughout my graduate career. Thanks for always being by my side even on the most difficult days.

## PREFACE

The first chapter of this dissertation is an overview of the current state-of-the-art in the enantioselective preparation of chiral boronic esters, versatile intermediates used in many stereospecific transformations. Giving a brief discussion on alternative methods, the introductory chapter mainly focuses on transition-metal-catalyzed asymmetric hydroboration (CAHB) directly relevant to the work in this thesis. The chapter also highlights current understanding of the mechanistic pathways along with experimental results. It serves as part of the invited perspective in preparation. The subsequent chapters highlight the innovation and significance of the methodology developed. Chapter two describes the two publications and a manuscript in preparation, introducing the unique direct routes to acyclic  $\gamma$ - and  $\delta$ -borylated carbonyl compounds, for which currently exists no alternative direct methods for their preparation. Chapter three including other two published manuscripts is a collaborative experimental and computational studies (in collaboration with Zhao-Di Yang and Rhitankar Pal, previous members in Zeng group, UNL chemistry) via CAHB of symmetrical cyclic substrates. The experimental work in chapter three also serves as an interesting approach, enantioselective desymmetrization towards the synthesis of quaternary or tetrasubstituted carbon stereogenic centers. Chapter four is part of published and in preparation manuscripts mentioned in chapters 2 and 3, but is separated to highlight the significance of the chemistry, mono- and bi-functionalizations of  $\gamma$ - and  $\delta$ -borylated carbonyl derivatives obtained from CAHB as well as to understand the stereochemical aspects of the conventional palladium-catalyzed cross-coupling reactions. The last chapter is the combined experimental procedures for substrates, intermediates, and products discussed in the previous chapters.

## TABLE OF CONTENTS

**CHAPTER ONE**

1.1 Chiral boronic esters – Useful synthetic intermediates .....	1
1.2 Recent development in the preparation of chiral boronic esters .....	8
1.3 Stoichiometric asymmetric hydroboration of alkenes.....	13
1.4 Transition-metal-catalyzed asymmetric hydroboration of alkenes .....	17
1.5 Mechanistic implications in transition-metal-catalyzed hydroboration of alkenes..	36
1.6 Summary .....	47
1.7 References .....	49

**CHAPTER TWO**

2.1 Enantioselective $\gamma$ -borylation of $\beta,\gamma$ -unsaturated amides and esters .....	67
2.2 Enantioselective $\gamma$ -borylation of $\gamma,\delta$ -unsaturated amides .....	71
2.3 Enantioselective $\delta$ -borylation of $\gamma,\delta$ -unsaturated carbonyl derivatives .....	85
2.4 Concluding remarks .....	100
2.5 References .....	102

**CHAPTER THREE**

3.1 Some selected desymmetrization methodologies.....	106
3.2 Enantioselective desymmetrization to all-carbon quaternary stereocenters via $\gamma$ - borylation of cyclic $\gamma,\delta$ -unsaturated amides .....	109
3.3 Deuterium-labeling studies .....	122
3.4 Computational studies – Mechanistic insights into directed CAHB.....	131

3.5 Concluding remarks .....	139
3.6 References .....	141

#### CHAPTER FOUR

4.1 Stereoretentive transformations of chiral boronic esters .....	145
4.2 Stereochemical aspects in coordination-directed palladium-catalyzed cross-coupling reactions) .....	150
4.3 Concluding remarks .....	165
4.4 References .....	166

#### CHAPTER FIVE

5.1 Experimental details .....	170
5.2 Preparation of substrates and intermediates .....	176
5.3 Procedures for directed catalytic asymmetric hydroboration (CAHB) with or without oxidation.....	231
5.4 Procedures for preparation of trifluoroborate salts from boronic esters .....	281
5.5 Procedures for directed Suzuki–Miyaura reactions .....	287
5.6 Other stereospecific transformations of organoboranes .....	302
5.7 Preparation of chiral ligands and palladium pre-catalyst .....	309
5.8 References .....	314

## LIST OF FIGURES

## CHAPTER ONE

<b>Figure 1.</b> Some selected stereosepecific transformations of C–B bonds.....	1
<b>Figure 2.</b> Preparation of biologically active molecules via protodeboronation methodology.....	4
<b>Figure 3.</b> Selected examples of recent developments in the preparation of chiral boronic esters.....	12
<b>Figure 4.</b> Brief hydroboration history.....	13
<b>Figure 5.</b> Rhodium-catalyzed hydroboration of styrene and styrenyl derivatives .....	19
<b>Figure 6.</b> Tang’s directed rhodium-catalyzed CAHB of vinyl arenes.....	20
<b>Figure 7.</b> Reversal in regioselective CAHB of styrene using rhodium and iridium catalysts .....	21
<b>Figure 8.</b> Iridium-catalyzed hydroboration of 1,1-disubstituted vinyl arenes .....	22
<b>Figure 9.</b> Fe- and Co-catalyzed hydroboration of 1,1-disubstituted vinyl arenes .....	23
<b>Figure 10.</b> Recent advancement for asymmetric hydroboration of gem-diaryl alkenes using copper(I) catalyst .....	24
<b>Figure 11.</b> Yun’s $\alpha$ -selective copper(I)-catalyzed hydroboration of vinyl arenes .....	25
<b>Figure 12.</b> Hoveyda’s $\beta$ -selective Cu-NHC-catalyzed hydroboration of vinyl arenes .....	26
<b>Figure 13.</b> Copper(I)-catalyzed hydroboration of dehydroamino acid methyl esters .....	26
<b>Figure 14.</b> Copper(I)-catalyzed borylative aromatization of p-quinone methides .....	27
<b>Figure 15.</b> Temperature dependence in regioselective Cu(I)-catalyzed hydroboration of cyclic 1,3-dienes .....	27
<b>Figure 16.</b> Cu(I)-catalyzed asymmetric hydroboration of unactivated alkenes .....	29



<b>Figure 17.</b> Effect of directing groups in CAHB of methyldene substrates leading to complementary regio- and $\pi$ -facial selectivities .....	30
<b>Figure 18.</b> Directed Rh(I)-catalyzed asymmetric hydroboration of different alkene substitution patterns.....	31
<b>Figure 19.</b> Enantioswitching in Rh(I)-catalyzed asymmetric hydroboration of (Z)-1,2,2-trisubstituted alkenes.....	33
<b>Figure 20.</b> Effect of borane on Weinreb amide-directed CAHB of 1,2-disubstituted alkenes .....	34
<b>Figure 21.</b> Proposed reversal enantioselective catalytic pathways of cobalt-catalyzed asymmetric hydroboration of 1,1-disubstituted vinyl arenes.....	36
<b>Figure 22.</b> Effect of boranes on regioselectivity of Cu(I)-catalyzed hydroboration of vinyl arenes .....	38
<b>Figure 23.</b> Ester-directed Cu(I)-catalyzed hydroboration of $\alpha$ -dehydroamino acid methyl esters.....	40
<b>Figure 24.</b> A. Discovery of oxidative addition of tmdBH and catBH to Wilkinson's catalyst by Kono and Ito.....	41
<b>Figure 25.</b> Proposed mechanistic pathway for Rh(I)-catalyzed hydroboration.....	42
<b>Figure 26.</b> Effect of metal precursors on regio- and enantioselectivity .....	43
<b>Figure 27.</b> Fernández's calculations for most stable isomers of H-Rh-BINAP-borane-styrene complex employing catBH and pinBH.....	44
<b>Figure 28.</b> Proposed simplified mechanistic pathway for Rh(I)-catalyzed hydroboration of two-point binding substrates .....	45

<b>Figure 29.</b> Tang's proposed mechanism for amide-directed CAHB of $\alpha$ -arylenamides illustrating the crucial roles of diborane reagent and NH acidic proton .....	46
---	----

## CHAPTER TWO

<b>Figure 1.</b> Enantioselective conjugate borylation and C–H borylation for the preparations of chiral $\beta$ -borylated of carbonyl compounds .....	68
<b>Figure 2.</b> Contrasting regio- and $\pi$ -facial selectivity of 1,2- and 1,1-disubstituted alkenes .....	69
<b>Figure 3.</b> Enantioselective $\gamma$ -borylation of $\beta,\gamma$ -unsaturated amides and esters.....	70
<b>Figure 4.</b> Comparing $\pi$ -facial discrimination in CAHB of $\beta,\gamma$ - and $\gamma,\delta$ -unsaturated phenyl amides.....	72
<b>Figure 5.</b> Temperature and amount of catalyst and borane effects on CAHB of $\gamma,\delta$ -unsaturated amide <b>7b</b> .....	76
<b>Figure 6.</b> Ligand:metal ratio studies on CAHB of $\gamma,\delta$ -unsaturated amide <b>7b</b> suggest that 1:1 ligand:metal ratio is sufficient to form an active catalyst .....	78
<b>Figure 7.</b> Substrate scope for CAHB of $\gamma,\delta$ -unsaturated amides.....	80
<b>Figure 8.</b> Current limitations of CAHB of $\gamma,\delta$ -unsaturated amides.....	82
<b>Figure 9.</b> Proof of absolute configuration of alcohols <b>9b–d</b> via comparing optical rotation with known lactone ( <i>R</i> )- <b>13</b> .....	83
<b>Figure 10.</b> Additional evidence for the absolute configuration of ( <i>S</i> )- <b>9n</b> via $^1\text{H}$ NMR analysis of Mosher's ester ( <i>S,S</i> )- <b>14</b> .....	84
<b>Figure 11.</b> Effect of vinyl substituents on regioselectivity and $\pi$ -facial selectivity of CAHB of $\gamma,\delta$ -unsaturated amides.....	85

<b>Figure 12.</b> Six-step synthetic routes for $\gamma,\delta$ -unsaturated amides .....	87
<b>Figure 13.</b> Preparation of $\gamma,\delta$ -unsaturated amides via Claisen-Johnson rearrangement and the potential problem with benzylic alcohol derivatives .....	88
<b>Figure 14.</b> Preparation of aryl/ heteroaryl substituted $\gamma,\delta$ -unsaturated amides <b>15</b> via Julia-typed olefination.....	89
<b>Figure 15.</b> Directing group and coordinating distance effects on $\delta$ -borylation of $\gamma,\delta$ -unsaturated carbonyl derivatives .....	90
<b>Figure 16.</b> Proposed catalytic cycle for CAHB of <b>15a</b> using <i>N</i> -aryl ligand scaffold involving Rh(I)-catalyzed concerted-metalation-deprotonation .....	92
<b>Figure 17.</b> Proposed catalytic cycle for CAHB of <b>15a</b> using <i>N</i> -aryl ligand scaffold involving Rh(III)-catalyzed concerted-metalation-deprotonation.....	94
<b>Figure 18.</b> Substrate scope for CAHB of aryl/ heteroaryl substituted $\gamma,\delta$ -unsaturated amides.....	96
<b>Figure 19.</b> CAHB of pre-installed $\alpha$ -chiral center aryl substituted $\gamma,\delta$ -unsaturated amides.....	98
<b>Figure 20.</b> Determination of absolute configuration of CAHB of <b>15e</b> via $^1\text{H}$ NMR analysis of Mosher's ester <b>22e</b> .....	99

### CHAPTER THREE

<b>Figure 1.</b> Selected desymmetrization methodologies .....	106
<b>Figure 2.</b> Current literature reports on enantioselective desymmetrization via CAHB toward the synthesis of molecules bearing quaternary carbon stereogenic centers product.....	108

<b>Figure 3.</b> CAHB of symmetric cyclic $\gamma,\delta$ -unsaturated amide <b>23a</b> , a model substrate for computational studies .....	109
<b>Figure 4.</b> Brief ligand and borane survey for CAHB of <b>23a</b> reveals moderate levels of enantioswitching.....	112
<b>Figure 5.</b> 1:2 Rh:Ligand ratio reveals linear relationship between the enantiomeric excess of ligand <b>T1a</b> (blue) and <b>T3c</b> (red) and that of the product <b>26a</b> .....	115
<b>Figure 6.</b> 1:1 Rh:Ligand ratio reveals linear relationship between the enantiomeric excess of ligand <b>T1a</b> (blue) and <b>T3c</b> (red) and that of the product <b>26a</b> .....	116
<b>Figure 7.</b> Enantioselective desymmetrization towards stereogenic quaternary carbon centers via CAHB of <b>23</b> .....	117
<b>Figure 8.</b> Deuterium-labeling studies for CAHB of <b>23c</b> show little evidence for reversible C–H formation.....	123
<b>Figure 9.</b> $^1\text{H}$ NMR spectra illustrating the deuterium incorporation into $\gamma$ -hydroxy product <b>26c</b> .....	124
<b>Figure 10.</b> Deuterium-labeling studies for CAHB of <b>23c</b> using tmdBH under $\text{D}_2$ .....	126
<b>Figure 11.</b> $^1\text{H}$ NMR spectra illustrating the deuterium incorporation of $\gamma$ -hydroxy product <b>28c</b> .....	128
<b>Figure 12.</b> Potential hydrogenation pathways .....	129
<b>Figure 13.</b> Proposed formation of 1:1 mixture <b>26c:28c</b> via equal energies of reductive elimination versus potential $\text{D}_2$ -sigma bond metathesis .....	130
<b>Figure 14.</b> Preliminary studies by Dr. Smith found that the higher relative energy complex <b>A</b> correlates to a major product observed.....	132

<b>Figure 15.</b> Proposed mechanistic pathways to isomeric products (1 <i>R</i> *,3 <i>S</i> *)- and (1 <i>S</i> *,3 <i>R</i> *)- <b>26a</b> are differentiated via migratory insertion into Rh–H versus Rh–B bonds..	133
<b>Figure 16.</b> Comparison of the potential energy profiles for pathway <b>I</b> and <b>II</b> .....	134
<b>Figure 17.</b> Proposed other mechanistic pathways to major $\gamma$ -borylated product (1 <i>R</i> *,3 <i>S</i> *)- <b>26a</b> .....	135
<b>Figure 18.</b> Comparison of the potential energy profiles for pathway <b>I</b> , <b>I-1</b> and <b>I-2</b> ...	136
<b>Figure 19.</b> Proposed pathways <b>III-1</b> and <b>III-2</b> for the formation of isomerized alkene leading to minor regioisomer $\beta$ -borylated product <b>27</b> and the comparison of the potential energy profiles .....	137
<b>Figure 20.</b> CAHB of <b>23b</b> versus isomerized <b>23b</b> : both alkenes undergo CAHB leading to the major $\gamma$ -borylated product .....	138

## CHAPTER FOUR

<b>Figure 1.</b> Bi-functionalizations of oxime ether- and phosphonate containing chiral boronic esters.....	146
<b>Figure 2.</b> Bi-functionalizations of tert-butylester containing chiral boronic esters.....	147
<b>Figure 3.</b> Stereospecific transformations of organoboranes <b>8b–d</b> .....	149
<b>Figure 4.</b> Palladium-catalyzed cross-coupling of primary $\gamma$ -borylated amides and esters.....	152
<b>Figure 5.</b> Preparation of organotrifluoroborate salts .....	154
<b>Figure 6.</b> Palladium-catalyzed cross-coupling of cyclic $\gamma$ -organotrifluoroborate salt.	155

<b>Figure 7.</b> Proposed pathways for efficient cross-coupling illustrating the necessary feature of <i>N</i> -benzyl amide moiety .....	156
<b>Figure 8.</b> Unexpected influence of the amide substituent in Pd-catalyzed cross-coupling .....	157
<b>Figure 9.</b> X-ray analysis of <b>59</b> establishes Pd-catalyzed cross-coupling proceeds with stereoretention .....	158
<b>Figure 10.</b> Coordination-directed stereocontrol in Pd-catalyzed cross-coupling .....	159
<b>Figure 11.</b> Determination of absolute configuration of cross-coupled products via Pd-catalyzed cross-coupling of acyclic $\gamma$ -trifluoroborato amides .....	161
<b>Figure 12.</b> Unexpected protoboronation pathway for Suzuki–Miyaura cross-couplings of benzylic $\delta$ -borylated amides <b>72</b> .....	162
<b>Figure 13.</b> Palladium-catalyzed cross-coupling of benzylic $\delta$ - borylated benzyl amide <b>15a</b> .....	164

## LIST OF TABLES

## CHAPTER ONE

**Table 1.** Stoichiometric asymmetric hydroboration using chiral borane reagents. ....15

## CHAPTER TWO

**Table 1.** Evaluating the effects of ligands and boranes in CAHB of **7b** .....74

**Table 2.** Brief survey of ligand effect on CAHB of **15a** .....91

## CHAPTER THREE

**Table 1.** Optimization studies of enantioselective desymmetrization via CAHB of **23a** .....110

**Table 2.** Brief survey on CAHB of diene substrate **23j** reveals that tmdBH is crucial for high group- and enantioselectivity .....118

**Table 3.** CAHB of  $\alpha$ -phenyl **23c** under H<sub>2</sub> with different tmdBH loading: the role of borane is important for the reaction to proceed.....125

## CHAPTER FOUR

**Table 1.** Optimization studies for Suzuki–Miyaura cross-couplings of **67b** and **67d**.....160

**Table 2.** Optimization studies for Suzuki–Miyaura cross-couplings of **19e** .....163

## CHAPTER FIVE

**Table 1.** Crystal data and structure refinement for [C<sub>20</sub>H<sub>22</sub>ONBF<sub>3</sub>][K], **31k**.....172

**Table 2.** Crystal data and structure refinement for [C<sub>26</sub>H<sub>29</sub>N<sub>2</sub>O<sub>2</sub>][BF<sub>4</sub>], **59** .....174

## LIST OF SCHEMES

## CHAPTER ONE

- Scheme 1.** Selected examples of C–B to C–N bond formation. ....3
- Scheme 2.** Mechanistic comparison between retentive and invertive pathways. ....4
- Scheme 3.** Aggarwal's proposed mechanism of main group organometallic-assisted stereoretentive  $sp^2$ – $sp^3$  cross-coupling .....6
- Scheme 4.** Hoveyda's total synthesis of (–)-equisetin involving 3 steps using boronic esters. ....8

## CHAPTER TWO

- Scheme 1.** Recent methodologies for the preparations of chiral benzylic boronic esters. ....86

## CHAPTER THREE

- Scheme 1.** Determination of absolute configuration of CAHB of cyclic  $\gamma,\delta$ -unsaturated amides via x-ray crystallographic analysis of  $\gamma$ -trifluoroborato amide **31k**. ....121



## LIST OF ABBREVIATIONS

anhyd.	anhydrous
aq	aqueous
Ar	Aryl
BF <sub>4</sub>	Tetrafluoroborate
BINAP	2,2'-Bis(diphenylphosphino) 1,1'-binaphthyl
BINOL	1,1'-Bi-2,2'-naphthol
Bn	Benzylic/benzyl
Calcd.	calculated
CAHB	Catalytic asymmetric hydroboration
catBH	Catecholborane
CDI	1,1-carbonyldiimidazole
cod	Cyclooctadiene
DCC	<i>N,N'</i> -Dicyclohexylcarbodiimide
DCM	Dichloromethane
dr	Diastereomer ratio
DFT	Density functional theory
DMB	2,5-dimethylborolane
DMF	<i>N,N</i> -dimethylformamide
ee	Enantiomeric excess
equiv	Equivalent
Et	Ethyl

EtOAc	Ethyl acetate
EtOH	Ethanol
FTIR	Fourier-Transform Infrared
GC	Gas chromatography
h or hr	Hour
H <sub>2</sub>	Hydrogen
HCl	Hydrochloric Acid
HPLC	High-performance liquid chromatography
HRMS	High-resolution mass spectrometry
Hz	Hertz
(Ipc) <sub>2</sub> BH	Diisopinocampheylborane
(Ipc)BH <sub>2</sub>	Monoisopinocapheylborane
IR	Infrared
J	Coupling Constant
L	Ligand
M	Molarity
m-	Meta
Me	Methyl
MeOH	Methanol
min	Minutes
m.p.	Melting point
N <sub>2</sub>	Nitrogen
NaH	Sodium hydride

nb	Norbornadiene
NHC	<i>N</i> -heterocyclic carbene
NMR	Nuclear magnetic resonance
[O]	Oxidation
o-	Ortho
p-	Para
Pd/C	Palladium on carbon
Ph	Phenyl
pinBH	Pinacolborane
rac	Racemic
rt	Room temperature
satd.	saturated
SOCl <sub>2</sub>	Thionyl chloride
TADDOL	$\alpha,\alpha,\alpha',\alpha'$ -Tetraaryl-1,3-dioxolan-4,5-dimethanol
TBAF	Tetra-butyl ammonium fluoride
TIPS	Trisopropylsilyl chloride
<i>t</i> Bu	Tetra-butyl
THF	Tetrahydrofuran
TLC	Thin-layer chromatography
tmdBH	4,5,6-trimethyl-1,3,2-dioxaborinane

## CHAPTER ONE: INTRODUCTION

## 1.1 Chiral boronic esters – Useful synthetic intermediates

Chiral boronic esters are significantly useful synthetic intermediates for a growing number of stereospecific transformations. Figure 1 illustrates some selected stereospecific transformations of C–B bond to a wide range of other useful functionalities, including C–O, C–N, C–E (E = electrophile; e.g., nitrogen, oxygen, and halides), C–H, and C–C bond formations. Examples are shown in simplified theme for secondary organoboronates, but many of listed transformations work equally well for tertiary boronic esters.<sup>1</sup>

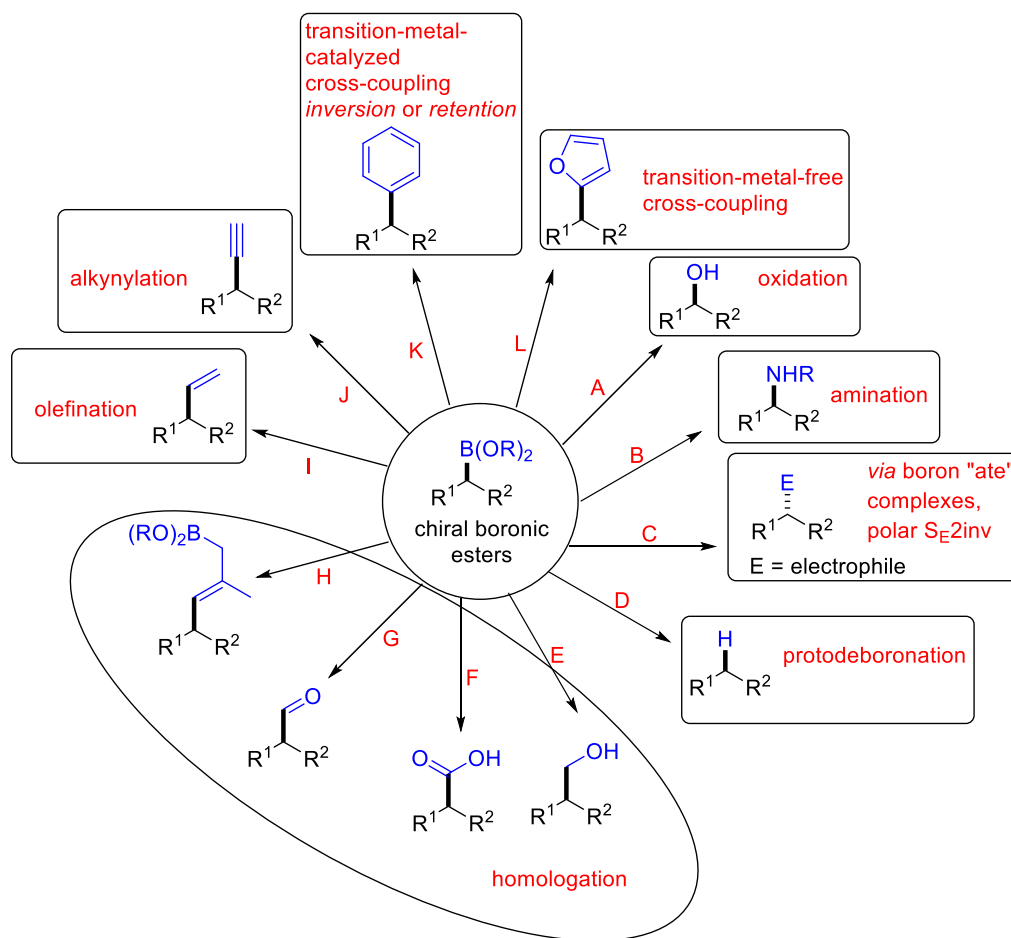
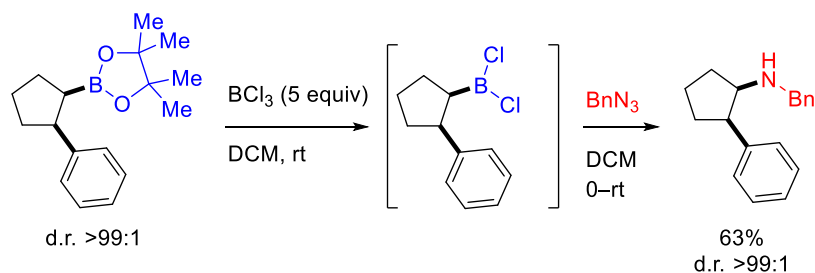


**Figure 1.** Some selected stereospecific transformations of C–B bonds

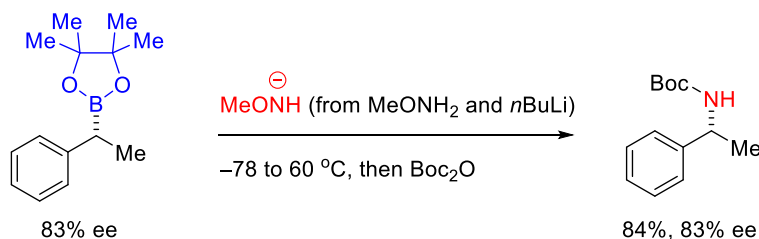
Among the examples shown in Figure 1, the stereospecific C–B to C–O bond formation via oxidation (Figure 1, route A) is the most commonly used method, in which the most widely used reagent is basic hydrogen peroxide developed by Brown and co-workers.<sup>2</sup> However, many functional groups (e.g., ester) could not be tolerated under the harsh conditions. Alternatively, when oxidizing boronic esters in the presence of versatile functional groups (e.g., ester), sodium perborate is a good choice.<sup>3</sup>

Building from the mechanism of oxidation of boronic esters by basic hydrogen peroxide, in which the peroxide attacks the empty p-orbital on the boron to form the “ate” complex followed by 1,2-metallate rearrangement and hydrolysis, many research groups sought other nucleophiles en route to new carbon–heteroatom bond formations. For example, C–B to C–N bond formation (Figure 1, route B) has been developed by Brown,<sup>4</sup> Matteson,<sup>5,6</sup> Knochel,<sup>7</sup> Morcken,<sup>8</sup> and Aggarwal.<sup>9</sup> The mechanisms of C–O and C–N bond formations are somewhat similar; however, since neutral nitrogen (e.g., amine containing a good leaving group or alkyl azide) is not as good a nucleophile as peroxide, the reaction conditions typically require a base for amine deprotonation (i.e., to enhance the amine nucleophilicity) or in case of azide nucleophile, a chlorine source (e.g., SiCl<sub>4</sub> or BCl<sub>3</sub>) are used to increase the Lewis acidity of the boron (i.e., converting the boronic ester to the corresponding dichloroborane) (Scheme 1). More than 80% of all drugs and drug candidates contain amine functionality; hence, the transformation of C–B to C–N bond further illustrates the importance of chiral boronic esters.

Knochel 2002

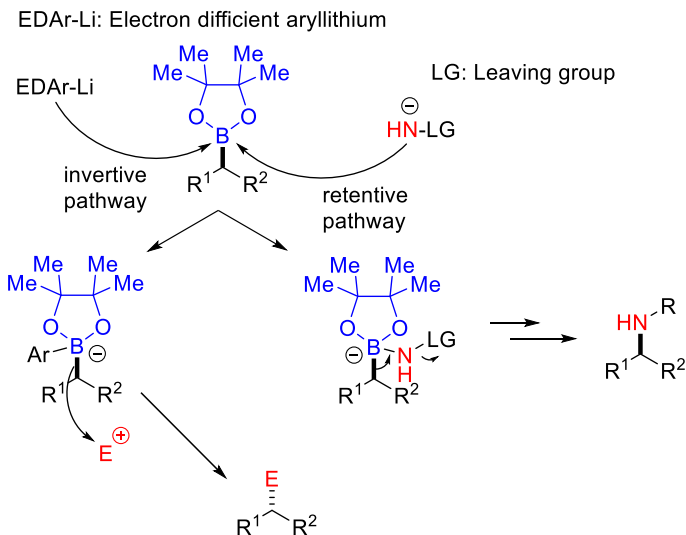


Morken 2012



**Scheme 1.** Selected examples of C–B to C–N bond formation

The two stereospecific transformations described above (i.e., C–B to C–O and C–N) proceed with stereoretention rationally explained by the 1,2-metallate shift pathway. To complement the stereoconfiguration, Aggarwal proposed a nucleophilic boron “ate” complex that could undergo invertive  $S_E2$  in the presence of an electrophile (Figure 1, route C and Scheme 2).<sup>10</sup> The methodology works quite well for halogenation (i.e., chlorination, iodination, bromination, and fluorination) as well as C–B to C–O and C–N bond formations.



**Scheme 2.** Mechanistic comparison between retentive and invertive pathways

Chiral boronic esters are useful not only in stereospecific transformation but also can be removed (i.e., C–B to C–H bond formation; Figure 1, route D) for late-stage functionalization purpose. Figure 2 illustrates some biologically active molecules prepared via protodeboronation methodology.<sup>1</sup>

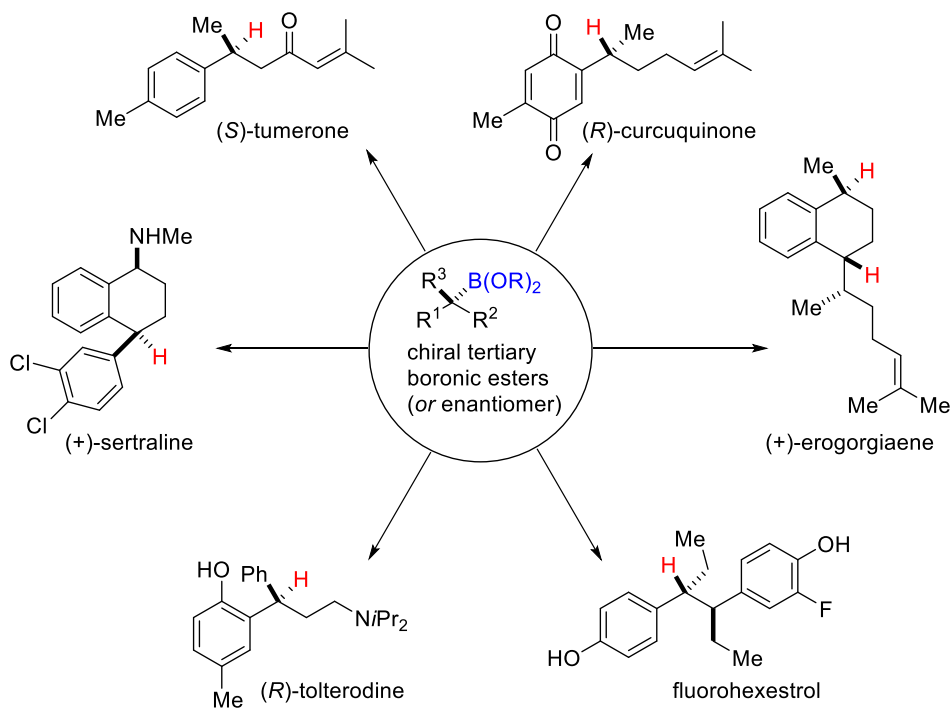


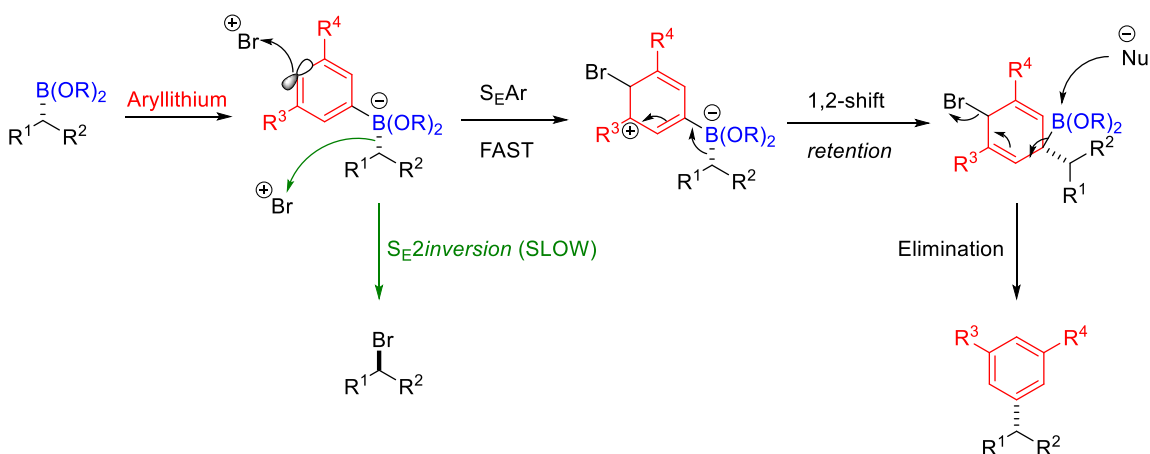
**Figure 2.** Preparation of biologically active molecules *via* protodeboronation methodology.

Though C–B to C–O bond formation is the most commonly used method, perhaps for analysis purpose, the stereospecific transformation to C–C bond has recently received extensive interest (Figure 1, routes E–L). Following initial report on one-carbon homologation using dihalomethane (e.g., iodochloromethane) to form enantioenriched primary alcohol after oxidation (Figure 1, route E) by Matteson<sup>11</sup> and co-workers, Crudden<sup>12</sup> *et. al* synthesized enantioenriched carboxylic acid (Figure 1, route F) and aldehyde (Figure 1, route G) via homologation/ oxidation using NaClO<sub>2</sub> and NaBO<sub>3</sub>, respectively. Later on, Aggarwal<sup>13</sup> and Fandrick<sup>14</sup> found that the method also works well for tertiary boronic esters. In addition, Aggarwal group applied Matteson's homologation following by Pd-catalyzed 1,3-borotropic shift to achieve three-carbon homologated primary boronic esters in essentially complete retention of configuration (Figure 1, route H).<sup>15</sup> Similarly, when vinyl Grignard or organolithium reagent is used in replacement of dihalomethane followed by treatment with I<sub>2</sub>/NaOMe or I<sub>2</sub>/TBAF, either alkene<sup>13,16,17</sup> or alkyne<sup>18</sup> is formed with complete stereoretention (Figure 1, routes I and J).

Besides the above C–C bond formations, Pd-catalyzed cross-coupling (e.g., Suzuki–Miyaura) is one of the most established methods in modern organic synthesis (Figure 1, route K).<sup>19–21</sup> Crudden,<sup>22,23</sup> Molander,<sup>24</sup> Suginome,<sup>25–27</sup> Hall,<sup>28,29</sup> Morken,<sup>30</sup> Biscoe,<sup>31</sup> and our group<sup>32,33</sup> have recently shown interest in the stereochemical aspects of the palladium-catalyzed cross-coupling of chiral secondary organoboron derivatives; the reactions could undergo either retention or inversion of configuration depending on the choice of substrates and catalysts. It is one of the main points of this thesis and will be

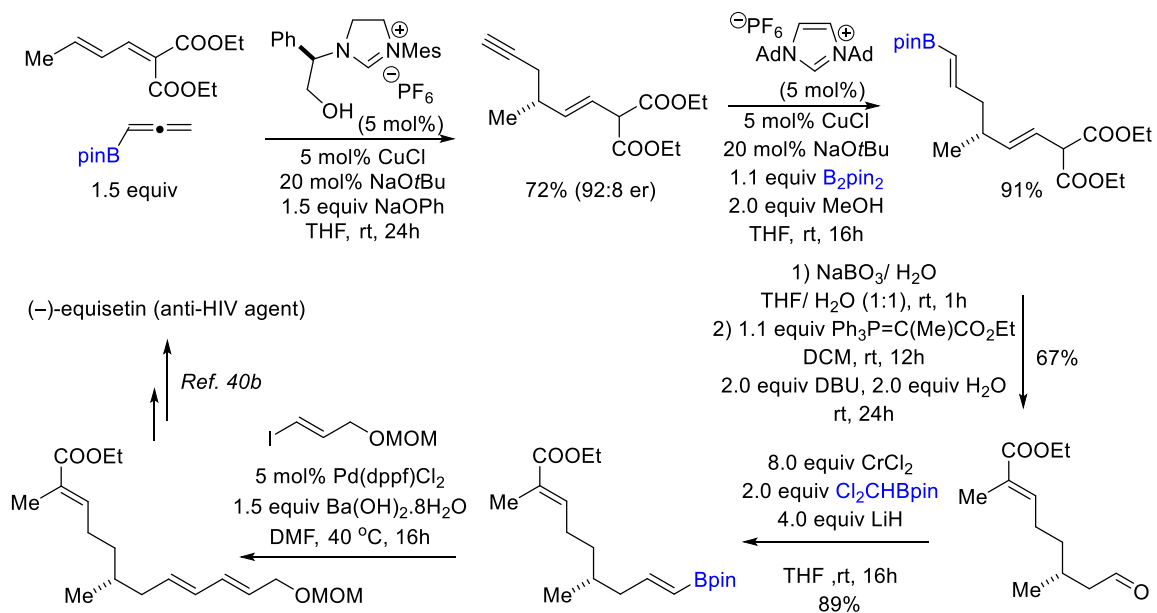


discussed in details *vide infra* (Chapter 4). In contrast to the conventional palladium-catalyzed cross-coupling, main group organometallic assisted  $sp^3$ – $sp^2$  cross-couplings developed by Aggarwal<sup>34–37</sup> (Figure 1, route L) undergo  $S_EAr$  and stereoretentive 1,2-metallate shift as shown in Scheme 3.



**Scheme 3.** Aggarwal's proposed mechanism of main group organometallic-assisted stereoretentive  $sp^2$ – $sp^3$  cross-coupling.

In addition to those versatile transformations described above, boronic esters have been applied to many syntheses of natural products and pharmaceutical compounds.<sup>38–43</sup> For example, Hoveyda and co-workers introduced the synthesis of *anti*-HIV agent (–)-equisetin, in which 3 steps utilizing transformations of boronic esters (Scheme 4).<sup>40</sup>



**Scheme 4.** Hoveyda's total synthesis of (-)-equisetin involving 3 steps using boronic esters.

## 1.2 Recent development in the preparation of chiral boronic esters

Since chiral boronic esters are valuable synthetic intermediates as shown in section 1.1, an extensive assortment of asymmetric routes for their preparation have been carried out by many research groups. Among all of the available methodologies, transition-metal-catalyzed asymmetric hydroboration (CAHB) of alkenes is arguably the most attractive approach mostly due to the atom-economic nature of the transformation.<sup>44</sup> Enantioselective hydroboration of activated alkenes (i.e., vinyl arene derivatives, conjugated alkenes, or conjugated carbonyl compounds) have been extensively studied by many research groups and will be discussed in details *vide infra* in this chapter (section 1.4). Takacs group, on the other hand, is interested in enantioselective hydroboration of unactivated alkenes utilizing coordinating functional groups (e.g., carbonyl derivatives) to give functionalized, chiral boronic esters. Previous work by Dr. Sean M. Smith<sup>45-48</sup> (University of Nebraska, 2012) opened access to  $\beta$ -borylated carbonyl derivatives via carbonyl directed CAHB; work by Mr. Suman Chakrabarty<sup>49</sup> and Ms. Veronika Shoba<sup>50</sup> involving phosphonate and oxime ether-directed CAHB, respectively, produced chiral tertiary boronic esters which are only accessible by a few alternative methods (Chapter 1.4.2). These studies demonstrated that the selectivity of hydroboration is highly dependent not only on directing group but also on alkene substitution patterns, the choice of catalyst systems and borane reagents. Experiments discussed in this dissertation will amplify mentioned above discoveries with novel direct routes to chiral secondary  $\gamma$ - and  $\delta$ -borylated carbonyl derivatives as well as their applications to a wide range of stereospecific transformations demonstrating the synthetic utility of the organoboron intermediates (Chapters 2–4).

Apart from CAHB, there are recently extensive developments for the enantioselective preparation of chiral boronic esters (Figure 3). Most recently, the Yu group at Scripps reported amide-directed palladium-catalyzed C–H  $\beta$ -borylation of small ring systems highlighting the first and only one enantioselective version using the same methodology up to date (Figure 3A).<sup>51</sup> Shortly before that, the Fu group reported stereoconvergent alkyl–alkyl cross couplings of racemic  $\alpha$ -haloboronates with organozinc reagents using Nickel catalysts (Figure 3B).<sup>52</sup> The method allows access to stereogenic secondary boronic esters bearing multiple chiral centers via an iterative homologation process. Using mechanistically different method but with similar approach, Aggarwal's lithiation-borylation/ Matteson's homologation also provides entry to multiple contiguous stereocenters (Figure 3C).<sup>53</sup> The methodology en routes to several natural products (i.e., (+)-kalkitoxin and (+)-hydroxyphthioceranic acid)<sup>54</sup> and highlights one of a few methods for the preparation of chiral tertiary boronic esters.<sup>55</sup> Several alternative methods for the synthesis of chiral tertiary boronic esters are independently reported by Shibasaki<sup>56,57</sup>/ Yun<sup>58</sup>/ Hoveyda<sup>59,60</sup> via enantioselective conjugate borylation (Figure 3D) and Tang<sup>61</sup> via directed CAHB (see Figure 6 for Tang's example); Hoveyda and co-workers also independently developed an efficient copper-catalyzed allylic substitution with B<sub>2</sub>pin<sub>2</sub> affording tertiary allylboronic esters (Figure 3E).<sup>62</sup> Compared to tertiary boronic esters, chiral primary and secondary organoboronates are thought to be more easily accessed but are not less useful (i.e., the current applications of tertiary boronic esters are limited to main group organometallic-assisted transformations mainly developed by Aggarwal<sup>1</sup> group). Consequently, many research groups have developed a wide range of methodologies for the asymmetric preparation of the latter. For example,

using different substitution patterns of alkenes (i.e., disubstituted alkenes as opposed to trisubstituted alkenes as shown in Figure 3D) in conjugate borylation, Hoveyda along with other groups reported the enantioselective synthesis of chiral secondary boronic esters.<sup>63</sup> Not restricted to conjugate borylation, Hoveyda and co-workers developed an enantioselective copper-catalyzed allylic substitution with diborylmethane to generate synthetic useful chiral primary homoallylic boronic esters and well as illustrate their applications in synthesis (Figure 3F).<sup>64</sup> Similarly, Niu and co-workers independently reported the same approach using silver-assisted, iridium-catalyzed allylation.<sup>65</sup> The Morcken group is one of the most active groups in this area (i.e., preparation of chiral boronic esters). His group has developed a number of methods for the enantioselective preparation of chiral secondary organoboranes including asymmetric hydrogenation of vinyl boronates (Figure 3G)<sup>66-68</sup> and Pt-catalyzed diboration<sup>69</sup> followed by Pd-catalyzed group-selective cross-couplings<sup>70</sup> of diboranes (Figure 3H). Recently, his group found that chiral carbohydrates also serve as efficient catalysts for enantioselective diboration reactions.<sup>71</sup> In addition to those, Morcken and co-workers have also developed palladium-catalyzed enantioselective conjunctive cross-coupling reactions (Figure 3I).<sup>72-74</sup> The groups of Yun and Miura are also very active in this area. For instance, besides conjugate borylation as discussed above, Yun and co-workers also reported several different examples of asymmetric reactions with vinyl boronates (Figure 3J).<sup>75</sup> Miura group, in addition to independent report of asymmetric reactions with vinyl boronates,<sup>76</sup> has developed the three-component coupling generating chiral  $\alpha$ -amino boronic esters in high yield and enantioselectivity (Figure 3K).<sup>77</sup> Referring to the three-component coupling, the Toste<sup>78</sup> and Liao<sup>79</sup> groups independently reported enantioselective palladium-catalyzed

1,1-arylboration (Figure 3L) and copper-catalyzed 1,2-allylboration (Figure 3M), respectively. Referring to the formation of chiral  $\alpha$ -amino boronic esters, Liao<sup>80</sup> and Ellman<sup>81</sup> groups independently introduced asymmetric borylation of imine using different approaches; while Ellman and co-workers pioneered a copper-catalyzed borylation of chiral *N*-(*tert*-butanesulfinyl)aldimines, Liao group reported a copper-catalyzed borylation of prochiral *N*-Boc-imines using a chiral *tert*-butyl sulfoxide–phosphine ligand (Figure 3N illustrated Ellman’s example). In addition to CAHB and the methodologies discussed above, there are several other attractive approaches including enantioselective B–H insertion (Figure 3O), independently reported by Zhou<sup>82</sup> and Xu<sup>83</sup> groups, enantioselective nucleophilic addition to aldehyde (Figure 3P), separately reported by Ito<sup>84</sup> and Meek,<sup>85</sup> and stereospecific Miyaura borylation (Figure 3Q) obtained by Watson and co-workers.<sup>86,87</sup>

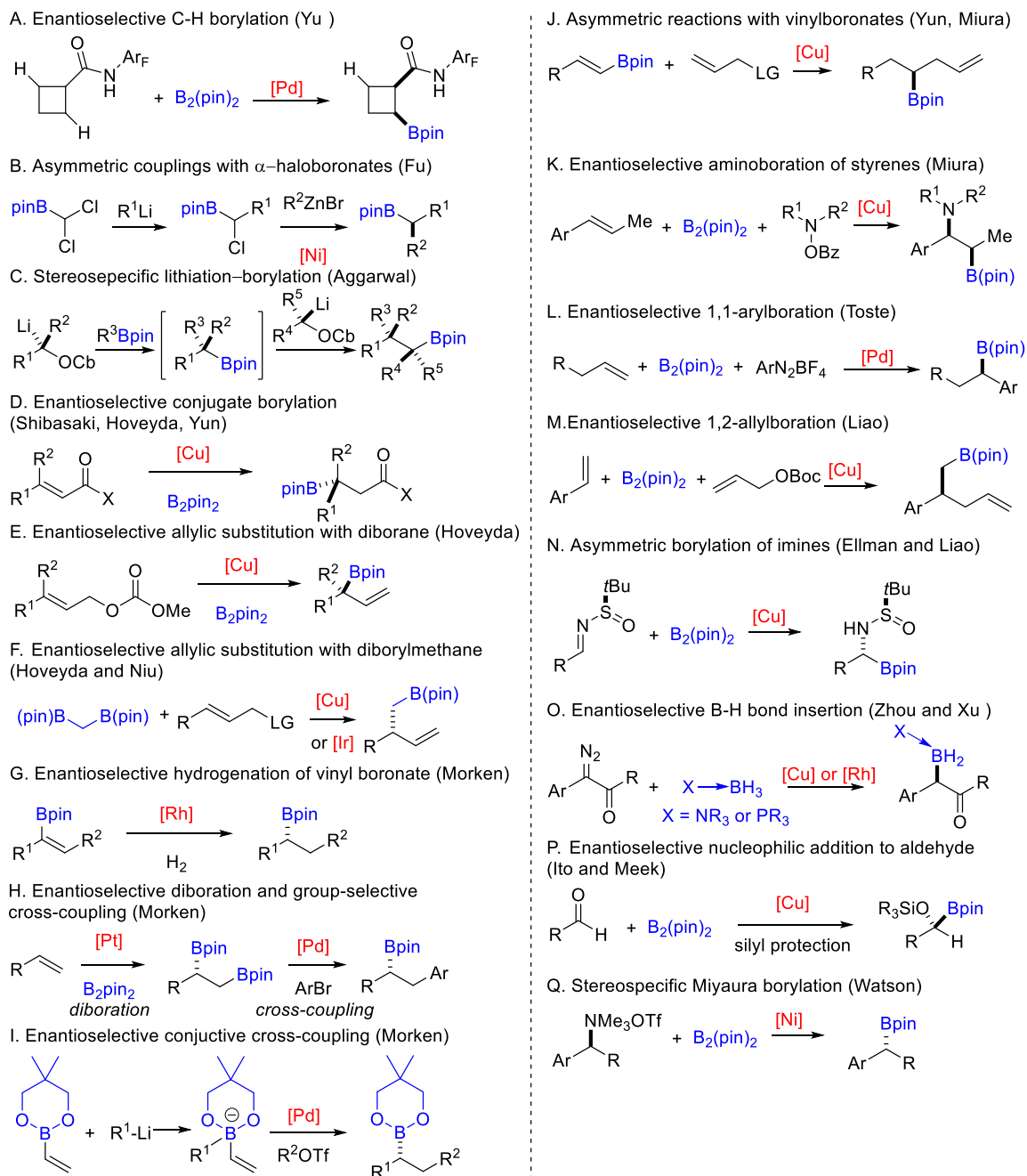


**Figure 3.** Selected examples of recent developments in the preparation of chiral boronic esters

### 1.3 Stoichiometric asymmetric hydroboration of alkenes

Despite the effectiveness of alternative methods for generation of chiral boronic esters discussed in section 1.2, asymmetric hydroboration remains the most attractive method highlighted by the discovery of H. C. Brown in 1956 resulting in the Nobel Prize in 1979.<sup>88</sup> The history of hydroboration is briefly shown in Figure 4.

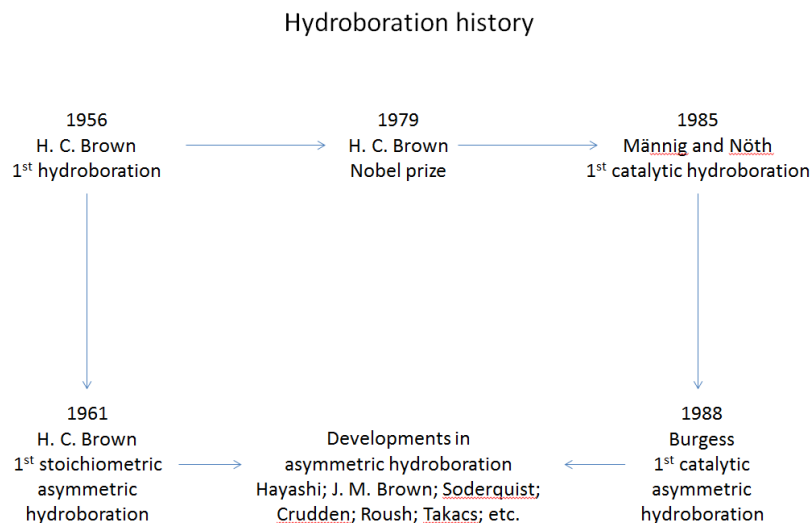


**Figure 4.** Brief hydroboration history.

Five years after the initial discovery, Brown showed that the asymmetric version could be performed using a chiral borane reagent (i.e., diisopinocampheylborane **(Ipc)<sub>2</sub>BH**, Table 1).<sup>89–92</sup> The **(Ipc)<sub>2</sub>BH** provides excellent enantioselectivity for *cis*-alkenes but poor selectivity for *trans*- and trisubstituted alkenes. The observations could be explained by steric hindrance; the size of *trans*- and trisubstituted alkenes could be too large for the reagent.<sup>93</sup> To solve the problem, monoisopinocampheylborane **(Ipc)BH<sub>2</sub>** was synthesized in essentially complete enantiopurity (i.e.; 100% ee).<sup>94</sup> The borane reagent successfully improved the selectivity for *trans*- and trisubstituted alkenes (results shown in Table 1 for direct comparison see refs 95–97 for better selectivity) from moderate to excellent selectivity.<sup>95–97</sup> However, in contrast to the di- discussed above, the mono-



version of the borane provided poor selectivity for *cis*-alkenes. These Brown's reagents **(Ipc)<sub>2</sub>BH** and **(Ipc)BH<sub>2</sub>** are apparently complementary to each other giving good selectivity for all *cis*-, *trans*-, and trisubstituted alkenes. In 1985, Masamune introduced a C<sub>2</sub>-symmetric dimethylborolane (**DMB**) which also provides excellent selectivity for all alkenes discussed above.<sup>98</sup> Even though Masamune's **DMB** seems to be more effective compared to Brown's reagents, the seven-step synthesis of the otherwise simple looking borane dramatically decreases its practicality. It is worth noting that both Brown's and Masamune's reagents are not effective for 1,1-disubstituted alkenes (i.e., methyldene substrates). In 2008, Soderquist and co-workers developed bicyclic boranes labeled **[3.3.2]-Ph** and **[3.3.2]-TMS** in Table 1.<sup>99</sup> The Soderquist's borane reagents provide good selectivity for not only the three types of alkenes discussed above but also the more challenging sub-class of alkenes, methyldene substrates in which the steric demand between the alkene substituents is significantly different (e.g., methyl vs. *tert*-butyl or phenyl vs. deuterium). The 1,1-disubstituted alkene is considered more challenge than its other substituent patterns because it is not easy for the catalysts to recognize or effectively differentiate between the prochiral enantiotopic faces.<sup>100</sup>

**Table 1.** Stoichiometric asymmetric hydroboration using chiral borane reagents. Color code: **excellent selectivity**, **moderate selectivity**, and poor selectivity

	Brown		Masamune	Soderquist			
	$(\text{Ipc})_2\text{BH}$	$(\text{Ipc})\text{BH}_2$	DMB	[3.3.2]-Ph	[3.3.2]-TMS		
	<i>trans</i> -alkenes	<i>cis</i> -alkenes	tri-substituted alkenes	1,1-disubstituted alkenes (methylidene substrates)			
$(\text{Ipc})_2\text{BH}$	14% ee	99% ee	15% ee	32% ee	—	—	—
$(\text{Ipc})\text{BH}_2$	73% ee	24% ee	53% ee	—	—	5% ee	—
DMB	99% ee	98% ee	98% ee	—	—	—	—
[3.3.2]-Ph	96% ee	32% ee	74% ee	38% ee	92% ee	78% ee	92% ee
[3.3.2]-TMS	95% ee	84% ee	—	52% ee	56% ee	66% ee	98% ee

Though the development of asymmetric hydroboration obtained by Brown, Masamune, and Soderquist is very much appreciated, the stoichiometric use of the chiral sources (i.e., borane reagents) is not the most efficient method. In addition, the above reagents are either not easy to make or quite reactive, and thus controlling the chemo- and enantioselectivity becomes a big challenge. To overcome the problem, many research groups have been seeking for a catalytic version using substoichiometric amount of the chiral sources. As shown in Figure 4, after H. C. Brown's Nobel Prize, in 1985 Männig and Nöth introduced the first catalytic hydroboration using catecholborane and Wilkinson's catalyst.<sup>101</sup> Though the first catalytic asymmetric hydroboration was credited to Burgess in 1988 using catecholborane (catBH) in the presence of neutral rhodium-DIOP or rhodium-BINAP,<sup>102</sup> the products obtained were in low enantioinduction ranging from racemic up to 69% ee. Shortly thereafter, Hayashi and coworkers introduced the first cationic rhodium-catalyzed asymmetric hydroboration of styrenyl derivatives with (+)-BINAP and catBH resulting in exclusively benzylic boronic esters with excellent

enantioselectivity (85–96% ee).<sup>103</sup> After that, there is an extensive development in this area which will be discussed in details in the next section 1.4.

## **1.4 Transition-metal-catalyzed asymmetric hydroboration of alkenes**

Compared to stoichiometric asymmetric hydroboration discussed in section 1.3, the transition-metal-catalyzed asymmetric hydroboration received much of interest. The developments of catalytic asymmetric hydroboration of activated substrates (e.g., vinyl arenes) were extensively studied by many research groups and have been reviewed by Crudden,<sup>104,105</sup> Guiry,<sup>106</sup> Westcott,<sup>107</sup> and J. M. Brown.<sup>108</sup> This section will cover materials mostly developed after those reviews; materials were covered in those reviews will only be mentioned when being related. In this dissertation, vinyl arenes, conjugated alkenes, and conjugate carbonyl compounds are referred to as activated substrates. Some might also consider substrates bearing functional groups to be activated substrates, in which the alkene is activated by the functional group either with electronic, steric, stereoelectronic, or coordinating effects. However, substrates that are not vinyl arenes, conjugated alkenes, and conjugate carbonyl compounds will be considered unactivated substrates herein; they are unactivated alkenes utilizing directing functional groups. Consequently, this section will be divided into two main subsections: catalytic asymmetric hydroboration of vinyl arenes and related conjugated alkenes (i.e., activated substrates) and of non-vinyl arenes (unactivated substrates).

### **1.4.1 Catalytic asymmetric hydroboration of vinyl arenes and related conjugated alkenes**

#### **1.4.1a Rhodium catalysis**

Among the transition metals, rhodium has a long-standing history. For example, the first catalytic hydroboration by Männig and Nöth<sup>101</sup> and the first catalytic asymmetric

hydroboration by either Burgess<sup>102</sup> or Hayashi<sup>103</sup> were all carried out by rhodium metal precursors. Figure 5 illustrates some successful examples of rhodium-catalyzed asymmetric hydroboration of styrene (i.e., **A**,  $R^1 = H$ ,  $R^2 = H$ ). After Hayashi's initial report highlighting the effective bidentate P,P-ligand (i.e., BINAP), several groups have found some other effective bidentate ligands including QUINAP,<sup>109</sup> PYPHOS,<sup>110</sup> JOSIPHOS,<sup>111</sup> or the ferrocenylpyrazole derivative **E**. Though those catalyst systems provide excellent selectivity for styrene, the substrate scope and the catalyst tunability remain limited; for example, for a long time, 78 and 74% ee were the best results obtained for 4-chlorostyrene **B** ( $R^1 = Cl$ ,  $R^2 = H$ ) and 4-trifluoromethylstyrene **C** ( $R^1 = CF_3$ ,  $R^2 = H$ ), respectively using QUINAP. To overcome the problem, Takacs group showed that monodentate ligands Taddol-derived phosphite **F** and phosphoramidite **G** could tolerate the electronic effect of substrates **B** and **C** resulting in 94 and 90% ee, respectively.<sup>112</sup>

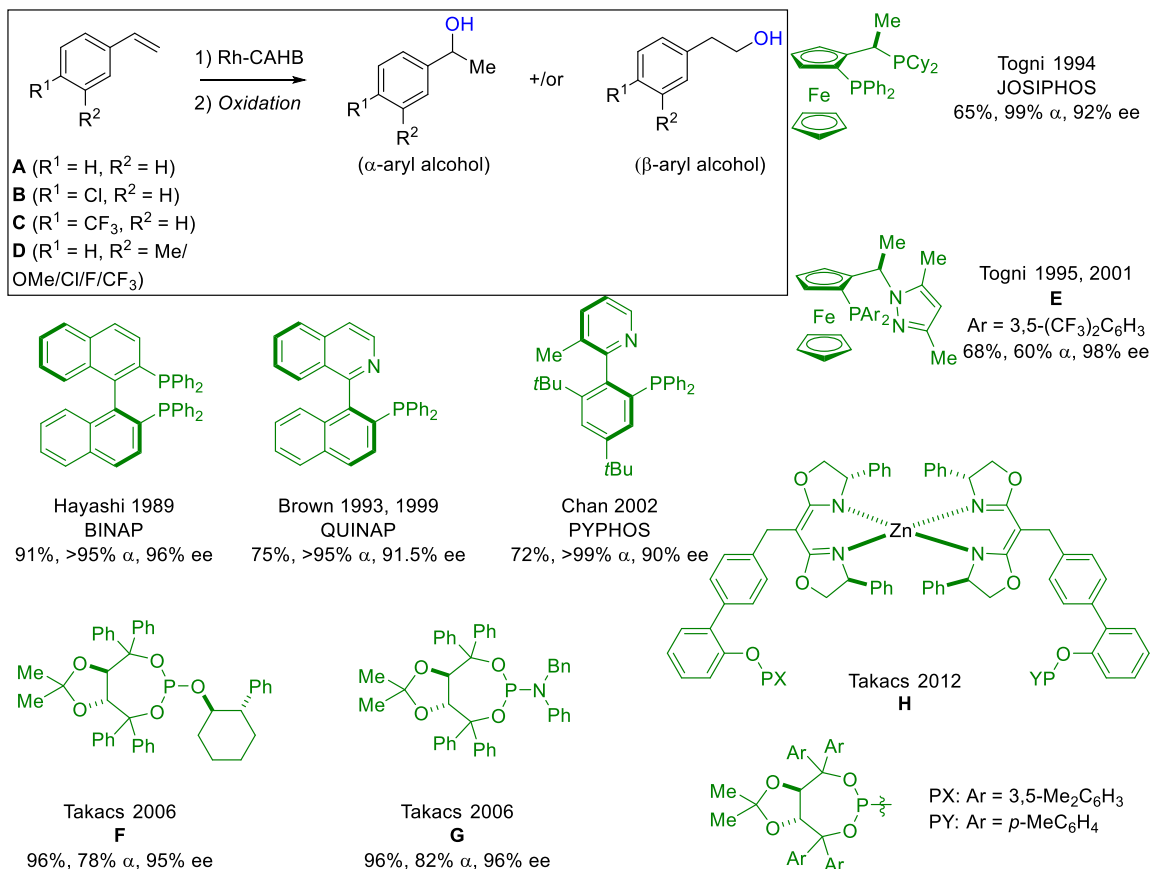


**Figure 5.** Rhodium-catalyzed hydroboration of styrene and styrenyl derivatives

To further introduce catalyst tuning, Takacs group presented a two-step optimization strategy using heterobimetallic catalyst systems: ligand/catalyst scaffold and ligating group.<sup>113</sup> There was no results obtained for styrene **A** but focused on the more challenging substrates and finding the general catalyst could well tolerate the electronic differentiation at meta position. The most general optimized catalyst system **H** performed hydroboration of *meta*-substituted substrates **D** with excellent enantioselectivities (93–94% ee) using as low as 0.05% rhodium catalyst.

In the case of CAHB of vinyl arenes, the most attractive example is perhaps the one obtained by Tang's group due to several reasons, (i) different from other examples, it is directed CAHB, (ii) the products are not only tertiary boronic esters but also  $\alpha$ -amino

boronic acid derivatives, extensively used in medicinal chemistry (Figure 6).<sup>61</sup> Using cationic Rh(I) catalyst precursor in conjunction with a chiral phosphine ligand (*R*)-BI-DIME, amide-directed CAHB of  $\alpha$ -arylenamides provides access to a series of chiral tertiary  $\alpha$ -amino boronic esters in excellent enantioselectivity (up to 99% ee). One major drawback of this transformation is that a diborane (i.e., B<sub>2</sub>pin<sub>2</sub>) is required for high enantioselectivity; the use of pinacolborane (pinBH) generates the same product in much lower ee with otherwise the same reaction conditions illustrating that the reaction is not atom-economical. It is also worth noting that the NH acidic proton is important; only trace amounts of borylated products was obtained using tertiary amide.

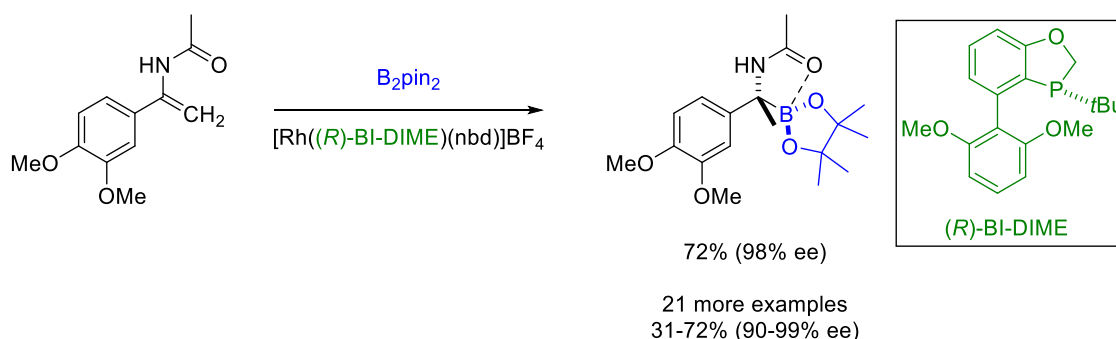


**Figure 6.** Tang's directed rhodium-catalyzed CAHB of vinyl arenes

#### 1.4.1b Iridium catalysis

In 2004, Crudden and co-workers used a cationic rhodium(I) precursor (i.e., Rh(COD)<sub>2</sub>BF<sub>4</sub>)/ JOSIPHOS (used by Togni in 1994 with catBH, Figure 5) in conjunction with pinacolborane (pinBH) instead of catecholborane (catBH) to show the reversal in enantioselectivity (Figure 7).<sup>114</sup> In the same paper, Crudden also showed that with the use of iridium catalyst, she obtained complete reversal in regioselectivity. Based upon similar observation of CAHB of diazines introduced by Bonin and Micoun, it was proposed that

reversal in enantioselectivity takes place due to a change in mechanism from Rh–H insertion to Ir–B insertion (see section 1.5 for details).<sup>115</sup>

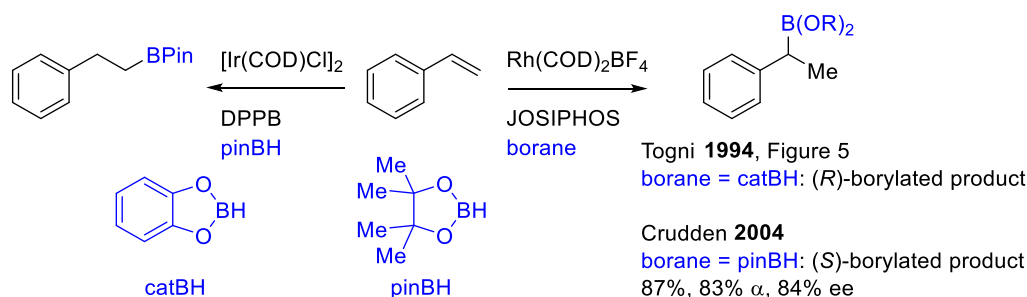


**Figure 7.** Reversal in regioselective CAHB of styrene using rhodium and iridium catalysts

Recognizing the complementary regiocontrol of iridium catalyst precursor, in 2011 Mazet and co-workers applied it to geminal  $\alpha$ -substituted styrene (i.e., 1,1-disubstituted alkenes) to introduce asymmetric CAHB (Figure 8).<sup>116</sup> This was also an important accomplishment at that time due to the hardly controlled enantioselectivity of a barely prochiral sub-class of alkenes, methylenes. In 2015, Diéguez *et. al* expanded the substrate scope using slightly modified bidentate P,N ligand (Figure 8).<sup>117</sup> The generality of both catalyst systems is only applied to substrates bearing significant differences in steric demand of the alkene substituents; moderate to poor selectivities are obtained for other substrates with otherwise the same reaction conditions. Iridium catalysts are considered more effective for regio- and diastereoselectivity control compared to rhodium catalysts in some previous findings;<sup>118–121</sup> however, in term of enantioselectivity, it still remains a challenging problem.



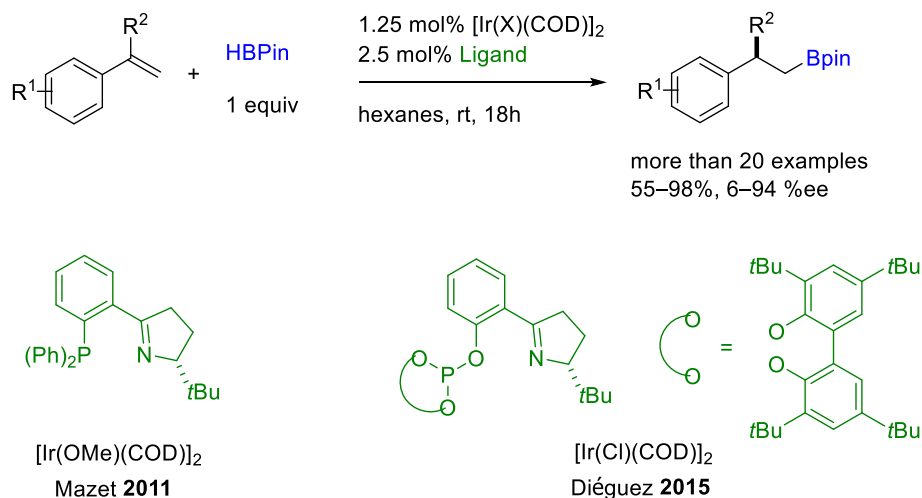


**Figure 8.** Iridium-catalyzed hydroboration of 1,1-disubstituted vinyl arenes

### 1.4.1c Cobalt and iron catalysis

In the past decade, many research groups have focused on the base-metal catalysts due to their low cost, high earth abundance, as well as environmentally benign nature.<sup>122–137</sup> Similar to iridium catalysts, iron and cobalt catalysts are found to typically produce a complementary selectivity to rhodium catalysts for catalytic hydroboration of vinyl arenes except for a few examples.<sup>122–124</sup> Up to date, successful enantioselective hydroboration using iron and cobalt catalysts are limited to geminal  $\alpha$ -substituted styrenes (i.e., 1,1-disubstituted vinyl arenes). However, cobalt and iron catalysts seem to dominate the area as their generality are applied to ca. 90 examples; many of which results in good yields and excellent enantioselectivities (Figure 9).

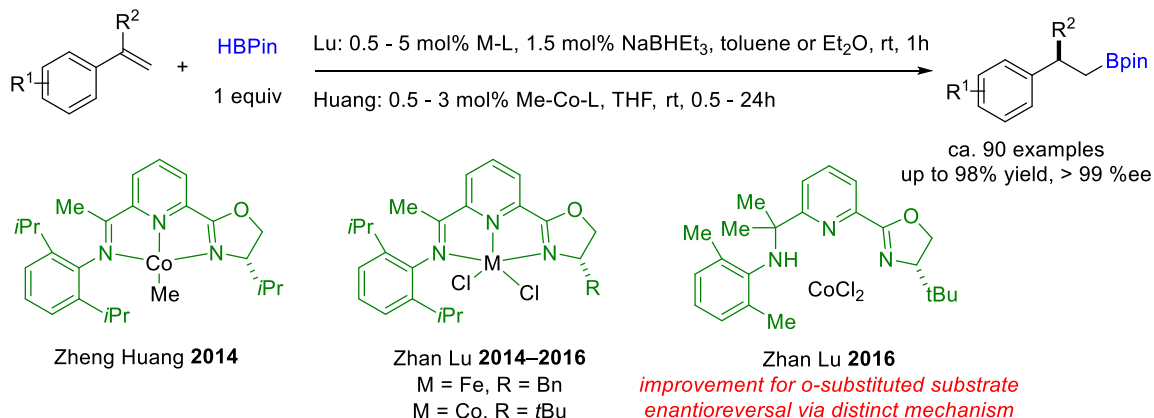


**Figure 9.** Fe- and Co-catalyzed hydroboration of 1,1-disubstituted vinyl arenes

The mechanism of Fe- and Co-catalyzed hydroboration reactions is distinct depending on the ligand employed (i.e., oxazoline iminopyridine (OIP) *versus* oxazoline aminoisopropylpyridine (OAP); see section 1.5 for mechanistic details). Interestingly, Co-OAP- and Co(Fe)-OIP-catalyzed hydroborations were achieved with opposite stereoconfigurations. In the case of OIP ligands, the generation of the M–H active catalyst species, however, is slightly different; Lu’s<sup>138–140</sup> work shows the M–H formed by the activating reagent, NaB(R)<sub>3</sub>H, whereas, Huang’s<sup>141</sup> studies claim the hydride source is not necessary, and the M–H is presumably formed by the addition of pinBH. By slightly modified the OIP along with the novel OAP ligands and the activating reagent, in 2016, Lu and coworkers showed the Co-catalyst systems efficiently catalyze hydroboration of sterically hindered 1,1-disubstituted styrenyl derivatives (i.e., *ortho*-substituted substrates), which were problematic substrates in previous studies.<sup>140</sup>

### 1.4.1d Copper catalysis

Though iron- and cobalt-catalysts employing OAP and OIP ligands seem to be the best catalyst system for asymmetric hydroboration of gem-arylalkyl alkenes as illustrated in Figure 9, the current limitation is of substrates bearing 1,1-diaryl alkenes; the substrates are neither reactive nor selective. For instance, in the same work showing excellent selectivity for hydroboration of gem-arylalkyl alkenes, Huang and co-workers pointed out that the current catalyst system (i.e., cobalt with OIP ligand) is not efficient for gem-diaryl alkenes (Figure 10A).<sup>141</sup> Recently, Xiong group found that copper system

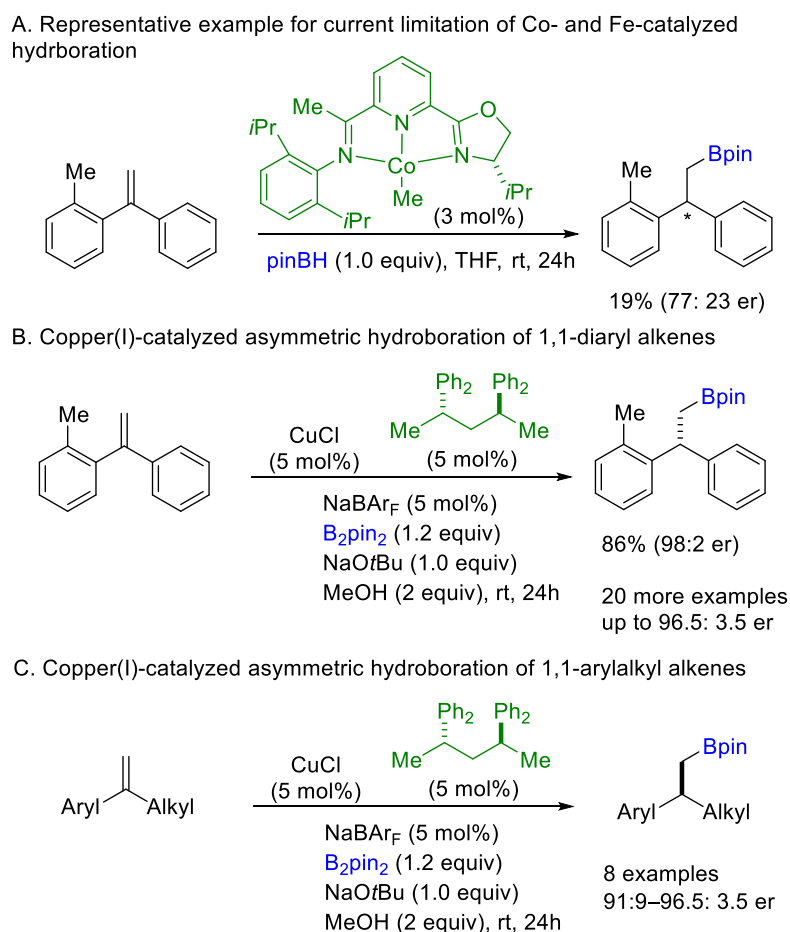


**Figure 10.** Recent advancement for asymmetric hydroboration of gem-diaryl alkenes using copper(I) catalyst.

could fix the problem; a series of 1,1-diaryl substituted alkene efficiently undergoes copper(I)-catalyzed hydroboration with high yield and enantioselectivity (Figure 10B).<sup>142</sup> The generality of the catalyst system can also be applied for gem-arylalkyl alkenes (Figure 10C).

While iridium-, cobalt-, and iron-catalyzed hydroboration reactions are currently limited to 1,1-disubstituted alkenes, along with rhodium, copper catalysts have been shown to facilitate hydroboration of different classes of alkenes. The first enantioselective copper-catalyzed hydroboration was carried out by Yun and co-workers in 2009 for styrenes.<sup>143</sup> With the use of Tangphos ligand, styrenes undergo copper-catalyzed hydroboration to afford benzylic boronic esters in good yield and excellent enantioselectivity (Figure 11). Later on, the same group found that DTBM-Segphos is more reactive for  $\beta$ -substituted vinyl arenes;<sup>144</sup> i.e., Tangphos is also selective but less reactive. Both ligands afford the same regioisomers (i.e., benzylic boronic ester/  $\alpha$ -selective) in high yield and enantioselectivity (Figure 11).

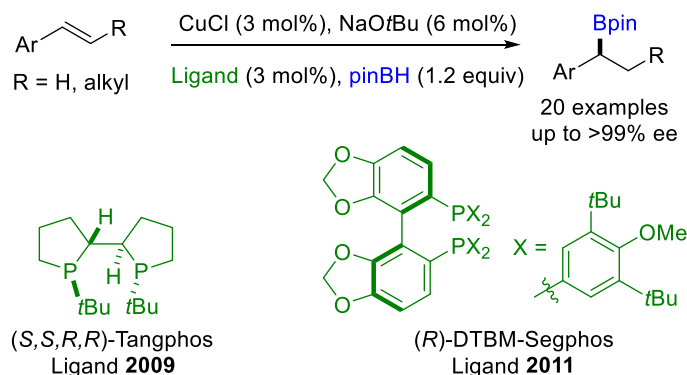


**Figure 11.** Yun's  $\alpha$ -selective copper(I)-catalyzed hydroboration of vinyl arenes

It is worth to note that the Yun's hydroboration uses pinBH as the boron source resulting in  $\alpha$ -selective hydroboration of vinyl arenes. On the other hand, replacement of pinBH by B<sub>2</sub>pin<sub>2</sub> gives the rise to complement regioselectivity (i.e.,  $\beta$ -selective). For

example, Cu-NHC-catalyzed hydroboration of both  $\alpha$ - and  $\beta$ -substituted vinyl arenes employing  $B_2pin_2$  provide  $\beta$ -borylated products (Figure 12).<sup>145,146</sup>

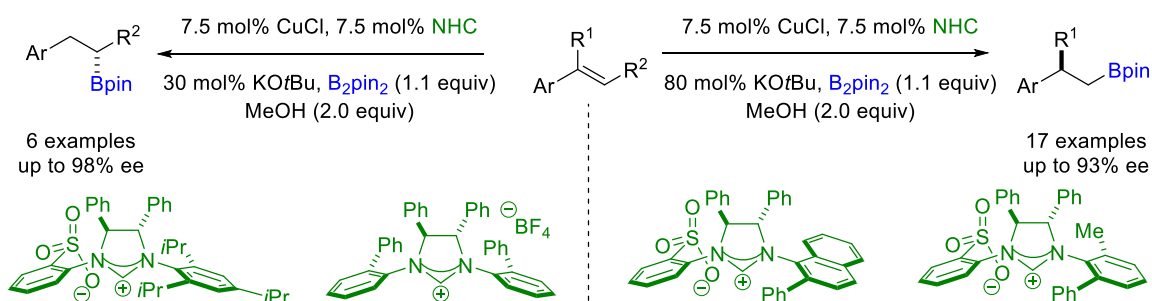


**Figure 12.** Hoveyda's  $\beta$ -selective Cu-NHC-catalyzed hydroboration of vinyl arenes

Different from the above examples, Tian and Lin claimed that their work on Cu(I)-catalyzed hydroboration of dehydroamino acid methyl esters was achieved via ester-directed asymmetric hydroboration (see section 1.5 for mechanistic details).<sup>147</sup> Although the work is not diastereoselective (i.e.,  $dr \sim 1:1$ ), the two diastereoisomers can be separated in total good yield with each high enantioselectivity (Figure 13). Another drawback of the methodology is that 4–5 equiv of  $B_2pin_2$  is necessary for high conversion; it is not clear what result was obtained with pinBH. Systematically, it can also be considered as a conjugate borylation process.

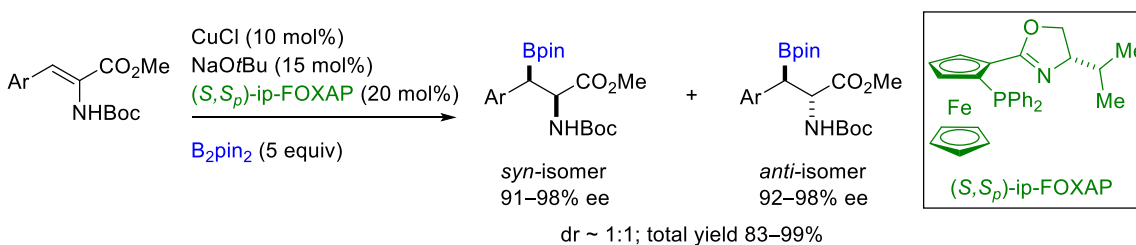


**Figure 13.** Copper(I)-catalyzed hydroboration of dehydroamino acid methyl esters

Similarly, Tortosa's work on *p*-quinone methides could be considered as either hydroboration or conjugate borylation (Figure 14).<sup>148</sup> Different from conventional conjugate borylation, the driving force in this case is aromatization making this process a

unique example. In addition, this methodology highlights one of a few examples producing highly enantioenriched diaryl substituted benzylic boronic esters.<sup>149,150</sup>

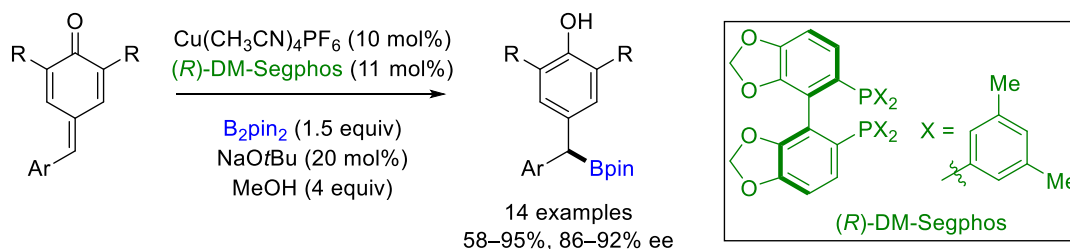


**Figure 14.** Copper(I)-catalyzed borylative aromatization of *p*-quinone methides

Though Ito's substrate is not vinyl arene but conjugate diene (i.e., 1,3-diene), it is considered to belong to activated substrate category.<sup>151</sup> A series of cyclic 1,3-diene substrates undergo Cu(I)-catalyzed hydroboration resulting in either allylic- or homoallylicboronic esters with temperature being the most important factor of regiocontrol (Figure 15).

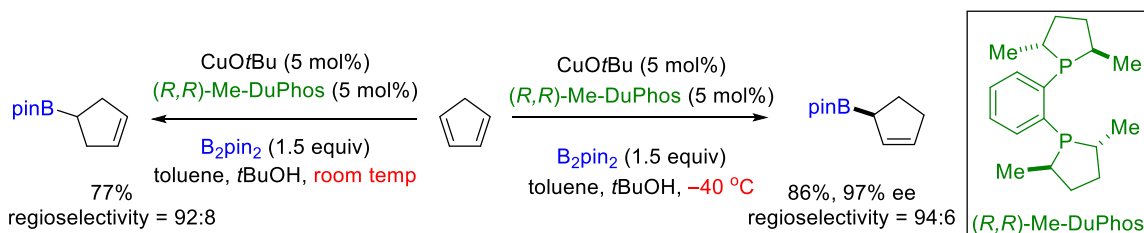


**Figure 15.** Temperature dependence in regioselective Cu(I)-catalyzed hydroboration of cyclic 1,3-dienes.

#### 1.4.2 Catalytic asymmetric hydroboration of non-vinyl arenes

Thus far, catalytic asymmetric hydroboration of unactivated alkenes was achieved only with rhodium and copper catalysts. The story of rhodium in this category started with Gevorgyan's on the enantioselective desymmetrization of a few examples of cyclopropenes via Rh(I)-catalyzed asymmetric hydroboration.<sup>152</sup> After that, besides

Takacs' Rh(I)-catalyzed CAHB, there are only four examples using copper up to date in which three of them are enantioselective desymmetrizations of cyclic substrates (Figure 16A). In 2014, Tian and co-workers introduced a series of cyclopropenes substrates bearing an aryl and a methylester group at the tetrasubstituted carbon; copper(I)-catalyzed CAHB of these substrates affords solely *trans*-product in high yield and enantioselectivity.<sup>153</sup> The *trans*-diastereoselectivity is claimed due to the steric effect of the methylester group as well as the weak coordination of copper to the carboxyl group. Tortosa and co-workers also applied the copper catalyst on enantioselective hydroboration of cyclopropenes<sup>154</sup> via desymmetrization. Later on, the same group with slightly modified reaction conditions was able to carry out desymmetrization of cyclobutenes.<sup>155</sup> Notably, both systems do not involve the coordinating functional group indicating that the high diastereoselectivity is completely controlled by steric effect. In 2016, Xi and Hartwig reported the only example of Cu(I)-catalyzed asymmetric hydroboration of acyclic aliphatic internal alkenes in which the regioselectivity is controlled by the electronic effect of the directing group employed (Figure 16 B).<sup>156</sup>

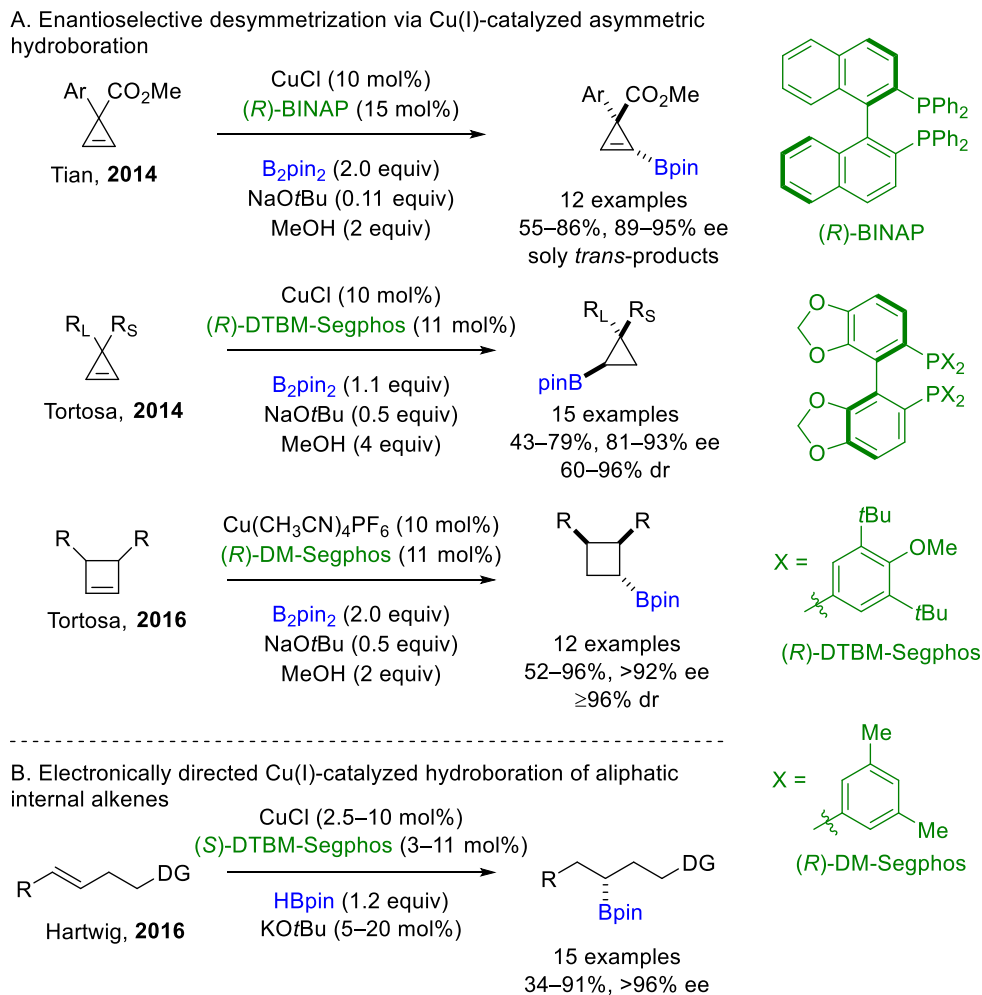


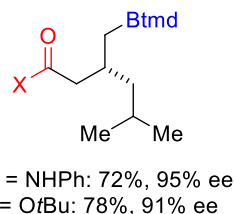
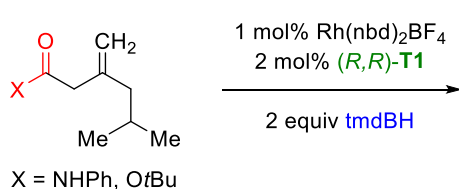
**Figure 16.** Cu(I)-catalyzed asymmetric hydroboration of unactivated alkenes

Takacs group has been actively involved in catalytic asymmetric hydroboration of unactivated alkenes utilizing rhodium catalyst and coordinating functional groups since 2008. The group found that the controlling factors for regio- and enantioselectivity are varied as a function of directing groups (e.g., carbonyl, oxime ether, phosphonate), substitution patterns (e.g., disubstituted, trisubstituted), nature of substituents (e.g., aryl, alkyl), ligands (e.g., phosphites, phosphoramidites), and boranes (e.g., pinBH, tmdBH). For examples, with similar system, carbonyl-directed CAHB of methyldene substrates differs from oxime-ether in several important aspects, including (i) the borane attacks



from opposite  $\pi$ -face, from the top face in the case of carbonyl and from the bottom in the case of oxime, and thus (ii) giving rise to complementary regioselectivity; carbonyl-directed CAHB affords  $\gamma$ -primary boronic esters while oxime ether-directed CAHB generates  $\beta$ -tertiary organoboranes (Figure 17). One might notice that different hydroborating agents were used (tmdBH for carbonyl- and pinBH for oxime-directed CAHB); however, choice of borane reagents was based only on slightly improved enantioselectivity. While the carbonyl case highlighted the first high regio- and enantioselective CAHB of unactivated 1,1-disubstituted alkenes producing primary boronic esters, the oxime ether case is interesting as one of a few examples for the introduction of enantioselective boron delivery to tertiary carbon centers.

#### Carbonyl-directed CAHB



#### Oxime ether-directed CAHB

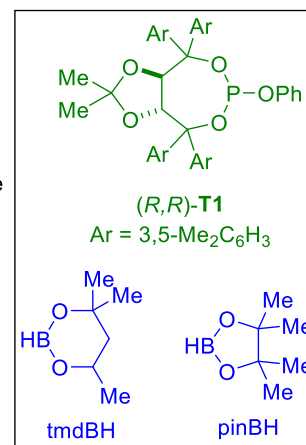
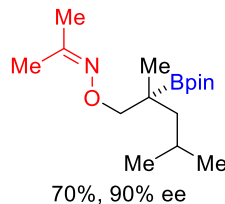
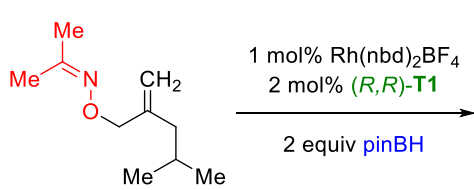
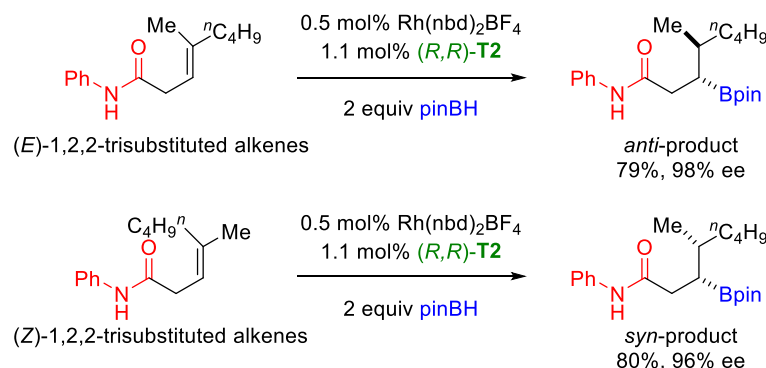


**Figure 17.** Effect of directing groups in CAHB of methylidene substrates leading to complementary regio- and  $\pi$ -facial selectivities

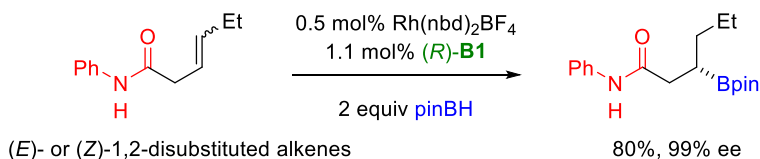
We have been more successful to find efficient CAHB conditions for 1,1- 1,2- and 1,2,2-substituted alkenes using carbonyl directing groups, when 1,1,2-substitution pattern was successfully hydroborated utilizing oxime ethers and phosphonates. (Figure 18). It is not that surprising in case of carbonyl-directed CAHB of 1,2,2-trisubstituted

alkenes in term of high regio- and diastereoselectivity; the boron is more likely to attach to the less substituted carbon and in the *syn* fashion along with hydrogen giving rise to *syn*- and *anti*-products from (*Z*)-alkenes and (*E*)-alkenes, respectively. In the case of 1,2-disubstituted alkenes, the boron prefers the carbon double bond proximal to the carbonyl-directing group illustrating the crucial role of the coordinating effect for high regioselectivity. In addition to the example of 1,1-disubstituted alkenes shown in Figure

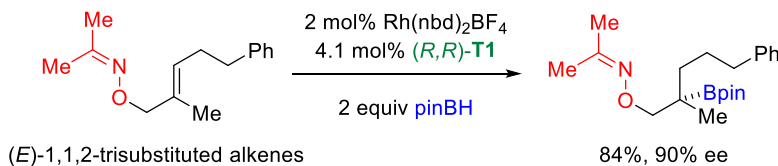
**A. Amide-directed CAHB of 1,2,2-trisubstituted alkenes**



**B. Amide-directed CAHB of 1,2-disubstituted alkenes**



**C. Oxime ether-directed CAHB of 1,1,2-trisubstituted alkenes**



**D. Phosphonate-directed CAHB of 1,1,2-trisubstituted alkenes**

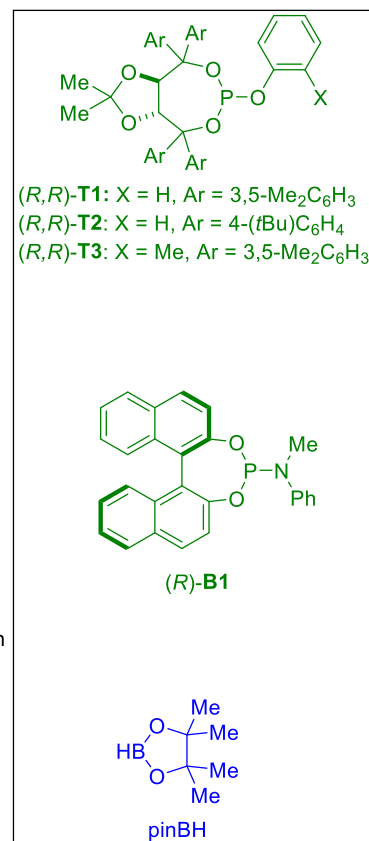
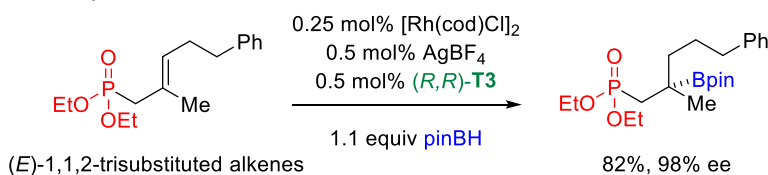


**Figure 18.** Directed Rh(I)-catalyzed asymmetric hydroboration of different alkene substitution patterns

17, oxime ether is also the efficient directing group for CAHB of 1,1,2-trisubstituted alkene (Figure 18C). Interestingly, oxime ether-directed CAHB of these two classes of alkene affords the enantiomeric products with the same sense of  $\pi$ -facial selectivity (both are bottom face borylation according to the structure drawn). Shortly thereafter, phosphonate was found to be as good directing group as oxime ether for CAHB of 1,1,2-trisubstituted alkenes generating the same regio- and  $\pi$ -facial selective borylated products (Figure 18D). Notably, despite the difference in the effect of directing groups and alkene substitution patterns, all of the substrates shown in Figure 18 have the same sense of  $\pi$ -facial selectivity (i.e., bottom approach as illustrated). In addition, it is fair to say that up to this point that TADDOL-derived phosphites (labeled **T** in Figure 18) and BINOL-derived phosphoramidites (labeled **B** in Figure 18) demonstrated the most successful results; while BINOL-derived phosphoramidite is the best choice for 1,2-disubstituted alkenes, TADDOL-derived phosphite is superior ligand for most of substitution patterns. This statement was further supported with experiments described in this dissertation (Chapter 2 and 3).

Though ligands **T** and **B** discussed above are the most successful ligands, it does not mean that other related ligands do not provide any positive results. For example, by slightly modified the ligand backbone from phosphite to phosphoramidite while keeping the stereoconfiguration of the TADDOL the same, amide-directed CAHB of 1,2,2-disubstituted alkenes gives rise to essentially complete enantio reversal (Figure 19).<sup>47</sup> Even though the TADDOL-phosphoramidite is not as selective as its phosphite analogue, the interesting results in hetero combination experiments might lead to new catalyst design. The mechanistic understanding of the enantio switching is not yet clear.

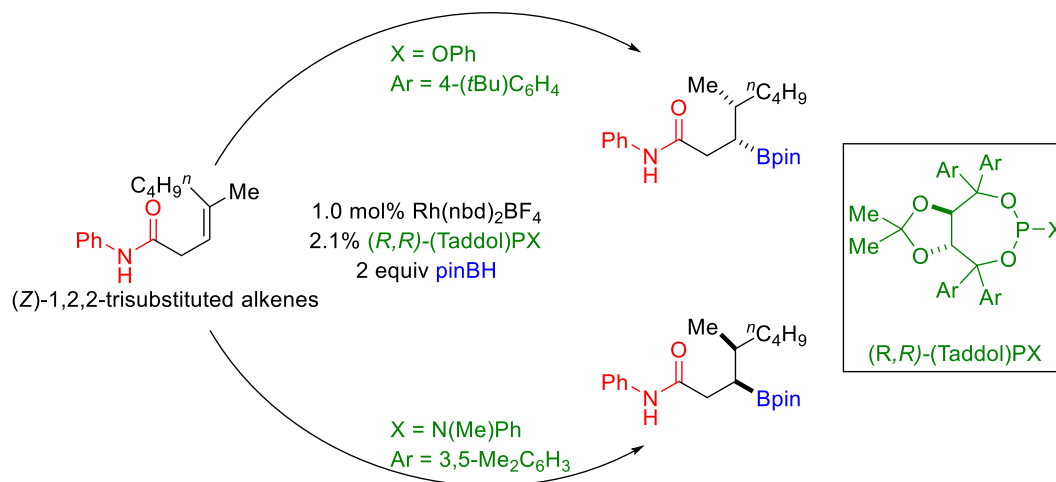


**Figure 19.** Enantioswitching in Rh(I)-catalyzed asymmetric hydroboration of  $(Z)\text{-1,2,2-}$ trisubstituted alkenes

In addition to the controlling factors discussed above, the nature of the borane reagents is also important. The later studies were typically carried out using pinBH and tmdBH based upon borane optimization studies obtained by Smith and Takacs.<sup>48</sup> The detailed results for one of the substrates studied (all give similar trends) are shown in Figure 20 illustrating that the yield and enantioselectivity vary widely as a function of borane. Importantly, both enantiopure  $(R)$ - and  $(S)$ -tmdBH gave similar results as compared to the racemic one.

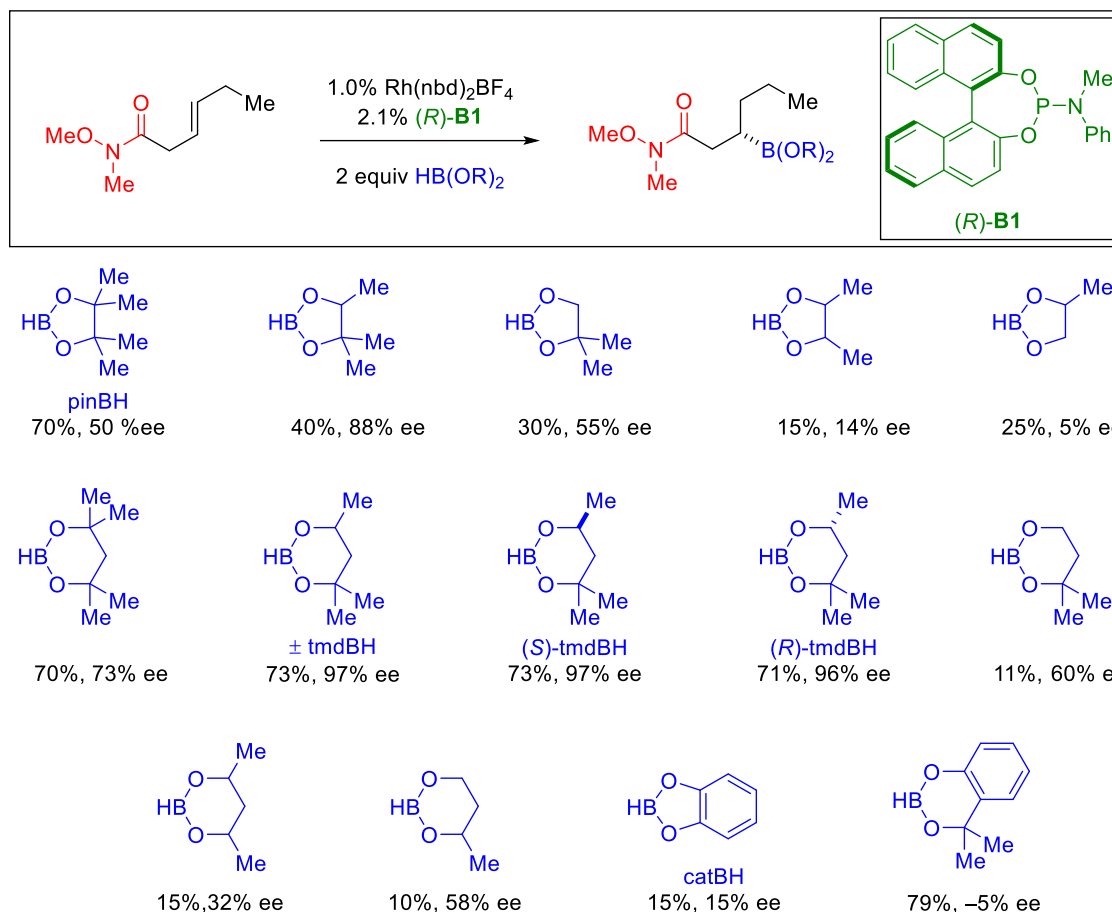


**Figure 20.** Effect of borane on Weinreb amide-directed CAHB of 1,2-disubstituted alkenes.

The above brief discussion in Rh(I)-catalyzed asymmetric hydroboration of unactivated alkenes had been carried out by Dr. Sean M. Smith, Ms. Veronika M. Shoba, and Mr. Suman Chakrabarty. The methodology gives rise to highly selective primary, secondary, and tertiary boronic esters. All borylated products are β-selective except for the case of carbonyl-directed CAHB of 1,1-disubstituted alkenes (Figure 17) carried out by Dr. Smith with my collaboration highlighting the first direct γ-selective borylation which will be discussed more details in Chapter 2. Other examples in this dissertation include synthesis of for γ- and δ-borylation of carbonyl compounds; currently no other

alternative methods for their direct enantioselective preparations have been reported. Besides the controlling factors mentioned above, work in this thesis will also show the effects of alkene substituents (aryl *versus* alkyl) in regioselectivity as well as alkene environment (cyclic *versus* acyclic) in groupselectivity.

### 1.5 Mechanistic implications in transition-metal catalyzed hydroboration of alkenes

The mechanism of transition-metal-catalyzed hydroboration of alkenes is thought to depend on the nature of the substrate, the metal precursor employed, the ligand used, and even the nature of the borane reagents. For example, recently, Zhang and Lu proposed that with a slight change in the nature of the ligand employed, the catalytic pathways could be mechanistically distinct from each other resulting in reversal of enantioselectivity (Figure 21).<sup>140</sup> With the use of an amine ligand, which has a flexible arm undergoes Co(0)/Co(II) catalytic cycle (i.e., mechanistically involving oxidative addition and reductive elimination steps, cycle I). On the other hand, when a rigid ligand side arm, imine, is employed, the reaction undergoes cycle II without changing the oxidation state of the metal (i.e., Co(I) cycle). The distinct proposed mechanisms are

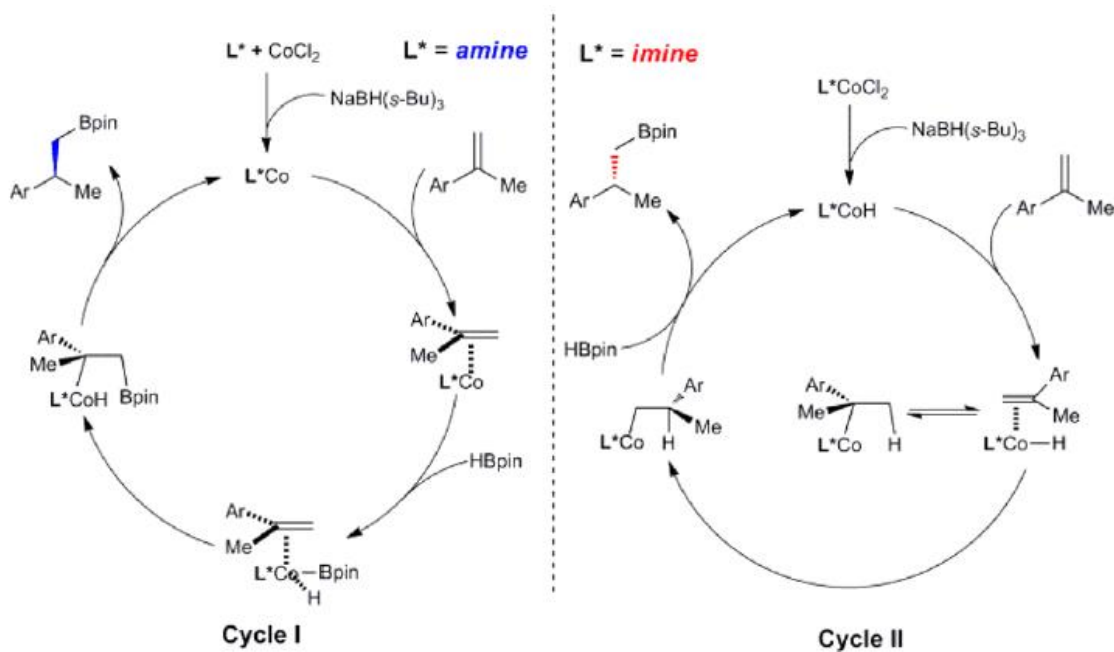


**Figure 21.** Proposed reversal enantioselective catalytic pathways of cobalt-catalyzed asymmetric hydroboration of 1,1-disubstituted vinyl arenes. Adapted with permission from reference 140. Copyright (2016) American Chemical Society.

reasonable as many findings before and after this study are either, (i) oxidative addition/reductive elimination or (ii) maintaining the metal's oxidation state (i.e., redox neutral) throughout the catalytic cycle. The previous studies by the same group<sup>130-140</sup> as well as Zhang<sup>141</sup> and co-workers on the same class of alkenes (i.e., methyldiene substrates) using cobalt- and iron catalysts in conjunction with similar imine ligands support proposed catalytic cycle II.

### 1.5.1 Catalytic pathways without changing oxidation state of the metal precursor

The discovery of this pathway perhaps is credited to Yun and co-workers for their Cu(I)-catalyzed hydroboration of styrenes in 2009.<sup>143</sup> The  $\sigma$ -bond metathesis between Cu–C and B–B is challenging to recognize and advocate.<sup>157</sup> The same applies to Yun's proposal of metathesis between Cu–C(sp<sup>3</sup>) and pinBH to generate the catalytically active Cu–H species (Figure 22, cycle A). However, DFT calculations were carried out to support the proposed mechanism; the results demonstrated that  $\sigma$ -bond metathesis, in fact, could take place and what is more, the addition of Cu–H to styrene is the rate-limiting step.<sup>158</sup> In 2011, the same group found that changing ligand from Tangphos to DTBM-Segphos with otherwise the same reaction conditions does not lead to reversal in selectivity; however, the latter ligand was found to improve either reactivity or enantioselectivity for the hydroboration of  $\beta$ -substituted vinyl arenes.<sup>144</sup> Preliminary DFT calculations were carried out to prove the efficiency of the DTBM-Segphos ligand; Segphos acts as a monodentate ligand due to steric hinderance around the phosphines, which might be responsible for the decreased stabilization of the reaction–catalyst complex. Using similar reaction conditions (i.e., CuCl and DTMB-Segphos), Hartwig and co-workers successfully carried out asymmetric hydroboration of a series of aliphatic



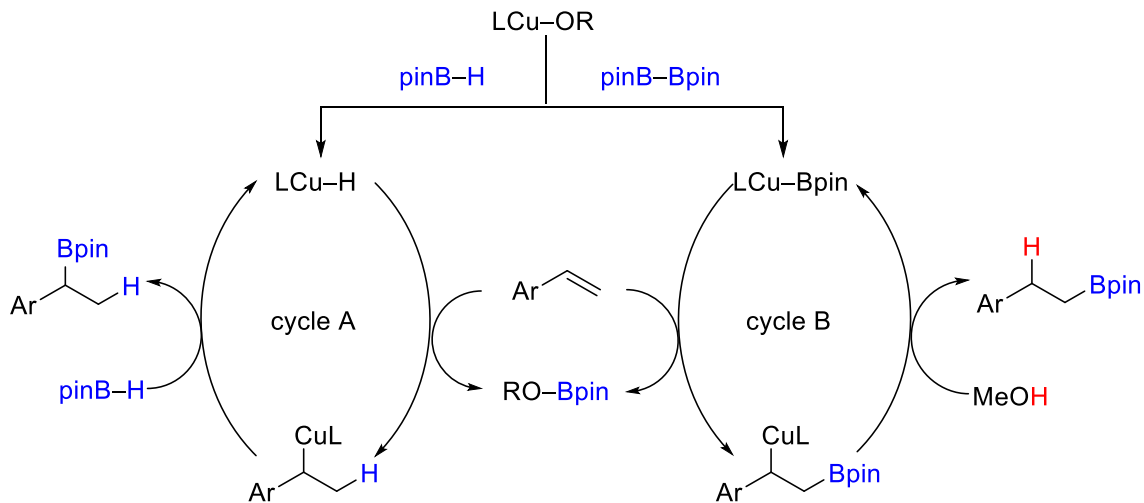


**Figure 22.** Effect of boranes on regioselectivity of Cu(I)-catalyzed hydroboration of vinyl arenes.

internal alkenes.<sup>156</sup> The transformation presumably undergoes similar mechanistic cycle A with the aid of DFT calculations to illustrate the effect of the proximal polar group in regio- and enantioselectivity.

In contrast to the above studies, Cu(I)-catalyzed hydroboration of vinyl arenes employing different types of ligand and using diborane (e.g.,  $B_2pin_2$ ) undergoes catalytic cycle B (Figure 22) resulting in complementary regioselectivity.<sup>145,146,159</sup> For example, similar to cycle A, starting from LCu-alkoxide, reaction with  $B_2pin_2$  generates LCu-Bpin instead of Cu-hydride.<sup>160-162</sup> In the next step, LCu still favors the more stabilized position (i.e., benzylic position); however, C-B migratory insertion generates the intermediate that complement the one in cycle A (i.e., C-H migratory insertion). In addition, reactions following cycle B require a proton additive (e.g., methanol) for the last step, stereoretentive Cu-C protonation to afford the desired product. There are also several examples of aliphatic terminal alkenes in which the use of the diborane is crucial for the pathway shown in cycle B.<sup>163,164</sup> In these studies, the steric effect of the ligands employed

is also responsible for regioselectivity. Similarly, Cu(I)-catalyzed hydroboration of cyclic 1,3-dienes using B<sub>2</sub>pin<sub>2</sub> by Ito<sup>151</sup> and coworkers also proceed in similar fashion to cycle B (Figure 22); however, the formation of allyl-copper species after Cu–B addition requires the protonation by alcohol occurring via S<sub>E</sub>2' pathway instead of stereoretentive Cu–C protonation.

Different from the above pathways, Cu(I)-CAHB of  $\alpha$ -dehydroamino acid methyl esters could be undergo either conjugate borylation or ester-directed Cu(I)-catalyzed hydroboration (Figure 23).<sup>147</sup> However, due to the pro-tertiary nature of the  $\alpha$ -carbon, it is less likely for the CuL to add to this carbon for conjugate borylation to happen. Another evidence for directed hydroboration pathway is that the product obtained is a nearly 1:1 mixture of diastereomers indicating the enantiodetermine step, LCu–C formation, is not likely to occur. On the other hand, after several first steps (as in Figure 21, cycle B) to generate LCu–Bpin species, copper can coordinate to the ester carbonyl directing group following by Bpin conjugate addition to afford copper-enolate species. Finally, protonation by alcohol gives the desired borylated product and regenerates the active catalyst.

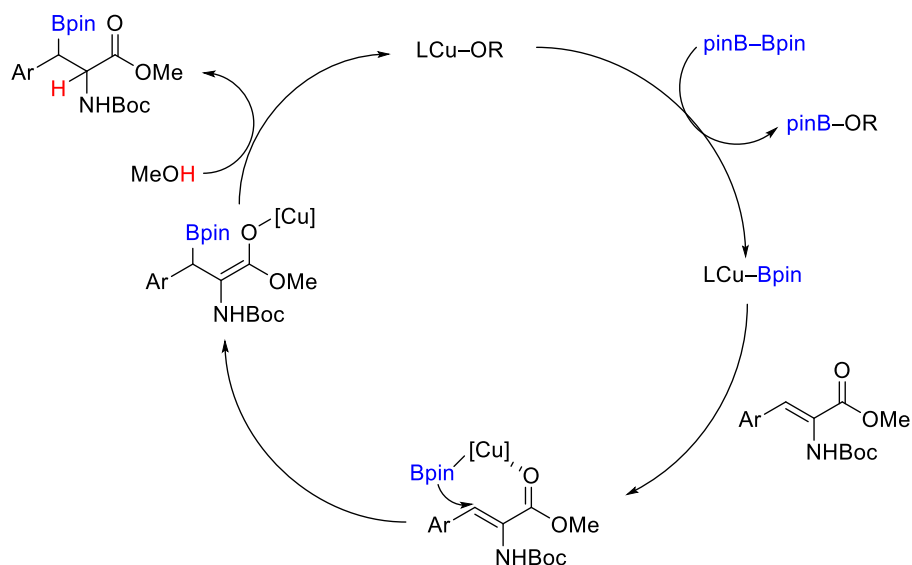


**Figure 23.** Ester-directed Cu(I)-catalyzed hydroboration of  $\alpha$ -dehydroamino acid methyl esters.

### 1.5.2 Catalytic pathways involving oxidative addition/ reductive elimination

The discovery of this pathway is credited to Kono and Ito<sup>165</sup> for their finding in oxidative addition of 4,4,6-trimethyl-1,3,2-dioxaborinane (tmdBH) and catecholborane (catBH) to Wilkinson's catalyst ( $\text{Rh}(\text{PPh}_3)_3\text{Cl}$ ) and to Männig and Nöth<sup>101</sup> for their first report on the rhodium(I)-catalyzed hydroboration of alkenes using Wilkinson's catalyst and catecholborane (catBH) (Figure 24).

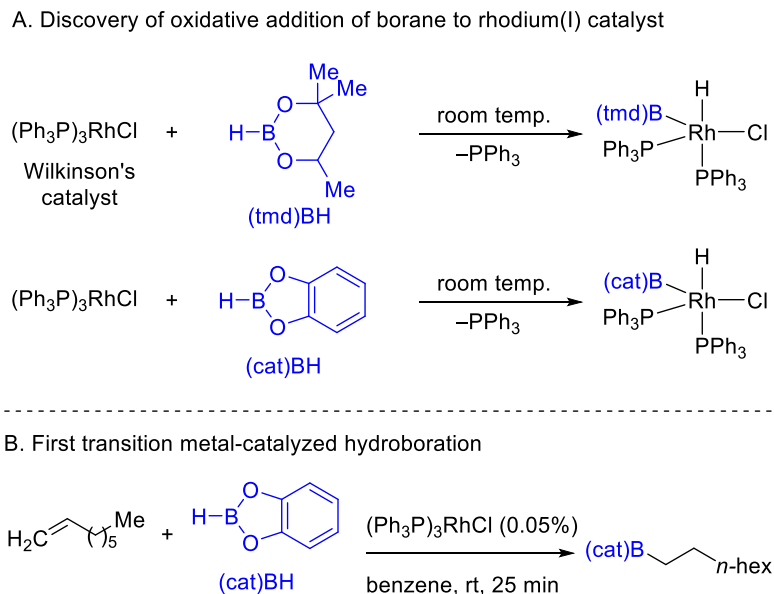


**Figure 24.** A. Discovery of oxidative addition of tmdBH and catBH to Wilkinson's catalyst by Kono and Ito; B. First example of Rh(I)-catalyzed hydroboration of alkenes by Männig and Nöth.

In the first introduction of Rh(I)-catalyzed hydroboration, Männig and Nöth also proposed the generally accepted mechanism which later supported by Evans and Fu (Figure 25).<sup>118,119</sup> First, one equivalent of  $\text{PPh}_3$  ligand is dissociated from Wilkinson's catalyst to generate the active catalyst Rh(I) (intermediate **I**). Oxidative addition of borane  $\text{HB}(\text{OR})_2$  to Rh(I) gives Rh(III) intermediate **II**. Next, alkene chelation with dissociation of another equivalent of  $\text{PPh}_3$  ligand forms intermediate **III**. Migratory  $\text{C}=\text{C}$  double insertion to  $\text{Rh}-\text{H}$  generate either branched alkyl-Rh **IV-a** or its linear regioisomer alkyl-Rh **IV-b**. Reductive elimination of either **IV-a** or **IV-b** affords the desired corresponding borylated product and regenerates active catalyst species **I** to continue the catalytic cycle. Recently, Schomaker group proposed a similar mechanism for Nickel(0)/Nickel(II) catalytic cycle in which the regioselectivity is controlled by the size of the

ligand in migratory insertion step.<sup>166</sup> While small NHC ligand affords branched alkyl-Ni **IV-a**, large NHC ligand prefers linear alkyl-Ni **IV-b**.

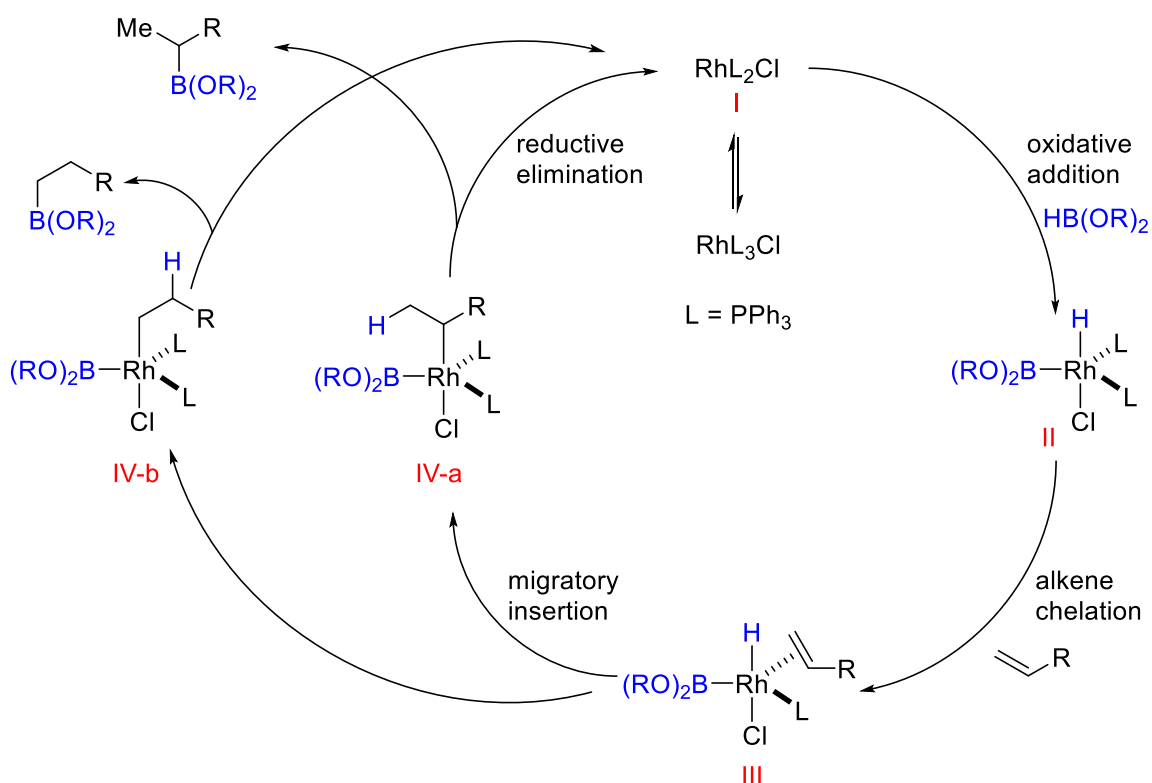


**Figure 25.** Proposed mechanistic pathway for Rh(I)-catalyzed hydroboration

In 1992, Burgess suggested a similar mechanism to one shown in Figure 24.<sup>167</sup> However, according to Burgess' proposal, alkene chelation step does not require the dissociation of the phosphine ligand to afford intermediate III as an octahedral structure instead (i.e., associative mechanism). Several *ab initio* studies were also carried out; work by Morokuma<sup>168</sup> and co-workers supports the associative pathway, while Schleyer<sup>169</sup> group favors the dissociative mechanism.

In another computational study, Ziegler<sup>170</sup> found that alkene insertion to Rh–B followed by reductive C–H formation is also possible. While hydride migration is slightly more favorable for associative mechanism, boron migration seems to be more compatible

with dissociative pathway. This proposal, in principle, makes the mechanistic understanding of Rh(I)-catalyzed hydroboration more difficult. Perhaps, there should be an *ab initio* study using iridium(I) catalyst precursor, which might facilitate the possibility of metal–boron bond migratory insertion. In fact, Rablen and Hartwig showed that insertion into the Ir–B bond is favored by 8 kcal/ mol over the insertion into the Ir–H bond based upon theoretical studies on bond dissociation energies.<sup>171</sup> Experimentally, Bonin and Micouin<sup>115</sup> and later on Crudden<sup>114</sup> showed the strong effect of these metal precursors in migratory insertion step resulting in reversal of enantio- and regioselectivity, respectively (Figure 26).

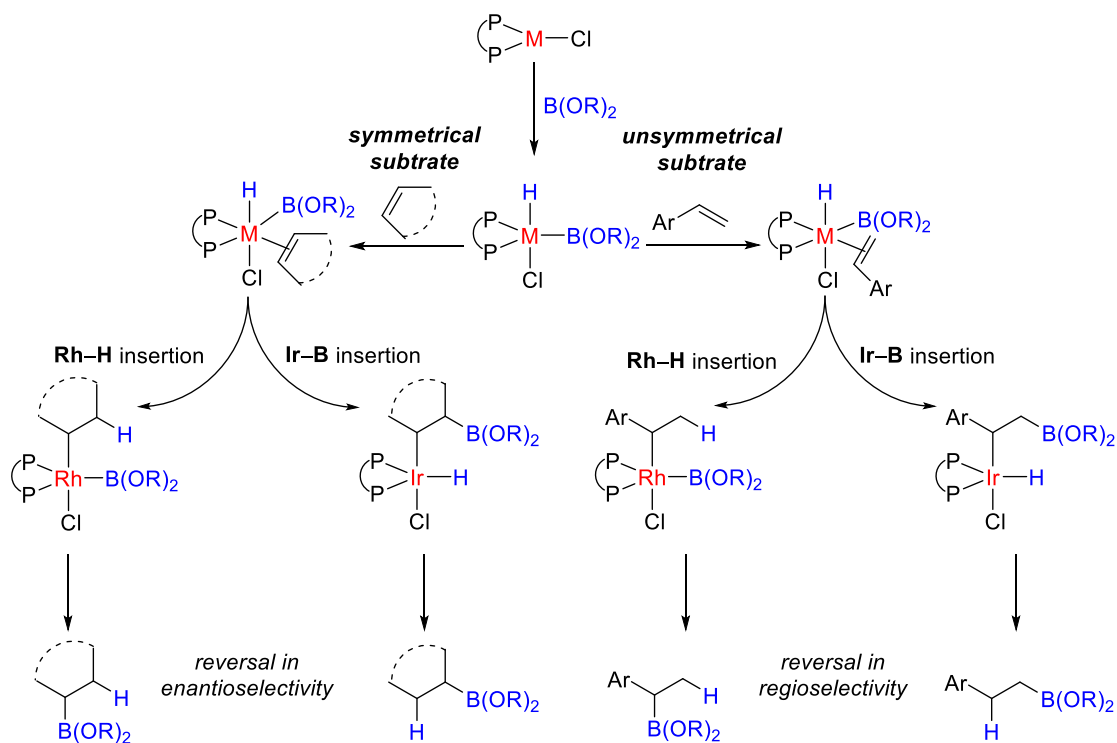


**Figure 26.** Effect of metal precursors on regio- and enantioselectivity

Enantioswitching was also observed to be effected by ligands employed or the nature of the borane reagents. As a recall from section 1.4, Smith and Takacs<sup>47</sup> showed that relatively small changes in ligand substituents could lead to complete enantioreversal

while the absolute stereochemistry of the ligands remains the same. The distinct mechanism for this effect is not yet clear. Fernández<sup>172</sup> and Crudden<sup>114</sup> independently reported the effect of boranes (i.e., pinBH and catBH) in conjunction with P,P-bidentate (i.e., BINAP and JOSIPHOS) ligands led to the reversal in enantioselectivity. Crudden claimed that unfavorable steric interactions between Bpin and PPh<sub>2</sub> are responsible for the change in enantioselectivity; this statement was supported by Fernández's computational studies (Figure 27).

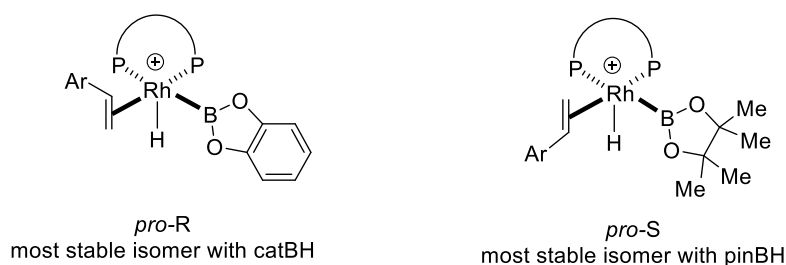


**Figure 27.** Fernández's calculations for most stable isomers of H-Rh-BINAP-borane-styrene complex employing catBH and pinBH

Building up from Fernández's model of cationic rhodium complex illustrated in Figure 27 for a one-point binding substrate (i.e., no coordinating group), this dissertation will show the model DFT calculations for two-point binding substrates which will be discussed in details in Chapter 3. To reduce the computing times, a proposed symmetric ligand (caged phosphine ligand), a symmetric borane (pinBH instead of tmdBH using experimentally), and a symmetric cyclopentene-based substrate will be used. The combination of computational and experimental studies provides better outlook of the mechanistic pathways. This dissertation will discuss in details the current understanding, limitation, as well as alternative pathways which should be also considered. The simplified proposed mechanistic cycle is illustrated in Figure 28. Though it look similar

to the one-point binding substrates illustrated in Figure 25, there are some significant differences, including (i) the two-point binding mechanism require cationic rhodium as an active catalyst species while the one-point binding substrates, in theory, can used both neutral and cationic metal precursors, (ii) the regioselectivity is mainly controlled by the proximity effect of the directing group rather than by the formation of stabilized benzylic alkyl-Rh intermediate as in case of simple vinyl arenes (i.e., one-point binding mechanism).

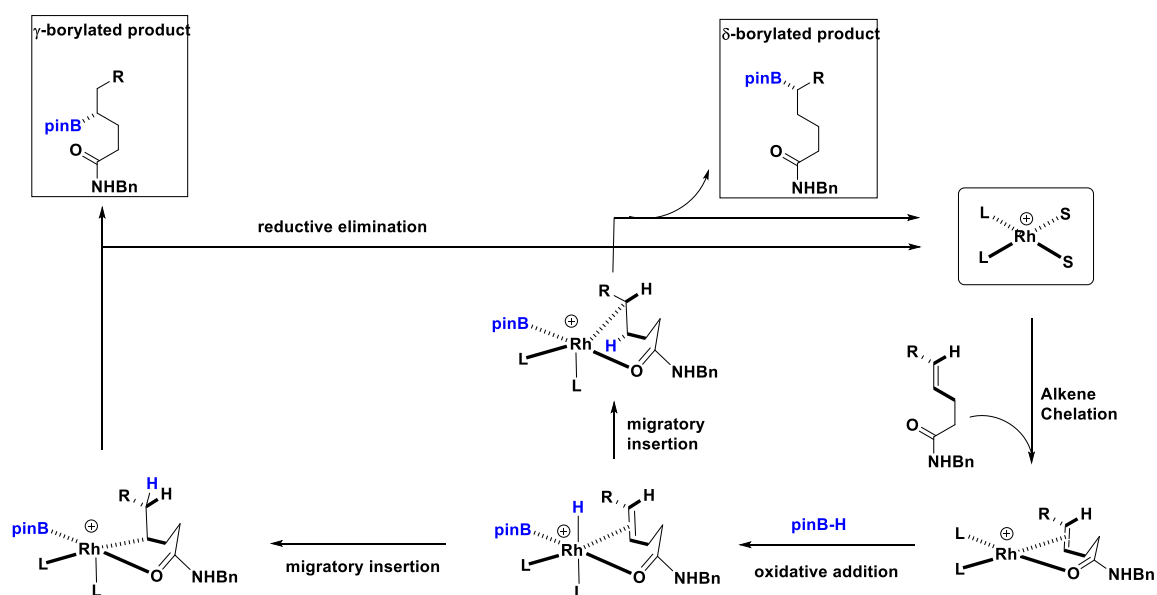


**Figure 28.** Proposed simplified mechanistic pathway for Rh(I)-catalyzed hydroboration of two-point binding substrates

It is worth to note that in Takacs' two-point binding systems, there is a wide range of functional group compatibility. For instance, it is not restricted to the secondary amide (i.e., benzyl amide) coordinating group as shown in Figure 28 (i.e., other functional groups such as ester, oxime ether, phosphonate, and later on in this dissertation, tertiary amide (e.g., morpholine and Weinreb amides) can also be applied) indicating the acidic NH proton does not play the crucial rule in the reaction mechanism. On the other hand,



Tang's amide-directed CAHB requires a secondary amide and diborane reagent (i.e.,  $B_2pin_2$ ) for high conversion and enantioselectivity, respectively (recalled from Figure 6).<sup>61</sup> Therefore, though in the two-point binding framework, Tang's proposed mechanism is quite different from Takacs' as illustrated in Figure 28. The main differences include, (i) oxidative addition of diborane to generate Rh-diborane complex, (ii) presence of an extra step for H–B exchange after alkene chelation (Figure 29).

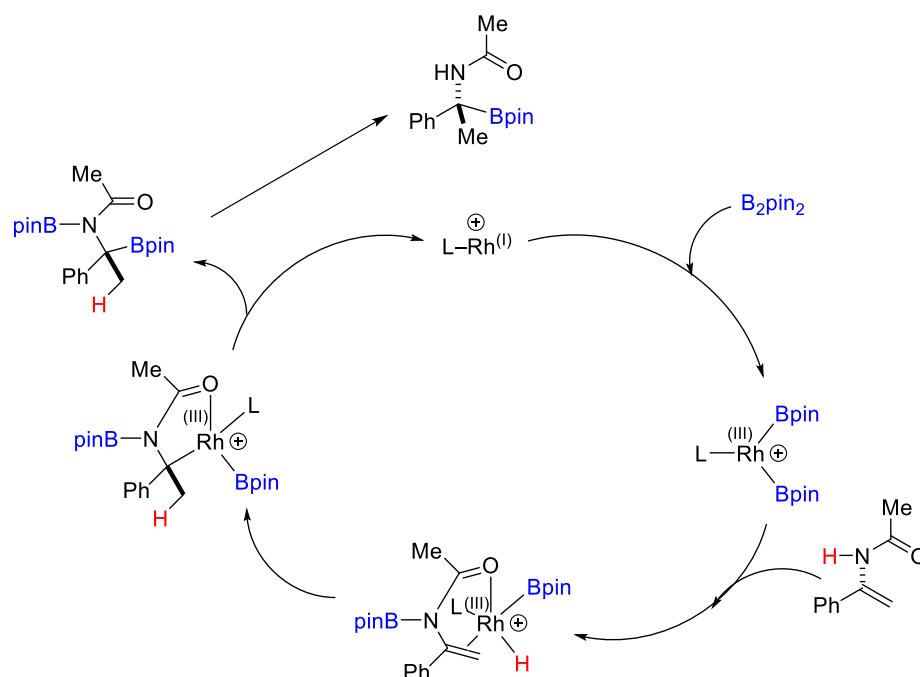


**Figure 29.** Tang's proposed mechanism for amide-directed CAHB of  $\alpha$ -arylenamides illustrating the crucial roles of diborane reagent and NH acidic proton.

## 1.6 Summary

Chiral boronic esters are versatile intermediates because of their widely used stereospecific transformations to other classes of interest. Among the functionalization methodologies, conventional Pd-catalyzed Suzuki–Miyaura cross-coupling of secondary boronic esters has recently attracted great deal attention due to the interest of understanding their stereochemical aspects. Herein, the configuration of the cross-coupling reaction will be discussed, rationalized and compared to the information provided in current literature.

In addition to the applications in stereospecific transformations, organoboranes have been recently used in total synthesis of natural products or other compounds of interest. Consequently, many research groups have been seeking for enantioselective methods for their preparations including stoichiometric reagents, stereoconvergent couplings of alpha-haloboronates, enantioselective allyl- and arylborylation, enantioselective allylic substitution with diborylmethane, enantioselective aminoborylation, enantioselective B–H bond insertion, enantioselective C–H borylation, enantioselective conjugate borylation, enantioselective conjunctive cross-coupling, enantioselective diboration, group selective cross-coupling of diboranes, enantioselective nucleophilic addition to aldehydes, enantioselective homologation of organoboron via lithiation-borylation, stereospecific catalytic Miyaura borylation, asymmetric reactions with vinylboronates, etc.

Despite the fact that many effective methodologies having been carried out, transition-metal-catalyzed asymmetric hydroboration has a long-standing story and is the most attractive method due to the atom-economic nature of the transformation. The

current literature on CAHB is still largely limited to vinyl arene substrates with a few exceptions from Hartwig, Tortosa, and other groups. Early carbonyl-directed CAHB in Takacs group obtained by Dr. Sean M. Smith and recently oxime ether-directed CAHB by Ms. Veronika Shoba and phosphonate-directed CAHB by Mr. Suman Chakrabarty made a great impact on the extension of the substrate scopes. Phosphonates and oxime ethers are particularly interesting due to their ability to direct the boron towards the tertiary carbon centers. Directed CAHB of  $\beta,\gamma$ -unsaturated carbonyl compounds along with enantioselective conjugate borylation and enantioselective C–H borylation mark a few direct routes to  $\beta$ -borylated carbonyl derivatives. With a more challenging further remote coordinating distance, directed CAHB of  $\gamma,\delta$ -unsaturated carbonyl compounds opens the first direct route to stereogenic  $\gamma$ - and  $\delta$ -borylated carbonyl derivatives (the first direct route to non-stereogenic  $\gamma$ -borylated amides and esters carried out in collaboration with Dr. Sean Smith in directed CAHB of geminal  $\gamma,\delta$ -unsaturated amides and esters will also be discussed).

To gain knowledge for better understanding of mechanistic pathways of CAHB with two-point binding substrates, collaborative experimental and computational studies of symmetric cyclic  $\gamma,\delta$ -unsaturated amides were carried out. The computational results suggest the catalytic cycle that is supported by the experimental results. However, some experimental results are in good agreement with alternative pathways that has not been theoretically considered yet.

## 1.7 References

- [1] Sanford, C.; Aggarwal, V. K., "Stereospecific Functionalizations and Transformations of Secondary and Tertiary Boronic Esters," *Chem. Commun.*, **2017**, 53, 5481–5494.
- [2] Brown, H. C.; Zweifel, G., "Hydroboration. IX. The Hydroboration of Cyclic and Bicyclic Olefins–Stereochemistry of the Hydroboration Reaction," *J. Am. Chem. Soc.*, **1961**, 83, 2544–2551.
- [3] Kabalka, G. W.; Shoup, T. M.; Goudgaon, N. M., "Sodium Perborate: A Mild and Convenient Reagent for Efficiently Oxidizing Trialkylboranes," *Tetrahedron Lett.*, **1989**, 30, 1483–1486.
- [4] Brown, H. C.; Kim, K. W.; Cole, T. E.; Singaram, B., "Chiral Synthesis via Organoboranes. 8. Synthetic Utility of Boronic Esters of Essentially 100% Optical Purity. Synthesis of Primary Amines of Very High Enantiomeric Purities," *J. Am. Chem. Soc.*, **1986**, 108, 6761–6764.
- [5] Matteson, D. S.; Kim, G. Y., "Asymmetric Alkyldifluoroboranes and Their Use in Secondary Amine Synthesis," *Org. Lett.*, **2002**, 4, 2513–2515.
- [6] Kim, B. J.; Matteson, D. S., "Conversion of Alkyltrifluoroborates in to Alkyldichloroboranes with Tetrachlorosilane in Coordinating Solvents," *Angew. Chem., Int. Ed.*, **2004**, 43, 3056–3058.
- [7] Hupe, E.; Marek, I.; Knochel, P., "Diastereoselective Reduction of Alkenylboronic Esters as a New Method for Controlling the Stereochemistry of up to Three Adjacent Centers in Cyclic and Acyclic Molecules," *Org. Lett.*, **2002**, 4, 2861–2863.
- [8] Mlynarski, S. N.; Karns, A. S.; Morken, J. P., "Direct Stereospecific Amination of Alkyl and Aryl Pinacol Boronates," *J. Am. Chem. Soc.*, **2012**, 134, 16449–16451.
- [9] Bagutski, V.; Elford, T. G.; Aggarwal, V. K., "Synthesis of Highly Enantioenriched C-Tertiary Amines From Boronic Esters: Application to the Synthesis of Igmesine," *Angew. Chem., Int. Ed.*, **2011**, 50, 1080–1083.
- [10] Larouche-Gauthier, R.; Elford, T. G.; Aggarwal, V. K., "Ate Complexes of Secondary Boronic Esters as Chiral Organometallic-Type Nucleophiles for Asymmetric Synthesis," *J. Am. Chem. Soc.*, **2011**, 133, 16794–16797.

- [11] Sadhu, K. M.; Matteson, D. S., "(Chloromethyl)lithium: Efficient Generation and Capture by Boronic Esters and a Simple Preparation of Diisopropyl (chloromethyl)boronate," *Organometallics*, **1985**, *4*, 1687–1689.
- [12] Chen, A.; Ren, L.; Crudden, C. M., "Catalytic Asymmetric Hydrocarboxylation and Hydrohydroxymethylation. A Two-Step Approach to the Enantioselective Functionalization of Vinylarenes," *J. Org. Chem.*, **1999**, *64*, 9704–9710.
- [13] Sonawane, R. P.; Jheengut, V.; Rabalakos, C.; Larouche-Gauthier, R.; Scott, H. K.; Aggarwal, V. K., "Enantioselective Construction of Quaternary Stereogenic Centers from Tertiary Boronic Esters: Methodology and Applications," *Angew. Chem., Int. Ed.*, **2011**, *50*, 3760–3763.
- [14] Fandrick, K. R.; Mulder, J. A.; Patel, N. D.; Gao, J.; Konrad, M.; Archer, E.; Buono, F. G.; Duran, A.; Schmid, R.; Daeubler, J.; Desrosiers, J.-N.; Zeng, X.; Rodriguez, S.; Ma, S.; Qu, B.; Li, Z.; Fandrick, D. R.; Grinberg, N.; Lee, H.; Bosanac, T.; Takahashi, H.; Chen, Z.; Bartolozzi, A.; Nemoto, P.; Busacca, C. A.; Song, J. J.; Yee, N. K.; Mahaney, P. E.; Senanayake, C. H., "Development of an Asymmetric Synthesis of a Chiral Quaternary FLAP Inhibitor," *J. Org. Chem.*, **2015**, *80*, 1651–1660.
- [15] Unsworth, P. J.; Leonori, D.; Aggarwal, V. K., "Stereocontrolled Synthesis of 1,5-Stereogenic Centers through Three-Carbon Homologation of Boronic Esters," *Angew. Chem., Int. Ed.*, **2014**, *53*, 9846–9850.
- [16] Evans, D. A.; Crawford, T. C.; Thomas, R. C.; Walker, J. A., "Studies Directed toward the Synthesis of Prostaglandins. Useful Boron-Mediated Olefin Syntheses," *J. Org. Chem.*, **1976**, *41*, 3947–3953.
- [17] Fletcher, C. J.; Blair, D. J.; Wheelhouse, K. M. P.; Aggarwal, V. K., "The Total Synthesis of (-)-Aplysin via a Lithiation-borylation-propenylation Sequence," *Tetrahedron*, **2012**, *68*, 7598–7604.
- [18] Wang, Y.; Noble, A.; Myers, E. L.; Aggarwal, V. K., "Enantiospecific Alkynylation of Alkylboronic Esters," *Angew. Chem., Int. Ed.*, **2016**, *55*, 4270–4274.
- [19] Magano, J.; Dunetz, J. R., "Large-Scale Applications of Transition Metal-Catalyzed Couplings for the Synthesis of Pharmaceuticals," *Chem. Rev.*, **2011**, *111*, 2177–2250.
- [20] Suzuki, A., "Cross-Coupling Reactions of Organoboranes: An Easy Way to Construct C–C Bonds," *Angew. Chem., Int. Ed.*, **2011**, *50*, 6722–6737.

- [21] Cherney, A. H.; Kadunce, N. T.; Reisman, S. E., “Enantioselective and Enantiospecific Transition Metal-Catalyzed Cross-Coupling Reactions of Organometallic Reagents to Construct C–C Bonds,” *Chem. Rev.*, **2015**, *115*, 9587–9652.
- [22] Glasspoole, B. W.; Oderinde, M. S.; Moore, B. D.; Antoft-Finch, A.; Crudden, C. M., “Highly Chemoselective and Enantiospecific Suzuki–Miyaura Cross Couplings of Benzylic Organoboronic Esters,” *Synthesis*, **2013**, *45*, 1759–1763.
- [23] Matthew, S. C.; Glasspoole, B. W.; Eisenberger, P.; Crudden, C. M., “Synthesis of Enantiomerically Enriched Triarylmethanes by Enantiospecific Suzuki–Miyaura Cross-Coupling Reactions,” *J. Am. Chem. Soc.*, **2014**, *136*, 5828–5831.
- [24] Sandrock, D. L.; Jean-Gerard, L.; Chen, C.; Dreher, S. D.; Molander, G. A., “Stereospecific Cross-Coupling of Secondary Alkyl  $\beta$ -Trifluoroboratoamides,” *J. Am. Chem. Soc.*, **2010**, *132*, 17108–17110.
- [25] Ohmura, T.; Awano, T.; Suginome, M., “Stereospecific Suzuki–Miyaura Coupling of Chiral  $\alpha$ -(Acylamino)benzylboronic Esters with Inversion of Configuration,” *J. Am. Chem. Soc.*, **2010**, *132*, 13191–13193.
- [26] Awano, T.; Ohmura, T.; Suginome, M., “Inversion or Retention? Effects of Acidic Additives on the Stereochemical Course in Enantiospecific Suzuki–Miyaura Coupling of  $\alpha$ -(Acetylamino)benzylboronic Esters,” *J. Am. Chem. Soc.*, **2011**, *133*, 20738–20741.
- [27] Daini, M.; Suginome, M., “Palladium-Catalyzed, Stereoselective, Cyclizative Alkenylboration of Carbon–Carbon Double Bonds through Activation of a Boron–Chlorine Bond,” *J. Am. Chem. Soc.*, **2011**, *133*, 4758–4761.
- [28] Lee, J. C.; McDonald, R.; Hall, D. G., “Enantioselective Preparation and Chemoselective Cross-Coupling of 1,1-Diboron Compounds,” *Nat. Chem.*, **2011**, *3*, 894–899.
- [29] Lee, J. C. H.; Sun, H.-Y.; Hall, D. G., “Optimization of Reaction and Substrate Activation in the Stereoselective Cross-Coupling of Chiral 3,3-Diboronyl Amides,” *J. Org. Chem.*, **2015**, *80*, 7134–7143.
- [30] Blaisdell, T. P.; Morken, J. P., “Hydroxyl-Directed Cross-Coupling: A Scalable Synthesis of Debromohamigeran E and Other Targets of Interest,” *J. Am. Chem. Soc.*, **2015**, *137*, 8712–8715.

- [31] Li, L.; Zhao, S.; Joshi-Pangu, A.; Diane, M.; Biscoe, M. R., "Stereospecific Pd-Catalyzed Cross-Coupling Reactions of Secondary Alkylboron Nucleophiles and Aryl Chlorides," *J. Am. Chem. Soc.*, **2014**, *136*, 14027–14030.
- [32] Hoang, G. L.; Yang, Z.-D.; Smith, S. M.; Pal, R.; Miska, J. L.; Pérez, D. E.; Petler, L. S. W.; Zeng, X. C.; Takacs, J. M., "Enantioselective Desymmetrization via Carbonyl-Directed Catalytic Asymmetric Hydroboration and Suzuki–Miyaura Cross-Coupling," *Org. Lett.*, **2015**, *17*, 940–943.
- [33] Hoang, G. L.; Takacs, J. M., "Enantioselective  $\gamma$ -Borylation of Unsaturated Amides and Stereoretentive Suzuki–Miyaura Cross-Coupling," *Chem. Sci.*, **2017**, *8*, 4511–4516.
- [34] Bonet, A.; Odachowski, M.; Leonori, D.; Essafi, S.; Aggarwal, V. K., "Enantiospecific  $sp^2$ – $sp^3$  Coupling of Secondary and Tertiary Boronic Esters," *Nat. Chem.*, **2014**, *6*, 584–589.
- [35] Llaveria, J.; Leonori, D.; Aggarwal, V. K., "Stereospecific Coupling of Boronic Esters with *N*-Heteroaromatic Compounds," *J. Am. Chem. Soc.*, **2015**, *137*, 10958–10961.
- [36] Sanford, C.; Rasappan, R.; Aggarwal, V. K., "Synthesis of Enantioenriched Alkylfluorides by the Fluorination of Boronate Complexes," *J. Am. Chem. Soc.*, **2015**, *137*, 10100–10103.
- [37] Odachowski, M.; Bonet, A.; Essafi, S.; Conti-Ramsden, P.; Harvey, J. N.; Leonori, D.; Aggarwal, V. K., "Development of Enantiospecific Coupling of Secondary and Tertiary Boronic Esters with Aromatic Compounds," *J. Am. Chem. Soc.*, **2016**, *138*, 9521–9532.
- [38] Soriano-Ursúa, M. A.; Das, B. C.; Trujillo-Ferrara, J. G. "Boron-Containing Compounds: Chemico-Biological Properties and Expanding Medicinal Potential in Prevention, Diagnosis and Therapy," *Expert Opinion on Therapeutic Patents* **2014**, *24*, 485–500; and references cited therein.
- [39] Baker, S. J.; Ding, C. Z.; Akama, T.; Zhang, Y.-K.; Hernandez, V.; Xia, Y. "Therapeutic Potential of Boron-Containing Compounds," *Future Med. Chem.* **2009**, *1*, 1275–1288; and references cited therein.
- [40] (a) Meng, F.; Li, X.; Torker, S.; Shi, Y.; Hoveyda, A. H. "Catalytic Enantioselective 1,6-Conjugate Additions of Propargyl and Allyl Groups," *Nature* **2016**, *537*, 387–393;

(b) Yuki, K.; Shindo, M.; Shishido, K., "Enantioselective Total Synthesis of (–)-Equisetin Using a Me<sub>3</sub>Al-Mediated Intramolecular Diels–Alder Reaction," *Tetrahedron Lett.*, **2001**, *42*, 2517–2519.

[41] Mlynarski, S. N.; Schuster, C. H.; Morken, J. P., "Asymmetric Synthesis from Terminal Alkenes by Cascades of Diboration and Cross-Coupling," *Nature*, **2014**, *505*, 386–390.

[42] Meng, F.; McGrath, K. P.; Hoveyda, A. M., "Multifunctional Organoboron Compounds for Scalable Natural Product Synthesis," *Nature*, **2014**, *513*, 367–374.

[43] Burns, M.; Essafi, S.; Bame, J. R.; Bull, S. P.; Webster, M. P.; Balieu, S.; Dale, J. W.; Butts, C. P.; Harvey, J. N.; Aggarwal, V. K., "Assembly-line Synthesis of Organic Molecules with Tailored Shapes," *Nature*, **2014**, *513*, 183–188.

[44] Collins, B. S. L.; Wilson, C. M.; Myers, E. L.; Aggarwal, V. K., "Asymmetric Synthesis of Secondary and Tertiary Boronic Esters," *Angew. Chem., Int. Ed.*, **2017**, *56*, Accepted. DOI: 10.1002/anie.201701963.

[45] Smith, S. M.; Thacker, N. C.; Takacs, J. M., "Efficient Amide-Directed Catalytic Asymmetric Hydroboration," *J. Am. Chem. Soc.*, **2008**, *130*, 3734–3735.

[46] Smith, S. M.; Takacs, J. M., "Amide-Directed Catalytic Asymmetric Hydroboration of Trisubstituted Alkenes," *J. Am. Chem. Soc.*, **2010**, *132*, 1740–1741.

[47] Smith, S. M.; Takacs, J. M., "Remarkable Levels of Enantioswitching in Catalytic Asymmetric Hydroboration," *Org. Lett.*, **2010**, *12*, 4612–4615.

[48] Smith, S. M.; Uteuliyev, M.; Takacs, J. M., "Catalytic Asymmetric Hydroboration of  $\beta,\gamma$ -Unsaturated Weinreb Amides: Striking Influence of the Borane," *Chem. Commun.*, **2011**, *47*, 7812–7814.

[49] Chakrabarty, S.; Takacs, J. M., "Synthesis of Chiral Tertiary Boronic Esters: Phosphonate-Directed Catalytic Asymmetric Hydroboration of Trisubstituted Alkenes," *J. Am. Chem. Soc.*, **2017**, *139*, 6066–6069.

[50] Shoba, V. M.; Thacker, N. C.; Bochat, A. J.; Takacs, J. M., "Synthesis of Chiral Tertiary Boronic Esters by Oxime-Directed Catalytic Asymmetric Hydroboration," *Angew. Chem., Int. Ed.*, **2016**, *55*, 1465–1469.



- [51] He, J.; Shao, Q.; Wu, Q.; Yu, J.-Q., "Pd(II)-Catalyzed Enantioselective C(sp<sup>3</sup>)-H Borylation," *J. Am. Chem. Soc.*, **2017**, *139*, 3344–3347.
- [52] Schmidt, J.; Choi, J.; Liu, A. T.; Slusarczyk, M.; Fu, G. C., "A General, Modular Method for the Catalytic Asymmetric Synthesis of Alkylboronate Esters," *Science*, **2016**, *354*, 1265–1269.
- [53] Burns, M.; Essafi, S.; Bame, J. R.; Bull, S. P.; Webster, M. P.; Balieu, S.; Dale, J. W.; Butts, C. P.; Harvey, J. N.; Aggarwal, V. K., "Assembly-Line Synthesis of Organic Molecules with Tailored Shapes," *Nature*, **2014**, *513*, 183–188.
- [54] Balieu, S.; Hallett, G. E.; Burns, M.; Bootwicha, T.; Studley, J.; Aggarwal, V. K., "Toward Ideality: The Synthesis of (+)-Kalkitoxin and (+)-Hydroxyphthioceranic Acid by Assembly-Line Synthesis," *J. Am. Chem. Soc.*, **2015**, *137*, 4398–4403.
- [55] For a review on lithiation–borylation methodology and its application in synthesis, see: Leonori, D.; Aggarwal, V. K., "Lithiation–Borylation Methodology and Its Application in Synthesis," *Acc. Chem. Res.*, 2014, *47*, 3174–3183.
- [56] Chen, I.-H.; Yin, L.; Itano, W.; Kanai, M.; Shibasaki, M., "Catalytic Asymmetric Synthesis of Chiral Tertiary Organoboronic Esters through Conjugate Boration of  $\beta$ -Substituted Cyclic Enones," *J. Am. Chem. Soc.*, **2009**, *131*, 11664–11665.
- [57] Chen, I.-H.; Yin, L.; Kanai, M.; Shibasaki, M., "Copper(I)–Secondary Diamine Complex-Catalyzed Enantioselective Conjugate Boration of Linear  $\beta,\beta$ -Disubstituted Enones," *Org. Lett.*, **2010**, *12*, 4098–4101.
- [58] Feng, X.; Yun, J., "Conjugate Boration of  $\beta,\beta$ -Disubstituted Unsaturated Esters: Asymmetric Synthesis of Functionalized Chiral Tertiary Organoboronic Esters," *Chem. Eur. J.*, **2010**, *16*, 13609–13612.
- [59] O'Brien, J. M.; Lee, K.-S.; Hoveyda, A. H., "Enantioselective Synthesis of Boron-Substituted Quaternary Carbons by NHC–Cu-Catalyzed Boronate Conjugate Additions to Unsaturated Carboxylic Esters, Ketones, or Thioesters," *J. Am. Chem. Soc.*, **2010**, *132*, 10630–10633.
- [60] Radomkit, S.; Hoveyda, A. H., "Enantioselective Synthesis of Boron-Substituted Quaternary Carbon Stereogenic Centers through NHC-Catalyzed Conjugate Additions of (Pinacolato)boron Units to Enones," *Angew. Chem., Int. Ed.*, **2014**, *53*, 3387–3391.

- [61] Hu, N.; Zhao, G.; Zhang, Y.; Liu, X.; Li, G.; Tang, W., "Synthesis of Chiral  $\alpha$ -Amino Tertiary Boronic Esters by Enantioselective Hydroboration of  $\alpha$ -Arylenamides," *J. Am. Chem. Soc.*, **2015**, *137*, 6746–6749.
- [62] Guzman-Martinez, A.; Hoveyda, A. H., "Enantioselective Synthesis of Allylboronates Bearing a Tertiary or Quaternary B-Substituted Stereogenic Carbon by NHC-Cu-Catalyzed Substitution Reactions," *J. Am. Chem. Soc.*, 2010, *132*, 10634–10637.
- [63] For recent selected examples, see: (a) Jiang, Q.; Guo, T.; Yu, Z., "Copper-Catalyzed Asymmetric Borylation: Construction of a Stereogenic Carbon Center Bearing Both  $\text{CF}_3$  and Organoboron Functional Groups," *J. Org. Chem.*, **2017**, *82*, 1951–1960; (b) Xie, J.-B.; Lin, S.; Qiao, S.; Li, G., "Asymmetric Catalytic Enantio- and Diastereoselective Boron Conjugate Addition Reactions of  $\alpha$ -Functionalized  $\alpha,\beta$ -Unsaturated Carbonyl Substrates," *Org. Lett.*, **2016**, *18*, 3926–3929; (c) Niu, Z.; Chen, J.; Chen, Z.; Ma, M.; Song, C.; Ma, Y., "Application of Bidentate Oxazoline–Carbene Ligands with Planar and Central Chirality in Asymmetric  $\beta$ -Boration of  $\alpha,\beta$ -Unsaturated Esters," *J. Org. Chem.*, **2015**, *80*, 602–608; (d) Luo, Y.; Roy, I. D.; Madec, A. G. E.; Lam, H. W., "Enantioselective Synthesis of Allylboronates and Allylic Alcohols by Copper-Catalyzed 1,6-Boration," *Angew. Chem., Int. Ed.*, **2014**, *53*, 4186–4190; (e) Wu, H.; Randomket, S.; O'Brien, J. M.; Hoveyda, A. H., "Metal-Free Catalytic Enantioselective C–B Bond Formation: (Pinacolato)boron Conjugate Additions to  $\alpha,\beta$ -Unsaturated Ketones, Esters, Weinreb Amides, and Aldehydes Promoted by Chiral N-Heterocyclic Carbenes," *J. Am. Chem. Soc.*, **2012**, *134*, 8277–8285.
- [64] Shi, Y.; Hoveyda, A. H., "Catalytic  $\text{S}_{\text{N}}2'$ - and Enantioselective Allylic Substitution with a Diborylmethane Reagent and Application in Synthesis," *Angew. Chem., Int. Ed.*, **2016**, *55*, 3455–3458.
- [65] Zhang, M.; Li, R.-Z.; Mou, Z.-D.; Cao, C.-G.; Liu, J.; Chen, Y.-W.; Niu, D., "Silver-Assisted, Iridium-Catalyzed Allylation of Bis[(pinacolato)boryl]methane Allows the Synthesis of Enantioenriched Homoallylic Organoboronic esters," *ACS Catal.*, **2016**, *6*, 3381–3386.
- [66] Moran, W. J.; Morken, J. P., "Rh-Catalyzed Enantioselective Hydrogenation of Vinyl Boronates for the Construction of Secondary Boronic Esters," *Org. Lett.*, **2006**, *8*, 2413–2415.
- [67] Morgan, J. B.; Morken, J. P., "Catalytic Enantioselective Hydrogenation of Vinyl Bis(boronates)," *J. Am. Chem. Soc.*, **2004**, *126*, 15338–15339.

[68] For a recent review, see: Verendel, J. J.; Pàmies, O.; Diéguez, M.; Andersson, P. G., “Asymmetric Hydrogenation of Olefins Using Chiral Crabtree-type Catalysts: Scope and Limitations,” *Chem. Rev.*, **2014**, *114*, 2130–2169.

[69] For recent examples, see: (a) Blaisdell, T. P.; Caya, T. C.; Zhang, L.; Sanz-Marco, A.; Morken, J. P., “Hydroxyl-Directed Stereoselective Diboration of Alkenes,” *J. Am. Chem. Soc.*, **2014**, *136*, 9264–9267; (b) Coombs, J. R.; Haeffner, F.; Kliman, L. T.; Morken, J. P., “Scope and Mechanism of the Pt-Catalyzed Enantioselective Diboration of Monosubstituted Alkenes,” *J. Am. Chem. Soc.*, **2013**, *135*, 11222–11231; (c) Ferris, G. E.; Hong, K.; Roundtree, I. A.; Morken, J. P., “A Catalytic Enantioselective Tandem Allylation Strategy for Rapid Terpene Construction: Application to the Synthesis of Pumilaside Aglycon,” *J. Am. Chem. Soc.*, **2013**, *135*, 2501–2504.

[70] Mlynarski, S. N.; Schuster, C. H.; Morken, J. P., “Asymmetric Synthesis from Terminal Alkenes by Cascades of Diboration and Cross-Coupling,” *Nature*, **2014**, *505*, 386–390.

[71] Fang, L.; Yan, L.; Haeffner, F.; Morken, J. P., “Carbohydrate-Catalyzed Enantioselective Alkene Diboration: Enhanced Reactivity of 1,2-Bonded Diboron Complexes,” *J. Am. Chem. Soc.*, **2016**, *138*, 2508–2511.

[72] Zhang, L.; Lovinger, G. J.; Edelstein, E. K.; Szymaniak, A. A.; Chierchia, M. P.; Morken, J. P., “Catalytic Conjunctive Cross-Coupling Enabled by Metal-Induced Metallate Rearrangement,” *Science*, **2016**, *351*, 70–74.

[73] Lovinger, G. J.; Aparece, M. D.; Morken, J. P., “Pd-Catalyzed Conjunctive Cross-Coupling between Grignard-Derived Boron “Ate” Complexes and C(sp<sup>2</sup>) Halides or Triflates: NaOTf as a Grignard Activator and Halide Scavenger,” *J. Am. Chem. Soc.*, **2017**, *139*, 3153–3160.

[74] Edelstein, E. K.; Namirembe, S.; Morken, J. P., “Enantioselective Conjunctive Cross-Coupling of Bis(alkenyl)borates: A General Synthesis of Chiral Allylboron Reagents,” *J. Am. Chem. Soc.*, **2017**, *139*, 5027–5030.

[75] Han, J. T.; Jang, W. J.; Kim, N.; Yun, J., “Asymmetric Synthesis of Borylalkanes via Copper-Catalyzed Enantioselective Hydroallylation,” *J. Am. Chem. Soc.*, **2016**, *138*, 15146–15149.

[76] Nishikawa, D.; Hirano, K.; Miura, M., "Asymmetric Synthesis of  $\alpha$ -Aminoboronic Acid Derivatives by Copper-Catalyzed Enantioselective Hydroamination," *J. Am. Chem. Soc.*, **2015**, *137*, 15620–15623.

[77] Nishikawa, D.; Hirano, K.; Miura, M., "Copper-Catalyzed Regio- and Stereoselective Aminoboration of Alkenylboronates," *Org. Lett.*, **2016**, *18*, 4856–4859.

[78] Nelson, H. M.; Williams, B. D.; Miró, J.; Toste, F. D., "Enantioselective 1,1-Arylborylation of Alkenes: Merging Chiral Anion Phase Transfer with Pd Catalysis," *J. Am. Chem. Soc.*, **2015**, *137*, 3213–3216.

[79] Jia, T.; Cao, P.; Wang, B.; Lou, Y.; Yin, X.; Wang, M.; Liao, J., "A Cu/Pd Cooperative Catalysis for Enantioselective Allylboration of Alkenes," *J. Am. Chem. Soc.*, **2015**, *137*, 13760–13763.

[80] Wang, D.; Cao, P.; Wang, B.; Jia, T.; Lou, Y.; Wang, M.; Liao, J., "Copper(I)-Catalyzed Asymmetric Pinacolboryl Addition of *N*-Boc-imines Using a Chiral Sulfoxide–Phosphine Ligand," *Org. Lett.*, **2015**, *17*, 2420–2423.

[81] Beenen, M. A.; An, C.; Ellman, J. A., "Asymmetric Copper-Catalyzed Synthesis of  $\alpha$ -Amino Boronate Esters from *N*-*tert*-Butanesulfinyl Aldimines," *J. Am. Chem. Soc.*, **2008**, *130*, 6910–6911.

[82] Cheng, Q.-Q.; Zhu, S.-F.; Zhang, Y.-Z.; Xie, X.-L.; Zhou, Q.-L., "Copper-Catalyzed B–H Bond Insertion Reaction: A Highly Efficient and Enantioselective C–B Bond-Forming Reaction with Amine–Borane and Phosphine–Borane Adducts," *J. Am. Chem. Soc.*, **2013**, *135*, 14094–14097.

[83] Chen, D.; Zhang, X.; Qi, W.-Y.; Xu, B.; Xu, M.-H., "Rhodium(I)-Catalyzed Asymmetric Carbene Insertion into B–H Bonds: Highly Enantioselective Access to Functionalized Organoboranes," *J. Am. Chem. Soc.*, **2015**, *137*, 5268–5271.

[84] Kubota, K.; Yamamoto, E.; Ito, H., "Copper(I)-Catalyzed Enantioselective Nucleophilic Borylation of Aldehydes: An Efficient Route to Enantiomerically Enriched  $\alpha$ -Alkoxyorganoboronate Esters," *J. Am. Chem. Soc.*, **2015**, *137*, 420–424.

[85] Joannou, M. V.; Moyer, B. S.; Meek, S. J., "Enantio- and Diastereoselective Synthesis of 1,2-Hydroxyboronates through Cu-Catalyzed Additions of Alkylboronates to Aldehydes," *J. Am. Chem. Soc.*, **2015**, *137*, 6176–6179.

- [86] Zhou, Q.; Srinivas, H. D.; Zhang, S.; Watson, M. P., "Accessing Both Retention and Inversion Pathways in Stereospecific, Nickel-Catalyzed Miyaura Borylations of Allylic Pivalates," *J. Am. Chem. Soc.*, **2016**, *138*, 11989–11995.
- [87] Basch, C. H.; Cobb, K. M.; Watson, M. P., "Nickel-Catalyzed Borylation of Benzylic Ammonium Salts: Stereospecific Synthesis of Enantioenriched Benzylic Boronates," *Org. Lett.*, **2016**, *18*, 136–139.
- [88] Brown, H. C.; Subba Rao, B. C., "A New Technique for the Conversion of Olefins into Organoboranes and Related Alcohols," *J. Am. Chem. Soc.*, **1956**, *78*, 5694–5695.
- [89] Brown, H. C.; Zweifel, G., "Hydroboration as a Convenient Procedure for the Asymmetric Synthesis of Alcohols of High Optical Purity," *J. Am. Chem. Soc.*, **1961**, *83*, 486–487.
- [90] Zweifel, G.; Ayyangar, N. R.; Brown, H. C., "Hydroboration. XVII. An Examination of Several Representative Dialkylboranes as Selective Hydroborating Agents," *J. Am. Chem. Soc.*, **1963**, *85*, 2072–2076.
- [91] Zweifel, G.; Ayyangar, N. R.; MuneKata, T.; Brown, H. C., "Hydroboration. XX. Reaction of Diisopinocampheylborane with Representative 2-Methyl-1-alkenes. A Convenient Synthesis of Optically Active 2-Methyl-1-alkanols." *J. Am. Chem. Soc.* **1964**, *86*, 1076–1079.
- [92] Brown, J. M.; Nguyen, B. N. In *In Stereoselective Hydroboration and Diboration of Carbon–Carbon Double Bonds*. Section Title: Organometallic and Organometalloidal Compounds; **2011**; Vol. 1, pp 295–324.
- [93] Brown, H. C.; Singaram, B., "Development of a Simple General Procedure for Synthesis of Pure Enantiomers via Chiral Organoboranes," *Acc. Chem. Res.*, **1988**, *21*, 287–293.
- [94] Brown, H. C.; Schwier, J. R.; Singaram, B., "Simple Synthesis of Monoisopinocampheylborane of High Optical Purity." *J. Org. Chem.*, **1978**, *43*, 4395–4397.
- [95] Brown, H. C.; Jadhav, P. K.; Mandal, A. K., "Hydroboration. 62. Monoisopinocampheylborane; An Excellent Chiral Hydroborating Agent for Trans-Disubstituted and Trisubstituted Alkenes. Evidence for a Strong Steric Dependence in such Asymmetric Hydroborations," *J. Org. Chem.*, **1982**, *47*, 5074–5083.

- [96] Brown, H. C.; Vara Prasad, J. V. N.; Gupta, A.; Bakshi, R. K., "Hydroboration. 80. Preparation of Trans-2-Phenylcyclopentyl- and Trans-2-Phenylcyclohexylboronates of Very High Enantiomeric Purities," *J. Org. Chem.*, **1987**, *52*, 310–311.
- [97] Brown, H. C.; Singaram, B., "Hydroboration. 68. Chiral Synthesis via Organoboranes. 1. A Simple Procedure to Achieve Products of Essentially 100% Optical Purity in Hydroboration of Alkenes with Monoisopinocampheylborane. Synthesis of Boronic Esters and Derived Products of Very High Enantiomeric Purities," *J. Am. Chem. Soc.*, **1984**, *106*, 1797–1800.
- [98] Masamune, S.; Kim, B. M.; Petersen, J. S.; Sato, T.; Veenstra, S. J.; Imai, T., "Organoboron Compounds in Organic Synthesis. 1. Asymmetric Hydroboration," *J. Am. Chem. Soc.*, **1985**, *107*, 4549–4551.
- [99] Gonzalez, A. Z.; Román, J. G.; Gonzalez, E.; Martinez, J.; Medina, J. R.; Matos, K.; Soderquist, J. A., "9-Borabicyclo[3.3.2]decanes and the Asymmetric Hydroboration of 1,1-Disubstituted Alkenes," *J. Am. Chem. Soc.*, **2008**, *130*, 9218–9219.
- [100] Thomas, S. P.; Aggarwal, V. K., "Asymmetric Hydroboration of 1,1-Disubstituted Alkenes," *Angew. Chem., Int. Ed.*, **2009**, *48*, 1896–1898.
- [101] Männig, D.; Nöth, H., "Catalytic Hydroboration with Rhodium Complexes," *Angew. Chem., Int. Ed.*, **1985**, *24*, 878–879.
- [102] Burgess, K.; Ohlmeyer, M. J., "Enantioselective Hydroboration Mediated by Homochiral Rhodium Catalysts," *J. Org. Chem.*, **1988**, *53*, 5178–5179.
- [103] Hayashi, T.; Matsumoto, Y.; Ito, Y., "Catalytic Asymmetric Hydroboration of Styrenes," *J. Am. Chem. Soc.*, **1989**, *111*, 3426–3428; (b) Hayashi, T.; Matsumoto, Y.; Ito, Y., "Asymmetric Hydroboration of Styrenes Catalyzed by Cationic Chiral Phosphine-Rhodium(I) Complexes," *Tetrahedron: Asymmetry*, **1991**, *2*, 601–612.
- [104] Crudden, C. M.; Edwards, D., "Catalytic Asymmetric Hydroboration: Recent Advances and Applications in Carbon–Carbon Bond-Forming Reactions," *Eur. J. Org. Chem.*, **2003**, 4695–4712.
- [105] Crudden, C. M.; Glasspoole, B. W.; Lata, C. J., "Expanding the Scope of Organoboron Species: Carbon–Carbon Bond Formation with Retention of Configuration," *Chem. Commun.*, **2009**, 6704–6716.

- [106] Carroll, A.-M.; O'Sullivan, T. P.; Guiry, P. J., "The Development of Enantioselective Rhodium-Catalysed Hydroboration of Olefins," *Adv. Synth. Cat.*, **2005**, *347*, 609–631.
- [107] Vogels, C.M.; Wescott, S. A., "Recent Advances in Organic Synthesis Using Transition Metal-Catalyzed Hydroborations," *Curr. Org. Chem.*, **2005**, *9*, 687–699.
- [108] (a) Brown, J. M.; Hulmes, D. I.; Layzell, T. P., "Effective Asymmetric Hydroboration Catalysed by a Rhodium Complex of 1-(2-Diphenylphosphino-1-naphthyl)isoquinoline," *J. Chem. Soc., Chem. Commun.*, **1993**, 1673–1674; (b) Doucet, H.; Fernandez, E.; Layzell, T. P.; Brown, J. M., "The Scope of Catalytic Asymmetric Hydroboration/Oxidation with Rhodium Complexes of 1,1'-(2-Diarylphosphino-1-naphthyl)isoquinolines," *Chem. Eur. J.*, **1999**, *5*, 1320–1330.
- [109] Kwong, F. Y.; Yang, Q.; Mak, T. C. W.; Chan, A. S. C.; Chan, K. S., "A New Atropisomeric P,N Ligand for Rhodium-Catalyzed Asymmetric Hydroboration," *J. Org. Chem.*, **2002**, *67*, 2769–2777.
- [110] Togni, A.; Breutel, C.; Schnyder, A.; Spindler, F.; Landert, H.; Tijani, A., "A Novel Easily Accessible Chiral Ferrocenyldiphosphine for Highly Enantioselective Hydrogenation, Allylic Alkylation, and Hydroboration Reactions," *J. Am. Chem. Soc.*, **1994**, *116*, 4062–4066.
- [111] (a) Schnyder, A.; Hintermann, L.; Togni, A., "Strong Electronic Effects on Enantioselectivity in Rhodium-Catalyzed Hydroborations with Novel Pyrazole-Containing Ferrocenyl Ligands," *Angew. Chem., Int. Ed.*, **1995**, *34*, 931–933; (b) Kollner, C.; Togni, A., "Synthesis, Characterization, and Application in Asymmetric Catalysis of Dendrimers Containing Chiral Ferrocenyl Diphosphines," *Can. J. Chem.*, **2001**, *79*, 1762–1774.
- [112] Moteki, S. A.; Wu, D.; Chandra, K. L.; Reddy, D. S.; Takacs, J. M., "TADDOL-Derived Phosphites and Phosphoramidites for Efficient Rhodium-Catalyzed Asymmetric Hydroboration," *Org. Lett.*, **2006**, *8*, 3097–3100.
- [113] Moteki, S. A.; Toyama, K.; Liu, Z.; Ma, J.; Holmes, A. E.; Takacs, J. M., "Two-Stage Optimization of a Supramolecular Catalyst for Catalytic Asymmetric Hydroboration," *Chem. Commun.*, **2012**, *48*, 263–265.

- [114] Crudden, C. M.; Hleba, Y. B.; Chen, A. C., "Regio- and Enantiocontrol in the Room-Temperature Hydroboration of Vinyl Arenes with Pinacol Borane," *J. Am. Chem. Soc.*, **2004**, *126*, 9200–9201.
- [115] Luna, A. P.; Bonin, M.; Micouin, L.; Husson, H.-P., "Reversal of Enantioselectivity in the Asymmetric Rhodium- versus Iridium-Catalyzed Hydroboration of Meso Substrates," *J. Am. Chem. Soc.*, **2002**, *124*, 12098–12099.
- [116] Mazet, C.; Gérard, D., "Highly Regio- and Enantioselective Catalytic Asymmetric Hydroboration of  $\alpha$ -Substituted Styrenyl Derivatives," *Chem. Commun*, **2011**, *47*, 298–300.
- [117] Magre, M.; Biosca, M.; Pàmies, O.; Diéguez, M., "Filling the Gaps in the Challenging Asymmetric Hydroboration of 1,1-Disubstituted Alkenes with Simple Phosphite-Based Phosphinooxazoline Iridium Catalysts," *ChemCatChem*, **2015**, *7*, 114–120.
- [118] Evans, D. A.; Fu, G. C., "Amide-Directed, Iridium-catalyzed Hydroboration of Olefins: Documentation of Regio- and Stereochemical Control in Cyclic and Acyclic Systems," *J. Am. Chem. Soc.*, **1991**, *113*, 4042–4043.
- [119] Evans, D. A.; Fu, G. C.; Hoveyda, A. H., "Rhodium(I)- and Iridium(I)-Catalyzed Hydroboration Reactions: Scope and Synthetic Applications," *J. Am. Chem. Soc.*, **1992**, *114*, 6671–6679.
- [120] Hoveyda, A. H.; Evans, D. A.; Fu, G. C., "Substrate-Directable Chemical Reactions," *Chem. Rev.*, **1993**, *93*, 1307–1370.
- [121] Brinkman, J. A.; Nguyen, T. T.; Sowa Jr., J. R., "Trifluoromethyl-Substituted Indenyl Rhodium and Iridium Complexes Are Highly Selective Catalysts for Directed Hydroboration Reactions," *Org. Lett.*, **2000**, *2*, 981–983.
- [122] Peng, J.; Docherty, J. H.; Dominey, A. P.; Thomas, S. P., "Cobalt-Catalysed Markovnikov Selective Hydroboration of Vinylarenes," *Chem. Commun.*, 2017, *53*, 4726–4729
- [123] Chen, X.; Cheng, Z.; Lu, Z., "Iron-Catalyzed, Markovnikov-Selective Hydroboration of Styrenes," *Org. Lett.*, **2017**, *19*, 969–971.



- [124] MacNair, A. J.; Millet, C. R. P.; Nichol, G. S.; Ironmonger, A.; Thomas, S. P., "Markovnikov-Selective, Activator-Free Iron-Catalyzed Vinylarene Hydroboration," *ACS Catal.*, **2016**, *6*, 7217–7221.
- [125] Liu, Y.; Zhou, Y.; Wang, H.; Qu, J., "FeCl<sub>2</sub>-Catalyzed Hydroboration of Aryl Alkenes with Bis(pinacolato)diboron," *RSC Adv.*, **2015**, *5*, 73705–73713.
- [126] Tseng, K.-N. T.; Kampf, J. W.; Szymczak, N. K., "Regulation of Iron-Catalyzed Olefin Hydroboration by Ligand Modifications at a Remote Site," *ACS Catal.*, **2015**, *5*, 411–415.
- [127] Zheng, J.; Sortais, J.- B.; Darcel, C., "[NHC]Fe(CO)<sub>4</sub>] Efficient Pre-catalyst for Selective Hydroboration of Alkenes," *ChemCatChem*, **2014**, *6*, 763–766.
- [128] Zhang, L.; Peng, D.; Leng, X.; Huang, Z., "Iron-Catalyzed, Atom-Economical, Chemo- and Regioselective Alkene Hydroboration with Pinacolborane," *Angew. Chem., Int. Ed.*, **2013**, *52*, 3676–3680.
- [129] Zhang, L.; Huang, Z., "Iron-Catalyzed Alkene Hydroboration with Pinacolborane," *Synlett*, **2013**, *24*, 1745–1747; and references cited therein.
- [130] Obligacion, J. V.; Chirik, P. J., "Highly Selective Bis(imino)pyridine Iron-Catalyzed Alkene Hydroboration," *Org. Lett.*, **2013**, *15*, 2680–2683.
- [131] Greenhalgh, M. D.; Thomas, S. P., "Chemo-, Regio-, and Stereoselective Iron-Catalysed Hydroboration of Alkenes and Alkynes," *Chem. Commun.*, **2013**, *49*, 11230–11232.
- [132] Wu, J. Y.; Moreau, B.; Ritter, T., "Iron-Catalyzed 1,4-Hydroboration of 1,3-Dienes," *J. Am. Chem. Soc.*, **2009**, *131*, 12915–12917.
- [133] Palmer, W. N.; Diao, T.; Pappas, I.; Chirik, P. J., "High-Activity Cobalt Catalysts for Alkene Hydroboration with Electronically Responsive Terpyridine and  $\alpha$ -Diimine Ligands," *ACS Catal.*, **2015**, *5*, 622–626.
- [134] Scheuermann, M. L.; Johnson, E. J.; Chirik, P. J., "Alkene Isomerization–Hydroboration Promoted by Phosphine-Ligated Cobalt Catalysts," *Org. Lett.*, **2015**, *17*, 2716–2719.

- [135] Zhang, L.; Zuo, Z.; Leng, X.; Huang, Z., "A Cobalt-Catalyzed Alkene Hydroboration with Pinacolborane," *Angew. Chem., Int. Ed.*, **2014**, *53*, 2696–2700.
- [136] Ruddy, A. J.; Sydora, O. L.; Small, B. L.; Stradiotto, M.; Turculet, L., "(*N*-Phosphinoamidinate)cobalt-Catalyzed Hydroboration: Alkene Isomerization Affords Terminal Selectivity," *Chem. Eur. J.*, **2014**, *20*, 13918–13922.
- [137] Obligacion, J. V.; Chirik, P. J., "Bis(imino)pyridine Cobalt-Catalyzed Alkene Isomerization–Hydroboration: A Strategy for Remote Hydrofunctionalization with Terminal Selectivity," *J. Am. Chem. Soc.*, **2013**, *135*, 19107–19110.
- [138] Chen, J.; Xi, T.; Ren, X.; Cheng, B.; Guo, J.; Lu, Z., "Asymmetric Cobalt Catalysts for Hydroboration of 1,1-Disubstituted Alkenes," *Org. Chem. Front.*, **2014**, *1*, 1306–1309.
- [139] Chen, J.; Xi, T.; Lu, Z., "Iminopyridine Oxazoline Iron Catalyst for Asymmetric Hydroboration of 1,1-Disubstituted Aryl Alkenes," *Org. Lett.*, **2014**, *16*, 6452–6455.
- [140] Zhang, H.; Lu, Z., "Dual-Stereocontrol Asymmetric Cobalt-Catalyzed Hydroboration of Sterically Hindered Styrenes," *ACS Catal.*, **2016**, *6*, 6596–6600.
- [141] Zhang, L.; Zuo, Z.; Wan, X.; Huang, Z., "Cobalt-Catalyzed Enantioselective Hydroboration of 1,1-Disubstituted Aryl Alkenes," *J. Am. Chem. Soc.*, **2014**, *136*, 15501–15504.
- [142] Wang, Z.; He, X.; Zhang, R.; Zhang, G.; Xu, G.; Zhang, Q.; Xiong, T.; Zhang, Q., "Copper-Catalyzed Asymmetric Hydroboration of 1,1-Disubstituted Alkenes," *Org. Lett.*, **2017**, *19*, 3067–3070.
- [143] Noh, D.; Chea, H.; Ju, J.; Yun, J., "Highly Regio- and Enantioselective Copper-Catalyzed Hydroboration of Styrenes," *Angew. Chem., Int. Ed.*, **2009**, *48*, 6062–6064.
- [144] Noh, D.; Yoon, S. K.; Won, J.; Lee, J. Y.; Yun, J., "An Efficient Copper(I)-Catalyst System for the Asymmetric Hydroboration of  $\beta$ -Substituted Vinylarenes with Pinacolborane," *Chem. Asian J.*, **2011**, *6*, 1967–1969
- [145] Lee, Y.; Hoveyda, A. H., "Efficient Boron–Copper Additions to Aryl-Substituted Alkenes Promoted by NHC–Based Catalysts. Enantioselective Cu-Catalyzed Hydroboration Reactions," *J. Am. Chem. Soc.*, **2009**, *131*, 3160–3161.

- [146] Corberán, R.; Mszar, N. W.; Hoveyda, A. H., “NHC-Cu-Catalyzed Enantioselective Hydroboration of Acyclic and Exocyclic 1,1-Disubstituted Aryl Alkenes,” *Angew. Chem., Int. Ed.*, **2011**, *50*, 7079–7082.
- [147] He, Z.-T.; Zhao, Y.-S.; Tian, P.; Wang, C.-C.; Dong, H.-Q.; Lin, G.-Q., “Copper-Catalyzed Asymmetric Hydroboration of  $\alpha$ -Dehydroamino Acid Derivatives: Facile Synthesis of Chiral  $\beta$ -Hydroxy- $\alpha$ -amino Acids,” *Org. Lett.*, **2014**, *16*, 1426–1429.
- [148] Jarava-Barrera, C.; Parra, A.; López, A.; Cruz-Acosta, F.; Collado-Sanz, D.; Cárdenas, D. J.; Tortosa, M., “Copper-Catalyzed Borylative Aromatization of *p*-Quinone Methides: Enantioselective Synthesis of Dibenzyllic Boronates,” *ACS Catal.*, **2016**, *6*, 442–446.
- [149] Nambo, M.; Crudden, C. M., “Recent Advances in the Synthesis of Triarylmethanes by Transition Metal Catalysis,” *ACS Catal.*, **2015**, *5*, 4734–4742.
- [150] Matthew, S. C.; Glasspoole, B. W.; Eisenberger, P.; Crudden, C. M., “Synthesis of Enantiomerically Enriched Triarylmethanes by Enantiospecific Suzuki–Miyaura Cross-Coupling Reactions,” *J. Am. Chem. Soc.*, **2014**, *136*, 5828–5831.
- [151] Sasaki, Y.; Zhong, C.; Sawamura, M.; Ito, H., “Copper(I)-Catalyzed Asymmetric Monoborylation of 1,3-Dienes: Synthesis of Enantioenriched Cyclic Homoallyl- and Allylboronates,” *J. Am. Chem. Soc.*, **2010**, *132*, 1226–1227.
- [152] Rubina, M.; Rubin, M.; Gevorgyan, V., “Catalytic Enantioselective Hydroboration of Cyclopropenes,” *J. Am. Chem. Soc.*, **2003**, *125*, 7198–7199.
- [153] Tian, B.; Liu, Q.; Tong, X.; Tian, P.; Lin, G.-Q., “Copper(I)-Catalyzed Enantioselective Hydroboration of Cyclopropenes: Facile Synthesis of Optically Active Cyclopropylboronates,” *Org. Chem. Front.*, **2014**, *1*, 1116–1122.
- [154] Parra, A.; Amenós, L.; Guisán-Ceinos, M.; López, A.; Ruano, J. L. G.; Tortosa, M., “Copper-Catalyzed Diastereo- and Enantioselective Desymmetrization of Cyclopropenes: Synthesis of Cyclopropylboronates,” *J. Am. Chem. Soc.*, **2014**, *136*, 15833–15836.
- [155] Guisán-Ceinos, M.; Parra, A.; Martín-Heras, V.; Tortosa, M., “Enantioselective Synthesis of Cyclobutylboronates via a Copper-Catalyzed Desymmetrization Approach,” *Angew. Chem., Int. Ed.*, **2016**, *55*, 6969–6972.

[156] Xi, Y.; Hartwig, J. F., "Diverse Asymmetric Hydrofunctionalization of Aliphatic Internal Alkenes through Catalytic Regioselective Hydroboration," *J. Am. Chem. Soc.*, **2016**, *138*, 6703–6706.

[157] Dang, L.; Lin, Z.; Marder, T., "DFT Studies on the Borylation of  $\alpha,\beta$ -Unsaturated Carbonyl Compounds Catalyzed by Phosphine Copper(I) Boryl Complexes and Observations on the Interconversion between O- and C-Bound Enolates of Cu, B, and Si," *Organometallics*, **2008**, *27*, 4443–4454.

[158] Won, J.; Noh, D.; Yun, J.; Lee, J. Y., "Catalytic Activity of Phosphine–Copper Complexes for Hydroboration of Styrene with Pinacolborane: Experiment and Theory," *J. Phys. Chem.*, **2010**, *114*, 12112–12115.

[159] Hong, S.; Liu, M.; Zhang, W.; Zeng, Q.; Deng, W., "Copper-Catalyzed Hydroboration of Arylalkenes at Room Temperature," *Tetrahedron Lett.*, **2015**, *56*, 2297–2302.

[160] Laitar, D. S.; Müller, P.; Sadighi, J. P., "Efficient Homogeneous Catalysis in the Reduction of CO<sub>2</sub> to CO," *J. Am. Chem. Soc.*, **2005**, *127*, 17196–17197.

[161] Lillo, V.; Fructos, M. R.; Ramírez, J.; Braga, A. A. C.; Maseras, F.; Díaz-Requejo, M. M.; Pérez, P. J.; Fernández, E., "A Valuable, Inexpensive Cu<sup>I</sup>/N-Heterocycle Carbene Catalyst for the Selective Diboration of Styrene," *Chem. Eur. J.*, **2007**, *13*, 2614–2621.

[162] Dang, L.; Zhao, H.; Lin, Z.; Marder, T. B., "Understanding the Higher Reactivity of B<sub>2</sub>cat<sub>2</sub> versus B<sub>2</sub>pin<sub>2</sub> in Copper(I)-Catalyzed Alkene Diboration Reactions," *Organometallics*, **2008**, *27*, 1178–1186.

[163] Iwamoto, H.; Kubota, K.; Ito, H., "Highly Selective Markovnikov Hydroboration of Alkyl-Substituted Terminal Alkenes with a Phosphine–Copper(I) Catalyst," *Chem. Commun.*, **2016**, *52*, 5916–5919.

[164] Kerchner, H. A.; Montgomery, J., "Synthesis of Secondary and Tertiary Alkylboranes via Formal Hydroboration of Terminal and 1,1-Disubstituted Alkenes," *Org. Lett.*, **2016**, *18*, 5760–5763.

[165] Kono, H.; Ito, K.; Nagai, Y., "Oxidative Addition of 4,4,6-Trimethyl-1,3,2-Dioxaborinane and Benzo[1,3,2]dioxaborole to Tris(triphenylphosphine)halogenrhodium," *Chem. Lett.*, **1975**, 1095–1096.

[166] Touney, E. E.; Hovel, R. V.; Buttke, C. T.; Freidberg, M. D.; Guzei, I. A.; Schomaker, J. M., "Heteroleptic Nickel Complexes for the Markovnikov-Selective Hydroboration of Styrenes," *Organometallics*, **2016**, *35*, 3436–3439.

[167] Burgess, K.; Donk, W. A. V. d.; Westcott, S. A.; Marder, T. B.; Baker, R. T.; Calabrese, J. C., "Reactions of Catecholborane with Wilkinson's Catalyst: Implications for Transition Metal-Catalyzed Hydroborations of Alkenes," *J. Am. Chem. Soc.*, **1992**, *114*, 9350–9359.

[168] Musaev, D. G.; Mebel, A. M.; Morokuma, K., "An ab Initio Molecular Orbital Study of the Mechanism of the Rhodium(I)-Catalyzed Olefin Hydroboration Reaction," *J. Am. Chem. Soc.*, **1994**, *116*, 10693–10702.

[169] Dorigo, A. E.; Schleyer, P. v. R., "An Ab Initio Investigation of the Rh<sup>I</sup>-Catalyzed Hydroboration of C=C Bonds: Evidence for Hydrogen Migration in the Key Step," *Angew. Chem., Int. Ed.*, **1995**, *34*, 115–118.

[170] Widauer, C.; Grützmacher, H.; Ziegler, T., "Comparative Density Functional Study of Associative and Dissociative Mechanisms in the Rhodium(I)-Catalyzed Olefin Hydroboration Reactions," *Organometallics*, **2000**, *19*, 2097–2107.

[171] Rablen, P. R.; Hartwig, J. F.; Nolan, S. P., "First Transition Metal-Boryl Bond Energy and Quantitation of Large Differences in Sequential Bond Dissociation Energies of Boranes," *J. Am. Chem. Soc.*, **1994**, *116*, 4121–4122.

[172] Segarra, A. M.; Daura-Oller, E.; Claver, C.; Poblet, J. M.; Bo, C.; Fernández, E., "In Quest of Factors That Control the Enantioselective Catalytic Markovnikov Hydroboration/ Oxidation of Vinylarenes," *Chem. Eur. J.*, **2004**, *10*, 6456 – 6467.

CHAPTER 2: ENANTIOSELECTIVE  $\gamma$ - AND  $\delta$ -BORYLATION OF ACYCLIC  $\beta,\gamma$ -  
AND  $\gamma,\delta$ -UNSATURATED CARBONYL DERIVATIVES

**2.1 Enantioselective  $\gamma$ -borylation of  $\beta,\gamma$ -unsaturated amides and esters<sup>1</sup>**

The work described in this section 2.1 was in collaboration with Dr. Sean M. Smith, a previous member of the Takacs group. I was involved in this project when first joining the group. At that time, the optimization studies were done; using the best performing conditions, I obtained several CAHB of substrates which were later used for Suzuki–Miyaura cross-coupling reactions (i.e., **4b** and **4h–j**) as well as transformations of the latter.

This work was already included in Dr. Smith's thesis (University of Nebraska, 2012) as the highlight of the first highly regio- and enantioselective CAHB of unactivated 1,1-disubstituted alkenes (i.e., methyldene substrates). However, I would like to summarize it herein as a different approach – first general direct asymmetric route to  $\gamma$ -borylation of carbonyl derivatives illustrating the innovation of this work. In addition, it is significant because the formation of the  $\gamma$ -borylated products broadens the range of structures that can subsequently be accessed from chiral boronic ester products. While conjugate addition<sup>2</sup> and C–H activation<sup>3</sup> methodologies provide efficient alternatives to CAHB for enantioselective  $\beta$ -borylation of carbonyl compounds (Figure 1), direct  $\gamma$ -borylation is unique to CAHB.

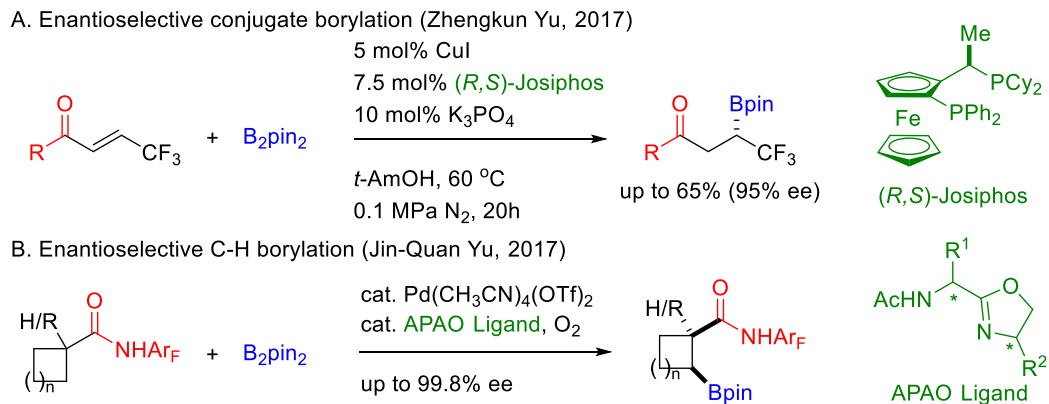


**Figure 1.** Enantioselective conjugate borylation and C–H borylation for the preparations of chiral  $\beta$ -borylated of carbonyl compounds.

In contrast to the CAHB of 1,2-disubstituted alkenes (e.g., **1a**) previously reported,<sup>4</sup> CAHB of these methylenes substrates (e.g., **3a**) differs in two important aspects (Figure 2). (i) The methylenes undergo CAHB, using 1% [Rh(nbd)<sub>2</sub>BF<sub>4</sub>]/2 (*R,R*)-**T1**] and 4,4,6-trimethyl-1,3,2-dioxaborinane (tmdBH), with complementary regioselectivity. While 1,2-disubstituted alkene **1a** generates  $\beta$ -borylated amide **2a**, 1,1-disubstituted alkene **3a** affords  $\gamma$ -borylated amide **4a**. (ii) Using the same catalyst system, the borane (i.e., tmdBH) adds to opposite faces of the alkene; borane adds to the top face for methylenes (for the perspective illustrated) *versus* bottom face addition in the isomeric 1,2-disubstituted alkenes.

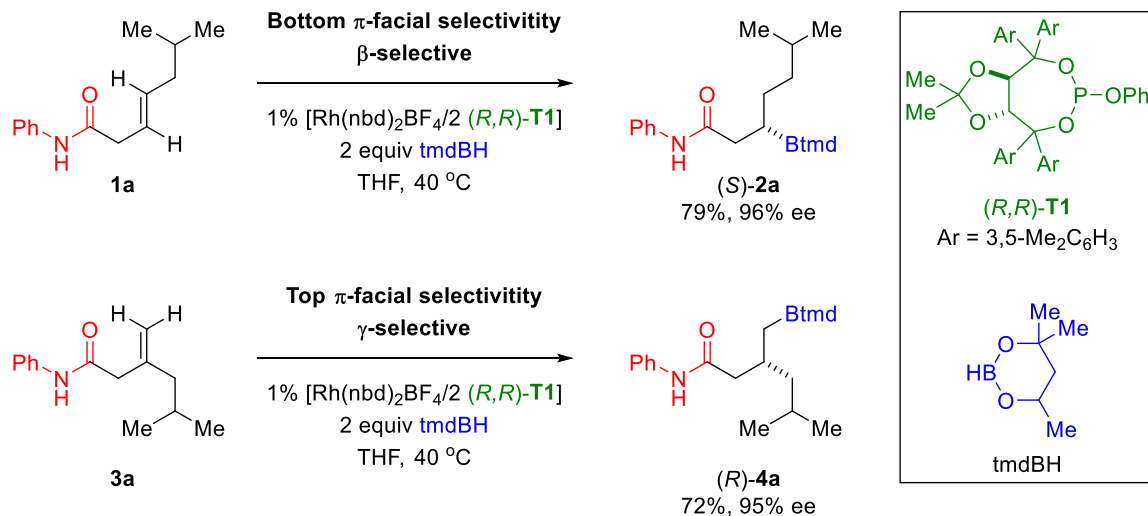


**Figure 2.** Contrasting regio- and  $\pi$ -facial selectivity of 1,2- and 1,1-disubstituted alkenes.

Having developed an efficient catalyst system for enantioselective  $\gamma$ -borylation of 1,1-disubstituted unsaturated amide **3a**, we explored the substrate scope (i.e., **3b–j**) to illustrate some of the current advances and limitations (Figure 3). Phenyl amide substrates bearing small substituents (i.e., **3b–c**, R = Me or Et) exhibits more modest regioselectivity (5–6:1); however, CAHB proceeds in good yield and a high level of enantioinduction (54–60%, 92–94% ee). Substrates with larger side chains including primary alkyl (i.e., **3d–e**) or secondary alkyl (i.e., **3f**), and aryl (i.e., **3g**) substituents predominantly provide  $\gamma$ -borylated products **4d–g** in excellent yield and enantioselectivity (regioselectivity >20:1, 70–73%, 90–94% ee). The versatile functional group *tert*-butyl ester also acts as an efficient directing group; CAHBs of  $\beta,\gamma$ -unsaturated *tert*-butyl esters **3h–j** proceed with good yield and high enantioselectivity (62–78%, 92–94% ee). Similar to the phenyl amide cases, *tert*-butyl ester substrates bearing small substituents exhibits lower regioselectivity (i.e., **3i–j**, R = Me or Et).



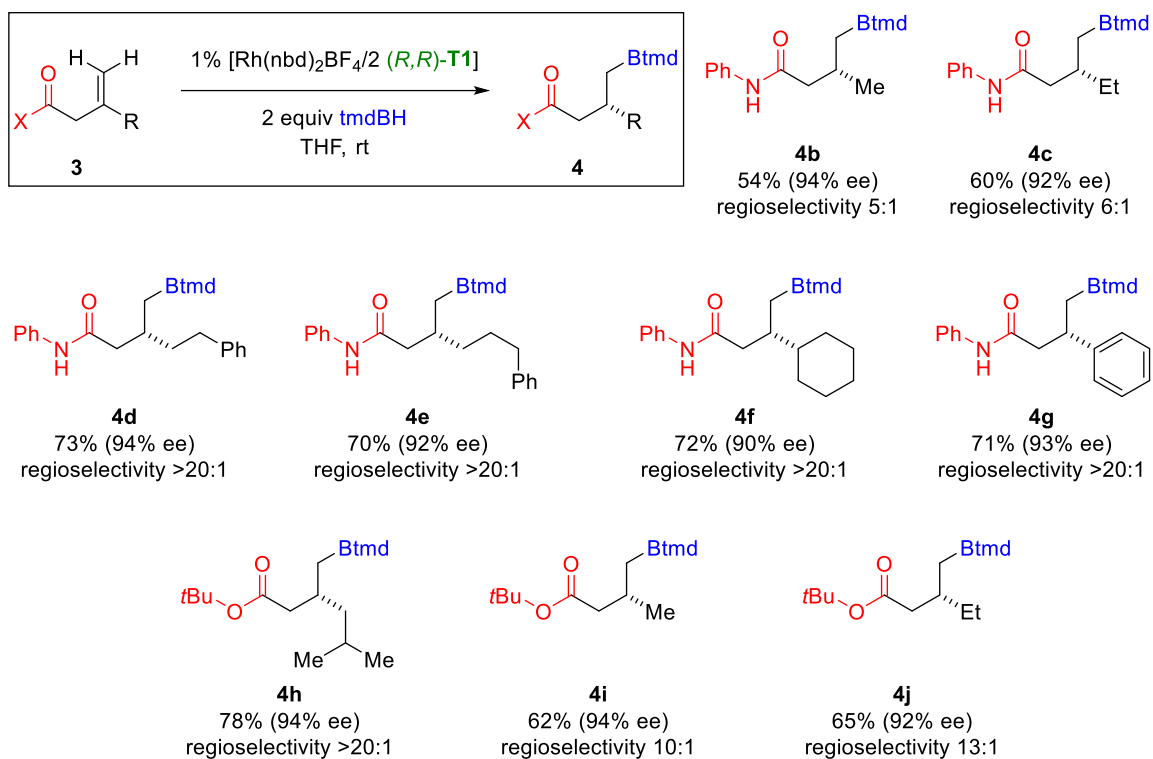
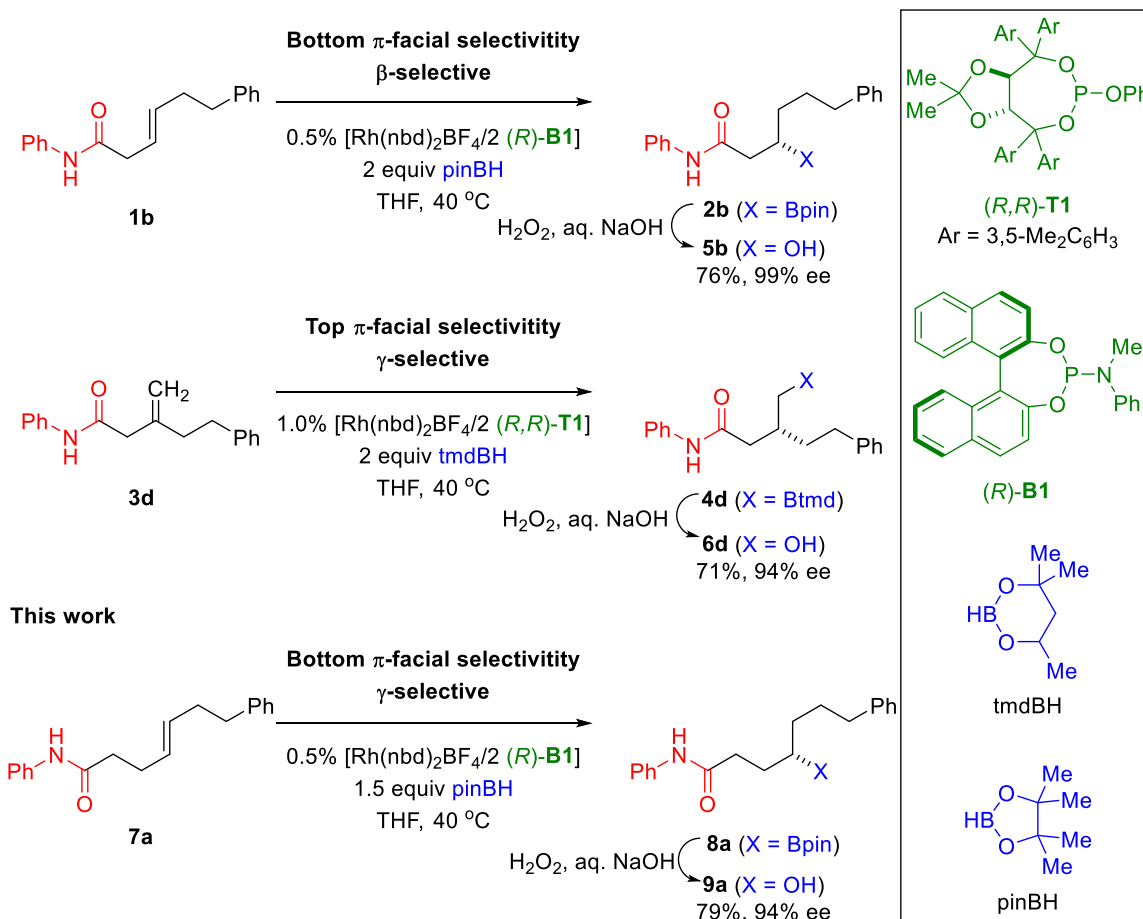


**Figure 3.** Enantioselective  $\gamma$ -borylation of  $\beta,\gamma$ -unsaturated amides and esters

## 2.2 Enantioselective $\gamma$ -borylation of $\gamma,\delta$ -unsaturated amides<sup>5</sup>

The work in section 2.1 introduced the first general direct asymmetric route to  $\gamma$ -borylated carbonyl compounds; however, due to the substitution pattern the boronic esters generated do not bear boron at a secondary or tertiary carbon stereocenter. To address the latter and to consider the challenge of further distal coordination in CAHB reactions, we sought a direct route to secondary  $\gamma$ -borylated carbonyl compounds. CAHB of  $\gamma,\delta$ -unsaturated amide **7a** undergoes highly  $\gamma$ -selective borylation in excellent yield and with high enantioselectivity (Figure 4). It differs from the previous  $\beta,\gamma$ -unsaturated amides<sup>1,4</sup> (i.e., **1** and **3**) in a number of important aspects. (i)  $\beta$ - and  $\gamma$ -Borylation of isomeric  $\beta,\gamma$ -substrates (e.g., **1b** and **3d**) differ in the sense of stereinduction (i.e.,  $\pi$ -facial discrimination). In contrast,  $\beta$ -borylation of  $\beta,\gamma$ -unsaturated amide **1b** and  $\gamma$ -borylation of the one-carbon homologue  $\gamma,\delta$ -unsaturated amide **7a** add to the same face of the alkene. (ii) CAHB of **7a** is more efficient; it is not necessary to use 2 equivalents of borane to effect complete hydroboration. As shown in previous studies of CAHB of  $\beta,\gamma$ -unsaturated carbonyl compounds, complete conversion of starting material requires an excess (2 equiv) of borane; i.e., using only one equivalent of borane fails to consume all starting material regardless of the amount of time and catalyst loading. The results indicate the borane is apparently being consumed in an undesired side-reaction (e.g., the reported rhodium-catalyzed formation of tris(pinacolato)diboron).<sup>6,7</sup> In the present case, CAHB of  $\gamma,\delta$ -unsaturated amides **7** requires only a slight excess of pinBH (i.e., 1.1 equiv). However, 1.5 equiv is typically used to facilitate faster conversion and/or permit the use of lower catalyst loading; optimization studies are discussed below, *vide infra*.

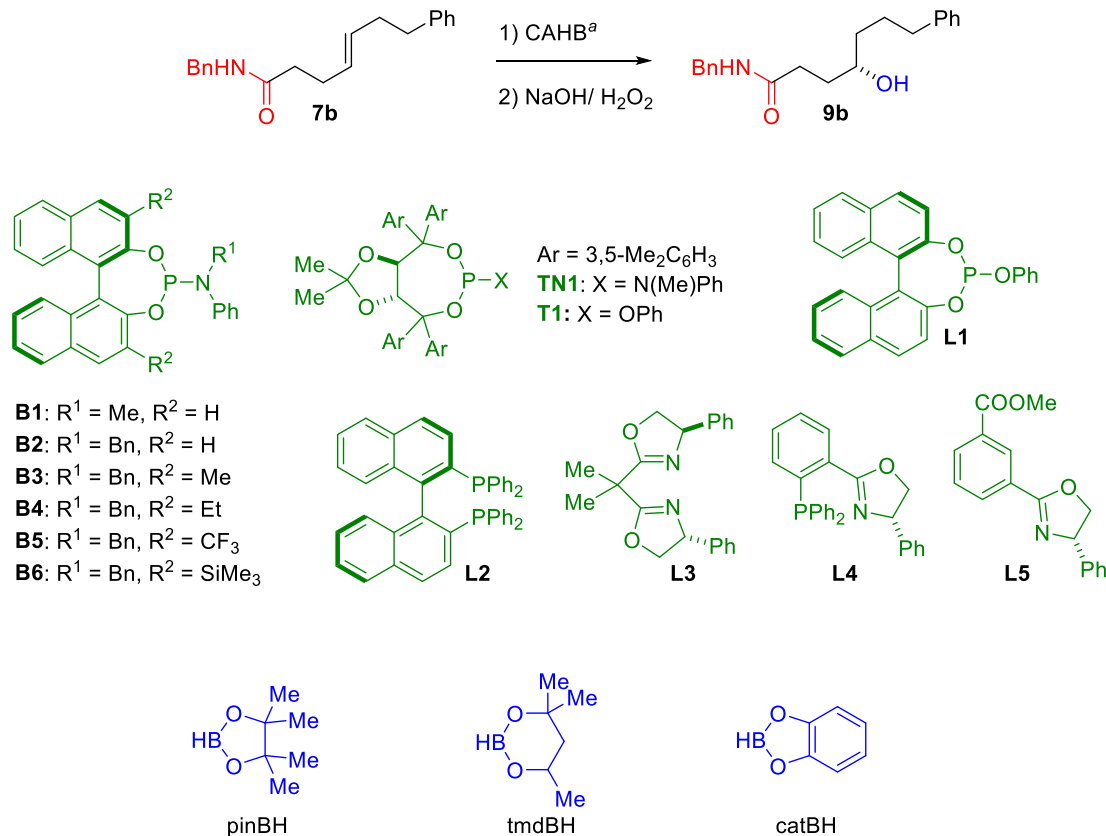
## Previous work



**Figure 4.** Comparing  $\pi$ -facial discrimination in CAHB of  $\beta,\gamma$ - and  $\gamma,\delta$ -unsaturated phenyl amides

Given the promising results obtained for CAHB of the one-carbon further remote  $\gamma,\delta$ -unsaturated phenyl amide **7a**, we wanted to focus this study on more versatile amides (i.e., benzyl amide, Weinreb amide, and morpholine amide). It is worth noting that the benzyl amide is not an efficient directing group for  $\beta,\gamma$ -unsaturated systems.<sup>4</sup> An extensive optimization study evaluating the effect of ligands, boranes, and the ligand:metal ratio are obtained for CAHB of  $\gamma,\delta$ -unsaturated benzyl amide **7b** (Table 1 and Figures 3–4). First, the effects of using various ligands and boranes are evaluated as shown in Table 1. Though tmdBH is very efficient in both  $\beta$ - and  $\gamma$ -borylation of  $\beta,\gamma$ -

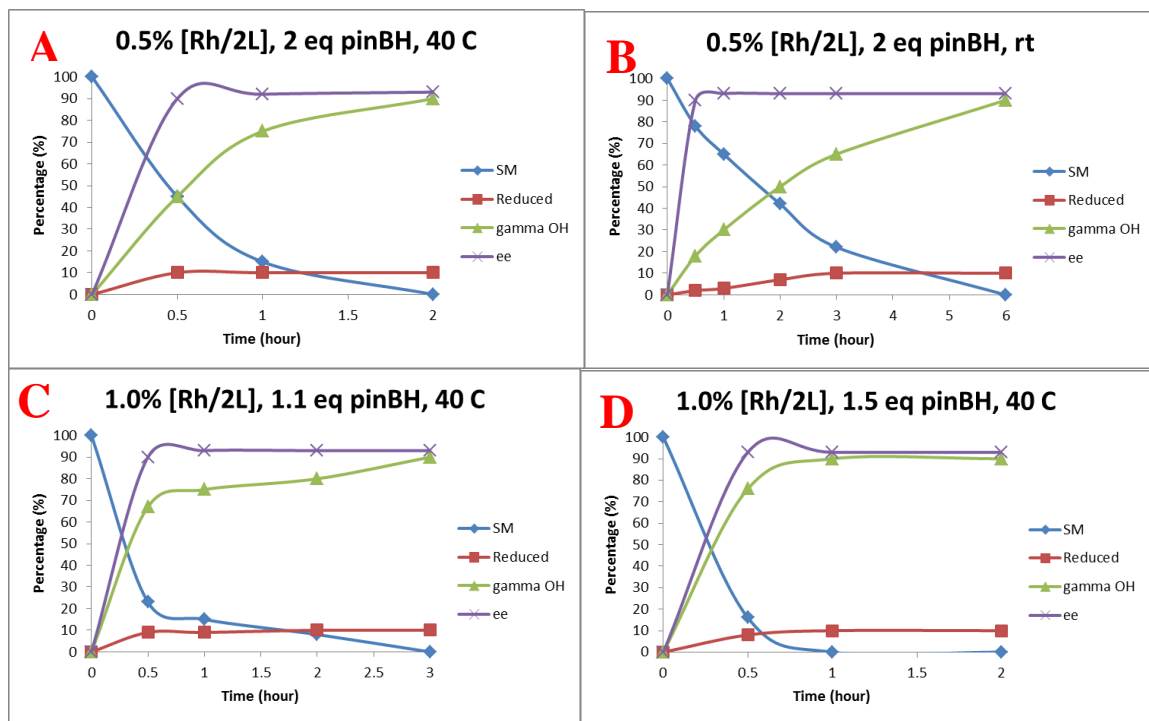
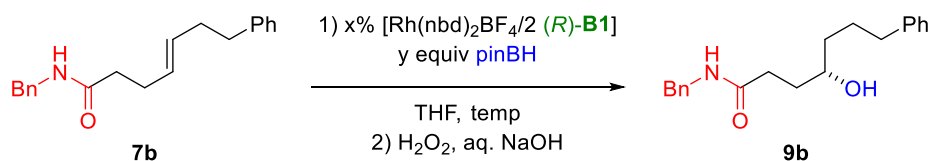
unsaturated carbonyl derivatives (Figure 1), it is much less reactive and selective for hydroboration in the present study (Table 1, entries 14–26). In some cases (entries 16–18), the conversions are good (as little as 11% starting material left over); however, there is only trace amount of the desired  $\gamma$ -borylated product observed; the major side-products obtained are reduced products in all cases. Catecholborane (catBH, entries 27–39) gives good yield in many cases; however, the products obtained are nearly racemic. On the other hand, pinacolborane (pinBH, entries 1–13) is quite effective. In conjunction with pinBH, simple BINOL-derived phosphonamidite ligands **B1–2** are among the successful catalyst systems (entries 1–2). The effect of 3,3'-substituents of varying steric and electronic character on BINOL-derived phosphonamidite ligands (i.e., **B3–6**, entries 3–6) are also tested. Except for **B6** (R = TMS, entry 6), which gives results similar to **B1** and **B2**, other derivatives proceed in lower yield and enantioselectivity (entries 3–5); the major side-products using these derivatives are either reduced products or those derived from alkene isomerization to the styrenyl derivative (i.e., vinyl arene). Simple TADDOL-derived phosphonamidite **TN1** and phosphite **T1** give high yield and regioselectivity for  $\gamma$ -borylation but only exhibit moderate enantioselectivity (entries 7–8). In contrast to BINOL-derived phosphonamidite ligands, BINOL-derived phosphite **L1** and BINAP **L2** are not reactive (i.e., 80–84% starting **7b** is recovered; entries 9–10). The oxazoline-containing monodentate and bidentate ligands **L3–5** are not selective for hydroboration pathway (entries 11–13); although starting material was consumed in these cases, only small amounts of hydroborated products were formed (14–24%).

**Table 1.** Evaluating the effects of ligands and boranes in CAHB of **7b**

Ligand	<b>B1 (pinBH)</b>				<b>B2 (tmdBH)</b>				<b>B3 (catBH)</b>			
	Entry	<b>5d</b>	<b>7d</b>	% ee	Entry	<b>5d</b>	<b>7d</b>	% ee	Entry	<b>5d</b>	<b>7d</b>	% ee
<b>B1</b>	<b>1</b>	<b>0</b>	<b>91</b>	<b>93</b>	14	80	12	n.d.	27	0	81	37
<b>B2</b>	<b>2</b>	<b>0</b>	<b>95</b>	<b>90</b>	15	60	15	n.d.	28	0	83	30
<b>B3</b>	3	0	64	87	16	35	0	n.d.	29	–		
<b>B4</b>	4	0	52	85	17	27	5	n.d.	30	–		
<b>B5</b>	5	0	19	85	18	11	0	n.d.	31	–		
<b>B6</b>	<b>6</b>	<b>0</b>	<b>90</b>	<b>90</b>	19	70	10	n.d.	32	–		
<b>TN1</b>	7	0	70	–43 <sup>b</sup>	22	>90	0	n.d.	33	18	69	–8 <sup>b</sup>
<b>T1</b>	8	0	85	46	23	>90	0	n.d.	34	10	76	48
<b>L1</b>	9	80	0	n.d.	20	>90	0	n.d.	35	0	60	n.d.
<b>L2</b>	10	84	0	n.d.	21	>90	0	n.d.	36	30	57	n.d.
<b>L3</b>	11	0	14	n.d.	24	>90	0	n.d.	37	0	40	n.d.
<b>L4</b>	12	50	17	n.d.	25	80	11	n.d.	38	22	67	–16 <sup>c</sup>
<b>L5</b>	13	0	24	n.d.	26	75	0	n.d.	39	6	36	n.d.

<sup>a</sup> CAHB conditions: 0.0528 mmol **5d**, 1.0 mol% Rh(*nbd*)<sub>2</sub>BF<sub>4</sub>, 1.0 mol% bidentate ligand or 2.0 mol% monodentate ligand, 2.0 equiv. borane, THF (C = 0.106 M), 40 °C, 5h; yield was reported as crude <sup>1</sup>H NMR yield using mesitylene as an internal standard and an average of two experiments generally exhibiting a spread of ±2%; % ee was determined by chiral HPLC Chiralpak-IC column; n.d. = not determined. <sup>b</sup> Enantioselectivity observed when using (*R*)-**TN1**. <sup>c</sup> (*S*)-**L4** was used.

With the best performing borane and ligand (i.e., pinBH and **B1**) identified, we next evaluate the effects of catalyst loading, amount of borane, and temperature for CAHB/ oxidation of **7b** (Figure 5). The study was carried out in six different conditions **A–F**; the x-axis represents the reaction time and the y-axis stands for the yield of four components: starting material (SM, blue), reduced product (red), the desired  $\gamma$ -hydroxy product **9b** (green), and the enantiomer excess of **9b** (ee, purple). Condition **A** is the same as the optimal condition obtained from Table 1 (entry 1, 0.5% Rh/2 **B1**, 2.0 equiv pinBH, 40 °C); brief kinetic results here show that all starting materials were consumed after 2 hours with good yield and enantioselectivity of **9b** (90%, 93% ee). According to Curtin–



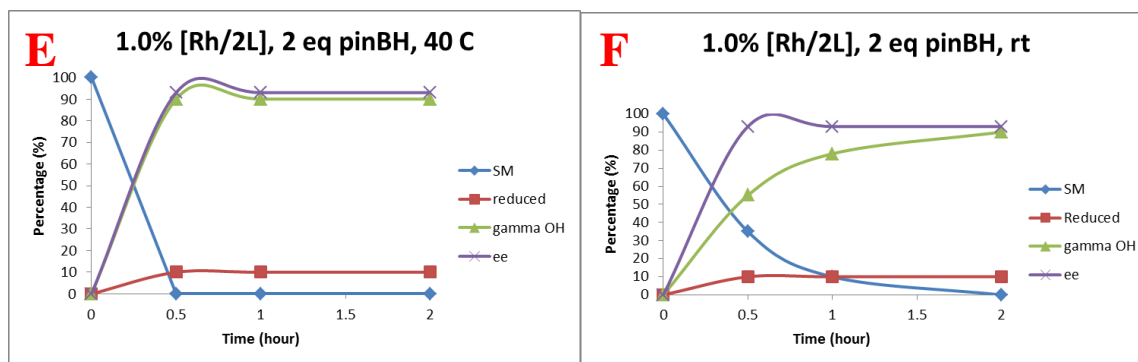


**Figure 5.** Temperature and amount of catalyst and borane effects on CAHB of  $\gamma,\delta$ -unsaturated amide **7b**

Hammett principle, lower the reaction temperature would lead to higher ee; however, condition **B** run at room temperature with otherwise the same reaction conditions as **A** affords the same results at the slower rate (6h for complete conversion). Notably and as highlighted above, condition **C** with slight excess of borane (i.e., 1.1 equiv pinBH) is also effective; however, it is still slower (3h for complete conversion) than **A** even with higher catalyst loading (1.0% Rh/2 **B1**) affording the same final results. Similar conditions to **C**, but increasing the amount of borane to 1.5 (**D**) and 2.0 (**E**) equiv push the reactions to completion in 1 and 0.5 hours, respectively. Condition **F** run at room temperature once again does not help to enhance the ee; the reaction maybe too fast for the Curtin–Hammett principle to be applied. Several conclusions from the optimization studies are shown in Figure 3; these include, (i) the catalyst loading can go as low as 0.5% without loss of yield or prolonged reaction time, (ii) increasing temperature from room temperature to 40 °C provides not only faster rate but also retain high selectivity, and (iii) as discussed above (Figure 2), in contrast to the CAHB of  $\beta,\gamma$ -systems only a slight excess of borane is required (as low as 1.1 equiv) for complete consumption of starting material. In addition, the graphs indicate that the reduced product forms at the

beginning of the reaction and reaching its maximum yield (i.e., 10%) before the borylation reaction is complete. The competing hydrogenation pathway is currently under investigation by Veronika Shoba, a current Ph.D. candidate in the Takacs lab.<sup>8</sup>

It is worth noting that the cationic rhodium catalyst precursor used above (i.e.,  $\text{Rh}(\text{nbd})_2\text{BF}_4$ ) is essential for the two-point binding substrates (i.e., alkenes utilizing the directing group). Neutral rhodium (e.g.,  $[\text{Rh}(\text{COD})\text{Cl}]_2$ ) is indeed ineffective resulting in no reaction. It is because the counterion (e.g.,  $\text{BF}_4^-$ ) of the cationic rhodium is ready to dissociate giving open binding sites for not only the alkene but also the directing group to bind to the metal. In addition, the 1:2 Rh:Ligand ratio (i.e.,  $[\text{Rh}(\text{nbd})_2\text{BF}_4/2 \mathbf{B1}]$ ) employed is suggested by early work in the Takacs group.<sup>9</sup> Can we use 1:1 Rh:Ligand (e.g.,  $[\text{Rh}(\text{nbd})_2\text{BF}_4/ \mathbf{B1}]$ ) as the missing coordination can be replaced by the coordinating solvent (i.e., THF)? To probe the question, several metal:ligand ratios were carried out for CAHB of **7b** (Figure 4). The color codes and labels are similar to Figure 5 with x-axis now represents the ligand:rhodium ratios ranking from 1:1.1–1:2  $\text{Rh}(\text{nbd})_2\text{BF}_4:\mathbf{B1}$ . All conditions are the same as depicted in the Scheme of Figure 6 with different reaction times (0.5–2 hours). Interestingly, with 1.1:1 ligand:metal ratio, the conversion is even faster than the suggested one; only approximate 2% of starting material left over after 0.5 hour, while the case of 2:1 ratio provides only slightly more than half conversion (i.e., 57%). After 2 hours, the reaction goes to completion in all cases. While the 1:1 ligand:rhodium catalyst is decidedly faster, the final yield of borylated product using the 2:1 ligand:metal ratio is higher (90% *versus* 84%) due to lower amounts of the reduced product formed. In addition, with more ligand, the level of enantioselectivity is also slightly higher (86% ee *versus* 93% ee). The results indicate that 1:1 ligand:metal ratio is



sufficient to form an active catalyst; however, having excess ligand reduces the unwanted side reaction and enhances the enantioselectivity. The results obtained using a 1.8:1 ligand:metal ratio are as good as 2:1; however, we settled on using the 2:1 ratio in further investigations as well as for publication purposes.

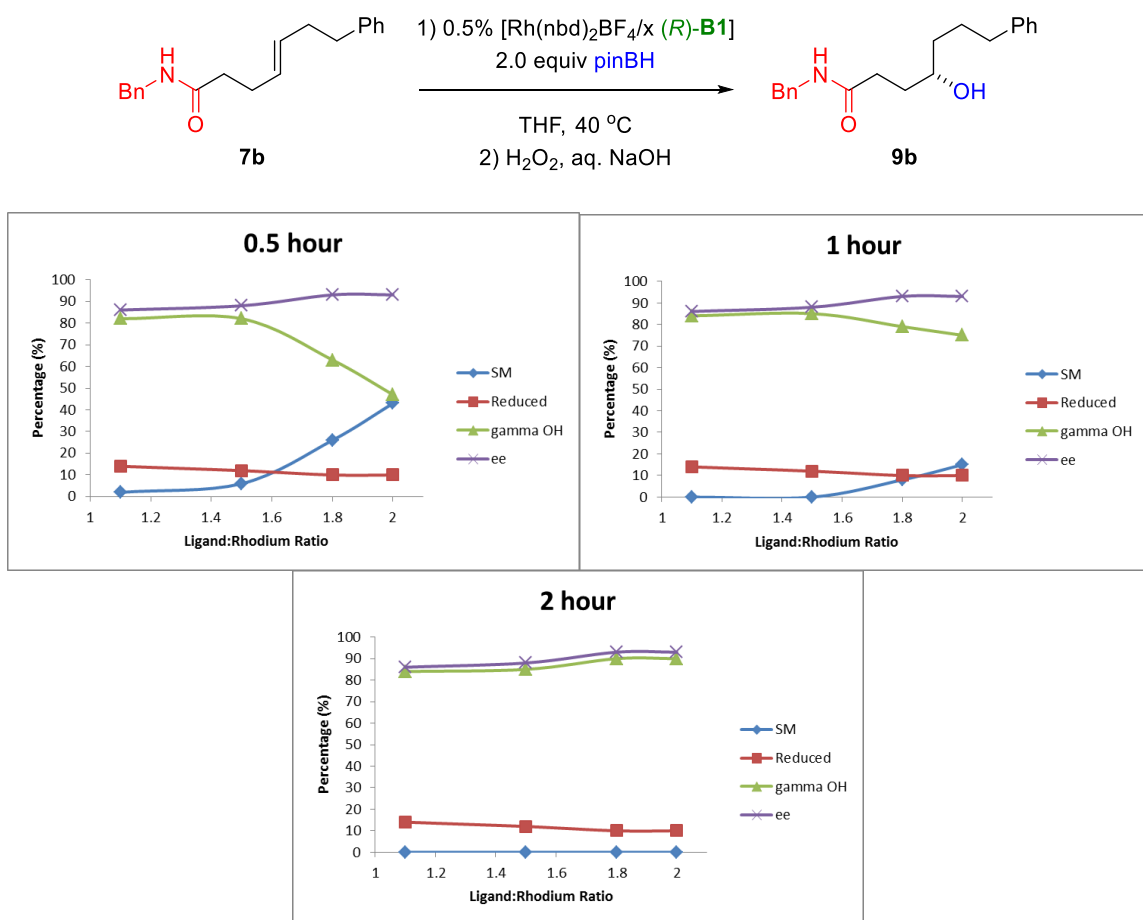


**Figure 6.** Ligand:metal ratio studies on CAHB of  $\gamma,\delta$ -unsaturated amide **7b** suggest that 1:1 ligand:metal ratio is sufficient to form an active catalyst; however, having excess ligand reduces the unwanted side reaction and enhances the enantioselectivity.

To further explore the generality of the optimized catalyst system, CAHB of a series of  $\gamma,\delta$ -unsaturated amides **7b–m** varying in their amide and the vinyl substituents

were converted to their  $\gamma$ -borylated intermediates and oxidized to their  $\gamma$ -hydroxy amides **9b–m** (Figure 7). As expected from previous CAHB of  $\beta,\gamma$ -unsaturated amides,<sup>4</sup> the *E/Z*-alkene geometry of the 1,2-disubstituted alkene moiety only slightly effect affects the results; e.g., comparable results are obtained for CAHB of (*E*)- and (*Z*)-**7b** (78%, 94:6 er). Along with the secondary amides (i.e., *N*-phenyl and *N*-benzyl) discussed above, the more labile tertiary amides (i.e., Weinreb and morpholine) **7c** and **7d** are also well tolerated under the reaction conditions resulting in high yield and enantioselectivity (68–81%, 89–92% ee). Among the amide series, secondary amides give the highest  $\gamma$ -selectivity (>20:1), and thus *N*-benzyl amide was chosen for further exploring the substrate scope. *N*-benzyl amide substrates **7e–g** bearing heteroaromatic ring systems also undergo CAHB/oxidation effectively yielding **9e–g** (59–72%, 84–88% ee). Not only *n*-alkyl but also certain branched alkyl substituents (i.e., **7h–j**) are well tolerated under the standard reaction conditions. In particular, substrate **7j** bearing a pre-installed chiral center and two double bond moieties undergoes CAHB selectively on the proximal double bond with respect to the amide directing group with essentially complete catalyst controlled; CAHB/ oxidation with (*R*)-**B2** affords (4*S*,7*S*)-**7j** and with (*S*)-**B2** affords (4*R*,7*S*)-**7j** in similar yield and diastereoselectivity. Oxygen- containing compounds (i.e., silyl ether and chiral acetal) **7k–m** are also good substrates. Chiral acetal **7l** again undergoes catalyst controlled  $\gamma$ -borylation with high diastereoselectivity.

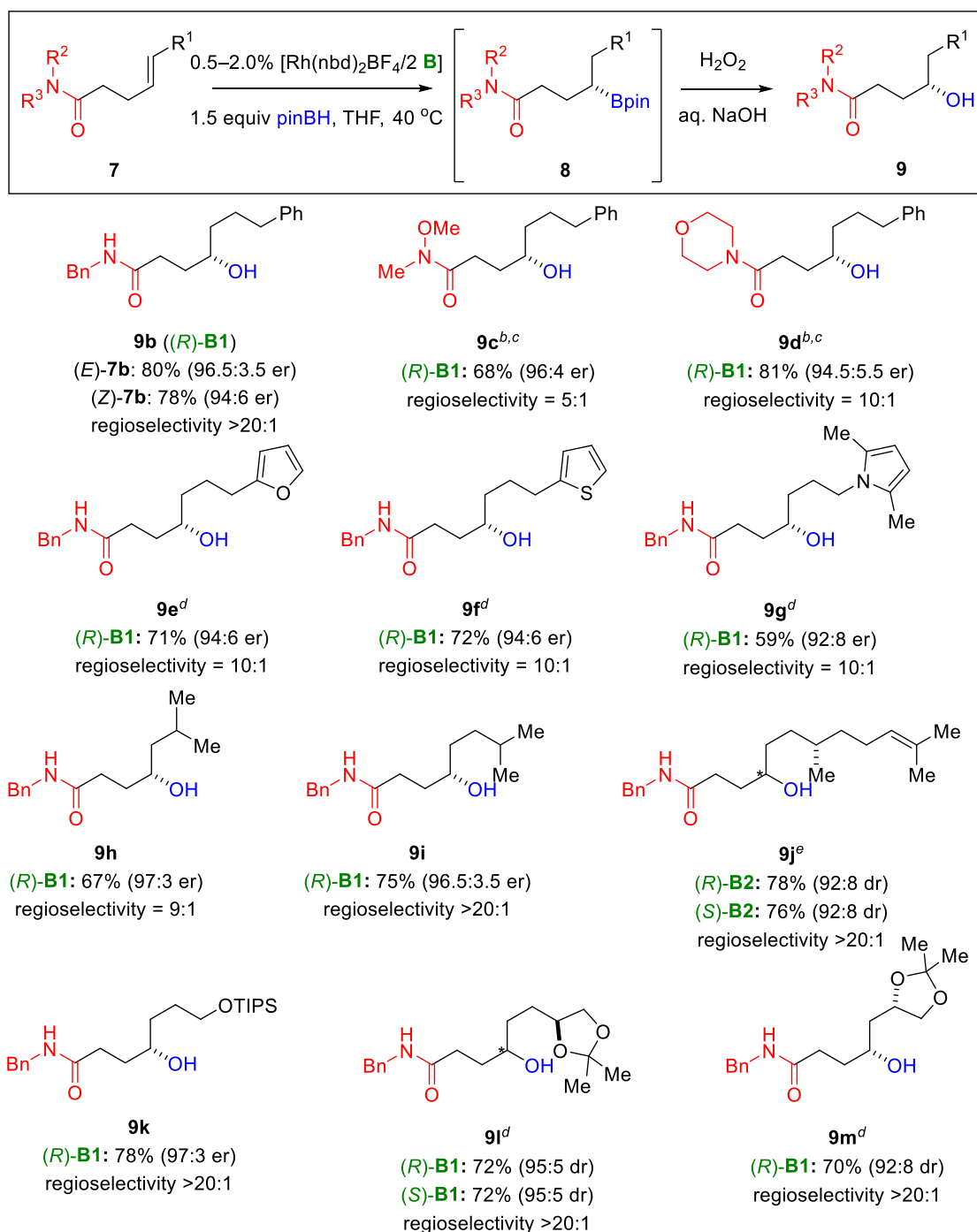


**Figure 7.** Substrate scope for CAHB of  $\gamma,\delta$ -unsaturated amides.

<sup>a</sup> Unless otherwise noted all reaction use 0.5%  $[\text{Rh}(\text{nbd})_2\text{BF}_4/2 \text{ B1}]$ , 1.5 equiv.  $\text{pinBH}$ , THF, 40 °C (12 h) followed by oxidation using  $\text{H}_2\text{O}_2/\text{aq. NaOH}$ . Unless otherwise noted, the isolated yield is that of the major regioisomer and reflects the average of three experiments generally exhibiting a spread of 2%; regioselectivity is determined from the crude  $^1\text{H}$  NMR of **9**. Enantiomer ratios (er) are determined by chiral HPLC analysis; diastereomer ratios (dr) are determined for the purified mixture of diastereomers by integrating major and minor  $^{13}\text{C}$  NMR resonances. <sup>b</sup> 2.0%  $[\text{Rh}(\text{nbd})_2\text{BF}_4/2 \text{ B1}]$ . <sup>c</sup> Oxidation conditions:  $\text{NaBO}_3/\text{H}_2\text{O}$ . <sup>d</sup> 1.0%  $[\text{Rh}(\text{nbd})_2\text{BF}_4/2 \text{ B1}]$ . <sup>e</sup> 1.0%  $[\text{Rh}(\text{nbd})_2\text{BF}_4/2 \text{ B2}]$ .

Despite the generality of the catalyst system to the broad range of substrates shown in Figure 7, there are still some limitations found in the current study (Figure 8). For example, substrate **7m**, which is similar to substrate **7l** in bearing chiral acetal moiety, but one which is in closer proximity to the site of hydroboration, shows a strong matched/mismatched effect. While the matched case using (*R*)-**B1** affords (*R,S*)-**7m** (70%, 92:8 dr) as shown in Figure 5, the catalyst employing (*S*)-**B1** gives rise to a complex mixture of regioisomers **10**. A substrate in which vinyl substituent is small (e.g., **7n**, R = Me) exhibits only modest regioselectivity (3:1) even though CAHB proceeds in good yield and high enantioselectivity (61%, 90% ee). Recall that ester functionality is found to be good directing group in  $\gamma$ -borylation of geminal  $\beta,\gamma$ -unsaturated carbonyl derivatives (section 2.1). However, attempted  $\gamma$ -borylation of  $\gamma,\delta$ -unsaturated ester **11** yields only trace amounts of borylated product; in this example, there is evidence for alkene isomerization.<sup>10</sup>

In spite of successful CAHB of  $\gamma,\delta$ -unsaturated amides, our attempts to carry out CAHB for a one carbon homologue  $\delta,\varepsilon$ -unsaturated amide **12** was less efficient and less regioselective under the standard conditions. In individual reactions, CAHB of **12** required 2% catalyst loading for complete consumption of starting material (56%, 1.5:1 regioselectivity), whereas 0.5% is sufficient in the case of **7b**. However, the direct competition of **12** and **7b** for limiting pinBH (1:1:1 proportions of each) affords only a modest excess of recovered **12** (74% recovered) relative to recovered **7b** (61% recovered). The results suggest that **7b** is consumed only slightly faster than **12** by active catalyst. A relatively slow conversion of rhodium precatalyst to active catalyst by **12** in the absence of **7b** could account of the conflicting observations.

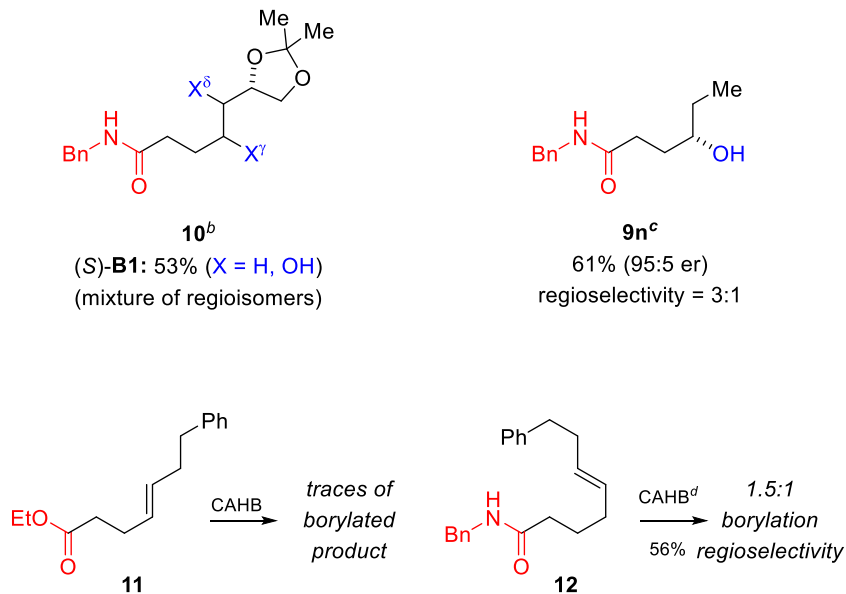


**Figure 8.** Current limitations of CAHB of  $\gamma,\delta$ -unsaturated amides.

<sup>a</sup> Standard conditions as shown in Figure 5. <sup>b</sup> 1.0% [Rh(*nbd*)<sub>2</sub>BF<sub>4</sub>/2 **B1**]. <sup>c</sup> *er* is determined by <sup>19</sup>F NMR of the corresponding Mosher ester. <sup>d</sup> 2.0% [Rh(*nbd*)<sub>2</sub>BF<sub>4</sub>/2 (*R*)-**B1**].

In order to prove the absolute configuration of the  $\gamma$ -borylation products derived from  $\gamma,\delta$ -unsaturated amides,  $\gamma$ -borylated Weinreb amide **7c** was treated with H<sub>2</sub>O<sub>2</sub>/aq. NaOH to afford the enantiomer of the known chiral 5-substituted- $\gamma$ -lactone (*R*)-**13** (Figure 9).<sup>11</sup> The opposite sign of optical rotation showed that CAHB products have the (*S*)-configuration. To further confirm the assignment, (*S*)-**13** and **9d** were converted to **9b**, both products exhibiting the same order of elution by chiral HPLC.

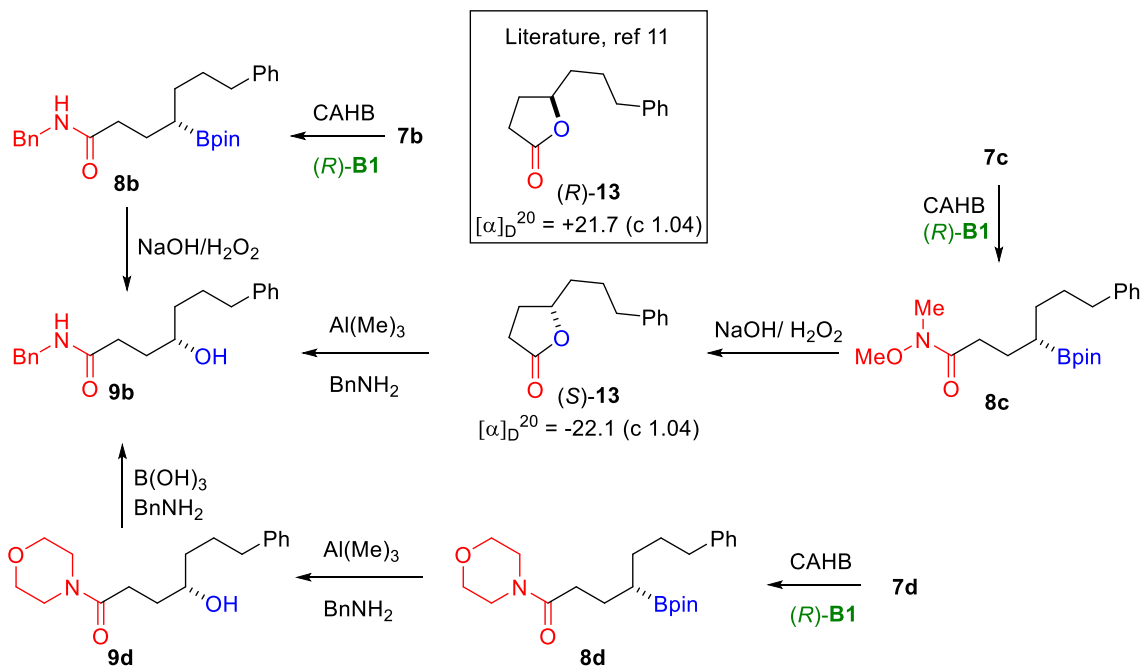


**Figure 9.** Proof of absolute configuration of alcohols **9b–d** via comparing optical rotation with known lactone  $(R)$ -**13**.

In addition to the chemical correlation and comparison of optical rotation depicted in Figure 9, Mosher's ester analysis provides additional evidence for the absolute configuration. Figure 10 illustrates the  $^1\text{H}$  NMR regions of NH and methyl groups of Mosher's ester **14**, prepared from **7n** (obtained from CAHB of **7n** with  $(R)$ -**B1**) and  $(S)$ -Mosher acid, respectively). From the figures, the major NH is more downfield, whereas, the major methyl group is more upfield. According to Feng Shao's<sup>12</sup> protocol for determination of absolute configuration using Mosher's ester analysis, the NH is on the same side of the methoxy group and the methyl group is on the opposite side of the methoxy group resulting in  $S,S$ -configuration of **14**. The method might not be reliable for determining absolute configuration of **9n** by itself since both NH and methyl groups are quite far away from the Mosher ester chiral center. However, the result is consistent with correlation to the known lactone  $(R)$ -**13** as described above.

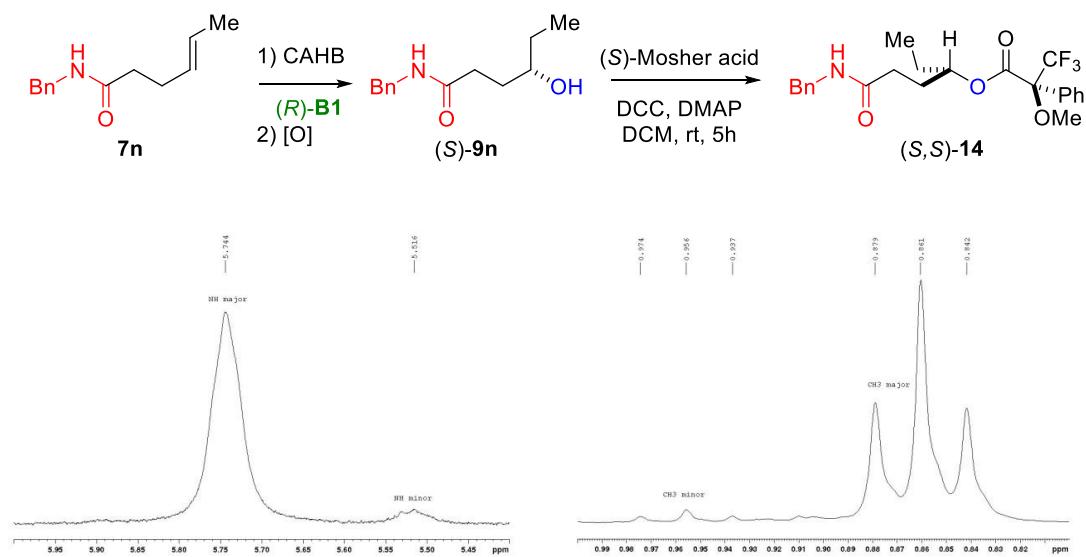


**Figure 10.** Additional evidence for the absolute configuration of (S)-9n via <sup>1</sup>H NMR analysis of Mosher's ester (S,S)-14.

### 2.3 Enantioselective $\delta$ -borylation of $\gamma,\delta$ -unsaturated carbonyl derivatives

In contrast to the results described above,  $\gamma,\delta$ -unsaturated amides bearing aryl substituents (i.e., vinyl arene substrates) behave much differently. For example, substrate **15a** (R = Ph) (Figure 11) gives predominantly opposite regioisomer (i.e.,  $\delta$ -selective borylation) to generate chiral benzylic boronic esters and the corresponding benzylic alcohols (**16a**) after oxidation. In addition, the borane adds to the opposite face of the alkene, that is, to the top face of the alkene (as illustrated in Figure 11) as opposed to the previous study of **7**.

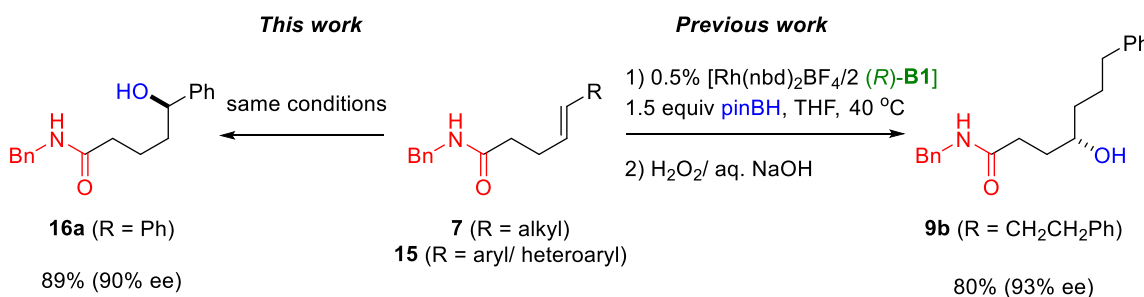
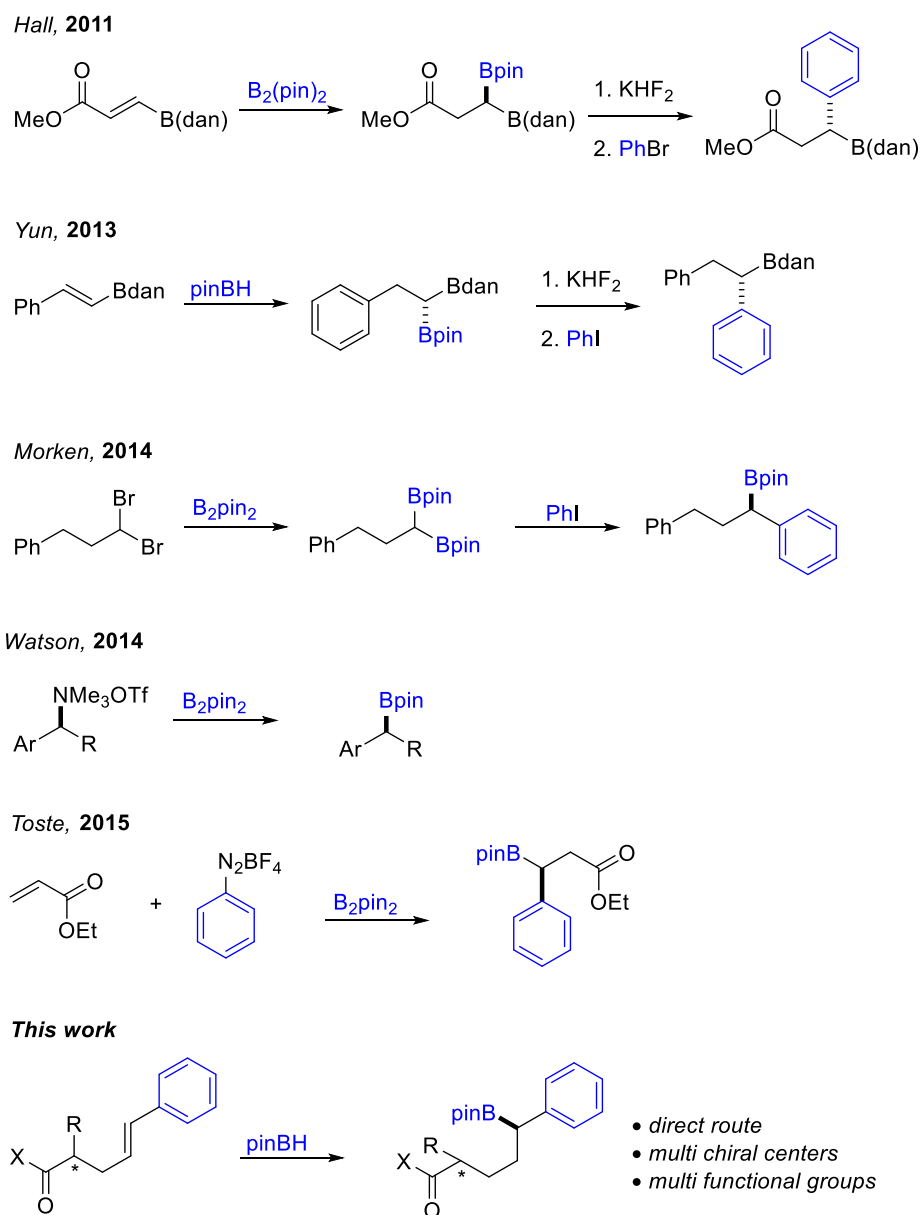


**Figure 11.** Effect of vinyl substituents on regioselectivity and  $\pi$ -facial selectivity of CAHB of  $\gamma,\delta$ -unsaturated amides.

Benzylic boronic esters are attractive building blocks for complex biologically active natural products and pharmaceuticals,<sup>13</sup> and consequently have been the focus of a variety of synthetic methods. Besides conventional methods such as asymmetric hydroboration of vinyl arenes,<sup>14–19</sup> enantioselective allylic borylation,<sup>20</sup> enantioselective conjugate borylation,<sup>21</sup> and asymmetric hydrogenation of vinyl boronates,<sup>22</sup> there has been significant interest in developing new enantioselective methods for their preparations. Scheme 1 shows several recent methodologies. Hall,<sup>23</sup> Yun,<sup>24</sup> and Morken<sup>25</sup> independently reported group selective cross-coupling of diborane. While Hall’s and Yun’s work exploit stereoretentive Pd-catalyzed cross-coupling of chiral diboranes,



Morcken's approach uses enantiotopic group-selective cross-coupling using a chiral palladium catalyst. Watson constructed the targeted derivatives via stereospecific Miyaura borylation of a chiral ammonium salt precursor.<sup>26</sup> Toste and co-workers developed a new strategy for a three component coupling using alpha-olefins,



**Scheme 1.** Recent methodologies for the preparations of chiral benzylic boronic esters.

aryldiazonium salts, and bis(pinacolato)diboron; the enantioselective is controlled by a cooperative chiral anion phase transfer catalyst and a palladium catalyst.<sup>27</sup> Though the CAHB of vinyl arenes has long been known,<sup>14-19</sup> high levels of enantioselectivity are often limited to simple sterene (i.e., vinyl arene) derivatives. This work introduced similar approach resulting in bifunctional chiral benzylic boronic esters bearing multi-chiral centers in some cases (*vide infra*).

Synthesizing the appropriate substrate(s) is always a potential challenge for every project. For example, benzyl amide substrates bearing alkyl (e.g., **7b**) and aryl (e.g., **15a**) are prepared in overall good yield by the six-step synthetic routes depicted in Figure 12. However, several of the steps are overnight reactions and the time-consuming route reduces its practicality.

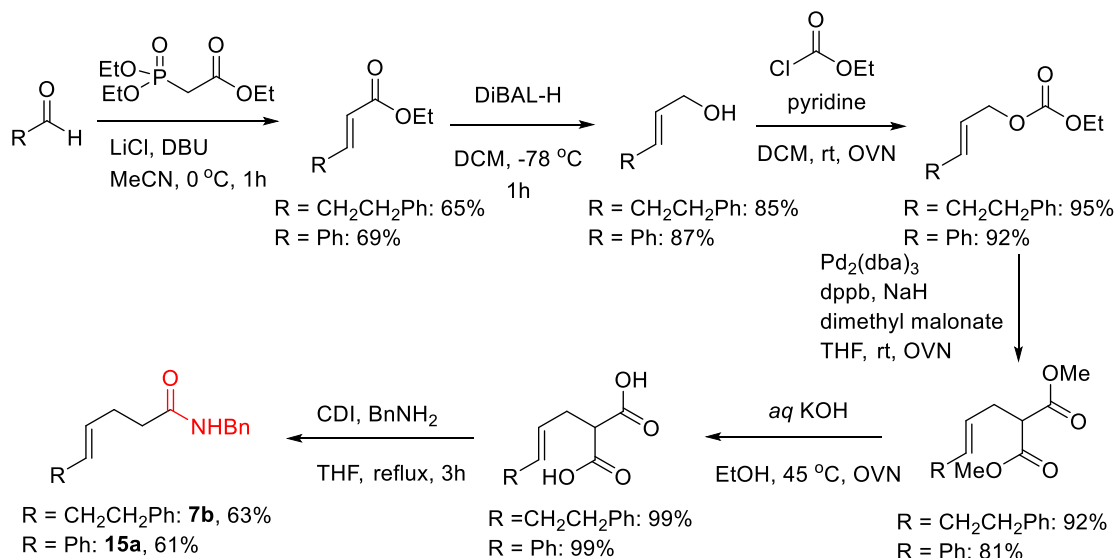
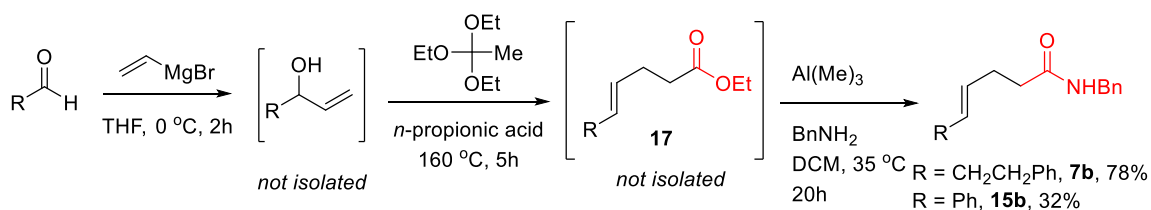


**Figure 12.** Six-step synthetic routes for  $\gamma,\delta$ -unsaturated amides

We sought a shorter synthetic strategy and found that Claisen-Johnson rearrangement methodology worked well for the alkyl-substituted substrates such as **7b** (Figure 13). However, when the same method was applied for aryl-substituted substrates

(e.g., **15a**), the benzylic alcohol intermediate, formed upon addition of the vinyl Grignard, suffered from competing pathways; a low yield of the desired  $\gamma,\delta$ -unsaturated ethyl ester **17** was obtained after the Claisen-Johnson rearrangement. Though the ethyl ester intermediate was reported as to be formed in good yield by this route,<sup>28</sup> we always see a nearly 1:1 mixture with allylic alcohol **18** obtained via the competitive pathway proposed in Figure 11. In our hands, similar results were found for other benzylic aldehyde derivatives.



Possible mechanism for potential problem when R = Ph in Claisen-Johnson rearrangement

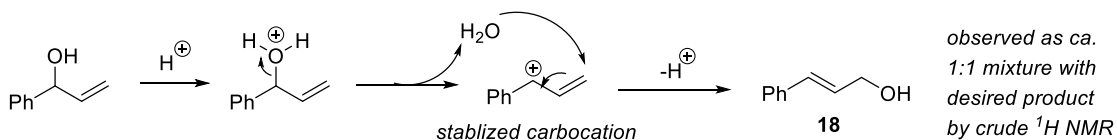


**Figure 13.** Preparation of  $\gamma,\delta$ -unsaturated amides via Claisen-Johnson rearrangement and the potential problem with benzylic alcohol derivatives

Several other routes, including ones involving Heck reaction and Claisen-Ireland rearrangements, were explored.<sup>29</sup> Ultimately, we found that Julia olefination<sup>29</sup> worked best in our hands. The modified Julia reagent (Figure 14) was easily prepared and used as the common intermediate to afford the desired  $\gamma,\delta$ -unsaturated amides **15** in just two extra steps.

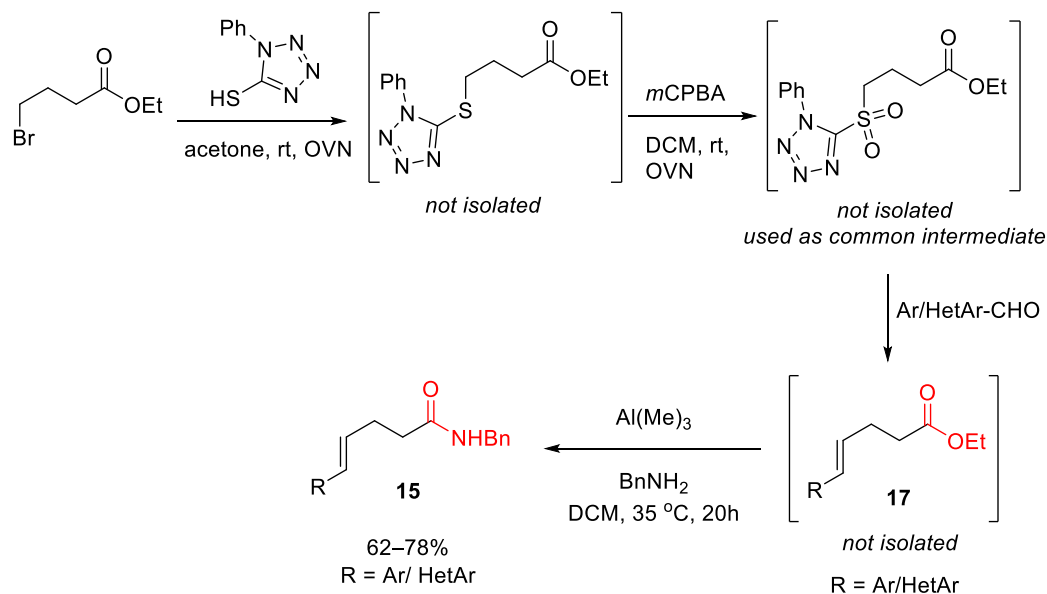


**Figure 14.** Preparation of aryl/ heteroaryl substituted  $\gamma,\delta$ -unsaturated amides **15** via Julia-typed olefination.

As mentioned above, CAHB of **15a** (at the time unexpectedly) affords the benzylic alcohol **16a** after oxidation. Does the strong electronic effect of the vinyl arene moiety simply override the directing group effect? We tested the several potential directing-groups to probe this question (Figure 15). Non-coordinating functional group silyl ether **15b** and weak coordinating functional group ester **15c** undergo CAHB standard conditions in high regioselectivity (>20:1) and yield (75–77%) suggesting that the potential directing group plays no role. However, the level of enantioselectivity is reduced, ranging from 85:15 to 90:10 er. *N*-Benzyl amide **15a**, another secondary amide **15d** (i.e., *N*-phenyl) and tertiary amide **15e** (i.e., morpholine) are all good substrates; the latter two afford  $\delta$ -borylated products **19d** (76%, 94:6 er) and **19e** (78%, 95.5:4.5 er), respectively. While the ratios change only mostly in terms of the percentages of the minor enantiomer formed, those changes are energetically significant when expressed as the difference in free energy between competing diastereotopic transition states.<sup>30</sup>

In addition to probing the effect of varying the directing group, we asked whether the one carbon homologue **15f** (i.e., the substrate in which the alkene is further remote to the amide directing group) behaved in the same manner under the standard conditions. Substrate **15f** once again predominate the benzylic selective affording  $\epsilon$ -borylated product **19f** in high yield (78%), regioselectivity (>20:1) with somewhat lower enantioselectivity (90.5:9.5 er). The results suggest that the electronic effect of the aryl substituent is stronger than the directing group effect in determining regioselectivity, however, the coordination to the directing group still may play an important role in the mechanism to explain the higher enantioselectivity that is observed for stronger coordinating functional groups (i.e., amides *versus* ester and OTIPS;  $\gamma,\delta$ -amide *versus*  $\delta,\epsilon$ -amide).

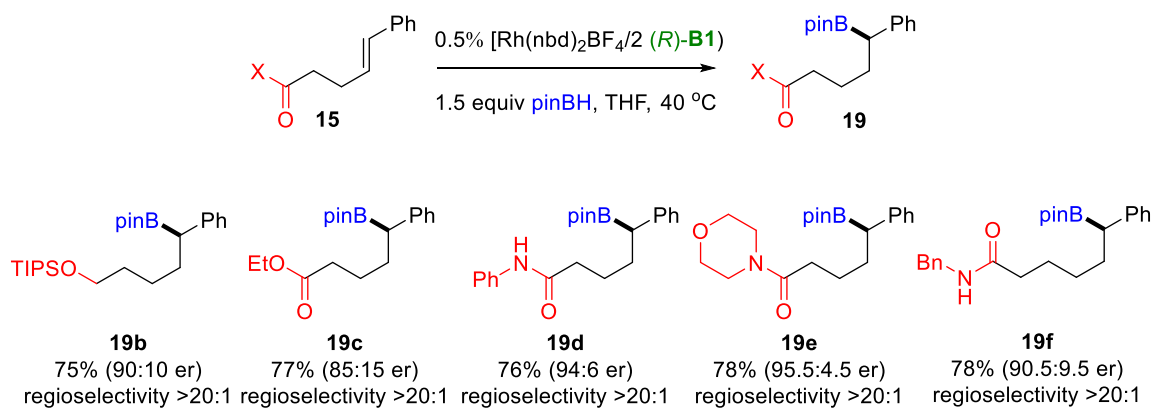
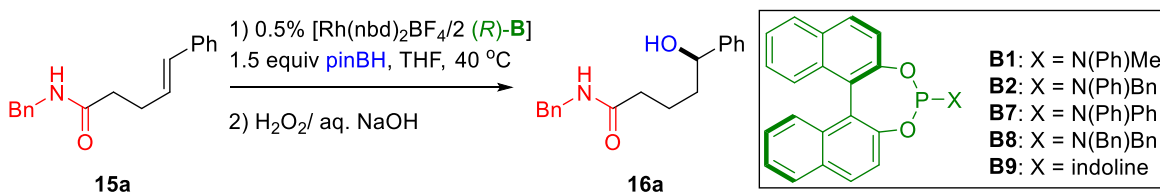


**Figure 15.** Directing group and coordinating distance effects on  $\delta$ -borylation of  $\gamma,\delta$ -unsaturated carbonyl derivatives

To probe why the *N*-aryl phosphoramidite ligands are efficient ligands for CAHB under the conditions employed, we carried out a brief survey of BINOL-derived phosphoramidites **B1–2** and **B7–9** for substrate **15a** (Table 2). The results indicate that the *N*-aryl moiety is needed for good conversion (entries 1–4, **B1**, **2**, and **7**). It is also

worth noting that a 1:1 Rh:L ratio (entry 2) is also efficient using **B1**. However, the level of enantioselectivity is little lower (94:6 vs. 95:5 er), and the yield drops from 89% to 81% reflecting the formation of more reduced product. Thus, we propose that the 1:1 Rh:L is essential to form the active catalyst, but additional ligand slows other competing pathways and enhances the enantioselectivity. Ligands **B1–2** with one *N*-phenyl substituent are among the best ligands found thus far. These afford the desired product **16a** in high yield and enantioselectivity (87–89%, 95:5 er). Ligand **B7** with an *N,N*-diphenyl substituent also afford **16a** in good yield (87%) and regioselectivity (>20:1) but with a lower er in this case (85:15). For a few other substrates, **B7** proves more optimal (*vide infra*). Ligands **B8**, which lacks an *N*-aryl substituent, and **B9**, which bear in indoline substituent, are not as effective resulting; we find lower conversion (50–80%), lower mode selectivity and lower regioselectivity (<4:1) (entries 5 and 6).

**Table 2.** Brief survey of ligand effect on CAHB of **15a**<sup>a</sup>



entry	ligand	conv (%)	rr	yield (%)	er
1	<b>B1</b>	100	>20:1	89	95:5
2 <sup>b</sup>	<b>B1</b>	100	>20:1	81	94:6
3	<b>B2</b>	100	>20:1	87	95:5
4	<b>B7</b>	100	>20:1	87	85:15
5	<b>B8</b>	50	3.5:1	18	—
6	<b>B9</b>	80	3:1	28	—

<sup>a</sup> Standard conditions. <sup>b</sup> 1:1 Rh:L was used.

The studies described above lead us to conclude that (i) regioselectivity is largely controlled by the aryl electronic effect, (ii) enantioselectivity is enhanced by the directing

group coordination effect, (iii) 1:1 Rh:L ratio is essential for the formation of the active catalyst, and (iv) the *N*-aryl scaffold is crucial for high reactivity and selectivity. Based on these conclusions, we propose as a working model the catalytic cycle illustrated in Figure 16. First, the Rh(I)-catalyst used in our CAHB is proposed to undergo concerted metalation/deprotonation (CMD) with the *N*-aryl of BINOL-derived phosphoramidite to generate the active catalyst species **A** and release HBF<sub>4</sub> to begin the catalytic cycle. Notably, *N*-aryl BINOL-derived phosphoramidite acts like a bidentate though it is designed for a monodentate ligand. After alkene **15a** chelation to form intermediate **B**,

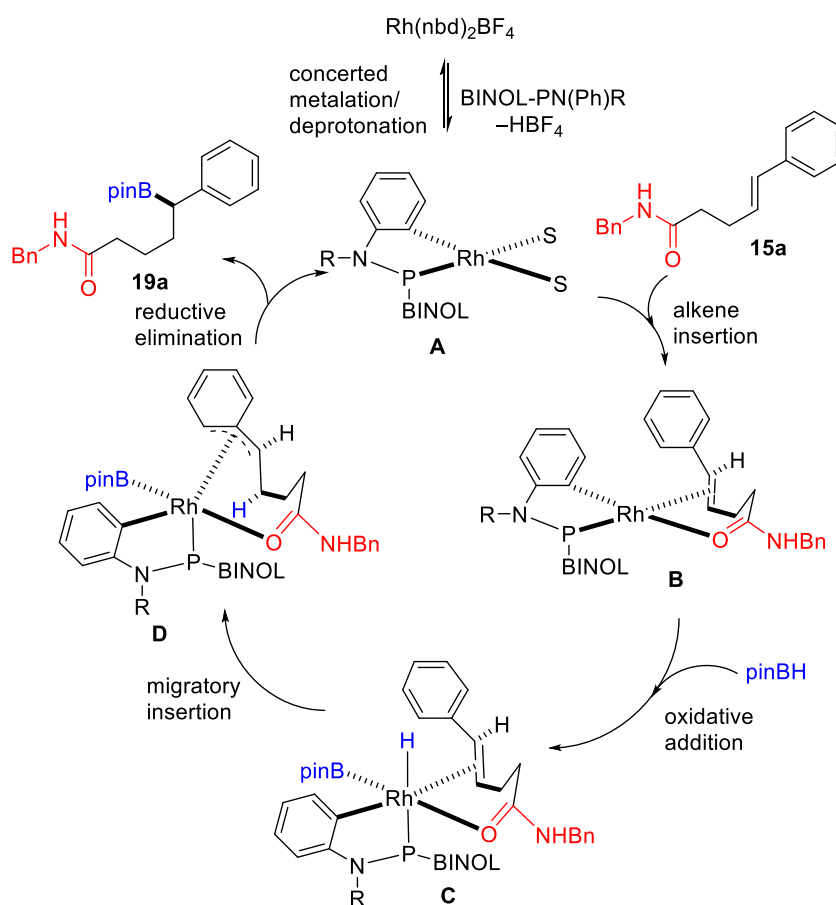


**Figure 16.** Proposed catalytic cycle for CAHB of **15a** using *N*-aryl ligand scaffold involving Rh(I)-catalyzed concerted-metalation-deprotonation

oxidative addition of pinacolborane (pinBH) affords Rh(III) octahedral species **C**. Since the regioselectivity is controlled by the aryl alkene substituent, migratory insertion of Rh–H would generate intermediate **D** following by reductive elimination to form the desired borylated product **19a** and regenerate the active catalyst **A**.

It should be addressed that rhodium(I) has been used in many C–H activation reactions; however, all of them are suggested to undergo oxidative addition to form Rh(III)–H intermediate or coordination facilitated by deprotonation with an adjacent basic nitrogen.<sup>31</sup> There is no precedent in literature on concerted metalation/deprotonation (CMD) for Rh(I); the proposed mechanism, which needs further study to be confirmed, could lead to another thoughtful and innovative project. Alternatively, Rh(III), the well-known metal precursor used in CMD,<sup>31</sup> can be generated in the presence of pinBH prior to CMD step (Figure 17).



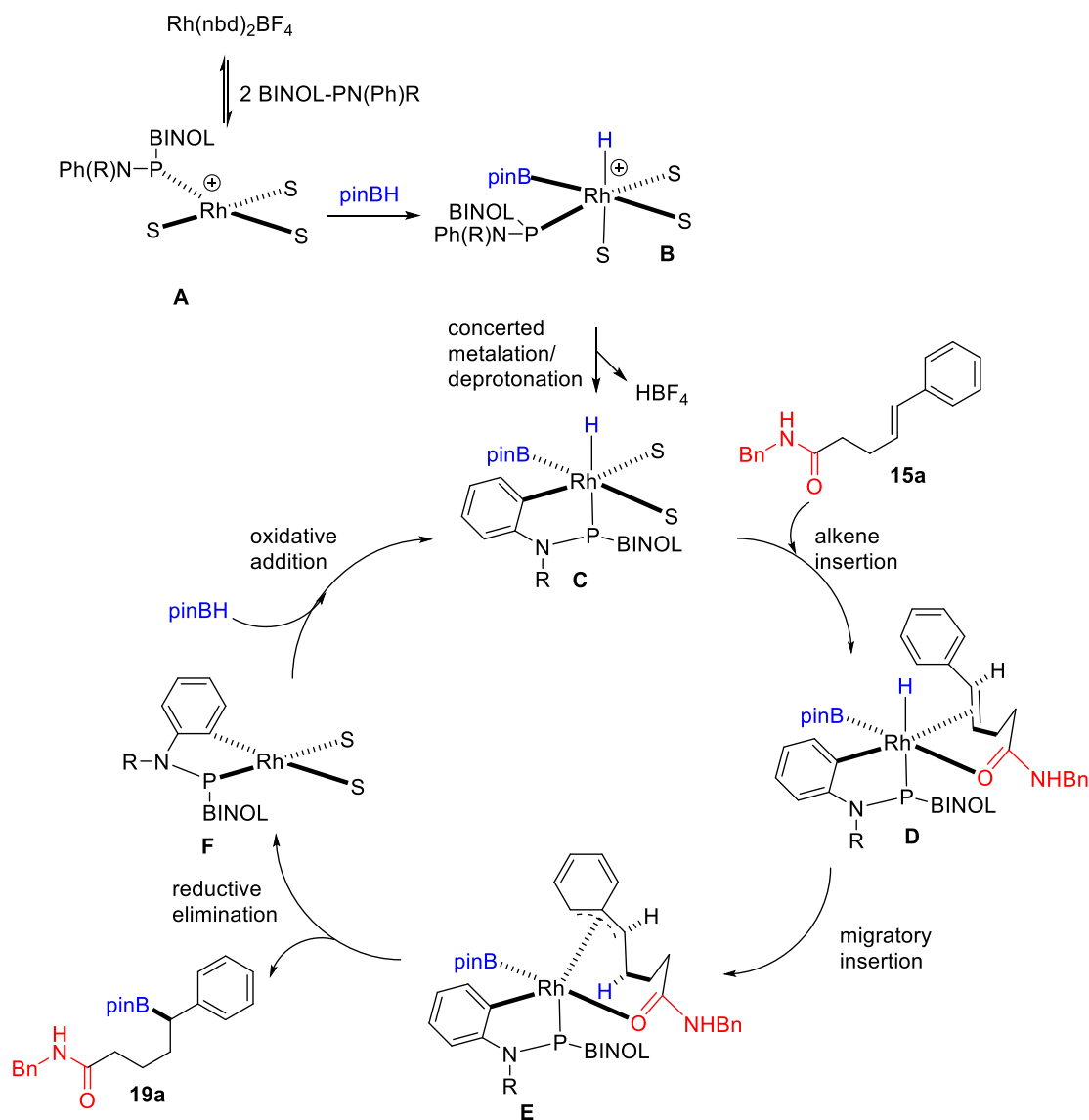


**Figure 17.** Proposed catalytic cycle for CAHB of **15a** using *N*-aryl ligand scaffold involving Rh(III)-catalyzed concerted-metalation-deprotonation

To further probe the generality of the reaction, a series of  $\gamma,\delta$ -unsaturated benzyl amides **15g–t** was prepared and evaluated in CAHB using ligands **B1–2** and **B7** (Figure 18). Although with *N,N*-diphenyl ligand **B7** gives lower ee for substrate **15a**, it gives the highest levels of enantioselectivity for several substrates. For example, substrate **15g**, which bears a 4- $\text{CF}_3$ -Ph substituent, undergoes CAHB with **B7** to afford  $\delta$ -borylated

product **19g** in high yield and enantioselectivity (78%, 95:5 er); **B1** and **B2** give comparable yields but only 91:9 and 90:10 er, respectively. Other substrates bearing different electron withdrawing groups at *para* position (i.e., **15h–i**) also well tolerated under standard conditions affording **19h–i** in high yield and enantioselectivity (75–77%, 95:5 er). In particular, **19i** bearing a 4-chlorophenyl substituent, could in principle be used in subsequent cross-coupling if desired. Substrates with alkoxy substituents at *meta*- and *para*-positions of the aryl ring (e.g., **15j–k**) also undergo efficient CAHB (72–79%, 96:4–97:3 er). However, when the methoxy group is appended to the *ortho*-position (e.g., **15l**), only moderate enantioselectivity (85.5:14.5 er) was obtained; nonetheless CAHB proceeds in good yield (82%) and high regioselectivity (>20:1). Substrate **15m**, another *ortho*-substituted aryl derivative is a good substrate affording **19m** in good yield and enantioselectivity (84%, 93:7 er). A series of heteroaromatic substituted substrates **15n–q** also undergo CAHB efficiently, although sluggishly; three equivalents of borane are needed for complete conversion in 12 hours (69–73%, 92:8–97:3 er).

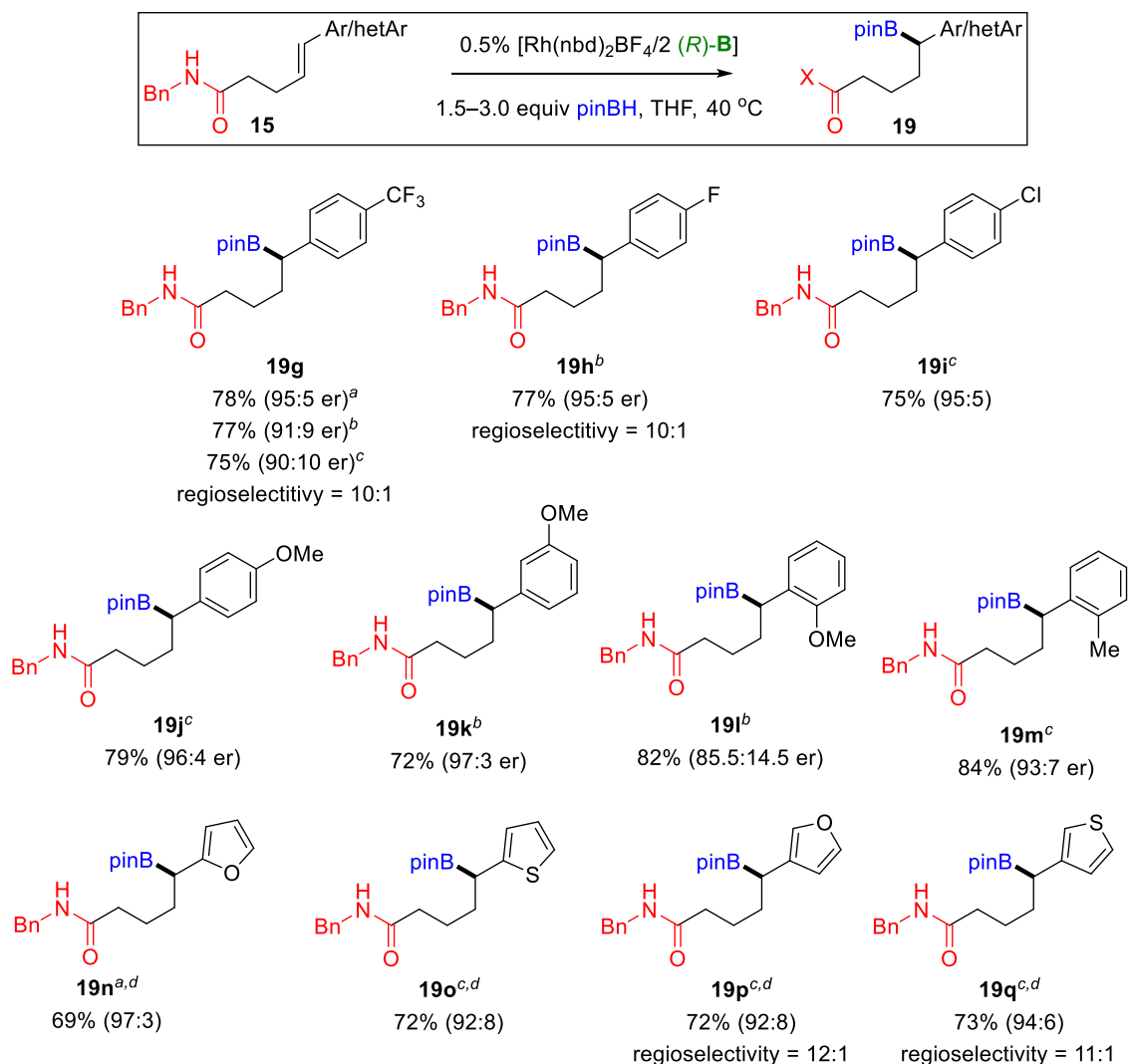
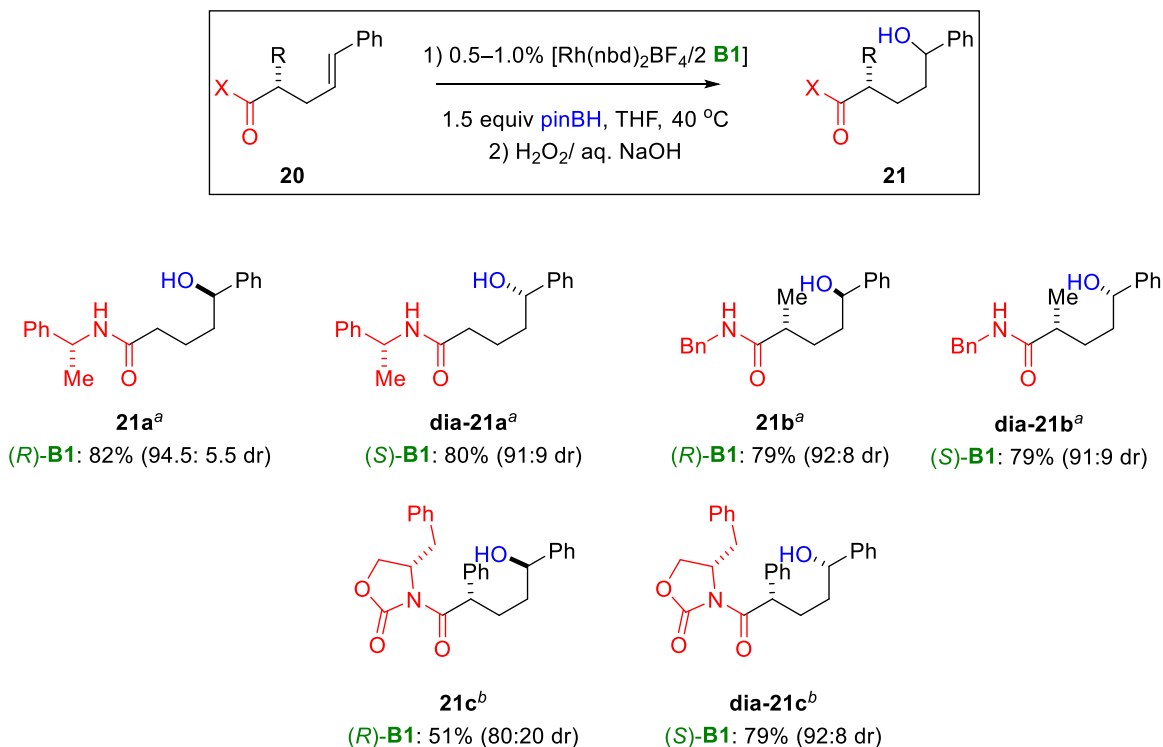


**Figure 18.** Substrate scope for CAHB of aryl/ heteroaryl substituted  $\gamma,\delta$ -unsaturated amides.

Unless otherwise noted all reaction use 0.5%  $[Rh(nbd)_2BF_4/2 \text{ B}]$ , 1.5 equiv.  $pinBH$ , THF, 40 °C (12 h). Unless otherwise noted, the isolated yield is that of the major regioisomer and reflects the average of three experiments generally exhibiting a spread of 2%; regioselectivity is determined from the crude  $^1H$  NMR of **19** and is greater than 20:1 unless otherwise noted. Enantiomer ratios (er) are determined by  $^{19}F$  NMR of the corresponding Mosher's ester. <sup>a</sup> **B7** was used. <sup>b</sup> **B1** was used. <sup>c</sup> **B2** was used. <sup>d</sup> 3.0 equiv  $pinBH$  was used.

We examined several variations of chiral substrates in the vinyl arene series (Figure 19). Substrate **20a** bearing a chiral *N*-phenethyl amide undergoes CAHB with largely catalyst control; CAHB/ oxidation with (*R*)-**B1** affords **21a** in comparable yield (82%) and enantioselectivity (94.5:5.5 dr) with the parent substrate **15a**; (*S*)-**B1** generates

the diastereomer **dia-21a** in similar yield but with a somewhat diminished diastereomer ratio (80%, 91:9 dr). Benzyl amide substrate with chiral  $\alpha$ -methylated center also undergoes catalyst controlled  $\delta$ -borylation yielding two diastereomers **21b** and **dia-21b** in the same results (79%, 91:9–92:8 dr). We found it interesting that Evans' chiral auxiliary-containing **20c** is also good substrate, albeit exhibiting a stronger matched/mismatched effect. While (*R*)-**B1** generates **dia-21c** with high yield and dr (79%, 92:8 dr), the mismatched ligand (*S*)-**B1** gives **21c** in much lower selectivity (51%, 80:20 dr). The origin of the matched/mismatched response is not yet clear; it could be predominantly influenced by either the chiral auxiliary or the relatively sterically demanding  $\alpha$ -phenyl substituent. CAHB of **20d** and **20e** will be obtained shortly to address the issue. In addition, substrates bearing chiral centers at both  $\alpha$ - and  $\beta$ -positions are also worth exploring. These proposed substrates could be made via Evans' chiral auxiliary enolate alkylation<sup>32</sup>/aldolization.<sup>33</sup>



Potential substrates for future outlook:

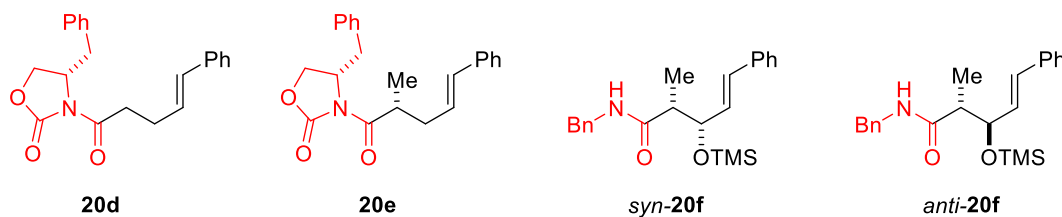


**Figure 19.** CAHB of pre-installed  $\alpha$ -chiral center aryl substituted  $\gamma,\delta$ -unsaturated amides.

Unless otherwise noted all reaction use  $[Rh(nbd)2BF4/2 \mathbf{B1}]$ , 1.5 equiv. *pinBH*, THF, 40 °C (12 h) followed by oxidation using  $H_2O_2/aq$  NaOH ( $NaBO_3$  for **20c**). Unless otherwise noted, the isolated yield is that of the major regioisomer and reflects the average of two experiments generally exhibiting a spread of 2%; regioselectivity is determined from the crude  $^1H$  NMR of **21** and is greater than 20:1 unless otherwise noted. Diastereomer ratios (*dr*) are determined for the purified mixture of diastereomers by integrating major and minor  $^1H$  or  $^{13}C$  NMR resonances. <sup>a</sup> 0.5%  $[Rh(nbd)2BF4/2 \mathbf{B1}]$ . <sup>b</sup> 1.0%  $[Rh(nbd)2BF4/2 \mathbf{B1}]$ .

The absolute configuration of  $\delta$ -borylation of  $\gamma,\delta$ -unsaturated amides was obtained via  $^1H$  NMR analysis of Mosher's ester **22e**; the latter is synthesized from the morpholine amide substrate **15e** via CAHB/ oxidation and DCC condensation with (*S*)-Mosher acid (Figure 20). The secondary benzylic Mosher's ester (e.g., **22e**) is deemed a

trustworthy source for determining absolute configurations. According to Feng Shao's<sup>12</sup> and co-workers, the major benzylic methyne proton is more downfield, it is on the same side of the methoxy group and on the opposite side of the phenyl group resulting in *R,S*-configuration of **22e** and thus *R*-configuration of **16e**.

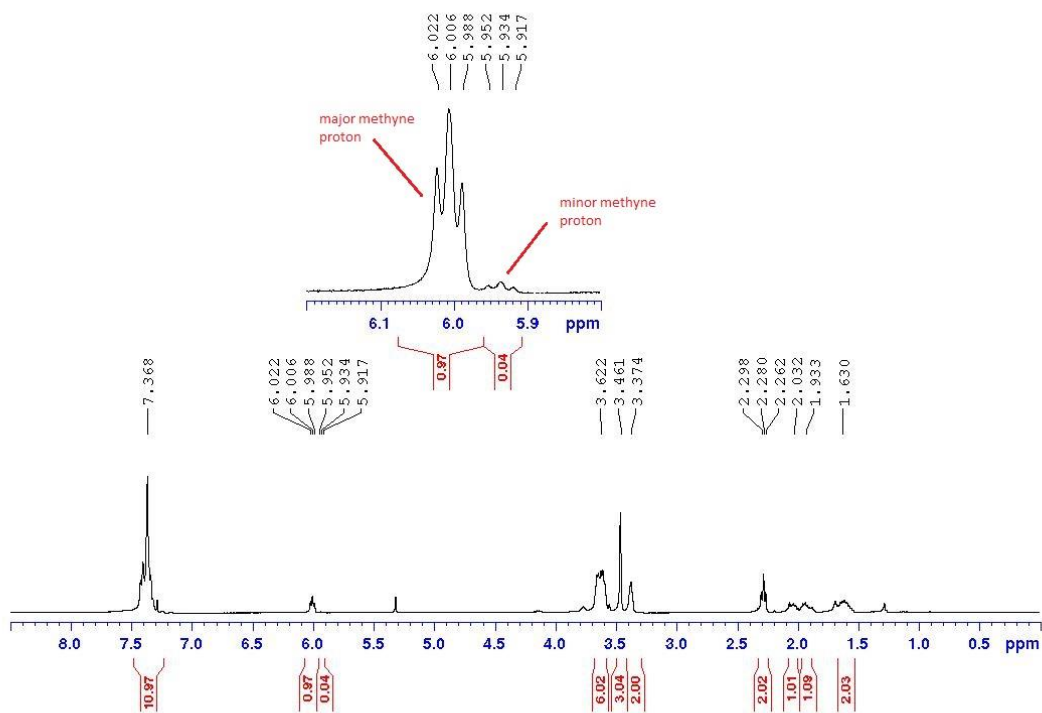
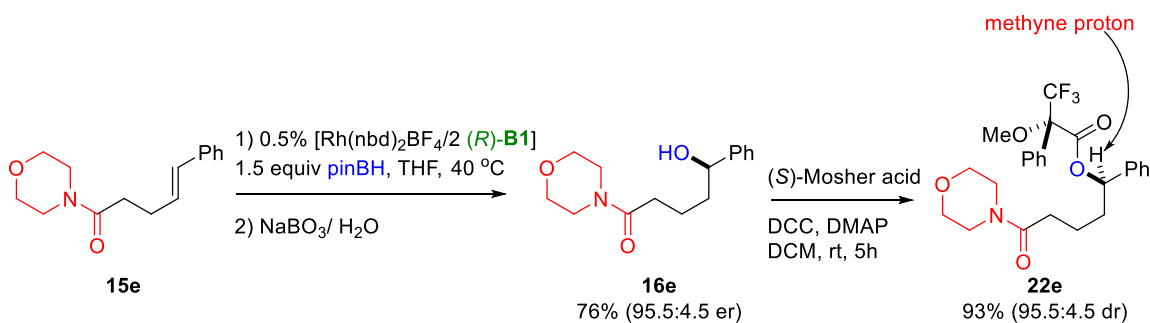


**Figure 20.** Determination of absolute configuration of CAHB of **15e** via <sup>1</sup>H NMR analysis of Mosher's ester **22e**

## 2.4 Concluding remarks

In summary, CAHBs of  $\beta,\gamma$ - and  $\gamma,\delta$ -unsaturated carbonyl derivatives provide a novel direct route to acyclic  $\gamma$ - and  $\delta$ -borylated carbonyl compounds highlighting the innovation of the dissertation. In particular, the methodology has opened a door to the more challenging substrates with further coordinating distance as compared to the previous studies. In addition, the electronic effect of the aryl substituents has proven to be overridden the carbonyl coordinating effect; however, the choice of a suitable directing group is still crucial to achieve high level of enantioinduction. The significances of these versatile intermediates will be emphasized via mono- and bifunctionalizations in Chapter four.

Not only the well-defined directing group, but also a suitable catalyst system as well as a choice of borane reagent are highly responsible for the current success. While *tmdBH* is better than *pinBH* for  $\beta,\gamma$ -substrates, it is essentially not reactive and selectivity for  $\gamma,\delta$ -systems; *pinBH*, on the other hand, are quite effective for the longer coordinating distance. Moreover, ligands also have crucial role in order to obtain high enantioselectivity; TADDOL-derived phosphite (i.e., **T1**) is the best choice for 1,1-disubstituted alkenes (i.e., methyldene substrates), whereas BINOL-derived phosphoramidites (i.e., **B1**, **B2**, and **B7**) give best performance for 1,2-disubstituted alkenes. Interestingly, in this study, we also find that *N*-aryl moiety of the **B** ligand family is required for good conversion perhaps due to the possibility for concerted metalation/deprotonation.

In some cases of pre-installed chiral substrates, the system is found to be essentially catalyst controlled in most cases to achieve both diastereomers in good yield

and high diastereoselectivity. In addition, substrate bearing two different alkene environments undergoes completely group-selective in which only the alkene proximal to the directing group gets hydroborated. Though not being mentioned in this thesis, CAHB of other sub-classes of alkenes (i.e., 1,2,2- and 1,1,2-trisubstituted alkenes) should be of interest to the scientific community.



## 2.5 References

- [1] Smith, S. M.; Hoang, G. L.; Pal, R.; Khaled, M. O. B.; Pelter, L. S. W.; Zeng, X. C.; Takacs, J. M., “ $\gamma$ -Selective Directed Catalytic Asymmetric Hydroboration of 1,1-Disubstituted Alkenes,” *Chem. Commun.*, **2012**, 48, 12180–12182.
- [2] (a) Jiang, Q.; Guo, T.; Yu, Z., “Copper-Catalyzed Asymmetric Borylation: Construction of a Stereogenic Carbon Center Bearing Both  $\text{CF}_3$  and Organoboron Functional Group,” *J. Org. Chem.*, **2017**, 82, 1951–1960; (b) Jarava-Barrera, C.; Parra, A.; López, A.; Cruz-Acosta, F.; Collado-Sanz, D.; Cárdenas, D. J.; Tortosa, M., “Copper-Catalyzed Borylative Aromatization of *p*-Quinone Methides: Enantioselective Synthesis of Dibenzyl Boronates,” *ACS Catal.*, **2016**, 6, 442–446; (c) Xie, J.-B.; Lin, S.; Qiao, S.; Li, G., “Asymmetric Catalytic Enantio- and Diastereoselective Boron Conjugate Addition Reactions of  $\alpha$ -Functionalized  $\alpha,\beta$ -Unsaturated Carbonyl Substrates,” *Org. Lett.*, **2016**, 18, 3926–3929; (d) Wu, H.; Garcia, J. M.; Haeffner, F.; Radomkit, S.; Zhugralin, A. R.; Hoveyda, A. H., “Mechanism of NHC-Catalyzed Conjugate Additions of Diboron and Bososilane Reagents to  $\alpha,\beta$ -Unsaturated Carbonyl Compounds,” *J. Am. Chem. Soc.*, **2015**, 137, 10585–10602; (e) Niu, Z.; Chen, J.; Chen, Z.; Ma, M.; Song, C.; Ma, Y., “Application of Bidentate Oxazoline–Carbene Ligands with Planar and Central Chirality in Asymmetric  $\beta$ -Boration of  $\alpha,\beta$ -Unsaturated Esters,” *J. Org. Chem.*, **2015**, 80, 602–608; (f) Luo, Y.; Roy, I. D.; Madec, A. G. E.; Lam, H. W., “Enantioselective Synthesis of Allylboronates and Allylic Alcohols by Copper-Catalyzed 1,6-Boration,” *Angew. Chem., Int. Ed.* **2014**, 53, 4186–4190; (g) Radomkiet, S.; Hoveyda, A. H., “Enantioselective Synthesis of Boron-Substituted Quaternary Carbon Stereogenic Centers through NHC-Catalyzed Conjugate Additions of (Pinacolato)boron Units to Enones,” *Angew. Chem., Int. Ed.*, **2014**, 53, 3387–3391.
- [3] He, J.; Shao, Q.; Wu, Q.; Yu, J.-Q., “Pd(II)-Catalyzed Enantioselective  $\text{C}(\text{sp}^3)\text{-H}$  Borylation,” *J. Am. Chem. Soc.*, **2017**, 139, 3344–3347.
- [4] Smith, S. M.; Thacker, N. C.; Takacs, J. M., “Efficient Amide-Directed Catalytic Asymmetric Hydroboration,” *J. Am. Chem. Soc.*, **2008**, 130, 3734–3735.
- [5] Hoang, G. L.; Takacs, J. M., “Enantioselective  $\gamma$ -Borylation and Stereoretentive Suzuki–Miyaura Cross-Coupling,” *Chem. Sci.*, **2017**, 8, 4511–4516.
- [6] Hadebe, S. W.; Robinson, R. S., “Rhodium-Catalyzed Hydroboration Reactions with Sulfur and Nitrogen Analogues of Catecholborane,” *Eur. J. Org. Chem.* **2006**, 4898–4904.

- [7] Burgess, K.; van der Donk, W. A.; Westcott, S. A.; Marder, T. B.; Baker, R. T.; Calabrese, J. C., "Reaction of Catecholborane with Wilkinson's Catalyst: Implications for Transition Metal-Catalyzed Hydroboration of Alkenes," *J. Am. Chem. Soc.* **1992**, *114*, 9350–9359.
- [8] Shoba, V. M.; Takacs, J. M., "Remarkably Facile Borane-Promoted, Rhodium-Catalyzed Asymmetric Hydrogenation of Tri- and Tetrasubstituted Alkenes," *J. Am. Chem. Soc.*, **2017**, *139*, 5740–5743.
- [9] Smith, S. M.; Takacs, J. M., "Remarkable Levels of Enantioswitching in Catalytic Asymmetric Hydroboration," *Org. Lett.*, **2010**, *12*, 4612–4615.
- [10] Scheuermann, M. L.; Johnson, E. J.; Chirik, P. J., "Alkene Isomerization–Hydroboration Promoted by Phosphine-Ligated Cobalt Catalysts," *Org. Lett.*, **2015**, *17*, 2716–2719.
- [11] (a) Larsen, C. H.; Ridway, B. H.; Shaw, J. T.; Smith, D. M.; Woerpel, K. A., "Stereoselective C-Glycosylation Reactions of Ribose Derivatives: Electronic Effects of Five-Membered Ring Oxocarbenium Ions," *J. Am. Chem. Soc.*, 2005, **127**, 10879–10884; (b) Aquino, M.; Cardani, S.; Fronza, G.; Fuganti, C.; Fernandez, R. P.; Tagliani, A., "Baker's Yeast Reduction of Arylalkyl and Arylalkenyl  $\gamma$ - and  $\delta$ -Keto Acids," *Tetrahedron*, 1991, **47**, 7887–7896.
- [12] Hoye, T. R.; Jeffrey, C. S.; Shao, F., "Mosher Ester Analysis for the Determination of Absolute Configuration of Stereogenic (Chiral) Carbinol Carbons," *Nature Protocols*, **2007**, *2*, 2451–2458.
- [13] (a) Hall, D. G., *Boronic Acids*, 2nd ed.; Wiley-VCH: Weinheim, **2011**; (b) Crudden, C. M.; Edwards, D., "Catalytic Asymmetric Hydroboration: Recent Advances and Applications in Carbon–Carbon Bond-Forming Reactions," *Eur. J. Org. Chem.*, **2003**, 4695–4712.
- [14] For a recent review, see: Carroll, A.-M.; O'Sullivan, T. P.; Guiry, P. J., "The Development of Enantioselective Rhodium-Catalysed Hydroboration of Olefins," *Adv. Synth. Cat.*, **2005**, *347*, 609–631.
- [15] Moteki, S. A.; Wu, D.; Chandra, K. L.; Reddy, D. S.; Takacs, J. M., "TADDOL-Derived Phosphites and Phosphoramidites for Efficient Rhodium-Catalyzed Asymmetric Hydroboration," *Org. Lett.*, **2006**, *8*, 3097–3100.

- [16] Moteki, S. A.; Toyama, K.; Liu, Z.; Ma, J.; Holmes, A. E.; Takacs, J. M., "Two-Stage Optimization of a Supramolecular Catalyst for Catalytic Asymmetric Hydroboration," *Chem. Commun.*, **2012**, 48, 263–265.
- [17] Hu, N.; Zhao, G.; Zhang, Y.; Liu, X.; Li, G.; Tang, W., "Synthesis of Chiral  $\alpha$ -Amino Tertiary Boronic Esters by Enantioselective Hydroboration of  $\alpha$ -Arylenamides," *J. Am. Chem. Soc.*, **2015**, 137, 6746–6749.
- [18] Noh, D.; Chea, H.; Ju, J.; Yun, J., "Highly Regio- and Enantioselective Copper-Catalyzed Hydroboration of Styrenes," *Angew. Chem., Int. Ed.*, **2009**, 48, 6062–6064.
- [19] Noh, D.; Yoon, S. K.; Won, J.; Lee, J. Y.; Yun, J., "An Efficient Copper(I)-Catalyst System for the Asymmetric Hydroboration of  $\beta$ -Substituted Vinylarenes with Pinacolborane," *Chem. Asian J.*, **2011**, 6, 1967–1969
- [20] Guzman-Martinez, A.; Hoveyda, A. H., "Enantioselective Synthesis of Allylboronates Bearing a Tertiary or Quaternary B-Substituted Stereogenic Carbon by NHC-Cu-Catalyzed Substitution Reactions," *J. Am. Chem. Soc.*, **2010**, 132, 10634–10637.
- [21] For a recent review, see: Calow, A. D.; Whiting, A., "Catalytic Methodologies for The  $\beta$ -Boration of Conjugated Electron Deficient Alkenes," *Org. Biomol. Chem.*, **2012**, 10, 5485–5497.
- [22] For a recent review, see: Verendel, J. J.; Pàmies, O.; Diéguez, M.; Andersson, P. G., "Asymmetric Hydrogenation of Olefins Using Chiral Crabtree-type Catalysts: Scope and Limitations," *Chem. Rev.*, **2014**, 114, 2130–2169.
- [23] Lee, J. C.; McDonald, R.; Hall, D. G., "Enantioselective Preparation and Chemoselective Cross-Coupling of 1,1-Diboron Compounds," *Nat. Chem.*, **2011**, 3, 894–899.
- [24] Feng, X.; Jeon, H.; Yun, J., "Regio- and Enantioselective Copper(I)-Catalyzed Hydroboration of Borylalkenes: Asymmetric Synthesis of 1,1-Diborylalkanes," *Angew. Chem., Int. Ed.*, **2013**, 52, 3989–3992.
- [25] Sun, C.; Potter, B.; Morcken, J. P., "A Catalytic Enantiotopic-Group-Selective Suzuki Reaction for the Construction of Chiral Organoboronates," *J. Am. Chem. Soc.*, **2014**, 136, 6534–6537.

- [26] Basch, C. H.; Cobb, K. M.; Watson, M. P., "Nickel-Catalyzed Borylation of Benzylic Ammonium Salts: Stereospecific Synthesis of Enantioenriched Benzylic Boronates," *Org. Lett.*, **2016**, *18*, 136–139.
- [27] Nelson, H. M.; Williams, B. D.; Miró, J.; Toste, F. D., "Enantioselective 1,1-Arylborylation of Alkenes: Merging Chiral Anion Phase Transfer with Pd Catalysis," *J. Am. Chem. Soc.*, **2015**, *137*, 3213–3216.
- [28] Joosten, A.; Lambert, É.; Vasse, J.-L.; Szymoniak, J., "Diastereoselective Access to *trans*-2-Substituted Cyclopentylamines," *Org. Lett.*, **2010**, *12*, 5128–5131.
- [29] Musacchio, A. J.; Nguyen, L. Q.; Beard, G. H.; Knowles, R. R., "Catalytic Olefin Hydroamination with Aminium Radical Cations: A Photoredox Method for Direct C–N Bond Formation," *J. Am. Chem. Soc.*, **2014**, *136*, 12217–12220.
- [30] Burés, J.; Armstrong, A.; Blackmond, D. G., "Curtin–Hammett Paradigm for Stereocontrol in Organocatalysis by Diarylprolinol Ether Catalysts," *J. Am. Chem. Soc.*, **2012**, *134*, 6741–6750.
- [31] (a) Colby, D. A.; Tsai, A. S.; Bergman, R. G.; Ellman, J. A., "Rhodium Catalyzed Chelation-Assisted C–H Bond Functionalization Reactions," *Acc. Chem. Res.*, **2012**, *45*, 814–825; (b) Lewis, J. C.; Berman, A. M.; Bergman, R. G.; Ellman, J. A., "Rh(I)-Catalyzed Arylation of Heterocycles via C–H Bond Activation: Expanded Scope through Mechanistic Insight," *J. Am. Chem. Soc.*, **2008**, *130*, 2493–2500.
- [32] Heravi, M. M.; Zadsirjan, V.; Farajpour, B., "Applications of Oxazolidinones as Chiral Auxiliaries in the Asymmetric Alkylation Reaction Applied to Total Synthesis," *RSC Adv.*, **2016**, *6*, 30498–30551.
- [33] Evans, D. A.; Tedrow, J. S.; Shaw, J. T.; Downey, C. W., "Diastereoselective Magnesium Halide-Catalyzed *anti*-Aldol Reactions of Chiral N-Acyloxazolidinones," *J. Am. Chem. Soc.*, **2002**, *124*, 392–393.

CHAPTER 3: ENANTIOSELECTIVE  $\gamma$ -BORYLATION OF CYCLIC  $\gamma,\delta$ -  
UNSATURATED AMIDES: DESYMMETRIZATION TO QUATERNARY  
STEREOCENTERS AND MAPPING OUT THE CATALYTIC CYCLE WITH THE  
AID OF COMPUTATIONAL STUDIES

### 3.1 Some selected desymmetrization methodologies

Enantioselective desymmetrization of prochiral or *meso* compounds has recently attracted much interest for the synthesis of enantioenriched molecules.<sup>1</sup> The majority of this methodology is categorized as shown in Figure 1, including nucleophilic ring-opening of cyclic substrates,<sup>2</sup> desymmetrization of *meso* difunctional compounds,<sup>3</sup> oxidative desymmetrization,<sup>4</sup> inter- and intramolecular C–C bond formation,<sup>5</sup> and reductive desymmetrization.<sup>1</sup>

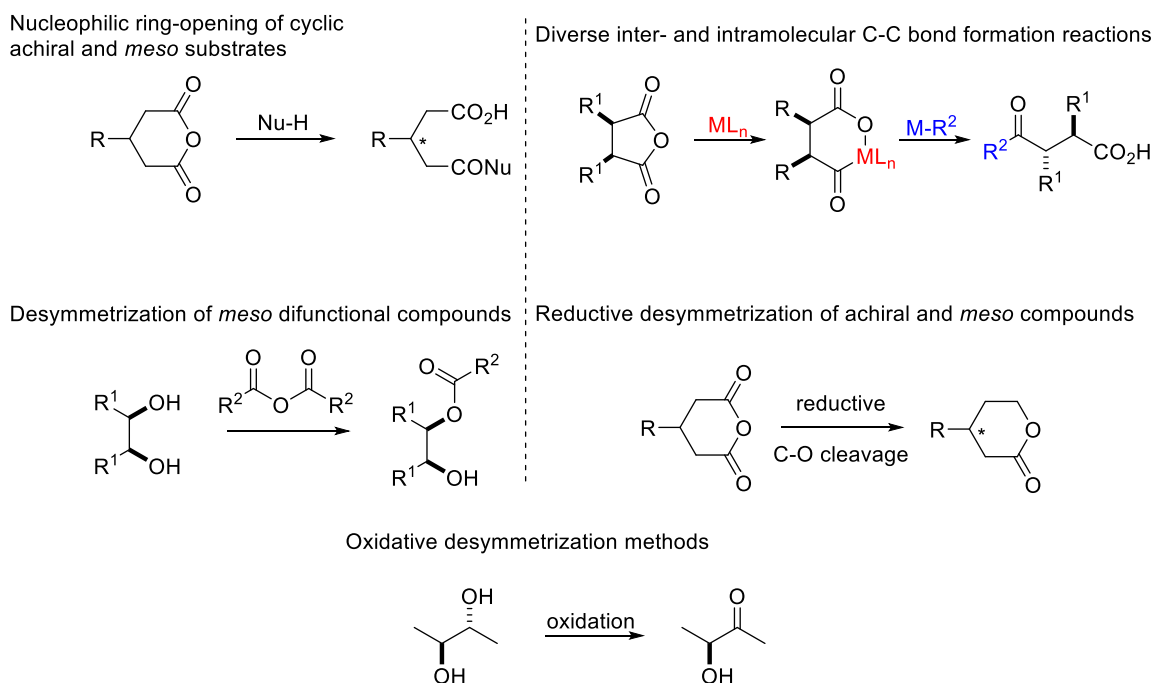


**Figure 1.** Selected desymmetrization methodologies

In addition to the above methods, enantioselective desymmetrization is recently highlighted as the most powerful approach to constructing quaternary or tetrasubstituted carbon stereogenic centers, existing widely in natural products, drugs, and bioactive molecules.<sup>6</sup>

Despite the rapid growth of interest, there is only a few catalytic enantioselective desymmetrization obtained via asymmetric hydroboration toward the synthesis of molecules bearing quaternary carbon stereogenic centers (Figure 2). Previous reports are based upon the enantioselective hydroboration of cyclopropene derivatives. In 2003, Gevorgyan introduced the directed Rh(I)-catalyzed hydroboration of a few cyclopropane-derived substrates. High yield and enantioselectivity with complete *cis*-diastereoselection is attributed to carbonyl-directed CAHB.<sup>7</sup> With similar substrates, Tian and co-workers on the other hand reported the exclusive formation of *trans*-products using a chiral copper(I) catalyst.<sup>8</sup> The formation of the latter was explained by the steric hindrance of the methyl ester group overriding the weak coordination of copper to the carboxyl group. Similarly, Tortosa's system does not involve the coordinating functional group indicating that the high diastereoselectivity is completely controlled by steric effect of the larger group (i.e.; R<sub>L</sub>).<sup>9</sup>

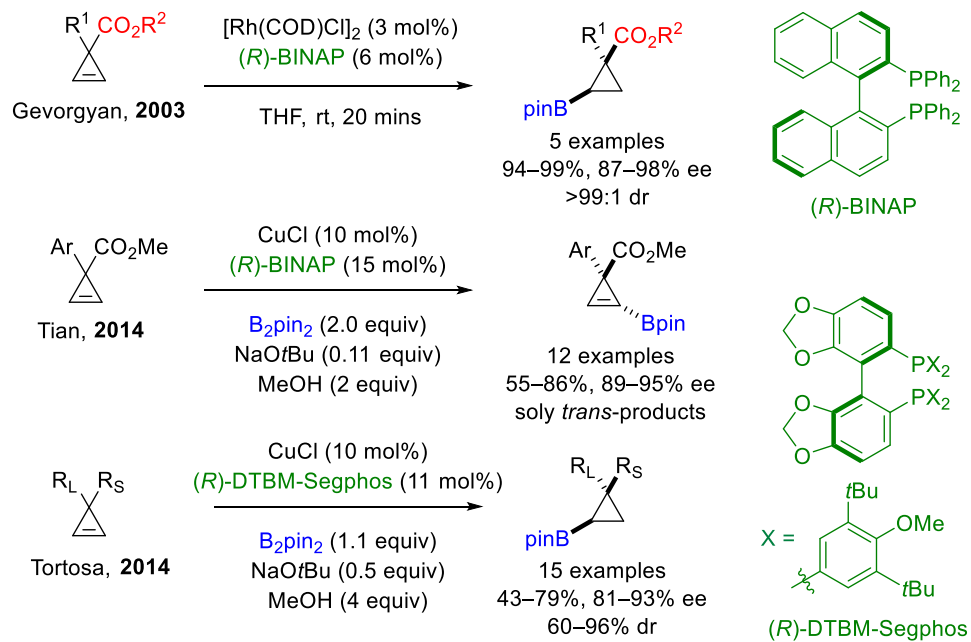


**Figure 2.** Current literature reports on enantioselective desymmetrization via CAHB toward the synthesis of molecules bearing quaternary carbon stereogenic centers product

### 3.2 Enantioselective desymmetrization to all-carbon quaternary stereocenters via $\gamma$ -borylation of cyclic $\gamma,\delta$ -unsaturated amides<sup>10</sup>

Inspired by the approach, we examined the homologous symmetric cyclic cyclopentene-derived substrate **23**. Three reasons were important in selecting this structural motif: (i) we would like to achieve  $\gamma$ -borylation using the more challenging substrates (i.e., longer coordinating distance), symmetric cyclic  $\gamma,\delta$ -unsaturated amides **23**, to complement  $\beta$ -borylation of cyclopropene-based substrates reported in literature (Figure 2), (ii) a series of non- $\alpha$ -hydrogen substrates (i.e., **23a**) should generate  $\alpha$ -quaternary carbon stereogenic centers after enantioselective desymmetrization via CAHB, and (iii) the symmetric substrate is, in principle, a good choice for computational studies (Figure 3) described later in this chapter.

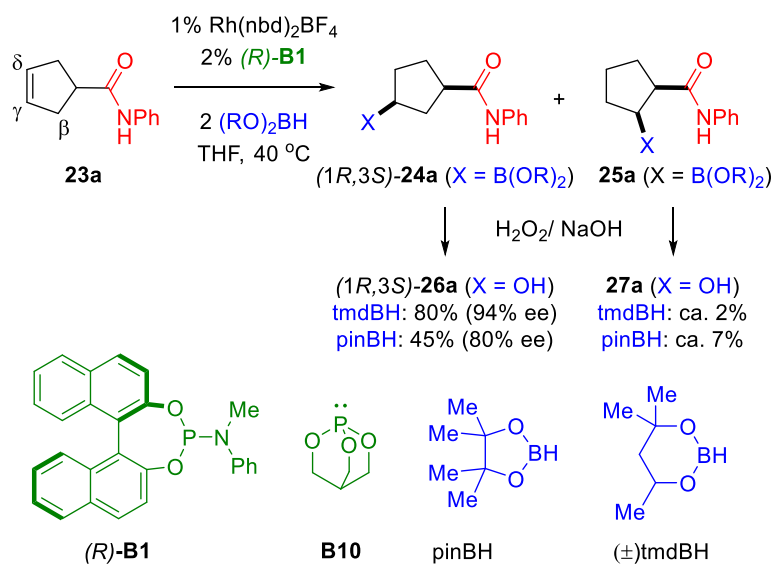


**Figure 3.** CAHB of symmetric cyclic  $\gamma,\delta$ -unsaturated amide **23a**, a model substrate for computational studies. Copyright (2014) ACS AuthorChoice (ref. 30).

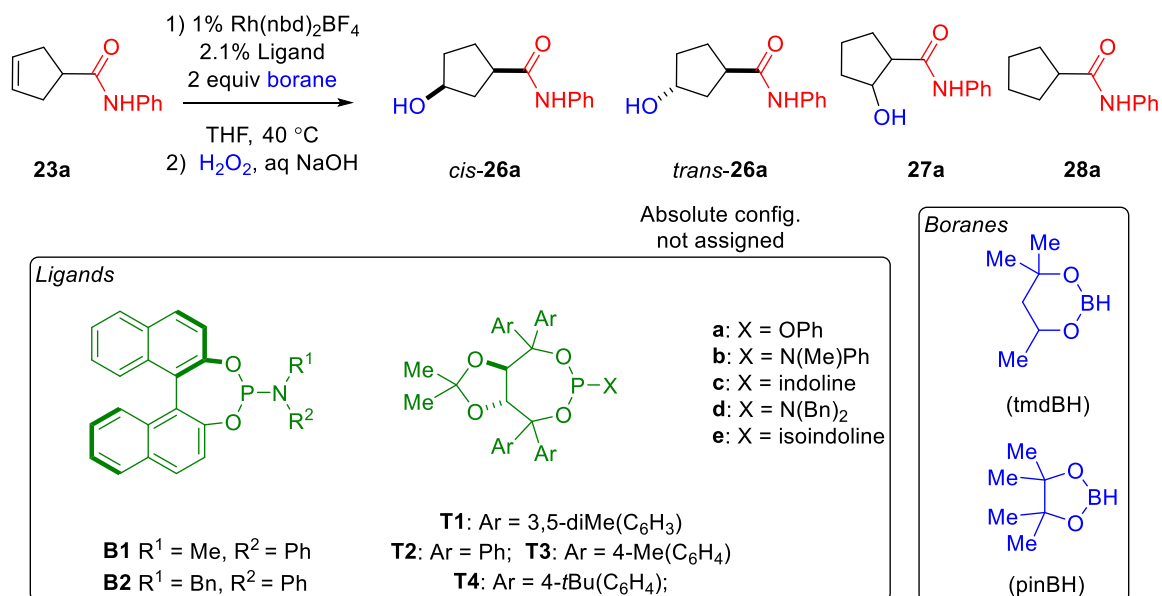
In contrast to the related acyclic  $\gamma,\delta$ -unsaturated amides discussed in Chapter 2, tmdBH, rather than pinBH, illustrates the best selectivity for the cyclic substrate **23a**. It



affords (1*R*,3*S*)-**26a** in 80% yield and 94% ee after CAHB/ oxidation; pinBH generates (1*R*,3*S*)-**26a** in much lower yield (45%) and enantioinduction (80% ee). In spite of pinBH's poor performance in practice, asymmetric structures render the computational study more time-consuming. Therefore, pinBH along with the caged-phosphite ligand **B10** are used as model compounds in density functional theory (DFT) calculations to reduce the computing time. The computational details will be discussed in later section 3.4.

CAHB of the parent substrate **23a** was screened with pinBH and tmdBH using a broad collection of simple, chiral TADDOL- and BINOL-derived ligands initial optimization studies. The results are summarized in Table 1.

**Table 1.** Optimization studies of enantioselective desymmetrization via CAHB of **23a**



#### A. Enantioselective desymmetrization via CAHB of **23a** with tmdBH.

Entry	Ligand	Abs. Config. ( <i>cis</i> - <b>26a</b> )	% ee ( <i>cis</i> - <b>26a</b> )	% Yield ( <i>cis</i> - <b>26a</b> )	% Yield ( <i>trans</i> - <b>26a</b> )	% Yield ( <b>27a</b> )	% Yield ( <b>28a</b> )
1	<b>B1</b>	(1 <i>R</i> ,3 <i>S</i> )	94	80	1	2	14
2	<b>B2</b>	(1 <i>R</i> ,3 <i>S</i> )	94	80	1	1	12
3	<b>T1a</b>	(1 <i>R</i> ,3 <i>S</i> )	83	70	1	3	25

4	<b>T2a</b>	(1 <i>R</i> ,3 <i>S</i> )	88	60	2	4	27
5	<b>T3a</b>	(1 <i>R</i> ,3 <i>S</i> )	87	59	2	4	32
6	<b>T4a</b>	(1 <i>R</i> ,3 <i>S</i> )	92	65	1	3	25
7	<b>T1b</b>	(1 <i>R</i> ,3 <i>S</i> )	26	35	2	4	55
8	<b>T2b</b>	(1 <i>R</i> ,3 <i>S</i> )	35	47	3	5	41
9	<b>T3b</b>	(1 <i>R</i> ,3 <i>S</i> )	23	45	2	5	45
10	<b>T4b</b>	(1 <i>R</i> ,3 <i>S</i> )	30	37	3	4	52
11	<b>T1c</b>	(1 <i>R</i> ,3 <i>S</i> )	11	9	3	5	81
12	<b>T2c</b>	(1 <i>R</i> ,3 <i>S</i> )	10	29	1	5	60
13	<b>T3c</b>	(1 <i>S</i> ,3 <i>R</i> )	40	22	1	4	68
14	<b>T4c</b>	(1 <i>R</i> ,3 <i>S</i> )	49	30	2	6	60
15	<b>T1d</b>	(1 <i>R</i> ,3 <i>S</i> )	20	2	2	4	81
16	<b>T2d</b>	(1 <i>R</i> ,3 <i>S</i> )	1	2	2	16	71
17	<b>T3d</b>	(1 <i>R</i> ,3 <i>S</i> )	2	5	3	17	69
18	<b>T4d</b>	(1 <i>R</i> ,3 <i>S</i> )	11	9	3	19	65
19	<b>T1e</b>	(1 <i>R</i> ,3 <i>S</i> )	11	5	2	4	71
20	<b>T3e</b>	(1 <i>S</i> ,3 <i>R</i> )	45	8	2	7	74
21	<b>T4e</b>	(1 <i>R</i> ,3 <i>S</i> )	50	9	3	7	70

#### B. Enantioselective desymmetrization via CAHB of **23a** with pinBH.

Entry	Ligand	Abs. Config. ( <i>cis</i> - <b>26a</b> )	% ee ( <i>cis</i> - <b>26a</b> )	% Yield ( <i>cis</i> - <b>26a</b> )	% Yield ( <i>trans</i> - <b>26a</b> )	% Yield ( <b>27a</b> )	% Yield ( <b>28a</b> )
22	<b>B1</b>	(1 <i>R</i> ,3 <i>S</i> )	80	45	3	7	25
23	<b>B2</b>	(1 <i>R</i> ,3 <i>S</i> )	81	52	3	8	28
24	<b>T1a</b>	(1 <i>R</i> ,3 <i>S</i> )	70	59	8	13	17
25	<b>T2a</b>	(1 <i>R</i> ,3 <i>S</i> )	60	66	8	7	16
26	<b>T3a</b>	(1 <i>R</i> ,3 <i>S</i> )	55	60	10	7	20
27	<b>T4a</b>	(1 <i>R</i> ,3 <i>S</i> )	68	62	9	8	18
28	<b>T1b</b>	(1 <i>S</i> ,3 <i>R</i> )	60	62	4	14	17
29	<b>T2b</b>	(1 <i>S</i> ,3 <i>R</i> )	75	64	6	11	16
30	<b>T3b</b>	(1 <i>S</i> ,3 <i>R</i> )	65	66	5	12	14
31	<b>T4b</b>	(1 <i>S</i> ,3 <i>R</i> )	60	62	4	15	16
32	<b>T1c</b>	(1 <i>S</i> ,3 <i>R</i> )	6	25	4	22	47
33	<b>T2c</b>	(1 <i>S</i> ,3 <i>R</i> )	60	75	5	8	15
34	<b>T3c</b>	(1 <i>S</i> ,3 <i>R</i> )	78	77	7	6	14
35	<b>T4c</b>	(1 <i>R</i> ,3 <i>S</i> )	15	63	4	15	16
36	<b>T1d</b>	(1 <i>S</i> ,3 <i>R</i> )	10	11	19	10	51
37	<b>T2d</b>	(1 <i>S</i> ,3 <i>R</i> )	13	48	8	18	20
38	<b>T3d</b>	(1 <i>S</i> ,3 <i>R</i> )	50	46	5	25	20
39	<b>T4d</b>	(1 <i>S</i> ,3 <i>R</i> )	10	23	34	8	22
40	<b>T1e</b>	(1 <i>R</i> ,3 <i>S</i> )	5	27	5	22	31
41	<b>T3e</b>	(1 <i>S</i> ,3 <i>R</i> )	70	55	8	12	19
42	<b>T4e</b>	(1 <i>R</i> ,3 <i>S</i> )	2	40	17	15	25

The results shown in Table 1 lead to several important conclusions, including (i) (BINOL)-derived phosphoramidites (i.e., **B1–2**) in conjunction with tmdBH gives the best catalyst/borane combination for this substrate (i.e., entries 1–2), (ii) tmdBH in

combination with certain ligands are much favorable for hydrogenation pathway giving reduced product **28a** in up to 81% yield (e.g., entries 11–21), (iii) with pinBH, changing from a TADDOL-derived phenyl phosphite (i.e., X = OPh, entries 24–27) to a TADDOL-derived phosphoramidite (i.e., X = NR<sup>1</sup>R<sup>2</sup>, entries 28–33 and 35–40) usually leads to enantioswitching with a few exceptions (entries 34, 41 and 42). To illustrate the latter aspect, see the graph in Figure 4. The blue data is obtained from experiments with tmdBH, the red data correspond to pinBH; negative numbers indicate predominantly the (1*S*,3*R*) absolute configuration while the positive numbers for percent ee are for predominantly the (1*R*,3*S*) absolute configuration. Most of the TADDOL-derived phosphoramidite ligands (i.e., **T1b–T4e**) in conjunction with pinBH give negative ee while using BINOL-derived phosphoramidites **B1/B2** and TADDOL-derived phosphite **T1–5a** give positive values.

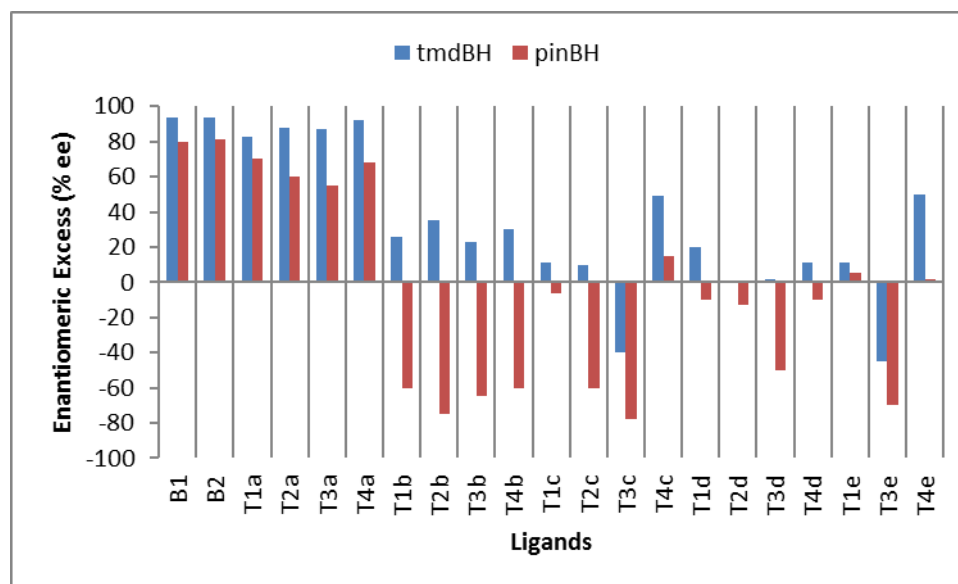


**Figure 4.** Brief ligand and borane survey for CAHB of **23a** reveals moderate levels of enantioswitching. Adapted with permission from reference 10. Copyright (2015) American Chemical Society.

The observed enantio reversal is in qualitative agreement with the previous report from the Takacs group of a high level of enantio switching in CAHB of a series of acyclic  $\beta,\gamma$ -unsaturated amides.<sup>11</sup> In principle, both enantiomeric products can be obtained via asymmetric catalysis by preparing both enantiomers of the catalyst. However, many chiral sources are available predominately in one absolute configuration; the other enantiomer might only be accessed by complicated synthetic routes or kinetic resolution of the racemic mixture. Therefore, uncovering additional strategies by which both enantiomers can be obtained from a single chiral source of interest in the community.<sup>12</sup> The work described above again demonstrates an ability to use modest changes in ligand substituents, while preserving the absolute configuration, to effect enantio switching. Though this interesting feature is difficult to predict and rationalize and further catalyst designs are required to reach high level of enantioselectivity in this case, it is consistent with the previous study.<sup>11</sup> Thus, the effect might be generalized as “TADDOL-derived phosphites and TADDOL-derived phosphoramidites in conjunction with pinBH can potentially provide enantio reversal in carbonyl-directed CAHB, at least for rhodium(I) catalyst system; modification of the ligand backbones might be needed to enhance the enantioselectivity.”

It is expected that the level of asymmetric induction obtained with a chiral catalyst should be dependent on the enantiomeric purity of the catalyst. Often a linear relationship is observed when a single chiral ligand is present in a chiral metal catalyst; that is, the product enantioselectivity is directly proportional to the enantiomeric excess of the chiral ligand employed in the reaction. However, many reports in literature have shown to deviate from this expectation resulting in a so-called nonlinear effect.<sup>13</sup> It is

now widely used as a mechanistic tool and most commonly to suggest multiple ligands are present in the active catalyst.<sup>14</sup> In the same report of enantioswitching discussed above, Smith and Takacs also report a negative nonlinear effect ((-)-NLE) and positive nonlinear effect ((+)-NLE) for TADDOL-derived phosphites and TADDOL-derived phosphoramidites, respectively.<sup>11</sup> The results suggest that the heterochiral combination (i.e.,  $L_R L_S Rh^+$ ) is more reactive for phosphite ligands (i.e., (-)-NLE), whereas it is more stable and less reactive than the homochiral (i.e.,  $L_R L_R Rh^+$  or  $L_S L_S Rh^+$ ) species in the case of phosphoramidites (i.e., (+)-NLE). In either case, it is suggested that two ligands are bound to the rhodium in the active catalyst species.<sup>12,13</sup> However, earlier in this dissertation (i.e., Chapters 2.2 and 2.3), we have shown that 1:1 Rh:L ratio is effective for the CAHB of acyclic  $\gamma,\delta$ -unsaturated amide derivatives. In order to have better understanding of mechanistic implications, we therefore carried out a NLE study of the cyclic substrate. The two best ligands in term of enantioversional (i.e., **T1a** and **T3c**) are chosen for this investigation (Figure 5). The blue data represent the change in enantiomeric excess of **T1a**, and the red data points are obtained varying **T3a**. The y-axis illustrates the enantiomeric excess of CAHB/ oxidation product **26a**, in which negative numbers correspond to formation of the (1*S*,3*R*)-diastereomer, while the positive numbers are for formation of the (1*R*,3*S*)-diastereomer. Viewing from left-to-right of the x-axis is the variation from pure (*S,S*)- to (*R,R*)-ligands. We were surprised to find that in contrast to the results obtained by Smith and Takacs, this work shows that both TADDOL-derived phosphite **T1a** and phosphoramidite **T3c** ligands afford an essentially linear relationship in the case of 1:2 Rh:Ligand ratio. The results could indicate that only chiral 1:2 Rh:Ligand catalysts (i.e.,  $L_R L_R Rh^+$  or  $L_S L_S Rh^+$ ) are most likely involved in CAHB of the

cyclic  $\gamma,\delta$ -unsaturated amide **23**; the heterochiral combination (i.e.,  $L_R L_S Rh^+$ ) is either not formed or is unreactive.<sup>13,15</sup> The result is also consistent with a 1:1 Rh:Ligand complex being the active catalyst.

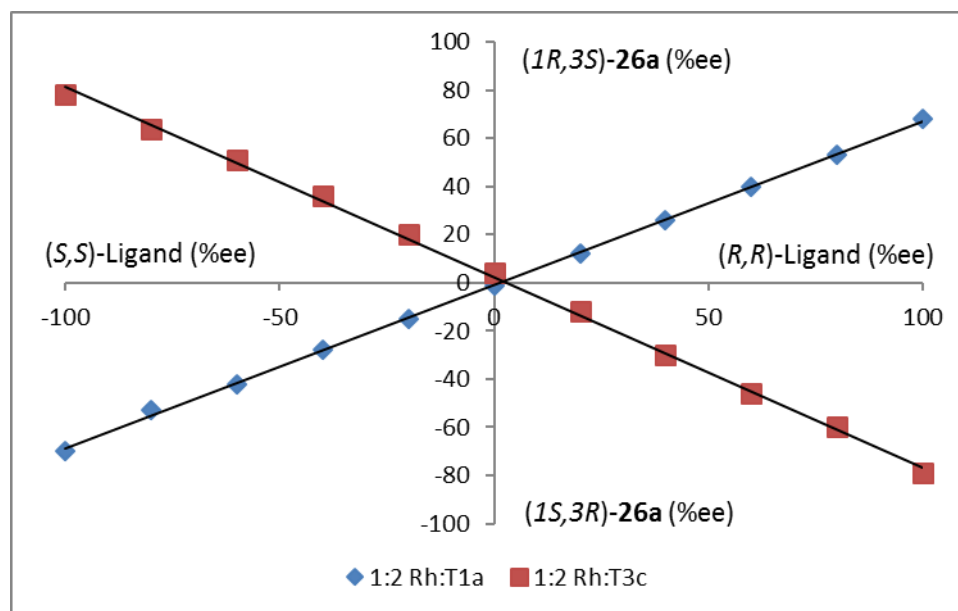


**Figure 5.** 1:2 Rh:Ligand ratio reveals linear relationship between the enantiomeric excess of ligand **T1a** (blue) and **T3c** (red) and that of the product **26a**.

From the results obtained for the case of 1:2 Rh:L ratio (Figure 5), we expected similar trends should be observed for 1:1 Rh:L ratio. Indeed, a linear relationship was obtained, although the percent enantiomeric excess of product obtained using enantiomerically pure ligand was lower using the 1:1 Rh:L combination (Figure 6). In agreement with CAHB of acyclic  $\gamma,\delta$ -unsaturated carbonyl compounds discussed in Chapter 2, we now hypothesize that a 1:1 Rh:L complex might be the active chiral catalyst. The presence of excess chiral ligand enhances the enantioselectivity, perhaps by pushing an equilibrium towards complete complex formation. Another possibility is that the two complexes (i.e., 1:2 Rh:L and 1:1 Rh:L) might generate two different active

catalysts. The computational studies discussed in the next sections will focus on  $^+\text{RhL}_2$  complex based upon the results built at the early stage; however, the pathway involving  $^+\text{RhL}$  should now also be considered.

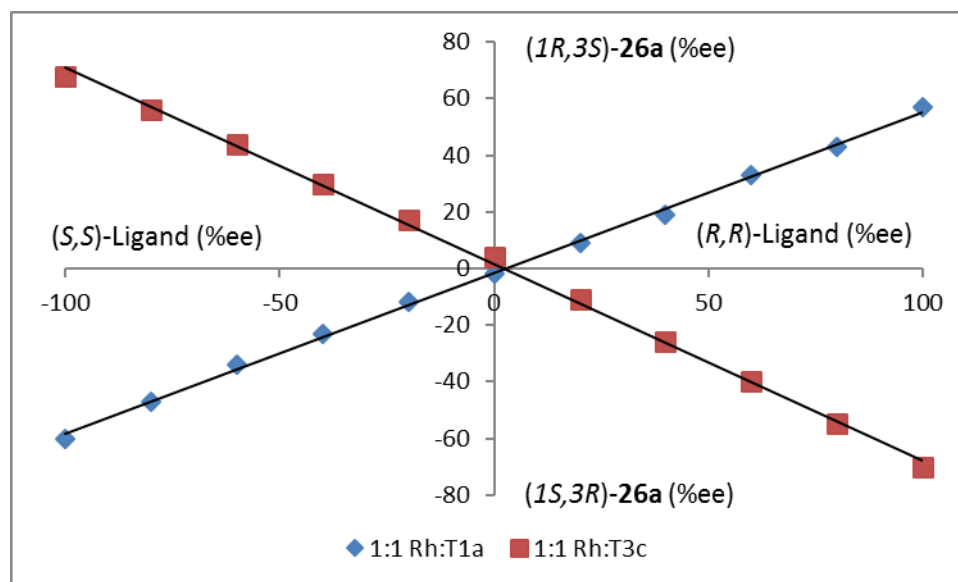


**Figure 6.** 1:1 Rh:Ligand ratio reveals linear relationship between the enantiomeric excess of ligand **T1a** (blue) and **T3c** (red) and that of the product **26a**.

With the optimized conditions employing *tmdBH* and ligand **B2** from our brief ligand and borane survey, a series of  $\alpha$ -substituted cyclopentene-based substrates **23a–l** is subjected to CAHB afford secondary  $\gamma$ -borylated amides **26a–l** bearing stereogenic quaternary  $\alpha$ -carbon centers (Figure 7). Along with the parent  $\alpha$ -hydrogen phenyl amide substrate **23a**, other phenyl amides with  $\alpha$ -substituted quaternary carbon including alkyl (i.e., **23b**, R = Me), aryl (i.e., **23c**, R = Ph), and trifluoromethyl 1 (i.e., **23b**, R = CF<sub>3</sub>) efficiently undergo CAHB affording the *cis* isomer in high yield (65–78%) and enantioselectivity (96:4–97:3 er). Corresponding benzyl amides **23e–h** are also good substrates giving comparable diastereoselectivity and yield, albeit with somewhat slightly

lower enantioselectivity (92:8–96:4 er). Substrates **23i** and **23j**, each contain two different alkenes, but undergo CAHB selectively with the endocyclic double bond leaving the other untouched; **26i** and **26j** are formed in good yield (75–80%) and high enantioselectivity (97:3–99:1 er). The observed products could be explained by the preferred orientation of the carbonyl oxygen which leads to greater reactivity for the

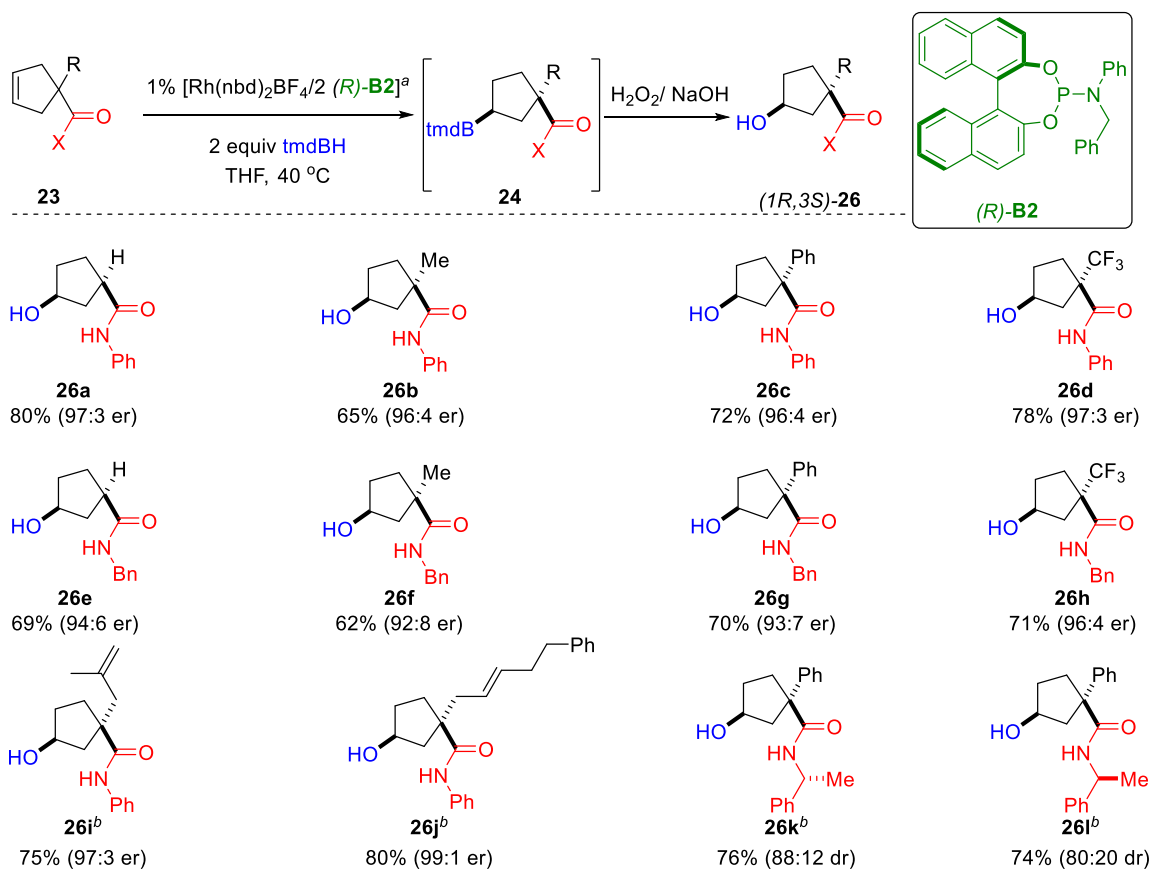


**Figure 7.** Enantioselective desymmetrization towards stereogenic quaternary carbon centers via CAHB of **23**

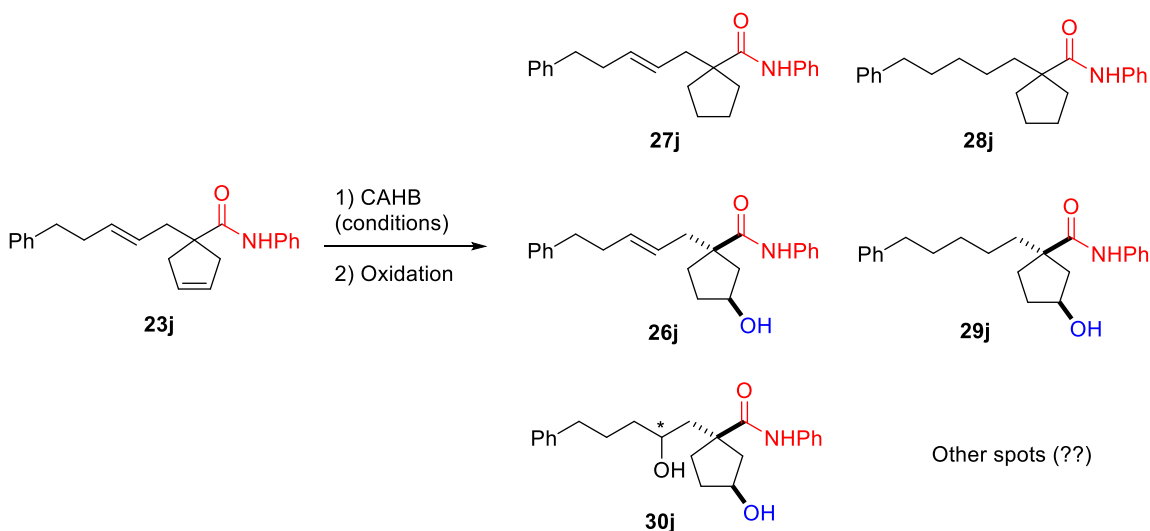
<sup>a</sup> Unless otherwise noted all reaction use 1.0%  $[Rh(nbd)_2BF_4/2 \text{ B2}]$ , 2.0 equiv.  $tmdBH$ , THF, 40 °C (12 h) followed by oxidation using  $H_2O_2/aq. NaOH$ . Unless otherwise noted, the isolated yield is that of the major diastereomer (*cis*) and reflects the average of two experiments generally exhibiting a spread of 2%. Enantiomer ratios (*er*) are determined by chiral HPLC analysis; diastereomer ratios (*dr*) are determined for the purified mixture of diastereomers by integrating major and minor  $^1H$  NMR resonances. <sup>b</sup> 2.0%  $[Rh(nbd)_2BF_4/2 \text{ B2}]$ .



endocyclic double bond and highlights unusual group selectivity in the CAHB. In contrast, chiral substrates **23k** and **23l** exhibit somewhat lower stereoselectivity and exhibit a matched/mismatched diastereomer effect with enantiomeric catalysts. Nonetheless, CAHB proceeds with high *cis/trans*-diastereoselectivity (i.e., solely *cis* product is obtained) and high yield (74–76%). In addition, these chiral substrates will be used to confirm structural assignments for both CAHB and product functionalization (*vide infra*).

CAHB of diene **23j**, which bears two similarly substituted alkenes with the same coordinating distance (i.e.,  $\gamma,\delta$  with respect to the carbonyl moiety), selects for the endocyclic alkene as depicted in Figure 7. This observation is consistent with tmdBH being an ineffective borane reagent for the related acyclic  $\gamma,\delta$ -unsaturated substrates discussed in Chapter 2. Consequently, we would like to understand a little more on the selectivity of this substrate; Table 2 summarizes the results of some selected CAHB conditions.

**Table 2.** Brief survey on CAHB of diene substrate **23j** reveals that tmdBH is crucial for high group- and enantioselectivity.



Conditions	Isomerized + Reduced + SM <sup>a</sup>	Reduced <b>27j</b>	Reduced <b>28j</b>	Alcohol <b>26j</b> <sup>b</sup>		Alcohol <b>29j</b> <sup>b</sup>		Alcohol <b>30j</b> <sup>c</sup>	Others <sup>d</sup>
	Yield	Yield	Yield	Yield	er	Yield	er	Yield	Yield
<b>A</b>	0	15	0	80	99:1	trace	–	0	0
B	20	–	–	73	99:1	trace	–	0	0
C	78	–	–	18	98:2	0	–	0	0
D	trace	–	–	27	94:6	11	–	17	30
E	trace	0	18	0	–	65	88:12	0	0
F	trace	–	–	10	–	10	–	19	45

General CAHB conditions: *x* mol% [Rh(nbd)<sub>2</sub>BF<sub>4</sub>/2 **B2**], *y* equiv borane, N<sub>2</sub> or H<sub>2</sub>, THF, 40 °C, 18h

Condition A: 2 mol% cat., 2 equiv tmdBH, N<sub>2</sub>

Condition B: 1 mol% cat., 2 equiv tmdBH, N<sub>2</sub>

Condition C: 1 mol% cat., 2 equiv tmdBH, H<sub>2</sub>

Condition D: 1 mol% cat., 2 equiv pinBH, N<sub>2</sub>

Condition E: 1 mol% cat., 2 equiv pinBH, H<sub>2</sub>

Condition F: 1 mol% cat., 4 equiv pinBH, N<sub>2</sub>

<sup>a</sup> In case the reaction did not go to completion, the mixture of isomerized alkenes ( $\beta,\gamma$ -endocyclic alkenes obtained via  $\beta$ -hydride elimination), reduced products, and starting material could not be separated via column chromatography

<sup>b</sup> In case of little selectivity, alcohol **26j** and alcohol **28j** could not be separated via column chromatography

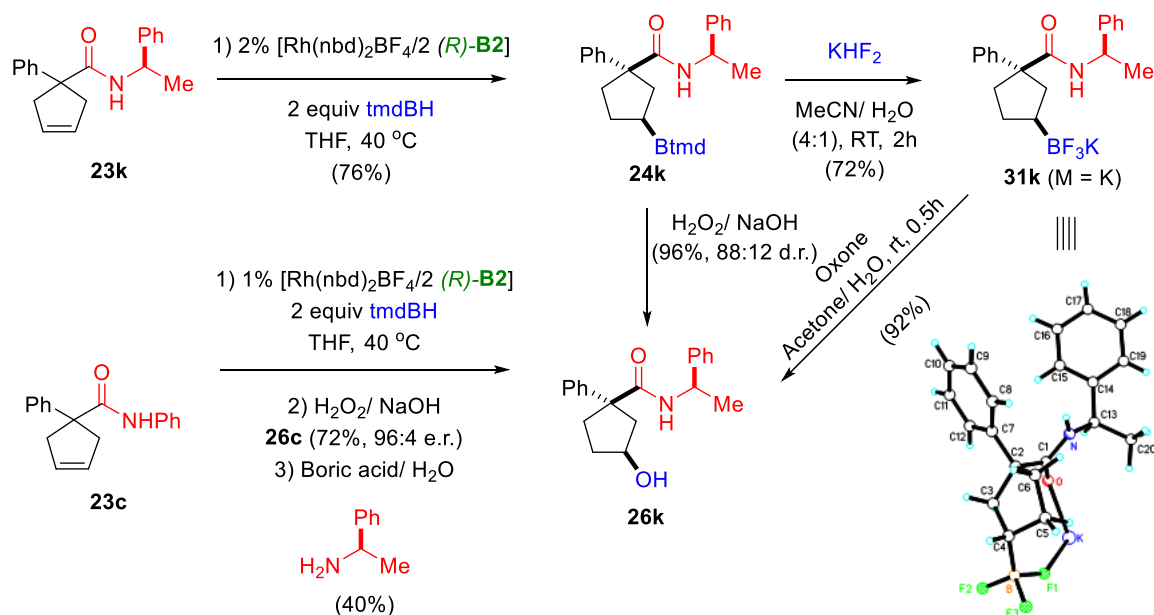
<sup>c</sup> Alcohol **30j** was reported after subtracting the yield of pinacol diol (a side product of oxidation of pinacolato boronic esters) using <sup>1</sup>H NMR mole ratio (the mixture might be separated, but not with conditions used to separate all other possible products)

<sup>d</sup> Other spots indicate other alcohols as they are more polar than alcohols **26j** and **28j**; their identifications are not yet determined

Condition A are the optimized conditions; CAHB of diene **23j** requires 2% catalyst loading for complete conversion. In addition to major alcohol **26j** obtained in high yield and selectivity (80%, 99:1 er), monoreduced product **27j** is also isolated in significant amount (15%) suggesting that under the standard condition, the competing hydrogenation pathway is also selective for the endocyclic alkene. Reducing the catalyst loading to 1% leads to an incomplete conversion but similar selectivity (condition B). Building on the contemporaneous results obtained by V. Shoba, the reaction was carried out under a hydrogen atmosphere; however, unexpectedly, the reactivity was low and a complex mixture of products obtained (condition C). Borane tmdBH is indeed crucial for high group- and enantioselectivity; several conditions using pinBH were carried out

(conditions D–F) but the results obtained were rather complicated mixtures. Some insights gleaned from reactions using pinBH include (i) pinBH is more reactive than tmdBH (all conditions using pinBH went to completion) and (ii) pinBH is more selective for hydroboration mode of cyclopentene ring. Under condition D (N<sub>2</sub> atmosphere) only a trace amount of reduced product was isolated; even under condition E (H<sub>2</sub> atmosphere), alcohol **30j** was the major product (65%) albeit with modest enantioselectivity (88:12).

As mentioned above, the chiral amide substrate **23k** proved useful for structural studies. Although CAHB proceeds with only modest diastereoselectivity (88:12 dr), the major diastereomer could be further functionalized to confirm the stereochemical course of CAHB (Scheme 1). Our first attempts to grow crystal of  $\gamma$ -hydroxy **26k** were unsuccessful. We turned to the corresponding trifluoroborate salt as a potentially more suitable candidate for x-ray crystallographic analysis. The isolated boronic ester **24k** was converted to **31k** by the method developed in Molander group.<sup>16</sup> Crystals suitable for x-ray analysis were grown by vapor diffusion method initially with minimum amount of 3:1 diethylether:methanol. The crystal structure of **31k** was determined by Dr. Victor Day (University of Kansas). The structure clearly establishes the stereochemistry of the boron-bearing carbon stereocenter relative to the pre-existing amide side chain stereocenter thus establishing the absolute stereochemical course of the CAHB. To further confirm the assignment for achiral amide substrates such as **23c**,  $\gamma$ -hydroxy amide **26c** was transamidated to **26k** via boric acid-catalyzed reaction resulting in formation of the same major diastereomer as that obtained from **23k**.



**Scheme 1.** Determination of absolute configuration of CAHB of cyclic  $\gamma,\delta$ -unsaturated amides via x-ray crystallographic analysis of  $\gamma$ -trifluoroborato amide **31k**. Adapted with permission from reference 10. Copyright (2015) American Chemical Society.

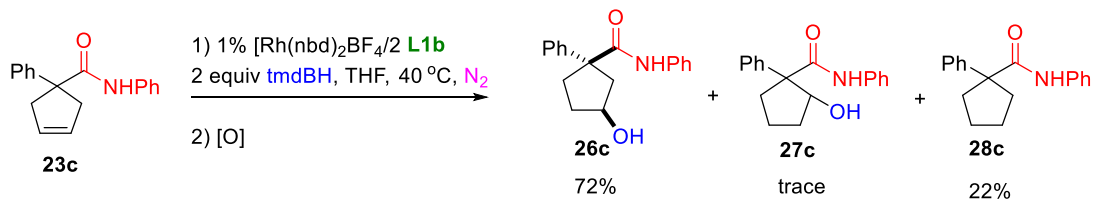
### 3.3 Deuterium-labeling studies

Deuterium-labeling studies for CAHB have been carried out by several groups to probe the mechanism of the reaction, in particular the degree of reversibility of certain steps in proposed mechanisms.<sup>17–19</sup> The absence of deuterium scrambling often suggests that the migratory insertion of Rh–H(D) into C=C double bond is irreversible. The level of deuterium scrambling is found to vary as a function of the substrate and borane employed in the reaction. Previous D-labeling studies in the Takacs' group obtained by Dr. Sean M. Smith (University of Nebraska, 2012) on Rh(I)-catalyzed CAHB of a series of  $\beta,\gamma$ -unsaturated amides suggested some important aspects, including (i) the stereospecific *syn*-addition of borane to alkenes, (ii) the absence of deuterium scrambling or isomerization indicating the migratory insertion of Rh–H(D) to C=C double bond is irreversible, and (iii) the mechanism involves a one-step oxidative addition of borane to the rhodium as supported by the lack of scrambling in a double-labeling experiment.

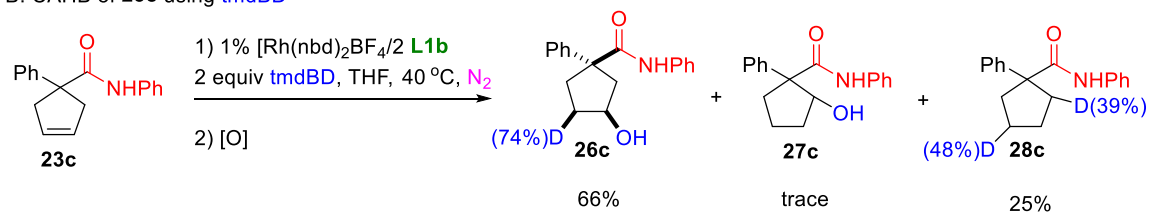
For comparison to the previous studies in the group as well as to support computational studies discussed later in this chapter, several sets of deuterium-labeling reactions were carried out. First the  $\alpha$ -phenyl substituted substrate **23c** was chosen to study the extent of deuterium incorporation into the major product after CAHB/oxidation, *cis*-hydroxy amide **26c**. CAHB of **23c** was carried out under similar conditions using several different borane sources (Figure 8); inset 8A illustrates the reference reaction using tmdBH. Using either deuterated borane reagent, tmdBD or pinBD, the major product is **26c** with high deuterium incorporation at one position (i.e., the  $\delta$ -carbon). The <sup>1</sup>H NMR spectra of **26c** as well as the deuterated versions are shown in Figure 9. The

spectra show little evidence for reversible C–H formation except based on the formation of **28c** with tmdBD.

A. CAHB of **23c** using tmdBH



B. CAHB of **23c** using tmdBD



C. CAHB of **23c** using pinBD

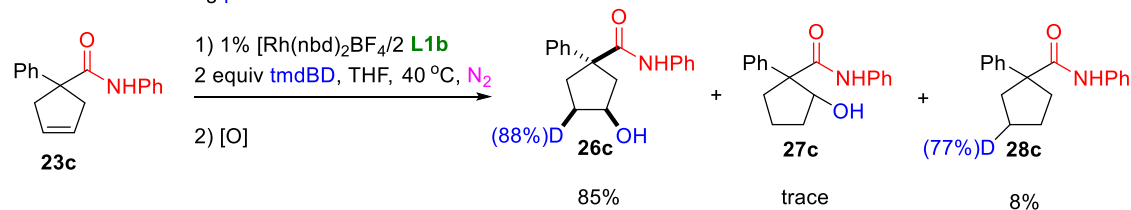
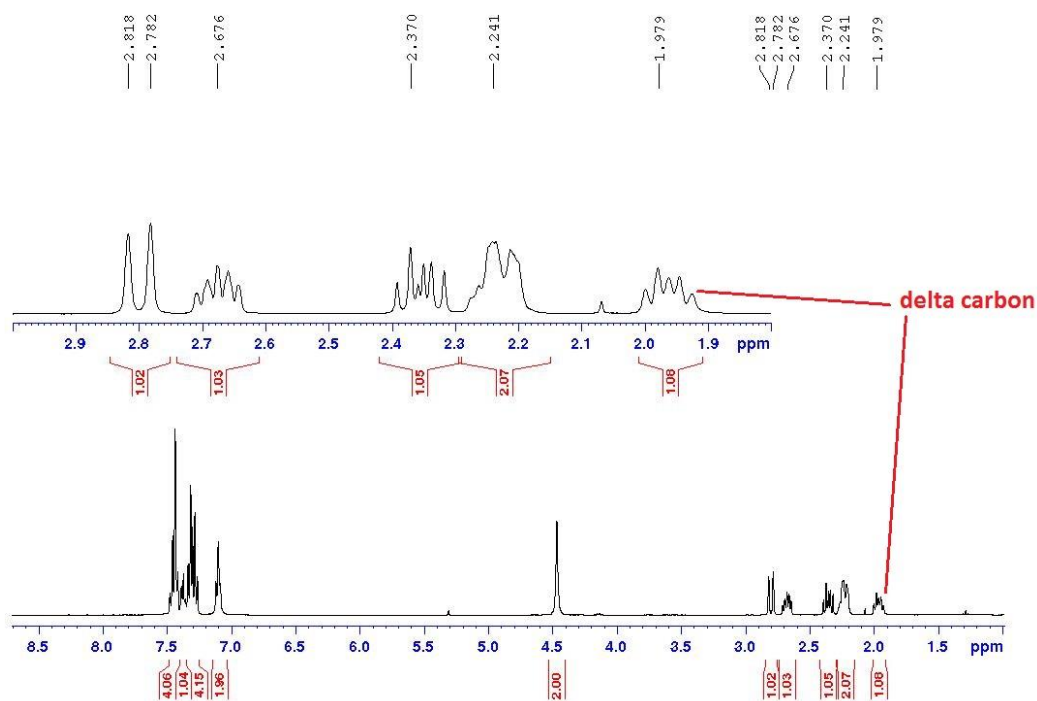
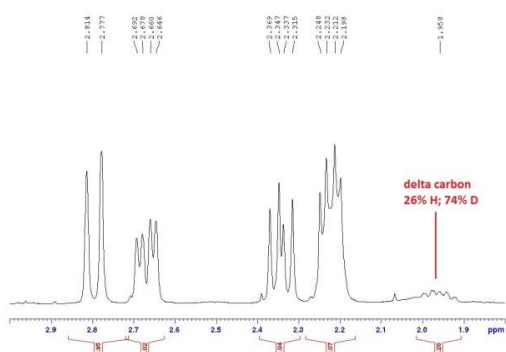


**Figure 8.** Deuterium-labeling studies for CAHB of **23c** show little evidence for reversible C–H formation

A.  $^1\text{H}$  NMR spectrum of **26c** using tmdBH (no deuterium incorporation)



B.  $^1\text{H}$  NMR spectrum of **26c** using tmdBD (74% deuterium incorporation at  $\delta$ -carbon)



C.  $^1\text{H}$  NMR spectrum of **26c** using pinBD (88% deuterium incorporation at  $\delta$ -carbon)

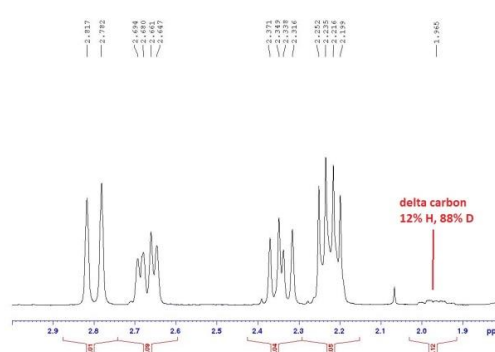
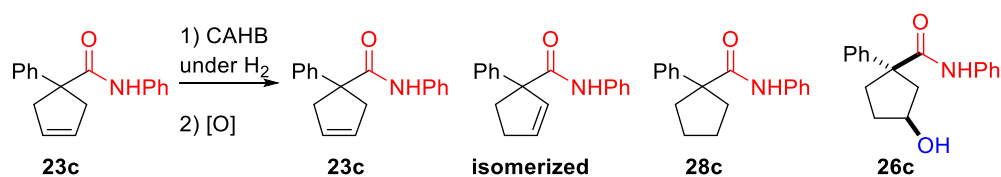


**Figure 9.**  $^1\text{H}$  NMR spectra illustrating the deuterium incorporation into  $\gamma$ -hydroxy product **26c**

Hydrogenation is a major competing pathway in most reported transition-metal-catalyzed hydroborations<sup>20-27</sup> and is also observed in this study. For example, as illustrated in Figure 8, up to 25% of the reduced product is formed under the optimal conditions for CAHB of **23c**; certain ligands (e.g., **T1d**) afford the hydrogenation product **28a** in up to 81% yield (Table 1). In effort to better understand the mechanism of the hydrogenated pathway, some selected deuterium-labeling studies under the conditions shown in Figure 8 were carried out (Table 3 and Figure 10). By adding a hydrogen source (e.g., methanol, water), Ms. Veronika Shoba was subsequently able to turn the undesired products into useful compounds.<sup>28</sup>

**Table 3.** CAHB of  $\alpha$ -phenyl **23c** under H<sub>2</sub> with different tmdBH loading: the role of borane is important for the reaction to proceed



Equiv of tmdBH	Starting material	Isomerized	Reduced <b>28c</b>	Alcohol <b>26c</b>
0	37	59	0	0
0.5	5	39	44	7
1.0	0	0	66	30
1.5	0	0	62	35
2.0	0	0	42	45

Conditions: 1% [Rh(nbd)<sub>2</sub>BF<sub>4</sub>]/2 (*R*)-**B2**, THF, 40 °C, 20h

Table 3 shows the results obtained by varying the amount of borane (i.e., tmdBH) in reactions set up under a hydrogen atmosphere (i.e., hydrogen balloon). The results indicate that the presence of borane is required for the reaction to proceed; without the borane, only significant amounts of recovered starting material and the corresponding isomerized alkene are obtained as an inseparable mixture (mole ratio determined by <sup>1</sup>H



NMR). Increasing the amount of borane employed leads to more alcohol product **26c** (up to 45% with 2 equiv tmdBH) via hydroboration pathway. To be consistent with the conditions throughout the studies, we chose 2.0 equiv of tmdBH for further investigation on D-labeling (Figure 10).

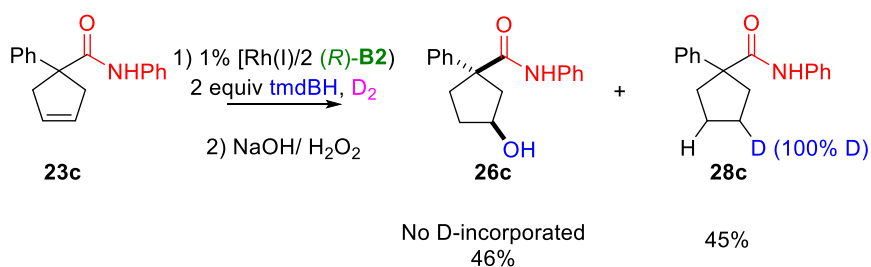
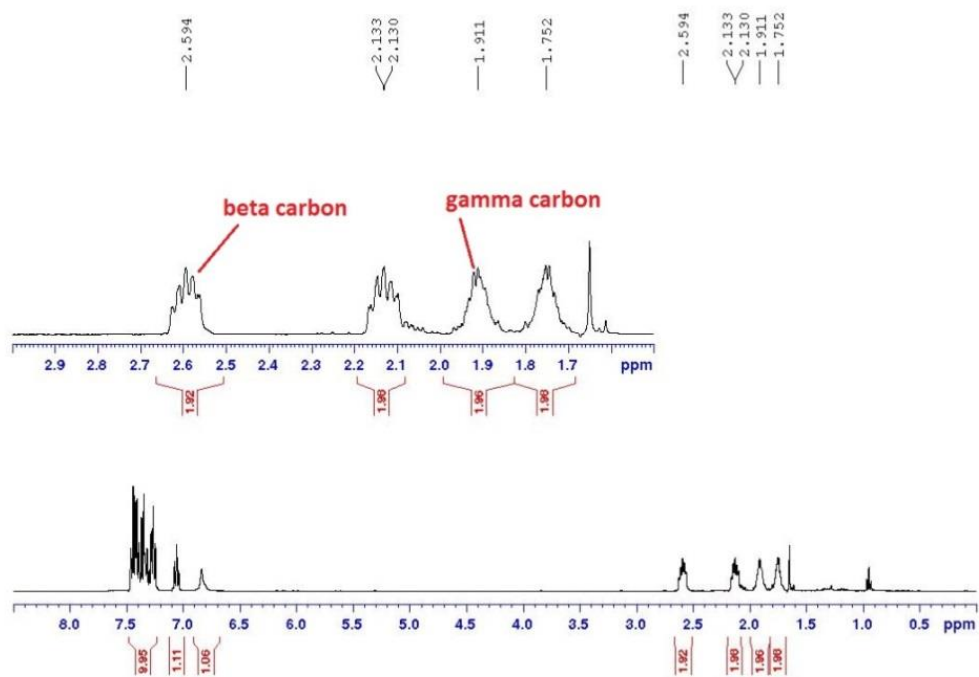


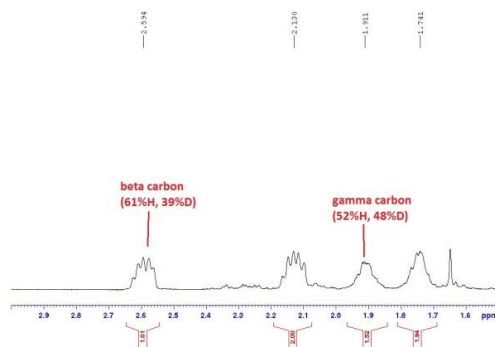
**Figure 10.** Deuterium-labeling studies for CAHB of **23c** using tmdBH under  $D_2$ .

In agreement with the results in Table 3, CAHB of **23c** employing tmdBH under a deuterium atmosphere afford nearly 1:1 ratio of hydroboration:hydrogenation products (i.e., **26c**:**28c**). In addition, there is no deuterium incorporated to **26c**, whereas 100% D is labeled at  $\gamma$ -carbon of reduced product **28c**. The conclusion is based on  $^1H$  NMR analysis; the  $^1H$  NMR spectra of **28c** as well as the deuterated versions using different conditions are shown in Figure 11.

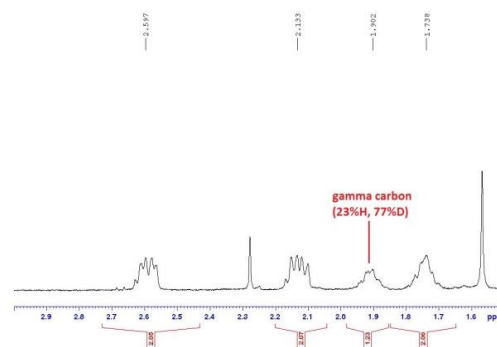
A.  $^1\text{H}$  NMR spectrum of **28c** using tmdBH (no deuterium incorporation)



B.  $^1\text{H}$  NMR spectrum of **28c** using tmdBD under nitrogen (39% deuterium incorporation at  $\beta$ -carbon, 48% deuterium incorporation at  $\gamma$ -carbon)



C.  $^1\text{H}$  NMR spectrum of **28c** using pinBD under nitrogen (no deuterium incorporation at  $\beta$ -carbon, 77% deuterium incorporation at  $\gamma$ -carbon)



D.  $^1\text{H}$  NMR spectrum of **28c** using tmdBH under  $\text{D}_2$  gas (no deuterium incorporation at  $\beta$ -carbon, 100% deuterium incorporation at  $\gamma$ -carbon)

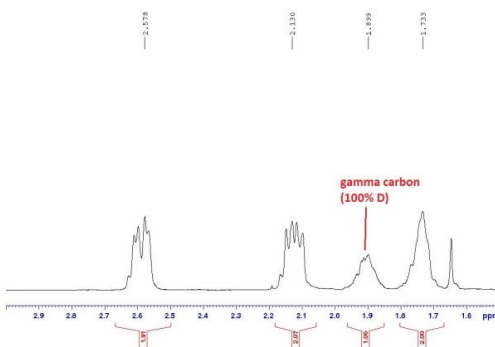


**Figure 11.**  $^1\text{H}$  NMR spectra illustrating the deuterium incorporation of  $\gamma$ -hydroxy product **28c**

Based upon the preliminary results of D-incorporation as well as the crucial role of borane, the proposed simplified mechanistic pathways for the formation of reduced product **28c** under different conditions are illustrated in Figure 12. After alkene chelation to form the common intermediate **A**, under  $\text{D}_2/\text{H}_2$  atmosphere in theory could potentially undergo oxidative addition of  $\text{D}_2/\text{H}_2$  to generate intermediate **B** (path I) to afford the di-deuterated product, but this is not observed. Therefore, path I is eliminated from the

possible pathways. Some precedents in literature on  $\sigma$ -bond metathesis suggest that the reaction employed tmdBH under  $D_2$  could potentially undergo competitive  $D_2$ -sigma bond metathesis leading to 100%-mono-D incorporated reduced product **28c** (path II).<sup>29</sup> Similarly, path III using pinBD under hydrogen is proposed to proceed with  $H_2$ -sigma bond metathesis to produce an enantiomer of mono-D incorporated reduced product **28c** obtained via path II.

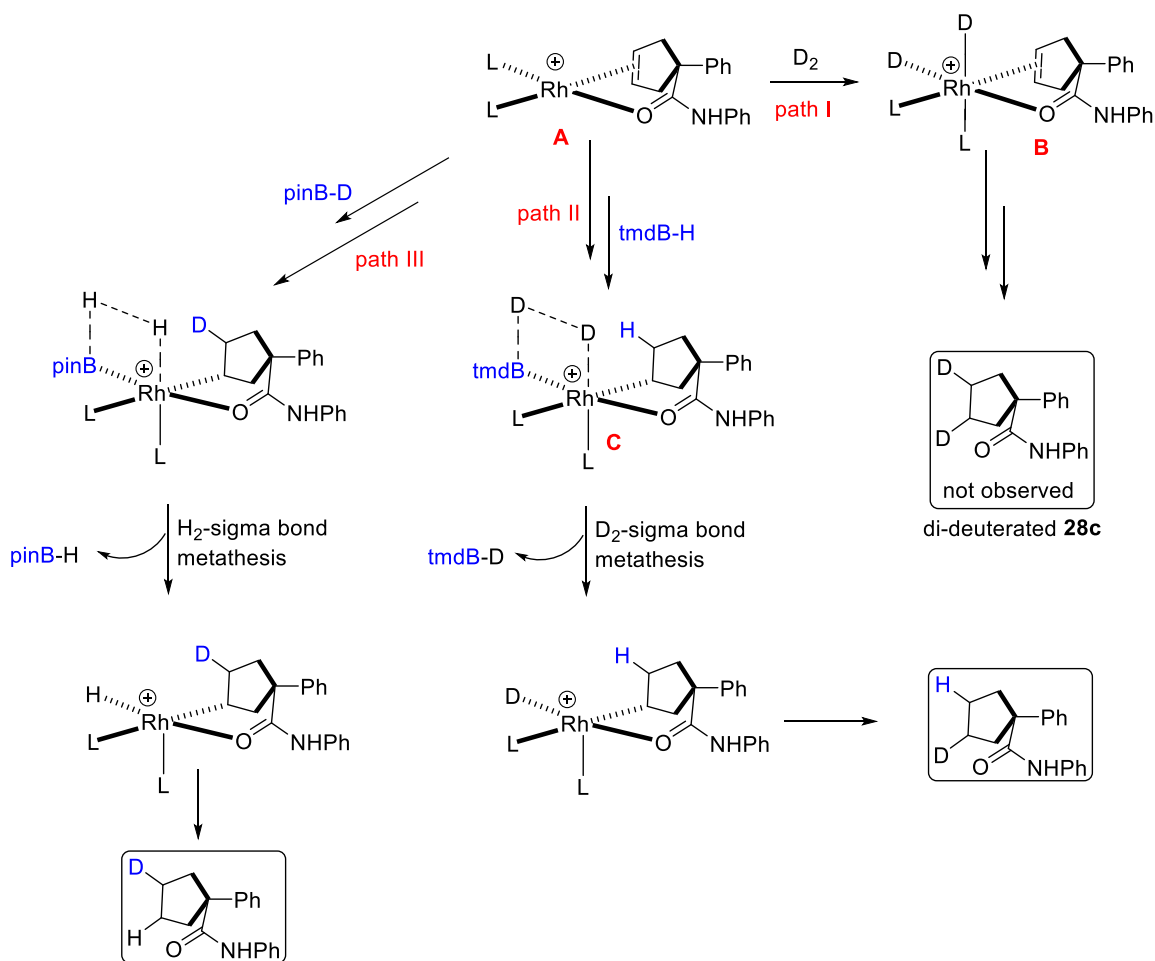


**Figure 12.** Potential hydrogenation pathways.

In addition to the potential hydrogen pathways depicted in Figure 12, the observation of 1:1 reduced:alcohol (i.e., **26c:28c**) could be explained by competing

reductive elimination (to the right) *versus* D<sub>2</sub>-sigma bond metathesis (to the left) as illustrated in Figure 13. These two pathways perhaps undergo with overall the same energies leading to the nearly 1:1 mixture of the mode selectivity products (i.e., hydrogenation *versus* hydroboration).

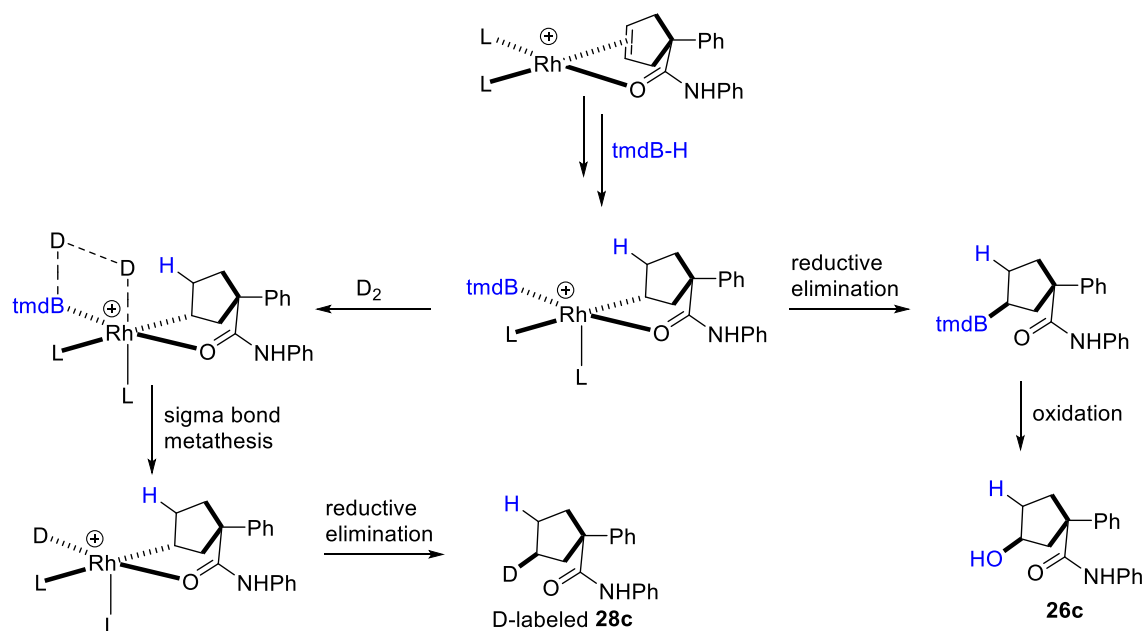


**Figure 13.** Proposed formation of 1:1 mixture **26c:28c** via equal energies of reductive elimination *versus* potential D<sub>2</sub>-sigma bond metathesis

### 3.4 Computational studies – Mechanistic insights into directed CAHB<sup>30</sup>

Chapter 1.5 has introduced some current literature on experimental and computational investigations into the mechanism of CAHB mainly focusing on one point binding substrates (e.g., vinyl arenes).<sup>31-34</sup> Building from those work as well as some preliminary calculations obtained by Dr. Sean M. Smith (University of Nebraska, 2012) in collaboration with Dr. Rhitankar Pal (UNL Chemistry alumni), this section summarizes density functional theory (DFT) calculations on a model compound and catalyst illustrating some current understanding of the mechanistic pathways for CAHB of a two point binding substrate (i.e., an otherwise unactivated alkene whose reaction is promoted by a nearby carbonyl directing group). Though it was later suggested by experimental work that a 1:1 rhodium:ligand complex forms the active catalyst (Chapters 2.2, 2.3, and 3.2), the calculations discussed below focus on a model catalyst complex employing 1:2 rhodium:ligand, which at the time was consistent with the experimental results obtained in the Takacs group.<sup>11,35-37</sup> The 1:1 rhodium:ligand model, however, should be explored in future studies. It should also be noted that the symmetric cyclic alkene (i.e., **23a**) used for DFT calculations differs from other acyclic substrates that the enantiodetermining step reflects *re/si* site selectivity rather than  $\pi$ -facial discrimination.

In Dr. Sean M. Smith's dissertation (University of Nebraska, 2012), models of diastereomeric complexes **A** and **B** were evaluated to see whether the observed enantiomeric product could be predicted (Figure 14). Interestingly, complex **B** which is calculated to be 3.8 kcal/mol lower in energy than **A**, however, it leads to the minor enantiomer (1*S*,3*R*)-**26a**. Those results indicated that the partitioning between the

diastereomeric reaction pathways could not be directly determined from the relative stabilities of complexes **A** and **B**.

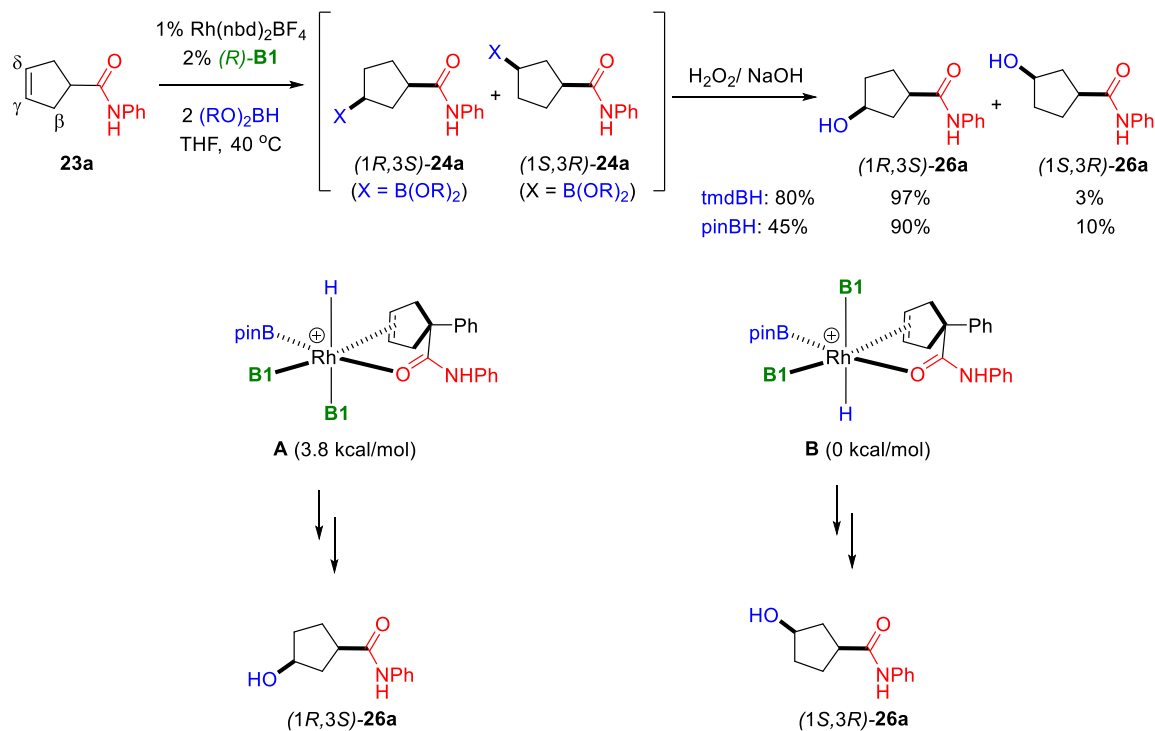


**Figure 14.** Preliminary studies by Dr. Smith found that the higher relative energy complex **A** correlates to a major product observed.

To address the problem, DFT calculations in this dissertation consider the differentiation between migratory insertion into the Rh–H bond (pathway **I**) and into the Rh–B (pathway **II**) bond (Figure 15). Unless otherwise noted, the computation work described herein was done in collaboration with Dr. Zhao-Di Yang (UNL Chemistry alumni), Dr. Rhitankar Pal (UNL Chemistry alumni), Prof. Liberty S. W. Pelter (Purdue University Calumet Chemistry), and Prof. Xiao C. Zeng (UNL Chemistry); Dr. Yang is most responsible for the published computational results presented below. DFT calculations for the model reaction are carried out using B3LYP method implemented in the Gaussian 09 package;<sup>38</sup> gradient optimizations were done with LANL2DZ for Rh

atom and  $6-31+G^{**}$  for all non-metal atoms. In addition, the sum of the free energies of all reactants (i.e.,  $[\text{Rh}(\mathbf{B10})_2\text{S}_2]^+ + \text{substrate } \mathbf{23a} + \text{pinBH}$ , where  $\text{S} = \text{solvent} = \text{THF}$ ) is set to zero.

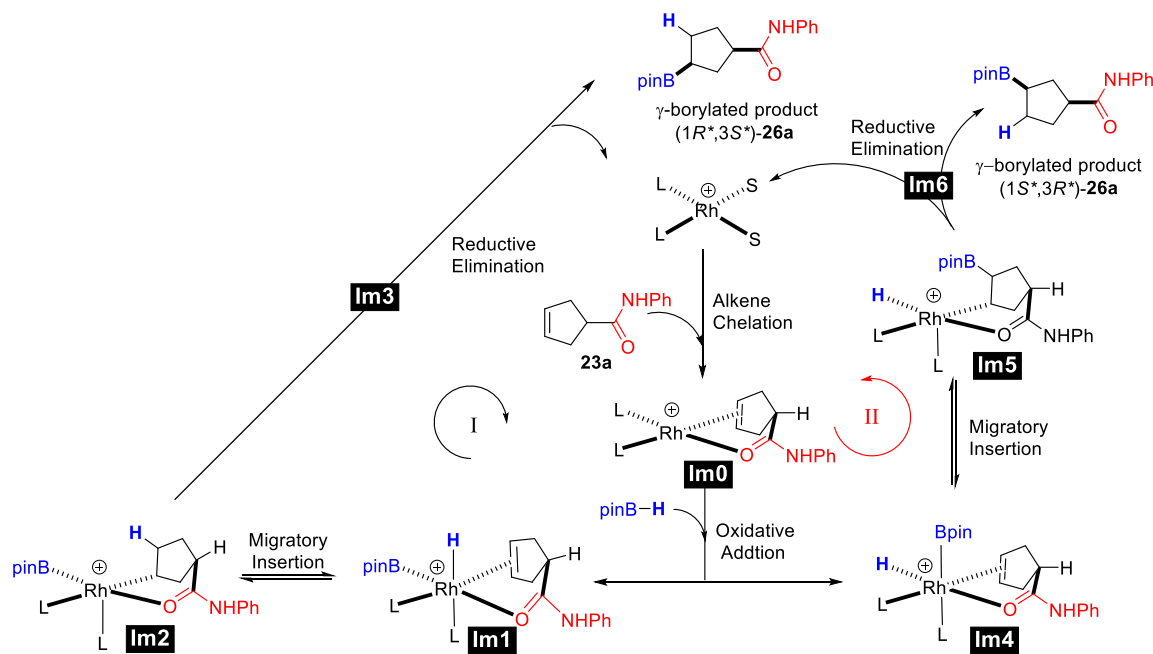


**Figure 15.** Proposed mechanistic pathways to isomeric products  $(1R^*,3S^*)$ - and  $(1S^*,3R^*)$ -**26a** are differentiated via migratory insertion into Rh–H versus Rh–B bonds. Adapted with permission from reference 30. Copyright (2014) American Chemical Society; ACS AuthorChoice.

Figure 15 shows the proposed competing pathways for the model reaction. The model reaction uses an achiral ligand and therefore the sense of asymmetric induction is not under investigation here, just the potential competing pathways. After alkene chelation of **23a** to a cationic rhodium(I) complex, the initial **Intermediate (Im0)** is formed. **pinBH** can be added either parallel or perpendicular to form **Im1** or **Im4**, respectively. **Im1** is aligned to undergo migratory insertion into the Rh–H bond to afford **Im2**. Reductive elimination via **Im3** affords the major isomer  $(1R^*,3S^*)$ -**26a** and regenerate



the active catalyst, **Im4** proceeds with similar pathways with differentiation in migratory insertion into Rh–B bond to form **Im5**, **Im6**, and finally the minor isomer (1*S*\*,3*R*\*)-**26a**. As a recall, (1*R*\*,3*S*\*) and (1*S*\*,3*R*\*) are for denoting the relative but not the absolute configuration as the ligand **B10** employed in this computational study is achiral.<sup>39</sup> The energy profiles of these two pathways (i.e., pathways **I** and **II**) are depicted in Figure 16.

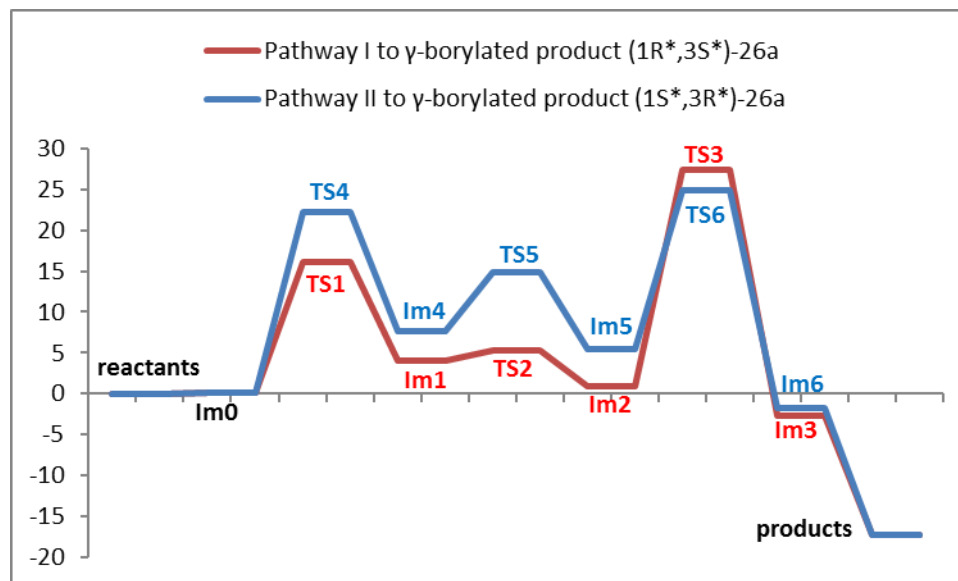


**Figure 16.** Comparison of the potential energy profiles for pathway **I** and **II**.

Although pathway **I** undergoes with overall lower energies to afford the major  $\gamma$ -borylated product (1*R*\*,3*S*\*)-**26a**, the transition state of reductive elimination step (i.e., **TS3**) with potentially high energy (i.e., 26.5 kcal/mol) make it difficult for the pinB group to migrate directly to  $\delta$ -carbon. The high energy profile of **TS3** is proposed due to the agostic interaction between Rh–HC $\delta$ . In order to enhance the reductive elimination step, we proposed other two possible pathways in which pathway **I-1** with the addition of THF and pathway **I-2** involving an unusual amide bond rotation both having ability to break the high energy barrier Rh–HC $\delta$  agostic interaction (Figure 17).

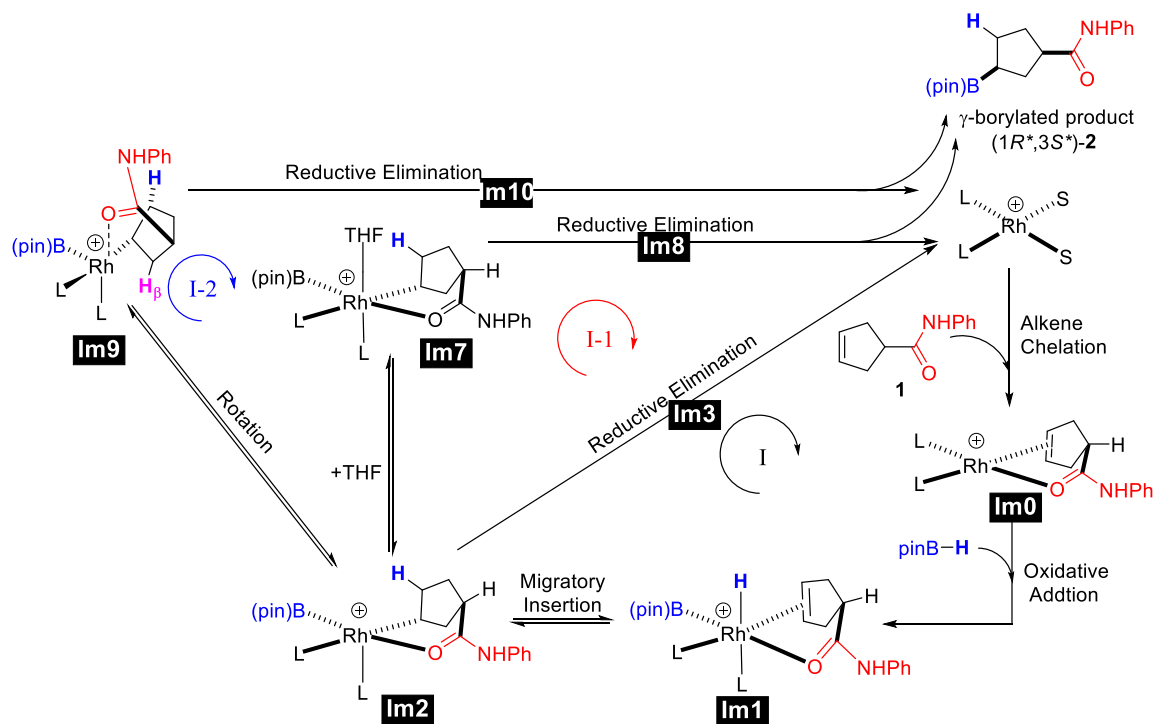


**Figure 17.** Proposed other mechanistic pathways to major  $\gamma$ -borylated product  $(1R^*,3S^*)$ -**26a**. Adapted with permission from reference 30. Copyright (2014) American Chemical Society; ACS AuthorChoice.

As illustrated in Figure 17, starting from **Im2**, pathway **I-1** with the reintroduction of THF to form a stable hexacoordinate octahedral complex **Im7** (**TS7** energy is only 7.82 kcal/mol from **Im2**) which then can undergo reductive elimination to produce  $(1R^*,3S^*)$ -**26a** via **Im8**. Another alternative pathway **I-2** shows that the Rh-coordinated carbonyl group of the amide functionality in **Im2** rotates approximately 78 degree from an equatorial to an axial position to afford **Im9** (**TS9** energy is approximately the same (7.74 kcal/mol) as THF addition in pathway **I-1**). In addition, the long Rh–H distances in the two proposed alternative pathways **I-1** and **I-2** (3.092 and 3.057 Å, respectively, as compared to 1.944 Å in **Im2**) indicate that Rh–HC<sub>8</sub> agostic interaction has been broken. The energy profiles for these alternative pathways are shown in Figure 18.

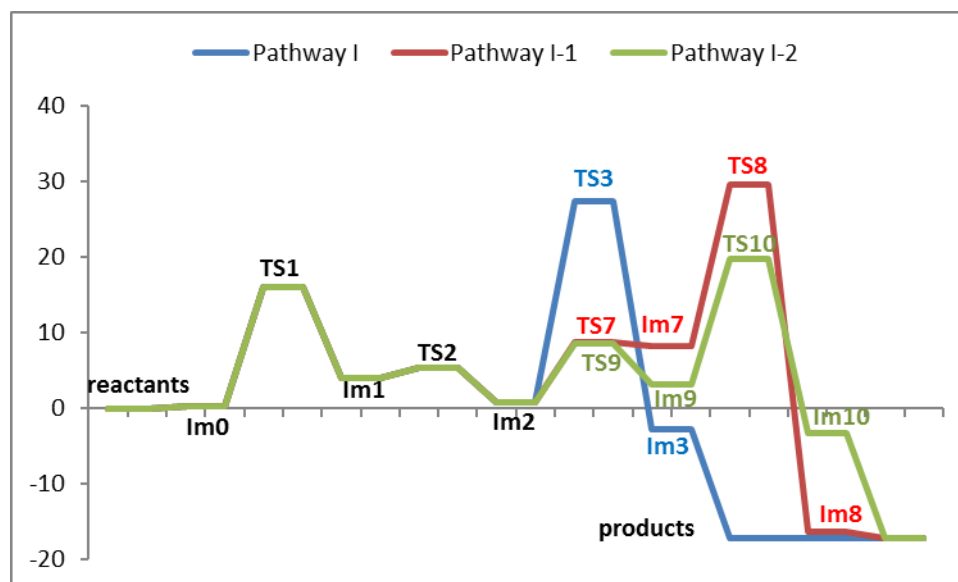


**Figure 18.** Comparison of the potential energy profiles for pathway **I**, **I-1** and **I-2**.

The overall energy diagrams of possible pathways leading to (1*R*\*,3*S*\*)-**26a** suggest that pathway **II-2** with unusual amide bond rotation is the most favorable pathway. However, the amide rotation also opens accessibility to  $\beta$ -hydride elimination accounting for the competing formation of  $\beta$ -borylated product **27** observed experimentally in some cases (Figure 19). According to DFT data, **III-2** starting from **Im9** is an overall lower energy pathway as compared to **III-1** beginning from **Im2** for the formation of **Im14** and **Im12**, respectively; these two intermediates can potentially afford the isomerized alkene of **23a**; DFT calculations for the beyond stages have not been obtained.

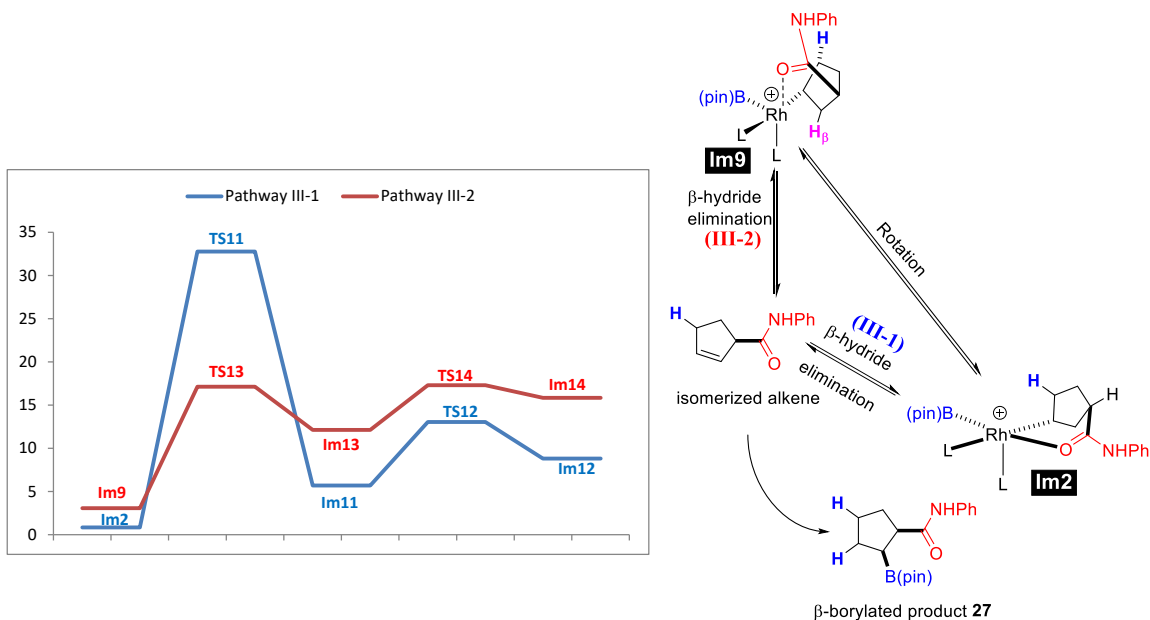


**Figure 19.** Proposed pathways **III-1** and **III-2** for the formation of isomerized alkene leading to minor regioisomer  $\beta$ -borylated product **27** and the comparison of the potential energy profiles. Adapted with permission from reference 30. Copyright (2014) American Chemical Society; ACS AuthorChoice.

It is worth noting that the highest energy barrier of pathway **III-2** (i.e., **TS14** = 17.30 kcal/mol), the major pathway leading to the formation of isomerized alkene then potentially the minor regioisomer  $\beta$ -borylated product **27**, is even ca. 2.5 kcal/mol lower than the highest energy barrier of the most favorable pathway **I-2** (i.e., **TS10** = 19.84 kcal/mol). The preliminary results suggest that the calculation beyond **Im14** must be obtained for the definite answer since CAHB of the isomerized alkene can also potentially give  $\gamma$ -borylated **26** as the major product. Initial experimental results revealed that CAHB of isomerized **23b** still afford  $\gamma$ -borylated **26b** as the major product with somewhat lower enantioselectivity (Figure 20).

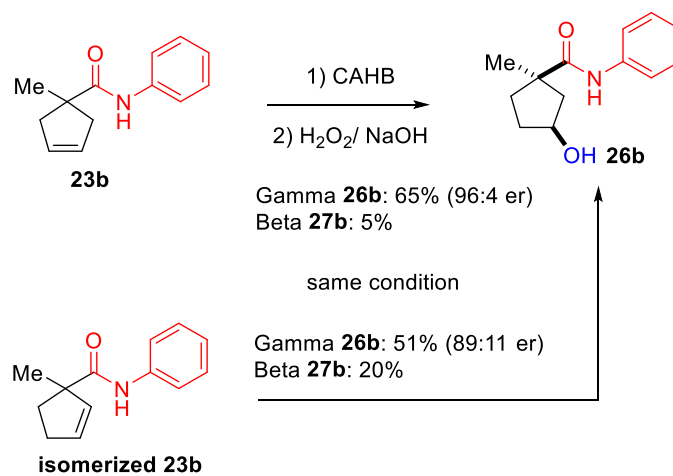


**Figure 20.** CAHB of **23b** versus isomerized **23b**: both alkenes undergo CAHB leading to the major  $\gamma$ -borylated product. *CAHB/oxidation conditions as shown in Figure 7.*

### 3.5 Concluding remarks

In complementary to literature reports on CAHB of cyclopropenes, the experimental work in this Chapter described the only enantioselective desymmetrization via CAHB of cyclopentene-based substrates. The method allows the accessibility to a series of secondary  $\gamma$ -boronic esters or alcohols (after oxidation) in conjunction with the stereogenic  $\alpha$ -quaternary carbon centers bearing alkyl-, aryl-, or trifluoromethyl side chains in the same molecule. Substrates bearing two alkene moieties undergo essentially selective CAHB for endocyclic alkenes. Though the chiral substrate with chiral center on *N*-amide side chain only provides modest stereoselectivity, its CAHB also proceeds with high diastereoselectivity (i.e., solely *cis* product) and yield; further transformation to the corresponding trifluoroborate salt is used to determine the reaction configuration via x-ray crystallographic analysis.

Preliminary results of deuterium-labeling studies suggest Rh–H(D) migratory insertion into either C=C alkene starting material or isomerized alkene is irreversible. Some simplified mechanistic pathways of the major competitive hydrogenation mode selectivity are also proposed based upon deuterium-labeling data.

Though experimental results (i.e., essentially linear relationship) suggest that the model 1:1 rhodium:ligand should also be theoretically considered, DFT calculations applied 1:2 rhodium:ligand based upon early studies in the group. The computational work supports the essential role of a directing group in the two-point binding motif leading to the solely *cis* product and in agreement with experimental studies. Migratory insertion of the coordinated alkene into the Rh–H to generate the major isomer  $\gamma$ -borylated (1*R*\*,3*S*\*)-**26a** is more favorable than Rh–B bond suggesting the *re/si* site

selectivity is responsible for enantioselective desymmetrization when chiral ligand is experimentally applied. Among the potential pathways leading to (1*R*\*,3*S*\*)-**26a**, **I-2** involving unusual amide bond rotation is found to be the most favorable pathway with reductive elimination is the rate-determining step. Additionally, **I-2** can potentially undergo  $\beta$ -hydride elimination to generate the isomerized alkene which can subsequently afford the minor regioisomer  $\beta$ -borylated product **27**; however, DFT calculations beyond this stage have not been obtained yet.

### 3.6 References

- [1] Fernández-Pérez, H.; Etayo, P.; Lao, J. R.; Núñez-Rico, J. L.; Vidal-Ferran, A., “Catalytic Enantioselective Reductive Desymmetrization of Achiral and *Meso* Compounds,” *Chem. Commun.*, **2013**, *49*, 10666–10675.
- [2] Villegas, M. D. D.; Gálves, J. A.; Etayo, P.; Badorrey, R.; López-R.-D.-V., P., “Recent advances in enantioselective organocatalyzed anhydride desymmetrization and its application to the synthesis of valuable enantiopure compounds,” *Chem. Soc. Rev.*, **2011**, *40*, 5564–5587.
- [3] Enríquez-G., A.; Kündig, E. P., “Desymmetrisation of *Meso*-Diols Mediated by Non-Enzymatic Acyl Transfer Catalysts,” *Chem. Soc. Rev.*, **2012**, *41*, 7803–7831.
- [4] García-U., E.; Alfonso, I.; Gotor, V., “Update 1 of: Enantioselective Enzymatic Desymmetrizations in Organic Synthesis,” *Chem. Rev.*, **2011**, *111*, PR110–PR180.
- [5] Johnson, J. B.; Rovis, R., “Enantioselective Cross-Coupling of Anhydrides with Organozinc Reagents: The Controlled Formation of Carbon–Carbon Bonds through the Nucleophilic Interception of Metalacycles,” *Acc. Chem. Res.*, **2008**, *41*, 327–338.
- [6] Zeng, X.-P.; Cao, Z.-Y., Cao, Wang, Y.-H.; Zhou, F.; Zhou, J., “Catalytic Enantioselective Desymmetrization Reactions to All-Carbon Quaternary Stereocenters,” *Chem. Rev.*, **2016**, *116*, 7330–7396.
- [7] Rubina, M.; Rubin, M.; Gevorgyan, V., “Catalytic Enantioselective Hydroboration of Cyclopropenes,” *J. Am. Chem. Soc.*, **2003**, *125*, 7198–7199.
- [8] Tian, B.; Liu, Q.; Tong, X.; Tian, P.; Lin, G.-Q., “Copper(I)-Catalyzed Enantioselective Hydroboration of Cyclopropenes: Facile Synthesis of Optically Active Cyclopropylboronates,” *Org. Chem. Front.*, **2014**, *1*, 1116–1122.
- [9] Parra, A.; Amenós, L.; Guisán-Ceinos, M.; López, A.; Ruano, J. L. G.; Tortosa, M., “Copper-Catalyzed Diastereo- and Enantioselective Desymmetrization of Cyclopropenes: Synthesis of Cyclopropylboronates,” *J. Am. Chem. Soc.*, **2014**, *136*, 15833–15836.
- [10] Hoang, G. L.; Yang, Z.-D.; Smith, S. M.; Pal, R.; Miska, J. L.; Pérez, D. E.; Petler, L. S. W.; Zeng, X. C.; Takacs, J. M., “Enantioselective Desymmetrization via Carbonyl-Directed Catalytic Asymmetric Hydroboration and Suzuki–Miyaura Cross-Coupling,” *Org. Lett.*, **2015**, *17*, 940–943.



- [11] Smith, S. M.; Takacs, J. M., "Remarkable Levels of Enantioswitching in Catalytic Asymmetric Hydroboration," *Org. Lett.*, **2010**, *12*, 4612–4615.
- [12] Escorihuela, J.; Burguete, M. I.; Luis, S. V., "New Advances in Dual Stereocontrol for Asymmetric Reactions," *Chem. Soc. Rev.*, **2013**, *42*, 5595–5617.
- [13] Satyanarayana, T.; Abraham, S.; Kagan, H. B., "Nonlinear Effects in Asymmetric Catalysis," *Angew. Chem., Int. Ed.*, **2009**, *48*, 456–494.
- [14] Blackmond, D. G., "Kinetic Aspects of Nonlinear Effects in Asymmetric Catalysis," *Acc. Chem. Res.*, **2000**, *33*, 402–411.
- [15] Zhao, L.; Ma, Y.; Duan, W.; He, F.; Chen, J.; Song, C., "Asymmetric  $\beta$ -Boration of  $\alpha,\beta$ -Unsaturated *N*-Acyloxazolidinones by [2.2]Paracyclophane-Based Bifunctional Catalyst," *Org. Lett.*, **2012**, *14*, 5780–5783.
- [16] Molander, G. A.; Shin, I.; Jean-Gérard, L., "Palladium-Catalyzed Suzuki–Miyaura Cross-Coupling Reactions of Enantiomerically Enriched Potassium  $\beta$ -Trifluoroboratoamides with Various Aryl- and Hetaryl Chlorides," *Org. Lett.*, **2010**, *12*, 4384–4387.
- [17] Evans, D. A.; Fu, G. C., "The Rhodium-Catalyzed Hydroboration of Olefins: A Mechanistic Investigation," *J. Org. Chem.*, **1990**, *55*, 2280–2282.
- [18] Evans, D. A.; Fu, G. C.; Anderson, B. A., "Mechanistic Study of The Rhodium(I)-Catalyzed Hydroboration Reaction," *J. Am. Chem. Soc.*, **1992**, *114*, 6679–6685.
- [19] Edwards, D. R.; Hleba, Y. B.; Lata, C. J.; Calhoun, L. A.; Crudden, C. M., "Regioselectivity of the Rhodium-Catalyzed Hydroboration of Vinyl Arenes: Electronic Twists and Mechanistic Shifts," *Angew. Chem., Int. Ed.*, **2007**, *46*, 7799–7802.
- [20] Palmer, W. N.; Diao, T.; Pappas, I.; Chirik, P., "High-Activity Cobalt Catalysts for Alkene Hydroboration with Electronically Responsive Terpyridine and  $\alpha$ -Diimine Ligands," *ACS Catal.*, **2015**, *5*, 622–626.
- [21] Hu, N.; Zhao, G.; Zhang, Y.; Liu, X.; Li, G.; Tang, W., "Synthesis of Chiral  $\alpha$ -Amino Tertiary Boronic Esters by Enantioselective Hydroboration of  $\alpha$ -Arylenamides," *J. Am. Chem. Soc.*, **2015**, *137*, 6746–6749.

- [22] Zhang, L.; Peng, D.; Leng, X.; Huang, Z., “Iron-Catalyzed, Atom-Economical, Chemo- and Regioselective Alkene Hydroboration with Pinacolborane,” *Angew. Chem., Int. Ed.*, **2013**, *52*, 3676–3680.
- [23] Obligacion, J. V.; Chirik, P. J., “Highly Selective Bis(imino)pyridine Iron-Catalyzed Alkene Hydroboration,” *Org. Lett.*, **2013**, *15*, 2680–2683.
- [24] Fritschi, C. B.; Wernitz, S. M.; Vogels, C. M.; Shaver, M. P.; Decken, A.; Bell, A.; Westcott, S. A., “4,4,5,5-Tetraphenyl-1,3,2-dioxaborolane: A Bulky Borane for the Transition Metal Catalysed Hydroboration of Alkenes,” *Eur. J. Inorg. Chem.*, **2008**, 779–785.
- [25] Lillo, V.; Fernandez, E.; Segarra, A. M., “Catalytic Asymmetric Hydroboration of Heterofunctional Allylic Substrates: An Efficient Heterogenized Version,” *Tetrahedron: Asymmetry*, **2007**, *18*, 911–914.
- [26] Caballero, A.; SaboEtienne, S., “Ruthenium-Catalyzed Hydroboration and Dehydrogenative Borylation of Linear and Cyclic Alkenes with Pinacolborane,” *Organometallics*, **2007**, *26*, 1191–1195.
- [27] Coapes, R. B.; Souza, F. E. S.; Thomas, R. L.; Hall, J. J.; Marder, T. B., “Rhodium Catalysed Dehydrogenative Borylation of Vinylarenes and 1,1-Disubstituted Alkenes without Sacrificial Hydrogenation—A Route to 1,1-Disubstituted Vinylboronates,” *Chem. Commun.*, **2003**, 614–615.
- [28] Shoba, V. M.; Thacker, N. C.; Bochat, A. J.; Takacs, J. M., “Synthesis of Chiral Tertiary Boronic Esters by Oxime-Directed Catalytic Asymmetric Hydroboration,” *Angew. Chem., Int. Ed.*, **2016**, *55*, 1465–1469.
- [29] Perutz, R. N.; Sabo-Etienne, S., “The  $\sigma$ -CAM Mechanism:  $\sigma$ -Complexes as the Basis of  $\sigma$ -Bond Metathesis at Late-Transition-Metal Centers,” *Angew. Chem., Int. Ed.*, **2007**, *46*, 2578–2592.
- [30] Yang, Z.-D.; Pal, R.; Hoang, G. L.; Takacs, J. M., “Mechanistic Insights into Carbonyl-Directed Rhodium-Catalyzed Hydroboration: ab Initio Study of a Cyclic  $\gamma,\delta$ -Unsaturated Amide,” *ACS Catal.*, **2014**, 763–773.
- [31] Musaev, D. G.; Mebel, A. M.; Morokuma, K., “An ab Initio Molecular Orbital Study of the Mechanism of the Rhodium(I)-Catalyzed Olefin Hydroboration Reaction,” *J. Am. Chem. Soc.*, **1994**, *116*, 10693–10702.

[32] Dorigo, A. E.; Schleyer, P. v. R., “An Ab Initio Investigation of the Rh<sup>I</sup>-Catalyzed Hydroboration of C=C Bonds: Evidence for Hydrogen Migration in the Key Step,” *Angew. Chem., Int. Ed.*, **1995**, *34*, 115–118.

[33] Widauer, C.; Grützmacher, H.; Ziegler, T., “Comparative Density Functional Study of Associative and Dissociative Mechanisms in the Rhodium(I)-Catalyzed Olefin Hydroboration Reactions,” *Organometallics*, **2000**, *19*, 2097–2107.

[34] Segarra, A. M.; Daura-Oller, E.; Claver, C.; Poblet, J. M.; Bo, C.; Fernández, E., “In Quest of Factors That Control the Enantioselective Catalytic Markovnikov Hydroboration/ Oxidation of Vinylarenes,” *Chem. Eur. J.*, **2004**, *10*, 6456 – 6467.

[35] Smith, S. M.; Hoang, G. L.; Pal, R.; Khaled, M. O. B.; Pelter, L. S. W.; Zeng, X. C.; Takacs, J. M., “ $\gamma$ -Selective Directed Catalytic Asymmetric Hydroboration of 1,1-Disubstituted Alkenes,” *Chem. Commun.*, **2012**, *48*, 12180–12182.

[36] Smith, S. M.; Thacker, N. C.; Takacs, J. M., “Efficient Amide-Directed Catalytic Asymmetric Hydroboration,” *J. Am. Chem. Soc.*, **2008**, *130*, 3734–3735.

[37] Smith, S. M.; Takacs, J. M., “Amide-Directed Catalytic Asymmetric Hydroboration of Trisubstituted Alkenes,” *J. Am. Chem. Soc.*, **2010**, *132*, 1740–1741.

[38] Frisch, M. J.; Trucks, G. W.; Schlegel, H. B.; Scuseria, G. E.; Robb, M. A.; Cheeseman, J. R.; Scalmani, G.; Barone, V.; Mennucci, B.; Petersson, G. A.; Nakatsuji, H.; Caricato, M.; Li, X.; Hratchian, H. P.; Izmaylov, A. F.; Bloino, J.; Zheng, G.; Sonnenberg, J. L.; Hada, M.; Ehara, M.; Toyota, K.; Fukuda, R.; Hasegawa, J.; Ishida, M.; Nakajima, T.; Honda, Y.; Kitao, O.; Nakai, H.; Vreven, T.; Montgomery, J. A., Jr.; Peralta, J. E.; Ogliaro, F.; Bearpark, M.; Heyd, J. J.; Brothers, E.; Kudin, K. N.; Staroverov, V. N.; Kobayashi, R.; Normand, J.; Raghavachari, K.; Rendell, A.; Burant, J. C.; Iyengar, S. S.; Tomasi, J.; Cossi, M.; Rega, N.; Millam, J. M.; Klene, M.; Knox, J. E.; Cross, J. B.; Bakken, V.; Adamo, C.; Jaramillo, J.; Gomperts, R.; Stratmann, R. E.; Yazyev, O.; Austin, A. J.; Cammi, R.; Pomelli, C.; Ochterski, J. W.; Martin, R. L.; Morokuma, K.; Zakrzewski, V. G.; Voth, G. A.; Salvador, P.; Dannenberg, J. J.; Dapprich, S.; Daniels, A. D.; Farkas, O.; Foresman, J. B.; Ortiz, J. V.; Cioslowski, J.; Fox, D. J. Gaussian, Inc., Wallingford, CT, 2009.

[39] Cross, L. W.; Klyne, W., “Iupac Commission on Nomenclature of Organic Chemistry. Rules for the Nomenclature of Organic Chemistry. Section E: Stereochemistry (Recommendations 1974),” *Pure. Appl. Chem.*, **1976**, *45*, 11–30.

CHAPTER 4: APPLICATIONS OF CHIRAL BORONIC ESTERS IN  
STEREOSPECIFIC TRANSFORMATIONS AND UNDERSTANDING THE  
STEREOCHEMICAL ASPECTS IN COORDINATION-DIRECTED PALLADIUM-  
CATALYZED CROSS-COUPPLING REACTIONS

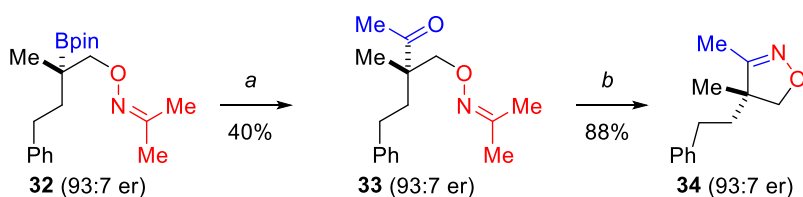
#### 4.1 Stereoretentive transformations of chiral boronic esters

One of the main reasons for the growth in the development of enantioselective preparation of organoboranes over the last couple decades is their subsequent use in stereospecific transformations.<sup>1</sup> The utility of the chiral boronic esters obtained via CAHB described in Chapters 2 and 3 will be highlighted herein in that context. The stereochemical course of the chemical reactions shown in this section is retention of configuration (i.e., stereoretention) via stereoretentive 1,2-metallate shift (see Chapter 1 for a representative mechanism). In addition, with the directing group in the same molecule, it will open opportunities for functionalized organoboranes. While the development of efficient methods for the CAHB of unactivated alkenes is a popular and worthwhile goal, CAHB of functionalized substrates directly afford functionalized organoboranes which are often the ultimate goal.

With respect to the synthetic utility of functionalized organoboranes, the Takacs group converted oxime ether- and phosphonate-containing chiral boronic esters to several targets of interest by utilizing both the directing group functionality as well as the C–B bond in subsequent reactions (Figure 1).<sup>2,3</sup> In case of oxime ether (Figure 1A),<sup>2</sup> treatment of **32** with lithiated ethyl vinyl ether followed by hydrolysis generates keto oxime **33**. The oxime ether is then treated with acid to yield 4,4,5-trisubstituted isoxazoline **34** via

cyclization. The methodology developed by Shoba and Takacs introduces the first example of a chiral 4,4,5-trisubstituted isoxazoline; the structure complements the known 5,5-disubstituted isoxazolines found in many biologically active natural products.<sup>4</sup> Recently, Chakrabarty and Takacs introduced a formal total synthesis of the natural product (*S*)-(+)-bakuchiol methyl ether **38** via manipulation of the phosphonate-containing boronic ester **35** (Figure 1B).<sup>3</sup> The work highlights the synthetic usefulness of not only boronic ester moiety but also the phosphonate functionality which is used for olefination.

A. Synthesis of 4,4,5-trisubstituted isoxazoline via bi-functionalizations of oxime ether-containing boronic esters



B. Synthesis of (*S*)-(+)-Bakuchiol methyl ether via bi-functionalizations of phosphonate-containing boronic esters

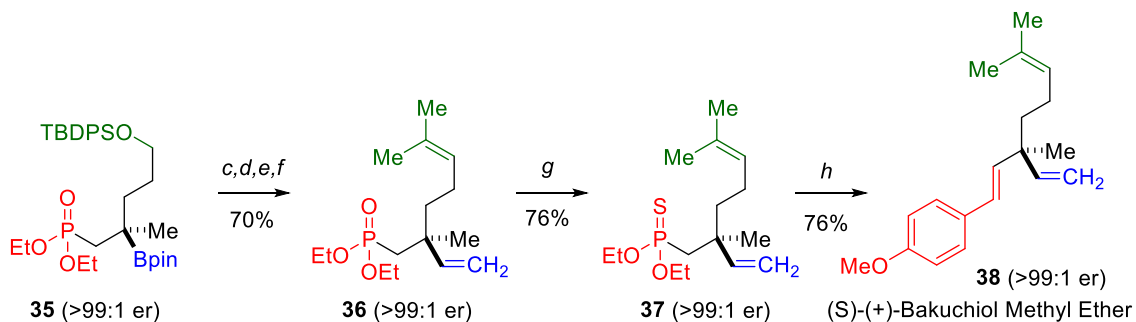


**Figure 1.** Bi-functionalizations of oxime ether- and phosphonate containing chiral boronic esters

*Conditions:* (a) (i)  $\text{LiC}(\text{OEt})=\text{CH}_2$ ,  $-78^\circ\text{C}$ , THF, (ii)  $\text{I}_2$ , (iii) NaOMe, MeOH; (b) HCl/H<sub>2</sub>O/MeOH (1:1:1),  $40^\circ\text{C}$ ; (c) (i)  $\text{CH}_2=\text{CHMgBr}$ , THF,  $-78^\circ\text{C}$ , (ii)  $\text{I}_2$ , MeOH,  $-78^\circ\text{C}$ , (iii) NaOMe, MeOH, (iv)  $\text{Na}_2\text{S}_2\text{O}_3$  (aq.); (d) TBAF, H<sub>2</sub>O; (e) DMSO, Py.SO<sub>3</sub>, Hünig's base; (f)  $(\text{CH}_3)_2\text{CH}=\text{PPh}_3$ ; (g) Lawesson's Reagent, Toluene Reflux; (h) *n*BuLi, 4-methoxy-benzaldehyde.

Among the stereospecific transformations of C–B bond, the stereoretentive C–B to C–O oxidation is the most common and, given the relative ease of characterizing

alcohols, has until recently been the standard way to analyze the products of CAHB. Oxidations of boronic esters bearing no or relatively robust functional groups (e.g., phenyl amides, benzyl amides) are usually carried out under rather harsh oxidation conditions, such as basic aqueous hydrogen peroxide (aq.  $\text{H}_2\text{O}_2/\text{NaOH}$ ).<sup>5</sup> However, with compounds containing more labile functional groups (e.g., esters), milder conditions employing sodium perborate should be used to keep the other functionality intact.<sup>6</sup> For example, treatment  $\gamma$ -borylated esters with aq.  $\text{H}_2\text{O}_2$  affords the labile  $\gamma$ -hydroxyester which spontaneously lactonizes to generate the  $\gamma$ -lactone. This was used in collaboration with Dr. Sean M. Smith as shown in Figure 2.<sup>7</sup> CAHBs of  $\beta$ -benzyl substituted **39a** and **39b** under standard conditions (see Chapter 2.1 for more details) afford  $\gamma$ -borylated *tert*-

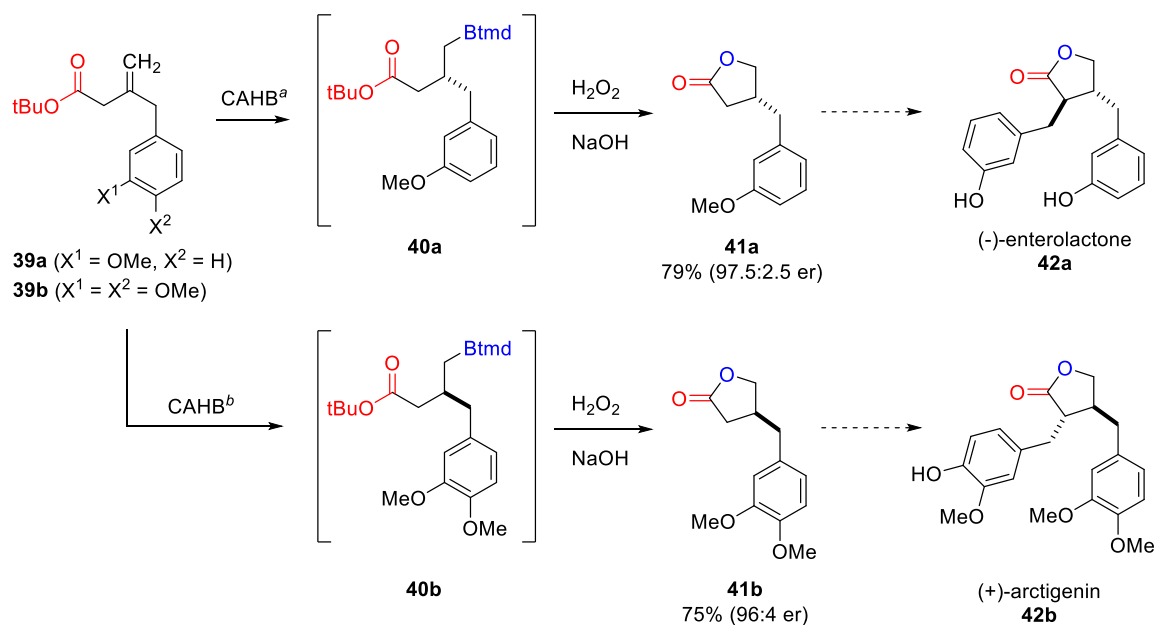


**Figure 2.** Bi-functionalizations of *tert*-butylester containing chiral boronic esters.

Reproduced from Ref. 7 with permission from The Royal Society of Chemistry.

CAHB Conditions: <sup>a</sup> 1%  $[\text{Rh}(\text{nbd})_2\text{BF}_4]/2$  (*R,R*)-**TI**], 2 equiv *tmdBH*, THF, 40 °C. <sup>b</sup> 1%  $[\text{Rh}(\text{nbd})_2\text{BF}_4]/2$  (*S,S*)-**TI**], 2 equiv *tmdBH*, THF, 40 °C.

butylester **40a** and **40b**; in *situ* treatment with aq. H<sub>2</sub>O<sub>2</sub> affords  $\beta$ -benzyl substituted  $\gamma$ -lactones **41a** and **41b** in high yield (75–79%) and enantioselectivity (96:4–97.5:2.5 er). These  $\beta$ -benzyl substituted  $\gamma$ -lactones have been used in syntheses of the lignan natural products (–)-enterolactone and (+)-arctigenin via diastereoselective alkylation.<sup>8</sup>

$\gamma$ -Borylated boronic ester bearing Weinreb amide functionality also undergoes CAHB/ oxidation to produce a  $\gamma$ -lactone in the same manner. Recently, we reported the formation of the known 5-substituted  $\gamma$ -lactone **13**<sup>9</sup> by oxidation of  $\gamma$ -borylated Weinreb amide **8c** to determine the absolute configuration of  $\gamma,\delta$ -unsaturated amide **7** produced by CAHB (Figure 3A; also see Chapter 2.2).<sup>10a</sup> In the same report, we highlight some useful stereospecific transformations of boronic esters **8b–d** many of which utilize both the C–B bond and the amide functionality (Figure 3). Compound **8d** underwent BCl<sub>3</sub>-assisted amination with benzyl azide under conditions reported by Knoche<sup>11</sup> to form the  $\gamma$ -amino acid derivative **43d** (Figure 3B). Using the same amination conditions with phenyl azide afforded the corresponding *N*-phenyl  $\gamma$ -amino acid en route to the 5-substituted- $\gamma$ -lactam **44** after acid catalyzed cyclization (Figure 3C). Aggarwal<sup>12</sup> has developed several methods using main group organometallic reagents to effect stereoretentive C–B to C–C bond construction. Two of these were successfully applied to generate **45d** and **46b** (Figure 3D and 3E). Benzyl amide derivative **8b** was efficiently converted to 1,4-aminoalcohol **47b** after oxidation of the C–B bond followed by amide reduction with LAH.

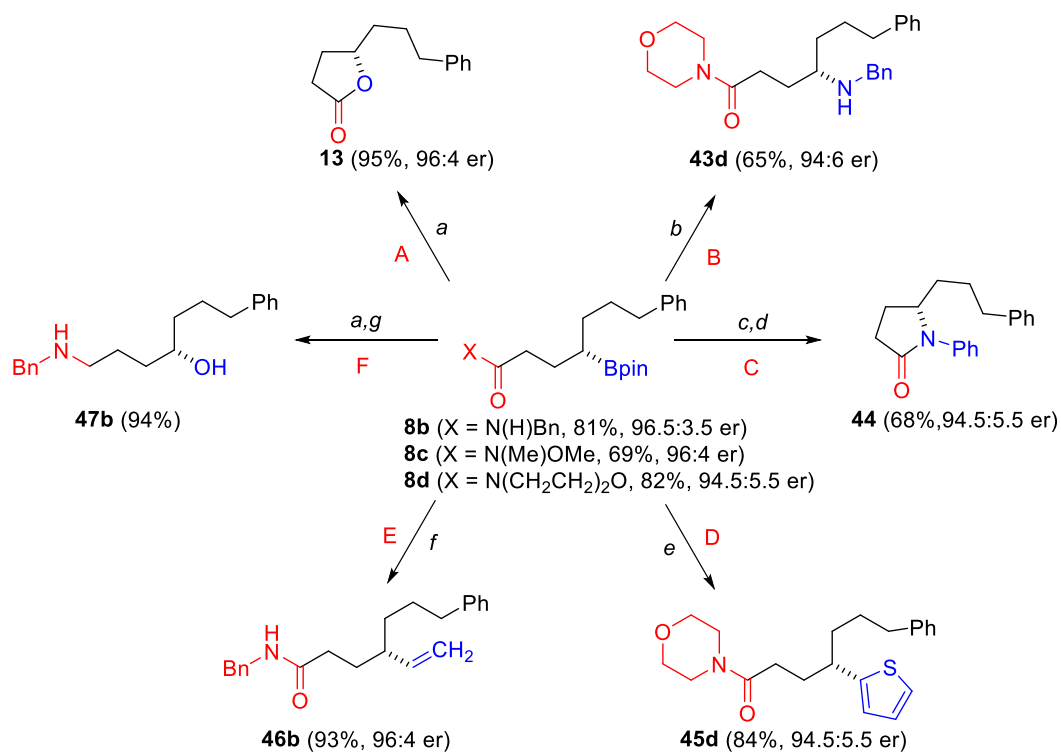


**Figure 3.** Stereospecific transformations of organoboranes **8b–d**. Reproduced from Ref. 10a with permission from The Royal Society of Chemistry.

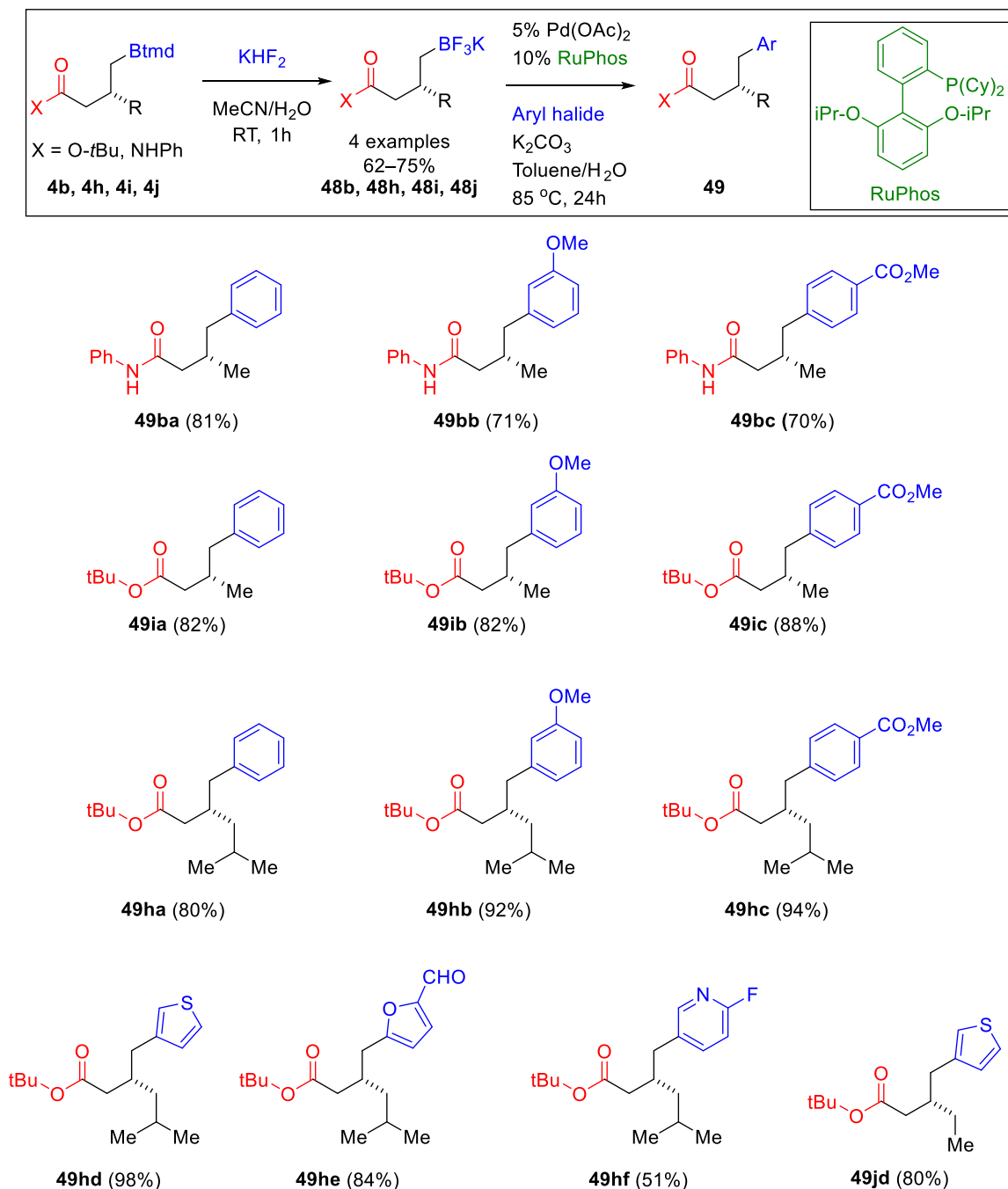
*Conditions:* (a) NaOH/H<sub>2</sub>O<sub>2</sub>; (b) BCl<sub>3</sub>, BnN<sub>3</sub>; (c) BCl<sub>3</sub>, PhN<sub>3</sub>; (d) 6M HCl; (e) (i) *n*-BuLi, thiophene, (ii) NBS; (f) (i) vinylMgBr, (ii) I<sub>2</sub>/NaOMe; (g) LiAlH<sub>4</sub> (LAH).



## 4.2 Stereochemical aspects in coordination-directed palladium-catalyzed cross-coupling reactions.

Palladium-catalyzed cross-coupling (e.g., Suzuki–Miyaura) is one of the most widely used methods in modern pharmaceutical synthesis.<sup>13–15</sup> For Pd-catalyzed cross-coupling reactions of  $sp^3$  boronic acid derivatives, trifluoroborate salts have found increasingly wide use due to the facts that: (i) compared to boronic acids and esters, trifluoroborate salts, monomeric in nature, are stable to air and aerobic moisture, (ii) with a tetrahedral geometry, due to the four groups bound to the boron center and exceptionally strong B–F bond, they are not Lewis acidic, and (iii) as salts, most trifluoroborate salts are free-flowing crystalline solids making them being easy to handle.<sup>16,17</sup> Despite the rapid growth in their use, organotrifluoroborate salts are not the active transmetalating species;<sup>18,19</sup> slow hydrolysis to the corresponding boronic acid is a key transformation in the reaction.<sup>20</sup> Though the mechanism suggests that the hydrolysis to boronic acid is crucial for the reactivity of organotrifluoroborate salts, boronic acids themselves are less frequently used in  $sp^3$  boron cross-coupling because it is typically a mixture of monomeric and trimeric boronic acid in nature; the latter makes an accurate assessment of stoichiometry challenging.<sup>17</sup> On the other hand, boronic esters are less reactive as well as less atom economical than boronic acids. In addition, the hydrolysis of boronic esters (e.g., pinacolboronates) to the boronic acids active species is rather complicated due to the high tendency of the liberated diol to regenerate the pinacol boronic esters; removing the pinacol is an example of driving the equilibrium in the forward direction.<sup>16</sup> Therefore,  $sp^3$  boron cross-coupling is less likely to involve the use of boronic esters except for a few examples using activated benzylic organoboranes.<sup>21–24</sup>

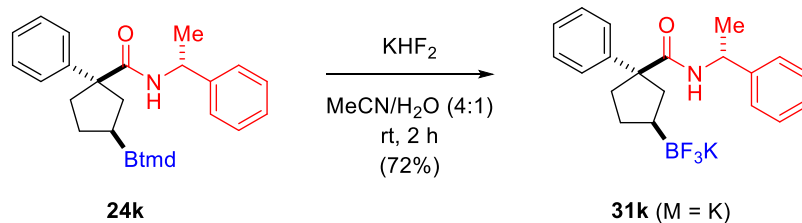
Using Molander's conditions without modification,<sup>25</sup> primary  $\gamma$ -borylated boronic esters **4b** and **4h–j**, obtained via CAHB of geminal  $\beta,\gamma$ -unsaturated amides and esters **3b** and **3h–j** (see Chapter 2.1), were converted to the corresponding trifluoroborate salts **48b** and **48h–j** (Figure 4) and successfully subjected to Pd-catalyzed cross-coupling with several representative aryl- and heteroaryl halides employing Molander's protocol.<sup>26</sup> The  $\gamma$ -trifluoroborato amides (i.e., **48b**) and esters (i.e., **48h–j**) are both well tolerated under the standard conditions affording cross-coupled products **49** in high yield (51–98%). Not only aryl halides but also heteroaryl halides are good coupling partners; in particular, **49jd** is the precursor to a chiral antispasmodic compound previously only reported as the racemate,<sup>27</sup> an example that highlights the utility of CAHB. In addition, the first successful cross-coupling of  $\gamma$ -borylated carbonyl derivatives, no examples of the latter have previously been reported, complements the examples using  $\beta$ -borylated carbonyl compounds.<sup>23,24,28,29</sup>



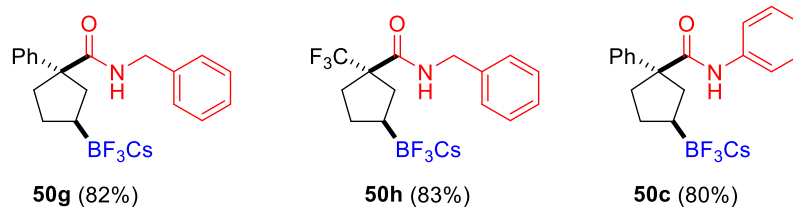
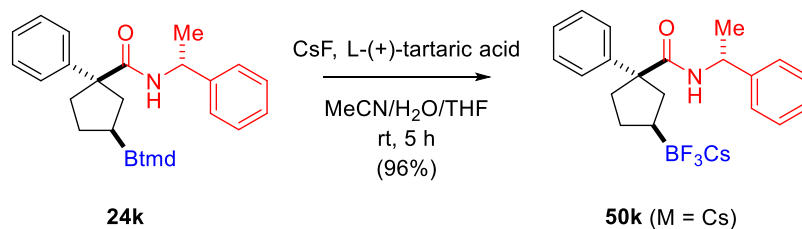
**Figure 4.** Palladium-catalyzed cross-coupling of primary  $\gamma$ -borylated amides and esters.

The stereochemical aspects of the palladium-catalyzed cross-coupling of chiral secondary organoboron derivatives have recently attracted a great deal of attention. Though

the above work on cross-coupling of primary  $\gamma$ -borylated carbonyl derivatives represents the first examples using  $\gamma$ -borylated derivatives, boron is not directly attached at the stereogenic center and thus does not address the key stereochemical issue of cross-coupling. However, we have introduced the first direct route to chiral secondary  $\gamma$ -borylated amides (see Chapter 3.2);<sup>10b</sup> Pd-catalyzed cross-coupling of the latter will address the question of the stereochemical course of cross-coupling: is it stereochemical retention or inversion?<sup>10</sup> Though first characterized in 1960,<sup>30</sup> the improved method for organotrifluoroborate salts to prevent the extensive etching of glassware was not introduced until 2012 by Lloyd-Jones and co-workers.<sup>31</sup> By applying this non-etching conditions (Figure 5B) to our chiral secondary  $\gamma$ -borylated amide **24k** (see Chapter 3.2),<sup>10b</sup> we found that the yield of trifluoroborate salt **50k** obtained are much higher (e.g., 96% *versus* 72% of **31k** (see Chapter 3.2)) than the method depicted in Figure 5A. The same method was also applied to other related  $\gamma$ -borylated amides **24** (see Chapter 3.2) affording **50c**, **50g**, and **50h** in good yield (80–83%).

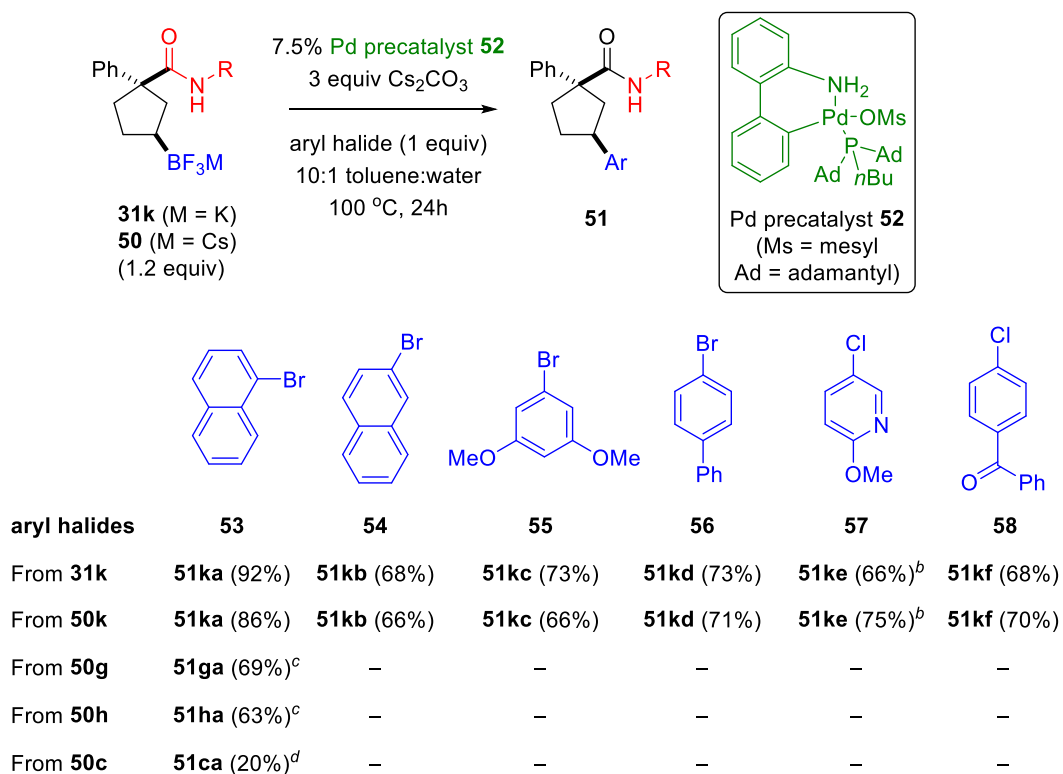
A. Preparation of potassium trifluoroborate salt using  $\text{KHF}_2$ 

## B. Preparation of cesium trifluoroborate salt using CsF

**Figure 5.** Preparation of organotrifluoroborate salts

Having developed an efficient method for the  $\gamma$ -borylation of cyclic  $\gamma,\delta$ -unsaturated amides as well as their conversions to the corresponding trifluoroborate salts, Suzuki–Miyaura cross-coupling of the latter was examined (Figure 6).<sup>10b</sup> Our first attempt with the potassium trifluoroborate salt of chiral phenethyl amide **31k** was successful; **31k** was cross-coupled with several representative aryl and heteroaryl halides affording **51ka–f** in high yield (66–92%). To the best of our knowledge, this is the first time the Buchwald cataCXium® A Pd G3 (**52**) was used in literature, even before it becomes commercially available.<sup>32</sup> The cesium trifluoroborate salt of chiral phenethyl amide **51k** performs as good as the potassium salt **31k**; it gives **51ka–f** in similar good

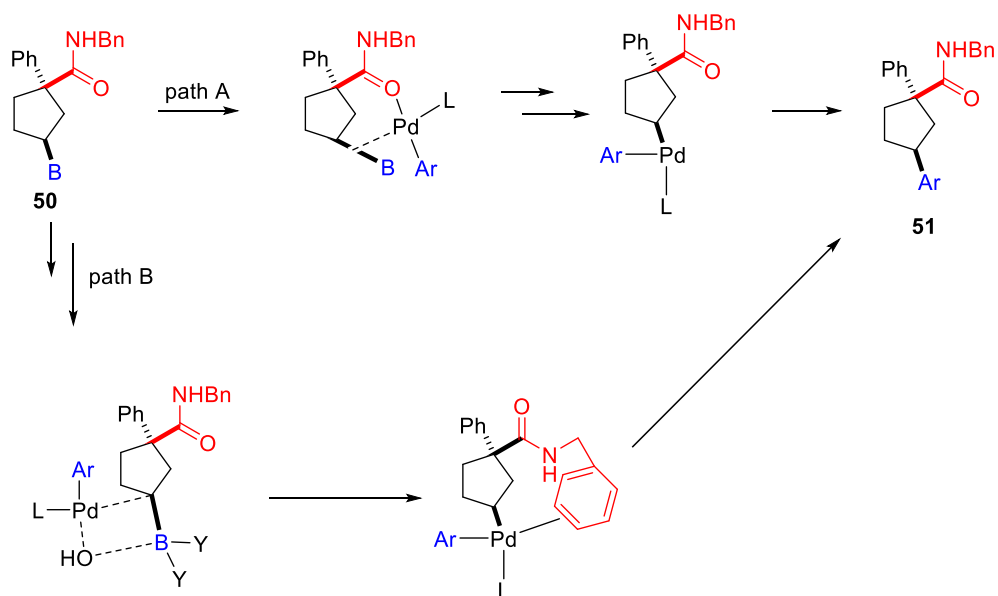
yield (66–86%) and was chosen for further investigation mostly due to higher yields in forming the salt. Benzyl amide trifluoroborate salts bearing  $\alpha$ -phenyl and  $\alpha$ -CF<sub>3</sub> quaternary carbon centers are also well tolerated under the standard conditions yielding **51ga** and **51ha**, respectively (63–69%). The spectral data of these two cross-coupled products indicate that the cross-coupling proceeds with high diastereoselectivity (e.g., the <sup>19</sup>F of **51ha** shows no more than 6% abundance in integrating a minor peak for another diastereomer). At first (*vide infra*), it seemed that the *N*-benzyl amide moiety seems to be crucial for the reactivity; phenyl amide trifluoroborate salt **50c** only produces **51ca** in 20% due to the low conversion of less than 35%; 85% of the corresponding alcohol (yield based on excess trifluoroborate) was obtained after Oxone oxidation.



**Figure 6.** Palladium-catalyzed cross-coupling of cyclic  $\gamma$ -organotrifluoroborate salt<sup>a</sup>

<sup>a</sup> Isolated yields based on limiting aryl halide, an average ( $\pm 2\%$ ) of two runs. <sup>b</sup> CsOH (5 equiv) replaces Cs<sub>2</sub>CO<sub>3</sub>. <sup>c</sup> Cross-coupling proceeds with high diastereoselectivity (ca. 94:6 dr). <sup>d</sup> Less than 35% conversion (85% of the corresponding alcohol (yield based on excess trifluoroborate) after Oxone oxidation was obtained)

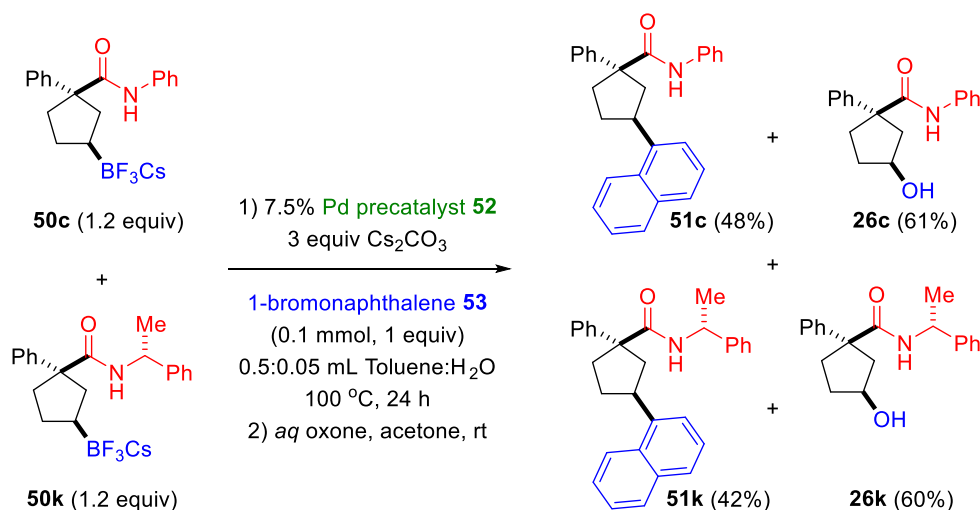
It is clear why the *N*-benzyl amide moiety should be a necessary element for cross-coupling. One might argue that the carbonyl of the phenyl amide is less Lewis basic and thus might not coordinate to the metal as well as does the carbonyl of the benzyl amide (Figure 7A). Another possibility, originally proposed by Molander<sup>33</sup> in his studies, is intramolecular hemilabile  $\pi$ -complexation of palladium by a suitably disposed benzyl substituent. In his studies, such a substituent was found to be a key element for enhancing the rate of transmetalation as well as facilitating cross-coupling with stereoretention (Figure 7B).



**Figure 7.** Proposed pathways for efficient cross-coupling illustrating the necessary feature of *N*-benzyl amide moiety.

To further probe the apparent unreactivity of the phenyl amide, a direct competition reaction with equal amount of the more reactive chiral phenethyl amide **50k** and the less reactive phenyl amide **50c** for a limiting amount of 1-bromonaphthalene **53** was carried out. Surprisingly, a nearly 1:1 mixture of cross-coupled products **51k** (42%)

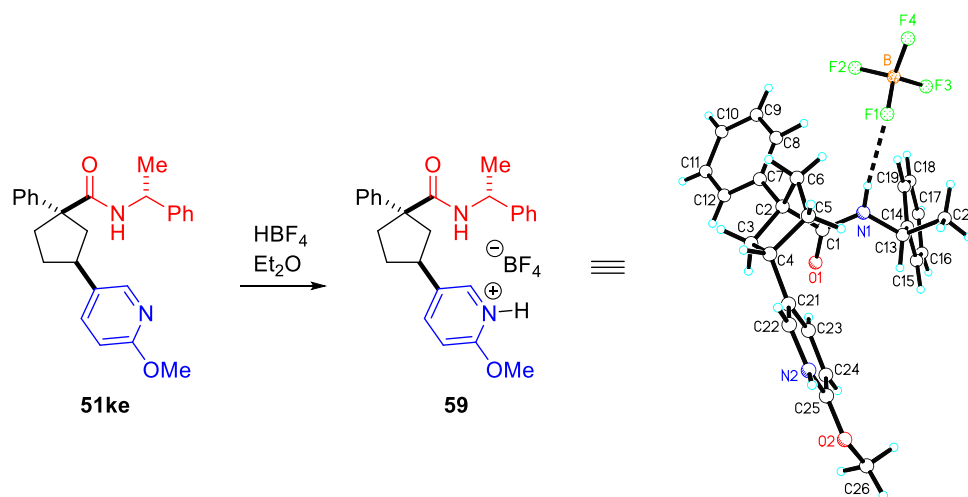
and **51c** (48%) is obtained and similar amount of the corresponding alcohols **26c** (61%) and **26k** (60%) were recovered after oxidation with Oxone (Figure 8). The surprising results observed raise doubt about the explanation in Figure 7 and suggest that **50c** is consumed as fast as **50k** by active catalyst. A relatively slow conversion of palladium precatalyst to active catalyst by **50c** in the absence of **50k** could account of the conflicting observations.



**Figure 8.** Unexpected influence of the amide substituent in Pd-catalyzed cross-coupling. Adapted with permission from reference 10b. Copyright (2015) American Chemical Society.

To prove the structural assignment of Suzuki–Miyaura cross-coupled products, a pyridine-based product **51ke** was converted to the corresponding tetrafluoroborate salt **59**; x-ray analysis of the resulting crystal confirms the structure as (1*R*,3*S*)-**59** establishing that the palladium-catalyzed cross-coupling proceeds with stereoretention (Figure 9).

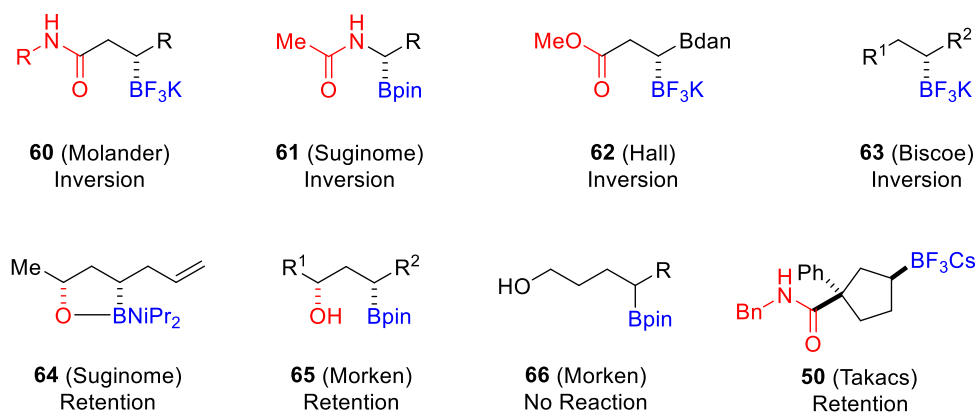




**Figure 9.** X-ray analysis of **59** establishes Pd-catalyzed cross-coupling proceeds with stereoretention. Adapted with permission from reference 10b. Copyright (2015) American Chemical Society.

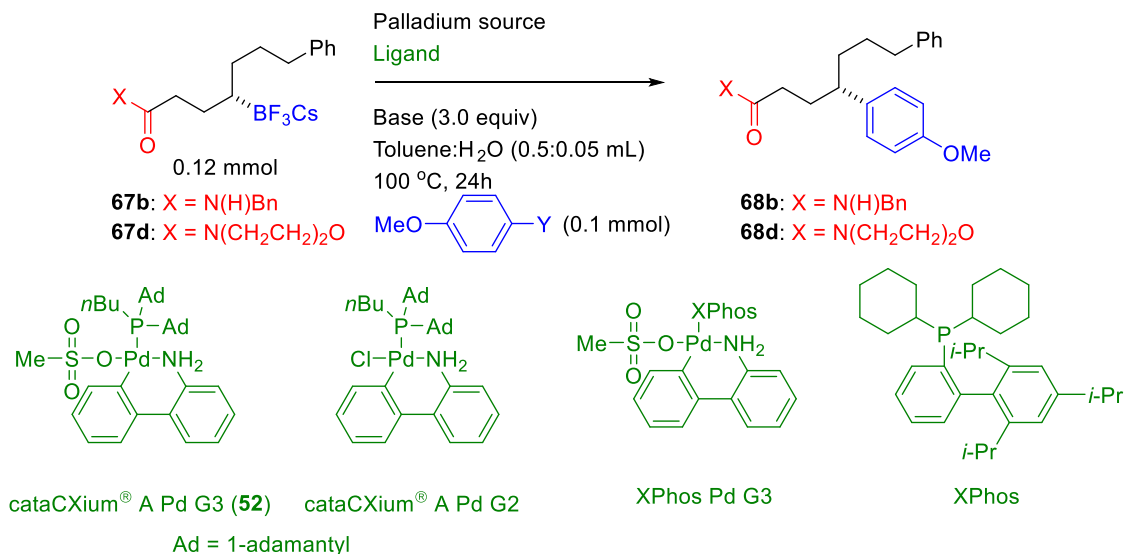
The above work should be of interest to a broad range of synthetic chemists, especially those with interests in organoboron chemistry, cross-coupling chemistry, and/or asymmetric catalysis. It is significant because it complements the previously reported  $\beta$ -borylated carbonyl derivatives (i.e., **60–62**), as well as simple substrates lacking functionality needed for coordination to boron during the course of transmetalation such as **63**, which proceed with stereoinversion as previously reported by Molander,<sup>26</sup> Suginome,<sup>23,24</sup> Hall,<sup>28,29</sup> and Biscoe,<sup>34</sup> respectively. Our work shows that  $\gamma$ -borylated amides **50** undergo Suzuki–Miyaura cross-coupling with stereoretention (Figure 10). It should be noted that Suginome<sup>35</sup> and Morcken<sup>36</sup> also reported stereoretentive Suzuki–Miyaura cross-couplings, however, those substrates (i.e., **64** and **65**) feature a physically closer distance relationship between boron and the donor substituent. It is proposed that a boracycle- or hydroxyl-directed, inner-sphere, retentive

transmetalation accounts for overall cross-coupling with stereoretention. When the hydroxyl is one-carbon further removed in **66** compared to **64** or **65**, but at a similar distance to **50**, the compound fails to cross-couple under the conditions employed for **65**.



**Figure 10.** Coordination-directed stereocontrol in Pd-catalyzed cross-coupling. Reproduced from Ref. 10a with permission from The Royal Society of Chemistry.

Our first attempts to cross-couple the acyclic  $\gamma$ -trifluoroborato benzyl amide **67b** (converted from the corresponding boronic ester **8b** using conditions described in Figure 5B) with 4-chloro- and 4-bromoanisole was unsuccessful (Table 1). Broader screening of  $\gamma$ -trifluoroborato benzyl amide **67b** along with the corresponding morpholino amide **67d** using different palladium sources, halides, bases, ligands, solvents reveals that the tertiary amide is much more successful in the cross-coupling; the reasons are not clear, but Hall has also reported similar observations with explanation.<sup>29</sup> Using the best conditions (i.e., entry 7), cross-coupling of **67d** (94.5:5.5 er) affords **68d** (52%) with essentially complete retention (94:6 er). None of the desired cross-coupled product **68b** was obtained under any of the conditions investigated.

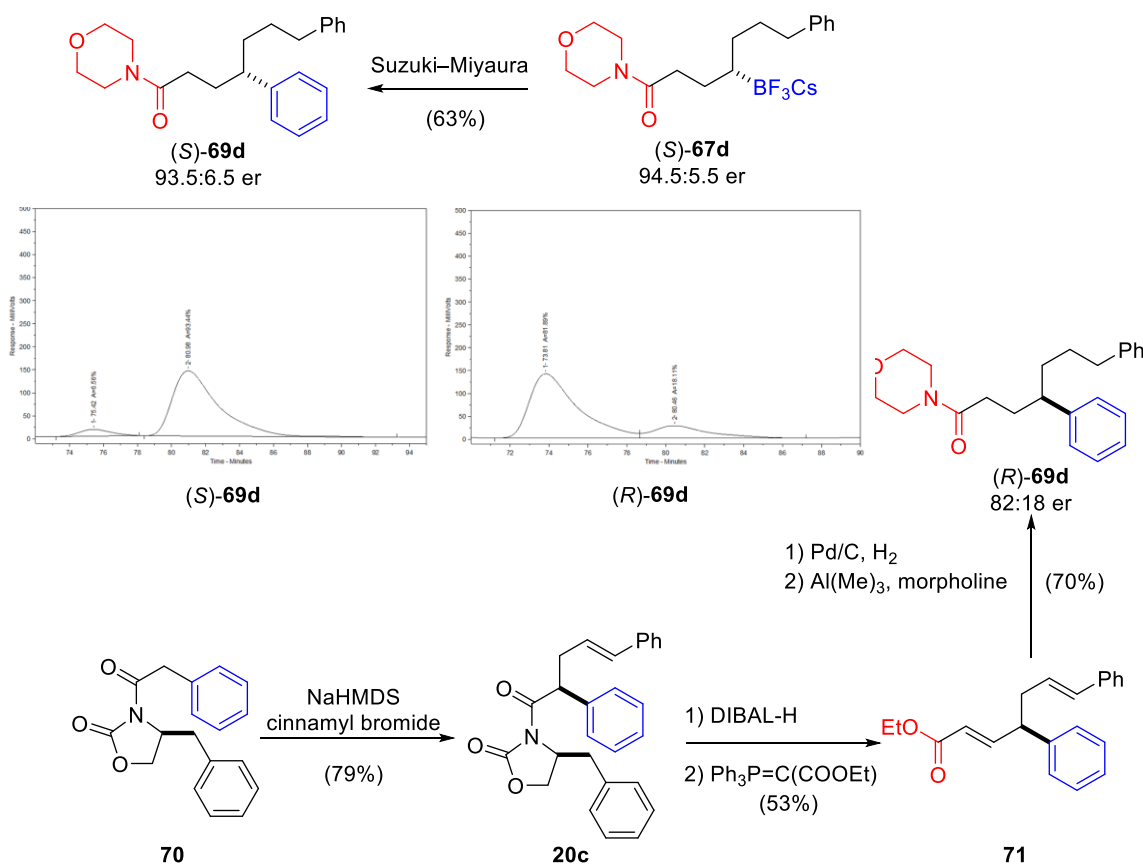
**Table 1.** Optimization studies for Suzuki–Miyaura cross-couplings of **67b** and **67d**.

Entry	Pd source	Ligand	Base	Y	<b>68b</b> (%)	<b>68d</b> (%)
1	Pd(OAc) <sub>2</sub>	XPhos	K <sub>2</sub> CO <sub>3</sub>	Cl	0	0
2	Pd <sub>2</sub> (dba) <sub>3</sub>	XPhos	K <sub>2</sub> CO <sub>3</sub>	Cl	0	38
3	Pd <sub>2</sub> (dba) <sub>3</sub>	P( <i>t</i> Bu) <sub>3</sub> .HBF <sub>4</sub>	K <sub>2</sub> CO <sub>3</sub>	Cl	0	10
4	Pd <sub>2</sub> (dba) <sub>3</sub>	cataCXium® A	K <sub>2</sub> CO <sub>3</sub>	Cl	0	15
5	XPhos Pd G3	–	K <sub>2</sub> CO <sub>3</sub>	Cl	0	21
6	<b>52</b>	–	K <sub>2</sub> CO <sub>3</sub>	Cl	0	49
<b>7</b>	<b>52</b>	–	<b>K<sub>2</sub>CO<sub>3</sub></b>	<b>Cl</b>	<b>0</b>	<b>52</b>
8 <sup>a</sup>	<b>52</b>	cataCXium® A	K <sub>2</sub> CO <sub>3</sub>	Cl	0	45
<b>9</b>	<b>52</b>	–	<b>Cs<sub>2</sub>CO<sub>3</sub></b>	<b>Cl</b>	<b>0</b>	<b>50</b>
10	<b>52</b>	–	K <sub>3</sub> PO <sub>4</sub>	Cl	0	47
11	<b>52</b>	–	CsOH	Cl	0	0
12	<b>52</b>	–	K <sub>2</sub> CO <sub>3</sub>	Br	0	45
13	<b>52</b>	–	Cs <sub>2</sub> CO <sub>3</sub>	Br	0	42
14 <sup>b</sup>	<b>52</b>	–	K <sub>2</sub> CO <sub>3</sub>	Cl	0	48
15 <sup>c</sup>	<b>52</b>	–	K <sub>2</sub> CO <sub>3</sub>	Cl	0	0
16 <sup>c</sup>	<b>52</b>	–	Cs <sub>2</sub> CO <sub>3</sub>	Cl	0	0

General conditions: 7.5 mol% Pd-precatalyst or 10 mol% Pd(OAc)<sub>2</sub> or 5 mol% Pd<sub>2</sub>(dba)<sub>3</sub>; 20 mol% ligand; isolated yield. <sup>a</sup> Additional 7.5 mol% cataCXium® A. <sup>b</sup> Toluene:H<sub>2</sub>O = 0.25:0.25 mL. <sup>c</sup> Bpin is used instead of BF<sub>3</sub>Cs.

To assign the structure of the Suzuki–Miyaura cross-coupling,  $\gamma$ -trifluoroborato morpholino amide (*S*)-**67d** (94.5:5.5 er, see Chapter 2.2 for the determination of absolute

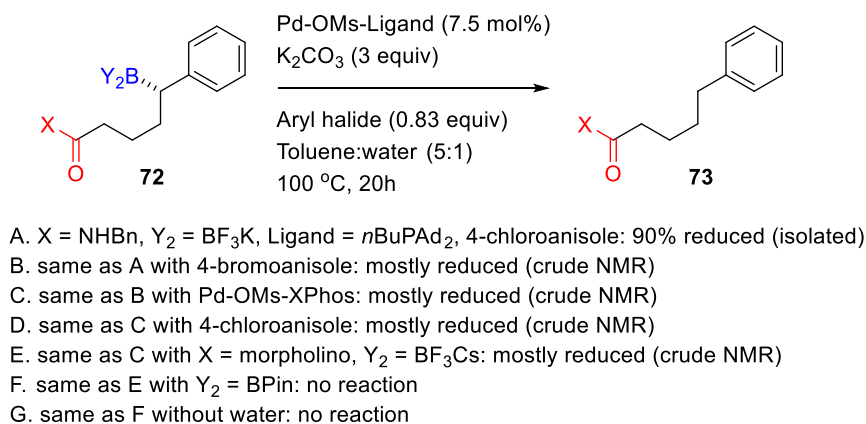
configuration) was cross-coupled with 4-chlorobenzene to afford (*S*)-**69d** in good yield and high stereoselectivity (Figure 11). Chiral HPLC analysis of (*S*)-**69d** was compared with authentic (*R*)-**69d** prepared via enolate allylation using the Evans chiral auxiliary via the following sequence: (i) *in situ* half reduction to aldehyde followed by Wadsworth-Horner-Emmons olefination, (ii) Pd/C hydrogenation, and (iii) amidation with morpholine.



**Figure 11.** Determination of absolute configuration of cross-coupled products via Pd-catalyzed cross-coupling of acyclic  $\gamma$ -trifluoroborato amides. Reproduced from Ref. 10a with permission from The Royal Society of Chemistry.

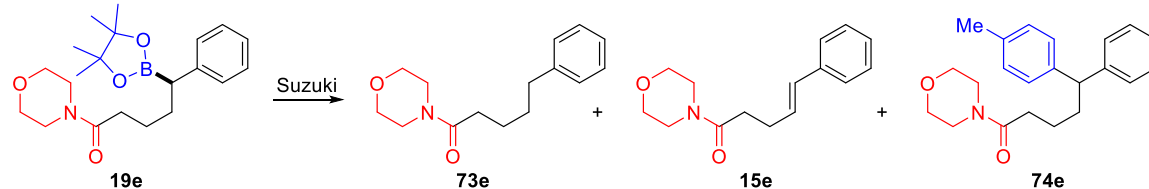
Our first attempts at Pd-catalyzed cross-coupling of benzylic  $\delta$ -borylated amides **72** using the above developed method was unsuccessful (Figure 12). The major product

observed is reduced product **73** presumably via protodeboronation pathway.<sup>37</sup> Further investigations using different palladium sources and ligands are still in progress.



**Figure 12.** Unexpected protoboronation pathway for Suzuki–Miyaura cross-couplings of benzylic  $\delta$ -borylated amides **72**.

Crudden and co-workers reported conditions for the cross-coupling conditions of benzylic boronic esters utilizing silver(I) oxide to facilitate the transmetallation step.<sup>21,22</sup> Using Crudden's conditions with benzylic  $\delta$ -borylated amides **19e** gave some **74e** (25%, condition A, Table 2), however, the reaction proceeds with low conversion (59%) and the yield of reduced product **73e** via protodeborylation is high (27%). Changing the solvent from toluene to THF, the reaction affords higher conversion increasing the yield of the cross-coupled product (40%, condition B). The base does have an important role for the cross-coupling mode selectivity; using cesium carbonate drastically increases the amounts of reduced **73e** (74–78%, conditions C and D) with no desired products observed. Finally, palladium sources and ligands illustrate the most important factors; conditions E–F improve the yield of cross-coupled product **74e** as high as 81%. Interestingly, simple triphenylphosphine ligand has been the best for the study; other triaryl- and trialkylphosphine ligands (e.g., P(*t*Bu)<sub>3</sub>) are under investigations.

**Table 2.** Optimization studies for Suzuki–Miyaura cross-couplings of **19e**.

Conditions	Unreacted (%) <sup>a</sup>	<b>19e</b>	<b>73e</b> (%) <sup>a</sup>	<b>15e</b> (%) <sup>a</sup>	<b>74e</b> (%) <sup>a</sup>
A	41		27	trace	25
B	21		33	trace	40
C	12		78	trace	trace
D	15		74	trace	trace
E	10		10	7	65
F	trace		15	15	62
G	trace		10	7	81

Condition A: 0.12 mmol **19e** (1.2 equiv), 0.1 mmol 4-iodotoluene (1.0 equiv), 8.1 mol% cataCXium® A Pd G3, 1.6 equiv Ag<sub>2</sub>O, 1.6 equiv K<sub>2</sub>CO<sub>3</sub>, Toluene, 100 °C, 20h.

Condition B: 0.12 mmol **19e** (1.2 equiv), 0.1 mmol 4-iodotoluene (1.0 equiv), 8.1 mol% cataCXium® A Pd G3, 1.6 equiv Ag<sub>2</sub>O, 1.6 equiv K<sub>2</sub>CO<sub>3</sub>, THF, 70 °C, 20h.

Condition C: 0.12 mmol **19e** (1.2 equiv), 0.1 mmol 4-iodotoluene (1.0 equiv), 8.1 mol% cataCXium® A Pd G3, 1.6 equiv Ag<sub>2</sub>O, 1.6 equiv Cs<sub>2</sub>CO<sub>3</sub>, THF, 70 °C, 20h.

Condition D: 0.12 mmol **19e** (1.2 equiv), 0.1 mmol 4-iodotoluene (1.0 equiv), 8.1 mol% cataCXium® A Pd G3, 1.6 equiv Ag<sub>2</sub>O, 1.6 equiv Cs<sub>2</sub>CO<sub>3</sub>, Toluene, 100 °C, 20h.

Condition E: 0.12 mmol **19e** (1.2 equiv), 0.1 mmol 4-iodotoluene (1.0 equiv), 8.1 mol% Pd<sub>2</sub>(dba)<sub>3</sub>, 10 mol% PPh<sub>3</sub>, 1.6 equiv Ag<sub>2</sub>O, THF, 65 °C, 20h.

Condition F: 0.12 mmol **19e** (1.2 equiv), 0.1 mmol 4-iodotoluene (1.0 equiv), 8 mol% Pd(PPh<sub>3</sub>)<sub>4</sub>, 1.6 equiv Ag<sub>2</sub>O, 1.6 equiv K<sub>2</sub>CO<sub>3</sub>, Et<sub>2</sub>O, 65 °C, 20h.

Condition G: 0.12 mmol **19e** (1.2 equiv), 0.1 mmol 4-iodotoluene (1.0 equiv), 8 mol% Pd(PPh<sub>3</sub>)<sub>4</sub>, 32 mol% PPh<sub>3</sub>, 1.6 equiv Ag<sub>2</sub>O, 1.6 equiv K<sub>2</sub>CO<sub>3</sub>, Et<sub>2</sub>O, 65 °C, 20h.

<sup>a</sup> Yield reported as crude <sup>1</sup>H NMR yield

Using the best performing conditions for cross-coupling of **19e** (i.e., condition G, Table 2), several other reactions have been carried out (Figure 13). Interestingly, in contrast to the acyclic  $\gamma$ -trifluoroborato amides discussed above, conditions developed by Crudden group are also effective for the benzyl amides. Cross-coupling of  $\delta$ -borylated benzyl amide **15a** with several representative aryl iodides afford **74a–77a** in good yield (68–79%). The level of enantiospecificity and the stereoretentive/stereoinvertive course of the Suzuki cross-coupling have not yet been determined.

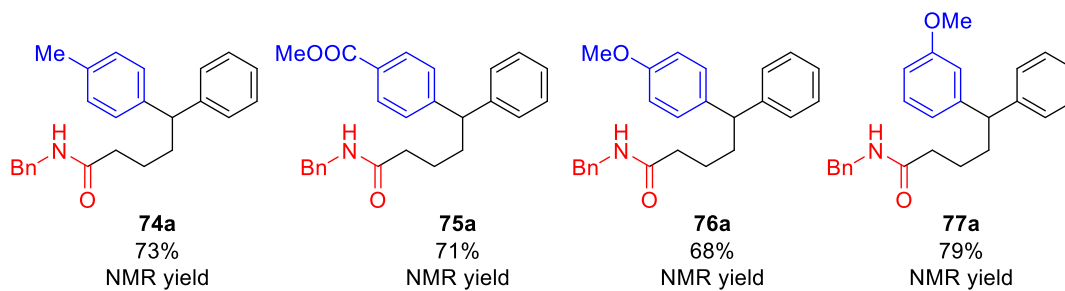
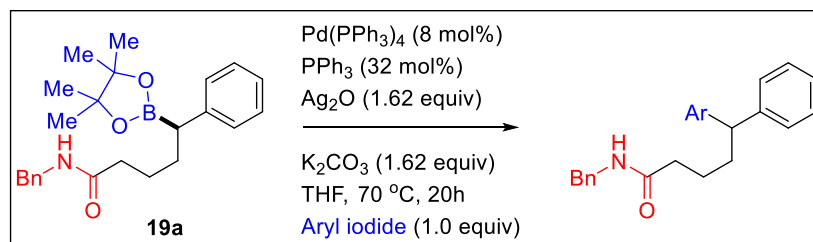


**Figure 13.** Palladium-catalyzed cross-coupling of benzylic  $\delta$ -borylated benzyl amide **15a**.

### 4.3 Concluding remarks

In contrast to similar  $\beta$ -borylated carbonyl derivatives reported in literature, both cyclic and acyclic  $\gamma$ -trifluoroborato amides undergo Suzuki–Miyaura cross-coupling with clean stereoretention. Initial results for cross-couplings of benzylic  $\delta$ -borylated amides are quite promising; however, the level of enantiospecificity and the stereoretentive/stereoinvertive course of the Suzuki cross-coupling have not yet been determined. Other stereospecific transformations of C–B bond are used to highlight the versatility of the bifunctional intermediates generated by  $\gamma$ -borylation, including conversion to lignan precursors, chiral  $\gamma$ -aminoacid derivatives, 1,4-amino alcohols, 5-substituted- $\gamma$ -lactones, and  $\gamma$ -lactam ring systems. Our results should be of interest to a broad range of chemists, especially those with interests in asymmetric catalysis, cross-coupling chemistry, asymmetric synthesis and organoboron chemistry.



#### 4.4 References

- [1] Sanford, C.; Aggarwal, V. K., "Stereospecific Functionalizations and Transformations of Secondary and Tertiary Boronic Esters," *Chem. Commun.*, **2017**, 53, 5481–5494.
- [2] Shoba, V. M.; Thacker, N. C.; Bochat, A. J.; Takacs, J. M., "Synthesis of Chiral Tertiary Boronic Esters by Oxime-Directed Catalytic Asymmetric Hydroboration," *Angew. Chem., Int. Ed.*, **2016**, 55, 1465–1469.
- [3] Chakrabarty, S.; Takacs, J. M., "Synthesis of Chiral Tertiary Boronic Esters: Phosphonate-Directed Catalytic Asymmetric Hydroboration of Trisubstituted Alkenes," *J. Am. Chem. Soc.*, **2017**, 139, 6066–6069.
- [4] K. Kaur, V. Kumar, A. K. Sharma, G. K. Gupta, "Isoxazoline Containing Natural Products as Anticancer Agents: A Review," *Eur. J. Med. Chem.*, **2014**, 77, 121–133.
- [5] Brown, H. C.; Zweifel, G., "Hydroboration. IX. The Hydroboration of Cyclic and Bicyclic Olefins—Stereochemistry of the Hydroboration Reaction," *J. Am. Chem. Soc.*, **1961**, 83, 2544–2551.
- [6] Kabalka, G. W.; Shoup, T. M.; Goudgaon, N. M., "Sodium Perborate: A Mild and Convenient Reagent for Efficiently Oxidizing Trialkylboranes," *Tetrahedron Lett.*, **1989**, 30, 1483–1486.
- [7] Smith, S. M.; Hoang, G. L.; Pal, R.; Khaled, M. O. B.; Pelter, L. S. W.; Zeng, X. C.; Takacs, J. M., "γ-Selective Directed Catalytic Asymmetric Hydroboration of 1,1-Disubstituted Alkenes," *Chem. Commun.*, **2012**, 48, 12180–12182.
- [8] Bode, J. W.; Doyle, M. P.; Protopopova, M. N.; Zhou, W.-L., "Intramolecular Regioselective Insertion into Unactivated Prochiral Carbon–Hydrogen Bonds with Diazoacetates of Primary Alcohols Catalyzed by Chiral Dirhodium(II) Carboxamidates. Highly Enantioselective Total Synthesis of Natural Lignan Lactones," *J. Org. Chem.*, **1996**, 61, 9146–9155.
- [9] (a) Larsen, C. H.; Ridway, B. H.; Shaw, J. T.; Smith, D. M.; Woerpel, K. A., "Stereoselective C-Glycosylation Reactions of Ribose Derivatives: Electronic Effects of Five-Membered Ring Oxocarbenium Ions," *J. Am. Chem. Soc.*, 2005, **127**, 10879–10884; (b) Aquino, M.; Cardani, S.; Fronza, G.; Fuganti, C.; Fernandez, R. P.; Tagliani, A., "Baker's Yeast Reduction of Arylalkyl and Arylalkenyl γ- and δ-Keto Acids," *Tetrahedron*, 1991, **47**, 7887–7896.

- [10] (a) Hoang, G. L.; Takacs, J. M., "Enantioselective  $\gamma$ -Borylation and Stereoretentive Suzuki–Miyaura Cross-Coupling," *Chem. Sci.*, **2017**, *8*, 4511–4516; (b) Hoang, G. L.; Yang, Z.-D.; Smith, S. M.; Pal, R.; Miska, J. L.; Pérez, D. E.; Petler, L. S. W.; Zeng, X. C.; Takacs, J. M., "Enantioselective Desymmetrization via Carbonyl-Directed Catalytic Asymmetric Hydroboration and Suzuki–Miyaura Cross-Coupling," *Org. Lett.*, **2015**, *17*, 940–943.
- [11] Hupe, E.; Marek, I.; Knochel, P., "Diastereoselective Reduction of Alkenylboronic Esters as a New Method for Controlling the Stereochemistry of up to Three Adjacent Centers in Cyclic and Acyclic Molecules," *Org. Lett.*, **2002**, *4*, 2861–2863.
- [12] (a) Odachowski, M.; Bonet, A.; Essafi, S.; Conti-Ramsden, P.; Harvey, J. N.; Leonori, D.; Aggarwal, V. K., "Development of Enantiospecific Coupling of Secondary and Tertiary Boronic Esters with Aromatic Compounds," *J. Am. Chem. Soc.*, **2016**, *138*, 9521–9532.; (b) Sonawane, R. P.; Jheengut, V.; Rabalakos, C.; Larouche-Gauthier, R.; Scott, H. K.; Aggarwal, V. K., "Enantioselective Construction of Quaternary Stereogenic Centers from Tertiary Boronic Esters: Methodology and Applications," *Angew. Chem., Int. Ed.*, **2011**, *50*, 3760–3763.
- [13] Magano, J.; Dunetz, J. R., "Large-Scale Applications of Transition Metal-Catalyzed Couplings for the Synthesis of Pharmaceuticals," *Chem. Rev.*, **2011**, *111*, 2177–2250.
- [14] Suzuki, A., "Cross-Coupling Reactions of Organoboranes: An Easy Way to Construct C–C Bonds," *Angew. Chem., Int. Ed.*, **2011**, *50*, 6722–6737
- [15] Cherney, A. H.; Kadunce, N. T.; Reisman, S. E., "Enantioselective and Enantiospecific Transition Metal-Catalyzed Cross-Coupling Reactions of Organometallic Reagents to Construct C–C Bonds," *Chem. Rev.*, **2015**, *115*, 9587–9652.
- [16] Lennox, A. J. J.; Lloyd-Jones, G. C., "Selection of Boron Reagents for Suzuki–Miyaura Coupling," *Chem. Soc. Rev.*, **2014**, *43*, 412–443.
- [17] Molander, G. A., "Organotrifluoroborates: Another Branch of the Mighty Oak," *J. Org. Chem.*, **2015**, *80*, 7837–7848.
- [18] Fu, G. C.; Littke, A. F.; Dai, C., "Versatile Catalysts for the Suzuki Cross-Coupling of Arylboronic Acids with Aryl and Vinyl Halides and Triflates under Mild Conditions," *J. Am. Chem. Soc.*, **2000**, *122*, 4020–4028.

- [19] Molander, G. A.; Biolatto, B., "Palladium-Catalyzed Suzuki–Miyaura Cross-Coupling Reactions of Potassium Aryl- and Heteroaryltrifluoroborates," *J. Org. Chem.*, **2003**, *68*, 4302–4314.
- [20] Butters, M.; Harvey, J. N.; Jover, J.; Lennox, A. J. J.; Lloyd-Jones, G. C.; Murray, P. M., "Aryl Trifluoroborates in Suzuki–Miyaura Coupling: The Roles of Endogenous Aryl Boronic Acid and Fluoride," *Angew. Chem., Int. Ed.*, **2010**, *49*, 5156–5160.
- [21] Glasspoole, B. W.; Oderinde, M. S.; Moore, B. D.; Antoft-Finch, A.; Crudden, C. M., "Highly Chemoselective and Enantiospecific Suzuki–Miyaura Cross Couplings of Benzylic Organoboronic Esters," *Synthesis*, **2013**, *45*, 1759–1763.
- [22] Matthew, S. C.; Glasspoole, B. W.; Eisenberger, P.; Crudden, C. M., "Synthesis of Enantiomerically Enriched Triarylmethanes by Enantiospecific Suzuki–Miyaura Cross-Coupling Reactions," *J. Am. Chem. Soc.*, **2014**, *136*, 5828–5831.
- [23] Ohmura, T.; Awano, T.; Suginome, M., "Stereospecific Suzuki–Miyaura Coupling of Chiral  $\alpha$ -(Acylamino)benzylboronic Esters with Inversion of Configuration," *J. Am. Chem. Soc.*, **2010**, *132*, 13191–13193.
- [24] Awano, T.; Ohmura, T.; Suginome, M., "Inversion or Retention? Effects of Acidic Additives on the Stereochemical Course in Enantiospecific Suzuki–Miyaura Coupling of  $\alpha$ -(Acetylamino)benzylboronic Esters," *J. Am. Chem. Soc.*, **2011**, *133*, 20738–20741.
- [25] Molander, G. A.; Shin, I.; Jean-Gérard, L., "Palladium-Catalyzed Suzuki–Miyaura Cross-Coupling Reactions of Enantiomerically Enriched Potassium  $\beta$ -Trifluoroboratoamides with Various Aryl- and Hetaryl Chlorides," *Org. Lett.*, **2010**, *12*, 4384–4387.
- [26] Sandrock, D. L.; Jean-Gerard, L.; Chen, C.; Dreher, S. D.; Molander, G. A., "Stereospecific Cross-Coupling of Secondary Alkyl  $\beta$ -Trifluoroboratoamides," *J. Am. Chem. Soc.*, **2010**, *132*, 17108–17110.
- [27] Blicke, F. F.; Leonard, F., "Antispasmodics. VIII," *J. Am. Chem. Soc.*, **1946**, *68*, 1934–1936.
- [28] Lee, J. C.; McDonald, R.; Hall, D. G., "Enantioselective Preparation and Chemoselective Cross-Coupling of 1,1-Diboron Compounds," *Nat. Chem.*, **2011**, *3*, 894–899.

- [29] Lee, J. C. H.; Sun, H.-Y.; Hall, D. G., "Optimization of Reaction and Substrate Activation in the Stereoselective Cross-Coupling of Chiral 3,3-Diboronyl Amides," *J. Org. Chem.*, **2015**, *80*, 7134–7143.
- [30] Chambers, R. D.; Clark, H. C.; Willis, C. J., "Some Salts of Trifluoromethylfluoroboric Acid," *J. Am. Chem. Soc.*, **1960**, *82*, 5298–5301.
- [31] Lennox, A. J. J.; Lloyd-Jones, G. C., "Preparation of Organotrifluoroborate Salts: Precipitation-Driven Equilibrium under Non-Etching Conditions," *Angew. Chem., Int. Ed.*, **2012**, *51*, 9385–9388.
- [32] N. C. Bruno, M. T. Tudge and S. L. Buchwald, "Design and Preparation of New Palladium Precatalysts for C-C and C-N Cross-Coupling Reactions," *Chem. Sci.*, **2013**, *4*, 916–920.
- [33] Molander, G. A.; Wisniewski, S. R., "Stereospecific Cross-Coupling of Secondary Organotrifluoroborates: Potassium 1-(Benzyloxy)alkyltrifluoroborates," *J. Am. Chem. Soc.*, **2012**, *134*, 16856–16868.
- [34] Li, L.; Zhao, S.; Joshi-Pangu, A.; Diane, M.; Biscoe, M. R., "Stereospecific Pd-Catalyzed Cross-Coupling Reactions of Secondary Alkylboron Nucleophiles and Aryl Chlorides," *J. Am. Chem. Soc.*, **2014**, *136*, 14027–14030.
- [35] Daini, M.; Suginome, M., "Palladium-Catalyzed, Stereoselective, Cyclizative Alkenylboration of Carbon–Carbon Double Bonds through Activation of a Boron–Chlorine Bond," *J. Am. Chem. Soc.*, **2011**, *133*, 4758–4761.
- [36] Blaisdell, T. P.; Morken, J. P., "Hydroxyl-Directed Cross-Coupling: A Scalable Synthesis of Debromohamigeran E and Other Targets of Interest," *J. Am. Chem. Soc.*, **2015**, *137*, 8712–8715.
- [37] (a) Fleckenstein, C. A.; Plenio, H., "Efficient Suzuki-Miyaura Coupling of (Hetero)aryl Chlorides with Thiophene- and Furanboronic Acids in Aqueous *n*-Butanol," *J. Org. Chem.*, **2008**, *73*, 3236–3244; (b) Lozada, J.; Liu, Z.; Perrin, D. M., "Base-Promoted Protodeboration of 2,6-Disubstituted Arylboronic Acids," *J. Org. Chem.*, **2014**, *79*, 5365–5368, and references cited therein

## CHAPTER 5: EXPERIMENTALS

**5.1 Experimental details****General procedures**

Reactions were carried out in a dry nitrogen atmosphere. Tetrahydrofuran (THF) was freshly distilled under sodium metal and benzophenone. HPLC solvents were filtered through Millipore filter paper. 4,4,5,5-tetramethyl-1,3,2-dioxaborolane (pinBH) was distilled immediately before use. All synthesized compounds were purified with flash chromatography using EMD Silica Gel 60 Geduran®, distilled via short path distillation, or triturated. Thin Layer Chromatography analyses were performed on Analtech Silica Gel HLF (0.25 mm) precoated analytical plates and visualized with use of handheld short wavelength UV light, Iodine stain (I<sub>2</sub> and EMD Silica Gel 60 Geduran®) and Vanillin stain (Ethanol, H<sub>2</sub>SO<sub>4</sub>, and vanillin). HPLC analyses were performed with use of an ISCO model 2360 HPLC and Chiral Technologies, Inc. chiral HPLC columns (Chiralcel-OJ-H, column: 250 x 4.6 mm; Chiralcel-AD, column: 250 x 4.6 mm; Chiralcel-OD, column: 250 x 4.6 mm; Chiralpak-IC, column: 250 x 4.6 mm; (S,S)-WHELK-O 1, column: 250 x 4.6 mm) and monitored with UV-VIS detector (Shimadzu SPD-10A<sub>VP</sub>/10A<sub>VP</sub>,  $\lambda = 210$  nm). Data were recorded and analyzed with ChromPerfect chromatography software (version 5.1.0). NMR spectra were recorded on 400 MHz and 300 MHz Bruker Advance NMR spectrometers using residue CHCl<sub>3</sub> ( $\delta$  7.27 ppm) or CDCl<sub>3</sub> ( $\delta$  77.0 ppm) for reference unless otherwise specified. Peaks are expressed as m (unresolved multiplet), q (quartet), t (triplet), d (doublet) or s (singlet). IR spectra were recorded using an Avatar 360 FT-IR. Optical rotations were measured as solutions, 1.0 g/100 mL in chloroform or methanol unless indicated otherwise, and recorded using an Autopol III automatic polarimeter. HRMS analyses were performed by the Nebraska Center for Mass

Spectrometry. Experimental procedures and characterization of compounds (i.e., **3a–j**, **4a–j**, **39a–41b**, **4b**, **4h–j**, **48b**, **48h–j** and **49**) in collaboration with Dr. Sean M. Smith were already described in his dissertation (University of Nebraska, 2012) and will not be shown herein. We thank Dr. Nathan C. Thacker for the preparation of deuterated boranes (University of Nebraska, 2014). We thank co-workers, especially Ms. Veronika M. Shoba for the share of catalysts used in optimization studies.

### **X-Ray Crystallographic Studies for [K][C<sub>20</sub>H<sub>22</sub>BF<sub>3</sub>NO], 31k**

A colorless single-domain crystal of [K][C<sub>20</sub>H<sub>22</sub>BF<sub>3</sub>NO], was suspended with Paratone N oil on a MiTeGen MicroMount and mounted on a goniometer head in a cold nitrogen stream at 100K for a single-crystal x-ray structure determination. Monochromatic x-rays were provided by a Bruker Diffraction System equipped with Helios multilayer optics, an APEX II CCD detector and a Bruker MicroSTAR microfocus rotating anode x-ray source operating at 45kV and 60mA. Intensity data were collected with the Bruker program SMART and diffracted intensities were measured with the Bruker program SAINT. The space group and crystallographic data are summarized in Table 1. The Bruker software package SHELXTL was used to solve the structure using “direct methods” techniques. All stages of weighted full-matrix least-squares refinement were conducted using  $F_o^2$  data with the SHELXTL Version 2010.3-0 software package.

The final structural model incorporated anisotropic thermal parameters for all non-hydrogen atoms and isotropic thermal parameters for all hydrogen atoms. All hydrogen atoms were located from a difference Fourier and included in the structural model as independent isotropic atoms whose parameters were allowed to vary in least-

squares refinement cycles. The absolute structure was determined experimentally using anomalous dispersion of the x-rays. The Flack absolute structure parameter refined to a final value of 0.034(7). The asymmetric unit consists of a single [K][C<sub>20</sub>H<sub>22</sub>BF<sub>3</sub>NO] formula unit. All thermal vibration ellipsoids are drawn at the 50% probability level.

**Table 1.** Crystal data and structure refinement for [C<sub>20</sub>H<sub>22</sub>ONBF<sub>3</sub>][K], **31k**

Identification code	q72d	
Empirical formula	C <sub>20</sub> H <sub>22</sub> B F <sub>3</sub> K N O	
Formula weight	399.30	
Temperature	100(2) K	
Wavelength	1.54178 Å	
Crystal system	Orthorhombic	
Space group	P2(1)2(1)2(1)	
Unit cell dimensions	a = 6.3906(3) Å	α = 90°.
	b = 7.7434(3) Å	β = 90°.
	c = 38.9797(17) Å	γ = 90°.
Volume	1928.91(14) Å <sup>3</sup>	
Z	4	
Density (calculated)	1.375 Mg/m <sup>3</sup>	

Absorption coefficient	2.742 mm <sup>-1</sup>
F(000)	832
Crystal size	0.11 x 0.04 x 0.03 mm <sup>3</sup>
Theta range for data collection	2.27 to 69.89°.
Index ranges	-7<=h<=7, -9<=k<=8, -46<=l<=37
Reflections collected	17786
Independent reflections	3401 [R(int) = 0.0300]
Completeness to theta = 66.00°	98.2 %
Absorption correction	Multi-scan
Max. and min. transmission	1.000 and 0.843
Refinement method	Full-matrix least-squares on F <sup>2</sup>
Data / restraints / parameters	3401 / 0 / 333
Goodness-of-fit on F <sup>2</sup>	1.044
Final R indices [I>2sigma(I)]	R1 = 0.0240, wR2 = 0.0592
R indices (all data)	R1 = 0.0252, wR2 = 0.0596
Absolute structure parameter	0.034(7)
Extinction coefficient	0.00069(12)



Largest diff. peak and hole 0.197 and -0.214 e.Å<sup>-3</sup>

### X-Ray Crystallographic Studies for [C<sub>26</sub>H<sub>29</sub>N<sub>2</sub>O<sub>2</sub>][BF<sub>4</sub>]

Using procedures described for [K][C<sub>20</sub>H<sub>22</sub>BF<sub>3</sub>NO] **31k**, the crystal data and structure refinement for for [C<sub>26</sub>H<sub>29</sub>N<sub>2</sub>O<sub>2</sub>][BF<sub>4</sub>], **59** are shown in Table 2.

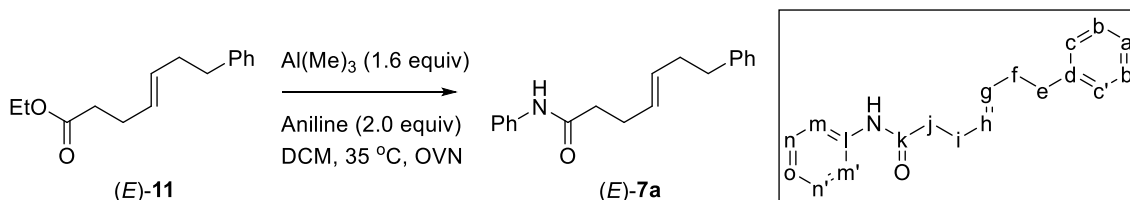
**Table 2.** Crystal data and structure refinement for [C<sub>26</sub>H<sub>29</sub>N<sub>2</sub>O<sub>2</sub>][BF<sub>4</sub>], **59**.

Identification code	q43e	
Empirical formula	C <sub>26</sub> H <sub>29</sub> B F <sub>4</sub> N <sub>2</sub> O <sub>2</sub>	
Formula weight	488.32	
Temperature	100(2) K	
Wavelength	1.54178 Å	
Crystal system	Orthorhombic	
Space group	P 21 21 21	
Unit cell dimensions	a = 8.4470(4) Å	α = 90°.
	b = 16.3195(8) Å	β = 90°.
	c = 17.2927(8) Å	γ = 90°.
Volume	2383.8(2) Å <sup>3</sup>	
Z	4	
Density (calculated)	1.361 Mg/m <sup>3</sup>	
Absorption coefficient	0.897 mm <sup>-1</sup>	

F(000)	1024
Crystal size	0.170 x 0.090 x 0.080 mm <sup>3</sup>
Theta range for data collection	3.724 to 69.959°.
Index ranges	-8<=h<=10, -19<=k<=18, -19<=l<=20
Reflections collected	20098
Independent reflections	4313 [R(int) = 0.0241]
Completeness to theta = 66.000°	100.0 %
Absorption correction	Multi-scan
Max. and min. transmission	1.000 and 0.924
Refinement method	Full-matrix least-squares on F <sup>2</sup>
Data / restraints / parameters	4313 / 0 / 432
Goodness-of-fit on F <sup>2</sup>	1.051
Final R indices [I>2sigma(I)]	R1 = 0.0410, wR2 = 0.1083
R indices (all data)	R1 = 0.0412, wR2 = 0.1085
Absolute structure parameter	0.16(6)
Extinction coefficient	n/a
Largest diff. peak and hole	0.461 and -0.406 e.Å <sup>-3</sup>

## 5.2 Preparation of substrates and intermediates

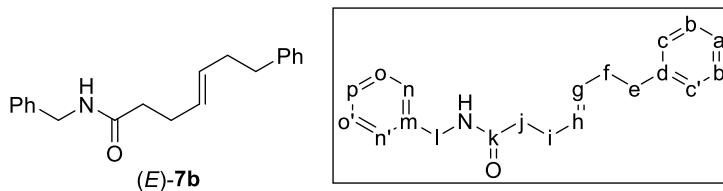
### General procedure for the preparation of (*E*)- $\gamma,\delta$ -unsaturated amides via trimethylaluminum mediated amide bond formation (GP1)



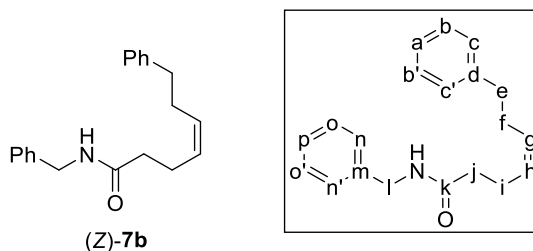
#### Preparation of (*E*)-7-phenyl-4-heptenecarboxylic acid phenyl amide ((*E*)-7a).

To a solution of aniline (2 equiv, 10 mmol, 0.91 mL) in DCM (20 mL) was slowly added trimethylaluminum (1.62 equiv, 2.0 M in hexanes, 8.1 mmol, 4.05 mL) at room temperature. The resulting mixture was stirred at room temp for 30 mins, and the corresponding ethyl ester ((*E*)-7-phenyl-4-heptenecarboxylic acid ethyl ester (*E*)-11, 5 mmol, 1.16g) was added dropwise. The resultant mixture was heated overnight at 35 °C. After cooling to room temperature, the reaction mixture was quenched with HCl (1M) and extracted with DCM (3 x 20 mL). The combined organic extracts were dried (anhyd. Na<sub>2</sub>SO<sub>4</sub>) and concentrated under reduced pressure. Flash chromatography on silica gel (80:20-60:40 hexanes:ethyl acetate) affords the title compound (992 mg, 71%) as a white solid: m.p. 106.0–107.0 °C; TLC analysis *R<sub>f</sub>* 0.65 (60:40 hexanes:ethyl acetate); <sup>1</sup>H NMR (400 MHz, CDCl<sub>3</sub>)  $\delta$  7.54 (2H, d, *J* = 7.8 Hz, m,m'), 7.48 (1H, br s, NH), 7.25–7.40 (4H, m, b,b',n,n'), 7.15–7.25 (3H, m, c,c',a), 7.13 (1H, t, *J* = 7.4 Hz, o), 5.40–5.70 (2H, m, g,h), 2.70 (2H, t, *J* = 7.4 Hz, e), 2.25–2.50 (6H, m, f,i,j); <sup>13</sup>C NMR (100 MHz, CDCl<sub>3</sub>)  $\delta$  171.03 (k), 142.00 (d), 138.06 (l), 131.30 (h), 129.10 (g), 129.05 (n,n'), 128.61 (b,b'), 128.40 (o), 125.92 (c,c'), 124.36 (a), 120.07 (m,m'), 37.65 (e), 36.01 (j), 34.44 (f), 28.60 (i); IR (neat) 3305 (N-H stretch), 3265, 2193, 1664 (C=O stretch), 1603, 1546, 1439, 972,

757, 693  $\text{cm}^{-1}$ ; HRMS (ESI) calcd. for  $\text{C}_{19}\text{H}_{21}\text{NNaO}$  ( $\text{M}+\text{Na}$ ): 302.1521, found 302.1531  $m/z$ .

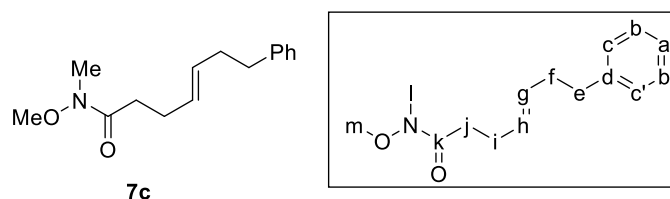


**(E)-7-phenyl-4-heptenecarboxylic acid benzyl amide ((E)-7b).** Following **GP1** with benzyl amine (2 equiv, 10 mmol, 1.1 mL) affords, after flash chromatography on silica gel (80:20-60:40 hexanes:ethyl acetate), the title compound (1.15 g, 78%) as a white solid: m.p. 65.5–66.5 °C; TLC analysis  $R_f$  0.4 (60:40 hexanes:ethyl acetate);  $^1\text{H}$  NMR (400 MHz,  $\text{CDCl}_3$ )  $\delta$  7.15–7.40 (10H, m, a,b,b',c,c',n,n',o,o',p), 5.89 (1H, br s, NH), 5.40–5.60 (2H, m, g,h), 4.44 (2H, d,  $J = 5.7$  Hz, l), 2.67 (2H, t,  $J = 7.3$  Hz, e), 2.20–2.40 (6H, m, f,i,j);  $^{13}\text{C}$  NMR (100 MHz,  $\text{CDCl}_3$ )  $\delta$  172.45 (k), 142.04 (d), 138.55 (m), 131.03 (h), 129.23 (g), 128.80 (b,b'), 128.61 (o,o'), 128.38 (c,c'), 127.93 (n,n'), 127.60 (p), 125.89 (a), 43.66 (l), 36.71 (j), 35.96 (e), 34.40 (f), 28.73 (i); IR (neat) 3285 (N-H stretch), 3028, 2915, 1635 ( $\text{C}=\text{O}$  stretch), 1537 (N-H bend), 1452, 1220, 965, 740, 694  $\text{cm}^{-1}$ ; HRMS (ESI) calcd. for  $\text{C}_{20}\text{H}_{23}\text{NNaO}$  ( $\text{M}+\text{Na}$ ): 316.1677, found 316.1681  $m/z$ .



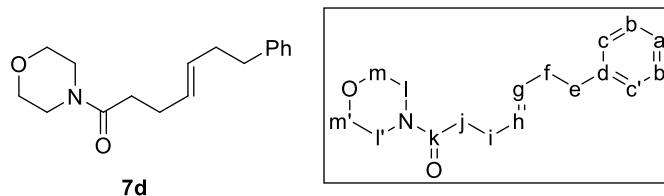
**(Z)-7-phenyl-4-heptenecarboxylic acid benzyl amide ((Z)-7b).** Following **GP1** with **(Z)-11** (5 mmol, 1.16g), benzyl amine (2 equiv, 10 mmol, 1.1 mL) affords, after flash chromatography on silica gel (80:20-60:40 hexanes:ethyl acetate), the title

compound (1.08 g, 73%) as a light yellow oil; TLC analysis  $R_f$  0.4 (60:40 hexanes:ethyl acetate);  $^1\text{H}$  NMR (400 MHz,  $\text{CDCl}_3$ )  $\delta$  7.15–7.40 (10H, m, a,b,b',c,c',n,n',o,o',p), 6.03 (1H, br s, NH), 5.45–5.55 (1H, m, h), 5.35–5.45 (1H, m, g), 4.41 (2H, d,  $J = 5.7$  Hz, l), 2.69 (2H, t,  $J = 7.8$  Hz, e), 2.41 (2H, q,  $J = 7.4$  Hz, f), 2.33 (2H, q,  $J = 7.4$  Hz, i), 2.08 (2H, t,  $J = 8.6$  Hz, j);  $^{13}\text{C}$  NMR (100 MHz,  $\text{CDCl}_3$ )  $\delta$  172.53 (k), 142.10 (d), 138.55 (m), 130.29 (h), 128.81 (b,b'), 128.78 (o,o'), 128.41 (g,c,c'), 127.92 (n,n'), 127.57 (p), 125.92 (a), 43.65 (l), 36.53 (j), 35.91 (e), 29.29 (f), 23.61 (i); IR (neat) 3285 (N-H stretch), 3026, 2922, 1642 (C=O stretch), 1543 (N-H bend), 1495, 1453, 728, 695  $\text{cm}^{-1}$ ; HRMS (ESI) calcd. for  $\text{C}_{20}\text{H}_{23}\text{NNaO}$  ( $\text{M}+\text{Na}$ ): 316.1677, found 316.1681  $m/z$ .

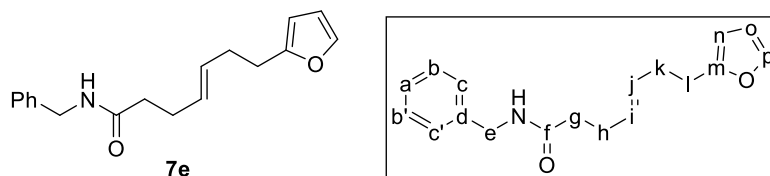


**(E)-7-phenyl-4-heptenecarboxylic acid Weinreb amide (7c).** Following **GPI** with *N*-methoxy-*N*-methylamine hydrochloride (5 equiv, 25 mmol, 2.4 g) and trimethylaluminum (5 equiv, 2.0 M in hexanes, 25 mmol, 12.5 mL) affords, after flash chromatography on silica gel (80:20-60:40 hexanes:ethyl acetate), the title compound (780 mg, 63%) as a yellow oil; TLC analysis  $R_f$  0.5 (60:40 hexanes:ethyl acetate);  $^1\text{H}$  NMR (400 MHz,  $\text{CDCl}_3$ )  $\delta$  7.25–7.35 (2H, m, b,b'), 7.15–7.25 (3H, m, a,c,c'), 5.45–5.65 (2H, m, g,h), 3.69 (3H, s, m), 3.20 (3H, s, l), 2.69 (2H, t,  $J = 7.4$  Hz, e), 2.49 (2H, m, j), 2.20–2.40 (4H, m, f,i);  $^{13}\text{C}$  NMR (100 MHz,  $\text{CDCl}_3$ )  $\delta$  174.14 (k), 142.16 (d), 130.50 (h), 129.63 (g), 128.59 (b,b'), 128.35 (c,c'), 125.84 (a), 61.33 (m), 36.10 (e), 34.50 (f), 32.30 (l), 32.01 (j), 27.65 (i) ; IR (neat) 2934 (C-H  $\text{sp}^3$  stretch), 1661 (C=O stretch), 1452,

1413, 1383 (C-N stretch), 969, 698  $\text{cm}^{-1}$ ; HRMS (ESI) calcd. for  $\text{C}_{15}\text{H}_{21}\text{NNaO}_2$  ( $\text{M}+\text{Na}$ ): 270.1470, found 270.1469  $m/z$ .



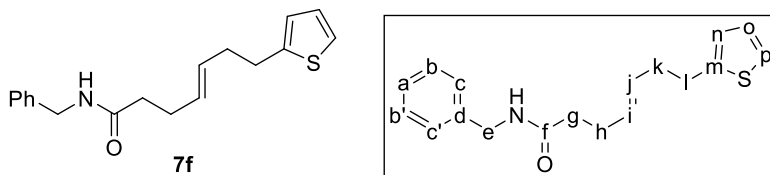
**(E)-7-phenyl-4-heptenecarboxylic acid morpholino amide (7d).** Following **GP1** with morpholine (2 equiv, 10 mmol, 0.87 mL) affords, after flash chromatography on silica gel (70:30-50:50 hexanes:ethyl acetate), the title compound (1.03 g, 75%) as a yellow oil; TLC analysis  $R_f$  0.4 (40:60 hexanes:ethyl acetate);  $^1\text{H}$  NMR (400 MHz,  $\text{CDCl}_3$ )  $\delta$  7.25–7.35 (2H, m, b,b'), 7.15–7.25 (3H, m, a,c,c'), 5.40–5.60 (2H, m, g,h), 3.55–3.70 (6H, m, l,l',m,m'), 3.35–3.50 (2H, m, l,l'), 2.68 (2H, t,  $J = 7.5$  Hz, e), 2.20–2.40 (6H, m, f,i,j);  $^{13}\text{C}$  NMR (100 MHz,  $\text{CDCl}_3$ )  $\delta$  171.23 (k), 142.05 (d), 131.68 (h), 129.47 (g), 128.59 (b,b'), 128.36 (c,c'), 125.87 (a), 67.05 and 66.76 (m,m'), 46.08 and 42.01 (l,l'), 36.04 (e), 34.46 (f), 33.13 (j), 28.28 (i); IR (neat) 2914 (C-H  $\text{sp}^3$  stretch), 2852, 1642 (C=O stretch), 1428, 1113, 968, 699  $\text{cm}^{-1}$ ; HRMS (ESI) calcd. for  $\text{C}_{17}\text{H}_{23}\text{NNaO}_2$  ( $\text{M}+\text{Na}$ ): 296.1626, found 296.1628  $m/z$ .



**(E)-7-(furan-2-yl)-4-heptenecarboxylic acid benzyl amide (7e).**<sup>1</sup> Following **GP1** with the corresponding ethyl ester ((E)-7-(furan-2-yl)-4-heptenecarboxylic acid ethyl ester, 5 mmol, 1.1 g) and benzyl amine (2 equiv, 10 mmol, 1.1 mL) affords, after

<sup>1</sup> The substrate should be used immediately after preparation or stored inside a glovebox to maintain its original quality

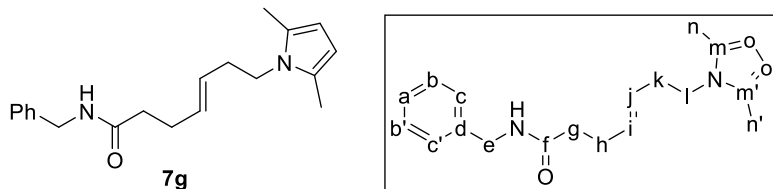
flash chromatography on silica gel (80:20-60:40 hexanes:ethyl acetate), the title compound (596 mg, 42%) as a white solid: m.p. 60.5–61.5 °C; TLC analysis  $R_f$  0.35 (60:40 hexanes:ethyl acetate);  $^1\text{H}$  NMR (400 MHz,  $\text{CDCl}_3$ )  $\delta$  7.25–7.40 (6H, m, a,b,b',c,c',p), 6.28 (1H, dd,  $J = 3.0$  Hz, 1.9 Hz, o), 5.98 (1H, dd,  $J = 3.1$  Hz, 0.6 Hz, n), 5.90 (1H, br s, NH), 5.40–5.60 (2H, m, i,j), 4.44 (2H, d,  $J = 5.7$  Hz, e), 2.67 (2H, t,  $J = 7.4$  Hz, l), 2.20–2.40 (6H, m, g,h,k);  $^{13}\text{C}$  NMR (100 MHz,  $\text{CDCl}_3$ )  $\delta$  172.40 (f), 155.78 (m), 140.89 (p), 138.51 (d), 130.53 (i), 129.50 (j), 128.80 (b,b'), 127.92 (c,c'), 127.60 (a), 110.17 (o), 105.03 (n), 43.66 (e), 36.64 (g), 31.02 (k), 28.68 (h), 28.07 (l); IR (neat) 3293 (N-H stretch), 2916, 1632 (C=O stretch), 1538 (N-H bend), 1506, 1453, 729, 695  $\text{cm}^{-1}$ ; HRMS (ESI) calcd. for  $\text{C}_{18}\text{H}_{21}\text{NNaO}_2$  (M+Na): 306.1470, found 306.1477  $m/z$ .



**(*E*)-7-(thiophen-2-yl)-4-heptenecarboxylic acid benzyl amide (7f).**<sup>2</sup> Following **GP1** with the corresponding ethyl ester ((*E*)-7-(thiophen-2-yl)-4-heptenecarboxylic acid ethyl ester, 5 mmol, 1.19g) and benzyl amine (2 equiv, 10 mmol, 1.1 mL) affords, after flash chromatography on silica gel (80:20-60:40 hexanes:ethyl acetate), the title compound (945 mg, 63%) as a white solid: m.p. 62.0–63.0 °C; TLC analysis  $R_f$  0.35 (60:40 hexanes:ethyl acetate);  $^1\text{H}$  NMR (400 MHz,  $\text{CDCl}_3$ )  $\delta$  7.30–7.40 (2H, m, b,b'), 7.25–7.30 (3H, m, a, c,c'), 7.12 (1H, dd,  $J = 5.2$  Hz, 0.8 Hz, p), 6.93 (1H, dd,  $J = 4.9$  Hz, 3.5 Hz, o), 6.79 (1H, d,  $J = 2.6$  Hz, n), 6.20 (1H, br s, NH), 5.40–5.60 (2H, m, i,j), 4.42 (2H, d,  $J = 5.7$  Hz, e), 2.87 (2H, t,  $J = 7.4$  Hz, l), 2.30–2.40 (4H, m, h,k), 2.26 (2H, t,  $J =$

<sup>2</sup> The substrate should be used immediately after preparation or stored inside a glovebox to maintain its original quality

7.1 Hz, g);  $^{13}\text{C}$  NMR (100 MHz,  $\text{CDCl}_3$ )  $\delta$  172.55 (f), 144.86 (m), 138.62 (d), 130.32 (i), 129.85 (j), 128.78 (b,b'), 127.89 (c,c'), 127.56 (a), 126.81 (o), 124.34 (p), 123.10 (n), 43.61 (e), 36.56 (g), 34.65 (k), 30.00 (h), 28.75 (l); IR (neat) 3291 (N-H stretch), 3030, 2915, 1629 (C=O stretch), 1531 (N-H bend), 1453, 968, 746, 693  $\text{cm}^{-1}$ ; HRMS (ESI) calcd. for  $\text{C}_{18}\text{H}_{21}\text{NNaOS}$  ( $\text{M}+\text{Na}$ ): 322.1242, found 322.1243  $m/z$ .

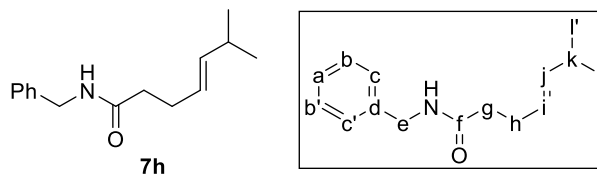


**(*E*)-7-(2,5-dimethyl-1*H*-pyrrol-1-yl)-4-heptenecarboxylic acid benzyl amide**

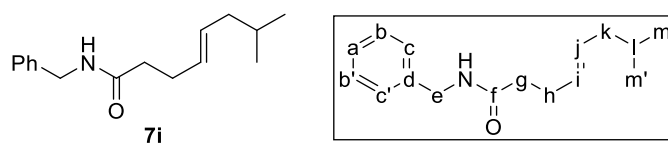
**(7g).**<sup>3</sup> Following **GP1** with the corresponding ethyl ester ((*E*)-7-(2,5-dimethyl-1*H*-pyrrol-1-yl)-4-heptenecarboxylic acid ethyl ester, 5 mmol, 1.25g) and benzyl amine (2 equiv, 10 mmol, 1.1 mL) affords, after flash chromatography on silica gel (80:20-60:40 hexanes:ethyl acetate), the title compound (840 mg, 54%) as a colorless oil; TLC analysis  $R_f$  0.5 (40:60 hexanes:ethyl acetate);  $^1\text{H}$  NMR (400 MHz,  $\text{CDCl}_3$ )  $\delta$  7.35–7.40 (2H, m, b,b'), 7.25–7.35 (3H, m, a,c,c'), 5.99 (1H, br s, NH), 5.77 (2H, s, o,o'), 5.40–5.50 (2H, m, i,j), 4.44 (2H, d,  $J = 5.8$  Hz, e), 3.76 (2H, t,  $J = 7.4$  Hz, l), 2.35–2.45 (2H, m, h), 2.25–2.35 (2H, m, k), 2.25 (2H, t,  $J = 7.0$  Hz, g, overlapping with n,n'), 2.23 (6H, s, n,n');  $^{13}\text{C}$  NMR (100 MHz,  $\text{CDCl}_3$ )  $\delta$  172.35 (f), 138.63 (d), 131.62 (i), 128.79 (b,b',m,m'), 127.92 (c,c'), 127.58 (a), 127.40 (j), 105.12 (o,o'), 43.63 (e), 43.48 (l), 36.51 (g), 34.18 (k), 28.80 (h), 12.73 (n,n'); IR (neat) 3283 (N-H stretch), 2914, 1643 (C=O stretch), 1539 (N-H bend), 1453, 1407, 970, 743, 697  $\text{cm}^{-1}$ ; HRMS (ESI) calcd. for  $\text{C}_{20}\text{H}_{26}\text{N}_2\text{NaO}$  ( $\text{M}+\text{Na}$ ): 333.1943, found 333.1950  $m/z$ .

<sup>3</sup> The substrate should be used immediately after preparation or stored inside a glovebox to maintain its original quality



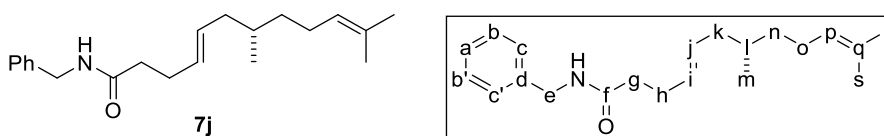


**(E)-6-methyl-4-heptenecarboxylic acid benzyl amide (7h).** Following **GP1** with the corresponding ethyl ester ((*E*)-6-methyl-4-heptenecarboxylic acid ethyl ester, 5 mmol, 0.85 g) and benzyl amine (2 equiv, 10 mmol, 1.1 mL) affords, after flash chromatography on silica gel (80:20-60:40 hexanes:ethyl acetate), the title compound (751 mg, 65%) as a white solid: m.p. 45.0–45.5 °C; TLC analysis  $R_f$  0.4 (60:40 hexanes:ethyl acetate);  $^1\text{H}$  NMR (400 MHz,  $\text{CDCl}_3$ )  $\delta$  7.15–7.40 (5H, m, a,b,b',c,c'), 6.08 (1H, br s, NH), 5.30–5.50 (2H, m, i,j), 4.42 (2H, d,  $J = 5.7$  Hz, e), 2.15–2.40 (5H, m, g,h,k), 0.95 (6H, d,  $J = 6.7$  Hz, l,l');  $^{13}\text{C}$  NMR (100 MHz,  $\text{CDCl}_3$ )  $\delta$  172.61 (f), 139.20 (d), 138.55 (j), 128.76 (b,b'), 127.88 (c,c'), 127.53 (i), 125.35 (a), 43.61 (e), 36.73 (g), 31.04 (k), 28.69 (h), 22.60 (l,l'); IR (neat) 3292 (N-H stretch), 2959, 2928, 2870, 1633 (C=O stretch), 1534 (N-H bend), 1454, 1407, 968, 746, 694  $\text{cm}^{-1}$ ; HRMS (ESI) calcd. for  $\text{C}_{15}\text{H}_{21}\text{NNaO}$  ( $\text{M}+\text{Na}$ ): 254.1521, found 254.1526  $m/z$ .



**(E)-7-methyl-4-octenecarboxylic acid benzyl amide (7i).** Following **GP1** with the corresponding ethyl ester ((*E*)-7-methyl-4-octenecarboxylic acid ethyl ester, 5 mmol, 0.92 g) and benzyl amine (2 equiv, 10 mmol, 1.1 mL) affords, after flash chromatography on silica gel (80:20-60:40 hexanes:ethyl acetate), the title compound (873 mg, 71%) as a white semi-solid; TLC analysis  $R_f$  0.4 (60:40 hexanes:ethyl acetate);  $^1\text{H}$  NMR (400 MHz,  $\text{CDCl}_3$ )  $\delta$  7.30–7.40 (2H, m, b,b'), 7.20–7.30 (3H, m, a,c,c'), 6.09 (1H, br s, NH), 5.35–

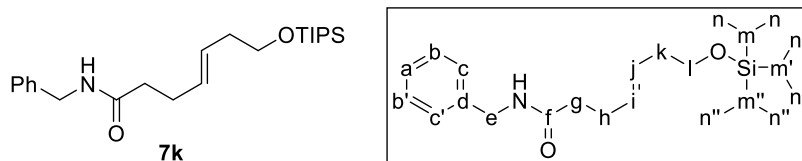
5.55 (2H, m, i,j), 4.42 (2H, d,  $J = 5.6$  Hz, e), 2.30–2.40 (2H, m, h), 2.25–2.30 (2H, m, g) 1.87 (2H, t,  $J = 6.6$  Hz, k), 1.50–1.65 (1H, m, l), 0.87 (6H, d,  $J = 6.6$  Hz, m,m') ;  $^{13}\text{C}$  NMR (100 MHz,  $\text{CDCl}_3$ )  $\delta$  172.57 (f), 138.55 (d), 130.78 (i), 129.52 (j), 128.76 (b,b'), 127.89 (c,c'), 127.53 (a), 43.63 (e), 42.00 (k), 36.75 (g), 28.79 (h), 28.45 (l), 22.37 (m,m'); IR (neat) 3286 (N-H stretch), 2953, 2923, 2868, 1642 (C=O stretch), 1544 (N-H bend), 1454, 967, 696  $\text{cm}^{-1}$ ; HRMS (ESI) calcd. for  $\text{C}_{16}\text{H}_{23}\text{NNaO}$  ( $\text{M}+\text{Na}$ ): 268.1677, found 268.1689  $m/z$ .



**(*S,E*)-7,11-dimethyl-4,10-dodecadienecarboxylic acid benzyl amide (7j).**

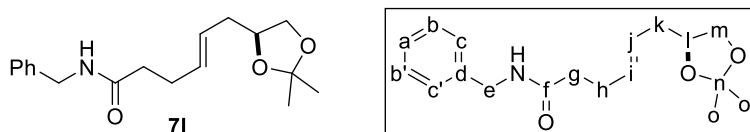
Following **GPI** with the corresponding ethyl ester ((*S,E*)-7,11-dimethyl-4,10-dodecadienecarboxylic acid ethyl ester, 5 mmol, 1.26 g) and benzyl amine (2 equiv, 10 mmol, 1.1 mL) affords, after flash chromatography on silica gel (80:20-60:40 hexanes:ethyl acetate), the title compound (1.14 g, 73%) as a colorless oil; TLC analysis  $R_f$  0.4 (60:40 hexanes:ethyl acetate);  $[\alpha]_D^{20} = +6.2^\circ$  ( $c$  2.0,  $\text{CHCl}_3$ );  $^1\text{H}$  NMR (400 MHz,  $\text{CDCl}_3$ )  $\delta$  7.30–7.35 (2H, m, b,b'), 7.25–7.30 (3H, m, a,c,c'), 6.22 (1H, br s, NH), 5.35–5.50 (2H, m, i,j), 5.11 (1H, tt,  $J = 7.2$  Hz, 1.3 Hz, p), 4.40 (2H, d,  $J = 5.8$  Hz, e), 2.30–2.40 (2H, m, h), 2.25–2.30 (2H, m, g), 1.90–2.05 (3H, m, k,o), 1.75–1.85 (1H, m, k), 1.70 (3H, s, r), 1.62 (3H, s, s), 1.40–1.50 (1H, m, l), 1.25–1.40 (1H, m, n), 1.10–1.20 (1H, m, n), 0.86 (3H, d,  $J = 6.6$  Hz, m);  $^{13}\text{C}$  NMR (100 MHz,  $\text{CDCl}_3$ )  $\delta$  172.62 (f), 138.58 (d), 131.17 (q), 130.47 (i), 129.69 (j), 128.73 (b,b'), 127.86 (c,c'), 127.49 (a), 124.98 (p), 43.60 (e), 40.05 (k), 36.77 (n), 36.71 (g), 32.77 (l), 28.83 (h), 25.85 (r), 25.70 (o), 19.46 (m), 17.77 (s); IR (neat) 3277 (N-H stretch), 2959, 2911, 1643 (C=O stretch), 1545 (N-H

bend), 1453, 968, 696  $\text{cm}^{-1}$ ; HRMS (ESI) calcd. for  $\text{C}_{21}\text{H}_{31}\text{NNaO}$  ( $\text{M}+\text{Na}$ ): 336.2303, found 336.2316  $m/z$ .



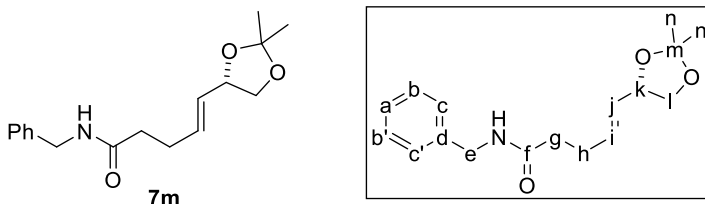
**(*E*)-7-((triisopropylsilyl)oxy)-4-heptenecarboxylic acid benzyl amide (7k).**

Following **GP1** with the corresponding ethyl ester ((*E*)-7-((triisopropylsilyl)oxy)-4-heptenecarboxylic acid ethyl ester, 5 mmol, 1.64 g) and benzyl amine (2 equiv, 10 mmol, 1.1 mL) affords, after flash chromatography on silica gel (80:20-60:40 hexanes:ethyl acetate), the title compound (1.46 g, 75%) as a colorless oil; TLC analysis  $R_f$  0.5 (60:40 hexanes:ethyl acetate);  $^1\text{H}$  NMR (400 MHz,  $\text{CDCl}_3$ )  $\delta$  7.20–7.40 (5H, m, a,b,b',c,c'), 6.14 (1H, br s, NH), 5.40–5.55 (2H, m, i,j), 4.41 (2H, d,  $J = 5.7$  Hz, e), 3.67 (2H, t,  $J = 6.8$  Hz, l), 2.20–2.40 (6H, m, g,h,k), 1.00–1.15 (21H, m, m,m',m'',n,n',n'');  $^{13}\text{C}$  NMR (100 MHz,  $\text{CDCl}_3$ )  $\delta$  172.55 (f), 138.55 (d), 130.49 (i), 128.75 (b,b'), 128.29 (j), 127.84 (c,c'), 127.51 (a), 63.44 (l), 43.61 (e), 36.52 (k), 36.50 (g), 28.85 (h), 18.14 (n,n',n''), 12.11 (m,m',m''); IR (neat) 3283 (N-H stretch), 2942, 2864, 1644 (C=O stretch), 1545 (N-H bend), 1455, 1100, 881, 679  $\text{cm}^{-1}$ ; HRMS (ESI) calcd. for  $\text{C}_{23}\text{H}_{39}\text{NNaO}_2\text{Si}$  ( $\text{M}+\text{Na}$ ): 412.2648, found 412.2652  $m/z$ .



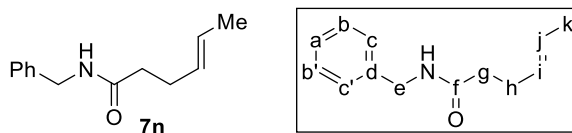
**(*S,E*)-6-(2,2-dimethyl-1,3-dioxolan-4-yl)-4-hexenecarboxylic acid benzyl amide (7l).** Following **GP1** with the corresponding ethyl ester ((*S,E*)-6-(2,2-dimethyl-1,3-dioxolan-4-yl)-4-hexenecarboxylic acid ethyl ester, 5 mmol, 1.2 g) and benzyl amine

(2 equiv, 10 mmol, 1.1 mL) affords, after flash chromatography on silica gel (60:40-30:70 hexanes:ethyl acetate), the title compound (1.05 g, 69%) as a white semi-solid; TLC analysis  $R_f$  0.25 (60:40 hexanes:ethyl acetate);  $[\alpha]_D^{20} = +19.2^\circ$  ( $c$  2.0,  $\text{CHCl}_3$ );  $^1\text{H}$  NMR (400 MHz,  $\text{CDCl}_3$ )  $\delta$  7.30–7.35 (2H, m, b,b'), 7.20–7.30 (3H, m, a,c,c'), 6.11 (1H, br s, NH), 5.40–5.60 (2H, m, i,j), 4.40 (2H, d,  $J = 5.7$  Hz, e), 4.00–4.10 (1H, m, l), 3.97 (1H, dd,  $J = 8.0$  Hz, 6.0 Hz, m), 3.52 (1H, dd,  $J = 7.9$  Hz, 7.0 Hz, m), 2.30–2.40 (3H, m, h,k), 2.25–2.30 (2H, m, g), 2.15–2.25 (1H, m, k), 1.40 (3H, s, o), 1.33 (3H, s, o');  $^{13}\text{C}$  NMR (100 MHz,  $\text{CDCl}_3$ )  $\delta$  172.32 (f), 138.53 (d), 131.82 (i), 128.76 (b,b'), 127.86 (c,c'), 127.54 (a), 126.52 (j), 109.00 (n), 75.53 (l), 68.92 (m), 43.60 (e), 36.92 (k), 36.37 (g), 28.70 (h), 27.01 and 25.74 (o,o'); IR (neat) 3291 (N-H stretch), 2984, 2933, 1643 (C=O stretch), 1541 (N-H bend), 1454, 1369, 1213, 1154, 1058, 969, 697  $\text{cm}^{-1}$ ; HRMS (ESI) calcd. for  $\text{C}_{18}\text{H}_{25}\text{NNaO}_3$  (M+Na): 236.1732, found 326.1739  $m/z$ .

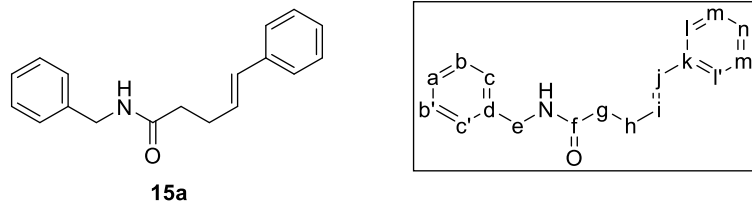


**(*S,E*)-5-(2,2-dimethyl-1,3-dioxolan-4-yl)-4-pentenecarboxylic acid benzyl amide (7m).** Following **GP1** with the corresponding ethyl ester ((*S,E*)-5-(2,2-dimethyl-1,3-dioxolan-4-yl)-4-pentenecarboxylic acid ethyl ester, 5 mmol, 1.14 g) and benzyl amine (2 equiv, 10 mmol, 1.1 mL) affords, after flash chromatography on silica gel (60:40-30:70 hexanes:ethyl acetate), the title compound (913 mg, 63%) as a colorless oil; TLC analysis  $R_f$  0.25 (60:40 hexanes:ethyl acetate);  $[\alpha]_D^{20} = +25.1^\circ$  ( $c$  2.0,  $\text{CHCl}_3$ );  $^1\text{H}$  NMR (400 MHz,  $\text{CDCl}_3$ )  $\delta$  7.30–7.35 (2H, m, b,b'), 7.25–7.30 (3H, m, a,c,c'), 6.02 (1H, br s, NH), 5.79 (1H, td,  $J = 15.3$  Hz, 6.5 Hz, i), 5.49 (1H, dd,  $J = 15.4$  Hz, 7.7 Hz, j),

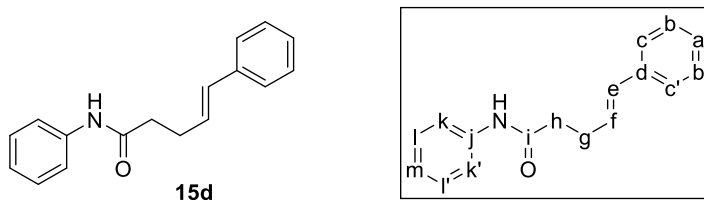
4.35–4.50 (1H, m, k), 4.41 (2H, d,  $J = 5.7$  Hz, e), 4.03 (1H, dd,  $J = 8.1$  Hz, 6.1 Hz, l), 3.52 (1H, dd,  $J = 8.0$  Hz, 8.0 Hz, l), 2.35–2.45 (2H, m, h), 2.25–2.35 (2H, m, g), 1.41 (3H, s, n), 1.38 (3H, s, n');  $^{13}\text{C}$  NMR (100 MHz,  $\text{CDCl}_3$ )  $\delta$  171.96 (f), 138.41 (d), 133.72 (i), 128.80 (b,b'), 128.77 (j), 127.91 (c,c'), 127.62 (a), 109.25 (m), 69.48 (k), 43.68 (e), 35.84 (g), 28.23 (h), 26.83 and 26.01 (n,n'); IR (neat) 3294 (N-H stretch), 2985, 2933, 2872, 1644 (C=O stretch), 1541 (N-H bend), 1454, 1369, 1244, 1213, 1155, 1057, 1028, 967, 859, 732, 697  $\text{cm}^{-1}$ ; HRMS (ESI) calcd. for  $\text{C}_{17}\text{H}_{23}\text{NNaO}_3$  (M+Na): 312.1576, found 312.1581  $m/z$ .



**(*E*)-4-hexenecarboxylic acid benzyl amide (7n).** Following **GP1** with the corresponding ethyl ester ((*E*)-4-hexenecarboxylic acid ethyl ester (5 mmol, 712 mg) and benzyl amine (2 equiv, 10 mmol, 1.1 mL) affords, after flash chromatography on silica gel (80:20-60:40 hexanes:ethyl acetate), the title compound (691 mg, 68%) as a white solid: m.p 58.5–59.5 °C; TLC analysis  $R_f$  0.4 (60:40 hexanes:ethyl acetate);  $^1\text{H}$  NMR (400 MHz,  $\text{CDCl}_3$ )  $\delta$  7.30–7.35 (2H, m, b,b'), 7.20–7.30 (3H, m, a,c,c'), 6.20 (1H, br s, NH), 5.25–5.55 (2H, m, i,j), 2.30–2.35 (2H, m, h), 2.20–2.30 (2H, m, g), 1.64 (3H, d,  $J = 5.8$  Hz, k);  $^{13}\text{C}$  NMR (100 MHz,  $\text{CDCl}_3$ )  $\delta$  172.64 (f), 138.59 (d), 129.64 (i), 128.74 (b,b'), 127.85 (c,c'), 127.49 (a), 126.43 (j), 43.58 (e), 36.60 (g), 28.75 (h), 18.00 (k); IR (neat) 3289 (N-H stretch), 2918, 1633 (C=O stretch), 1548 (N-H bend), 1493, 1452, 1234, 964, 747, 697  $\text{cm}^{-1}$ ; HRMS (ESI) calcd. for  $\text{C}_{13}\text{H}_{17}\text{NNaO}$  (M+Na): 226.1208, found 226.1208  $m/z$ .

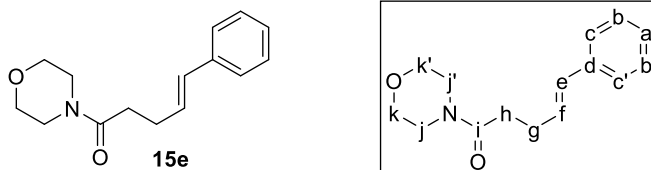


**(E)-5-phenyl-4-pentenecarboxylic acid benzyl amide (15a).** Following **GP1** with the corresponding ethyl ester ((*E*)- 5-phenyl-4-pentenecarboxylic acid ethyl ester (5 mmol, 1.02 g)) and benzyl amine (2 equiv, 10 mmol, 1.1 mL) affords, after flash chromatography on silica gel (80:20-60:40 hexanes:ethyl acetate), the title compound (1.05 g, 79%) as a white solid; TLC analysis  $R_f$  0.4 (60:40 hexanes:ethyl acetate);  $^1\text{H}$  NMR (400 MHz,  $\text{CDCl}_3$ )  $\delta$  7.20–7.40 (10H, m, a, b, b', c, c', l, l', m, m', n), 6.46 (1H, d,  $J = 15.8$  Hz, j), 6.22 (1H, dt,  $J = 15.8$  and 6.9 Hz, i), 6.07 (1H, br s, NH), 4.45 (2H, d,  $J = 5.7$  Hz, e), 2.55–2.65 (2H, m, h), 2.39 (2H, t,  $J = 7.4$  Hz, g);  $^{13}\text{C}$  NMR (100 MHz,  $\text{CDCl}_3$ )  $\delta$  172.10 (f), 138.40 (d), 137.42 (k), 131.30 (j), 128.81 (b, b'), 128.75 (i), 128.64 (l, l'), 127.90 (m, m'), 127.59 (n), 127.30 (a), 126.20 (c, c'), 43.72 (e), 36.51 (g), 29.13 (h).

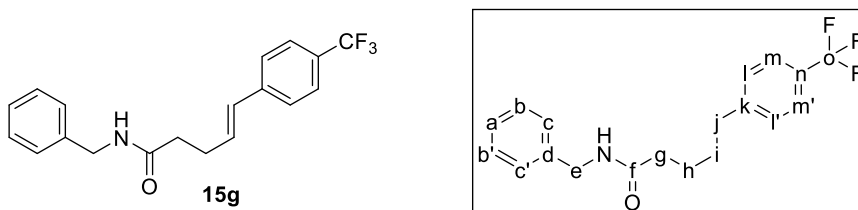


**(E)-5-phenyl-4-pentenecarboxylic acid phenyl amide (15d).** Following **GP1** with the corresponding ethyl ester ester ((*E*)- 5-phenyl-4-pentenecarboxylic acid ethyl ester (5 mmol, 1.02 g)) and aniline (2 equiv, 10 mmol, 0.91 mL) affords, after flash chromatography on silica gel (80:20-60:40 hexanes:ethyl acetate), the title compound (892 mg, 71%) as a white solid; TLC analysis  $R_f$  0.65 (60:40 hexanes:ethyl acetate);  $^1\text{H}$  NMR (400 MHz,  $\text{CDCl}_3$ )  $\delta$  7.53 (2H, d,  $J = 7.8$  Hz, k, k'), 7.30–40 (7H, m, b, b', c, c', l, l', NH), 7.24 (1H, t,  $J = 7.0$  Hz, a), 7.13 (1H, t,  $J = 7.3$  Hz, m), 6.51 (1H, d,  $J =$

15.8 Hz, e), 6.25 (1H, dt,  $J = 15.8$  and  $6.7$  Hz, f), 2.67 (2H, q,  $J = 7.1$  Hz, g), 2.55 (2H, t,  $J = 7.4$  Hz, h);  $^{13}\text{C}$  NMR (100 MHz,  $\text{CDCl}_3$ )  $\delta$  170.81 (i), 137.94 (j), 137.36 (d), 131.47 (e), 129.13 (l,l'), 128.67 (b,b'), 128.63 (m), 127.37 (f), 126.21 (c,c'), 124.44 (a), 120.04 (k,k'), 37.43 (h), 28.94 (g).

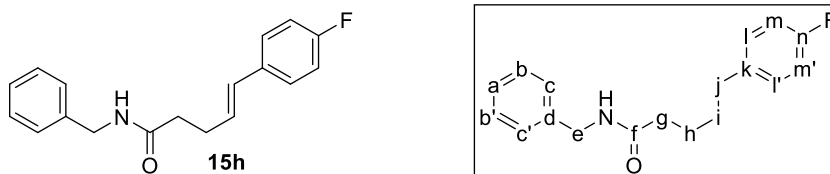


**(E)-5-phenyl-4-pentenecarboxylic acid morpholine amide (15e).** Following **GPI** the corresponding ethyl ester ester ((E)- 5-phenyl-4-pentenecarboxylic acid ethyl ester (5 mmol, 1.02 g)) and morpholine (2 equiv, 10 mmol, 0.87 mL) affords, after flash chromatography on silica gel (70:30-50:50 hexanes:ethyl acetate), the title compound (957 mg, 78%) as a yellow oil; TLC analysis  $R_f$  0.4 (40:60 hexanes:ethyl acetate);  $^1\text{H}$  NMR (400 MHz,  $\text{CDCl}_3$ )  $\delta$  7.34 (2H, d,  $J = 7.2$  Hz, c,c'), 7.29 (2H, t,  $J = 7.3$  Hz, b,b'), 7.20 (1H, t,  $J = 7.1$  Hz, a), 6.44 (1H, d,  $J = 15.9$  Hz, e), 6.26 (1H, dt,  $J = 15.9$  and  $6.8$  Hz, f), 3.60–3.70 (6H, m, j,j',k,k'), 3.45–3.50 (2H, m, j,j'), 2.57 (2H, q,  $J = 6.8$  Hz, h), 2.47 (2H, t,  $J = 7.5$  Hz, g);  $^{13}\text{C}$  NMR (100 MHz,  $\text{CDCl}_3$ )  $\delta$  170.91 (i), 137.50 (d), 130.94 (e), 129.24 (f), 128.64 (b,b'), 127.24 (a), 126.13 (c,c'), 67.02 and 66.72 (k,k'), 46.06 and 42.06 (j,j'), 32.86 (g), 28.67 (h).



**(E)-5-(4-trifluoromethyl)phenyl-4-pentenecarboxylic acid benzyl amide (15g).** Following **GPI** with the corresponding ethyl ester ((E)- 5-(4-

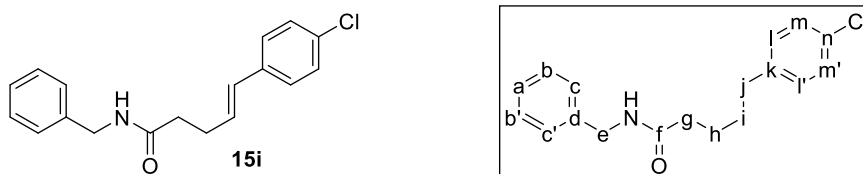
trifluoromethyl)phenyl-4-pentenecarboxylic acid ethyl ester (5 mmol, 1.36 g) and benzyl amine (2 equiv, 10 mmol, 1.1 mL) affords, after flash chromatography on silica gel (80:20-60:40 hexanes:ethyl acetate), the title compound (1.18 g, 71%) as a white solid; TLC analysis  $R_f$  0.4 (60:40 hexanes:ethyl acetate);  $^{19}\text{F}$  NMR (376 MHz,  $\text{CDCl}_3$ )  $\delta$  -62.44 ( $\text{CF}_3$ );  $^1\text{H}$  NMR (400 MHz,  $\text{CDCl}_3$ )  $\delta$  7.56 (2H, d,  $J = 8.2$  Hz, l,l'), 7.41 (2H, d,  $J = 8.2$  Hz, m,m'), 7.25–7.35 (5H, m, a,b,b',c,c'), 6.49 (1H, d,  $J = 15.8$  Hz, j), 6.34 (1H, dt,  $J = 15.8$  and 6.8 Hz, i), 5.81 (1H, br s, NH), 4.48 (2H, d,  $J = 5.7$  Hz, e), 2.64 (2H, q,  $J = 7.1$  Hz, h), 2.42 (2H, t,  $J = 7.3$  Hz, g);  $^{13}\text{C}$  NMR (100 MHz,  $\text{CDCl}_3$ )  $\delta$  171.75 (f), 140.90 (k), 138.32 (d), 131.62 (aryl), 130.08 (aryl), 128.83 (aryl), 127.92 (aryl), 127.68 (aryl), 126.31 (aryl), 125.57 (q,  $J = 4.1$  Hz, aryl), 43.76 (e), 36.17 (g), 29.04 (h).



**(*E*)-5-(4-fluoro)phenyl-4-pentenecarboxylic acid benzyl amide (15h).** Following **GP1** with the corresponding ethyl ester ((*E*)- 5-(4-fluoro)phenyl-4-pentenecarboxylic acid ethyl ester (5 mmol, 1.11 g) and benzyl amine (2 equiv, 10 mmol, 1.1 mL) affords, after flash chromatography on silica gel (80:20-60:40 hexanes:ethyl acetate), the title compound (1.06 g, 75%) as a white solid; TLC analysis  $R_f$  0.4 (60:40 hexanes:ethyl acetate);  $^{19}\text{F}$  NMR (376 MHz,  $\text{CDCl}_3$ )  $\delta$  -115.10 to -115.25 (m, F);  $^1\text{H}$  NMR (400 MHz,  $\text{CDCl}_3$ )  $\delta$  7.20–7.30 (7H, m, a,b,b',c,c',l,l'), 6.99 (2H, t,  $J = 8.7$  Hz, m,m'), 6.41 (1H, d,  $J = 15.8$  Hz, j), 6.13 (1H, dt,  $J = 15.8$  and 6.9 Hz, i), 5.99 (1H, br s, NH), 4.45 (2H, d,  $J = 5.7$  Hz, e), 2.58 (2H, q,  $J = 7.2$  Hz, h), 2.39 (2H, t,  $J = 7.4$  Hz, g);  $^{13}\text{C}$  NMR (100 MHz,  $\text{CDCl}_3$ )  $\delta$  172.08 (f), 163.40 and 160.96 (n), 138.40 (d), 133.61 and 133.58 (k), 130.10

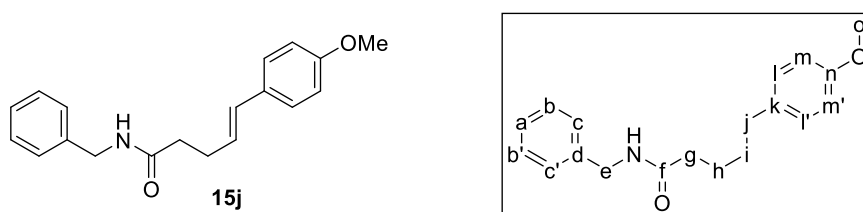


(j), 128.80 (b,b'), 128.50 and 128.48 (i), 127.88 (l,l'), 127.68 (a), 127.60 (c,c'), 115.59 and 115.37 (m,m'), 43.70 (e), 36.43 (g), 29.05 (h).



**(E)-5-(4-chlorophenyl)-4-pentenecarboxylic acid benzyl amide (15i).**

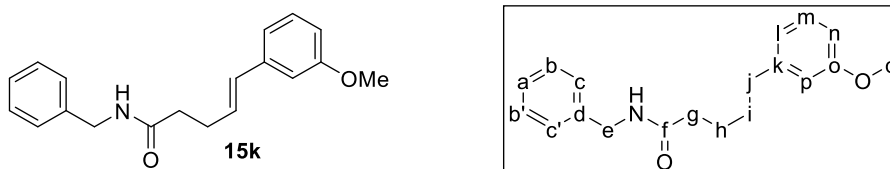
Following **GP1** with the corresponding ethyl ester ((*E*)- 5-(4-chlorophenyl)-4-pentenecarboxylic acid ethyl ester (5 mmol, 1.19 g) and benzyl amine (2 equiv, 10 mmol, 1.1 mL) affords, after flash chromatography on silica gel (80:20-60:40 hexanes:ethyl acetate), the title compound (1.17 g, 77%) as a white solid; TLC analysis  $R_f$  0.4 (60:40 hexanes:ethyl acetate); <sup>1</sup>H NMR (400 MHz, CDCl<sub>3</sub>)  $\delta$  7.20–7.30 (9H, m, a,b,b',c,c',l,l',m,m'), 6.39 (1H, d,  $J$  = 15.8 Hz, j), 6.19 (1H, dt,  $J$  = 15.8 and 6.9 Hz, i), 6.00 (1H, br s, NH), 4.45 (2H, d,  $J$  = 5.7 Hz, e), 2.59 (2H, q,  $J$  = 7.0 Hz, h), 2.39 (2H, t,  $J$  = 7.4 Hz, g); <sup>13</sup>C NMR (100 MHz, CDCl<sub>3</sub>)  $\delta$  172.00 (f), 138.39 (n), 135.93 (d), 132.83 (k), 130.07 (j), 129.52 (i), 128.81 (l,l'), 128.75 (b,b'), 127.89 (m,m'), 127.62 (a), 127.40 (c,c'), 43.71 (e), 36.30 (g), 29.06 (h).



**(E)-5-(4-methoxyphenyl)-4-pentenecarboxylic acid benzyl amide (15j).**

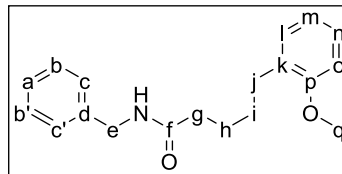
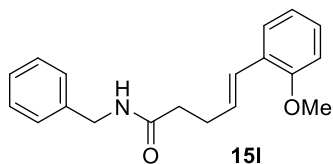
Following **GP1** with the corresponding ethyl ester ((*E*)- 5-(4-methoxyphenyl)-4-pentenecarboxylic acid ethyl ester (5 mmol, 1.17 g) and benzyl amine (2 equiv, 10 mmol, 1.1 mL) affords, after flash chromatography on silica gel (80:20-60:40 hexanes:ethyl

acetate), the title compound (1.11 g, 75%) as a white solid; TLC analysis  $R_f$  0.4 (60:40 hexanes:ethyl acetate);  $^1\text{H}$  NMR (400 MHz,  $\text{CDCl}_3$ )  $\delta$  7.20–7.30 (7H, m, a,b,b',c,c',l,l'), 6.85 (2H, d,  $J = 8.7$  Hz, m,m'), 6.39 (1H, d,  $J = 15.8$  Hz, j), 6.07 (1H, dt,  $J = 15.8$  and 6.9 Hz, i), 4.44 (2H, d,  $J = 5.8$  Hz, e), 3.82 (3H, s, o), 2.57 (2H, q,  $J = 7.3$  Hz, h), 2.38 (2H, t,  $J = 7.4$  Hz, g);  $^{13}\text{C}$  NMR (100 MHz,  $\text{CDCl}_3$ )  $\delta$  172.30 (f), 159.01 (n), 138.47 (d), 130.64 (j), 130.28 (k), 128.78 (l,l'), 127.87 (b,b'), 127.53 (a), 127.32 (c,c'), 126.57 (i), 114.06 (m,m'), 55.42 (o), 43.66 (e), 36.62 (g), 29.16 (h).



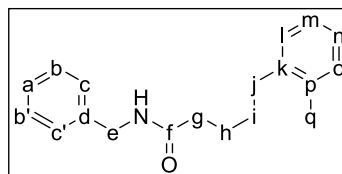
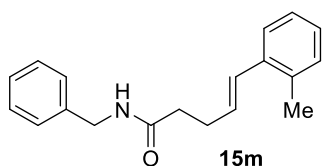
**(*E*)-5-(3-methoxy)phenyl-4-pentenecarboxylic acid benzyl amide (15k).**

Following **GP1** with the corresponding ethyl ester ((*E*)- 5-(3-methoxy)phenyl-4-pentenecarboxylic acid ethyl ester (5 mmol, 1.17 g) and benzyl amine (2 equiv, 10 mmol, 1.1 mL) affords, after flash chromatography on silica gel (80:20-60:40 hexanes:ethyl acetate), the title compound (1.07 g, 72%) as a white solid; TLC analysis  $R_f$  0.4 (60:40 hexanes:ethyl acetate);  $^1\text{H}$  NMR (400 MHz,  $\text{CDCl}_3$ )  $\delta$  7.20–7.30 (6H, m, a,b,b',c,c',m), 6.93 (1H, d,  $J = 7.6$  Hz, l), 6.88 (1H, d,  $J = 2.1$  Hz, p), 6.80 (1H, dd,  $J = 8.2$  and 2.5 Hz, n), 6.43 (1H, d,  $J = 15.8$  Hz, j), 6.22 (1H, dt,  $J = 15.8$  and 6.9 Hz, i), 5.95 (1H, br s), 4.45 (2H, d,  $J = 5.7$  Hz, e), 3.82 (3H, s, q), 2.60 (2H, q,  $J = 7.5$  Hz, h), 2.39 (2H, t,  $J = 7.5$  Hz, g);  $^{13}\text{C}$  NMR (100 MHz,  $\text{CDCl}_3$ )  $\delta$  172.12 (f), 159.92 (o), 138.90 (k), 138.38 (d), 131.19 (j), 129.61 (i), 129.12 (m), 128.81 (b,b'), 127.89 (c,c'), 127.59 (a), 118.87 (l), 112.94 (n), 111.59 (p), 55.33 (q), 43.72 (e), 36.43 (g), 29.08 (h).



**(E)-5-(2-methoxy)phenyl-4-pentenecarboxylic acid benzyl amide (15l).**

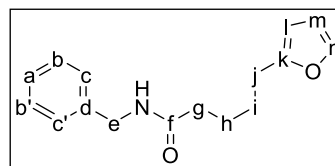
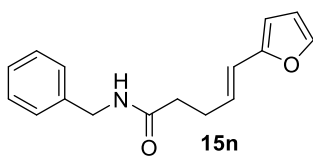
Following **GP1** with the corresponding ethyl ester ((E)- 5-(2-methoxy)phenyl-4-pentenecarboxylic acid ethyl ester (5 mmol, 1.17 g) and benzyl amine (2 equiv, 10 mmol, 1.1 mL) affords, after flash chromatography on silica gel (80:20-60:40 hexanes:ethyl acetate), the title compound (1.05 g, 71%) as a white solid; TLC analysis  $R_f$  0.4 (60:40 hexanes:ethyl acetate);  $^1\text{H}$  NMR (400 MHz,  $\text{CDCl}_3$ )  $\delta$  7.39 (1H, dd,  $J = 7.8$  and 1.6 Hz, n), 7.20–7.30 (6H, m, a,b,b',c,c',l), 6.93 (1H, t,  $J = 7.4$  Hz, m), 6.88 (1H, d,  $J = 8.2$  Hz, o), 6.80 (1H, d,  $J = 16.0$  Hz, j), 6.23 (1H, dt,  $J = 16.0$  and 6.9 Hz, i), 6.04 (1H, br s), 4.45 (2H, d,  $J = 5.8$  Hz, e), 3.83 (3H, s, q), 2.61 (2H, q,  $J = 7.3$  Hz, h), 2.40 (2H, t,  $J = 7.6$  Hz, g);  $^{13}\text{C}$  NMR (100 MHz,  $\text{CDCl}_3$ )  $\delta$  172.35 (f), 156.50 (p), 138.49 (d), 129.48 (j), 128.77 (b,b'), 128.33 (l), 127.88 (c,c'), 127.52 (a), 126.68 (n), 126.49 (k), 125.90 (i), 120.77 (m), 110.92 (o), 55.53 (q), 43.68 (e), 36.62 (g), 29.61 (h).



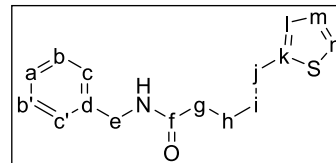
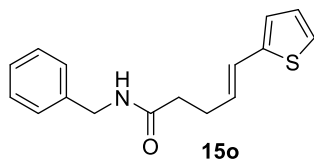
**(E)-5-(2-methyl)phenyl-4-pentenecarboxylic acid benzyl amide (15m).**

Following **GP1** with the corresponding ethyl ester ((E)- 5-(2-methyl)phenyl-4-pentenecarboxylic acid ethyl ester (5 mmol, 1.09 g) and benzyl amine (2 equiv, 10 mmol, 1.1 mL) affords, after flash chromatography on silica gel (80:20-60:40 hexanes:ethyl acetate), the title compound (992 mg, 71%) as a white solid; TLC analysis  $R_f$  0.4 (60:40 hexanes:ethyl acetate);  $^1\text{H}$  NMR (400 MHz,  $\text{CDCl}_3$ )  $\delta$  7.35–7.45 (1H, m, aryl), 7.25–7.35

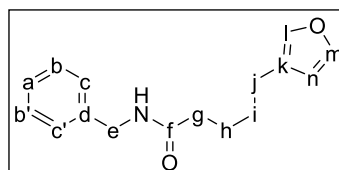
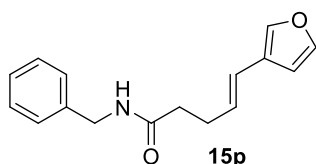
(5H, m, aryl), 7.10–7.20 (3H, m, aryl), 6.67 (1H, d,  $J = 15.6$  Hz, j), 6.10 (1H, dt,  $J = 15.6$  and 6.9 Hz, i), 5.97 (1H, br s), 4.47 (2H, d,  $J = 5.7$  Hz, e), 2.63 (2H, q,  $J = 7.3$  Hz, h), 2.42 (2H, t,  $J = 7.5$  Hz, g), 2.33 (3H, s, q);  $^{13}\text{C}$  NMR (100 MHz,  $\text{CDCl}_3$ )  $\delta$  172.15 (f), 138.41 (aryl), 136.54 (aryl), 135.19 (aryl), 130.34 (aryl), 130.09 (i), 129.14 (j), 128.82 (aryl), 127.91 (aryl), 127.61 (aryl), 127.25 (aryl), 126.16 (aryl), 125.61 (aryl), 43.72 (e), 36.67 (g), 29.47 (h), 19.93 (q).



**(E)-5-(2-furanyl)-4-pentenecarboxylic acid benzyl amide (15n).** Following **GP1** with the corresponding ethyl ester ((*E*)- 5-(2-furanyl)phenyl-4-pentenecarboxylic acid ethyl ester (5 mmol, 970 mg) and benzyl amine (2 equiv, 10 mmol, 1.1 mL) affords, after flash chromatography on silica gel (80:20-60:40 hexanes:ethyl acetate), the title compound (830 mg, 65%) as a light yellow solid;  $^1\text{H}$  NMR (400 MHz,  $\text{CDCl}_3$ )  $\delta$  7.20–7.35 (6H, m, a,b,b',c,c',n), 6.37 (1H, dd,  $J = 3.2$  and 1.9 Hz, l), 6.28 (1H, d,  $J = 15.9$  Hz, j), 6.10–6.20 (2H, m, i and m, *overlapped*), 5.95 (1H, br s), 4.45 (2H, d,  $J = 5.7$  Hz, e), 2.57 (2H, q,  $J = 7.2$  Hz, h), 2.37 (2H, t,  $J = 7.5$  Hz, g);  $^{13}\text{C}$  NMR (100 MHz,  $\text{CDCl}_3$ )  $\delta$  172.03 (f), 152.89 (k), 141.62 (n), 138.36 (d), 128.78 (b,b'), 127.87 (c,c'), 127.64 (i), 127.57 (a), 119.92 (j), 111.28 (m), 106.90 (l), 43.71 (e), 36.37 (g), 28.90 (h).

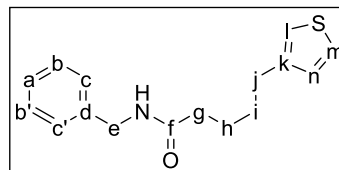
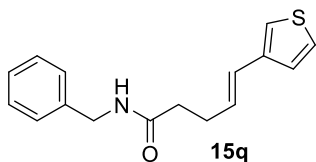


**(E)-5-(2-thiophenyl)-4-pentenecarboxylic acid benzyl amide (15o).** Following **GPI** with the corresponding ethyl ester ((E)- 5-(2-thiophenyl)phenyl-4-pentenecarboxylic acid ethyl ester (5 mmol, 1.05 g) and benzyl amine (2 equiv, 10 mmol, 1.1 mL) affords, after flash chromatography on silica gel (80:20-60:40 hexanes:ethyl acetate), the title compound (936 mg, 69%) as a white solid;  $^1\text{H}$  NMR (400 MHz,  $\text{CDCl}_3$ )  $\delta$  7.25–7.35 (5H, m, a,b,b',c,c'), 7.13 (1H, d,  $J = 5.0$  Hz, n), 6.96 (1H, dd,  $J = 5.0$  and 4.0 Hz, l), 6.89 (1H, d,  $J = 3.3$  Hz, m), 6.58 (1H, d,  $J = 15.7$  Hz, j), 6.06 (1H, dt,  $J = 15.7$  and 7.0 Hz, i), 5.91 (1H, br s), 4.46 (2H, d,  $J = 5.7$  Hz, e), 2.57 (2H, q,  $J = 7.2$  Hz, h), 2.38 (2H, t,  $J = 7.3$  Hz, g);  $^{13}\text{C}$  NMR (100 MHz,  $\text{CDCl}_3$ )  $\delta$  171.98 (f), 142.57 (k), 138.33 (d), 128.81 (b,b'), 128.56 (i), 127.87 (c,c'), 127.59 (a) , 127.39 (l), 124.98 (m), 124.60 (j). 123.67 (n), 43.73 (e), 36.36 (g), 28.92 (h).

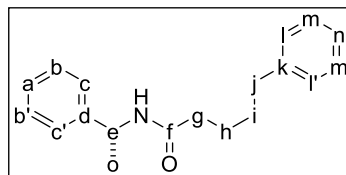
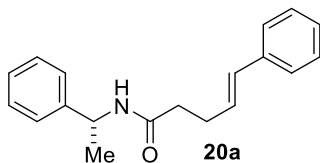


**(E)-5-(3-furanyl)-4-pentenecarboxylic acid benzyl amide (15p).** Following **GPI** with the corresponding ethyl ester ((E)- 5-(3-furanyl)phenyl-4-pentenecarboxylic acid ethyl ester (5 mmol, 970 mg) and benzyl amine (2 equiv, 10 mmol, 1.1 mL) affords, after flash chromatography on silica gel (80:20-60:40 hexanes:ethyl acetate), the title compound (870 mg, 68%) as a light yellow solid;  $^1\text{H}$  NMR (400 MHz,  $\text{CDCl}_3$ )  $\delta$  7.20–7.40 (7H, m, a,b,b',c,c',l,m), 6.49 (1H, d,  $J = 0$  Hz, n), 6.30 (1H, d,  $J = 15.8$  Hz, j), 5.94 (1H, dt,  $J = 15.8$  and 6.9 Hz, i), 5.89 (1H, br s), 4.46 (2H, d,  $J = 5.7$  Hz, e), 2.55 (2H, q,  $J$

= 7.4 Hz, h), 2.37 (2H, t,  $J = 7.4$  Hz, g);  $^{13}\text{C}$  NMR (100 MHz,  $\text{CDCl}_3$ )  $\delta$  172.10 (f), 143.50 (m), 139.90 (l), 138.40 (d), 128.81 (b,b'), 128.33 (i), 127.89 (c,c'), 127.61 (a), 124.21 (k), 120.94 (j), 107.60 (n), 43.70 (e), 36.49 (g), 28.97 (h).



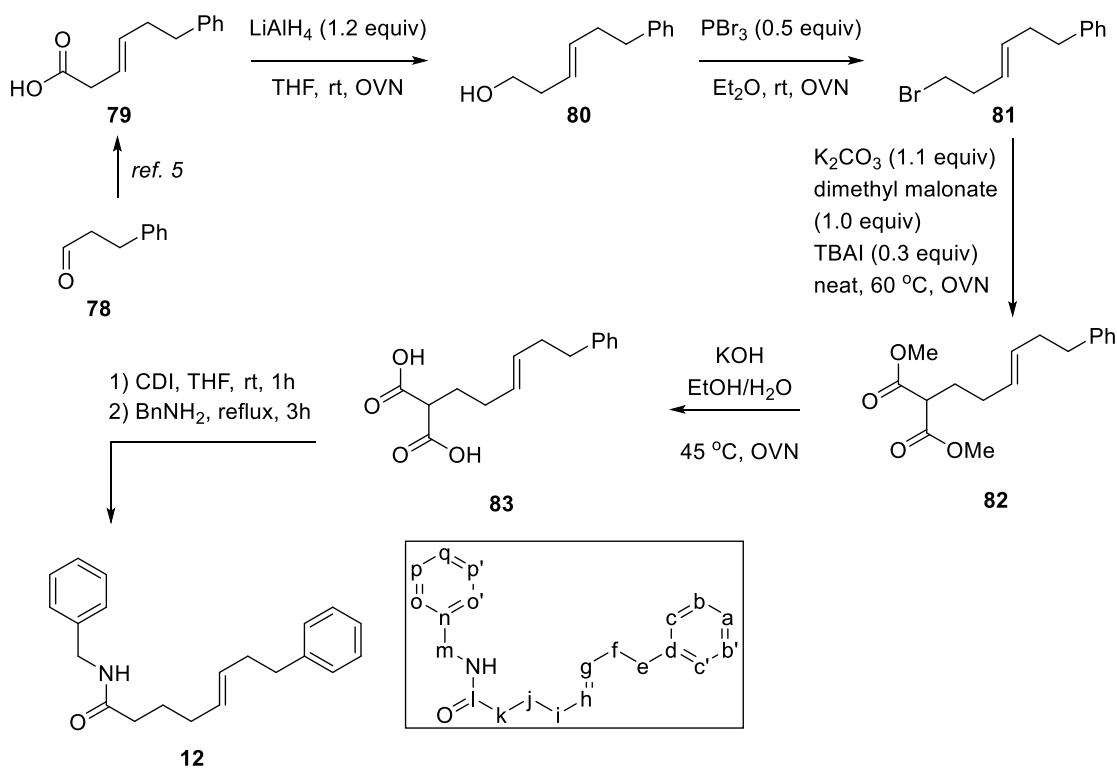
**(*E*)-5-(3-thiophenyl)-4-pentenecarboxylic acid benzyl amide (15q).** Following **GP1** with the corresponding ethyl ester ((*E*)- 5-(3-thiophenyl)phenyl-4-pentenecarboxylic acid ethyl ester (5 mmol, 1.05 g) and benzyl amine (2 equiv, 10 mmol, 1.1 mL) affords, after flash chromatography on silica gel (80:20-60:40 hexanes:ethyl acetate), the title compound (963 mg, 79%) as a white solid;  $^1\text{H}$  NMR (400 MHz,  $\text{CDCl}_3$ )  $\delta$  7.20–7.35 (6H, m, a,b,b',c,c',l), 7.17 (1H, dd,  $J = 5.0$  and 0 Hz, m), 7.07 (1H, dd,  $J = 2.2$  and 0 Hz, n), 6.46 (1H, d,  $J = 15.8$  Hz, j), 6.07 (1H, dt,  $J = 15.8$  and 6.9 Hz, i), 5.94 (1H, br s), 4.46 (2H, d,  $J = 5.7$  Hz, e), 2.57 (2H, q,  $J = 7.3$  Hz, h), 2.38 (2H, t,  $J = 7.4$  Hz, g);  $^{13}\text{C}$  NMR (100 MHz,  $\text{CDCl}_3$ )  $\delta$  172.11 (f), 140.03 (k), 138.40 (d), 128.80 (b,b'), 128.65 (i), 127.89 (c,c'), 127.60 (a), 126.01 (l), 125.60 (j), 125.03 (m), 121.23 (n), 43.70 (e), 36.49 (g), 29.01 (h).



**(*R,E*)-5-phenyl-4-pentenecarboxylic acid 1-phenylethyl amide (20a).** Following **GP1** with the corresponding ethyl ester ((*E*)- 5-phenyl-4-pentenecarboxylic acid ethyl ester (5 mmol, 1.02 g) and (*R*)-(+)- $\alpha$ -methylbenzylamine (2 equiv, 10 mmol, 1.3 mL) affords, after flash chromatography on silica gel (80:20-60:40 hexanes:ethyl

acetate), the title compound (1.06 g, 76%) as a white solid; TLC analysis  $R_f$  0.4 (60:40 hexanes:ethyl acetate);  $^1\text{H}$  NMR (400 MHz,  $\text{CDCl}_3$ )  $\delta$  7.20–7.40 (10H, m, a,b,b',c,c',l,l',m,m',n), 6.45 (1H, d,  $J = 15.8$  Hz, j), 6.21 (1H, dt,  $J = 15.8$  and 6.9 Hz, i), 5.94 (1H, d,  $J = 7.4$  Hz, NH), 5.15–5.20 (1H, m, e), 2.58 (2H, q,  $J = 6.9$  Hz, h), 2.30–2.40 (2H, m, g), 1.50 (3H, d,  $J = 6.9$  Hz, o);  $^{13}\text{C}$  NMR (100 MHz,  $\text{CDCl}_3$ )  $\delta$  171.33 (f), 143.32 (k), 137.44 (d), 131.25 (j), 128.82 (i), 128.77 (b,b'), 128. 128.64 (l,l'), 127.42 (n), 127.29 (a), 126.30 (m,m'), 126.19 (c,c'), 43.77 (e), 36.57 (g), 29.16 (h), 21.86 (o).

### Preparation sequence of $\gamma,\delta$ -unsaturated benzyl amide 12



To a cooled ( $0^\circ\text{C}$ ) solution of (*E*)-6-phenylhex-3-enoic acid<sup>5</sup> **79** (13.3 mmol, 2.53 g) in THF (50 mL) was added lithium aluminum hydride (LAH, 1.05 equiv, 14.0 mmol, 530 mg). The resulting mixture was warmed to room temperature and stirred overnight. The reaction mixture was quenched with 5N KOH (1 mL) and water (0.5 mL). Following

by 30-min stir, the resultant mixture was filtered through a pad of celite and wash with ethyl acetate (2 x 5 mL). The filtrate was dried (anhyd. Na<sub>2</sub>SO<sub>4</sub>) and concentrated under reduced pressure to give the crude yellow oil **S3** in quantitative yield which was used in the next step without further purification.

To a cooled (0 °C) solution of (*E*)-6-phenylhex-3-en-1-ol **80** (13.1 mmol, 2.31 g) in diethyl ether (20 mL) was added PBr<sub>3</sub> (0.5 equiv, 6.6 mmol, 0.62 mL) dropwise. The resultant mixture was slowly warmed to room temperature and stirred overnight. The reaction mixture was quenched with brine solution (20 mL). The organic layer was separated and the aqueous layer was washed with ethyl acetate (2 x 20 mL). The combined organic extracts were concentrated under reduced pressure, passed through a short pad of silica gel eluting with 20% ethyl acetate:hexanes (50 mL), and concentrated again under reduced pressure to afford the crude yellow oil **80** in 92% yield which was used in the next step without further purification.

A neat mixture of (*E*)-(6-bromohex-3-en-1-yl)benzene **81** (6 mmol, 1.43 g), dimethyl malonate (6 mmol, 1.0 equiv, 0.69 mL), K<sub>2</sub>CO<sub>3</sub> (6.6 mmol, 1.1 equiv, 910 mg) and TBAI (1.8 mmol, 0.3 equiv, 665 mg) was stirred vigorously at 60 °C for 24 hrs. The resultant mixture was cooled down to room temperature, diluted with ethyl acetate, filtered, washed with ethyl acetate (3 x 5 mL), and concentrated under reduced pressure to give the crude yellow oil **81** in 81% yield which was used in the next step without further purification.

To a solution of dimethyl (*E*)-2-(6-phenylhex-3-en-1-yl)malonate **82** (2.2 mmol, 635 mg) in EtOH:water (5 mL, 4:1) was added KOH (7.2 mmol, 3.2 equiv, 405 mg). The resultant mixture was heated to 45 °C. After a 16h stir, the mixture was cooled to room

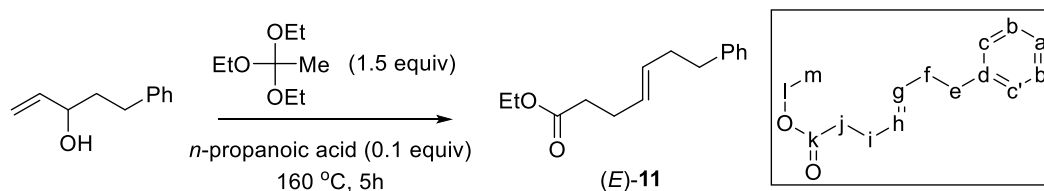


temperature, concentrated under reduced pressure and poured into a solution of diethyl ether:hexanes (5 mL, 1:4) and water (5 mL). The resulting mixture was acidified with conc. H<sub>2</sub>SO<sub>4</sub> (0.4 mL) and adjusted to pH = 1 by dilute HCl (3M). After extraction with EtOAc (3 x 10 mL), the organic layers were combined, dried (anhyd. Na<sub>2</sub>SO<sub>4</sub>) and concentrated under reduced pressure to give the crude off-white solid **82** in 96% yield which was used in the next step without further purification.

To a solution of (*E*)-2-(6-phenylhex-3-en-1-yl)malonic acid **83** (2.1 mmol, 550 mg) in THF (5 mL) was added CDI (2.3 mmol, 1.1 equiv, 372 mg) portion wise under positive nitrogen.<sup>6</sup> The resulting mixture was stirred at room temp for 2h, then benzyl amine (3.2 mmol, 1.5 equiv, 0.35 mL) was added in one portion. The resultant mixture was refluxed for 3h, cooled to room temp, and concentrated under reduced pressure. The obtained residue was then dissolved in 10 mL EtOAc and washed with a 10 mL aqueous solution of citric acid monohydrate (2.1 mmol, 1 equiv, 441 mg) and a saturated sodium bicarbonate (10 mL). The organic extract was dried (anhyd. Na<sub>2</sub>SO<sub>4</sub>) and concentrated under reduced pressure. Flash chromatography on silica gel (80:20-60:40 hexanes:ethyl acetate) affords the title compound **12** (473 mg, 73%) as a white solid: m.p. 67.0–68.0 °C; TLC analysis R<sub>f</sub> 0.4 (60:40 hexanes:ethyl acetate); <sup>1</sup>H NMR (400 MHz, CDCl<sub>3</sub>) δ 7.25–7.40 (7H, m, b,b',o,o',p,p',q), 7.15–7.25 (3H, m, a,c,c'), 5.68 (1H, br s, NH), 5.30–5.50 (2H, m, g,h), 4.44 (2H, d, *J* = 5.7 Hz, m), 2.69 (2H, t, *J* = 7.4 Hz, e), 2.34 (2H, q, *J* = 6.6 Hz, f), 2.11 (2H, t, *J* = 7.4 Hz, k), 2.04 (2H, q, *J* = 6.6 Hz, i), 1.65–1.80 (2H, m, j); <sup>13</sup>C NMR (100 MHz, CDCl<sub>3</sub>) δ 172.92 (l), 142.08 (d), 138.54 (n), 130.66 (g), 130.17 (h), 128.83 (b,b'), 128.64 (p,p'), 128.37 (c,c'), 128.00 (o,o'), 127.64 (q), 125.84 (a), 43.70 (m), 36.95 (e), 35.80 (k), 34.19 (f), 31.95 (i), 25.37 (j); IR (neat) 3290 (N-H stretch),

2924, 2848, 1629 (C=O stretch), 1550 (N-H bend), 1494, 1452, 726, 693  $\text{cm}^{-1}$ ; HRMS (ESI) calcd. for  $\text{C}_{21}\text{H}_{25}\text{NNaO}$  ( $\text{M}+\text{Na}$ ): 330.1834, found 330.1833  $m/z$ .

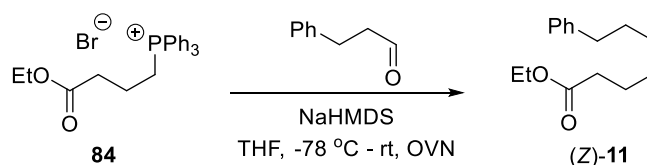
**General procedure for the preparation of (*E*)- $\gamma,\delta$ -unsaturated ethyl esters via Claisen-Johnson rearrangement (GP2)<sup>7</sup>**



**(*E*)-7-phenyl-4-heptenecarboxylic acid ethyl ester ((*E*)-11).**<sup>7</sup> A mixture of 5-phenylpent-1-en-3-ol (61.6 mmol, 10.1 g), triethyl orthoacetate (93.3 mmol, 1.5 equiv, 17.1 mL), and *n*-propanoic acid (6.6 mmol, 0.11 equiv, 0.5 mL) was heated with Dean-Stark apparatus at 160 °C for 5h. After cooling to room temperature, the reaction mixture was quenched with satd.  $\text{NaHCO}_3$  (10 mL), then dilute with DCM (100 mL) and HCl (1M, 100 mL). After a 2h stir, the organic layer was separated, and the aqueous layer was washed with DCM (2 x 50 mL). The organic layers were combined, dried (anhyd.  $\text{Na}_2\text{SO}_4$ ) and concentrated under reduced pressure affords, after flash chromatography on silica gel (95:5 hexanes:ethyl acetate), the title compound (11.9 g, 83%) as a yellow liquid; TLC analysis  $R_f$  0.4 (90:10 hexanes:ethyl acetate);  $^1\text{H}$  NMR (400 MHz,  $\text{CDCl}_3$ )  $\delta$  7.30–7.35 (2H, m, b,b'), 7.30–7.35 (3H, m, a,c,c'), 5.45–5.60 (2H, m, g,h), 4.18 (2H, q,  $J = 7.1$  Hz, l), 2.72 (2H, t,  $J = 7.3$  Hz, e), 2.30–2.40 (6H, m, f,i,j), 1.30 (3H, t,  $J = 7.1$  Hz, m);  $^{13}\text{C}$  NMR (100 MHz,  $\text{CDCl}_3$ )  $\delta$  173.27 (k), 142.07 (d), 130.85 (h), 128.96 (g), 128.59 (b,b'), 128.39 (c,c'), 125.90 (a), 60.35 (l), 36.09 (e), 34.49 (j), 34.44 (f), 28.04 (i), 14.42 (m); IR (neat) 2980, 2925, 1732 (C=O stretch), 1453, 1371, 1247, 1175, 1032, 968, 745, 698  $\text{cm}^{-1}$ ; HRMS (ESI) calcd. for  $\text{C}_{15}\text{H}_{20}\text{NaO}_2$  ( $\text{M}+\text{Na}$ ): 255.1361, found 255.1364  $m/z$ .

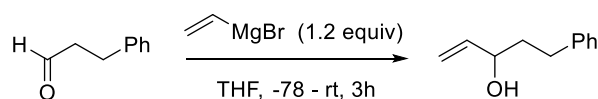
The above ester (*E*)-**11** was isolated via column chromatography for screening purpose. All other (*E*)-esters were pass through a short pad of silica gel eluting with 10% EtOAc:hexanes, concentrated under reduced pressure, and used without further purification. *Note:* the reaction was typically done under air. For furan-, thiophene-, and pyrrole-containing compounds, it should be done under nitrogen to prevent partial decomposition of the products.

**Preparation of (*Z*)-7-phenyl-4-heptenecarboxylic acid ethyl ester ((*Z*)-**11**) via Wittig reaction**



The Wittig reagent **84** was prepared from 4-bromobutyric acid ethyl ester and triphenylphosphine as previously reported in literature.<sup>8</sup> To a cooled (0 °C) solution of **84** (11 mmol, 5 g) in THF (40 mL) was added NaHMDS (1.1 equiv, 1M, 12 mmol, 12 mL) dropwise. The resultant mixture was stirred at 0 °C in 30 mins. After cooling down to -78 °C, 3-phenylpropanal (1.1 equiv, 12 mmol, 1.6 mL) was added dropwise. The resultant mixture was slowly warmed to room temp and stirred overnight. The reaction was quenched with satd. ammonium chloride (20 mL) and extracted with EtOAc (3 x 30 mL). The organic layers were combined, washed with brine, dried (anhyd. Na<sub>2</sub>SO<sub>4</sub>) and concentrated under reduced pressure. The obtained residue was dilute with minimum amount of DCM, passed through a short pad of silica gel eluting with 10% EtOAc:hexanes, concentrated under reduced pressure to give a crude (*Z*)-**11** as a yellow liquid (1.3 g, 51%), which was used in the next step without further purification.

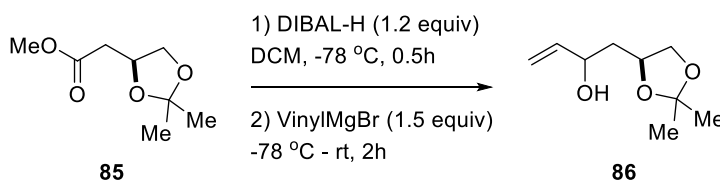
**General procedure for the preparation of allylic alcohol with aldehyde and vinyl magnesium bromide (GP3)<sup>7</sup>**



To a cooled (-78 °C) solution of vinyl magnesium bromide (140 mmol, 1.2 equiv, 1M, 140 mL) was added 3-phenylpropanal (120 mmol, 16 mL) dropwise. The resultant mixture was slowly warmed to room temp and stirred for a total of 3h. After quenching with satd. ammonium chloride, it was continued stirring for 15 more mins. The pH was adjusted to 3-4 using dilute HCl (1M). After extraction with EtOAc (3 x 100 mL), the organic layers were combined, washed with brine, dried (anhyd. Na<sub>2</sub>SO<sub>4</sub>) and concentrated under reduced pressure to give the crude yellow liquid (18.2 g, 93%) which was used in the next step without further purification.

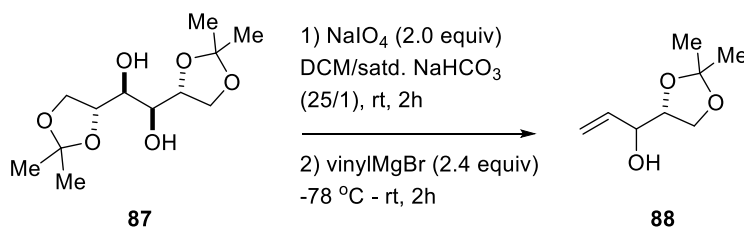
The above procedure was applied for all allylic alcohols, except for the two dioxolane-containing compounds.

**Preparations of dioxolane-containing allylic alcohols**



**1-((S)-2,2-dimethyl-1,3-dioxolan-4-yl)but-3-en-2-ol (86).** The preparation of (4S)-(2,2-dimethyl-[1,3]-dioxolan-4-yl) acetic acid methyl ester **85** from (L)-malic acid was previously reported in literature.<sup>9</sup> To the solution of ester **85** (20 mmol, 3.5 g) in DCM (80 mL) was slowly added DIBAL-H (1M, 1.2 equiv, 24 mmol, 24 mL) at -78 °C. The resulting mixture was stirred at -78 °C for 30 mins, then vinyl magnesium bromide (1M, 1.5 equiv, 30 mmol, 30 mL) was slowly added at the same temperature. The

resultant mixture was stirred at  $-78\text{ }^{\circ}\text{C}$  for 30 mins and allowed to warm to room temperature and stirred for another 1.5h. The reaction mixture was carefully quenched with NaOH (1M, 15 mL). After filtering through a pad of celite, a filtrate was washed with water and brine. The organic layer was dried (anhyd.  $\text{Na}_2\text{SO}_4$ ) and carefully concentrated under reduced pressure to give the crude yellow liquid (3.06 g, 89%) which was used in the next step without further purification.

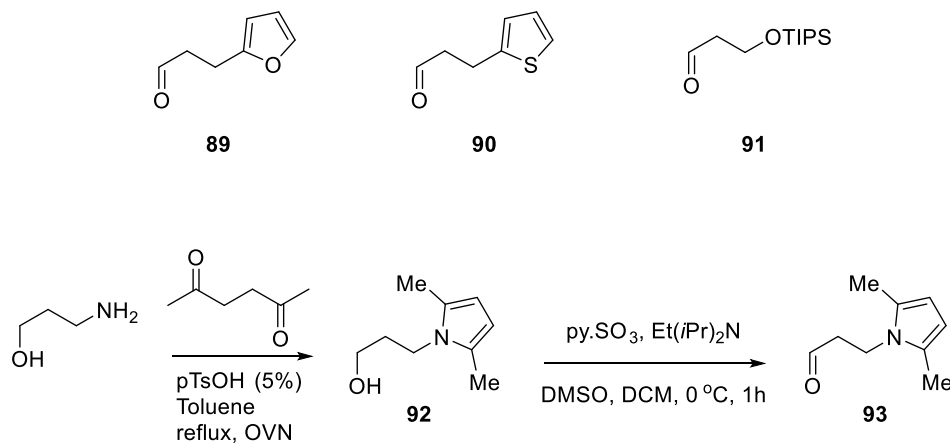


**1-((*R*)-2,2-dimethyl-1,3-dioxolan-4-yl)prop-2-en-1-ol (88).** The preparation of (1*S*,2*S*)-1,2-bis((*R*)-2,2-dimethyl-1,3-dioxolan-4-yl)ethane-1,2-diol **87** from (D)-mannitol was previously reported in literature.<sup>10</sup> To a solution of **87** (21.7 mmol, 5.7 g) in DCM (65 mL) was added satd.  $\text{NaHCO}_3$  (2.6 mL). While the resulting mixture is vigorously stirred,  $\text{NaIO}_4$  (2 equiv, 43.4 mmol, 9.3 g) was added portion wise. After stirring at room temp for 4h, the suspension was filtered through a pad of celite, flushed with nitrogen, and used in the next step without further purification.

To the above solution, vinyl magnesium bromide (2.4 equiv with respect to **87**, 1M, 52 mmol, 52 mL) was added slowly at  $-78\text{ }^{\circ}\text{C}$ . The resultant mixture was stirred at  $-78\text{ }^{\circ}\text{C}$  for 30 mins and allowed to warm to room temperature and stirred for another 1.5h. The reaction mixture was carefully quenched with NaOH (1M, 35 mL). After filtering through a pad of celite, a filtrate was washed with water and brine. The organic layer was dried (anhyd.  $\text{Na}_2\text{SO}_4$ ) and carefully concentrated under reduced pressure to give the

crude yellow liquid **88** (4.46 g, 65%) which was used in the next step without further purification.

### Preparations of aldehydes **89–91** and **93**



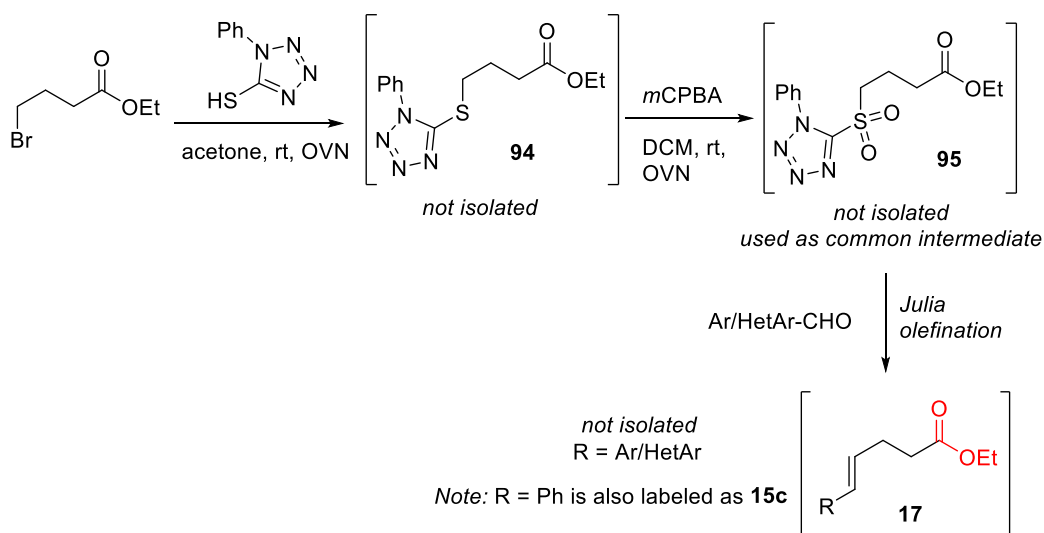
**89**,<sup>11</sup> **90**,<sup>12</sup> and **91**<sup>13</sup> were prepared as described in literature.

**3-(2,5-dimethyl-1H-pyrrol-1-yl)propanal (93).** The solution of 3-aminopropanol (59.7 mmol, 4.56 mL), 2,5-hexanedione (59.7 mmol, 7.0 mL), and *p*-toluenesulfonic acid monohydrate (0.05 equiv, 3 mmol, 570 mg) in toluene (50 mL) was reflux with Dean-Stark apparatus overnight. The resultant mixture was cooled to room temp and washed with water. The organic layer was separated and the aqueous layer was extracted with DCM (3 x 20 mL). The organic layers were combined, dried (anhyd. Na<sub>2</sub>SO<sub>4</sub>) and concentrated under reduced pressure to give crude **92** as a brown liquid in (9.1 g, quantitative) which was used in the next step without further purification.

To a cooled (0 °C) solution of crude **92** (13.7 mmol, 2.1 g) in DCM (40 mL) was added DMSO (6 equiv, 82.1 mmol, 5.8 mL), Et(*i*Pr)<sub>2</sub>N (3 equiv, 41 mmol, 7.1 mL) and sulfur trioxide pyridine complex (2 equiv, 27.4, 4.35 g) sequentially. The resultant mixture was stirred at 0 °C for 1h before quenching with brine (20 mL). The aqueous

layer was washed with Et<sub>2</sub>O (3 x 20 mL), and the combined organic layers were dried (anhyd. Na<sub>2</sub>SO<sub>4</sub>) and concentrated under reduced pressure to give crude **93** as a brown liquid (1.61 g, 78%) which was used in the next step without further purification.

**General procedure for the preparation of aryl/ heteroaryl substituted  $\gamma,\delta$ -unsaturated esters via Julia-typed olefination (GP4)<sup>14</sup>**

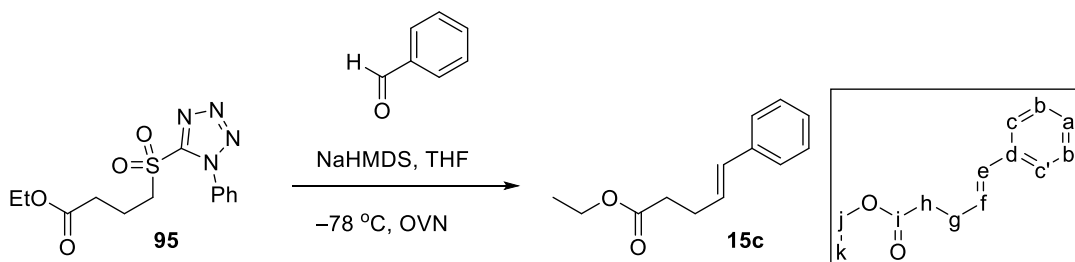


To a solution of 1-phenyl-1H-tetrazole-5-thiol (10.0 g, 56.1 mmol, 1 equiv) and K<sub>2</sub>CO<sub>3</sub> (15.5 g, 112.3 mmol, 2.0 equiv) in acetone (300 mL) was added ethyl 4-bromobutyrate (8.8 mL, 61.7 mmol, 1.1 equiv) under nitrogen atmosphere. The resulting mixture was stirred at room temperature overnight then filtered through a pad of celite and concentrated under reduced pressure to afford light yellow oil crude **94** (16.5 g, quantitative) used in the next step without further purification.

Inside a nitrogen glove bag, to a solution of **94** (16.4 g, 56 mmol, 1 equiv) in DCM (200 mL) was added m-CPBA (48.4 g, 278 mmol, 5 equiv) and NaHCO<sub>3</sub> (11.7 g, 140 mmol, 2.5 equiv). After an overnight stir, the resulting mixture was filtered, washed with EtOAc, and concentrated under reduced pressure. The residue was then dissolved in

the minimum amount of DCM and pushing through a plug of silica gel eluting with 1:1 EtOAc:hexanes to afford the Julia-typed intermediate **95** as light yellow solid (17.3 g, 95%). Crude **95** is used as a common intermediate for Julia olefination.

**Representative Julia olefination<sup>15</sup> example:**

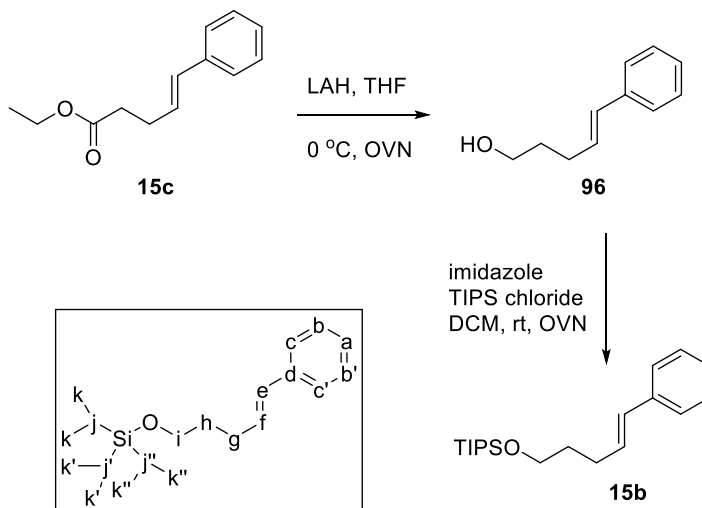


**(E)- 5-phenyl-4-pentenecarboxylic acid ethyl ester (R = Ph, 15c).** To a solution of Julia reagent **95** (1.6 g, 4.93 mmol, 1 equiv) in THF (25 mL) was added NaHMDS (2M, 2.7 mL, 5.43 mmol, 1.1 equiv) at  $-78\text{ }^{\circ}\text{C}$ . The resulting mixture was stirred at the same temperature for 30 mins then benzaldehyde (0.75 mL, 7.4 mmol, 1.5 equiv) was added dropwise. The resultant mixture was slowly warmed to room temperature and stir overnight after quenching with water and EtOAc. The organic layer was separated and the aqueous layer was extract with EtOAc (10 mL x 2). The combined organic layers were dried (anhydr.  $\text{Na}_2\text{SO}_4$ ) and concentrated under reduced pressure affords, after flash chromatography on silica gel (95:5 hexanes:ethyl acetate), the title compound (1.09 g, 72%) as a yellow liquid; TLC analysis  $R_f$  0.7 (90:10 hexanes:ethyl acetate);  $^1\text{H}$  NMR (400 MHz,  $\text{CDCl}_3$ )  $\delta$  7.30–7.40 (4H, m, b,b',c,c'), 7.24 (1H, t,  $J = 7.0$  Hz, a), 6.48 (1H, d,  $J = 15.8$  Hz, e), 6.25 (1H, dt,  $J = 15.8$  and 6.3 Hz, f), 4.19 (2H, q,  $J = 7.1$  Hz, j), 2.50–2.60 (4H, m, g,h), 1.30 (3H, t,  $J = 7.1$  Hz, k);  $^{13}\text{C}$  NMR (100 MHz,  $\text{CDCl}_3$ )  $\delta$  173.08 (i), 137.54 (d), 131.09 (f), 128.63 (b,b',e), 127.26 (a), 126.19 (c,c'), 60.51 (j), 34.20 (h), 28.45 (g), 14.41 k).



Ester **15c** was isolated for screening purpose. All other esters prepared via this method were pass through a short pad of silica gel eluting with 10% EtOAc:hexanes, concentrated under reduced pressure, and used without further purification.

### Preparation of OTIPS substrate **15b**

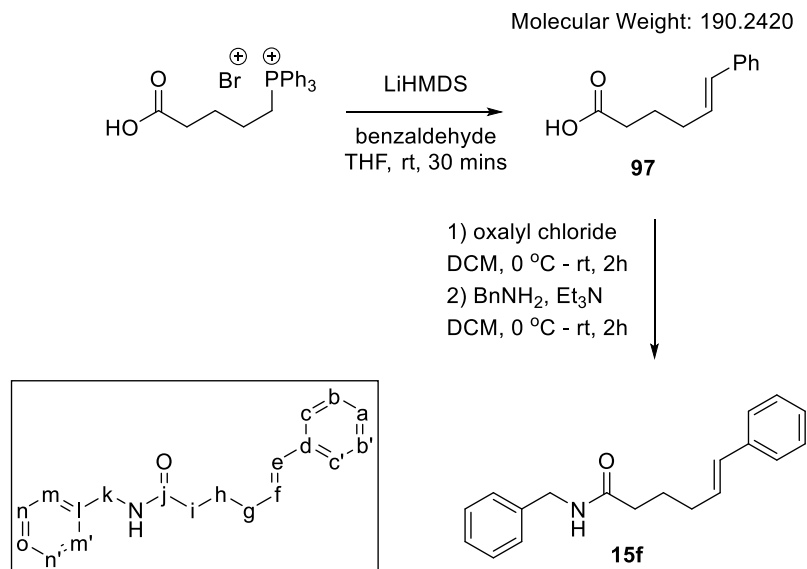


**(E)-triisopropyl((5-phenylpent-4-en-1-yl)oxy)silane (**15b**)**. To a cooled (0 °C) solution of (*E*)- 5-phenyl-4-pentenecarboxylic acid ethyl ester **15c** (3.3 mmol, 679 mg, 1 equiv) in THF (15 mL) was added lithium aluminum hydride (LAH, 1.05 equiv, 3.5 mmol, 133 mg). The resulting mixture was warmed to room temperature and stirred overnight. The reaction mixture was quenched with 5N KOH (0.3 mL) and water (0.15 mL). Following by 30-min stir, the resultant mixture was filtered through a pad of celite and wash with ethyl acetate (2 x 5 mL). The filtrate was dried (anhyd. Na<sub>2</sub>SO<sub>4</sub>) and concentrated under reduced pressure to give the crude yellow oil **96** in quantitative yield (535 mg) which was used in the next step without further purification.

To the solution of alcohol **96** (520 mg, 3.2 mmol, 1 equiv) and imidazole (435 mg, 6.4 mmol, 2 equiv) in DCM (10 mL) was added dropwise triisopropylsilyl chloride

(645 mg, 3.36 mmol, 1.05 equiv) at room temperature. The resultant mixture was stirred overnight then concentrated under reduced pressure affords, after flash chromatography on silica gel (95:5 hexanes:ethyl acetate), the title compound (814 mg, 80%) as a colorless liquid; TLC analysis  $R_f$  0.7 (90:10 hexanes:ethyl acetate);  $^1\text{H}$  NMR (400 MHz,  $\text{CDCl}_3$ )  $\delta$  7.41 (2H, d,  $J = 7.2$  Hz, c,c'), 7.36 (2H, t,  $J = 7.4$  Hz, b,b'), 7.26 (1H, t,  $J = 7.0$  Hz, a), 6.49 (1H, d,  $J = 15.8$  Hz, e), 6.32 (1H, dt,  $J = 15.8$  and 6.8 Hz, f), 3.83 (2H, d,  $J = 6.4$  Hz, i), 2.35–2.45 (2H, m, g), 1.75–1.85 (2H, m, h), 1.15–1.20 (21H, m, j,j',j'',k,k',k'');  $^{13}\text{C}$  NMR (100 MHz,  $\text{CDCl}_3$ )  $\delta$  138.06 (d), 130.78 (f), 130.21 (e), 128.61 (b,b'), 126.94 (a), 126.08 (c,c'), 62.88 (i), 32.81 (h), 29.54 (g), 18.22 (k,k',k''), 12.21 (j,j',j'').

**Preparation of  $\delta,\epsilon$ -unsaturated benzyl amide substrate 15f involving general procedure for the preparation of unsaturated amides via acid chloride intermediates (GP5)**

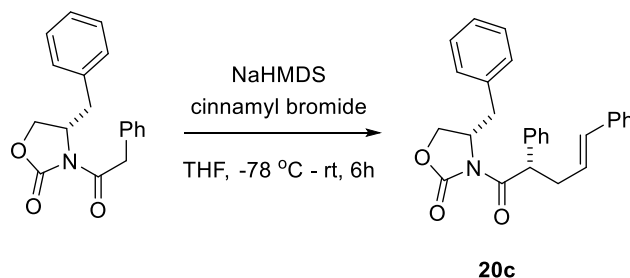


**(E)- 6-phenyl-5-hexanecarboxylic acid benzyl amide (15f).** To a solution of 4-(carboxybutyl)triphenylphosphonium bromide<sup>16</sup> (2.0 g, 4.5 mmol, 1 equiv) in THF (10 mL) was added LiHMDS (1.8 mL, 9.5 mmol, 2.1 equiv) over 10 mins at room temperature. After 15 min, benzaldehyde (0.5 mL, 4.5 mmol) was added dropwise at room temperature. After 15 min, water (15 mL) and ether (15 mL) were added. The organic phase was rinsed with water (10 mL). The combined aqueous solution was washed with EtOAc (15 mL), acidified (10% HCl), and extracted with EtOAc (2 x 15 mL). The combined organic extracts were dried and concentrated under reduced pressure to afford crude **97** (771 mg, 90%).

**(GP5)** To a cooled solution (0 °C) of the crude carboxylic acid **97** (750 mg, 3.94 mmol) in dichloromethane (20 mL) was added dropwise oxalyl chloride (1.35 mL, 4.0 equiv, 15.7 mmol) followed by 3 drops of DMF. The resultant mixture was slowly warmed to room temperature and stir for the total of 1.5 h. The reaction mixture was then concentrated. The resulting acid chloride was redissolved in dichloromethane (20 mL) and cooled to 0 °C. The resultant mixture was then added dropwise aniline (0.55 mL, 1.5 equiv, 5.85 mmol) followed by dropwise addition of triethylamine (1.1 mL, 2.0 equiv, 7.8 mmol). The reaction mixture was slowly warm to room temp and stir for the total of 1.5 h. Whereupon it was diluted, it was washed twice with HCl (3M), once with satd. NaHCO<sub>3</sub> solution, and once with brine. The organic extracts were dried (Na<sub>2</sub>SO<sub>4</sub>) and concentrated under reduced pressure affords, after flash chromatography on silica gel (80:20-60:40 hexanes:ethyl acetate), the mixture of 7:1 *E/Z* **15f** as a yellow solid; TLC analysis R<sub>f</sub> 0.4 (60:40 hexanes:ethyl acetate). The mixture of 7:1 *E/Z* **15f** was then diluted with a minimum amount of EtOAc following by addition of hexanes (9:1

hexanes:EtOAc). After 2 hours, the resultant mixture was filtered to afford the title compound (672 mg, 61%) as a white solid;  $^1\text{H}$  NMR (400 MHz,  $\text{CDCl}_3$ )  $\delta$  7.25–7.40 (9H, m, a,b,b',c,c',m,m',n,n'), 7.22 (1H, t,  $J = 6.7$  Hz, o), 6.39 (1H, d,  $J = 15.8$  Hz, e), 6.20 (1H, dt,  $J = 15.8$  and  $6.9$  Hz, f), 5.74 (1H, br s, NH), 4.46 (2H, d,  $J = 5.7$  Hz, k), 2.25–2.35 (4H, m, g, i), 1.85–1.95 (2H, m, h);  $^{13}\text{C}$  NMR (100 MHz,  $\text{CDCl}_3$ )  $\delta$  172.65 (j), 138.45 (l), 137.62 (d), 130.93 (e), 129.80 (f), 128.86 (n,n'), 128.63 (b,b'), 128.00 (c,c'), 128.67 (o), 127.14 (a), 126.08 (m,m'), 43.77 (k), 36.01 (i), 32.52 (g), 25.24 (h).

### General procedure for Evans' chiral auxiliary alkylation (GP6)<sup>17</sup>

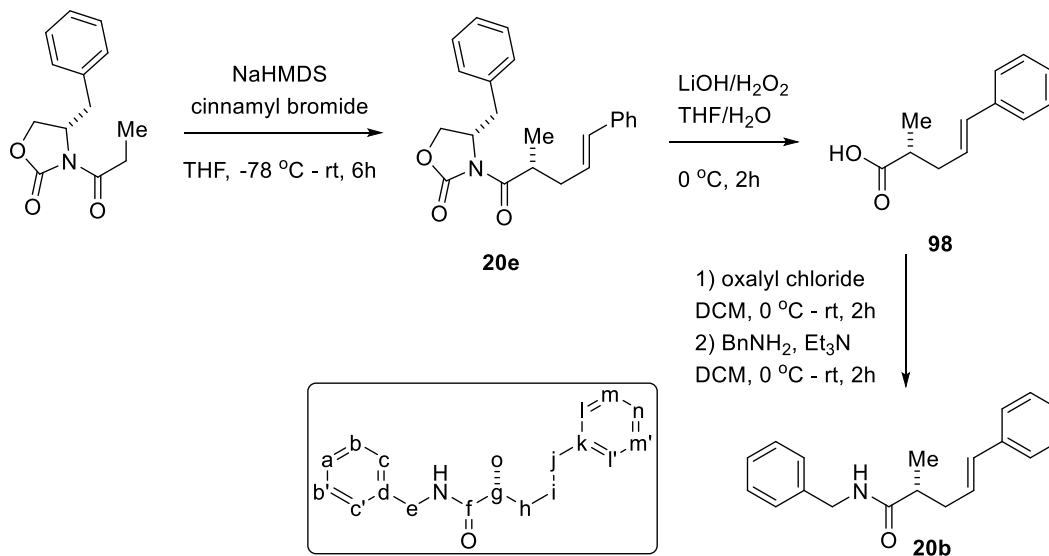


To a cooled ( $-78$  °C) solution of (*S*)-4-benzyl-3-(2-phenylacetyl)oxazolidin-2-one (4.4 mmol, 1.3 g) in THF (15 mL) was added NaHMDS (1.1 equiv, 2M, 4.84 mmol, 2.4 mL) dropwise. The resultant mixture was stirred at  $-78$  °C for 1h, and cinnamyl bromide (2 equiv, 8.8 mmol, 1.73 g) was added dropwise. The resulting mixture was slowly warmed to room temp and stirred for another 5h before quenching with water. The crude reaction was extracted with EtOAc (3 x 30 mL). The organic extracts were combined, dried (anhyd.  $\text{Na}_2\text{SO}_4$ ), and concentrated under reduced pressure. Flash chromatography on silica gel (75:25 hexanes:ethyl acetate) affords the title compound **S20** (1.43 g, 79%) as a white solid: 143.5–144.5 °C; TLC analysis  $R_f = 0.4$  (70:30 hexanes:ethyl acetate);  $[\alpha]_{\text{D}}^{20} = +121^\circ$  ( $c$  1.0,  $\text{CHCl}_3$ );  $^1\text{H}$  NMR (400 MHz,  $\text{CDCl}_3$ )  $\delta$  7.49 (2H, d,  $J = 7.3$  Hz),

7.25–7.45 (10H, m), 7.15–7.25 (3H, m), 6.54 (1H, d,  $J = 15.8$  Hz), 6.20–6.30 (1H, m), 5.33 (1H, dd,  $J = 9.0$  and  $6.2$  Hz), 4.60–4.70 (1H, m), 4.00–4.20 (2H, m), 3.32 (1H, dd,  $J = 13.4$  and  $3.1$  Hz), 3.05–3.20 (1H, m), 2.70–2.80 (2H, m);  $^{13}\text{C}$  NMR (100 MHz,  $\text{CDCl}_3$ )  $\delta$  173.64, 153.11, 138.36, 137.42, 135.34, 132.76, 129.54, 129.05, 128.84, 128.77, 128.65, 127.67, 127.44, 127.38, 127.01, 126.26, 65.88, 55.80, 48.87, 38.02, 37.96; IR (neat) 3029, 1762 (C=O stretch), 1691 (C=O stretch), 1494, 1392, 1369, 1349, 1243, 1224, 1210, 1185, 1109, 1053, 984, 969, 743, 716, 700, 690  $\text{cm}^{-1}$ ; HRMS (ESI) calcd. for  $\text{C}_{27}\text{H}_{25}\text{NNaO}_3$  ( $\text{M}+\text{Na}$ ): 434.1732, found 434.1738  $m/z$ .

### Preparation of pre-installed $\alpha$ -chiral center aryl substituted $\gamma,\delta$ -unsaturated amide

#### 20b

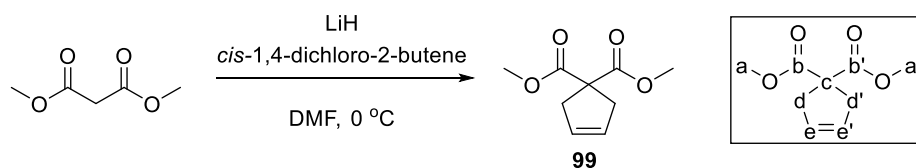


To cooled ( $0\text{ }^\circ\text{C}$ ) a solution of **20e** (prepared via **GP6** with (S)-4-benzyl-3-propionyloxazolidin-2-one, 665 mg, 1.9 mmol) in THF (30 mL) and water (10 mL) was added LiOH (150 mg, 3.8 mmol) and hydrogen peroxide (30%, 1.4 mL). The resulting mixture was stirred at the same temperature for 2h before quenching with aqueous  $\text{Na}_2\text{SO}_3$  (1.5M, 13 mL). The resultant mixture was then acidified with dilute HCl (1M) to

pH=1. Following by extraction with DCM (20 mL x 3), the combined organic layers dried (anhyd. Na<sub>2</sub>SO<sub>4</sub>), and concentrated under reduced pressure to afford crude acid **98** in quantitative yield used in the next step without further purification.

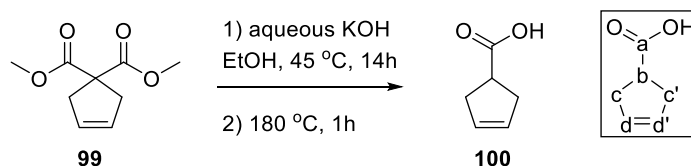
Following **GP5** for the preparation of unsaturated amides via acid chloride intermediates, crude acid **98** (1.9 mmol) affords, after flash chromatography on silica gel (80:20-60:40 hexanes:ethyl acetate), the title compound (814 mg, 80%) as a white solide; TLC analysis R<sub>f</sub> 0.4 (60:40 hexanes:ethyl acetate); <sup>1</sup>H NMR (300 MHz, CDCl<sub>3</sub>) δ 7.20–7.35 (10H, m, a,b,b',c,c',l,l',m,m',n), 6.44 (1H, d, *J* = 15.8 Hz, j), 6.21 (1H, dt, *J* = 15.8 and 7.3 Hz, i), 5.91 (1H, br s, NH), 4.55 (1H, dd, *J* = 14.7 and 8.2 Hz, e), 4.37( 1H, dd, *J* = 14.7 and 8.2 Hz, e) 2.50–2.70 (1H, m, h), 2.30–2.50 (2H, m, g,h), 1.25 (3H, d, *J* = 6.4 Hz, o); <sup>13</sup>C NMR (75 MHz, CDCl<sub>3</sub>) δ 175.49 (f), 138.41 (d), 137.33 (k), 132.17 (j), 128.68 (b,b'), 128.53 (l,l'), 127.75 (m,m'), 127.49 (i), 127.41 (a) 127.21 (n), 126.13 (c,c'), 43.44 (e), 41.92 (g), 37.74 (h), 17.68 (o).

### Preparation sequence of 3-cyclopentenecarboxylic acid.<sup>18</sup>



**Preparation of 3-cyclopentene-1,1-dicarboxylic acid dimethyl ester (**99**).**<sup>1</sup> To a cooled (0 °C) solution of dimethylmalonate (6.6 g, 50.0 mmol) in dry *N,N*-dimethylformamide (DMF, 75 mL) was added LiH (1.0 g, 126 mmol) under nitrogen atmosphere. The reaction was stirred at this temperature for 2 h, then *cis*-1,4-dichloro-2-butene (6.94 g, 55.5 mmol) was added dropwise, and the resultant mixture was slowly warm to room temperature. After 72 h, the mixture was diluted with 20% diethyl ether in hexanes (100

mL) and poured into cold water (100 mL). The organic layer was washed with brine (3 x 50 mL). The organic layer was dried ( $\text{Na}_2\text{SO}_4$ ) and concentrated under reduced pressure to afford the title compound (8.06 g, 87%) as a white solid: mp 169.5–171.0 °C;  $^1\text{H}$  NMR (300 MHz,  $\text{CDCl}_3$ )  $\delta$  5.59 (2H, s, e,e'), 3.72 (6H, s, a,a'), 3.01 (4H, s, d,d');  $^{13}\text{C}$  NMR (75 MHz,  $\text{CDCl}_3$ )  $\delta$  172.60 (b,b'), 127.76 (e,e'), 58.74 (c), 52.77 (a,a'), 40.90 (d,d'); IR (neat) 2983, 2897, 1720 (C=O stretch), 1430, 1258 (C-O-C antisymmetrical stretch), 752, 694 (O-C-O bend)  $\text{cm}^{-1}$ .

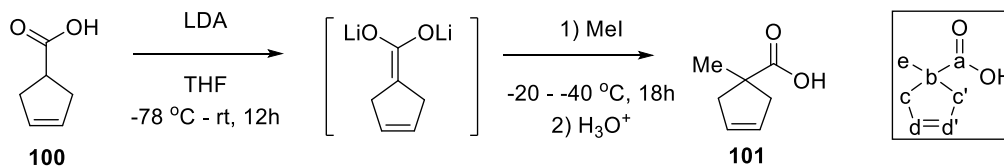


**Preparation of 3-cyclopentenecarboxylic acid (100).**<sup>18</sup> To the stirring solution of 3-cyclopentene-1,1-dicarboxylic acid dimethyl ester (5.01g, 27.2 mmol) in 4:1 ethanol:water (55 mL) was added KOH (5.02g, 89.1 mmol). The reaction was stirred at 45 °C for 14h. The reaction mixture was then concentrated under reduced pressure and poured into a solution of 1:4 ether:hexanes (20 mL) and water (30 mL). The mixture was acidified with concentrated sulfuric acid (ca. 4.5 mL) until pH = 1 and then extracted with ethyl acetate (3 x 30 mL). The combined organic layers were dried ( $\text{Na}_2\text{SO}_4$ ) and concentrated under reduced pressure to afford a crude white solid. The solid was heated at 180 °C for 1 h and then cooled to room temperature. Flash chromatography on silica gel (90:10 hexanes:ethyl acetate) affords the title compound (2.21 g, 73%, 2 steps) as a yellow oil: TLC analysis  $R_f$  0.35 (70:30 hexanes:ethyl acetate);  $^1\text{H}$  NMR (300 MHz,  $\text{CDCl}_3$ )  $\delta$  10.99 (1H, br s, OH), 5.68 (2H, s, d,d'), 3.25–3.10 (1H, m, b), 2.75–2.65 (4H, m, c,c');  $^{13}\text{C}$  NMR (75 MHz,  $\text{CDCl}_3$ )  $\delta$  182.88 (a), 128.91 (d,d'), 41.40 (b), 36.20 (c,c');

IR (neat) 3265 (O-H stretch), 3064, 2929, 1695 (C=O stretch), 1614 (C=C stretch), 1422, 931, 678  $\text{cm}^{-1}$ . HRMS (FAB) calcd. for  $\text{C}_6\text{H}_9\text{O}_2$  (M+H): 113.0603, found 113.1603  $m/z$ .

**General procedure for  $\alpha$ -alkylation of carboxylic acid via dianion intermediate**

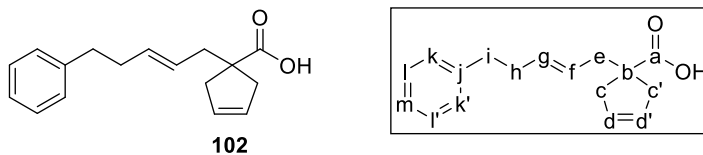
**(GP7).**



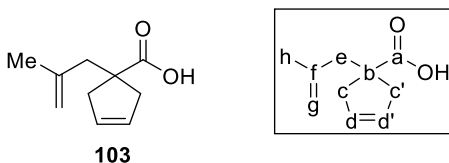
**Preparation of 1-methyl-3-cyclopentenecarboxylic acid (101).** To a cooled ( $-78\text{ }^\circ\text{C}$ ) solution of diisopropylamine (8.15 mL, 58.0 mmol) in THF (200 mL) was slowly added *n*-butyllithium (20.5 mL, 2.5 M solution in hexanes, 51.3 mmol). The resultant mixture was stirred at that temperature for 1 h followed by a 1 h-stir at room temperature. The reaction mixture was then cooled to  $-20\text{ }^\circ\text{C}$  –  $-40\text{ }^\circ\text{C}$  and a solution of 3-cyclopentenecarboxylic acid **100** (2.54 g, 22.6 mmol) in THF (15 mL) was slowly added over 1 h. The resultant mixture was slowly raised to room temperature and stir for the total of 12 h. After that, the mixture was cooled to  $-20\text{ }^\circ\text{C}$  –  $-40\text{ }^\circ\text{C}$  and methyl iodide (2.15 mL, 34.3 mmol) was added dropwise. The resultant mixture was slowly raised to room temperature and stir for the total of 18 h. The mixture was quenched with dilute HCl (3M) and extracted with ethyl acetate (3 x 25 mL). The combined organic layers were dried ( $\text{Na}_2\text{SO}_4$ ) and concentrated under reduced pressure. Flash chromatography on silica gel (80:20 hexanes:ethyl acetate) affords the title compound (2.45 g, 87%) as a dark oil: TLC analysis  $R_f$  0.40 (70:30 hexanes:ethyl acetate);  $^1\text{H}$  NMR (300 MHz,  $\text{CDCl}_3$ )  $\delta$  12.06 (1H, br s, OH), 5.63 (2H, s, d,d'), 2.97 (2H, d,  $J = 14.4$  Hz, c,c'), 2.27 (2H, d,  $J = 14.7$  Hz, c,c'), 1.35 (3H, s, e);  $^{13}\text{C}$  NMR (75 MHz,  $\text{CDCl}_3$ )  $\delta$  185.41 (a), 128.22 (d,d'), 47.71



(b), 44.53 (c,c'), 25.71 (e); IR (neat) 3195 (O-H stretch), 3064, 2970, 2917, 1695 (C=O stretch), 1467, 1405, 1287, 944, 670  $\text{cm}^{-1}$ . HRMS (EI) calcd. for  $\text{C}_7\text{H}_{10}\text{O}_2$ : 126.0681, found 126.0676  $m/z$ .



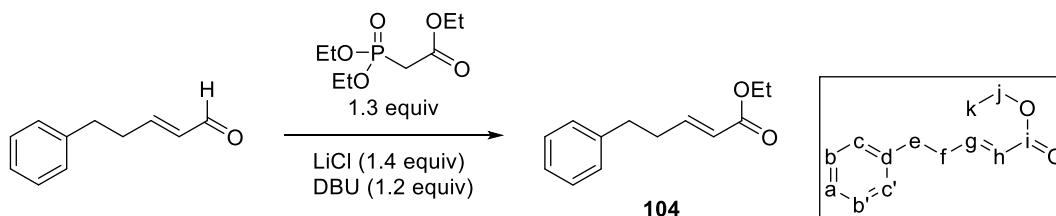
**(E)-1-(5-phenylpent-2-en-1-yl)cyclopent-3-ene-1-carboxylic acid (102).** Following **GP7** with diisopropylamine (4.5 mL, 32.0 mmol in 100 mL THF), *n*-butyllithium (11.3 mL, 2.5 M solution in hexanes, 28.3 mmol), 3-cyclopentenecarboxylic acid **100** (1.4 g, 12.5 mmol in 10 mL THF), and allylic bromide **106** (prepared *vide infra*) affords, after flash chromatography on silica gel (90:10 hexanes:ethyl acetate), the title compound (2.95 g, 92 %) as a yellow oil: TLC analysis  $R_f$  0.50 (70:30 hexanes:ethyl acetate);  $^1\text{H}$  NMR (300 MHz,  $\text{CDCl}_3$ )  $\delta$  12.05 (1H, br s, OH), 7.40–7.20 (5H, j, k,k',l,l',m), 5.63 (2H, s, d,d'), 5.60–5.40 (2H, m, f,g), 2.92 (2H, d,  $J = 14.7$  Hz, c,c'), 2.75–2.65 (2H, m, c,c'), 2.50–2.30 (6H, m, e,h,i);  $^{13}\text{C}$  NMR (75 MHz,  $\text{CDCl}_3$ )  $\delta$  184.34 (a), 141.92 (j), 133.56 (d,d'), 128.49 (g), 128.35 (l,l'), 128.31 (k,k'), 126.02 (m), 125.80 (f), 51.99 (b), 41.93 (e), 41.84 (c,c'), 36.00 (i), 34.41 (h); IR (neat) 2918 (O-H stretch), 1694 (C=O stretch), 1277, 1226 (C-O stretch), 967, 951 (O-H bend), 697, 670  $\text{cm}^{-1}$ . HRMS (ESI) calcd. for  $\text{C}_{17}\text{H}_{19}\text{Na}_2\text{O}_2$  (M-H+2Na): 301.1180, found 301.1190  $m/z$ .



**1-(2-methylallyl)cyclopent-3-ene-1-carboxylic acid (103).** Following **GP7** with diisopropylamine (4.5 mL, 32.0 mmol) in 100 mL THF, *n*-butyllithium (11.3 mL, 2.5 M

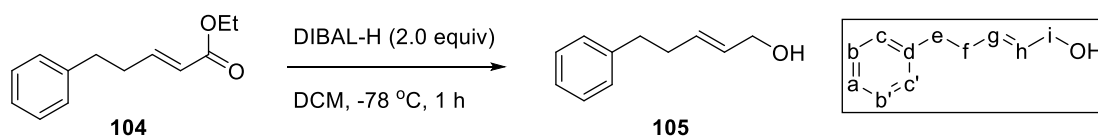
solution in hexanes, 28.3 mmol), 3-cyclopentenecarboxylic acid **100** (1.4 g, 12.5 mmol in 10 mL THF), and 3-bromo-2-methylpropene (1.9 mL, 18.8 mmol) affords, after flash chromatography on silica gel (90:10 hexanes:ethyl acetate), the title compound (1.85 g, 89 %) as a yellow oil: TLC analysis  $R_f$  0.55 (70:30 hexanes:ethyl acetate);  $^1\text{H}$  NMR (400 MHz,  $\text{CDCl}_3$ )  $\delta$  12.02 (1H, br s, OH), 5.63 (2H, s, d,d'), 4.84 (1H, s, g), 4.70 (1H, s, g), 2.96 (2H, d,  $J = 14.4$  Hz, c,c'), 2.52 (2H, s, e), 2.44 (2H, d,  $J = 14.8$  Hz, c,c'), 1.73 (3H, s, h);  $^{13}\text{C}$  NMR (100 MHz,  $\text{CDCl}_3$ )  $\delta$  184.59 (a), 142.39 (f), 128.36 (d,d'), 113.60 (g), 51.66 (a), 46.57 (e), 42.49 (c,c'), 23.21 (h); IR (neat) 2911 (O-H stretch), 1694 (C=O stretch), 1229 (C-O stretch), 951 (O-H bend), 893, 693, 663  $\text{cm}^{-1}$ . HRMS (ESI) calcd. for  $\text{C}_{10}\text{H}_{13}\text{Na}_2\text{O}_2$  (M-H+2Na): 211.0711, found 211.0719  $m/z$ .

**Preparation sequence of (*E*)-(5-bromopent-3-en-1-yl)benzene (106).**

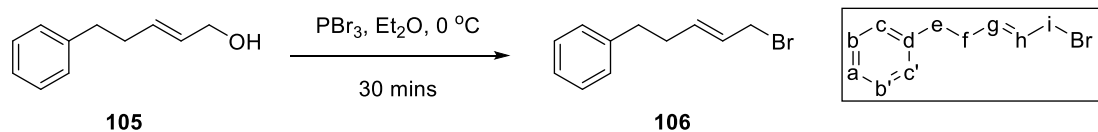


**Preparation of ethyl (*E*)-5-phenylpent-2-enoate (**104**).**<sup>19</sup> To a suspension of LiCl (2.21 g, 1.4 equiv, 52.0 mmol) in MeCN (50 mL) were added DBU (6.7 mL, 1.2 equiv, 45.0 mmol) and triethyl phosphonoacetate (9.7 mL, 1.3 equiv, 48.5 mmol). The resulting mixture was stirred at rt for 15 mins. After cooling to 0 °C, 3-phenylpropionaldehyde (4.9 mL, 37.2 mmol) was added slowly in 5 mins. The resultant mixture was slowly warmed to rt for the total of 1 h and quenched by saturated ammonium chloride. The resultant mixture was extracted with ethyl acetate (3 x 50 mL). The combined organic extracts were dried (anhyd.  $\text{Na}_2\text{SO}_4$ ) and concentrated under reduced pressure. Flash chromatography

on silica gel (95:5 hexanes:ethyl acetate) affords the title compound (6.9 g, 91%) as a colorless liquid: TLC analysis  $R_f$  0.50 (90:10 hexanes:ethyl acetate);  $^1\text{H}$  NMR (300 MHz,  $\text{CDCl}_3$ )  $\delta$  7.35–7.30 (2H, m, b,b'), 7.30–7.15 (3H, m, a,c,c'), 7.05 (1H, dt,  $J = 15.7$  and 6.8 Hz, g), 5.89 (1H, dt,  $J = 15.7$  and 1.5 Hz, h), 4.22 (2H, q,  $J = 15.7$  Hz, j), 2.81 (2H, t,  $J = 7.3$  Hz, e), 2.60–2.50 (2H, m, f) 1.32 (3H, t,  $J = 7.1$  Hz, k);  $^{13}\text{C}$  NMR (75 MHz,  $\text{CDCl}_3$ )  $\delta$  166.56 (i), 148.04 (g), 140.83 (d), 128.51 (b,b'), 128.35 (c,c'), 126.19 (a), 121.90 (h), 60.20 (j), 34.38 (e), 33.91 (f), 14.30 (k).

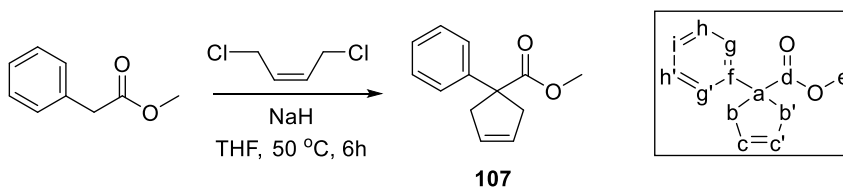


**Preparation of (*E*)-5-phenylpent-2-en-1-ol (105).**<sup>20</sup> To a solution of ester **104** (6.8 g, 33.3 mmol) in dichloromethane was added DIBAL-H (67 mL, 2.0 equiv, 67 mmol, 1M in hexane) slowly at  $-78$  °C. The resultant mixture was stirred at  $-78$  °C and carefully quenched with saturated aq. potassium sodium tartrate. The layers were separated and the aqueous layer was washed with dichloromethane (2 x 75 mL). The combined organic extracts were dried (anhyd.  $\text{Na}_2\text{SO}_4$ ) and concentrated under reduced pressure to afford the title compound (5.0 g, 93%) as a colorless liquid:  $^1\text{H}$  NMR (300 MHz,  $\text{CDCl}_3$ )  $\delta$  7.40–7.30 (2H, m, b,b'), 7.30–7.20 (3H, m, a,c,c'), 5.90–5.60 (2H, m, g,h), 4.11 (2H, d,  $J = 4.9$  Hz, i), 2.78 (2H, t,  $J = 7.3$  Hz, e), 2.50–2.40 (2H, m, f), 2.40–2.25 (1H, br s, OH);  $^{13}\text{C}$  NMR (75 MHz,  $\text{CDCl}_3$ )  $\delta$  141.79 (d), 132.04 (h), 129.71 (g), 128.49 (b,b'), 128.40 (c,c'), 125.94 (a), 63.49 (i), 35.61 (e), 34.04 (f).



**Preparation of (*E*)-(5-bromopent-3-en-1-yl)benzene (106).**<sup>20</sup> To a cooled (0 °C) solution of allylic alcohol **105** (5.0 g, 30.8 mmol) in Et<sub>2</sub>O (50 mL) was added phosphorous tribromide (1.45 mL, 0.5 equiv, 15.4 mmol). The resultant mixture was stirred at 0 °C for 30 mins and quenched by saturated brine solution. The layers were separated and the aqueous layer was washed with Et<sub>2</sub>O (2 x 30 mL). The combined organic extracts were dried (anhyd. Na<sub>2</sub>SO<sub>4</sub>) and concentrated under reduced pressure. The residue was passed through a short pad of silica and concentrated under reduced pressure to afford the title compound (6.6 g, 95%) as yellow liquid: <sup>1</sup>H NMR (300 MHz, CDCl<sub>3</sub>) δ 7.40–7.30 (2H, m, b,b'), 7.30–7.20 (3H, m, a,c,c'), 5.90–5.70 (2H, m, g,h), 3.98 (2H, d, *J* = 6.8 Hz, i), 2.75 (2H, t, *J* = 7.3 Hz, e), 2.50–2.40 (2H, m, f); <sup>13</sup>C NMR (75 MHz, CDCl<sub>3</sub>) δ 141.36 (d), 135.49 (h), 128.45 (b,b'), 128.41 (c,c'), 127.01 (g'), 126.01 (a), 35.24 (i), 33.82 (e), 33.34 (f).

**Preparation of methyl 1-phenyl-3-cyclopentenecarboxylate (107).**<sup>21</sup>

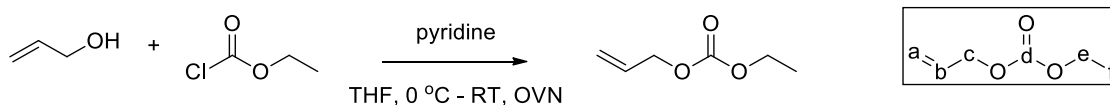


To a cooled (0 °C) solution of methyl phenylacetate (6.0 g, 39.6 mmol) in THF (80 mL) and *N,N'*-dimethylpropyleneurea (20 mL) was carefully added NaH (1.9 g, 79.7 mmol) and the mixture was stirred at 50 °C. After 2 h, the resultant mixture was allowed to cool to room temperature, and *cis*-1,4-dichloro-2-butene (5.2 mL, 47.3 mmol) was added dropwise. The resultant mixture was then stirred at 50 °C for 3 h. After cooling to room temperature, the mixture was quenched with saturated ammonium chloride and extracted

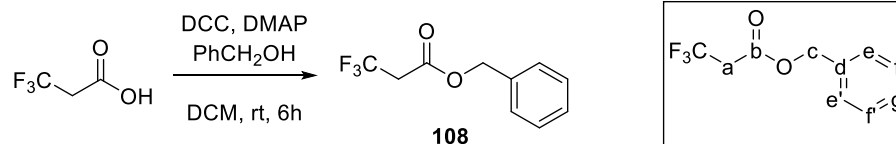
with ethyl acetate (2 x 25 mL). The combined organic layers were dried (Na<sub>2</sub>SO<sub>4</sub>) and concentrated under reduced pressure. Flash chromatography on silica gel (97:3 hexanes:ethyl acetate) affords the title compound (3.51 g, 44%) as a yellow oil: TLC analysis *R<sub>f</sub>* 0.80 (70:30 hexanes:ethyl acetate); <sup>1</sup>H NMR (300 MHz, CDCl<sub>3</sub>) δ 7.45–7.20 (5H, m, g,g',h,h',i), 5.82 (2H, s, c,c'), 3.68 (3H, s, e), 3.48 (2H, d, *J* = 14.6, b,b'), 2.82 (2H, d, *J* = 14.8, b,b'); <sup>13</sup>C NMR (75 MHz, CDCl<sub>3</sub>) δ 176.58 (d), 143.78 (f), 129.18 (g,g'), 128.44 (c,c'), 126.79 (h,h'), 126.58 (i), 58.42 (e), 52.49 (a), 42.88 (b,b').

**Preparation sequence of benzyl 1-(trifluoromethyl)cyclopent-3-enecarboxylate**

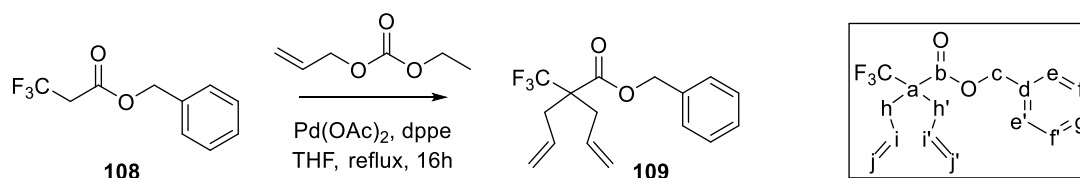
**(110).<sup>22</sup>**



**Preparation of allyl ethyl carbonate.** To a cooled (0 °C) solution of allylic alcohol (13.6 mL, 0.2 mol) and DMAP (0.6 g, 5 mmol) in dichloromethane (300 mL) was slowly added pyridine (32 mL, 2 equiv, 0.4 mol). Ethyl chloroformate (19.1 mL, 1 equiv, 0.2 mol) was added dropwise to the above mixture. The resultant mixture was slowly warmed to room temperature and stirred overnight. The reaction mixture was washed with water (3 x 100 mL). The organic extracts were dried (anhyd. Na<sub>2</sub>SO<sub>4</sub>) and concentrated under reduced pressure. Flash chromatography on silica gel (95:5 hexanes:ethyl acetate) affords the title (24.3 g, 93%) as a colorless liquid; TLC analysis *R<sub>f</sub>* 0.55 (90:10 hexanes:ethyl acetate); <sup>1</sup>H NMR (300 MHz, CDCl<sub>3</sub>) δ 6.05–5.80 (1H, m, b), 5.29 (1H, dd, *J* = 31.5 Hz, 17.1 Hz, a), 4.61 (2H, d, *J* = 5.7 Hz, c), 4.19 (2H, q, *J* = 7.1 Hz, e), 1.30 (3H, t, *J* = 7.1 Hz, f); <sup>13</sup>C NMR (75 MHz, CDCl<sub>3</sub>) δ 154.94 (d), 131.67 (b), 118.65 (a), 68.19 (c), 63.96 (e), 14.20 (f).

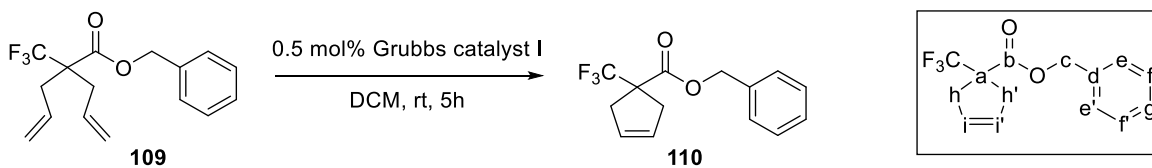


**Preparation of benzyl 3,3,3-trifluoropropanoate (108).**<sup>22</sup> Using the general procedure of DCC-mediated condensation with 3,3,3-trifluoropropanoic acid (3.0 g, 23.4 mmol), DMAP (72.0 mg, 0.025 equiv, 0.59 mmol), DCC (4.8 g, 1 equiv, 23.4 mmol), and benzyl alcohol (4.85 mL, 2 equiv, 46.8 mmol) affords, after flash chromatography on silica gel (90:10 hexanes:ethyl acetate), the title compound (4.9 g, 96%) as a colorless liquid: TLC analysis  $R_f$  0.55 (80:20 hexanes:ethyl acetate);  $^{19}\text{F}$  NMR (376 MHz,  $\text{CDCl}_3$ )  $\delta$  -63.43 (t,  $J$  = 9.6 Hz,  $\text{CF}_3$ );  $^1\text{H}$  NMR (400 MHz,  $\text{CDCl}_3$ )  $\delta$  7.50–7.35 (5H, m, e, e', f, f', g), 5.26 (2H, s, c), 3.26 (2H, q,  $J$  = 14.6, a);  $^{13}\text{C}$  NMR (100 MHz,  $\text{CDCl}_3$ )  $\delta$  163.00 (q,  $J$  = 4.1 Hz, b), 134.91 (d), 128.71 (f), 128.66 (e), 128.37 (g), 123.43 (q,  $J$  = 274.4 Hz,  $\text{CF}_3$ ), 67.50 (c), 39.59 (q,  $J$  = 30.9 Hz, a).



**Preparation of benzyl 2-allyl-2-(trifluoromethyl)pent-4-enoate (109).**<sup>22</sup> To a refluxed solution of  $\text{Pd}(\text{OAc})_2$  (203 mg, 0.04 equiv, 0.87 mmol) and 1,2-bis(diphenylphosphanyl)ethane (dppe; 1.07 g, 0.12 equiv, 2.6 mmol) in THF (50 mL) was added a solution of benzyl 3,3,3-trifluoropropanoate **108** (4.85 g, 22.2 mmol) and allyl ethyl carbonate (8.9 mL, 66.7 mmol, 3.0 equiv) in THF (250 mL) via cannula. After 16 h of reflux, the resultant mixture was cooled to rt and concentrated under reduced pressure. Flash chromatography on silica gel (95:5 hexanes:ethyl acetate) affords the title

compound (6.1 g, 92%) as a colorless oil: TLC analysis  $R_f$  0.85 (70:30 hexanes:ethyl acetate);  $^{19}\text{F}$  NMR (376 MHz,  $\text{CDCl}_3$ )  $\delta$  -68.05 (s,  $\text{CF}_3$ );  $^1\text{H}$  NMR (400 MHz,  $\text{CDCl}_3$ )  $\delta$  7.45–7.35 (5H, m, e,e',f,f',g), 5.85–5.70 (2H, m, i,i'), 5.24 (2H, s, c), 5.20–5.10 (4H, m, j,j'), 2.70–2.60 (4H, m, h,h');  $^{13}\text{C}$  NMR (100 MHz,  $\text{CDCl}_3$ )  $\delta$  168.40 (b), 135.11 (d), 131.50 (i,i'), 128.61 (f,f'), 128.46 (g), 128.23 (e,e'), 125.91 (q,  $J = 283.24$  Hz,  $\text{CF}_3$ ), 119.69 (j,j'), 67.49 (c), 55.94 (q,  $J = 23.14$  Hz, a), 36.19 (h,h').

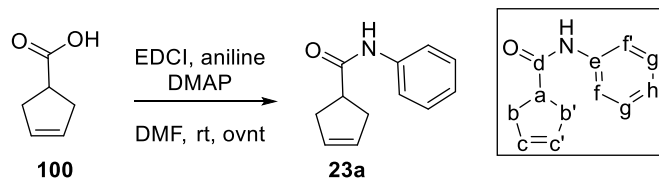


**Preparation of benzyl 1-(trifluoromethyl)cyclopent-3-enecarboxylate (110).**<sup>22</sup> A solution of diallyl benzyl ester **37** (599 mg, 2.0 mmol) and Grubbs' I catalyst (8.3 mg, 0.01 mmol, 0.005 equiv) in dichloromethane (20 mL) was stirred at rt for 5 h. The resultant mixture was then concentrated under reduced pressure. Flash chromatography on silica gel (90:10 hexanes:ethyl acetate) affords the title compound (535 mg, 99%) as a colorless oil: TLC analysis  $R_f$  0.75 (80:20 hexanes:ethyl acetate);  $^{19}\text{F}$  NMR (376 MHz,  $\text{CDCl}_3$ )  $\delta$  -72.73 (s,  $\text{CF}_3$ );  $^1\text{H}$  NMR (400 MHz,  $\text{CDCl}_3$ )  $\delta$  7.45–7.35 (5H, m, e,e',f,f',g), 5.67 (2H, s, i,i'), 5.27 (2H, s, c), 3.11 (2H, d,  $J = 15.2$ , h,h'), 2.92 (2H, d,  $J = 15.8$ , h,h');  $^{13}\text{C}$  NMR (100 MHz,  $\text{CDCl}_3$ )  $\delta$  170.12 (b), 135.29 (d), 128.63 (i,i'), 128.40 (f,f'), 127.89 (g), 127.67 (e,e'), 126.67 (q,  $J = 279.0$  Hz,  $\text{CF}_3$ ), 67.66 (c), 57.14 (q,  $J = 25.7$  Hz, a), 38.87 (h,h').

**General procedure for the preparation of  $\gamma,\delta$ -unsaturated carboxylic acids via hydrolysis of esters (GP8).**

To a carboxylate ester was added a solution of KOH 1 M in ethanol (5 equiv), and the reaction was heated at reflux for 2 h. The reaction mixture was cooled to rt and partially concentrated under reduced pressure. The residue was added water and extracted twice with dichloromethane. The aqueous layer was acidified until pH = 1 with HCl (3M) and extracted twice with dichloromethane. The combined organic extracts were dried ( $\text{Na}_2\text{SO}_4$ ) and concentrated under reduced pressure to afford a corresponding carboxylic acid which was used in the next step without further purification.

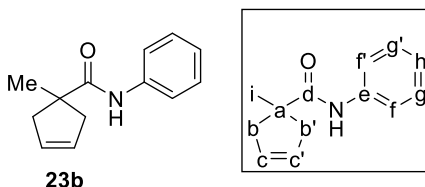
**General procedure for the preparation of  $\gamma,\delta$ -unsaturated phenyl amides via EDCI-mediated condensation (GP9).**



**Preparation of 3-cyclopentenecarboxylic acid phenyl amide (23a).** To a cooled (0 °C) degassed solution of 3-cyclopentenecarboxylic acid **100** (562 mg, 5.0 mmol) in *N,N*-dimethylformamide (DMF, 40 mL) was slowly added aniline (0.46 mL, 5.0 mmol). The resulting solution was stirred (0.5 h, 0 °C) and then *N*-(3-dimethylaminopropyl)-*N*'-ethylcarbodiimide hydrochloride (EDCI, 1.06 g, 5.5 mmol) and 4-(dimethylamino)pyridine (DMAP, 612 mg, 5.0 mmol) were added. The resulting mixture was allowed to slowly warm to room temperature and stirred overnight. The reaction mixture was quenched by the addition of satd. aq. sodium bicarbonate (50 mL) and



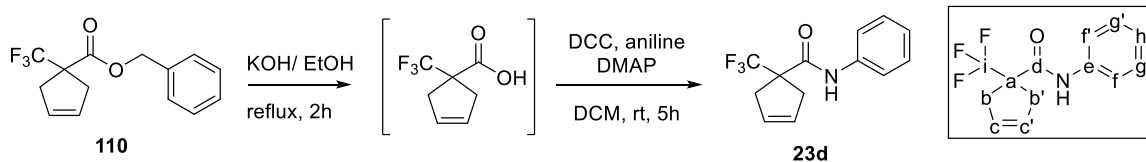
extracted with ethyl acetate (2 x 50 mL). The combined organic extracts were washed with HCl (3M, 2 x 30 mL) and dried (anhyd. Na<sub>2</sub>SO<sub>4</sub>) and concentrated under reduced pressure. Flash chromatography on silica gel (85:15 hexanes:ethyl acetate) affords the title (815 mg, 87%) as a white solid: mp 83.0–84.5 °C; TLC analysis *R<sub>f</sub>* 0.5 (75:25 hexanes:ethyl acetate); <sup>1</sup>H NMR (300 MHz, CDCl<sub>3</sub>) δ 7.97 (1H, br s, NH), 7.56 (2H, d, *J* = 7.8 Hz, f,f'), 7.30 (2H, t, *J* = 7.6 Hz, g,g'), 7.10 (1H, t, *J* = 7.4 Hz, h), 5.71 (2H, s, c,c'), 3.25–3.05 (1H, m, a), 2.85–2.55 (4H, m, b,b'); <sup>13</sup>C NMR (75 MHz, CDCl<sub>3</sub>) δ 174.80 (d), 138.23 (e), 129.19 (c,c'), 128.90 (g,g'), 124.13 (h), 120.10 (f,f'), 44.28 (a), 37.15 (b,b'); IR (neat) 3288 (N-H stretch), 3253, 3142, 1655 (C=O stretch), 1544 (N-H bend), 1439, 1310, 750 cm<sup>-1</sup>. HRMS (FAB) calcd. for C<sub>12</sub>H<sub>14</sub>NO (M+H): 188.0997, found 188.1081 *m/z*.



**1-methyl-3-cyclopentenecarboxylic acid phenyl amide (23b).** Following the general procedure, 3-cyclopentene-1-methylcarboxylic acid **101** (632 mg, 5.0 mmol) affords, after flash chromatography on silica gel (85:15 hexanes:ethyl acetate), the title compound (854 mg, 85%) as a white solid: mp 91.0–93.5 °C; TLC analysis *R<sub>f</sub>* 0.5 (75:25 hexanes:ethyl acetate); <sup>1</sup>H NMR (300 MHz, CDCl<sub>3</sub>) δ 7.52 (2H, d, *J* = 8.0 Hz, f,f'), 7.48 (1H, br s, NH), 7.30 (2H, t, *J* = 7.7 Hz, g,g'), 7.09 (1H, t, *J* = 7.4 Hz, h), 5.73 (2H, s, c,c'), 2.97 (2H, d, *J* = 14.5 Hz, b,b'), 2.36 (2H, d, *J* = 14.5 Hz, b,b'), 1.42 (3H, s, i); <sup>13</sup>C NMR (75 MHz, CDCl<sub>3</sub>) δ 176.73 (d), 138.21 (e), 129.13 (c,c'), 128.92 (g,g'), 124.13 (h), 120.09 (f,f'), 48.96 (a), 45.10 (b,b'), 26.14 (i); IR (neat) 3657 (N-H stretch), 2974, 2897,

1679 (C=O stretch), 1593 (C=C stretch), 1520 (N-H bend), 1438, 1303, 727  $\text{cm}^{-1}$ . HRMS (FAB) calcd. for  $\text{C}_{13}\text{H}_{16}\text{NO}$  (M+H): 202.1232, found 202.1228  $m/z$ .

**General procedure for the preparation of  $\gamma,\delta$ -unsaturated phenyl amides via DCC-mediated condensation (GP9).**



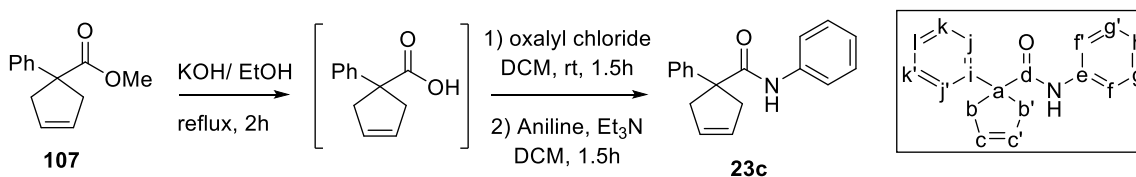
**Preparation of 1-(trifluoromethyl)-3-cyclopentenecarboxylic acid phenyl amide (5d).**

Using the general procedure for the preparation of  $\gamma,\delta$ -unsaturated carboxylic acids via hydrolysis of esters with benzyl ester **110** (501 mg, 1.85 mmol) affords the crude carboxylic acid (327 mg) as yellow oil used in the next step without further purification.

To a solution of the crude  $\gamma,\delta$ -unsaturated carboxylic acid (327 mg, 1.82 mmol) in dichloromethane (6 mL) was added DMAP (5.6 mg, 0.025 equiv, 0.046 mmol) and aniline (0.33 mL, 2 equiv, 3.64 mmol). The resultant mixture was stirred at 0 °C for 15 mins and DCC (374 mg, 1 equiv, 1.82 mmol) was added. The reaction mixture was slowly warm to rt and stir for 5 h. After filtration, the filtrate was washed twice with HCl (3M) and once with satd.  $\text{NaHCO}_3$ . The organic extracts were dried ( $\text{Na}_2\text{SO}_4$ ) and concentrated under reduced pressure. Flash chromatography on silica gel (90:10 hexanes:ethyl acetate) affords, the title compound (321 mg, 68%, 2 steps) as a white solid: mp 69.5–72.5 °C; TLC analysis  $R_f$  0.60 (70:30 hexanes:ethyl acetate);  $^{19}\text{F}$  NMR (376 MHz,  $\text{CDCl}_3$ )  $\delta$  -71.86 (s,  $\text{CF}_3$ );  $^1\text{H}$  NMR (400 MHz,  $\text{CDCl}_3$ )  $\delta$  7.52 (2H, d,  $J = 7.7$  Hz, f,f'), 7.60–7.45 (1H, m, NH), 7.36 (2H, t,  $J = 7.6$  Hz, g,g'), 7.17 (1H, t,  $J = 7.4$  Hz,

h), 5.74 (2H, s, c,c'), 3.21 (2H, d,  $J = 15.5$  Hz, b,b'), 2.97 (2H, d,  $J = 15.3$  Hz, b,b');  $^{13}\text{C}$  NMR (100 MHz,  $\text{CDCl}_3$ )  $\delta$  167.06 (d), 137.32 (e), 129.07 (c,c'), 128.05 (g,g'), 127.24 (q,  $J = 278.7$  Hz, i), 124.98 (h), 120.43 (f,f'), 58.11 (q,  $J = 24.7$ , a), 38.89 (q,  $J = 2.0$  Hz, b,b'); IR (neat) 3309 (N-H stretch), 2924, 2867, 1667 (C=O stretch), 1599 (C=C stretch), 1535 (N-H bend), 1476, 1301, 1263, 1148, 753, 739, 662 (C-F stretch)  $\text{cm}^{-1}$ . HRMS (ESI) calcd. for  $\text{C}_{13}\text{H}_{12}\text{F}_3\text{NaNO}$  ( $\text{M}+\text{Na}$ ): 278.0769, found 278.0766  $m/z$ .

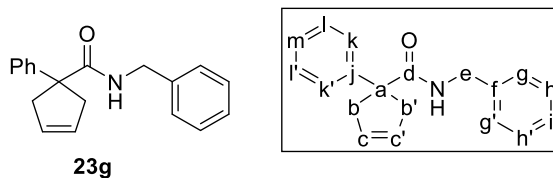
### Preparation of $\gamma,\delta$ -unsaturated amides via acid chloride intermediates via GP5.



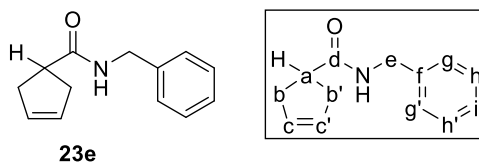
**Preparation of 1-phenyl-3-cyclopentenecarboxylic acid phenyl amide (23c).** Using the general procedure for the preparation of  $\gamma,\delta$ -unsaturated carboxylic acids via hydrolysis of esters (GP8) with methyl ester **107** (1.66 g, 8.2 mmol) affords the crude carboxylic acid (1.47 g) as yellow solid used in the next step without further purification.

Following GP5 the above crude acid affords, after flash chromatography on silica gel (90:10 hexanes:ethyl acetate) affords, the title compound (1.55 g, 72%, 3 steps) as a white solid: mp 90.5–92.5 °C; TLC analysis  $R_f$  0.6 (70:30 hexanes:ethyl acetate);  $^1\text{H}$  NMR (300 MHz,  $\text{CDCl}_3$ )  $\delta$  7.50–7.20 (9H, m, f,f',g,g',h,j,j',k,k'), 7.08 (1H, t,  $J = 7.4$  Hz, l), 5.81 (2H, s, c,c'), 3.43 (2H, d,  $J = 14.6$ , b,b'), 2.92 (2H, d,  $J = 14.6$ , b,b');  $^{13}\text{C}$  NMR (75 MHz,  $\text{CDCl}_3$ )  $\delta$  174.49 (d), 144.53 (e), 138.12 (i), 129.03 (j,j'), 128.90 (c,c'), 128.73 (k,k'), 127.28 (g,g'), 126.75 (h), 124.12 (l), 119.62 (f,f'), 59.24 (a), 43.89 (b,b'); IR (neat) 3286 (N-H stretch), 3056, 2846, 2917, 1648 (C=O stretch), 1595 (C=C stretch), 1518 (N-

H bend), 1497, 1436, 1312, 1239, 753, 742, 732, 688, 655  $\text{cm}^{-1}$ . HRMS (ESI) calcd. for  $\text{C}_{18}\text{H}_{17}\text{NaNO}$  ( $\text{M}+\text{Na}$ ): 286.1208, found 286.1197  $m/z$ .

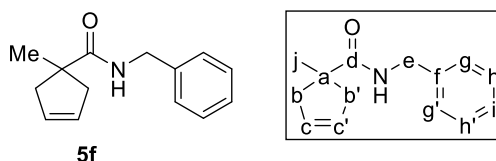


**1-phenyl-3-cyclopentenecarboxylic acid benzyl amide (23g).** Following **GP5** with benzylamine (1.28 mL, 1.5 equiv, 11.7 mmol) affords, after flash chromatography on silica gel (90:10 hexanes:ethyl acetate), the title compound (1.48 g, 65%, 3 steps) as a white solid: mp 68.0–70.5 °C; TLC analysis  $R_f$  0.50 (70:30 hexanes:ethyl acetate);  $^1\text{H}$  NMR (400 MHz,  $\text{CDCl}_3$ )  $\delta$  7.40–7.30 (4H, m, g,g',k,k'), 7.35–7.25 (4H, m, i,l,l',m), 7.13 (2H, d,  $J = 6.4$  Hz, h,h'), 5.79 (2H, s c,c'), 5.69 (1H, br s, NH), 4.41 (2H, d,  $J = 5.8$  Hz, e), 3.37 (2H, dd,  $J = 14.3$  Hz, b,b'), 2.85 (2H, d,  $J = 14.4$  Hz, b,b');  $^{13}\text{C}$  NMR (100 MHz,  $\text{CDCl}_3$ )  $\delta$  176.35 (d), 144.97 (f), 138.57 (j), 128.81 (c,c'), 128.75 (k,k'), 128.59 (l,l'), 127.37 (h,h'), 127.28 (m), 126.95 (g,g'), 126.74 (i), 58.44 (a), 43.83 (e), 43.80 (b,b'); IR (neat) 3393, 3351 (N-H stretch), 3057, 3029, 1637 (C=O stretch), 1518 (N-H bend), 1497, 1446, 1027, 1005, 718  $\text{cm}^{-1}$ . HRMS (ESI) calcd. for  $\text{C}_{19}\text{H}_{19}\text{NaNO}$  ( $\text{M}+\text{Na}$ ): 300.1364, found 300.1364  $m/z$ .



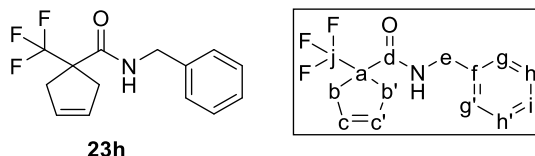
**3-cyclopentenecarboxylic acid benzyl amide (23e).** Following **GP5** with carboxylic acid **100** (562 mg, 5.0 mmol), oxalyl chloride (1.72 mL, 4.0 equiv, 20 mmol), triethyl amine (1.4 mL, 2.0 equiv, 10.0 mmol), and benzylamine (0.82 mL, 1.5 equiv, 7.5 mmol)

affords, after flash chromatography on silica gel (85–70:15–30 hexanes:ethyl acetate), the title compound (684 mg, 68%, 2 steps) as a white solid: mp 103.5–105.5 °C; TLC analysis  $R_f$  0.35 (70:30 hexanes:ethyl acetate);  $^1\text{H}$  NMR (400 MHz,  $\text{CDCl}_3$ )  $\delta$  7.40–7.30 (2H, m, h,h'), 7.35–7.25 (2H, m, g,g',i), 5.94 (1H, br s, NH), 5.70 (2H, s, c,c'), 4.46 (2H, d,  $J = 5.7$  Hz, e), 3.05–2.95 (1H, m, a), 2.75–2.60 (4H, m, b,b');  $^{13}\text{C}$  NMR (100 MHz,  $\text{CDCl}_3$ )  $\delta$  175.82 (d), 138.55 (f), 129.26 (c,c'), 128.71 (h,h'), 127.75 (g,g'), 127.46 (i), 43.62 (e), 43.51 (a), 37.02 (b,b'); IR (neat) 3271 (N-H stretch), 3054, 2898, 2837, 1635 (C=O stretch), 1551 (C=C stretch), 1497 (N-H bend), 1454, 1449, 1389, 1033, 746, 693  $\text{cm}^{-1}$ . HRMS (ESI) calcd. for  $\text{C}_{13}\text{H}_{15}\text{NaNO}$  ( $\text{M}+\text{Na}$ ): 224.1051, found 224.1059  $m/z$ .

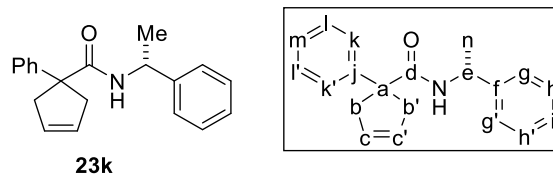


**1-methyl-3-cyclopentenecarboxylic acid benzyl amide (23f).** Following **GP5** with carboxylic acid **101** (632 mg, 5.0 mmol), oxalyl chloride (1.72 mL, 4.0 equiv, 20 mmol), triethyl amine (1.4 mL, 2.0 equiv, 10.0 mmol), and benzylamine (0.82 mL, 1.5 equiv, 7.5 mmol) affords, after flash chromatography on silica gel (85–70:15–30 hexanes:ethyl acetate), the title compound (667 mg, 62%, 2 steps) as a white solid: mp 72.5–74.5 °C; TLC analysis  $R_f$  0.40 (70:30 hexanes:ethyl acetate);  $^1\text{H}$  NMR (400 MHz,  $\text{CDCl}_3$ )  $\delta$  7.40–7.30 (2H, m, h,h'), 7.35–7.25 (2H, m, g,g',i), 5.91 (1H, br s, NH), 5.68 (2H, s, c,c'), 4.48 (2H, d,  $J = 5.7$  Hz, e), 2.89 (2H, d,  $J = 14.4$  Hz, b,b'), 2.29 (2H, d,  $J = 14.7$  Hz, b,b'), 1.35 (3H, s, j);  $^{13}\text{C}$  NMR (100 MHz,  $\text{CDCl}_3$ )  $\delta$  178.27 (d), 138.70 (f), 128.89 (c,c'), 128.72 (h,h'), 127.64 (g,g'), 127.43 (i), 48.17 (a), 45.12 (b,b'), 43.69 (e), 26.33 (j); IR (neat) 3369 (N-H stretch), 3305, 2916, 1637 (C=O stretch), 1528 (N-H bend), 1414,

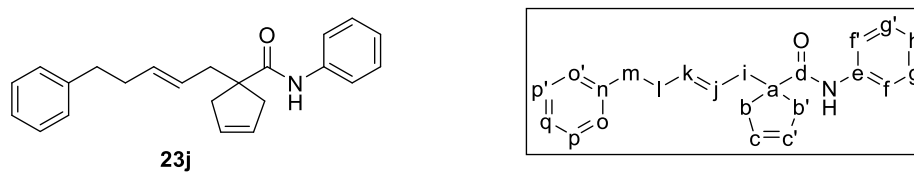
1289, 1235, 948, 714  $\text{cm}^{-1}$ . HRMS (ESI) calcd. for  $\text{C}_{14}\text{H}_{17}\text{NaNO}$  ( $\text{M}+\text{Na}$ ): 238.1208, found 238.1218  $m/z$ .



**1-(trifluoromethyl)-3-cyclopentenecarboxylic acid benzyl amide (23h).** Following **GP5** with carboxylic ester **110** (1.36 g, 5.0 mmol), oxalyl chloride (1.72 mL, 4.0 equiv, 20 mmol), triethyl amine (1.4 mL, 2.0 equiv, 10.0 mmol), and benzylamine (0.82 mL, 1.5 equiv, 7.5 mmol) affords, after flash chromatography on silica gel (90:10 hexanes:ethyl acetate), the title compound (702 mg, 52%, 3 steps) as a white solid: mp 77.5–78.5  $^{\circ}\text{C}$ ; TLC analysis  $R_f$  0.5 (70:30 hexanes:ethyl acetate);  $^{19}\text{F}$  NMR (282 MHz,  $\text{CDCl}_3$ )  $\delta$  -72.11 (s,  $\text{CF}_3$ );  $^1\text{H}$  NMR (300 MHz,  $\text{CDCl}_3$ )  $\delta$  7.45–7.20 (5H, m, g,g',h,h',i), 6.21 (1H, br s, NH), 5.68 (2H, s, c,c'), 4.51 (2H, d,  $J = 5.6$  Hz, e), 3.12 (2H, d,  $J = 15.6$  Hz, b,b'), 2.88 (2H, d,  $J = 15.4$  Hz, b,b');  $^{13}\text{C}$  NMR (75 MHz,  $\text{CDCl}_3$ )  $\delta$  169.04 (d), 137.72 (f), 128.82 (c,c'), 127.90 (h,h'), 127.67 (i), 127.53 (g,g'), 127.33 (q,  $J = 278.7$ , j), 57.28 (q,  $J = 24.6$ , a), 44.20 (e), 38.91 (b,b'); IR (neat) 3338 (N-H stretch), 3030, 2922, 1660 (C=O stretch), 1533 (C=C stretch), 1496 (N-H bend), 1419, 1302, 1127 (C-N stretch), 954, 712, 697, 655  $\text{cm}^{-1}$ . HRMS (ESI) calcd. for  $\text{C}_{14}\text{H}_{14}\text{F}_3\text{NaNO}$  ( $\text{M}+\text{Na}$ ): 292.0925, found 292.0923  $m/z$ .

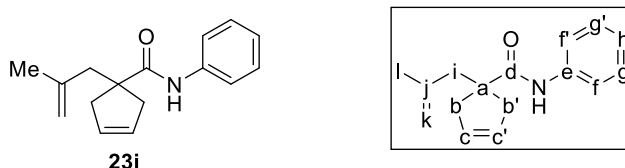


**(R)-1-phenyl-N-(1-phenylethyl)cyclopent-3-ene-1-carboxamide (23k).** Following **GP5** with (*R*)-(+)- $\alpha$ -methylbenzylamine (1.5 mL, 1.5 equiv, 11.7 mmol) affords, after flash chromatography on silica gel (90:10 hexanes:ethyl acetate), the title compound (1.67 g, 70%, 3 steps) as a white solid: mp 73.5–75.5 °C; TLC analysis  $R_f$  0.6 (70:30 hexanes:ethyl acetate);  $^1\text{H}$  NMR (300 MHz,  $\text{CDCl}_3$ )  $\delta$  7.45–7.20 (8H, m, h,h',i,k,k',l,l',m), 7.14 (2H, t,  $J = 6.7$  Hz, g,g'), 5.76 (2H, s, c,c'), 5.44 (1H, br s, NH), 5.20–5.05 (1H, m, e), 3.32 (2H, dd,  $J = 16.6$  and 10.5 Hz, b,b'), 2.81 (2H, dd,  $J = 15.9$  and 14.8 Hz, b,b'), 1.38 (3H, d,  $J = 6.9$  Hz, n);  $^{13}\text{C}$  NMR (75 MHz,  $\text{CDCl}_3$ )  $\delta$  175.46 (d), 145.11 (j), 143.35 (f), 128.76 and 128.66 (c,c'), 128.69 (k,k'), 128.52 (l,l'), 127.12 (h,h'), 126.89 (m), 126.64 (i), 125.90 (g,g'), 58.25 (a), 48.93 (e), 43.87 and 43.79 (b,b'), 21.60 (n); IR (neat) 3290 (N-H stretch), 3053, 1644 (C=O stretch), 1623 (C=C stretch), 1526 (N-H bend), 1493, 1444, 741, 695, 662  $\text{cm}^{-1}$ . HRMS (ESI) calcd. for  $\text{C}_{20}\text{H}_{21}\text{NaNO}$  ( $\text{M}+\text{Na}$ ): 314.1521, found 314.1510  $m/z$ .



**(E)-1-(5-phenyl-2-pentenyl)-3-cyclopentenecarboxylic acid phenyl amide (23j).** Following **GP5** with carboxylic acid **102** (1.40 g, 5.46 mmol), oxalyl chloride (1.88 mL, 4.0 equiv, 21.8 mmol), triethyl amine (1.53 mL, 2.0 equiv, 10.9 mmol), and aniline (0.77 mL, 1.5 equiv, 8.2 mmol) affords, after flash chromatography on silica gel (90:10

hexanes:ethyl acetate), the title compound (1.36 g, 75%, 2 steps) as a light yellow solid: mp 82.5–83.0 °C; TLC analysis  $R_f$  0.7 (70:30 hexanes:ethyl acetate);  $^1\text{H}$  NMR (400 MHz,  $\text{CDCl}_3$ )  $\delta$  7.51 (2H, dd,  $J = 8.7$  and  $1.2$  Hz, f,f'), 7.40–7.25 (4H, m, g,g',p,p'), 7.27 (1H, br s, NH), 7.25–7.15 (3H, m, o,o',q), 7.14 (1H, t,  $J = 7.4$  Hz, h), 5.73 (2H, s, c,c'), 5.65–5.45 (2H, m, j,k), 2.85 (2H, d,  $J = 14.4$  Hz, b,b'), 2.70 (2H, t,  $J = 7.3$  Hz, m), 2.50–2.40 (4H, m, b,b',i), 2.40–2.35 (2H, m, l);  $^{13}\text{C}$  NMR (100 MHz,  $\text{CDCl}_3$ )  $\delta$  175.54 (d), 141.85 (n), 138.15 (e), 133.74 (k), 129.13 (c,c'), 128.97 (g,g'), 128.51 (p,p'), 128.31 (o,o'), 126.44 (j), 125.82 (q), 124.15 (h), 120.03 (f), 53.00 (a), 42.38 (i), 42.16 (b,b'), 35.87 (m), 34.40 (l); IR (neat) 3329 (N-H stretch), 3060, 2916, 2844, 1659 (C=O stretch), 1598 (C=C stretch), 1529 (N-H bend), 1497, 1436, 1309, 1233, 976, 951, 755, 692, 677  $\text{cm}^{-1}$ . HRMS (ESI) calcd. for  $\text{C}_{23}\text{H}_{25}\text{NaNO}$  (M+Na): 354.1834, found 354.1833  $m/z$ .



**1-(2-methylallyl)-3-cyclopentenecarboxylic acid phenyl amide (23i).** Following **GP5** with carboxylic acid **103** (454 mg, 2.73 mmol), oxalyl chloride (0.94 mL, 4.0 equiv, 10.9 mmol), triethyl amine (0.77 mL, 2.0 equiv, 5.45 mmol), and aniline (0.39 mL, 1.5 equiv, 4.1 mmol) affords, after flash chromatography on silica gel (90:10 hexanes:ethyl acetate), the title compound (468 mg, 71%, 2 steps) as an off-white solid: mp 109.0–110.0 °C; TLC analysis  $R_f$  0.7 (70:30 hexanes:ethyl acetate);  $^1\text{H}$  NMR (400 MHz,  $\text{CDCl}_3$ )  $\delta$  7.51 (2H, d,  $J = 7.6$  Hz, f,f'), 7.40–7.30 (3H, m, g,g',NH), 7.12 (1H, t,  $J = 7.4$  Hz, h), 5.74 (2H, s, c,c'), 4.92 (1H, s, k), 4.75 (1H, s, k), 2.95 (2H, d,  $J = 14.5$  Hz, b,b'), 2.60–2.50 (4H, m, b,b',i), 1.76 (3H, s, l);  $^{13}\text{C}$  NMR (100 MHz,  $\text{CDCl}_3$ )  $\delta$  175.37 (d), 142.51 (j),

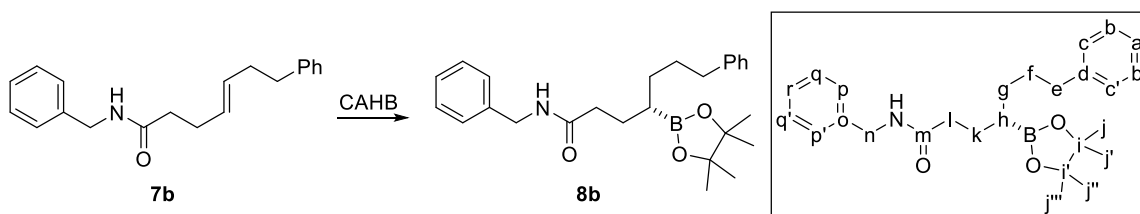


138.12 (e), 129.01 (c,c'), 128.97 (g,g'), 124.17 (h), 120.01 (f,f'), 114.21 (k), 52.90 (a), 46.78 (i), 42.99 (b,b'), 23.84 (l); IR (neat) 3240 (N-H stretch), 3066, 2925, 1646 (C=O stretch), 1597 (C=C stretch), 1531 (N-H bend), 1485, 1438, 951, 749, 729, 690, 661  $\text{cm}^{-1}$ . HRMS (ESI) calcd. for  $\text{C}_{16}\text{H}_{19}\text{NaNO}$  (M+Na): 264.1364, found 264.1357  $m/z$ .

### 5.3 Procedures for directed catalytic asymmetric hydroboration (CAHB) with or without oxidation

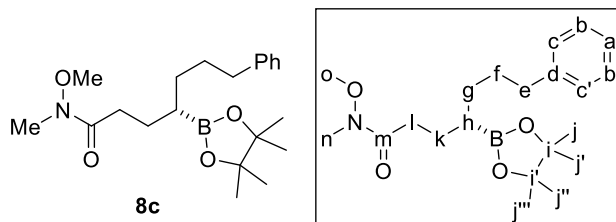
#### General procedure for CAHB of unsaturated carbonyl derivatives without subsequent oxidation. (GP10)

Note: **8b** and **8d** were obtained in a gram scale without loss in selectivity.

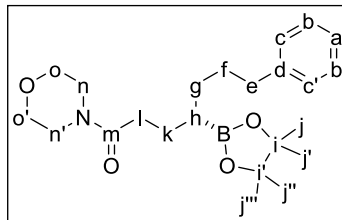
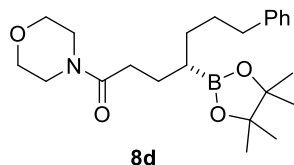


**(S)-7-phenyl-4-(4,4,5,5-tetramethyl-1,3,2-dioxaborolan-2-yl)heptanecarboxylic acid benzyl amide (8b).** To a yellow solution of 0.5 mol%  $[\text{Rh}(\text{nbd})_2\text{BF}_4/ 2(R)\text{-B1}]$  (i.e.,  $\text{Rh}(\text{nbd})_2\text{BF}_4$  (1.0 mg, 2.64  $\mu\text{mol}$ ) and  $(R)$ -(BINOL)PN(Me)Ph **B1** (2.23 mg, 5.28  $\mu\text{mol}$ )) in THF (2.0 mL) was added  $\gamma,\delta$ -unsaturated amide **7b** (1.08 g, 3.7 mmol) as a solution in THF (2.0 mL). To the resulting solution was added dropwise a solution of 4,4,5,5-tetramethyl-1,3,2-dioxaborolane (pinBH, 102 mg, 0.8 mmol, 1.5 equiv) in THF (1.0 mL). The mixture was then stirred at 40 °C for 12h. Afterwards, the reaction was concentrated under reduced pressure and purified via flash chromatography on silica gel (90:10-40:60 hexanes:ethyl acetate) to afford the title compound (1.26 g, 81%) as a yellow oil: TLC analysis  $R_f$  0.3 (60:40 hexanes:ethyl acetate);  $[\alpha]_D^{20} = +2.4^\circ$  ( $c$  2.0,  $\text{CHCl}_3$ );  $^{11}\text{B}$  NMR (128 MHz,  $\text{CDCl}_3$ )  $\delta$  34.51;  $^1\text{H}$  NMR (400 MHz,  $\text{CDCl}_3$ )  $\delta$  7.30–7.40 (2H, m, q,q'), 7.25–7.30 (5H, m, b,b',c,c',r), 7.15–7.25 (3H, m, a,p,p'), 6.00 (1H, br s, NH), 4.44 (2H, d,  $J = 5.8$  Hz, n), 2.61 (2H, t,  $J = 7.6$  Hz, e), 2.15–2.30 (2H, m, l), 1.70–1.85 (2H, m, k), 1.60–1.70 (2H, m, f), 1.50–1.60 (1H, m, g), 1.40–1.50 (1H, m, g), 1.23 (12H, s, j,j',j'',j'''), 1.00–1.10 (1H, m, h);  $^{13}\text{C}$  NMR (100 MHz,  $\text{CDCl}_3$ )  $\delta$  173.19 (m), 142.82 (d),

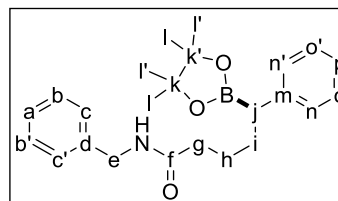
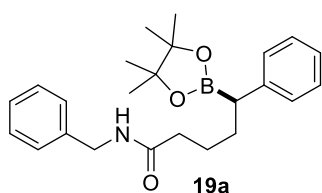
138.60 (o), 128.78 (q,q'), 128.51 (b,b'), 128.34 (c,c'), 128.00 (p,p'), 127.55 (r), 125.69 (a), 83.25 (i,i'), 43.72 (n), 36.50 (l), 36.26 (e), 30.98 (f), 30.94 (g), 27.49 (k), 24.95 (j,j',j'',j'''); IR (neat) 3285 (N-H stretch), 2976, 2926, 2856, 1644 (C=O stretch), 1541 (N-H bend), 1454, 1379 (C-N stretch), 1315, 1141, 747, 697  $\text{cm}^{-1}$ ; HRMS (ESI) calcd. for  $\text{C}_{26}\text{H}_{36}\text{BNNaO}_3$  (M+Na): 444.2686, found 444.2701  $m/z$ .



**(S)-7-phenyl-4-(4,4,5,5-tetramethyl-1,3,2-dioxaborolan-2-yl)heptanecarboxylic acid Weinreb amide (8c).** Following **GP10** with 2 mol%  $[\text{Rh}(\text{nbd})_2\text{BF}_4/ 2(R)\text{-B1}]$  and **7c** (130 mg, 0.528 mmol) affords, after flash chromatography on silica gel (90:10-50:50 hexanes:ethyl acetate), the title compound (136 mg, 69%) as a yellow oil: TLC analysis  $R_f$  0.4 (60:40 hexanes:ethyl acetate);  $[\alpha]_{\text{D}}^{20} = +5.1^\circ$  (c 2.0,  $\text{CHCl}_3$ );  $^{11}\text{B}$  NMR (128 MHz,  $\text{CDCl}_3$ )  $\delta$  33.87;  $^1\text{H}$  NMR (400 MHz,  $\text{CDCl}_3$ )  $\delta$  7.25–7.30 (2H, m, b,b'), 7.15–7.25 (3H, m, a,c,c'), 3.67 (3H, s, o), 3.18 (3H, s, n), 2.62 (2H, d,  $J = 7.6$  Hz, e), 2.30–2.60 (2H, m, l), 1.40–1.80 (6H, m, f,g,k), 1.26 (12H, s, j,j',j'',j'''), 1.00–1.15 (1H, m, h);  $^{13}\text{C}$  NMR (100 MHz,  $\text{CDCl}_3$ )  $\delta$  174.93 (m), 142.89 (d), 128.50 (b,b'), 128.31 (c,c'), 125.63 (a), 83.09 (i,i'), 61.29 (o), 36.30 (e), 32.28 (n), 31.71 (l), 31.01 (f), 31.00 (g), 26.30 (k), 24.97 and 24.93 (j,j',j'',j'''); IR (neat) 2976, 2930, 2857, 1663 (C=O stretch), 1380 (C-N stretch), 1314, 1142, 699  $\text{cm}^{-1}$ ; HRMS (ESI) calcd. for  $\text{C}_{21}\text{H}_{34}\text{BNNaO}_4$  (M+Na): 398.2479, found 398.2496  $m/z$ .

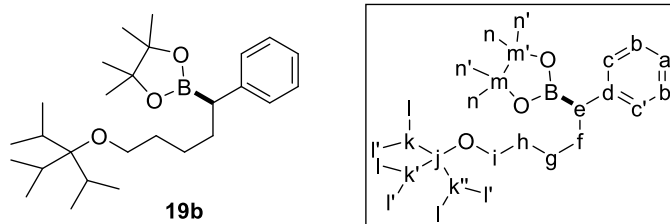


**(S)-7-phenyl-4-(4,4,5,5-tetramethyl-1,3,2-dioxaborolan-2-yl)heptanecarboxylic acid morpholino amide (8d).** Following **GP10** with 2 mol% [Rh(nbd)<sub>2</sub>BF<sub>4</sub>/ 2(*R*)-**B1**] and **7d** (1.01 g, 3.7 mmol) affords, after flash chromatography on silica gel (90:10-40:60 hexanes:ethyl acetate), the title compound (1.22 g, 82%) as a yellow oil: TLC analysis *R<sub>f</sub>* 0.4 (40:60 hexanes:ethyl acetate); [α]<sub>D</sub><sup>20</sup> = +0.3° (*c* 2.0, CHCl<sub>3</sub>); <sup>11</sup>B NMR (128 MHz, CDCl<sub>3</sub>) δ 34.34; <sup>1</sup>H NMR (400 MHz, CDCl<sub>3</sub>) δ 7.25–7.35 (2H, m, b,b'), 7.10–7.25 (3H, m, a,c,c'), 3.55–3.70 (6H, m, n,n',o,o'), 3.40–3.50 (2H, m, n,n'), 2.61 (2H, d, *J* = 7.2 Hz, e), 2.25–2.40 (2H, m, l), 1.40–1.80 (6H, m, f,g,k), 1.24 (12H, s, j,j',j'',j'''), 1.00–1.10 (1H, m, h); <sup>13</sup>C NMR (100 MHz, CDCl<sub>3</sub>) δ 172.11 (m), 144.78 (d), 128.49 (b,b'), 128.32 (c,c'), 125.67 (a), 83.17 (i,i'), 67.06 and 66.86 (o,o'), 46.19 and 41.95 (n,n'), 36.25 (e), 33.08 (l), 30.92 (f), 30.89 (g), 26.99 (k), 25.00 and 24.94 (j,j',j'',j'''); IR (neat) 2974, 2924, 2854, 1644 (C=O stretch), 1425, 1380 (C-N stretch), 1142, 1114, 699 cm<sup>-1</sup>; HRMS (ESI) calcd. for C<sub>23</sub>H<sub>36</sub>BNNaO<sub>4</sub> (M+Na): 424.2635, found 424.2648 *m/z*.



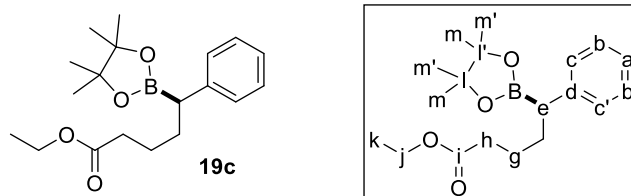
**(R)-5-phenyl-5-(4,4,5,5-tetramethyl-1,3,2-dioxaborolan-2-yl)pentanecarboxylic acid benzyl amide (19a).** Following **GP10** with **15a** (140 mg, 0.528 mmol) affords, after flash

chromatography on silica gel (95:5–90:10 DCM:ethyl acetate), the title compound (187 mg, 90%) as a yellow oil: TLC analysis  $R_f$  0.4 (40:60 hexanes:ethyl acetate); Enantiomeric excess was checked by converting to the corresponding Mosher's ester **22a** (general procedure *vide infra*); crude  $^{19}\text{F}$  NMR (375 MHz,  $\text{CDCl}_3$ ) shows  $\delta$   $-71.36$  (major 95%) and  $-71.61$  (minor 5%);  $^1\text{H}$  NMR (400 MHz,  $\text{CDCl}_3$ )  $\delta$  7.10–7.40 (10H, m, a,b,b',c,c',n,n',o,o',p), 5.76 (1H, br s, NH), 4.44 (2H, d,  $J = 5.6$  Hz, e), 2.32 (1H, t,  $J = 7.3$  Hz, j), 2.23 (2H, t,  $J = 7.4$  Hz, g), 1.80–1.95 (1H, m, h), 1.60–1.75 (3H, m, h,i), 1.20 (12H, d,  $J = 8.0$  Hz, l,l') ;  $^{13}\text{C}$  NMR (100 MHz,  $\text{CDCl}_3$ )  $\delta$  172.76 (f), 142.94 (m), 138.55 (d), 128.79 (b,b'), 128.48 (n,n',o,o'), 127.93 (c,c'), 127.56 (a), 125.43 (p), 83.52 (k,k'), 43.64 (e), 36.81 (g), 32.25 (h), 25.44 (i), 24.73 and 24.70 (l,l').

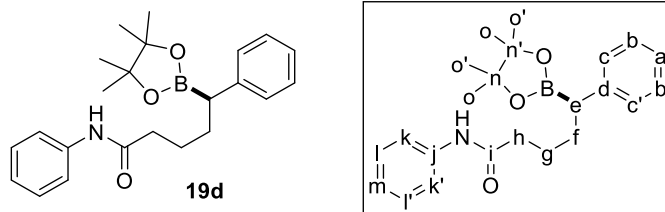


**(R)-2-(5-((3-isopropyl-2,4-dimethylpentan-3-yl)oxy)-1-phenylpentyl)-4,4,5,5-tetramethyl-1,3,2-dioxaborolane (19b)**. Following **GP10** with **15b** (168 mg, 0.528 mmol) affords, after flash chromatography on silica gel (95:5 hexanes:ethyl acetate), the title compound (170 mg, 75%) as a colorless oil: TLC analysis  $R_f$  0.7 (80:20 hexanes:ethyl acetate); Chiral HPLC analysis (Chiralcel-OD, 99:1 hexanes:isopropanol, flowrate = 1.0 mL/min) showed peaks at 35 minutes (10.0% (*S*)) and 42 minutes (90.0% (*R*));  $^1\text{H}$  NMR (400 MHz,  $\text{CDCl}_3$ )  $\delta$  7.20–7.30 (4H, m, b,b',c,c'), 7.10–7.20 (1H, m, a), 3.67 (2H, t,  $J = 6.6$  Hz, l), 2.34 (1H, t,  $J = 7.9$  Hz, e), 1.85–2.00 (1H, m, h), 1.65–1.75 (1H, m, h), 1.50–1.65 (2H, m, g), 1.30–1.45 (2H, m, f), 1.23 (12H, d,  $J = 7.4$  Hz, n,n'),

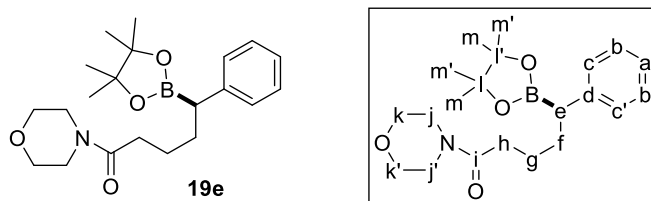
1.05–1.10 (21H, m, k,k',k'',l,l');  $^{13}\text{C}$  NMR (100 MHz,  $\text{CDCl}_3$ )  $\delta$  143.51 (d), 128.49 (b,b'), 128.34 (c,c'), 125.20 (a), 83.33 (m,m'), 63.57 (l), 33.24 (g), 32.70 (h), 25.77 (f), 24.74 and 24.71 (n,n'), 18.17 (l,l'), 12.14 (k,k',k'').



**(R)-5-phenyl-5-(4,4,5,5-tetramethyl-1,3,2-dioxaborolan-2-yl)pentanecarboxylic ethyl ester (19c).** Following **GP10** with **15c** (108 mg, 0.528 mmol) affords, after flash chromatography on silica gel (95:5 hexanes:ethyl acetate), the title compound (135 mg, 77%) as a yellow oil: TLC analysis  $R_f$  0.7 (80:20 hexanes:ethyl acetate); Enantiomeric excess was checked by converting to the corresponding Mosher's ester **22c** (general procedure *vide infra*); crude  $^{19}\text{F}$  NMR (375 MHz,  $\text{CDCl}_3$ ) shows  $\delta$   $-71.37$  (major 85%) and  $-71.56$  (minor 15%);  $^1\text{H}$  NMR (400 MHz,  $\text{CDCl}_3$ )  $\delta$  7.25–7.30 (2H, m, b,b'), 7.15–7.25 (2H, m, c,c'), 7.10–7.15 (1H, m, a), 4.12 (2H, q,  $J = 7.1$  Hz, j), 2.20–2.40 (3H, m, e,h), 1.85–1.95 (1H, m, g), 1.65–1.75 (1H, m, g), 1.55–1.65 (2H, m, f), 1.25 (3H, t,  $J = 7.2$  Hz, k), 1.22 (12H, d,  $J = 8.5$  Hz, m,m');  $^{13}\text{C}$  NMR (100 MHz,  $\text{CDCl}_3$ )  $\delta$  173.74 (i), 142.94 (d), 128.46 (b,b'), 128.43 (c,c'), 125.37 (a), 83.45 (l,l'), 60.23 (j), 34.48 (g), 32.10 (h), 24.74 and 24.69 (f,m,m'), 14.34 (k).

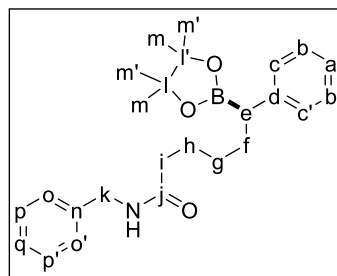
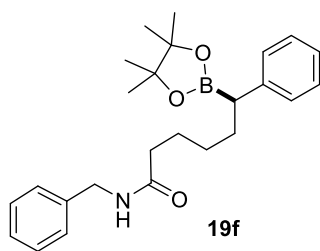


**(R)-5-phenyl-5-(4,4,5,5-tetramethyl-1,3,2-dioxaborolan-2-yl)pentanecarboxylic phenyl amide (19d).** Following **GP10** with **15d** (133 mg, 0.528 mmol) affords, after flash chromatography on silica gel (95:5–90:10 DCM:ethyl acetate), the title compound (152 mg, 76%) as a yellow oil: TLC analysis  $R_f$  0.6 (50:50 hexanes:ethyl acetate); Enantiomeric excess was checked by converting to the corresponding Mosher's ester **22d** (general procedure *vide infra*); crude  $^{19}\text{F}$  NMR (375 MHz,  $\text{CDCl}_3$ ) shows  $\delta$   $-71.39$  (major 94%) and  $-71.64$  (minor 6%);  $^1\text{H}$  NMR (400 MHz,  $\text{CDCl}_3$ )  $\delta$  7.51 (2H, d,  $J = 7.8$  Hz, k,k'), 7.20–7.35 (6H, m, b,b',c,c',l,l'), 7.16 (1H, t,  $J = 7.1$  Hz, a), 7.10 (1H, t,  $J = 7.1$  Hz, m), 2.30–2.40 (3H, e,h), 1.85–2.00 (1H, m, g), 1.65–1.80 (3H, m, f,g), 1.22 (12H, d,  $J = 9.2$  Hz, o,o');  $^{13}\text{C}$  NMR (100 MHz,  $\text{CDCl}_3$ )  $\delta$  171.31 (i), 142.90 (d), 138.11 (j), 129.04 (l,l'), 128.52 (b,b',c,c'), 125.49 (a), 124.23 (m), 120.00 (k,k'), 83.58 (n,n'), 37.79 (g), 32.14 (h), 25.36 (f), 24.76 and 24.73 (o,o').



**(R)-5-phenyl-5-(4,4,5,5-tetramethyl-1,3,2-dioxaborolan-2-yl)pentanecarboxylic phenyl amide (19d).** Following **GP10** with (*R*)-**B2** and **15d** (130 mg, 0.528 mmol) affords, after flash chromatography on silica gel (95:5–90:10 DCM:ethyl acetate), the title compound (154 mg, 78%) as a yellow oil: TLC analysis  $R_f$  0.4 (40:60 hexanes:ethyl

acetate); Enantiomeric excess was checked by converting to the corresponding Mosher's ester **22e** (general procedure *vide infra*); crude  $^{19}\text{F}$  NMR (375 MHz,  $\text{CDCl}_3$ ) shows  $\delta$  –71.22 (major 95.5%) and –71.61 (minor 4.5%);  $^1\text{H}$  NMR (400 MHz,  $\text{CDCl}_3$ )  $\delta$  7.15–7.25 (4H, m, b,b',c,c'), 7.12 (1H, t,  $J$  = 7.0 Hz, a), 3.55–3.65 (6H, m, j,j',k,k'), 3.30–3.35 (2H, m, j,j'), 2.20–2.35 (3H, m, e,h), 1.85–1.95 (1H, m, g), 1.65–1.75 (1H, m, g), 1.55–1.65 (2H, m, f), 1.19 (12H, d,  $J$  = 8.2 Hz, m,m');  $^{13}\text{C}$  NMR (100 MHz,  $\text{CDCl}_3$ )  $\delta$  171.76 (i), 142.90 (d), 128.48 (b,b'), 128.43 (c,c'), 125.39 (a), 83.46 (l,l'), 67.00 and 67.71 (k,k'), 46.10 and 41.91 (j, j'), 33.32 (g), 32.22 (h), 24.86 (f), 24.74 and 24.71 (m,m').

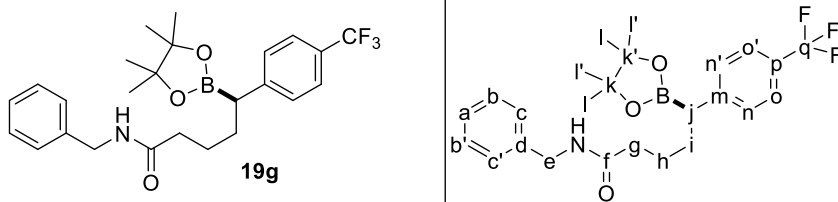


**(R)-6-phenyl-6-(4,4,5,5-tetramethyl-1,3,2-dioxaborolan-2-yl)hexanecarboxylic**

**benzyl amide (19f).** Following **GP10** with **15f** (148 mg, 0.528 mmol) affords, after flash chromatography on silica gel (95:5–90:10 DCM:ethyl acetate), the title compound (168 mg, 78%) as a yellow oil: TLC analysis  $R_f$  0.4 (40:60 hexanes:ethyl acetate); Chiral HPLC analysis (Chiralpak-IC, 60:40 hexanes:isopropanol, flowrate = 1.0 mL/min) showed peaks at 47 minutes (90.5% (*R*)) and 56 minutes (9.5% (*S*));  $^1\text{H}$  NMR (400 MHz,  $\text{CDCl}_3$ )  $\delta$  7.15–7.40 (9H, m, b,b',c,c',o,o',p,p',q), 7.14 (1H, t,  $J$  = 7.1 Hz, a), 5.72 (1H, br s, NH), 4.42 (2H, d,  $J$  = 5.7 Hz, k), 2.30 (1H, t  $J$  = 7.8 Hz, e), 2.18 (2H, t,  $J$  = 7.2 Hz, i), 1.80–1.90 (1H, m, h), 1.60–1.80 (3H, m, f,h), 1.25–1.40 (2H, m, g), 1.21 (12H, d,  $J$  = 8.6 Hz, m,m');  $^{13}\text{C}$  NMR (100 MHz,  $\text{CDCl}_3$ )  $\delta$  172.97 (j), 143.25 (n), 138.54 (d), 128.81

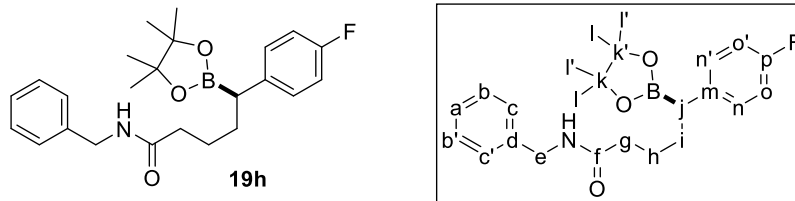


(b,b'), 128.48 (p,p'), 128.44 (c,c'), 127.92 (q), 125.30 (a), 83.41 (l,l'), 43.66 (k), 36.79 (i), 32.24 (h), 28.97 (g), 25.87 (f), 24.75 and 24.69 (m,m').

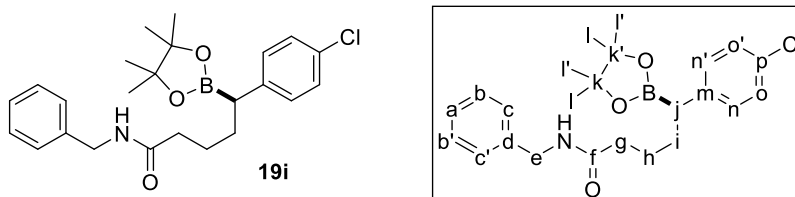


**(R)-5-(4-trifluoromethyl)phenyl-5-(4,4,5,5-tetramethyl-1,3,2-dioxaborolan-2-yl)**

**pentanecarboxylic acid benzyl amide (19g).** Following **GP10** with (*R*)-**B7** and **15g** (176 mg, 0.528 mmol) affords, after flash chromatography on silica gel (95:5–90:10 DCM:ethyl acetate), the title compound (190 mg, 78%) as a yellow oil: TLC analysis  $R_f$  0.4 (40:60 hexanes:ethyl acetate); Enantiomeric excess was checked by converting to the corresponding Mosher's ester **22g** (general procedure *vide infra*); crude  $^{19}\text{F}$  NMR (375 MHz,  $\text{CDCl}_3$ ) shows  $\delta$  –71.28 (major 95%) and –71.46 (minor 5%);  $^{19}\text{F}$  NMR (375 MHz,  $\text{CDCl}_3$ )  $\delta$  –62.17;  $^1\text{H}$  NMR (400 MHz,  $\text{CDCl}_3$ )  $\delta$  7.51 (2H, d,  $J$  = 8.1 Hz, o,o'), 7.25–7.35 (7H, m, a,b,b',c'c',n,n'), 5.87 (1H, br s, NH), 4.43 (2H, d,  $J$  = 5.5 Hz, e), 2.40 (1H, t,  $J$  = 7.2 Hz, j), 2.22 (2H, t,  $J$  = 7.4 Hz, g), 1.80–2.00 (1H, m, h), 1.60–1.80 (3H, m, h,i), 1.21 (12H, d,  $J$  = 5.9 Hz, l,l');  $^{13}\text{C}$  NMR (100 MHz,  $\text{CDCl}_3$ )  $\delta$  172.62 (f), 147.35 (m), 138.49 (d), 128.80 (aryl), 128.67 (aryl), 127.92 (aryl), 127.60 (aryl), 125.37 (q,  $J$  = 3.7 Hz, aryl), 83.79 (k,k'), 43.67 (e), 36.63 (g), 31.93 (h), 25.33 (i), 24.71 and 24.69 (l,l').

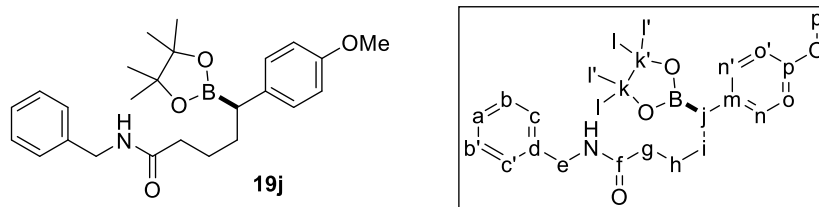


**(R)-5-(4-fluoro)phenyl-5-(4,4,5,5-tetramethyl-1,3,2-dioxaborolan-2-yl)pentanecarboxylic acid benzyl amide (19h).** Following **GP10** with **15h** (150 mg, 0.528 mmol) affords, after flash chromatography on silica gel (95:5–90:10 DCM:ethyl acetate), the title compound (167 mg, 77%) as a yellow oil: TLC analysis  $R_f$  0.4 (40:60 hexanes:ethyl acetate); Enantiomeric excess was checked by converting to the corresponding Mosher's ester **22h** (general procedure *vide infra*); crude  $^{19}\text{F}$  NMR (375 MHz,  $\text{CDCl}_3$ ) shows  $\delta$   $-71.25$  (major 95%) and  $-71.51$  (minor 5%);  $^{19}\text{F}$  NMR (375 MHz,  $\text{CDCl}_3$ )  $\delta$   $-118.4$  to  $-118.6$  (m, F);  $^1\text{H}$  NMR (400 MHz,  $\text{CDCl}_3$ )  $\delta$  7.25–7.40 (5H, m, aryl), 7.14 (2H, dd,  $J = 8.6$  and 5.5 Hz, aryl), 6.94 (2H,  $J = 8.8$  Hz, aryl), 4.44 (2H, d,  $J = 5.9$  Hz, e), 2.30 (1H, t,  $J = 7.3$  Hz, j), 2.22 (2H, t,  $J = 7.4$  Hz, g), 1.80–1.90 (1H, m, h), 1.60–1.75 (3H, m, f,h), 1.21 (12H, d,  $J = 6.8$  Hz, l,l') ;  $^{13}\text{C}$  NMR (100 MHz,  $\text{CDCl}_3$ )  $\delta$  172.69 (f), 162.31 and 159.89 (p), 138.54 (d), 129.74 (aryl), 129.66 (aryl), 128.79 (aryl), 127.83 (aryl), 127.59 (aryl), 115.29 and 115.08 (o,o'), 83.59 (k,k'), 43.65 (e), 36.73 (g), 32.35 (h), 25.33 (i), 24.72 and 24.69 (l,l').



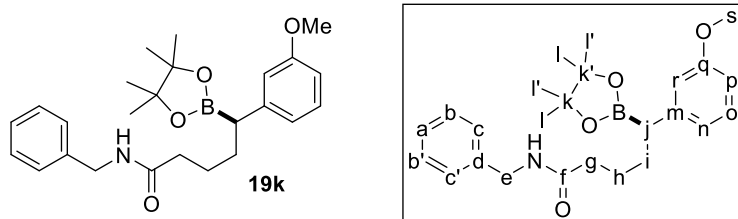
**(R)-5-(4-chloro)phenyl-5-(4,4,5,5-tetramethyl-1,3,2-dioxaborolan-2-yl)pentanecarboxylic acid benzyl amide (19i).** Following **GP10** with (*R*)-**B2** and **15i**

(158 mg, 0.528 mmol) affords, after flash chromatography on silica gel (95:5–90:10 DCM:ethyl acetate), the title compound (169 mg, 75%) as a yellow oil: TLC analysis  $R_f$  0.4 (40:60 hexanes:ethyl acetate); Enantiomeric excess was checked by converting to the corresponding Mosher's ester **22i** (general procedure *vide infra*); crude  $^{19}\text{F}$  NMR (375 MHz,  $\text{CDCl}_3$ ) shows  $\delta$   $-71.35$  (major 95%) and  $-71.57$  (minor 5%);  $^1\text{H}$  NMR (400 MHz,  $\text{CDCl}_3$ )  $\delta$  7.25–7.35 (5H, m, a,b,b',o,o',p), 7.22 (2H, d,  $J = 8.4$  Hz, c,c'), 7.13 (2H,  $J = 8.4$  Hz, n,n'), 4.42 (2H, d,  $J = 5.7$  Hz, e), 2.29 (1H, t,  $J = 7.3$  Hz, j), 2.20 (2H, t,  $J = 7.4$  Hz, g), 1.80–1.90 (1H, m, h), 1.50–1.70 (3H, m, f,h), 1.21 (12H, d,  $J = 6.2$  Hz, l,l');  $^{13}\text{C}$  NMR (100 MHz,  $\text{CDCl}_3$ )  $\delta$  172.68 (f), 141.50 (m), 138.55 (d), 131.09 (p). 129.78 (n,n'), 128.79 (b,b'), 128.56 (o,o'), 127.92 (c,c'), 127.57 (a), 83.66 (k,k'), 43.63 (e), 36.67 (g), 32.10 (h), 25.55 (i), 24.73 and 24.70 (l,l').



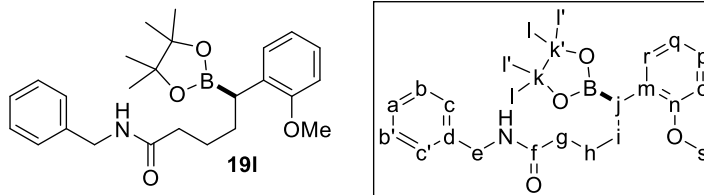
**(R)-5-(4-methoxyphenyl)-5-(4,4,5,5-tetramethyl-1,3,2-dioxaborolan-2-yl)pentanecarboxylic acid benzyl amide (19j)**. Following **GP10** with (*R*)-**B2** and **15j** (156 mg, 0.528 mmol) affords, after flash chromatography on silica gel (95:5–90:10 DCM:ethyl acetate), the title compound (177 mg, 79%) as a yellow oil: TLC analysis  $R_f$  0.4 (40:60 hexanes:ethyl acetate); Enantiomeric excess was checked by converting to the corresponding Mosher's ester **22j** (general procedure *vide infra*); crude  $^{19}\text{F}$  NMR (375 MHz,  $\text{CDCl}_3$ ) shows  $\delta$   $-71.40$  (major 96%) and  $-71.68$  (minor 4%);  $^1\text{H}$  NMR (400 MHz,  $\text{CDCl}_3$ )  $\delta$  7.20–7.35 (5H, m, a,b,b',c,c'), 7.10 (2H, d,  $J = 8.6$  Hz, n,n'), 6.80 (2H, d,  $J =$

8.6 Hz, o,o'), 5.94 (1H, br s, NH)), 4.41 (2H, d,  $J = 5.7$  Hz, e), 3.77 (3H, s, s), 2.15–2.30 (3H, m, g,j), 1.80–1.90 (1H, m, h), 1.55–1.70 (3H, m, h,i), 1.20 (12H, d,  $J = 7.6$  Hz, l,l');  $^{13}\text{C}$  NMR (100 MHz,  $\text{CDCl}_3$ )  $\delta$  172.92 (f), 157.51 (q), 138.59 (d), 134.90 (m), 129.34 (n,n'), 128.75 (b,b'), 127.90 (c,c'), 127.51 (a), 113.94 (o,o'), 83.46 (k,k'), 55.28 (s), 43.59 (e), 36.76 (g), 32.49 (h), 25.39 (i), 24.73 and 24.71 (l,l').

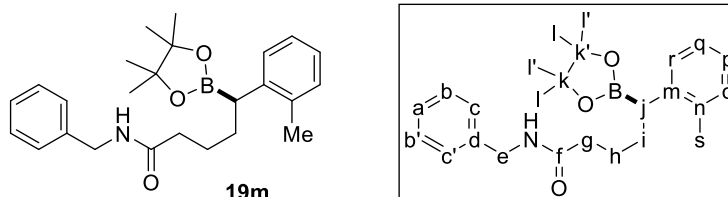


**(R)-5-(3-methoxyphenyl)-5-(4,4,5,5-tetramethyl-1,3,2-dioxaborolan-2-**

**yl)pentanecarboxylic acid benzyl amide (19k).** Following **GP10** with **15k** (156 mg, 0.528 mmol) affords, after flash chromatography on silica gel (95:5–90:10 DCM:ethyl acetate), the title compound (161 mg, 72%) as a yellow oil: TLC analysis  $R_f$  0.4 (40:60 hexanes:ethyl acetate); Chiral HPLC analysis (Chiralcel-AD, 60:40 hexanes:isopropanol, flowrate = 1.0 mL/min) showed peaks at 15 minutes (97.0% (*R*)) and 19 minutes (3.0% (*S*));  $^1\text{H}$  NMR (400 MHz,  $\text{CDCl}_3$ )  $\delta$  7.20–7.40 (5H, m, aryl), 7.17 (1H, t,  $J = 7.7$  Hz, aryl), 6.75–6.85 (2H, m, aryl), 6.71 (1H, d,  $J = 7.8$  Hz, aryl), 5.86 (1H, br s, NH)), 4.43 (2H, d,  $J = 5.5$  Hz, e), 3.79 (3H, s, s), 2.15–2.35 (3H, m, g,j), 1.80–1.95 (1H, m, h), 1.55–1.80 (3H, m, h,i), 1.21 (12H, d,  $J = 7.4$  Hz, l,l');  $^{13}\text{C}$  NMR (100 MHz,  $\text{CDCl}_3$ )  $\delta$  172.81 (f), 159.72 (q), 144.61 (m), 138.85 (d), 129.35 (o), 128.77 (b,b'), 127.90 (c,c'), 127.53 (a), 120.99 (n), 114.14 (p), 110.90 (r), 83.53 (k,k'), 55.18 (s), 43.62 (e), 36.79 (g), 32.26 (h), 25.46 (i), 24.73 (l,l').

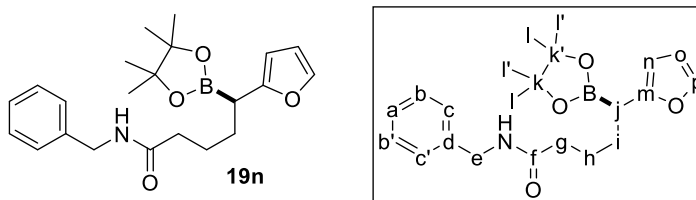


**(R)-5-(2-methoxy)phenyl-5-(4,4,5,5-tetramethyl-1,3,2-dioxaborolan-2-yl)pentanecarboxylic acid benzyl amide (19l).** Following **GP10** with **15l** (156 mg, 0.528 mmol) affords, after flash chromatography on silica gel (95:5–90:10 DCM:ethyl acetate), the title compound (183 mg, 82%) as a yellow oil: TLC analysis  $R_f$  0.4 (40:60 hexanes:ethyl acetate); Chiral HPLC analysis (Chiralcel-AD, 60:40 hexanes:isopropanol, flowrate = 1.0 mL/min) showed peaks at 17 minutes (85.5% (*R*)) and 23 minutes (14.5% (*S*));  $^1\text{H}$  NMR (400 MHz,  $\text{CDCl}_3$ )  $\delta$  7.30–7.35 (2H, m, b,b'), 7.25–7.30 (3H, m, a,c,c'), 7.10–7.20 (2H, m, q,r), 6.88 (1H, t,  $J = 7.0$  Hz, p), 6.82 (1H, d,  $J = 8.3$  Hz, o), 5.95 (1H, br s, NH), 4.42 (2H, dd,  $J = 5.5$  and 1.8 Hz, e), 3.77 (3H, s, s), 2.43 (1H, t,  $J = 6.9$  Hz, j), 2.22 (2H, td,  $J = 8.1$  and 2.8 Hz, g), 1.80–1.95 (1H, m, h), 1.55–1.75 (3H, m, h,i), 1.23 (12H, d,  $J = 8.9$  Hz, l,l');  $^{13}\text{C}$  NMR (100 MHz,  $\text{CDCl}_3$ )  $\delta$  173.14 (f), 157.04 (n), 138.68 (d), 131.87 (m), 130.12 (r), 128.74 (b,b'), 127.87 (c,c,'), 127.47 (a), 126.64 (q), 120.74 (p), 110.20 (o), 83.23 (k,k'), 55.15 (s), 43.56 (e), 36.84 (g), 30.54 (h), 25.47 (i), 24.90 and 24.77 (l,l').



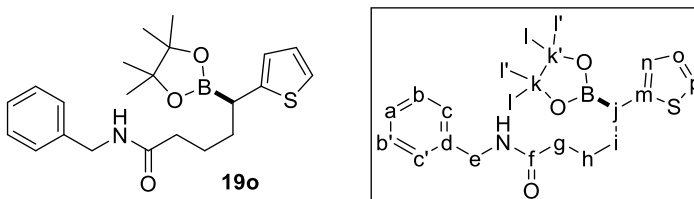
**(R)-5-(2-methyl)phenyl-5-(4,4,5,5-tetramethyl-1,3,2-dioxaborolan-2-yl)pentanecarboxylic acid benzyl amide (19m).** Following **GP10** with **15m** (148 mg,

0.528 mmol) affords, after flash chromatography on silica gel (95:5–90:10 DCM:ethyl acetate), the title compound (181 mg, 84%) as a yellow oil: TLC analysis  $R_f$  0.4 (40:60 hexanes:ethyl acetate); Chiral HPLC analysis (Chiralpak-IC, 60:40 hexanes:isopropanol, flowrate = 1.4 mL/min) showed peaks at 15 minutes (93.0% (*R*)) and 17 minutes (7.0% (*S*));  $^1\text{H}$  NMR (400 MHz,  $\text{CDCl}_3$ )  $\delta$  7.30–7.35 (2H, m, b,b'), 7.25–7.30 (3H, m, c,c',o), 7.19 (1H, d,  $J = 7.5$  Hz, a), 7.10–7.15 (2H, m, q,r), 7.00–7.10 (1H, m, p), 5.92 (1H, br s, NH), 4.43 (2H, d,  $J = 5.9$  Hz, e), 2.54 (1H, t,  $J = 7.0$  Hz, j), 2.34 (3H, s, s), 2.23 (2H, t,  $J = 6.8$  Hz, g), 1.85–2.00 (1H, m, h), 1.60–1.80 (3H, m, h,i), 1.21 (12H, d,  $J = 8.6$  Hz, l,l');  $^{13}\text{C}$  NMR (100 MHz,  $\text{CDCl}_3$ )  $\delta$  172.84 (f), 141.44 (m), 138.61 (d), 136.08 (n), 130.35 (o), 128.77 (b,b'), 127.91 (c,c'), 127.86 (r), 127.53 (a), 126.07 (p), 125.25 (q), 83.44 (k,k'), 43.61 (e), 36.90 (g), 31.86 (h), 25.64 (i), 24.80 and 24.70 (l,l'), 20.30 (s).



**(*R*)-5-(2-furanyl)-5-(4,4,5,5-tetramethyl-1,3,2-dioxaborolan-2-yl)pentanecarboxylic acid benzyl amide (19n).** Following **GP10** with 1 mol% [Rh/2 (*R*)-**B7**], 3 equiv pinBH and **15n** (135 mg, 0.528 mmol) affords, after flash chromatography on silica gel (95:5–90:10 DCM:ethyl acetate), the title compound (140 mg, 69%) as a yellow oil: TLC analysis  $R_f$  0.4 (40:60 hexanes:ethyl acetate); Enantiomeric excess was checked by converting to the corresponding Mosher's ester **22n** (general procedure *vide infra*); crude  $^{19}\text{F}$  NMR (375 MHz,  $\text{CDCl}_3$ ) shows  $\delta$   $-71.59$  (major 97%) and  $-72.00$  (minor 3%);  $^1\text{H}$  NMR (400 MHz,  $\text{CDCl}_3$ )  $\delta$  7.30–7.40 (2H, m, b,b'), 7.25–7.30 (4H, m, a,c,c',p), 6.27

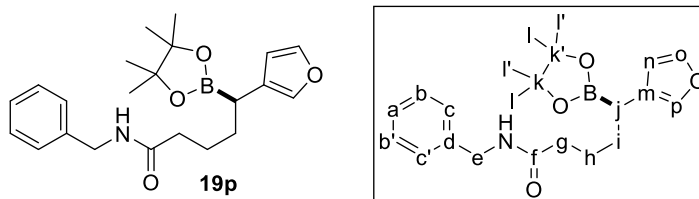
(1H, t,  $J = 2.5$  Hz, o), 6.03 (1H, d,  $J = 2.9$  Hz, n), 5.84 (1H, br s, NH), 4.45 (2H, d,  $J = 5.6$  Hz, e), 2.49 (1H, t,  $J = 7.1$  Hz, j), 2.23 (2H, t,  $J = 7.4$  Hz, g), 1.75–1.85 (2H, m, h), 1.65–1.75 (2H, m, i), 1.25 (12H, d,  $J = 2.8$  Hz, l,l');  $^{13}\text{C}$  NMR (100 MHz,  $\text{CDCl}_3$ )  $\delta$  172.74 (f), 156.37 (m), 140.86 (p), 138.54 (d), 128.78 (b,b'), 127.91 (c,c'), 127.55 (a), 110.29 (o), 105.10 (n), 83.83 (k,k'), 43.85 (e), 36.65 (g), 29.81 (h), 25.20 (i), 24.80 and 24.73 (l,l').



**(R)-5-(2-thiophenyl)-5-(4,4,5,5-tetramethyl-1,3,2-dioxaborolan-2-**

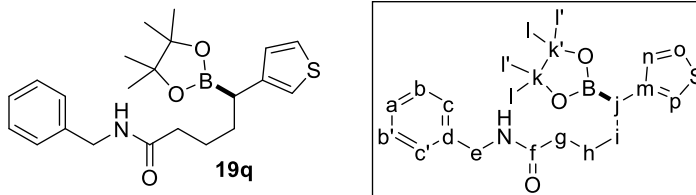
**yl)pentanecarboxylic acid benzyl amide (19o).** Following **GP10** with 1 mol% [Rh/2 (R)-**B2**], 3 equiv pinBH and **15o** (143 mg, 0.528 mmol) affords, after flash chromatography on silica gel (95:5–90:10 DCM:ethyl acetate), the title compound (152 mg, 72%) as a yellow oil: TLC analysis  $R_f$  0.4 (40:60 hexanes:ethyl acetate); Enantiomeric excess was checked by converting to the corresponding Mosher's ester **22o** (general procedure *vide infra*); crude  $^{19}\text{F}$  NMR (375 MHz,  $\text{CDCl}_3$ ) shows  $\delta$   $-71.32$  (major 92%) and  $-71.74$  (minor 8%);  $^1\text{H}$  NMR (400 MHz,  $\text{CDCl}_3$ )  $\delta$  7.30–7.40 (2H, m, b,b'), 7.25–7.30 (3H, m, a,c,c'), 7.09 (1H, dd,  $J = 5.1$  and 0.9 Hz, p), 6.91 (1H, dd,  $J = 5.1$  and 3.4 Hz, o), 6.81 (1H, d,  $J = 3.4$  Hz, n), 5.82 (1H, br s, NH), 4.44 (2H, d,  $J = 5.7$  Hz, e), 2.66 (1H, t,  $J = 7.1$  Hz, j), 2.24 (2H, t,  $J = 7.3$  Hz, g), 1.85–1.95 (1H, m, h), 1.65–1.80 (3H, m, h,i), 1.24 (12H, d,  $J = 4.3$  Hz, l,l');  $^{13}\text{C}$  NMR (100 MHz,  $\text{CDCl}_3$ )  $\delta$  172.66 (f),

145.87 (m), 138.53 (d), 128.80 (b,b'), 127.92 (c,c'), 127.57 (a), 126.88 (o), 124.09 (n), 122.78 (p), 83.84 (k,k'), 43.66 (e), 36.67 (g), 33.28 (h), 25.18 (i), 24.74 and 24.73 (l,l').



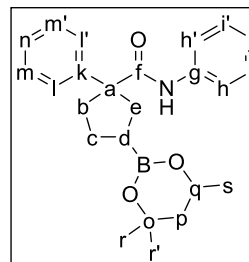
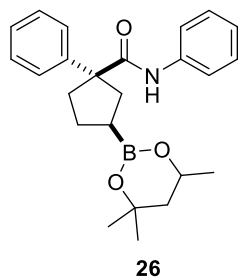
**(R)-5-(3-furanyl)-5-(4,4,5,5-tetramethyl-1,3,2-dioxaborolan-2-yl)pentanecarboxylic acid benzyl amide (19p)**. Following **GP10** with 1 mol% [Rh/2 (*R*)-**B2**], 3 equiv pinBH and **15p** (135 mg, 0.528 mmol) affords, after flash chromatography on silica gel (95:5–90:10 DCM:ethyl acetate), the title compound (146 mg, 72%) as a yellow oil: TLC analysis  $R_f$  0.4 (40:60 hexanes:ethyl acetate); Enantiomeric excess was checked by converting to the corresponding Mosher's ester **22p** (general procedure *vide infra*); crude <sup>19</sup>F NMR (375 MHz, CDCl<sub>3</sub>) shows  $\delta$  –71.59 (major 92%) and –72.00 (minor 8%); <sup>1</sup>H NMR (400 MHz, CDCl<sub>3</sub>)  $\delta$  7.20–7.40 (7H, m, a,b,b',c,c',o,p), 6.28 (1H, s, n), 5.90 (1H, br s, NH), 4.43 (2H, d,  $J$  = 5.6 Hz, e), 2.15–2.30 (3H, m, g,j), 1.60–1.80 (2H, m, h,i), 1.23 (12H, d,  $J$  = 0.0 Hz, l,l'); <sup>13</sup>C NMR (100 MHz, CDCl<sub>3</sub>)  $\delta$  172.90 (f), 142.62 (o), 138.89 (p), 138.55 (d), 128.77 (b,b'), 127.89 (c,c'), 127.54 (a), 125.20 (m), 111.13 (n), 83.59 (k,k'), 43.62 (e), 36.69 (g), 31.32 (h), 25.26 (i), 24.79 and 24.74 (l,l').





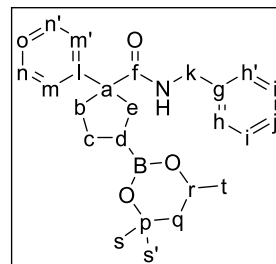
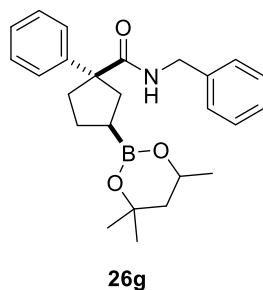
**(R)-5-(2-thiophenyl)-5-(4,4,5,5-tetramethyl-1,3,2-dioxaborolan-2-**

**yl)pentanecarboxylic acid benzyl amide (19o).** Following **GP10** with 1 mol% [Rh/2 (R)-**B2**], 3 equiv pinBH and **15o** (143 mg, 0.528 mmol) affords, after flash chromatography on silica gel (95:5–90:10 DCM:ethyl acetate), the title compound (154 mg, 73%) as a yellow oil: TLC analysis  $R_f$  0.4 (40:60 hexanes:ethyl acetate); Enantiomeric excess was checked by converting to the corresponding Mosher's ester **22o** (general procedure *vide infra*); crude  $^{19}\text{F}$  NMR (375 MHz,  $\text{CDCl}_3$ ) shows  $\delta$   $-71.34$  (major 94%) and  $-71.60$  (minor 6%);  $^1\text{H}$  NMR (400 MHz,  $\text{CDCl}_3$ )  $\delta$  7.30–7.35 (2H, m, b,b'), 7.25–7.30 (3H, m, a,c,c'), 7.22 (1H, dd,  $J = 4.8$  and 3.0 Hz, o), 6.90–7.00 (2H, m, n,p), 5.91 (1H, br s, NH), 4.43 (2H, d,  $J = 5.7$  Hz, e), 2.48 (1H, t,  $J = 7.1$  Hz, j), 2.22 (2H, t,  $J = 7.4$  Hz, g), 1.80–1.90 (1H, m, h), 1.60–1.80 (3H, m, h,i), 1.21 (12H, d,  $J = 4.2$  Hz, l,l');  $^{13}\text{C}$  NMR (100 MHz,  $\text{CDCl}_3$ )  $\delta$  172.82 (f), 142.67 (m), 138.57 (d), 128.78 (b,b'), 128.30 (n), 127.92 (c,c'), 127.55 (a), 125.07 (o), 119.70 (p), 83.58 (k,k'), 43.63 (e), 36.72 (g), 31.88 (h), 25.40 (i), 24.77 and 24.72 (l,l').



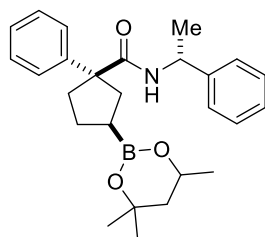
**(1*R*,3*S*)-1-phenyl-3-(4,4,6-trimethyl-1,3,2-dioxaborinan-2-yl)-1-**

**cyclopentanecarboxylic acid phenyl amide (26c).** Following **GP10** with 1 mol% [**Rh/2 (R)-B2**], 2 equiv tmdBH and **23c** (139.2 mg, 0.528 mmol) affords, after flash chromatography on silica gel (90:10 hexanes:ethyl acetate), the title compound (151 mg, 73%) as a light yellow solid: mp 112.5–114.0 °C; TLC analysis  $R_f$  0.75 (70:30 hexanes:ethyl acetate);  $^1\text{H}$  NMR (400 MHz,  $\text{CDCl}_3$ )  $\delta$  7.46 (1H, d,  $J = 7.4$  Hz, l,l'), 7.45–7.35 (4H, m, h,h',m,m'), 7.35–7.20 (2H, m, i,i',j), 7.05 (1H, t,  $J = 7.4$  Hz, n), 6.92 (1H, d,  $J = 18.6$  Hz, NH), 4.25–4.10 (2H, m, q), 2.60–2.45 (2H, m, b,e), 2.40–2.25 (2H, m, b), 2.20–2.10 (2H, m, e), 1.95–1.80 (3H, m, c), 1.76 (1H, dd,  $J = 13.9$  and 3.0 Hz, p), 1.46 (1H, dd,  $J = 12.5$  and 12.5 Hz, p), 1.40–1.30 (1H, m, d), 1.27 (6H, d,  $J = 3.9$  Hz, r,r'), 1.24 (3H, dd,  $J = 6.2$  and 4.1 Hz, s);  $^{13}\text{C}$  NMR (100 MHz,  $\text{CDCl}_3$ )  $\delta$  174.95 and 174.91 (f), 143.63 and 143.57 (k), 138.33 and 138.30 (g), 128.84 (i,i'), 128.79 (m,m'), 127.04 (j), 127.03 (l,l'), 123.87 and 123.85 (n), 119.60 and 119.55 (h,h'), 70.52 and 70.50 (o), 64.69 and 64.62 (q), 61.03 and 61.02 (a), 45.93 and 45.89 (p), 39.40 and 39.31 (b), 37.67 (e), 31.27 and 31.24 (r,r'), 28.10 and 28.07 (d), 26.60 and 26.53 (c), 23.20 and 23.18 (s); IR (neat) 3408 (N-H stretch), 2971, 1677 (C=O stretch), 1596 (N-H bend), 1519, 1493, 1436, 1303 (C-O stretch), 1208 (C-N stretch), 1163, 700, 690  $\text{cm}^{-1}$ .

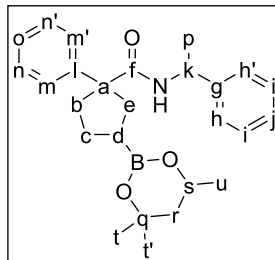


**(1*R*,3*S*)-1-phenyl-3-(4,4,6-trimethyl-1,3,2-dioxaborinan-2-yl)-1-**

**cyclopentanecarboxylic acid benzyl amide (26g).** Following **GP10** with 1 mol% [Rh/2 (*R*)-**B2**], 2 equiv tmdBH and **23g** (146.5 mg, 0.528 mmol) affords, after flash chromatography on silica gel (90:10 hexanes:ethyl acetate), the title compound (154.2 mg, 72%) as a yellow oil: TLC analysis  $R_f$  0.6 (70:30 hexanes:ethyl acetate);  $^1\text{H}$  NMR (400 MHz,  $\text{CDCl}_3$ )  $\delta$  7.45–7.35 (2H, m, m,m'), 7.35–7.30 (2H, m, i,i'), 7.30–7.20 (2H, m, j,n,n',o), 7.15–7.05 (2H, m, h,h'), 5.70 (1H, d,  $J = 31.3$  Hz, NH), 4.50–4.30 (2H, m, k), 4.20–3.95 (1H, m, r), 2.55–2.40 (2H, m, b,e), 2.30–2.10 (2H, m, b,e), 1.85–1.70 (3H, m, c,q), 1.44 (1H, dd,  $J = 13.8$  and 11.7 Hz, q), 1.26 (6H, s, s,s'), 1.23 (3H, dd,  $J = 6.2$  and 6.2 Hz, t), 1.35–1.15 (1H, m, d);  $^{13}\text{C}$  NMR (100 MHz,  $\text{CDCl}_3$ )  $\delta$  176.77 and 176.71 (f), 144.13 and 144.04 (l), 138.83 and 138.82 (g), 128.54 (i,i'), 128.51 (n,n'), 127.31 and 127.25 (h,h'), 127.13 and 127.12 (m,m'), 127.07 and 127.06 (j), 126.70 and 126.68 (o), 70.50 and 70.47 (p), 64.64 and 64.59 (r), 60.18 and 60.15 (a), 45.92 and 45.87 (q), 43.57 and 43.52 (k), 39.17 and 39.03 (b), 37.65 and 37.61 (e), 31.26 and 31.24 (s,s'), 28.09 and 28.05 (d), 26.54 and 26.52 (c), 23.21 and 23.20 (t); IR (neat) 3339 (N-H stretch), 2970, 1645 (C=O stretch), 1600 (N-H bend), 1512 (C=C stretch, aromatic), 1300 (C-O stretch), 1207, 724, 696  $\text{cm}^{-1}$ .

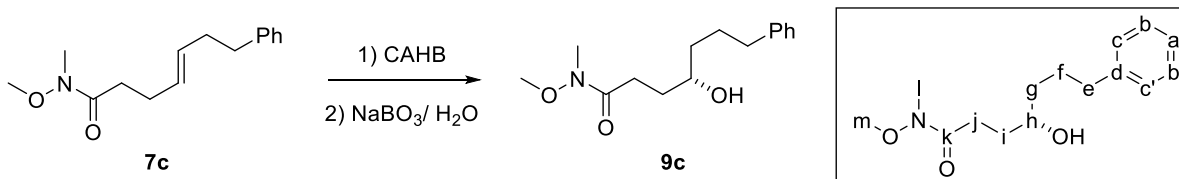


26k



**(1*R*,3*S*)-1-phenyl-*N*-((*R*)-1-phenylethyl)-3-(4,4,6-trimethyl-1,3,2-dioxaborinan-2-yl)cyclopentane-1-carboxamide (26k).** Following **GP10** with 2 mol% [Rh/2 (*R*)-**B2**], 2 equiv tmdBH and **26k** (154 mg, 0.528 mmol) affords, after flash chromatography on silica gel (90:10 hexanes:ethyl acetate), the title compound (173.1 mg, 78%) as a yellow oil: TLC analysis  $R_f$  0.7 (70:30 hexanes:ethyl acetate);  $^1\text{H}$  NMR (300 MHz,  $\text{CDCl}_3$ )  $\delta$  7.40–7.20 (8H, m, f,g,h,h',i,i',j,m,m',n,n'), 7.15–7.05 (2H, m, j,o), 5.47 (1H, dd,  $J = 11.2$  and  $1.9$  Hz, NH), 5.15–5.00 (1H, m, k), 4.20–4.00 (1H, m, s), 2.50–2.30 (2H, m, b,e), 2.30–2.05 (2H, m, b,e), 1.85–1.70 (3H, m, c,r), 1.50–1.40 (1H, m, r), 1.34 (3H, dd,  $J = 6.8$  and  $4.0$  Hz, p), 1.25 (6H, s, t,t'), 1.23 (3H, d,  $J = 6.2$  Hz, u), 1.30–1.20 (1H, m, d);  $^{13}\text{C}$  NMR (75 MHz,  $\text{CDCl}_3$ )  $\delta$  175.96 and 175.89 (f), 144.22 and 144.05 (l), 143.58 and 143.57 (g), 128.51 and 128.48 (i,i'), 128.42 (n,n'), 127.04 and 127.02 (h,h'), 126.95 (m,m'), 126.68 and 126.64 (j), 125.90 and 125.86 (o), 70.40 (q), 64.58 and 64.54 (s), 60.10 and 60.06 (a), 48.55 (k), 45.92 and 45.88 (r), 39.33 and 39.04 (b), 37.60 and 37.49 (e), 31.26 and 31.23 (t,t'), 28.07 and 28.03 (d), 26.55 (c), 23.23 and 23.19 (u), 21.75 and 21.69 (p); IR (neat) 3345 (N-H stretch), 2970, 2932, 1649 (C=O stretch), 1600 (N-H bend), 1493 (C=C stretch, aromatic), 1446, 1300 (C-O stretch), 1207, 765, 697  $\text{cm}^{-1}$ .

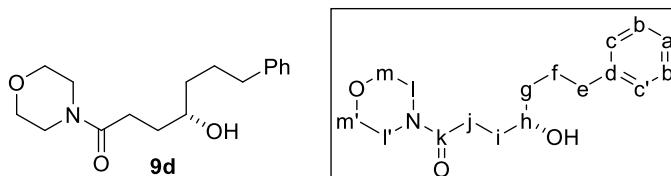
**General procedure for CAHB-oxidation sequence with NaBO<sub>3</sub>/ H<sub>2</sub>O (GP11).**



**(S)-4-hydroxy-7-phenylheptanecarboxylic acid Weinreb amide (9c).**

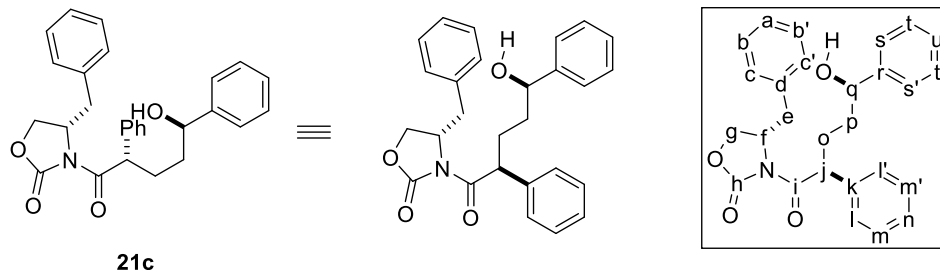
Following **GP10** with 2 mol% [Rh/2 (*R*)-**B1**] and **7c** (130 mg, 0.528 mmol) without purification, the obtained residue was taken up in THF (1.5 mL) and water (1.5 mL). NaBO<sub>3</sub>-tetrahydrate (231 mg, 1.5 mmol) was added to the resultant mixture. After a 5 h vigorous stir, the reaction was diluted with water (3 mL) and EtOAc (5 mL). The organic layer was separated and the aqueous layer was extracted with EtOAc (2 x 3 mL). The combined organic layers were dried (anhyd. Na<sub>2</sub>SO<sub>4</sub>) and concentrated under reduced pressure affords, after flash chromatography on silica gel (80:20-20:80 hexanes:ethyl acetate), the title compound (95 mg, 68%) as a colorless oil; TLC analysis R<sub>f</sub> 0.5 (0:100 hexanes:ethyl acetate); [α]<sub>D</sub><sup>20</sup> = -12.5° (*c* 2.0, CHCl<sub>3</sub>); er of **9c** was determined by using harsh oxidation (NaOH/H<sub>2</sub>O<sub>2</sub>) instead of NaBO<sub>3</sub>-tetrahydrate to form lactone **13** followed by Al(Me)<sub>3</sub>-assisted transamidation with benzyl amine to generate **9b** (**GP1**): Chiral HPLC analysis (Chiralpak-IC, 60:40 hexanes:isopropanol, flow rate = 1.3 mL/min) showed peaks at 26 minutes (4.0% (*R*)) and 30 minutes (96.0% (*S*)); <sup>1</sup>H NMR (400 MHz, CDCl<sub>3</sub>) δ 7.25–7.30 (2H, m, b,b'), 7.15–7.25 (3H, m, a,c,c'), 3.70 (3H, s, m), 3.60–3.70 (1H, m, h, *overlapping with* m), 3.20 (3H, s, l), 2.74 (1H, br s, OH), 2.66 (2H, t, *J* = 7.6 Hz, e), 2.50–2.70 (2H, m, j, *overlapping with* e), 1.80–1.90 (2H, m, f,i), 1.65–1.75 (2H, m, f,i), 1.45–1.65 (2H, m, g); <sup>13</sup>C NMR (100 MHz, CDCl<sub>3</sub>) δ 175.19 (k), 142.55 (d),

128.54 (b,b'), 128.38 (c,c'), 125.78 (a), 71.45 (h), 61.35 (m), 37.36 (g), 35.99 (e), 32.37 (l), 31.74 (i), 28.63 (j), 27.62 (f); IR (neat) 3430 (O-H stretch), 2933, 2858, 1639 (C=O stretch), 1452, 1416, 1386, 1177, 994, 748, 699  $\text{cm}^{-1}$ ; HRMS (ESI) calcd. for  $\text{C}_{15}\text{H}_{23}\text{NNaO}_3$  (M+Na): 288.1576, found 288.1583  $m/z$ .



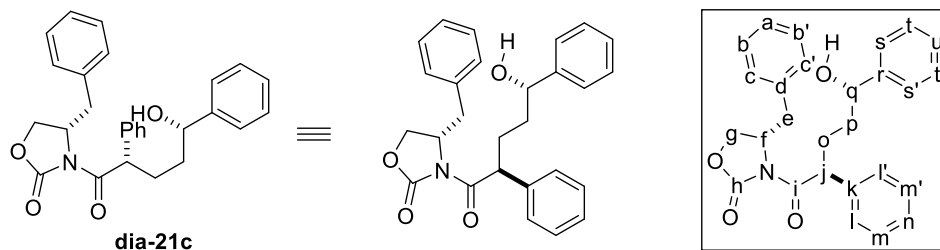
**(S)-4-hydroxy-7-phenyl-heptanecarboxylic acid morpholino amide (9d).**

Following **GP11** with **9d** (144 mg, 0.528 mmol) affords, after flash chromatography on silica gel (80:20-70:30 hexanes:ethyl acetate, then switch to 50:50-20:80 hexanes:acetone), the title compound (125 mg, 81%) as a colorless oil; TLC analysis  $R_f$  0.7 (20:80 hexanes:acetone);  $[\alpha]_D^{20} = -5.1^\circ$  (c 2.0,  $\text{CHCl}_3$ ); er of **7c** was determined by boric acid-catalyzed transamidation with benzyl amine to form the corresponding benzyl amide **9b**.<sup>11</sup> Chiral HPLC analysis (Chiralpak-IC, 60:40 hexanes:isopropanol, flow rate = 1.3 mL/min) showed peaks at 28 minutes (5.5 0% (*R*)) and 31 minutes (94.5% (*S*));  $^1\text{H}$  NMR (400 MHz,  $\text{CDCl}_3$ )  $\delta$  7.25–7.30 (2H, m, b,b'), 7.15–7.20 (3H, m, a,c,c'), 3.55–3.70 (7H, m, h,l,l',m,m'), 3.40–3.50 (2H, m, l,l'), 2.64 (2H, t,  $J = 7.6$  Hz, e), 2.46 (2H, t,  $J = 7.0$  Hz, j), 1.75–1.90 (2H, m, f,i), 1.60–1.75 (2H, m, f,i), 1.45–1.60 (2H, m, g);  $^{13}\text{C}$  NMR (100 MHz,  $\text{CDCl}_3$ )  $\delta$  172.44 (k), 142.50 (d), 128.53 (b,b'), 128.39 (c,c'), 125.83 (a), 71.28 (h), 66.95 and 66.68 (m,m'), 46.11 and 42.14 (l,l'), 37.44 (g), 35.97 (e), 32.11 (i), 29.75 (j), 27.62 (f); IR (neat) 3418 (O-H stretch), 2919, 2855, 1622 (C=O stretch), 1432, 1271, 1232, 1114, 1068, 1031, 748, 699  $\text{cm}^{-1}$ ; HRMS (ESI) calcd. for  $\text{C}_{17}\text{H}_{25}\text{NNaO}_3$  (M+Na): 314.1732, found 314.1743  $m/z$ .



**(*S*)-4-benzyl-3-((*2S,5R*)-5-hydroxy-2,5-diphenylpentanoyl)oxazolidin-2-one (21c).**

Following **GP11** with 1 mol% [Rh/2 (*R*)-**B1**] and **20c** (109 mg, 0.264 mmol) affords, after flash chromatography on silica gel (90:10 hexanes:ethyl acetate), the title compound (58 mg, 51%) as a white solid; TLC analysis  $R_f$  0.6 (70:30 hexanes:ethyl acetate);  $^1\text{H}$  NMR (400 MHz,  $\text{CDCl}_3$ )  $\delta$  7.20–7.40 (15H, m, aryl), 5.09 (1H, t,  $J = 7.3$  Hz, f), 4.74 (0.16H, t,  $J = 6.5$  Hz, q), 4.70 (0.83H, t,  $J = 6.1$  Hz, q), 4.55–4.65 (1H, m, j), 4.11 (1H, dd,  $J = 9.0$  and 2.2 Hz, g), 4.04 (1H, dd,  $J = 7.9$  and 0 Hz, g), 3.38 (1H, dd,  $J = 13.3$  and 3.2 Hz, e), 2.79 (1H, dd,  $J = 13.2$  and 9.8 Hz, e), 2.30–2.40 (0.8H, m, o), 2.15–2.25 (0.2H, m, o), 1.95–2.05 (0.2H, m, o), 1.65–1.90 (2.8H, m, o,p);  $^{13}\text{C}$  NMR (100 MHz,  $\text{CDCl}_3$ )  $\delta$  174.06 (i), 153.09 (h), 144.46, 138.52, 135.46, 129.55, 129.09, 128.80, 128.76, 128.65, 127.77, 127.56, 127.47, 126.03, 74.49 (q), 65.96 (g), 55.96 (f), 48.56 (j), 38.17 (e), 36.80 (p), 30.51 (o).

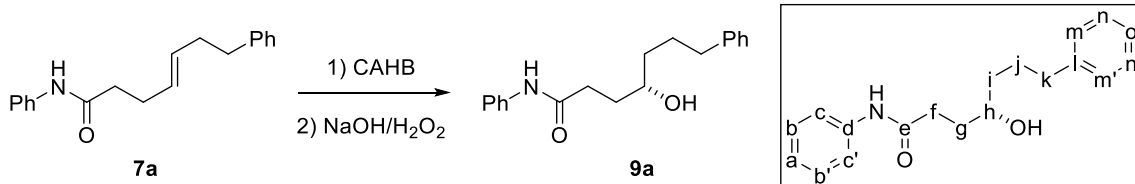


**(*S*)-4-benzyl-3-((*2S,5S*)-5-hydroxy-2,5-diphenylpentanoyl)oxazolidin-2-one (dia-21c).**

Following **GP11** with 1 mol% [Rh/2 (*S*)-**B1**] and **20c** (109 mg, 0.264 mmol) affords,

after flash chromatography on silica gel (90:10 hexanes:ethyl acetate), the title compound (89 mg, 79%) as a white solid; TLC analysis  $R_f$  0.6 (70:30 hexanes:ethyl acetate);  $^1\text{H}$  NMR (400 MHz,  $\text{CDCl}_3$ )  $\delta$  7.20–7.40 (15H, m, aryl), 5.09 (1H, t,  $J = 7.6$  Hz, f), 4.74 (0.92H, t,  $J = 6.5$  Hz, q), 4.70 (0.08H, t,  $J = 6.3$  Hz, q), 4.55–4.65 (1H, m, j), 4.12 (1H, dd,  $J = 9.1$  and 2.4 Hz, g), 4.05 (1H, dd,  $J = 7.8$  and 0 Hz, g), 3.37 (1H, dd,  $J = 13.3$  and 3.2 Hz, e), 2.79 (1H, dd,  $J = 13.3$  and 9.8 Hz, e), 2.30–2.40 (0.08H, m, o), 2.15–2.25 (0.92H, m, o), 2.00–2.05 (0.92H, m, o), 1.65–1.90 (2.08H, m, o,p);  $^{13}\text{C}$  NMR (100 MHz,  $\text{CDCl}_3$ )  $\delta$  174.07 (i), 153.14 (h), 144.51, 138.40, 135.43, 129.55, 129.09, 128.84, 128.78, 128.62, 127.70, 127.59, 127.48, 125.96, 73.96 (q), 66.03 (g), 55.95 (f), 48.43 (j), 38.16 (e), 36.80773 (p), 30.33 (o).

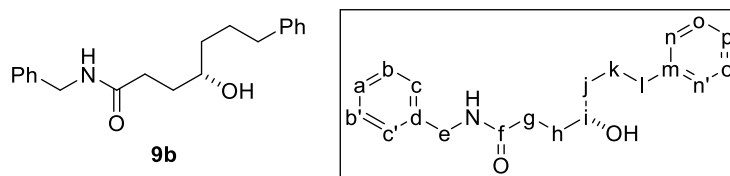
**General procedure for CAHB-oxidation sequence with  $\text{H}_2\text{O}_2$  (GP12).**



**(S)-4-hydroxy-7-phenyl-heptanecarboxylic acid phenyl amide (9a).** Following **GP10** with **7a** (148 mg, 0.528 mmol) without purification, the resultant mixture was diluted with THF (10 mL) followed by addition of methanol (8 mL), sodium hydroxide (6 mL of a 3.0 M soln.), and the slow addition of  $\text{H}_2\text{O}_2$  (1.0 mL of a 30% solution). The resulting mixture stirred (2 h) and then extracted with dichloromethane (3 x 15 mL). The combined organic extracts were dried (anhyd.  $\text{Na}_2\text{SO}_4$ ) and concentrated under reduced pressure. Flash chromatography on silica gel (90:10-40:60 hexanes:ethyl acetate) affords the title compound (124 mg, 79%) as a white solid: m.p. 119.5–120.5 °C; TLC analysis  $R_f$



0.3 (40:60 hexanes:ethyl acetate);  $[\alpha]_D^{20} = +7.5^\circ$  ( $c$  1.0, MeOH); Chiral HPLC analysis (Chiralpak-IB, 70:30 hexanes:isopropanol, flow rate = 1.4 mL/min) showed peaks at 41 minutes (3.0% (*R*)) and 44 minutes (97.0% (*S*));  $^1\text{H NMR}$  (400 MHz,  $\text{CDCl}_3$ )  $\delta$  7.70 (1H, br s, NH), 7.51 (2H, d,  $J = 7.7$  Hz, c,c'), 7.25–7.35 (4H, m, b,b',m,m'), 7.15–7.25 (3H, m, b,b',n,n',o), 7.12 (1H, t,  $J = 7.3$  Hz, a), 3.60–3.80 (1H, m, h), 2.65 (2H, t,  $J = 7.8$  Hz, k), 2.45–2.60 (3H, m, f, OH), 1.90–2.00 (1H, m, g), 1.70–1.85 (3H, m, g,j), 1.50–1.60 (2H, m, i);  $^{13}\text{C NMR}$  (100 MHz,  $\text{CDCl}_3$ )  $\delta$  172.03 (e), 142.34 (l), 137.98 (d), 129.11 (b,b'), 128.53 (n,n'), 128.44 (m,m'), 125.90 (o), 124.43 (a), 120.02 (c,c'), 71.46 (h), 37.41 (i), 35.91 (k), 34.32 (f), 32.48 (g), 27.55 (j); IR (neat) 3670 (N-H stretch, O-H stretch), 3279, 3247, 2950, 2911, 1659 (C=O stretch), 1600 (N-H bend), 1543, 1496, 1412 (C-N stretch), 754, 689  $\text{cm}^{-1}$ ; HRMS (ESI) calcd. for  $\text{C}_{19}\text{H}_{23}\text{NNaO}_2$  ( $\text{M}+\text{Na}$ ): 320.1626, found 320.1631  $m/z$ .

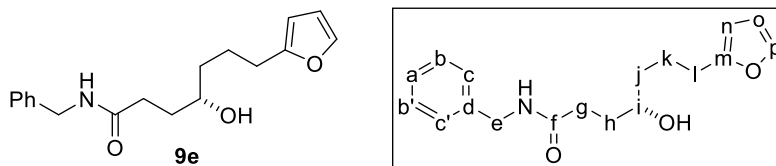


**(*S*)-4-hydroxy-7-phenyl-4-heptanecarboxylic acid benzyl amide (9b).**

Following **GP12** with (*E*)-**7b** (155 mg, 0.528 mmol) affords, after flash chromatography on silica gel (80:20–20:80 hexanes:ethyl acetate), the title compound (131 mg, 80%) as a white solid: m.p. 88.5–89.5 °C; TLC analysis  $R_f$  0.4 (0:100 hexanes:ethyl acetate);  $[\alpha]_D^{20} = -7.9^\circ$  ( $c$  1.0,  $\text{CHCl}_3$ ); Chiral HPLC analysis (Chiralpak-IC, 60:40 hexanes:isopropanol, flow rate = 1.3 mL/min) showed peaks at 28 minutes (3.5% (*R*)) and 32 minutes (96.5% (*S*));  $^1\text{H NMR}$  (400 MHz,  $\text{CDCl}_3$ )  $\delta$  7.10–7.40 (10H, a,b,b',c,c',n,n',o,o',p), 6.28 (1H, br s, NH), 4.40 (2H, d,  $J = 5.7$  Hz, e), 3.55–3.70 (1H, m, i), 3.19 (1H, d,  $J = 4.2$  Hz, OH), 2.64

(2H, t,  $J = 7.6$  Hz, l), 2.36 (2H, td,  $J = 7.3$  and 2.8 Hz, g), 1.70–1.90 (2H, m, h,k), 1.60–1.70 (2H, m, h,k), 1.40–1.60 (2H, m, j);  $^{13}\text{C}$  NMR (100 MHz,  $\text{CDCl}_3$ )  $\delta$  173.76 (f), 142.48 (m), 138.30 (d), 128.82 (b,b'), 128.54 (o,o'), 128.42 (n,n'), 127.89 (c,c'), 127.64 (a), 125.85 (p), 71.29 (i), 43.79 (e), 37.31 (j), 35.95 (l), 33.23 (g), 32.72 (h), 27.61 (k); IR (neat) 3306 (N-H stretch, O-H stretch), 3025, 2937, 2919, 2867, 1637 (C=O stretch), 1546 (N-H bend), 1495, 1442, 1234, 724, 694  $\text{cm}^{-1}$ ; HRMS (ESI) calcd. for  $\text{C}_{20}\text{H}_{25}\text{NNaO}_2$  (M+Na): 334.1783, found 334.1781  $m/z$ .

Following **GP12** with (*Z*)-**7b** (155 mg, 0.528 mmol) affords, after flash chromatography on silica gel (80:20-20:80 hexanes:ethyl acetate), the title compound (128 mg, 78%) as a white solid: m.p. 88.0–99.5 °C; TLC analysis  $R_f$  0.4 (0:100 hexanes:ethyl acetate);  $[\alpha]_D^{20} = -7.8^\circ$  ( $c$  1.0,  $\text{CHCl}_3$ ); Chiral HPLC analysis (Chiralpak-IC, 60:40 hexanes:isopropanol, flow rate = 1.3 mL/min) showed peaks at 27 minutes (6.0% (*R*)) and 31 minutes (94.0% (*S*)); spectroscopic data matched with (*S*)-**9b** obtained from (*E*)-**7b** as shown above.

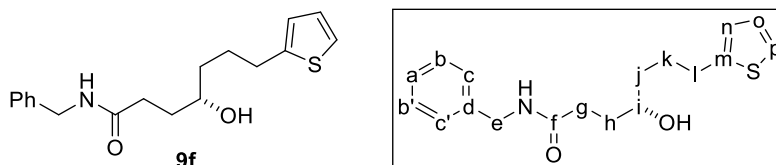


**(*S*)-7-(furan-2-yl)-4-hydroxyheptanecarboxylic acid benzyl amide (7e).**<sup>4</sup>

Following **GP12** with 1.0 mol%  $[\text{Rh}(\text{nbd})_2\text{BF}_4]$  2(*R*)-**B1** and **7e** (150 mg, 0.528 mmol) affords, after flash chromatography on silica gel (80:20-20:80 hexanes:ethyl acetate), the title compound (113 mg, 71%) as a light yellow solid: m.p. 72.5–74.0 °C; TLC analysis

<sup>4</sup> A pseudo-racemate was prepared for HPLC analysis by combining crude reactions mixtures obtained by CAHB using (*R*)- and (*S*)-**B1** then oxidizing and isolating the resulting alcohol

$R_f$  0.35 (0:100 hexanes:ethyl acetate);  $[\alpha]_D^{20} = -6.1^\circ$  ( $c$  2.0,  $\text{CHCl}_3$ ); Chiral HPLC analysis (Chiralpak-IB, 60:40 hexanes:isopropanol, flowrate = 1.4 mL/min) showed peaks at 18 minutes (94.0% ( $S$ )) and 47 minutes (6.0% ( $R$ ));  $^1\text{H}$  NMR (400 MHz,  $\text{CDCl}_3$ )  $\delta$  7.20–7.40 (6H, a,b,b',c,c',p), 6.29 (1H, dd,  $J = 2.9$  and 2.0 Hz, o), 6.26 (1H, br s, NH, overlapping with o), 6.00 (1H, d,  $J = 3.0$  Hz, n), 4.42 (2H, d,  $J = 5.7$  Hz, e), 3.55–3.70 (1H, m, i), 2.85–3.45 (1H, br s, OH), 2.65 (2H, t,  $J = 7.4$  Hz, l), 2.38 (2H, td,  $J = 7.2$  and 3.4 Hz, g), 1.75–1.90 (2H, m, h,k), 1.60–1.75 (2H, m, h,k), 1.40–1.60 (2H, m, j);  $^{13}\text{C}$  NMR (100 MHz,  $\text{CDCl}_3$ )  $\delta$  173.72 (f), 156.17 (m), 140.86 (p), 138.28 (d), 128.83 (b,b'), 127.90 (c,c'), 127.65 (a), 110.20 (o), 104.97 (n), 71.16 (i), 43.80 (e), 43.79 (e), 37.16 (j), 33.25 (g), 32.70 (h), 27.98 (l), 24.33 (k); IR (neat) 3288 (N-H stretch, O-H stretch), 2919, 1632 (C=O stretch), 1534, 1453, 1090, 1006, 723, 695  $\text{cm}^{-1}$ ; HRMS (ESI) calcd. for  $\text{C}_{18}\text{H}_{23}\text{NNaO}_3$  ( $M+\text{Na}$ ): 324.1576, found 324.1573  $m/z$ .

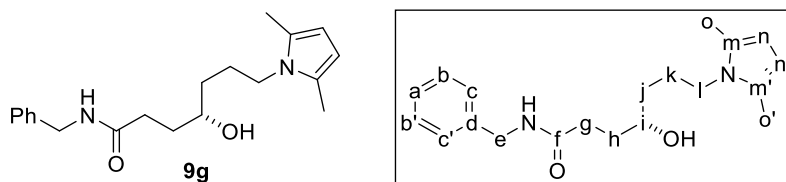


**( $S$ )-4-hydroxy-7-(thiophen-2-yl)-heptanecarboxylic acid benzyl amide (**9f**).<sup>5</sup>**

Following **GP12** with 1.0 mol%  $[\text{Rh}(\text{nbd})_2\text{BF}_4/ 2(R)\text{-B1}]$  and **7f** (158 mg, 0.528 mmol) affords, after flash chromatography on silica gel (80:20-20:80 hexanes:ethyl acetate), the title compound (121 mg, 72%) as a white solid: m.p. 73.5–74.5  $^\circ\text{C}$ ; TLC analysis  $R_f$  0.35 (0:100 hexanes:ethyl acetate);  $[\alpha]_D^{20} = -4.7^\circ$  ( $c$  1.5,  $\text{CHCl}_3$ ); Chiral HPLC analysis (Chiralpak-IB, 60:40 hexanes:isopropanol, flowrate = 1.4 mL/min) showed peaks at 28 minutes (94.0% ( $S$ )) and 109 minutes (6.0% ( $R$ ));  $^1\text{H}$  NMR (400 MHz,  $\text{CDCl}_3$ )  $\delta$  7.35–

<sup>5</sup> A pseudo-racemate was prepared for HPLC analysis by combining crude reactions mixtures obtained by CAHB using ( $R$ )- and ( $S$ )-**B1** then oxidizing and isolating the resulting alcohol

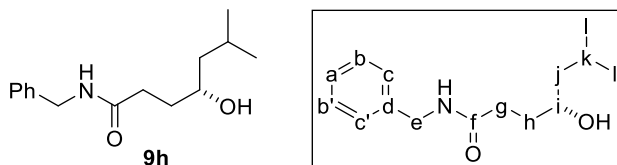
7.40 (2H, b,b'), 7.25–7.35 (3H, a,c,c'), 7.12 (1H, dd,  $J = 5.1$  and  $1.0$  Hz, p), 6.93 (1H, dd,  $J = 5.0$  and  $3.4$  Hz, o), 6.80 (1H, dd,  $J = 3.3$  and  $0.8$  Hz, n), 6.16 (1H, br s, NH), 4.43 (2H, d,  $J = 5.7$  Hz, e), 3.60–3.70 (1H, m, i), 2.86 (2H, t,  $J = 7.5$  Hz, l), 2.39 (2H, td,  $J = 7.2$  and  $3.8$  Hz, g), 1.80–1.90 (2H, m, h,k), 1.65–1.80 (2H, m, h,k), 1.45–1.60 (2H, m, j);  $^{13}\text{C}$  NMR (100 MHz,  $\text{CDCl}_3$ )  $\delta$  173.67 (f), 145.36 (m), 138.26 (d), 128.85 (b,b'), 127.92 (c,c'), 127.68 (a), 126.82 (o), 124.27 (n), 123.02 (p), 71.20 (i), 43.84 (e), 37.11 (j), 33.27 (g), 32.68 (h), 29.94 (l), 27.97 (k); IR (neat) 3291 (N-H stretch, O-H stretch), 2917, 2849, 1630 (C=O stretch), 1534, 1453, 691  $\text{cm}^{-1}$ ; HRMS (ESI) calcd. for  $\text{C}_{18}\text{H}_{23}\text{NNaO}_2\text{S}$  (M+Na): 340.1347, found 340.1354  $m/z$ .



**(S)-7-(2,5-dimethyl-1H-pyrrol-1-yl)-4-hydroxyheptanecarboxylic acid benzyl amide (9g).**<sup>6</sup> Following **GP12** with 1.0 mol%  $[\text{Rh}(\text{nbd})_2\text{BF}_4/ 2(R)\text{-B1}]$  and **7g** (164 mg, 0.528 mmol) affords, after flash chromatography on silica gel (80:20-20:80 hexanes:ethyl acetate), the title compound (102 mg, 59%) as a yellow oil; TLC analysis  $R_f$  0.4 (0:100 hexanes:ethyl acetate);  $[\alpha]_{\text{D}}^{20} = -7.1^\circ$  ( $c$  1.8,  $\text{CHCl}_3$ ); Chiral HPLC analysis (Chiralpak-IC, 60:40 hexanes:isopropanol, flowrate = 1.4 mL/min) showed peaks at 42 minutes (8.0% (*R*)) and 54 minutes (92.0% (*S*));  $^1\text{H}$  NMR (400 MHz,  $\text{CDCl}_3$ )  $\delta$  7.25–7.40 (5H, a,b,b',c,c'), 6.10 (1H, br s, NH), 5.78 (2H, s, n,n'), 4.43 (2H, d,  $J = 5.7$  Hz, e), 3.77 (2H, t,  $J = 7.6$  Hz, l), 3.55–3.70 (1H, m, i), 2.30–2.45 (2H, m, g), 2.24 (6H, s, o,o'), 1.75–1.90

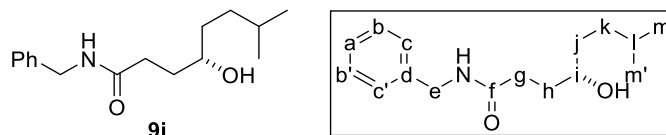
<sup>6</sup> A pseudo-racemate was prepared for HPLC analysis by combining crude reactions mixtures obtained by CAHB using (*R*)- and (*S*)-**B1** then oxidizing and isolating the resulting alcohol

(2H, m, h,k), 1.65–1.75 (2H, m, h,k), 1.45–1.55 (2H, m, j);  $^{13}\text{C}$  NMR (100 MHz,  $\text{CDCl}_3$ )  $\delta$  173.61 (f), 138.17 (d), 128.87 (b,b'), 127.92 (c,c'), 127.72 (a), 127.48 (m,m'), 105.19 (n,n'), 71.14 (i), 43.87 (e), 43.60 (l), 34.82 (j), 33.22 (g), 32.66 (h), 27.36 (k), 12.68 (o,o'); IR (neat) 3285 (N-H stretch, O-H stretch), 2923, 1643 (C=O stretch), 1541, 1453, 1407, 1298, 742, 697  $\text{cm}^{-1}$ ; HRMS (ESI) calcd. for  $\text{C}_{20}\text{H}_{28}\text{N}_2\text{NaO}_2$  (M+Na): 351.2048, found 351.2059  $m/z$ .

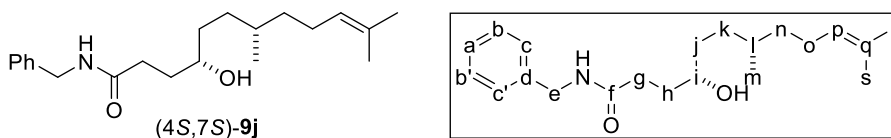


**(S)-4-hydroxy-6-methylheptanecarboxylic acid benzyl amide (9h).** Following **GP12** with **7h** (122 mg, 0.528 mmol) affords, after flash chromatography on silica gel (80:20-20:80 hexanes:ethyl acetate), the title compound (88 mg, 67%) as a white solid: m.p. 50.5–51.5  $^{\circ}\text{C}$ ; TLC analysis  $R_f$  0.4 (0:100 hexanes:ethyl acetate);  $[\alpha]_{\text{D}}^{20} = -18.4^{\circ}$  ( $c$  2.0,  $\text{CHCl}_3$ ); Chiral HPLC analysis (Chiralpak-IC, 90:10 hexanes:isopropanol, flowrate = 1.4 mL/min) showed peaks at 96 minutes (3.0% (*R*)) and 103 minutes (97.0% (*S*));  $^1\text{H}$  NMR (400 MHz,  $\text{CDCl}_3$ )  $\delta$  7.30–7.40 (2H, b,b'), 7.25–7.30 (3H, a,c,c'), 6.21 (1H, br s, NH), 4.43 (2H, d,  $J = 5.7$  Hz, e), 3.65–3.75 (1H, m, i), 2.60–3.00 (1H, br s, OH), 2.40 (2H, td,  $J = 7.6$  and 2.6 Hz, g), 1.80–1.90 (1H, m, h), 1.70–1.80 (1H, m, k), 1.60–1.70 (1H, m, h), 1.40–1.50 (1H, m, j), 1.20–1.25 (1H, m, j), 0.92 (6H, dd,  $J = 6.2$  and 5.4 Hz, l,l');  $^{13}\text{C}$  NMR (100 MHz,  $\text{CDCl}_3$ )  $\delta$  173.70 (f), 138.34 (d), 128.82 (b,b'), 127.89 (c,c'), 127.63 (a), 69.42 (i), 47.04 (j), 43.79 (e), 33.26 (h), 33.24 (g), 24.73 (k), 23.47 and 22.28 (l,l'); IR (neat) 3284 (N-H stretch, O-H stretch), 2952, 2916, 2868, 1643 (C=O stretch),

1546, 1453, 696  $\text{cm}^{-1}$ ; HRMS (ESI) calcd. for  $\text{C}_{15}\text{H}_{23}\text{NNaO}_2$  ( $\text{M}+\text{Na}$ ): 272.1626, found 272.1638  $m/z$ .

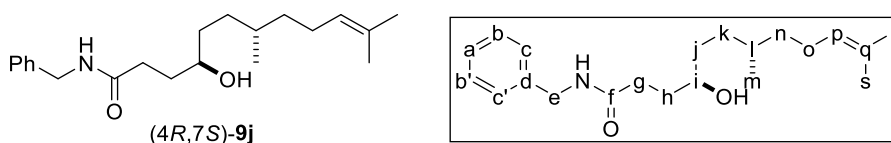


**(S)-4-hydroxy-7-methyloctanecarboxylic acid benzyl amide (9i).** Following **GP12** with **7i** (130 mg, 0.528 mmol) affords, after flash chromatography on silica gel (80:20-20:80 hexanes:ethyl acetate), the title compound (104 mg, 75%) as a white solid: m.p. 61.0–62.0 °C; TLC analysis  $R_f$  0.4 (0:100 hexanes:ethyl acetate);  $[\alpha]_D^{20} = -5.9^\circ$  ( $c$  2.0,  $\text{CHCl}_3$ ); Chiral HPLC analysis (Chiralcel-OD, 60:40 hexanes:isopropanol, flowrate = 1.0 mL/min) showed peaks at 11 minutes (96.5% (*S*)) and 16 minutes (3.5% (*R*));  $^1\text{H}$  NMR (400 MHz,  $\text{CDCl}_3$ )  $\delta$  7.30–7.35 (2H, b,b'), 7.20–7.30 (a,c,c'), 6.49 (1H, br s, NH), 4.39 (2H, d,  $J = 5.7$  Hz, e), 3.50–3.60 (1H, m, i), 3.26 (1H, br s, OH), 2.30–2.45 (2H, m, g), 1.80–1.90 (1H, m, h), 1.60–1.70 (1H, m, h), 1.50–1.60 (1H, m, l), 1.40–1.50 (2H, m, j), 1.25–1.35 (1H, m, k), 1.15–1.25 (1H, m, k) 0.89 (6H, dd,  $J = 6.6$  and 1.6 Hz, m,m');  $^{13}\text{C}$  NMR (100 MHz,  $\text{CDCl}_3$ )  $\delta$  173.90 (f), 138.36 (d), 128.78 (b,b'), 127.84 (c,c'), 127.57 (a), 71.72 (i), 43.72 (e), 35.60 (j), 34.97 (k), 33.23 (g), 32.75 (h), 28.20 (l), 22.76 and 22.68 (m,m'); IR (neat) 3452 (N-H stretch), 3294 (O-H stretch), 2951, 2931, 2901, 2868, 1615 (C=O stretch), 1545, 1454, 1249, 1063, 1029, 723, 692  $\text{cm}^{-1}$ ; HRMS (ESI) calcd. for  $\text{C}_{16}\text{H}_{25}\text{NNaO}_2$  ( $\text{M}+\text{Na}$ ): 286.1783, found 286.1785  $m/z$ .



**(4S,7S)-4-hydroxy-7,11-dimethyl-10-dodecenecarboxylic acid benzyl amide**

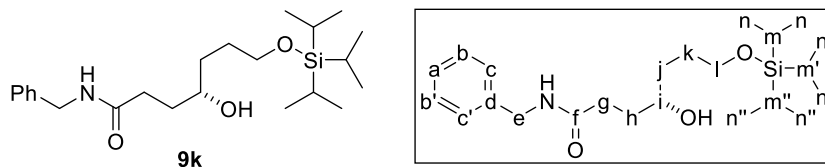
**((4S,7S)-9j).** Following **GP12** with 1.0 mol% [Rh(nbd)<sub>2</sub>BF<sub>4</sub>/ 2(*R*)-**B2**] and **7j** (167 mg, 0.528 mmol) affords, after flash chromatography on silica gel (80:20-20:80 hexanes:ethyl acetate), the title compound (137 mg, 78%) as a white solid: m.p. 72.0–73.0 °C; TLC analysis *R<sub>f</sub>* 0.5 (0:100 hexanes:ethyl acetate); [α]<sub>D</sub><sup>20</sup> = –2.5° (*c* 1.0, CHCl<sub>3</sub>); <sup>1</sup>H NMR (400 MHz, CDCl<sub>3</sub>) δ 7.20–7.40 (5H, a,b,b',c,c'), 6.30 (1H, br s, NH), 5.11 (1H, t, *J* = 5.8 Hz, p), 4.42 (2H, d, *J* = 5.5 Hz, e), 3.45–3.65 (1H, m, i), 3.05 (1H, br s, OH), 2.30–2.45 (2H, m, g), 1.80–2.05 (3H, m, o,h), 1.70 (3H, s, r), 1.62 (3H, s, s), 1.20–1.50 (6H, m, h,j,l,n), 1.15–1.20 (2H, m, k), 0.89 (3H, d, *J* = 5.5 Hz, m); <sup>13</sup>C NMR (100 MHz, CDCl<sub>3</sub>) δ 173.77 (f), 138.33 (d), 131.19 (q), 128.80 (b,b'), 127.88 (c,c'), 127.61 (a), 125.01 (p), 71.92 (major diastereomer, 92%, i), 71.82 (minor diastereomer, 8%, i), 43.78 (e), 37.19 (minor diastereomer, 7%, l), 37.12 (major diastereomer, 93%, l), 35.29 (n), 33.26 (g), 32.99 (h), 32.65 (j and k *overlapping*), 25.83 (r), 25.64 (o), 19.67 (m), 17.77 (s); IR (neat) 3300 (N-H stretch, O-H stretch), 2962, 2911, 2849, 1642 (C=O stretch), 1552, 1452, 1344, 1256, 695 cm<sup>-1</sup>; HRMS (ESI) calcd. for C<sub>21</sub>H<sub>33</sub>NNaO<sub>2</sub> (M+Na): 354.2409, found 354.2414 *m/z*.



**(4R,7S)-4-hydroxy-7,11-dimethyl-10-dodecenecarboxylic acid benzyl amide**

**((4R,7S)-9j).** Following **GP12** with 1.0 mol% [Rh(nbd)<sub>2</sub>BF<sub>4</sub>/ 2(*S*)-**B2**] and **7j** (167 mg, 0.528 mmol) affords, after flash chromatography on silica gel (80:20-20:80 hexanes:ethyl

acetate), the title compound (133 mg, 76%) as a white semi-solid; TLC analysis  $R_f$  0.5 (0:100 hexanes:ethyl acetate);  $[\alpha]_D^{20} = +6.5^\circ$  ( $c$  1.0,  $\text{CHCl}_3$ );  $^1\text{H NMR}$  (400 MHz,  $\text{CDCl}_3$ )  $\delta$  7.30–7.35 (2H, m, b,b'), 7.25–7.30 (3H, m, a,c,c'), 6.30 (1H, br s, NH), 5.11 (1H, t,  $J = 6.2$  Hz, p), 4.42 (2H, d,  $J = 5.7$  Hz, e), 3.45–3.70 (1H, m, i), 3.04 (1H, br s, OH), 2.30–2.45 (2H, m, g), 1.80–2.05 (3H, m, o,h), 1.70 (3H, s, r), 1.62 (3H, s, s), 1.20–1.50 (7H, m, h,j,k,l,n), 1.10–1.20 (1H, m, k), 0.89 (3H, d,  $J = 6.4$  Hz, m);  $^{13}\text{C NMR}$  (100 MHz,  $\text{CDCl}_3$ )  $\delta$  173.77 (f), 138.33 (d), 131.19 (q), 128.80 (b,b'), 127.88 (c,c'), 127.61 (a), 125.02 (p), 71.92 (minor diastereomer, 7%, i), 71.82 (major diastereomer, 93%, i), 43.78 (e), 37.19 (major diastereomer, 92%, l), 37.12 (minor diastereomer, 8%, l), 35.28 (n), 33.29 (g), 32.94 (h), 32.75 (k), 32.58 (j), 25.83 (r), 25.65 (o), 19.61 (m), 17.77 (s); IR (neat) 3271 (N-H stretch, O-H stretch), 2912, 2851, 1651 (C=O stretch), 1616, 1538 1453, 727, 694  $\text{cm}^{-1}$ ; HRMS (ESI) calcd. for  $\text{C}_{21}\text{H}_{33}\text{NNaO}_2$  ( $\text{M}+\text{Na}$ ): 354.2409, found 354.2412  $m/z$ .

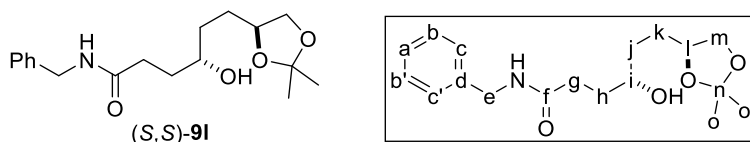


**(S)-4-hydroxy-7-((triisopropylsilyloxy)heptanecarboxylic acid benzyl amide**

**(9k).** Following **GP12** with **7k** (206 mg, 0.528 mmol) affords, after flash chromatography on silica gel (80:20-20:80 hexanes:ethyl acetate), the title compound (168 mg, 78%) as a colorless oil; TLC analysis  $R_f$  0.4 (20:80 hexanes:ethyl acetate);  $[\alpha]_D^{20} = +7.1^\circ$  ( $c$  2.0,  $\text{CHCl}_3$ ); Chiral HPLC analysis (Chiralpak-IC, 80:20 hexanes:isopropanol, flowrate = 1.4 mL/min) showed peaks at 29 minutes (3.0% (*R*)) and 35 minutes (97.0% (*S*));  $^1\text{H NMR}$  (400 MHz,  $\text{CDCl}_3$ )  $\delta$  7.30–7.35 (2H, b,b'), 7.25–7.30 (3H, a,c,c'), 6.28 (1H, br s, NH), 4.44 (2H, dd,  $J = 5.6$  and 3.2 Hz, e), 3.70–3.85 (3H, m, l, OH), 3.60–3.70 (1H, m, i),

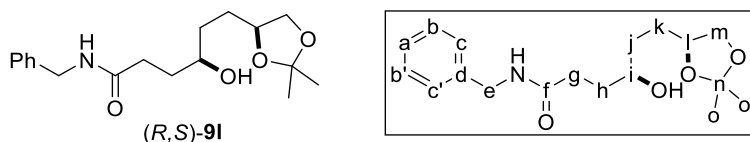


2.42 (2H, t,  $J = 7.0$  Hz, g), 1.85–1.95 (1H, m, h), 1.60–1.80 (4H, m, h,j,k), 1.50–1.60 (1H, m, j), 1.00–1.15 (3H, m, m,m',m''), *overlapping with n,n',n''*), 1.08 (18H, s, n,n',n'');  $^{13}\text{C}$  NMR (100 MHz,  $\text{CDCl}_3$ )  $\delta$  173.61 (f), 138.48 (d), 128.77 (b,b'), 127.88 (c,c'), 127.54 (a), 71.14 (i), 63.95 (l), 43.74 (e), 35.37 (j), 33.46 (g), 32.89 (h), 29.60 (k), 18.08 (n,n',n''), 12.02 (m,m',m''); IR (neat) 3289 (N-H stretch, O-H stretch), 2941, 2864, 1644 (C=O stretch), 1548, 1454, 1097, 881, 679  $\text{cm}^{-1}$ ; HRMS (ESI) calcd. for  $\text{C}_{23}\text{H}_{41}\text{NNaO}_3\text{Si}$  (M+Na): 430.2753, found 430.2763  $m/z$ .



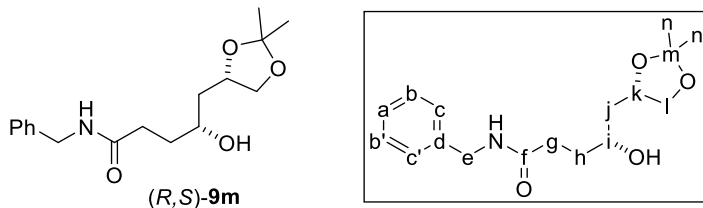
**(S,S)-4-hydroxy-6-(2,2-dimethyl-1,3-dioxolan-4-yl)hexanecarboxylic acid benzyl amide ((S,S)-9I).** Following **GP12** with 1.0 mol%  $[\text{Rh}(\text{nbd})_2\text{BF}_4/ 2(R)\text{-B1}]$  and **71** (160 mg, 0.528 mmol) affords, after flash chromatography on silica gel (70:30-0:100 hexanes:ethyl acetate), the title compound (122 mg, 72%) as a colorless oil; TLC analysis  $R_f$  0.25 (0:100 hexanes:ethyl acetate);  $[\alpha]_D^{20} = +10.1^\circ$  ( $c$  1.0,  $\text{CHCl}_3$ );  $^1\text{H}$  NMR (400 MHz,  $\text{CDCl}_3$ )  $\delta$  7.30–7.35 (2H, m, b,b'), 7.25–7.30 (3H, m, a,c,c'), 6.27 (1H, br s, NH), 4.42 (2H, d,  $J = 5.7$  Hz, e), 4.05–4.15 (1H, m, l), 4.05 (1H, dd,  $J = 6.0$  and 6.0 Hz, m), 3.60–3.70 (1H, m, i), 3.53 (1H, dd,  $J = 7.5$  and 7.5 Hz, m), 3.08 (1H, br s, OH), 2.40 (2H, t,  $J = 6.6$  Hz, g), 1.80–1.90 (1H, m, h), 1.60–1.80 (3H, m, h,k), 1.50–1.60 (2H, m, j), 1.41 (3H, s, o,o'), 1.36 (3H, s, o,o');  $^{13}\text{C}$  NMR (100 MHz,  $\text{CDCl}_3$ )  $\delta$  173.62 (f), 138.32 (d), 128.81 (b,b'), 127.87 (c,c'), 127.61 (a), 109.08 (n), 76.22 (l), 71.17 (major diastereomer, 96%, i), 71.02 (minor diastereomer, 4%, i), 69.56 (major diastereomer, 96%, m), 69.54 (minor diastereomer, 4%, m), 43.78 (e), 34.19 (major diastereomer, 95%, j), 34.01 (minor

diastereomer, 5%, j), 33.28 (g), 32.86 (h), 30.23 (k), 27.01 (o,o'), 25.83 (o,o'); IR (neat) 3298 (N-H stretch, O-H stretch), 2984, 2932, 2868, 1644 (C=O stretch), 1543, 1454, 1369, 1214, 1155, 1053, 698  $\text{cm}^{-1}$ ; HRMS (ESI) calcd. for  $\text{C}_{18}\text{H}_{27}\text{NNaO}_4$  (M+Na): 344.1838, found 344.1847  $m/z$ .

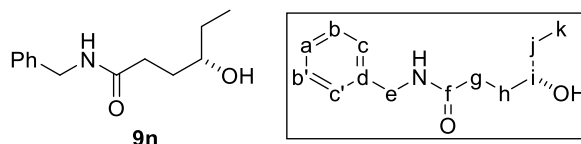


**(S,S)-4-hydroxy-6-(2,2-dimethyl-1,3-dioxolan-4-yl)hexanecarboxylic acid benzyl amide ((S,S)-91).** Following **GP12** with 1.0 mol%  $[\text{Rh}(\text{nbd})_2\text{BF}_4]$  / **2(S)-B1**] and **71** (160 mg, 0.528 mmol) affords, after flash chromatography on silica gel (70:30-0:100 hexanes:ethyl acetate), the title compound (122 mg, 72%) as a colorless oil; TLC analysis  $R_f$  0.25 (0:100 hexanes:ethyl acetate);  $[\alpha]_D^{20} = +22.3^\circ$  ( $c$  1.0,  $\text{CHCl}_3$ );  $^1\text{H}$  NMR (400 MHz,  $\text{CDCl}_3$ )  $\delta$  7.30–7.35 (2H, m, b,b'), 7.20–7.30 (3H, m, a,c,c'), 6.44 (1H, br s, NH), 4.39 (2H, d,  $J = 5.7$  Hz, e), 4.05–4.15 (1H, m, l), 4.02 (1H, dd,  $J = 7.6$  and 7.6 Hz, m), 3.55–3.75 (2H, m, i, OH), 3.50 (1H, dd,  $J = 7.2$  and 7.2 Hz, m), 2.36 (1H, t,  $J = 6.0$  Hz, g), 1.80–1.90 (1H, m, h), 1.55–1.80 (4H, m, h,j,k), 1.45–1.50 (1H, m, j), 1.40 (3H, s, o,o'), 1.35 (3H, s, o,o');  $^{13}\text{C}$  NMR (100 MHz,  $\text{CDCl}_3$ )  $\delta$  173.68 (f), 138.28 (d), 128.75 (b,b'), 127.79 (c,c'), 127.55 (a), 108.93 (n), 76.21 (l), 71.06 (minor diastereomer, 5%, i), 70.95 (major diastereomer, 95%, i), 69.61 (minor diastereomer, 5%, m), 69.51 (major diastereomer, 95%, m), 43.69 (e), 34.19 (minor diastereomer, 0%, j), 33.94 (major diastereomer, 100%, j), 33.18 (g), 32.73 (h), 29.79 (k), 26.99 (o,o'), 25.79 (o,o'); IR (neat) 3294 (N-H stretch, O-H stretch), 2984, 2931, 2869, 1644 (C=O stretch), 1542,

1454, 1369, 1214, 1054, 698  $\text{cm}^{-1}$ ; HRMS (ESI) calcd. for  $\text{C}_{18}\text{H}_{27}\text{NNaO}_4$  ( $\text{M}+\text{Na}$ ): 344.1838, found 344.1851  $m/z$ .

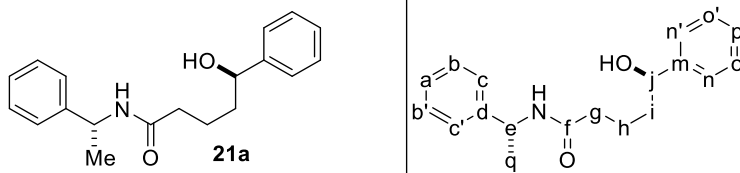


**(R,S)-5-(2,2-dimethyl-1,3-dioxolan-4-yl)-4-hydroxypentanecarboxylic acid benzyl amide ((R,S)-9m).** Following **GP12** with 1.0 mol%  $[\text{Rh}(\text{nbd})_2\text{BF}_4/ 2(S)\text{-B1}]$  and **7m** (153 mg, 0.528 mmol) affords, after flash chromatography on silica gel (70:30-0:100 hexanes:ethyl acetate), the title compound (114 mg, 70%) as a colorless oil; TLC analysis  $R_f$  0.25 (0:100 hexanes:ethyl acetate);  $[\alpha]_D^{20} = -3.5^\circ$  ( $c$  1.0,  $\text{CHCl}_3$ ); <sup>1</sup>H NMR (400 MHz,  $\text{CDCl}_3$ )  $\delta$  7.30–7.35 (2H, m, b,b'), 7.20–7.30 (3H, m, a,c,c'), 6.37 (1H, br s, NH), 4.40 (2H, d,  $J = 5.7$  Hz, e), 4.25–4.35 (1H, m, k), 4.07 (1H, dd,  $J = 8.0$  and 6.1 Hz, l), 3.80–3.90 (1H, m, i), 3.55 (1H, dd,  $J = 7.8$  and 7.8 Hz, l), 2.39 (1H, t,  $J = 6.9$  Hz, g), 1.80–1.90 (1H, m, h), 1.60–1.80 (3H, m, h,j), 1.40 (3H, s, n,n'), 1.35 (3H, s, n,n'); <sup>13</sup>C NMR (100 MHz,  $\text{CDCl}_3$ )  $\delta$  173.60 (f), 138.27 (d), 128.81 (b,b'), 127.86 (c,c'), 127.62 (a), 108.81 (m), 73.79 (k), 69.66 (major diastereomer, 92%, i), 69.49 (minor diastereomer, 8%, i), 68.58 (l), 43.77 (e), 40.67 (minor diastereomer, 7%, j), 40.56 (major diastereomer, 93%, j), 33.15 (g), 33.08 (h), 27.03 (n,n'), 25.78 (n,n'); IR (neat) 3304 (N-H stretch, O-H stretch), 2984, 2935, 2873, 1644 (C=O stretch), 1542, 1454, 1369, 1214, 1155, 1052, 698  $\text{cm}^{-1}$ ; HRMS (ESI) calcd. for  $\text{C}_{17}\text{H}_{25}\text{NNaO}_4$  ( $\text{M}+\text{Na}$ ): 330.1681, found 330.1690  $m/z$ .



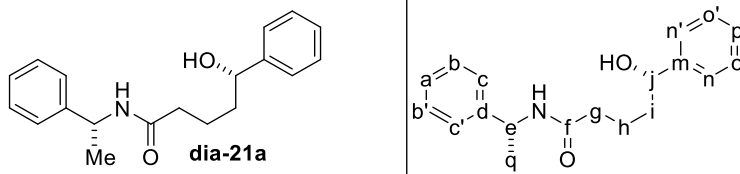
**(S)-4-hydroxy-hexanecarboxylic acid benzyl amide (9n).** Following **GP12** with **7n** (107 mg, 0.528 mmol) affords, after flash chromatography on silica gel (80:20-20:80 hexanes:ethyl acetate), the title compound (71 mg, 61%) as a white solid: m.p. 63.5–64.5 °C; TLC analysis  $R_f$  0.4 (0:100 hexanes:ethyl acetate);  $[\alpha]_D^{20} = +5.3^\circ$  ( $c$  1.44,  $\text{CHCl}_3$ );  $^1\text{H}$  NMR (300 MHz,  $\text{CDCl}_3$ )  $\delta$  7.20–7.40 (5H, m, a,b,b',c,c'), 6.48 (1H, br s, NH), 4.40 (2H, d,  $J = 5.2$  Hz, e), 3.40–3.60 (1H, m, i), 3.21 (1H, br s, OH), 2.37 (2H, t,  $J = 6.5$  Hz, g) 1.75–1.95 (1H, m, h), 1.55–1.75 (1H, m, h), 1.40–1.55 (2H, m, j), 0.93 (3H, t,  $J = 7.2$  Hz, k);  $^{13}\text{C}$  NMR (75 MHz,  $\text{CDCl}_3$ )  $\delta$  173.80 (f), 138.24 (d), 128.67 (b,b'), 127.74 (c,c'), 127.46 (a), 72.67 (i), 43.62 (e), 33.12 (g), 32.16 (h), 30.40 (j), 10.02 (k); IR (neat) 3280 (N-H stretch, O-H stretch), 2964, 2920, 2877, 1631 (C=O stretch), 1549 (N-H bend), 1493, 1326, 1264, 936, 729, 693  $\text{cm}^{-1}$ ; HRMS (ESI) calcd. for  $\text{C}_{13}\text{H}_{19}\text{NNaO}_2$  (M+Na): 244.1313, found 244.1316  $m/z$ .

Er of **7n** was determined by  $^{19}\text{F}$  NMR of the corresponding Mosher ester (*S,S*)-**14**:  $^{19}\text{F}$  NMR (376 MHz,  $\text{CDCl}_3$ )  $\delta$  -71.01 (s, 5%, minor,  $\text{CF}_3$ ), -71.08 (s, 95%, major,  $\text{CF}_3$ ); see **GP13** *vide infra*.



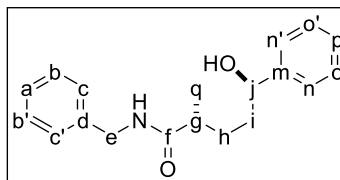
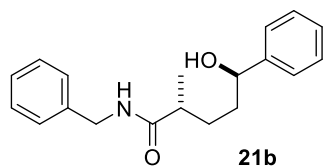
**(R)-5-hydroxy-5-phenyl-N-((R)-1-phenylethyl)pentanamide (21a).** Following **GP12** with **20a** (74 mg, 0.264 mmol) affords, after flash chromatography on silica gel

(80:20-20:80 hexanes:ethyl acetate), the title compound (64 mg, 82%) as a white solid; TLC analysis  $R_f$  0.4 (0:100 hexanes:ethyl acetate);  $^1\text{H}$  NMR (400 MHz,  $\text{CDCl}_3$ )  $\delta$  7.20–7.40 (10H, m, aryl), 6.05 (1H, d,  $J = 7.6$  Hz, NH), 5.05–5.15 (1H, m, e), 4.60–4.70 (1H, m, j), 2.60–3.10 (1H, br s, OH), 2.10–2.30 (2H, m, g), 1.60–1.80 (4H, m, h,i), 1.47 (3H, d,  $J = 6.9$  Hz, q);  $^{13}\text{C}$  NMR (100 MHz,  $\text{CDCl}_3$ )  $\delta$  172.24 (f), 144.92 (m), 143.40 (d), 128.77, 128.53, 127.53, 127.43, 126.31, 125.92, 74.02 (j), 48.78 (e), 38.52 (i), 36.29 (g), 22.02 (minor q, 5.5%), 21.97 (major q, 94.5%), 21.86 (h).



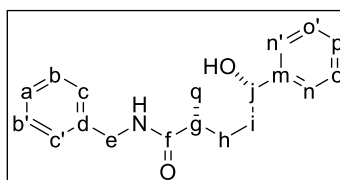
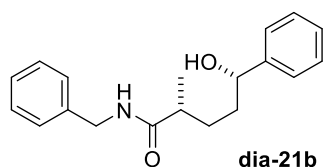
**(S)-5-hydroxy-5-phenyl-N-((R)-1-phenylethyl)pentanamide (dia-21a).**

Following **GP12** with (*S*)-**B1** and **20a** (74 mg, 0.264 mmol) affords, after flash chromatography on silica gel (80:20-20:80 hexanes:ethyl acetate), the title compound (62 mg, 80%) as a white solid; TLC analysis  $R_f$  0.4 (0:100 hexanes:ethyl acetate);  $^1\text{H}$  NMR (400 MHz,  $\text{CDCl}_3$ )  $\delta$  7.20–7.40 (10H, m, aryl), 6.04 (1H, d,  $J = 7.6$  Hz, NH), 5.05–5.15 (1H, m, e), 4.60–4.70 (1H, m, j), 2.60–3.10 (1H, br s, OH), 2.21 (2H, t,  $J = 6.6$  Hz, g), 1.60–1.85 (4H, m, h,i), 1.47 (3H, d,  $J = 6.9$  Hz, q);  $^{13}\text{C}$  NMR (100 MHz,  $\text{CDCl}_3$ )  $\delta$  172.23 (f), 144.90 (m), 143.39 (d), 128.76, 128.53, 127.53, 127.43, 126.32, 125.91, 74.07 (j), 48.78 (e), 38.50 (i), 36.33 (g), 22.02 (major q, 9.0%), 21.96 (major q, 91%), 21.86 (h).



**(2*R*,5*R*)-5-hydroxy-2-methyl-5-phenylpentanecarboxylic acid benzyl amide**

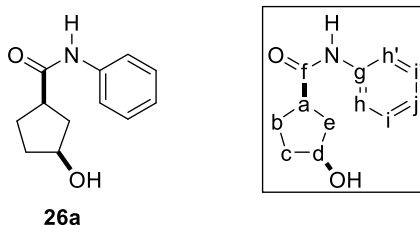
**(21b).** Following **GP12** with **20b** (74 mg, 0.264 mmol) affords, after flash chromatography on silica gel (80:20-20:80 hexanes:ethyl acetate), the title compound (62 mg, 79%) as a white solid; TLC analysis  $R_f$  0.4 (0:100 hexanes:ethyl acetate);  $^1\text{H}$  NMR (400 MHz,  $\text{CDCl}_3$ )  $\delta$  7.20–7.35 (10H, m, aryl), 6.206.25 (br s, minor 8.0%, NH), 6.05–6.20 (br s, major 92%, NH), 4.63 (1H, t,  $J = 6.2$  Hz, j), 4.38 (2H, d,  $J = 5.7$  Hz, e), 2.90 (1H, br s, OH), 2.20–2.30 (1H, m, g), 1.70–1.90 (3H, m, h,i), 1.55–1.65 (0.08H, m, minor i), 1.35–1.45 (0.92H, m, major i), 1.13 (3H, d,  $J = 6.9$  Hz, q);  $^{13}\text{C}$  NMR (100 MHz,  $\text{CDCl}_3$ )  $\delta$  176.46 (f), 144.88 (m), 138.61 (d), 128.78, 128.52, 127.87, 127.54, 127.53, 125.97, 74.31 (j), 43.49 (e), 41.27 (g), 36.95 (i), 30.42 (h), 18.16 (q).



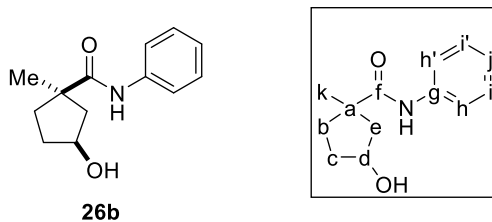
**(2*R*,5*S*)-5-hydroxy-2-methyl-5-phenylpentanecarboxylic acid benzyl amide**

**(dia-21b).** Following **GP12** with (*S*)-**B1** and **20b** (74 mg, 0.264 mmol) affords, after flash chromatography on silica gel (80:20-20:80 hexanes:ethyl acetate), the title compound (62 mg, 79%) as a white solid; TLC analysis  $R_f$  0.4 (0:100 hexanes:ethyl acetate);  $^1\text{H}$  NMR (400 MHz,  $\text{CDCl}_3$ )  $\delta$  7.20–7.35 (10H, m, aryl), 6.10–6.20 (br s, major 91.0%, NH), 6.05–6.10 (br s, minor 9.0%, NH), 4.60–4.65 (1H, m, j), 4.39 (2H, d,  $J = 5.6$  Hz, e), 2.82 (1H,

br s, OH), 2.20–2.35 (1H, m, g), 1.65–1.80 (3H, m, h,i), 1.50–1.65 (0.91H, m, major i), 1.35–1.45 (0.09H, m, minor i), 1.15 (3H, d,  $J = 6.8$  Hz, q);  $^{13}\text{C}$  NMR (100 MHz,  $\text{CDCl}_3$ )  $\delta$  176.54 (f), 144.97 (m), 138.61 (d), 128.79, 128.53, 127.90, 127.53, 127.53, 125.87, 74.35 (j), 43.51 (e), 41.16 (g), 36.91 (i), 30.82 (h), 18.24 (q).



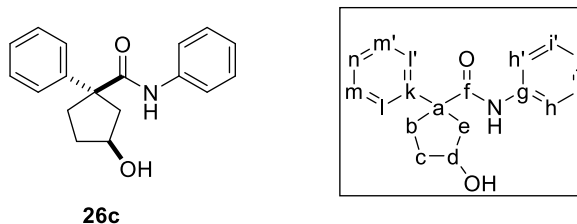
**(1R,3S)-3-hydroxycyclopentanecarboxylic acid phenyl amide (26a).** Following **GP12** with 1.0 mol%  $[\text{Rh}(\text{nbd})_2\text{BF}_4/ 2(R)\text{-B2}]$ , 2 equiv tmdBH, and **23a** (99.1 mg, 0.528 mmol), affords, after flash chromatography on silica gel (80–40:20–60 hexanes:ethyl acetate) affords the title compound (86.7 mg, 80%) as a white solid: mp 100.5–102.5 °C; TLC analysis  $R_f$  0.4 (50:50 hexanes:ethyl acetate);  $[\alpha]_D^{20} = -14^\circ$  ( $c$  1.0,  $\text{CHCl}_3$ ); Chiral HPLC analysis (Chiralpak-IC, 80:20 hexanes:isopropanol, flow rate = 1.0 mL/min) showed peaks at 56 minutes (3.0% (1S,3R)) and 64 minutes (97.0% (1R,3S));  $^1\text{H}$  NMR (400 MHz,  $\text{CDCl}_3$ )  $\delta$  8.84 (1H, br s, NH), 7.54 (2H, d,  $J = 7.9$  Hz, h,h'), 7.31 (2H, t,  $J = 7.8$  Hz, i,i'), 7.11 (1H, t,  $J = 7.3$  Hz, j), 4.56 (1H, d,  $J = 6.6$  Hz, d), 4.40 (1H, br s, OH), 3.05–2.90 (1H, m, a), 2.20–1.90 (5H, m, b,c,e), 1.80–1.65 (1H, m, c);  $^{13}\text{C}$  NMR (100 MHz,  $\text{CDCl}_3$ )  $\delta$  177.41 (f), 138.18 (a), 128.93 (i,i'), 124.32 (j), 120.11 (h,h'), 73.89 (d), 45.28 (a), 38.94 (e), 36.50 (b), 29.20 (c); IR (neat) 3677 (N-H stretch, O-H stretch), 2907, 2803, 1728 (C=O stretch), 1663, 1597 (N-H bend), 1565, 1389 (C-N stretch), 1238 (C-OH bend), 1050 (C-OH stretch)  $\text{cm}^{-1}$ ; HRMS (ESI) calcd. for  $\text{C}_{12}\text{H}_{15}\text{NNaO}_2$  ( $\text{M}+\text{Na}$ ): 228.1000, found 228.1002  $m/z$ .



**(1*R*, 3*S*)-3-hydroxy-1-methylcyclopentanecarboxylic acid phenyl amide (26b).**

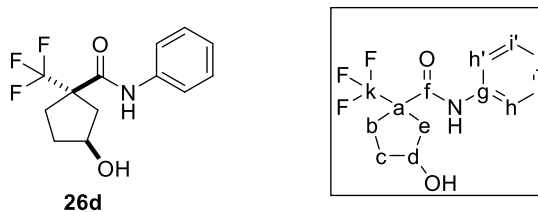
Following **GP12** with 1.0 mol% [Rh(nbd)<sub>2</sub>BF<sub>4</sub>/ 2(*R*)-**B2**], 2 equiv tmdBH, and **23b** (106.4 mg, 0.528 mmol) affords, after flash chromatography on silica gel (85:15 dichloromethane:ethyl acetate), the title compound (76.2 mg, 65 %) as a white solid: mp 91.0–93.5 °C; TLC analysis *R<sub>f</sub>* 0.5 (80:20 dichloromethane:ethyl acetate); [α]<sub>D</sub><sup>20</sup> = -13° (*c* 0.7, CHCl<sub>3</sub>); Chiral HPLC analysis (Chiralcel-OD, 90:10 hexanes:isopropanol, flow rate = 1.3 mL/min) showed peaks at 87 minutes (96.0% (1*R*,3*S*)) and 105 minutes (4.0% (1*S*,3*R*)); <sup>1</sup>H NMR (400 MHz, CDCl<sub>3</sub>) δ 8.94 (1H, br s, NH), 7.54 (2H, d, *J* = 7.6 Hz, h,h'), 7.31 (2H, t, *J* = 7.5 Hz, i,i'), 7.08 (1H, t, *J* = 7.4 Hz, j), 4.55 (1H, s, d), 3.44 (1H, br s, OH), 2.40 (1H, ddd, *J* = 18.8 Hz, 10.9 Hz, 7.9 Hz, b), 2.31 (1H, dd, *J* = 14.9 Hz, 1.6 Hz, e), 2.00–1.85 (2H, m, c), 1.80–1.70 (2H, m, b,e), 1.37 (3H, s, k); <sup>13</sup>C NMR (100 MHz, CDCl<sub>3</sub>) δ 178.32 (f), 138.78 (g), 128.88 (i,i'), 123.78 (j), 119.64 (h,h'), 75.18 (d), 48.98 (a), 47.64 (e), 38.52 (b), 36.03 (c), 25.91 (k); IR (neat) 3318 (O-H stretch, N-H stretch), 2962, 2901, 1663 (C=O stretch), 1536 (C-OH bend), 1495, 1434, 1311 (C-N stretch), 657 cm<sup>-1</sup>; HRMS (CI) calcd. for C<sub>13</sub>H<sub>18</sub>NO<sub>2</sub> (M+H): 220.1338, found 220.1346 *m/z*.



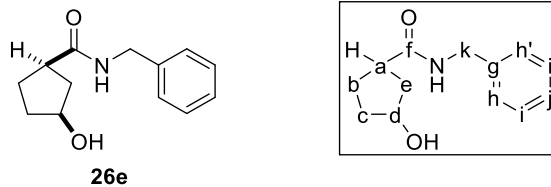


**(1*R*, 3*S*)-3-hydroxy-1-phenylcyclopentanecarboxylic acid phenyl amide (26c).**

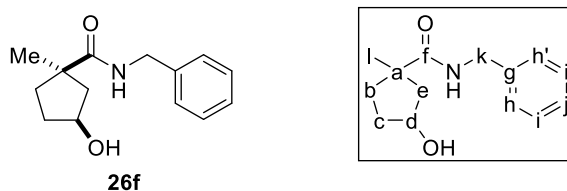
Following **GP12** with 1.0 mol% [Rh(nbd)<sub>2</sub>BF<sub>4</sub>/ 2(*R*)-**B2**], 2 equiv tmdBH, and **23c** (139.2 mg, 0.528 mmol) affords, after flash chromatography on silica gel (85:15 dichloromethane:ethyl acetate), the title compound (106.7 mg, 72 %) as a white solid: mp 113.5–114.5 °C; TLC analysis *R<sub>f</sub>* 0.5 (80:20 dichloromethane:ethyl acetate); [α]<sub>D</sub><sup>20</sup> = -43° (*c* 0.8, CHCl<sub>3</sub>); Chiral HPLC analysis (Chiralcel-OD, 60:40 hexanes:isopropanol, flowrate = 1.4 mL/min) showed peaks at 14 minutes (96.0% (1*R*,3*S*)) and 22 minutes (4.0% (1*S*,3*R*)); <sup>1</sup>H NMR (400 MHz, CDCl<sub>3</sub>) δ 7.50–7.40 (4H, m, h,h',i,i'), 7.40–7.35 (1H, m, j), 7.40–7.35 (4H, m, l,l',m,m'), 7.15–7.05 (2H, m, n,NH), 4.47 (2H, br s, d,OH), 2.80 (1H, d, *J* = 14.2 Hz, e), 2.75–2.60 (1H, m, b), 2.40–2.30 (1H, m, b), 2.30–2.20 (2H, m, c,e), 2.00–1.90 (1H, m, c); <sup>13</sup>C NMR (100 MHz, CDCl<sub>3</sub>) δ 177.02 (f), 143.60 (k), 137.42 (g), 129.34 (i,i'), 128.96 (m,m'), 127.81 (j), 127.19 (l,l'), 124.74 (n), 120.15 (h,h'), 73.01 (d), 59.39 (a), 47.12 (e), 36.33 (b), 36.01 (c); IR (neat) 3492 (O-H stretch), 3400 (N-H stretch), 2896, 1668 (C=O stretch), 1596 (C=C stretch), 1522 (C-OH bend), 1492, 1437, 1311 (C-N stretch), 1033, 751, 733, 691 cm<sup>-1</sup>; HRMS (ESI) calcd. for C<sub>18</sub>H<sub>19</sub>NNaO<sub>2</sub> (M+Na): 304.1313, found 304.1299 *m/z*.



(*1S*, *3S*)-3-hydroxy-1-(trifluoromethyl)cyclopentanecarboxylic acid phenyl amide (**26d**). Following **GP12** with 1.0 mol% [Rh(nbd)<sub>2</sub>BF<sub>4</sub>/ 2(*R*)-**B2**], 2 equiv tmdBH, and **23d** (135.2 mg, 0.528 mmol) affords, after flash chromatography on silica gel (90:10 dichloromethane:ethyl acetate), the title compound (111.9 mg, 78 %) as a white solid: mp 129.0–130.5 °C; TLC analysis R<sub>f</sub> 0.75 (80:20 dichloromethane:ethyl acetate); [α]<sub>D</sub><sup>20</sup> = -22° (*c* 1.3, CHCl<sub>3</sub>); Chiral HPLC analysis (Chiralpak-IC with OD guard column, 80:20 hexanes:isopropanol, flowrate = 1.0 mL/min) showed peaks at 14 minutes (97.0% (*1S,3S*)) and 21 minutes (3.0% (*1R,3R*)); <sup>19</sup>F NMR (282 MHz, CDCl<sub>3</sub>) δ -71.94; <sup>1</sup>H NMR (300 MHz, CDCl<sub>3</sub>) δ 9.53 (1H, br s, NH), 7.49 (2H, d, *J* = 7.6 Hz, h,h'), 7.30 (2H, t, *J* = 7.5 Hz, i,i'), 7.11 (1H, t, *J* = 7.4 Hz, j), 4.65 (1H, s, d), 3.88 (1H, br s, OH), 2.55–2.25 (4H, m, b,e), 2.10–1.95 (1H, m, c), 1.95–1.80 (1H, m, c); <sup>13</sup>C NMR (75 MHz, CDCl<sub>3</sub>) δ 170.51 (f), 137.92 (g), 128.95 (i,i'), 127.3 (q, *J* = 279 Hz, k), 124.52 (j), 120.00 (h,h'), 74.16 (d), 58.58 (q, *J* = 24 Hz, a), 40.88 (e), 36.20 (c), 32.21 (b); IR (neat) 3416 (O-H stretch), 3263 (N-H stretch), 3089, 2376, 1669 (C=O stretch), 1624, 1599 (C=C stretch), 1567 (C-OH bend), 1450, 1157, 1131, 752, 692, 653 cm<sup>-1</sup>; HRMS (ESI) calcd. for C<sub>13</sub>H<sub>14</sub>F<sub>3</sub>NNaO<sub>2</sub> (M+Na): 296.0874, found 296.0870 *m/z*.

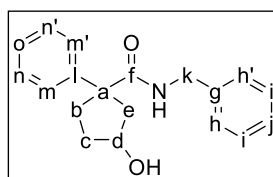
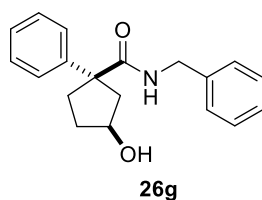


**(1*R*,3*S*)-3-hydroxycyclopentanecarboxylic acid benzyl amide (26e).** Following **GP12** with 1.0 mol% [Rh(nbd)<sub>2</sub>BF<sub>4</sub>/ 2(*R*)-**B2**], 2 equiv tmdBH, and **23e** (106.3 mg, 0.528 mmol) affords, after flash chromatography on silica gel (80–30:20–70 hexanes:ethyl acetate), the title compound (80.0 mg, 69 %) as a white solid: mp 115.5–116.0 °C; TLC analysis *R<sub>f</sub>* 0.3 (20:80 hexanes:ethyl acetate); [α]<sub>D</sub><sup>20</sup> = -12° (*c* 1.4, CHCl<sub>3</sub>); chiral HPLC analysis determined by converting to the corresponding phenyl amide **26a** using boric acid-catalyzed transamidation;<sup>23</sup> Chiralpak-IC, 80:20 hexanes:isopropanol, flow rate = 1.4 mL/min, showed peaks at 40 minutes (6.0% (1*S*,3*R*)) and 45 minutes (94.0% (1*R*,3*S*)). <sup>1</sup>H NMR (300 MHz, CDCl<sub>3</sub>) δ 7.40–7.20 (5H, m, h,h',i,i',j), 6.27 (1H, br s, NH), 4.45 (2H, d, *J* = 5.7 Hz, k), 4.40–4.25 (2H, m, d,OH), 2.85–2.70 (1H, m, a), 2.20–1.80 (5H, m, b,c,e), 1.80–1.60 (1H, m, c); <sup>13</sup>C NMR (75 MHz, CDCl<sub>3</sub>) δ 178.42 (f), 138.02 (g), 128.78 (i,i'), 127.74 (h,h'), 127.61 (j), 73.65 (d), 44.09 (a), 43.87 (k), 38.99 (e), 36.56 (c), 28.93 (b); IR (neat) 3259 (O-H stretch), 3085 (N-H stretch), 2937, 1634 (C=O stretch), 1573, 1551 (C=C stretch), 1233, 1001, 752, 727, 700 cm<sup>-1</sup>; HRMS (ESI) calcd. for C<sub>13</sub>H<sub>17</sub>NaNO<sub>2</sub> (M+Na): 242.1157, found 242.1153 *m/z*.



**(1*R*, 3*S*)-3-hydroxy-1-methylcyclopentanecarboxylic acid benzyl amide (26f).** Following **GP12** with 1.0 mol% [Rh(nbd)<sub>2</sub>BF<sub>4</sub>/ 2(*R*)-**B2**], 2 equiv tmdBH, and **23f** (114.0

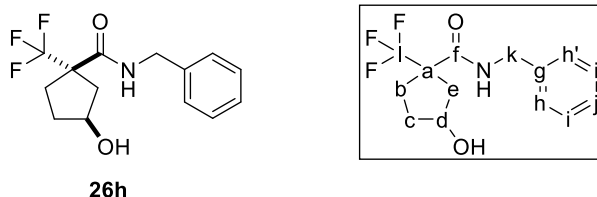
mg, 0.528 mmol) affords, after flash chromatography on silica gel (85:15 dichloromethane:ethyl acetate), the title compound (76.4 mg, 62 %) as a colorless oil: TLC analysis  $R_f$  0.4 (80:20 dichloromethane:ethyl acetate);  $[\alpha]_D^{20} = -12^\circ$  ( $c$  1.6,  $\text{CHCl}_3$ ); chiral HPLC analysis determined by converting to the corresponding phenyl amide **26b** using boric acid-catalyzed transamidation;<sup>23</sup> Chiral HPLC analysis (Chiralcel-OD, 90:10 hexanes:isopropanol, flow rate = 1.3 mL/min) showed peaks at 87 minutes (92.0% (1*R*,3*S*)) and 105 minutes (8.0% (1*S*,3*R*));  $^1\text{H}$  NMR (300 MHz,  $\text{CDCl}_3$ )  $\delta$  7.40–7.20 (5H, m, h,h',i,i',j), 6.60 (1H, br s, NH), 4.47 (2H, d,  $J = 5.6$  Hz, k), 4.45–4.35 (1H, m, d), 4.00 (1H, d,  $J = 7.2$  Hz, OH), 2.40–2.15 (2H, m, b,e), 1.95–1.80 (2H, m, c), 1.75–1.60 (2H, m, b,e), 1.32 (3H, s, l);  $^{13}\text{C}$  NMR (75 MHz,  $\text{CDCl}_3$ )  $\delta$  180.08 (f), 138.35 (g), 128.74 (i,i'), 127.61 (j), 127.47 (h,h'), 74.59 (d), 48.18 (e), 47.81 (a), 43.89 (k), 38.29 (b), 36.21 (c), 25.66 (l); IR (neat) 3299 (O-H stretch, N-H stretch), 2958, 1636 (C=O stretch), 1535 (C=C stretch), 1453 (C-OH bend), 1227, 1190, 961, 721, 696  $\text{cm}^{-1}$ ; HRMS (ESI) calcd. for  $\text{C}_{14}\text{H}_{19}\text{NaNO}_2$  (M+Na): 256.1313, found 256.1325  $m/z$ .



**(1*R*, 3*S*)-3-hydroxy-1-phenylcyclopentanecarboxylic acid benzyl amide (26g).**

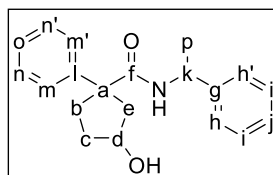
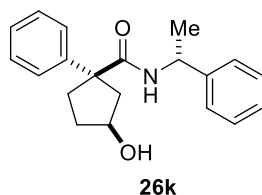
Following **GP12** with 1.0 mol%  $[\text{Rh}(\text{nbd})_2\text{BF}_4/ 2(R)\text{-B2}]$ , 2 equiv tmdBH, and **26g** (146.5 mg, 0.528 mmol) affords, after flash chromatography on silica gel (85:15 dichloromethane:ethyl acetate), the title compound (109.3 mg, 70 %) as a white solid: mp 91.0–93.5  $^\circ\text{C}$ ; TLC analysis  $R_f$  0.4 (80:20 dichloromethane:ethyl acetate);  $[\alpha]_D^{20} = -45^\circ$  ( $c$  1.3,  $\text{CHCl}_3$ ); Chiral HPLC analysis (Chiralpak-AD, 70:30 hexanes:isopropanol, flowrate

= 1.0 mL/min) showed peaks at 15 minutes (93.0% (1*R*,3*S*)) and 20 minutes (7.0% (1*S*,3*R*)); <sup>1</sup>H NMR (400 MHz, CDCl<sub>3</sub>) δ 7.45–7.30 (4H, m, i,i',n,n'), 7.35–7.25 (4H, m, h,h',j,o), 7.08 (2H, d, *J* = 6.5 Hz, m,m'), 5.61 (2H, br s, NH), 4.70 (1H, d, *J* = 10.1 Hz, OH), 4.45–4.35 (2H, m, d,k), 4.33 (1H, dd, *J* = 15.2 and 5.8 Hz, k), 2.75 (1H, dd, *J* = 14.1 and 1.3 Hz, e), 2.65–2.55 (1H, m, b), 2.35–2.25 (1H, m, b), 2.25–2.10 (1H, m, c,e), 2.00–1.90 (1H, m, c); <sup>13</sup>C NMR (100 MHz, CDCl<sub>3</sub>) δ 178.88 (f), 143.95 (l), 137.96 (g), 129.11 (i,i'), 128.67 (n,n'), 127.52 (h,h'), 127.41 (j), 127.17 (o), 127.01 (m,m'), 73.02 (d), 58.46 (a), 47.14 (e), 43.81 (k), 36.35 (b), 36.11 (c); IR (neat) 3316 (O-H stretch, N-H stretch), 1638 (C=O stretch), 1532 (C-OH bend), 1494, 1450, 1282, 1062, 1027, 992, 743, 719, 697, 662 cm<sup>-1</sup>; HRMS (ESI) calcd. for C<sub>19</sub>H<sub>21</sub>NaNO<sub>2</sub> (M+Na): 318.1470, found 318.1456 *m/z*.



**(1*S*, 3*S*)-3-hydroxy-1-(trifluoromethyl)cyclopentanecarboxylic acid benzyl amide (26h).** Following **GP12** with 1.0 mol% [Rh(nbd)<sub>2</sub>BF<sub>4</sub>/ 2(*R*)-**B2**], 2 equiv tmdBH, and **23h** (142.2 mg, 0.528 mmol) affords, after flash chromatography on silica gel (85:15 dichloromethane:ethyl acetate), the title compound (107.8 mg, 71 %) as a white solid: mp 100.5–102.0 °C; TLC analysis R<sub>f</sub> 0.5 (80:20 dichloromethane:ethyl acetate); [α]<sub>D</sub><sup>20</sup> = -16° (*c* 1.3, CHCl<sub>3</sub>); Chiral HPLC analysis (Chiralcel-OD, 70:30 hexanes:isopropanol, flowrate = 1.0 mL/min) showed peaks at 12 minutes (3.5% (1*R*,3*R*)) and 18 minutes (96.5% (1*S*,3*S*)); <sup>19</sup>F NMR (282 MHz, CDCl<sub>3</sub>) δ -71.04 (s, CF<sub>3</sub>); <sup>1</sup>H NMR (300 MHz, CDCl<sub>3</sub>) δ 7.45–7.20 (5H, m, h,h',i,i',j), 7.09 (1H, br s, NH), 4.60–4.40 (3H, m, d,k), 3.71

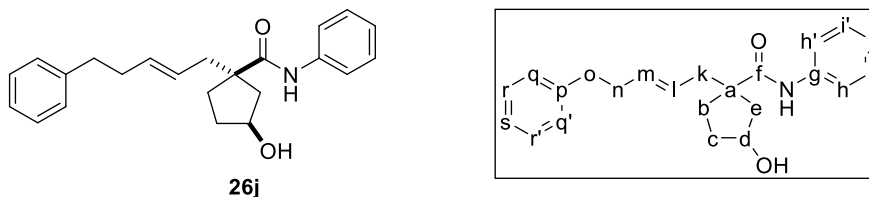
(1H, br s, OH), 2.50–2.15 (4H, m, b,e), 2.20–1.80 (2H, m, c); <sup>13</sup>C NMR (75 MHz, CDCl<sub>3</sub>) δ 171.70 (f), 137.58 (g), 129.29 (l), 128.80 (i,i'), 127.62 (j), 127.44 (h,h'), 73.57 (d), 57.96 (q, *J* = 24.5 Hz, a), 44.04 (k), 40.74 (e), 36.18 (c), 31.70 (b); IR (neat) 3421 (O-H stretch), 3311 (N-H stretch), 3269, 3084, 2944, 2360, 1657 (C=O stretch), 1526 (C-OH bend), 1455, 1362, 1301 (C-N stretch), 1169, 1123, 746, 696, 648 cm<sup>-1</sup>; HRMS (ESI) calcd. for C<sub>14</sub>H<sub>16</sub>F<sub>3</sub>NaNO<sub>2</sub> (M+Na): 310.1031, found 310.1026 *m/z*.



**(1*R*,3*S*)-3-hydroxy-1-phenyl-*N*-((*R*)-1-phenylethyl)cyclopentane-1-**

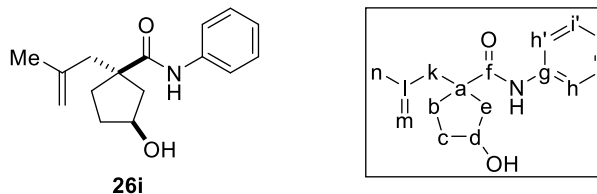
**carboxamide (26k).** Following **GP12** with 2.0 mol% [Rh(nbd)<sub>2</sub>BF<sub>4</sub>/ 2(*R*)-**B2**], 2 equiv tmdBH, and **23k** (154.2 mg, 0.528 mmol) affords, after flash chromatography on silica gel (85:15 dichloromethane:ethyl acetate), the title compound (124.3 mg, 76 %) as a white solid: mp 98.5–99.5 °C; TLC analysis *R<sub>f</sub>* 0.5 (80:20 dichloromethane:ethyl acetate); [α]<sub>D</sub><sup>20</sup> = -80° (*c* 1.3, CHCl<sub>3</sub>); <sup>1</sup>H NMR (400 MHz, CDCl<sub>3</sub>) δ 7.45–7.35 (2H, m, i,i'), 7.35–7.30 (3H, m, j,n,n'), 7.30–7.20 (3H, m, h,h',o), 6.99 (2H, d, *J* = 7.3 Hz, m,m'), 5.47 (1H, d, *J* = 6.9 Hz, NH), 5.05–4.95 (1H, m, k), 4.62 (1H, d, *J* = 10.0 Hz, OH), 4.45–4.35 (1H, m, d), 2.67 (1H, d, *J* = 14.2 Hz, e), 2.60–2.50 (1H, m, b), 2.35–2.25 (1H, m, b), 2.25–2.15 (1H, m, c), 2.10 (1H, d, *J* = 14.1 Hz and 6.8 Hz, e), 2.20–1.85 (1H, m, c), 1.34 (2.63H, d, *J* = 6.9 Hz, *p* major), 1.28 (0.33H, d, *J* = 6.7 Hz, *p* minor); the peaks at 1.34 and 1.28 ppm are used to determined the diastereoselectivity (88:12 major:minor); <sup>13</sup>C NMR (100 MHz, CDCl<sub>3</sub>) δ 177.84 (f), 143.99 (l), 143.00 (g), 129.04 (i,i'), 128.56 (n,n'), 127.46 (h,h'), 127.17 (j), 127.06 (o), 125.53 (m,m'), 72.84 (d), 58.43 (a), 49.16 (k), 46.86 (e),

36.12 (b), 35.99 (c), 22.00 (p, major), 21.69 (p, minor); IR (neat) 3368 (O-H stretch, N-H stretch), 1633 (C=O stretch), 1540 (C=C stretch), 1493, 1445, 1096, 760, 736, 695  $\text{cm}^{-1}$ ; HRMS (ESI) calcd. for  $\text{C}_{20}\text{H}_{23}\text{NaNO}_2$  (M+Na): 332.1626, found 332.1619  $m/z$ .



**(1*S*,3*S*)-3-hydroxy-1-((*E*)-5-phenylpent-2-en-1-yl)cyclopentanecarboxylic acid phenyl amide (**26j**).** Following **GP12** with 2.0 mol%  $[\text{Rh}(\text{nbd})_2\text{BF}_4/ 2(R)\text{-B2}]$ , 2 equiv tmdBH, and **26j** (175.0 mg, 0.528 mmol) affords, after flash chromatography on silica gel (90:10 dichloromethane:ethyl acetate), the title compound (147.9 mg, 80%) as a light yellow oil: TLC analysis  $R_f$  0.75 (80:20 dichloromethane:ethyl acetate);  $[\alpha]_D^{20} = +17^\circ$  ( $c$  1.8,  $\text{CHCl}_3$ ); Chiral HPLC analysis (Chiralpak-ASH with OD guard column, 70:30 hexanes:isopropanol, flowrate = 1.0 mL/min) showed peaks at 15 minutes (99.0% (1*S*,3*S*)) and 20 minutes (1.0% (1*R*,3*R*));  $^1\text{H}$  NMR (400 MHz,  $\text{CDCl}_3$ )  $\delta$  9.07 (1H, br s, NH), 7.54 (2H, d,  $J = 7.6$  Hz, h,h'), 7.35–7.25 (4H, m, i,i',r,r'), 7.25–7.15 (3H, m, j,q,q'), 7.10 (1H, t,  $J = 7.4$  Hz, s), 5.65–5.50 (2H, m, l,m), 4.55–4.45 (1H, m, d), 3.51 (1H, br s, OH), 2.71 (2H, t,  $J = 7.3$  Hz, o), 2.61 (1H, dd,  $J = 13.9$  Hz and 6.1 Hz, k), 2.45–2.35 (2H, m, b), 2.35–2.20 (2H, m, k,n), 2.12 (1H, d,  $J = 15.0$  Hz, e), 1.90–1.70 (4H, m, c,e,n);  $^{13}\text{C}$  NMR (100 MHz,  $\text{CDCl}_3$ )  $\delta$  177.56 (f), 141.81 (p), 138.82 (g), 133.54 (m), 128.90 (i,i'), 128.49 (r,r'), 128.31 (j), 127.18 (l), 125.81 (q,q'), 123.81(s), 119.72 (h,h'), 74.81 (d), 52.75 (a), 44.15 (e), 41.86 (k), 36.56 (n), 36.06 (c), 35.86 (o), 34.36 (b); IR (neat) 3296 (O-H stretch), 2935 (N-H stretch), 1660 (C=O stretch), 1597 (C=C stretch), 1555 (C-OH

bend), 1497, 1442, 1333, 1308 (C-N stretch), 1254, 960, 907, 752, 692  $\text{cm}^{-1}$ ; HRMS (ESI) calcd. for  $\text{C}_{23}\text{H}_{27}\text{NaNO}_2$  (M+Na): 372.1939, found 372.1939  $m/z$ .

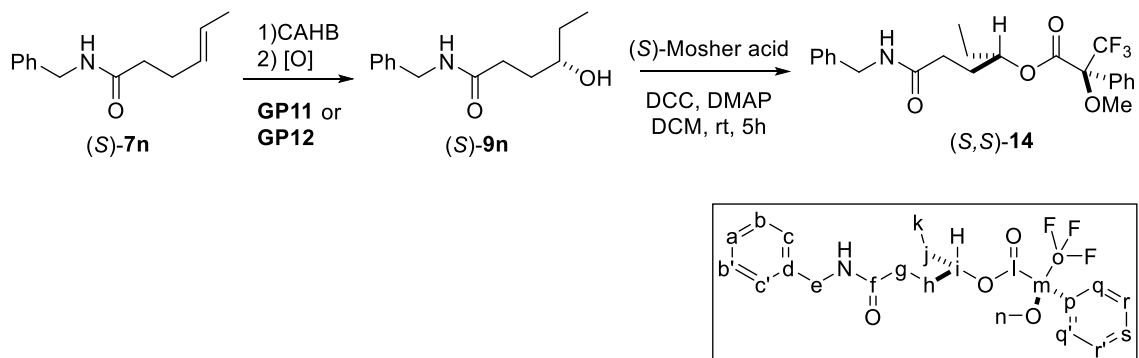


**(1*S*,3*S*)-3-hydroxy-1-(2-methylallyl)cyclopentanecarboxylic acid phenyl amide (26i).**

Following **GP12** with 2.0 mol%  $[\text{Rh}(\text{nbd})_2\text{BF}_4/ 2(R)\text{-B2}]$ , 2 equiv tmdBH, and **23i** (127.5 mg, 0.528 mmol) affords, after flash chromatography on silica gel (90:10 dichloromethane:ethyl acetate), the title compound (102.5 mg, 75%) as a white solid: mp 76.5–78.5  $^{\circ}\text{C}$ ; TLC analysis  $R_f$  0.6 (80:20 dichloromethane:ethyl acetate);  $[\alpha]_D^{20} = +10^{\circ}$  ( $c$  1.7,  $\text{CHCl}_3$ ); Chiral HPLC analysis (Chiralpak-AD, 80:20 hexanes:isopropanol, flowrate = 1.0 mL/min) showed peaks at 16 minutes (97.0% (1*S*,3*S*)) and 21 minutes (3.0% (1*R*,3*R*));  $^1\text{H}$  NMR (300 MHz,  $\text{CDCl}_3$ )  $\delta$  8.75 (1H, br s, NH), 7.52 (2H, d,  $J = 7.6$  Hz, h,h'), 7.31 (2H, t,  $J = 7.6$  Hz, i,i'), 7.10 (1H, t,  $J = 7.4$  Hz, j), 4.89 (1H, s, m), 4.72 (1H, s, m), 4.55–4.45 (1H, m, d), 3.46 (1H, br s, OH), 2.93 (1H, d,  $J = 15.4$  Hz, k), 2.40–2.30 (2H, m, b,e), 2.16 (1H, d,  $J = 15.4$  Hz, k), 2.20–1.80 (4H, m, b,c,e), 1.76 (3H, s, n);  $^{13}\text{C}$  NMR (75 MHz,  $\text{CDCl}_3$ )  $\delta$  177.01 (f), 143.01 (l), 138.57 (g), 128.90 (i,i'), 124.01 (j), 119.98 (h,h'), 113.76 (m), 74.29 (d), 52.79 (a), 47.14 (k), 44.38 (e), 38.60 (b), 35.45 (c), 23.86 (n); IR (neat) 3348 (O-H stretch), 3081 (N-H stretch), 2954, 2916, 1653 (C=O stretch), 1621, 1597 (C=C stretch), 1556 (C-OH bend), 1499, 1442, 1352 1307 (C-N stretch), 1259, 1072, 1027, 970, 959, 891, 750, 688  $\text{cm}^{-1}$ ; HRMS (ESI) calcd. for  $\text{C}_{16}\text{H}_{21}\text{NaNO}_2$  (M+Na): 282.1470, found 282.1459  $m/z$ .



**General procedure for preparation of Mosher's esters via CAHB/ oxidations and DCC condensation with (S)-Mosher acid (GP13): checking ee or determine absolute configuration purpose.**



**(S)-6-(benzylamino)-6-oxohexan-3-yl**

**(S)-3,3,3-trifluoro-2-methoxy-2-**

**phenylpropanoate ((S,S)-14).** Following **GP12** – CAHB/ oxidation of **7n** described

above to afford **(S)-9n**; to a solution of **9n** (0.06 mmol, 13.2 mg) and (S)-Mosher acid

(3.1 equiv, 0.186 mmol, 44 mg) in DCM (1 mL) was added DCC (3.1 equiv, 0.186 mmol,

38.6 mg) and DMAP (3.1 equiv, 0.186 mmol, 22.8 mg). The resultant mixture was stirred

at room temp for 5h then concentrated under vacuum. Flash column chromatography

(80:20-50:50 hexanes:ethyl acetate) affords the title compound (24 mg, 92%) as a white

semi-solid; TLC analysis  $R_f$  0.5 (50:50 hexanes:ethyl acetate);  $[\alpha]_D^{20} = -34.5^\circ$  ( $c$  1.87,

$\text{CHCl}_3$ );  $^{19}\text{F}$  NMR (376 MHz,  $\text{CDCl}_3$ )  $\delta$  -71.01 (s, 5%, minor,  $\text{CF}_3$ ), -71.08 (s, 95%,

major,  $\text{CF}_3$ );  $^1\text{H}$  NMR (400 MHz,  $\text{CDCl}_3$ )  $\delta$  7.50–7.60 (2H, m, r,r'), 7.25–7.45 (8H,

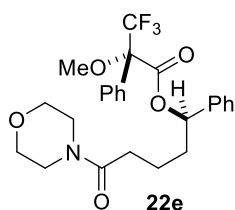
a,b,b',c,c',q,q',s), 5.74 (0.94H, br s, major NH), 5.52 (0.05H, br s, minor NH), 5.00–5.15

(1H, m, i), 4.44 (2H, d,  $J = 5.7$  Hz, e), 3.54 (3H, s, n), 2.05–2.30 (3H, m, g,h), 1.95–2.05

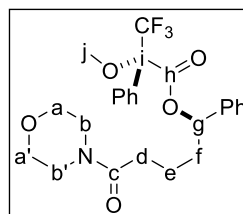
(1H, m, h), 1.60–1.70 (2H, m, j), 0.96 (0.12H, t,  $J = 7.4$  Hz, minor k), 0.86 (2.89H, t,  $J =$

7.4 Hz, major k);  $^{13}\text{C}$  NMR (100 MHz,  $\text{CDCl}_3$ )  $\delta$  171.60 (f), 166.59 (l), 138.26 (d),

132.26 (p), 129.74 (r,r'), 128.85 (b,b'), 128.57 (q,q'), 127.98 (c,c'), 127.70 (s), 127.54 (a), 123.50 (q,  $J = 287$  Hz, o), 84.79 and 84.52 (m), 78.16 (i), 55.47 (n), 43.82 (e), 32.21 (g), 29.38 (h), 26.82 (j), 9.37 (k); IR (neat) 3293 (N-H stretch), 2970, 2935, 1741 (C=O stretch), 1644 (C=O stretch), 1545 (N-H bend), 1452, 1258, 1165, 1121, 1016, 992, 715, 696  $\text{cm}^{-1}$ ; HRMS (ESI) calcd. for  $\text{C}_{23}\text{H}_{26}\text{F}_3\text{NNaO}_4$  (M+Na): 460.1712, found 460.1729  $m/z$ .



Molecular Weight: 479.4962



**(R)-5-morpholino-5-oxo-1-phenylpentyl**

**(S)-3,3,3-trifluoro-2-methoxy-2-**

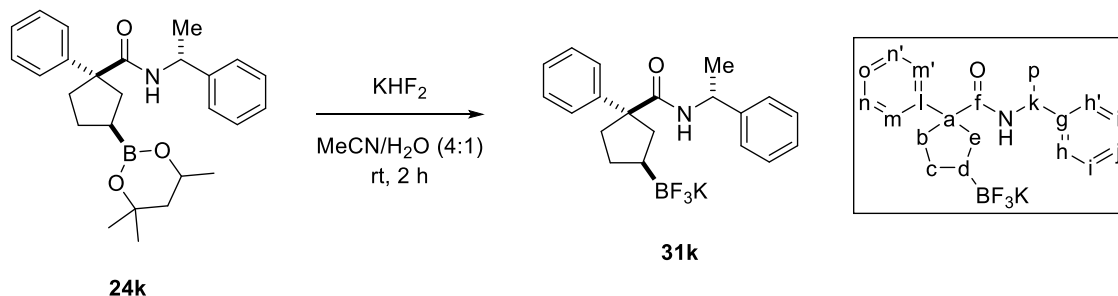
**phenylpropanoate (22e).** CAHB without oxidation described in **GP10** affords **19e**.

Boronic ester **19e** (0.06 mmol, 15.8 mg) was then oxidized with  $\text{NaBO}_3$  (**GP11**) to generate the crude corresponding alcohol subjected to **GP13**, affords, after flash column chromatography (80:20-50:50 hexanes:ethyl acetate) the title compound (26 mg, 90%) as a white semi-solid; TLC analysis  $R_f$  0.5 (50:50 hexanes:ethyl acetate);  $^{19}\text{F}$  NMR (375 MHz,  $\text{CDCl}_3$ )  $\delta$  -71.22 (s,  $\text{CF}_3$ , major 95.5%) and -71.61 (s,  $\text{CF}_3$ , minor 4.5%);  $^1\text{H}$  NMR (400 MHz,  $\text{CDCl}_3$ )  $\delta$  7.20–7.45 (10H, m, aryl), 6.01 (0.955H, t,  $J = 6.4$  Hz, g major), 5.93 (0.045H, t,  $J = 7.0$  Hz, g minor), 3.50–3.70 (6H, m, a,a',b,a'), 3.46 (3H, s, j), 3.35–3.40 (2H, m, b,b'), 2.28 (2H, t,  $J = 7.3$  Hz, d), 2.00–2.10 (1H, m, f), 1.85–2.00 (1H, m, f), 1.55–1.75 (2H, m, e);  $^{13}\text{C}$  NMR (100 MHz,  $\text{CDCl}_3$ )  $\delta$  170.01, 166.11, 138.88, 132.38, 129.66, 128.73, 128.70, 128.45, 127.55, 127.08, 78.55, 67.01, 66.68, 55.49, 45.98, 41.98, 35.41, 32.45, 20.93.

The two Mosher's esters above (i.e., **14** and **22e**) are isolated for proof of CAHB absolute configuration purpose; other benzylic boronic esters **19** applied this method to determine the ee were run at 0.02 mmol scale and the Mosher's esters were not isolated; the crude  $^{19}\text{F}$  NMR are essentially clean to obtain the ee.

## 5.4 Procedures for preparation of trifluoroborate salts from boronic esters

### General procedure for the preparation of potassium trifluoroborate salts (GP14).<sup>24</sup>



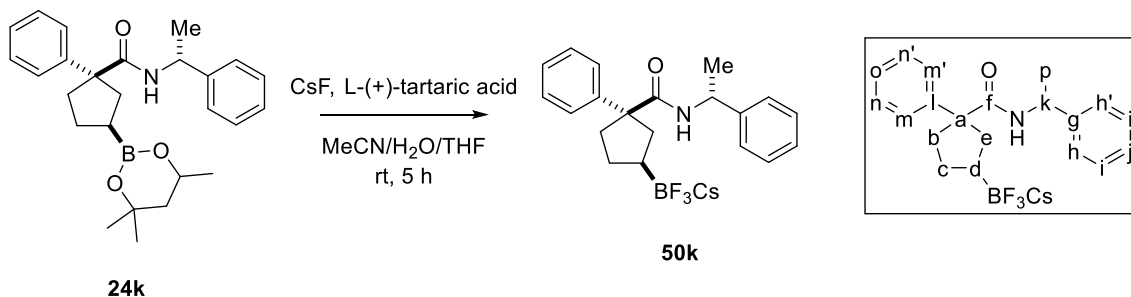
### Preparation of (1*R*,3*S*)-1-phenyl-*N*-((*R*)-1-phenylethyl)-3-

(trifluoroborato)cyclopentane-1-carboxamide, potassium salt (**31k**). To a solution of  $\gamma$ -dioxaborato amide **24k** (839 mg, 2.0 mmol, 1.0 equiv) in acetonitrile (MeCN, 4.0 mL) was slowly added a solution of KHF<sub>2</sub> (467 mg, 6.0 mmol, 3.0 equiv) in H<sub>2</sub>O (1.2 mL). After a 2 h stir, the reaction mixture was concentrated under reduced pressure and allowed to dry under vacuum. The resultant crude solid was extracted with acetone (2 x 5 mL) and the combined organic extracts were concentrated under reduced pressure. Diethyl ether (10.0 mL) was added to precipitate the product. Filtration affords the title compound (575 mg, 72%) as a white solid: mp 214.0–216.0 °C; [ $\alpha$ ]<sub>D</sub><sup>20</sup> = +17° (*c* 1.0, MeOH); <sup>19</sup>F NMR (282 MHz, MeOD)  $\delta$  -147.27 (s, BF<sub>3</sub>K); <sup>1</sup>H NMR (300 MHz, MeOD)  $\delta$  7.40 (2H, d, *J* = 7.5 Hz, h,h'), 7.35–7.10 (8H, m, i,i',j,m,m',n,n',o), 5.00–4.90 (1H, m, k), 2.30–2.10 (2H, m, b,e), 1.65–1.55 (2H, m, c), 1.36 (3H, d, *J* = 7.0 Hz, p), 1.05–0.85 (1H, m, d); <sup>13</sup>C NMR (75 MHz, MeOD)  $\delta$  178.16 (f), 145.39 (l), 144.11 (g), 127.86 (i,i'), 127.68 (n,n'), 126.58 (h,h'), 126.29 (m,m'), 125.69 (j), 125.61 (o), 60.20 (a), 48.86 (k), 38.82 (b), 37.25 (e), 26.24 (c), 20.78 (p); IR (neat) 3438 (N-H stretch), 2941, 2867, 1662 (C=O stretch), 1500 (N-H bend), 1461, 1446, 1320 (C-N stretch), 1172, 997, 958, 890,

696  $\text{cm}^{-1}$ ; HRMS (ESI) calcd. for  $\text{C}_{20}\text{H}_{22}\text{BF}_3\text{NO}$  (M-K): 360.1747, found 360.1761  $m/z$ .

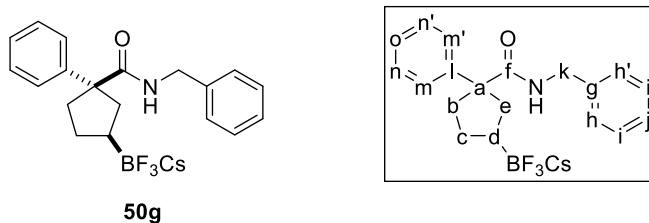
The salt was recrystallized (3:1  $\text{Et}_2\text{O}/\text{MeOH}$ ) to give off-white single crystals, and an X-ray crystal structure was obtained.

**General procedure for the preparation of cesium trifluoroborate salts (GP15).**<sup>25</sup>

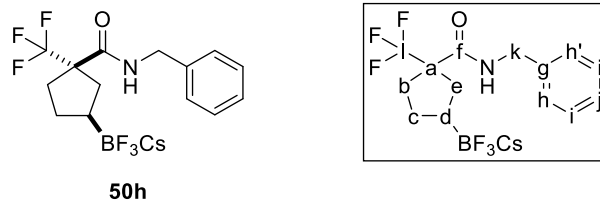


**Preparation of (1*R*,3*S*)-1-phenyl-*N*-((*R*)-1-phenylethyl)-3-(trifluoroborato)cyclopentane-1-carboxamide, cesium salt (50k).** To a solution of  $\gamma$ -dioxaborato amide **24k** (839 mg, 2.0 mmol, 1.0 equiv) in acetonitrile (MeCN, 8.0 mL) was added a solution of CsF (1.21 g, 8.0 mmol, 4.0 equiv) in  $\text{H}_2\text{O}$  (0.8 mL). The resultant mixture was stirred at room temp for 2 mins, and a solution of L-(+)-tartaric acid (614 mg, 4.1 mmol, 2.05 equiv) in THF (3.0 mL) was added dropwise. After a 5 h stir, the mixture was filtered, washed through with more MeCN, and the filtrate was concentrated under reduced pressure to afford the crude mixture of trifluoroborate salt. Afterward, diethyl ether was added to the crude mixture to dissolve undesired products. Following a decantation to remove the solvent and undesired products, the precipitate was further dried under vacuum to afford the title compound (947 mg, 96%) as an off-white solid: mp 246.0–247.5  $^{\circ}\text{C}$ ;  $[\alpha]_{\text{D}}^{20} = +16^{\circ}$  ( $c$  1.0, MeOH);  $^{19}\text{F}$  NMR (376 MHz, MeOD)  $\delta$  -145.41 (s,  $\text{BF}_3\text{Cs}$ );  $^1\text{H}$  NMR (400 MHz, MeOD)  $\delta$  7.40 (2H, d,  $J = 7.3$  Hz, h,h'), 7.35–7.15 (8H, m, i,i',j,m,m',n,n',o), 5.00–4.90 (1H, m, k), 2.35–2.20 (2H, m, b,e), 2.20–2.00 (2H, m, b,e), 1.70–1.55 (2H, m, c), 1.37 (3H, d,  $J = 7.0$  Hz, p), 1.05–0.80 (1H, m, d);  $^{13}\text{C}$  NMR (100

MHz, MeOD)  $\delta$  178.21 (f), 145.43 (l), 144.20 (g), 127.90 (i,i'), 127.69 (n,n'), 126.60 (h,h'), 126.32 (m,m'), 125.71 (j), 125.64 (o), 60.21 (a), 48.93 (k), 38.86 (b), 37.30 (e), 26.28 (c), 20.81 (p); IR (neat) 3441 (N-H stretch), 2941, 2851, 2830, 1659 (C=O stretch), 1497 (N-H bend), 1297 (C-N stretch), 929, 895, 696  $\text{cm}^{-1}$ ; HRMS (ESI) calcd. for  $\text{C}_{20}\text{H}_{22}\text{BF}_3\text{NO}$  (M-Cs): 360.1747, found 360.1736  $m/z$ .

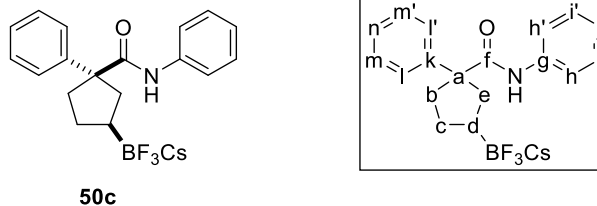


**(1R,3S)-1-phenyl-3-(trifluoroborato)1-1-cyclopentanecarboxylic acid benzyl amide, cesium salt (50g).** Following **GP15** with **24g** (203 mg, 0.50 mmol, 1.0 equiv) affords the title compound (196 mg, 82 %) as the white solid: mp 167.5–169.0 °C;  $[\alpha]_{\text{D}}^{20} = +3.2^\circ$  (c 1.0, MeOH);  $^{19}\text{F}$  NMR (376 MHz, MeOD)  $\delta$  -144.61 (s,  $\text{BF}_3\text{Cs}$ );  $^1\text{H}$  NMR (400 MHz, MeOD)  $\delta$  7.44 (2H, d,  $J = 7.2$  Hz, h,h'), 7.30 (2H, t,  $J = 7.4$  Hz, n,n'), 7.25–7.15 (4H, m, i,i',j,o), 7.12 (2H, d,  $J = 6.8$  Hz, m,m'), 4.40–4.25 (2H, m, k), 2.35–2.25 (2H, m, b,e), 2.20–2.05 (2H, m, b,e), 1.65–1.55 (2H, m, c), 1.05–0.85 (1H, m, d);  $^{13}\text{C}$  NMR (100 MHz, MeOD)  $\delta$  179.07 (f), 145.12 (l), 139.22 (g), 127.91 (i,i'), 127.79 (n,n'), 126.67 (h,h'), 126.59 (m,m'), 126.40 (j), 125.81 (o), 60.24 (a), 42.66 (k), 38.79 (b), 37.22 (e), 26.17 (c); IR (neat) 3354 (N-H stretch), 2936, 2872, 1656 (C=O stretch), 1628 (C=C stretch), 1514 (N-H bend), 1443, 1287 (C-N stretch), 1091, 948, 919, 897, 728, 696  $\text{cm}^{-1}$ ; HRMS (ESI) calcd. for  $\text{C}_{19}\text{H}_{20}\text{BF}_3\text{NO}$  (M-Cs): 346.1590, found 346.1573  $m/z$ .

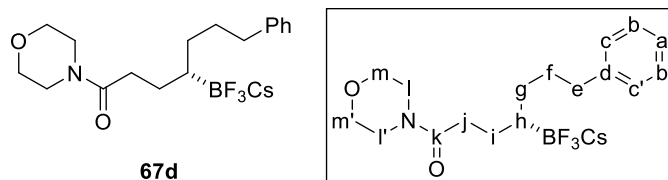


**(1*R*,3*S*)-1-trifluoromethyl-3-(trifluoroborato)-1-cyclopentanecarboxylic acid benzyl amide, cesium salt (50h).** Following **GP10** with **23h** (142.5 mg, 0.528 mmol) affords, after passing through a short pad of silica gel and concentrating under reduced pressure, the crude  $\gamma$ -dioxaborato amide **24h** as the dark oil used in the next step without further purification.

Following **GP15** with **24h** (200 mg, 0.50 mmol, 1.0 equiv) affords the title compound (147 mg, 59%, 2 steps) as a white foamy solid: mp 73.0–75.5 °C;  $[\alpha]_D^{20} = -26^\circ$  (*c* 2.0, CHCl<sub>3</sub>); <sup>19</sup>F NMR (376 MHz, CDCl<sub>3</sub>)  $\delta$  -69.90 (s, CF<sub>3</sub>), -133.70 (s, BF<sub>3</sub>Cs); <sup>1</sup>H NMR (400 MHz, CDCl<sub>3</sub>)  $\delta$  7.30–7.25 (2H, m, i,i'), 7.21 (1H, d, *J* = 7.1 Hz, j), 7.17 (1H, d, *J* = 7.0 Hz, h,h'), 6.51 (1H, br s, NH), 4.35 (2H, d, *J* = 5.2 Hz, k), 2.20–2.05 (2H, m, b,e), 2.05–1.95 (2H, m, e), 1.90–1.85 (1H, m, b), 1.75–1.60 (1H, m, c), 1.45–1.30 (1H, m, c), 1.05–0.85 (1H, m, d); <sup>13</sup>C NMR (100 MHz, CDCl<sub>3</sub>)  $\delta$  171.29 (f), 138.16 (g), 128.76 (i,i'), 127.46 (j), 127.11 (h,h'), 59.85 (q, *J* = 93.3 Hz, a), 43.95 (k), 34.84 (b), 33.71 (e), 29.37 (c); IR (neat) 3373 (N-H stretch), 2956, 2870, 1657 (C=O stretch), 1523 (N-H bend), 1497, 1454, 1293 (C-N stretch), 1273, 1146, 1090, 1001, 926, 895, 729, 697 cm<sup>-1</sup>; HRMS (ESI) calcd. for C<sub>14</sub>H<sub>15</sub>BF<sub>6</sub>NO (M-Cs): 338.1151, found 338.1179 *m/z*.



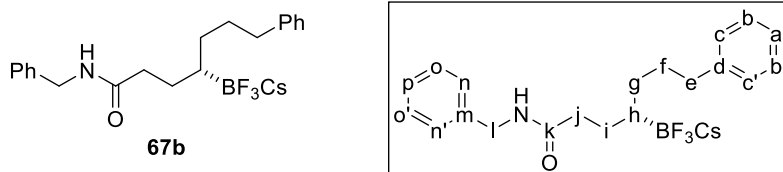
**(1*R*,3*S*)-1-phenyl-3-(trifluoroborato)-1-cyclopentanecarboxylic acid phenyl amide, cesium salt (50c).** Following **GP15** with **24c** (196 mg, 0.50 mmol, 1.0 equiv) affords the title compound (186 mg, 80 %) as the white solid: mp 173.5–177.0 °C;  $[\alpha]_D^{20} = +11^\circ$  (*c* 1.0, MeOH);  $^{19}\text{F}$  NMR (376 MHz, MeOD)  $\delta$  -144.25 (s,  $\text{BF}_3\text{Cs}$ );  $^1\text{H}$  NMR (400 MHz, MeOD)  $\delta$  7.50–7.40 (4H, m, h,h',l,l'), 7.33 (2H, t,  $J = 7.4$  Hz, m,m'), 7.26 (2H, t,  $J = 7.5$  Hz, i,i'), 7.21 (1H, t,  $J = 7.3$  Hz, j), 7.06 (1H, t,  $J = 7.4$  Hz, n), 2.50–2.30 (2H, m, b,e), 2.30–2.10 (2H, m, b,e), 1.75–1.60 (2H, m, c), 1.10–0.95 (1H, m, d);  $^{13}\text{C}$  NMR (100 MHz, MeOD)  $\delta$  177.61 (f), 145.34 (k), 138.55 (g), 128.18 (i,i'), 127.89 (m,m'), 126.51 (l,l'), 125.89 (j), 123.79 (n), 120.85 (h,h'), 61.13 (a), 38.97 (b), 37.77 (e), 26.60 (c); IR (neat) 3402 (N-H stretch), 2947, 2842, 1663 (C=O stretch), 1596 (C=C stretch), 1516 (N-H bend), 1493, 1436, 1311 (C-N stretch), 1241, 1080, 994, 901, 897, 745, 696  $\text{cm}^{-1}$ ; HRMS (ESI) calcd. for  $\text{C}_{18}\text{H}_{18}\text{BF}_3\text{NO}$  (M-Cs): 332.1434, found 332.1426  $m/z$ .



**(*S*)-7-phenyl-4-(trifluoroborato)heptanecarboxylic acid morpholino amide, cesium salt (67d).** Following **GP15** with **8d** (803 mg, 2.0 mmol, 1.0 equiv) afford the title compound (874 mg, 92%) as an off-white foamy solid: mp 61.5–62.5 °C;  $[\alpha]_D^{20} = +0.5^\circ$  (*c* 1.0,  $\text{CHCl}_3$ );  $^{19}\text{F}$  NMR (376 MHz,  $\text{CDCl}_3$ )  $\delta$  -133.36 (s,  $\text{BF}_3\text{Cs}$ );  $^1\text{H}$  NMR (400 MHz,  $\text{CDCl}_3$ )  $\delta$  7.25–7.30 (2H, m, b,b'), 7.15–7.20 (3H, m, a,c,c'), 3.55–3.60 (4H, m,



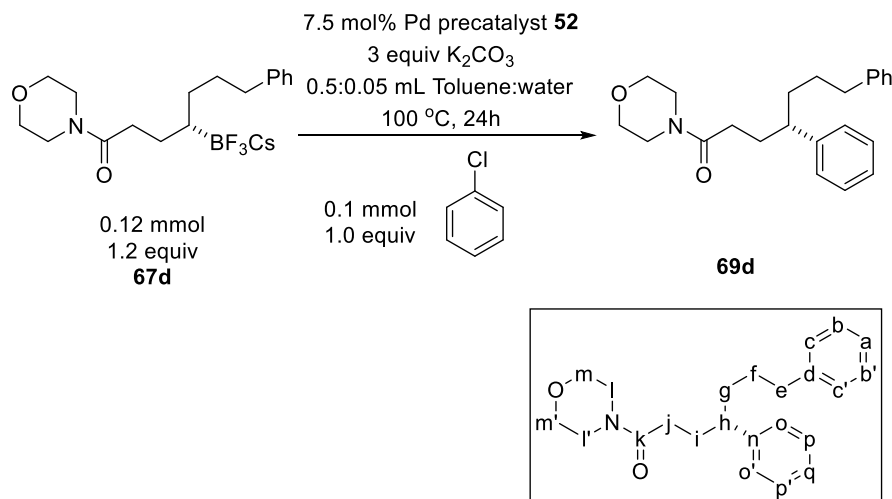
m,m'), 3.45–3.55 (2H, m, l,l'), 3.30–3.40 (2H, m, l,l'), 2.58 (2H, t,  $J = 6.9$  Hz, e), 2.25–2.35 (1H, m, j), 2.15–2.25 (1H, m, j), 1.50–1.70 (3H, m, f,i), 1.30–1.45 (2H, m, g,i), 1.10–1.25 (1H, m, g), 0.25–0.40 (1H, m, h);  $^{13}\text{C}$  NMR (100 MHz,  $\text{CDCl}_3$ )  $\delta$  173.90 (k), 143.63 (d), 128.68 (b,b'), 128.39 (c,c'), 125.64 (a), 66.94 and 66.86 (m,m'), 46.28 and 41.86 (l,l'), 36.70 (e), 31.79 (j), 31.07 (f), 30.09 (g), 26.60 (i); IR (neat) 2908, 2854, 1609 ( $\text{C}=\text{O}$  stretch), 1461 (N-H bend), 1434, 1240 ( $\text{C}-\text{N}$  stretch), 1114, 1064, 957, 932, 742, 702  $\text{cm}^{-1}$ ; HRMS (ESI) calcd. for  $\text{C}_{17}\text{H}_{24}\text{BF}_3\text{NO}_2$  (M-Cs): 342.1852, found 342.1852  $m/z$ .



**(S)-7-phenyl-4-(trifluoroborato)heptanecarboxylic acid benzyl amide, cesium salt (67b).** Following **GP15** with **8b** (421 mg, 1.0 mmol, 1.0 equiv) affords the title compound (396 mg, 80%) as a white foamy solid: mp 57.5–58.5 °C;  $[\alpha]_{\text{D}}^{20} = -2.9^\circ$  ( $c$  1.0, MeOH);  $^{19}\text{F}$  NMR (376 MHz, MeOD)  $\delta$  -131.52 (s,  $\text{BF}_3\text{Cs}$ );  $^1\text{H}$  NMR (400 MHz, MeOD)  $\delta$  7.00–7.40 (10H, m, a,b,b',c,c',n,n',o,o',p), 4.36 (2H, s, l), 2.56 (2H, t,  $J = 7.7$  Hz, e), 2.30 (2H, t,  $J = 8.1$  Hz, j), 1.55–1.80 (4H, m, f,i), 1.40–1.55 (1H, m, g), 1.20–1.30 (1H, m, g), 0.30–0.50 (1H, m, h);  $^{13}\text{C}$  NMR (100 MHz, MeOD)  $\delta$  177.08 (k), 143.66 (d), 138.97 (m), 128.16 (b,b'), 128.14 (o,o'), 127.76 (n,n'), 127.16 (c,c'), 126.74 (p), 124.94 (a), 42.67 (l), 36.67 (e), 36.01 (j), 31.06 (f), 30.79 (g), 27.83 (i); IR (neat) 3408 (N-H stretch), 3294 2919, 2852, 1640 ( $\text{C}=\text{O}$  stretch), 1521, 1495, 1452 (N-H bend), 1528, 912, 744, 697  $\text{cm}^{-1}$ ; HRMS (ESI) calcd. for  $\text{C}_{20}\text{H}_{24}\text{BF}_3\text{NO}$  (M-Cs): 362.1903, found 362.1897  $m/z$ .

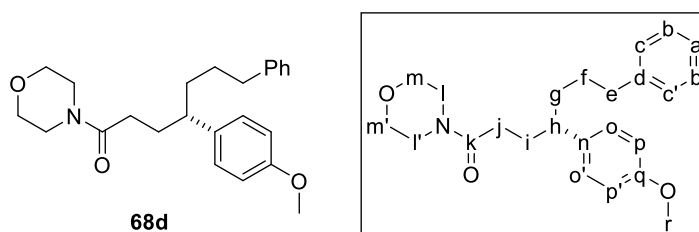
## 5.5 Procedures for directed Suzuki–Miyaura reactions

### General procedure for Suzuki-Miyaura cross-coupling reactions of secondary acyclic $\gamma$ -trifluoroborato amides (GP16).



**(S)-4,7-diphenylheptanecarboxylic acid morpholino amide ((S)-69d).** An 8-mL vial was charged with Buchwald cataCXium® A Pd G3 precatalyst **52** (5.5 mg, 0.0075 mmol, 0.075 equiv),  $K_2CO_3$  (42 mg, 0.3 mmol, 3.0 equiv),  $\gamma$ -trifluoroborato amide **67d** (57 mg, 0.12 mmol, 1.2 equiv), chlorobenzene (11.3 mg, 0.1 mmol, 1.0 equiv), toluene (0.5 mL), and water (0.05 mL). The resultant mixture was stirred at 100 °C for 24 h. After cooling to room temperature, the organic layer was separated, and water (1.0 mL) was added to the aqueous layer following by extraction with ethyl acetate (2 x 2 mL). The combined organic extracts were dried (anhyd.  $Na_2SO_4$ ) and concentrated under reduced pressure. Flash chromatography on silica gel (95:5–80:20 DCM:ethyl acetate) affords the title compound (22 mg, 63%) as a yellow oil; TLC analysis  $R_f = 0.4$  (80:20 DCM:ethyl acetate);  $[\alpha]_D^{20} = -3.7^\circ$  ( $c$  1.0,  $CHCl_3$ ); Chiral HPLC analysis (Chiralpak-IC, 80:20 hexanes:isopropanol, flowrate = 1.5 mL/min) showed peaks at 75 minutes (6.5% (*R*)) and 81 minutes (93.5% (*S*));  $^1H$  NMR (400 MHz,  $CDCl_3$ )  $\delta$  7.05–7.35 (10H, m,

a,b,b',c,c',o,o',p,p',q), 3.50–3.65 (6H, m, l,l',m,m'), 3.10–3.30 (2H, m, l,l'), 2.50–2.65 (3H, m, e,h), 2.05–2.15 (3H, m, i,j), 1.80–1.90 (1H, m, i), 1.60–1.75 (2H, m, g), 1.45–1.60 (2H, m, f);  $^{13}\text{C}$  NMR (100 MHz,  $\text{CDCl}_3$ )  $\delta$  171.72 (k), 144.84 (d), 142.55 (n), 128.60 (b,b'), 128.49 (p,p'), 128.33 (c,c'), 127.79 (o,o'), 126.42 (a), 125.74 (q), 67.01 and 66.67 (m,m'), 45.88 (l,l'), 45.61 (h), 41.95 (l,l'), 36.76 (g), 36.00 (e), 32.08 (i), 30.97 (j), 29.42 (f); IR (neat) 2919, 2851, 1644 (C=O stretch), 1452, 1426, 1230, 1114, 1029, 747, 699  $\text{cm}^{-1}$ ; HRMS (ESI) calcd. for  $\text{C}_{23}\text{H}_{29}\text{NNaO}_2$  ( $\text{M}+\text{Na}$ ): 374.2096, found 374.2106  $m/z$ .

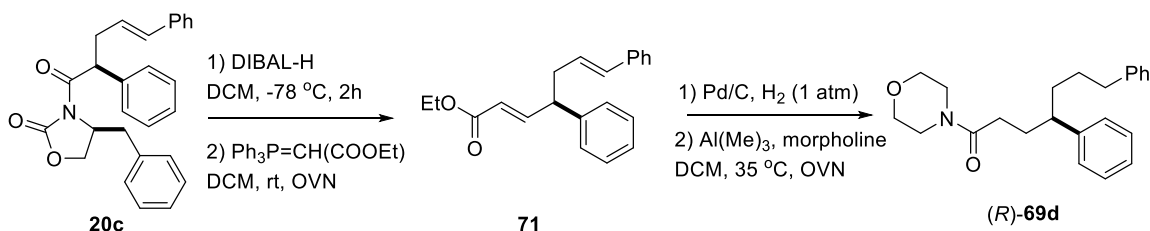


**(S)-4-(4-methoxyphenyl)-7-phenylheptanecarboxylic acid morpholino amide**

**(22c).** Following **GP16** with 4-chloroanisole (14.3 mg, 0.1 mmol, 1.0 equiv) affords, after flash chromatography on silica gel (95:5–80:20 DCM:ethyl acetate), the title compound (19.8 mg, 52%) as a yellow oil; TLC analysis  $R_f$  0.4 (80:20 DCM:ethyl acetate);  $[\alpha]_D^{20} = -7.1^\circ$  ( $c$  2.0,  $\text{CHCl}_3$ ); Chiral HPLC analysis ((*S,S*)-WHELK-O 1, 50:50 hexanes:isopropanol, flow rate = 1.0 mL/min) showed peaks at 25 minutes (6.0% (*R*)) and 28 minutes (94.0% (*S*));  $^1\text{H}$  NMR (400 MHz,  $\text{CDCl}_3$ )  $\delta$  7.26 (2H, t,  $J = 7.2$  Hz, o,o'), 7.17 (1H, t,  $J = 7.3$  Hz, a), 7.11 (2H, d,  $J = 7.1$  Hz, c,c'), 7.06 (2H, d,  $J = 8.6$  Hz, b,b'), 6.85 (2H, d,  $J = 8.6$  Hz, p,p'), 3.81 (3H, s, r), 3.60–3.65 (2H, m, m,m'), 3.55–3.60 (4H, m, l,l',m,m'), 3.15–3.30 (2H, m, l,l'), 2.45–2.65 (3H, m, e,h), 2.00–2.15 (3H, m, i,j), 1.75–1.85 (1H, m, i), 1.45–1.75 (4H, m, f,g);  $^{13}\text{C}$  NMR (100 MHz,  $\text{CDCl}_3$ )  $\delta$  171.80 (k), 158.12 (q), 142.60 (d), 136.77 (n), 128.61 (b,b'), 128.49 (c,c'), 128.32 (o,o'), 125.72 (a),

113.96 (p,p'), 67.02 and 66.69 (m,m'), 55.34 (r), 45.90 (l,l'), 44.76 (h), 41.95 (l,l'), 36.93 (g), 36.01 (e), 32.25 (i), 31.02 (j), 29.44 (f); IR (neat) 2920, 2852, 1643 (C=O stretch), 1510, 1426, 1244, 1113, 1030, 831, 700  $\text{cm}^{-1}$ ; HRMS (ESI) calcd. for  $\text{C}_{24}\text{H}_{31}\text{NNaO}_3$  (M+Na): 404.2202, found 404.2213  $m/z$ .

### An alternative synthetic route for (R)-69d



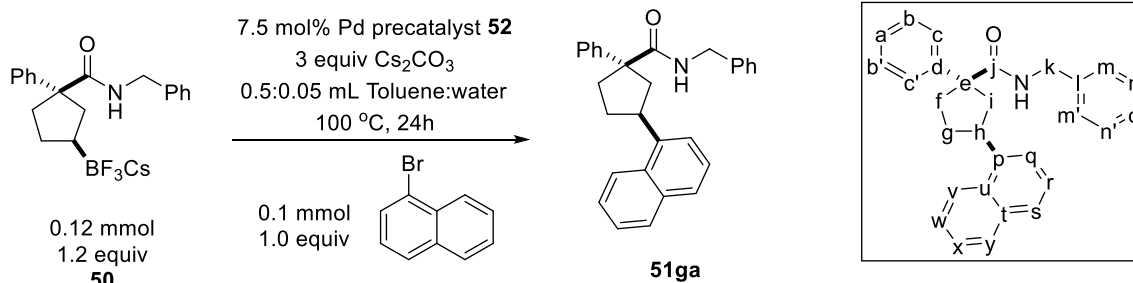
To a cooled ( $-78\text{ }^\circ\text{C}$ ) solution of **20c** (via **GP6** *vide supra*) (0.38 mmol, 156 mg) in DCM (2 mL) was added dropwise a solution of DIBAL-H (2 equiv, 1M, 0.76 mmol, 0.76 mL) dropwise. The resultant mixture was stirred at  $-78\text{ }^\circ\text{C}$  for 2h. After quenching with satd.  $\text{NH}_4\text{Cl}$  (1 mL), the Wittig reagent ( $\text{Ph}_3\text{P=CH(COOEt)}$ ), 1.2 equiv, 0.456 mmol, 160 mg) in DCM (1 mL) was added dropwise. The resultant mixture was stirred OVN at room temp and passed through a pad of celite and washed with DCM (3 x 3 mL). The filtrate was concentrated under reduced pressure to give a crude **71** (61.7 mg, 53%) used in the next step without further purification.

A solution of **71** (0.18 mmol, 55 mg) and Pd/C (10%, 0.1 equiv) in methanol (1 mL) was stirred under  $\text{H}_2$  (1 atm) for 5h. The resultant mixture was passed through a pad of celite and concentrated under reduced pressure to give a crude reduced product (55 mg, 99%) used in the next step without further purification.

Following **GP1** with the obtained reduced product (0.16 mmol, 50 mg) affords, after column chromatography (95:5–80:20 DCM:ethyl acetate), the title compound (*R*)-**69d** (40.2 mg, 71%) as a yellow oil; TLC analysis  $R_f = 0.4$  (80:20 DCM:ethyl acetate);  $[\alpha]_D^{20} = +3.2^\circ$  ( $c$  1.0,  $\text{CHCl}_3$ ); (Chiralpak-IC, 80:20 hexanes:isopropanol, flowrate = 1.5 mL/min) showed peaks at 74 minutes (82.0% (*R*)) and 80 minutes (18.0% (*S*)); spectroscopic data matched with (*S*)-**69d** obtained from Suzuki-Miyaura cross-coupling of (*S*)-**67d**.

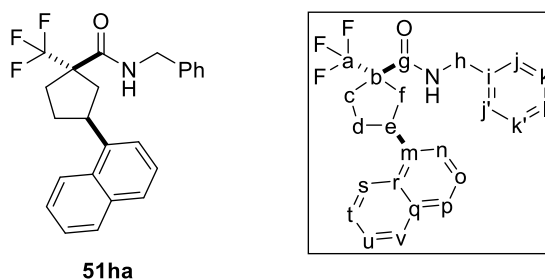
### General procedure for Suzuki-Miyaura cross-coupling reactions of secondary cyclic

#### $\gamma$ -trifluoroborato amides (GP16).



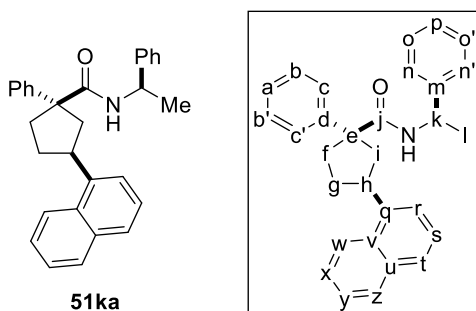
**(1*R*,3*S*)-3-(naphthalen-1-yl)-1-phenylcyclopentanecarboxylic acid benzyl amide (51ga)**. An 8-mL vial was charged with Pd precatalyst **52** (5.5 mg, 0.0075 mmol, 0.075 equiv),  $\text{Cs}_2\text{CO}_3$  (98 mg, 0.3 mmol, 3.0 equiv),  $\gamma$ -trifluoroborato amide **50g** ( $\text{R}^1 = \text{CF}_3$ ,  $\text{R}^2 = \text{CH}_2\text{Ph}$ ,  $\text{M} = \text{Cs}$ ) (57.5 mg, 0.12 mmol, 1.2 equiv), 1-bromonaphthalene **53** (20.7 mg, 0.1 mmol, 1.0 equiv), toluene (0.5 mL), and water (0.05 mL). The resultant mixture was stirred at 100 °C for 24 h. After cooling to room temperature, the organic layer was separated, and water (1.0 mL) was added to the aqueous layer following by extraction with ethyl acetate (2 x 2 mL). The combined organic extracts were dried (anhyd.  $\text{Na}_2\text{SO}_4$ ) and concentrated under reduced pressure. Flash chromatography on silica gel (90:10–

85:15 hexanes:ethyl acetate) affords the title compound (28.1 mg, 69%) as a yellow oil; TLC analysis  $R_f = 0.55$  (70:30 hexanes:ethyl acetate);  $[\alpha]_D^{20} = -3.2^\circ$  ( $c$  1.3,  $\text{CHCl}_3$ );  $^1\text{H}$  NMR (400 MHz,  $\text{CDCl}_3$ )  $\delta$  8.10–8.00 (1H, m, v), 7.95–7.85 (1H, m, y), 7.76 (1H, d,  $J = 8.2$  Hz, s), 7.69 (1H, d,  $J = 7.1$  Hz, q), 7.60–7.45 (6H, m, a,n,n',o,w,x), 7.40–7.35 (1H, m, r), 7.35–7.25 (4H, m, b,b',m,m'), 7.09 (2H, d,  $J = 6.4$  Hz, c,c'), 5.49 (1H, br s, NH), 4.45–4.35 (2H, m, k), 4.00–3.90 (1H, m, h), 2.95–2.80 (3H, m, f,i), 2.50–2.40 (1H, m, f), 2.40–2.30 (1H, m, g), 2.20–2.10 (1H, m, g);  $^{13}\text{C}$  NMR (100 MHz,  $\text{CDCl}_3$ )  $\delta$  176.52 (j), 143.90 (d), 140.67 (p), 138.47 (l), 133.90 (t), 132.12 (u), 129.12 (n,n'), 128.88 (y), 128.60 (b,b'), 127.30 (r), 127.27 (m,m'), 127.19 (c,c'), 126.97 (o,o'), 126.65 (s), 125.83 (w), 125.70 (a), 125.33 (x), 123.53 (v), 122.65 (q), 58.98 (e), 43.75 (k), 43.69 (i), 39.41 (h), 37.04 (f), 32.59 (g); IR (neat) 3325 (N-H stretch), 1646 (C=O stretch), 1598 (C=C stretch), 1533 (N-H bend), 1449, 1418, 1285, 795, 775, 718, 695  $\text{cm}^{-1}$ ; HRMS (ESI) calcd. for  $\text{C}_{29}\text{H}_{27}\text{NaNO}$  ( $\text{M}+\text{Na}$ ): 428.1990, found 428.1992  $m/z$ .



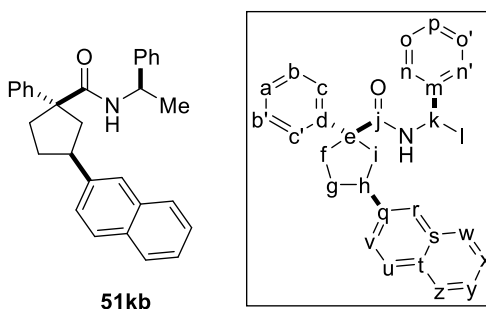
**(1S,3S)-3-(naphthalen-1-yl)-1-(trifluoromethyl)cyclopentanecarboxylic acid benzyl amide (51ha)**. Following **GP16** with 1-bromonaphthalene **53** (20.7 mg, 0.1 mmol, 1.0 equiv), cross-coupling of  $\gamma$ -trifluoroborato amide **50h** (56.5 mg, 0.12 mmol, 1.2 equiv) affords, after flash chromatography on silica gel (90:10 hexanes:ethyl acetate), the title compound (25.0 mg, 63%) as a yellow oil; TLC analysis  $R_f = 0.75$  (70:30 hexanes:ethyl

acetate);  $[\alpha]_{\text{D}}^{20} = -16^{\circ}$  (*c* 0.5,  $\text{CHCl}_3$ );  $^{19}\text{F}$  NMR (376 MHz,  $\text{CDCl}_3$ )  $\delta$  -70.47;  $^1\text{H}$  NMR (400 MHz,  $\text{CDCl}_3$ )  $\delta$  8.11 (1H, d,  $J = 8.4$  Hz, v), 7.90 (1H, dd,  $J = 7.6$  Hz, s), 7.77 (1H, dd,  $J = 7.9$  Hz, n), 7.60–7.40 (4H, m, l,p,t,u), 7.40–7.20 (5H, m, j,j',k,k',o), 6.12 (1H, br s, NH), 4.60–4.45 (2H, m, h), 4.10–3.95 (1H, m, e), 2.80–2.65 (2H, m, c,f), 2.60–2.55 (1H, m, f), 2.40–2.20 (2H, m, c,d), 2.20–2.10 (1H, m, d);  $^{13}\text{C}$  NMR (100 MHz,  $\text{CDCl}_3$ )  $\delta$  169.18 (g), 138.32 (m), 137.61 (i), 133.89 (q), 131.97 (r), 128.96 (v), 128.85 (k,k'), 127.70 (j,j'), 127.53 (o), 127.17 (l), 126.08 (p), 125.66 (t), 125.55 (u), 123.16 (s), 122.40 (n), 58.45 (d,  $J = 24$  Hz, b), 44.41 (h), 41.13 (e), 39.01 (f), 32.70 (d), 31.73 (c); IR (neat) 3341 (N-H stretch), 3052, 2957, 1657 (C=O stretch), 1598 (C=C stretch), 1522 (N-H bend), 1496, 1453, 1287, 1147, 1111, 777, 726, 695  $\text{cm}^{-1}$ ; HRMS (ESI) calcd. for  $\text{C}_{24}\text{H}_{22}\text{F}_3\text{NaNO}$  (M+Na): 420.1551, found 420.1534 *m/z*.



**Preparation of (1R,3S)-3-(naphthalen-1-yl)-1-phenyl-N-((R)-1-phenylethyl)cyclopentane-1-carboxamide (51ka).** Following **GP16** with 1-bromonaphthalene **53** (20.7 mg, 0.1 mmol, 1.0 equiv), cross-coupling of  $\gamma$ -trifluoroborato amide **50k** (59.2 mg, 0.12 mmol, 1.2 equiv) affords, after flash chromatography on silica gel (90:10–85:15 hexanes:ethyl acetate), the title compound (36.0 mg, 86%) as a yellow oil; TLC analysis  $R_f = 0.6$  (70:30 hexanes:ethyl acetate);  $[\alpha]_{\text{D}}^{20} = -20^{\circ}$  (*c* 1.0,  $\text{CHCl}_3$ );  $^1\text{H}$  NMR (400 MHz,  $\text{CDCl}_3$ )  $\delta$  8.05–8.00 (1H, m, w), 7.90–7.85 (1H, m, z), 7.80–7.70 (1H, m, t), 7.70–7.60 (1H, m, y), 7.55–7.45 (7H, m, a,c,c',n,p,o,o'), 7.40–7.35 (1H, m, s),

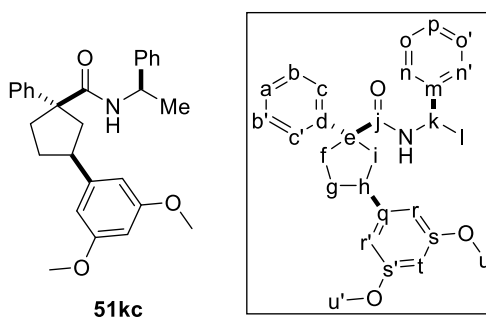
7.30–7.20 (3H, m, n',r,x), 7.07 (2H, d,  $J = 6.9$  Hz, b,b'), 5.34 (1H, br s, NH), 5.20–5.00 (1H, m, k), 4.00–3.85 (1H, m, h), 2.90–2.70 (3H, m, f,i), 2.50–2.40 (1H, m, f), 2.40–2.30 (1H, m, g), 2.20–2.10 (1H, m, g), 1.35 (3H, d,  $J = 6.9$  Hz, l);  $^{13}\text{C}$  NMR (100 MHz,  $\text{CDCl}_3$ )  $\delta$  175.63 (j), 144.10 (d), 143.33 (q), 140.65 (m), 133.87 (u), 132.10 (v), 129.07 (o,o'), 128.86 (z), 128.53 (b,b'), 127.25 (s), 127.08 (n,n'), 126.91 (c,c'), 126.60 (t), 125.83 (p), 125.72 (x), 125.67 (a), 125.29 (r), 123.50 (w), 122.69 (y), 58.94 (e), 48.88 (k), 43.57 (i), 37.47 (h), 37.01 (f), 32.71 (g), 21.82 (l); IR (neat) 3337 (N-H stretch), 3053, 2923, 1644 (C=O stretch), 1597 (C=C stretch), 1493 (N-H bend), 1445, 796, 777, 732, 696  $\text{cm}^{-1}$ ; HRMS (ESI) calcd. for  $\text{C}_{30}\text{H}_{29}\text{NaNO}$  ( $\text{M}+\text{Na}$ ): 442.2147, found 442.2151  $m/z$ .



**(1R,3S)-3-(naphthalen-2-yl)-1-phenyl-N-((R)-1-phenylethyl)cyclopentane-1-carboxamide (51kb).** Following **GP16** with 2-bromonaphthalene **54** (20.7 mg, 0.1 mmol, 1.0 equiv), cross-coupling of  $\gamma$ -trifluoroborato amide **50k** (59.2 mg, 0.12 mmol, 1.2 equiv) affords, after flash chromatography on silica gel (90:10–85:15 hexanes:ethyl acetate), the title compound (28.0 mg, 66%) as a yellow oil; TLC analysis  $R_f = 0.6$  (70:30 hexanes:ethyl acetate);  $[\alpha]_{\text{D}}^{20} = +48^\circ$  ( $c$  1.1,  $\text{CHCl}_3$ );  $^1\text{H}$  NMR (400 MHz,  $\text{CDCl}_3$ )  $\delta$  7.90–7.75 (3H, m, w,z,u), 7.75–7.70 (1H, m, r), 7.55–7.50 (1H, m, x), 7.50–7.40 (5H, m, c,c',o,o',y), 7.40–7.30 (2H, m, n,n'), 7.30–7.20 (3H, m, a,p,v), 7.09 (2H, d,  $J = 6.8$  Hz, b,b'), 5.35 (1H, br s, NH), 5.15–5.05 (1H, m, k), 3.40–3.20 (1H, m, h), 2.90–2.75 (2H, m,

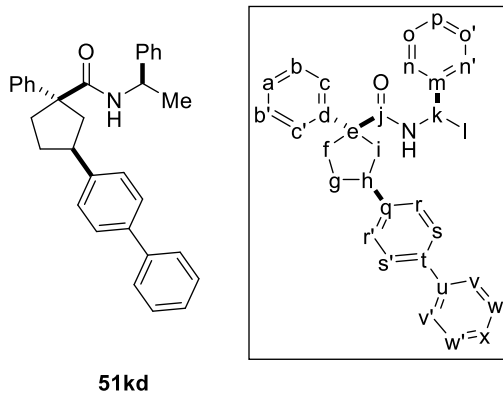


f,i), 2.75–2.65 (1H, m, i), 2.45–2.35 (1H, m, f), 2.35–2.20 (1H, m, g), 2.15–2.05 (1H, m, g), 1.37 (3H, d,  $J = 6.9$  Hz, l);  $^{13}\text{C}$  NMR (100 MHz,  $\text{CDCl}_3$ )  $\delta$  175.70 (j), 144.04 (d), 143.36 (q), 142.59 (m), 133.53 (s), 132.24 (t), 129.00 (o,o'), 128.71 (b,b'), 128.53 (z), 128.08 (w), 127.58 (u), 127.21 (n,n'), 127.09 (c,c'), 126.94 (p), 126.12 (x), 125.90 (a), 125.72 (v), 125.32 (y), 125.22 (r), 59.24 (e), 48.89 (k), 44.77 (i), 44.64 (h), 37.30 (f), 33.72 (g), 21.87 (l); IR (neat) 3325 (N-H stretch), 2920, 1708 (C=O stretch), 1644 (C=C stretch), 1598 (N-H bend), 1493, 1446, 888, 857, 817, 745, 696  $\text{cm}^{-1}$ ; HRMS (ESI) calcd. for  $\text{C}_{30}\text{H}_{29}\text{NaNO}$  ( $\text{M}+\text{Na}$ ): 442.2147, found 442.2151  $m/z$ .



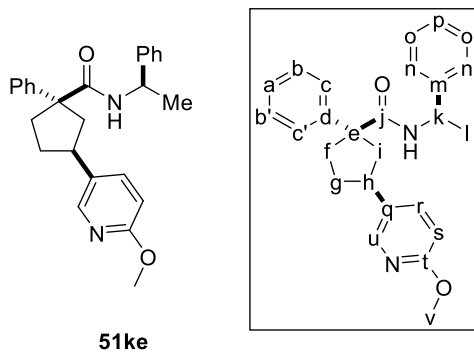
**(1*R*,3*S*)-3-(3,5-dimethoxyphenyl)-1-phenyl-*N*-((*R*)-1-phenylethyl)cyclopentane-1-carboxamide (51kc).** Following **GP16** with 1-bromo-3,5-dimethoxybenzene **55** (21.7 mg, 0.1 mmol, 1.0 equiv), cross-coupling of  $\gamma$ -trifluoroborato amide **50k** (59.2 mg, 0.12 mmol, 1.2 equiv) affords, after flash chromatography on silica gel (90:10–85:15 hexanes:ethyl acetate), the title compound (28.5 mg, 66%) as a yellow oil; TLC analysis  $R_f = 0.5$  (70:30 hexanes:ethyl acetate);  $[\alpha]_{\text{D}}^{20} = +15^\circ$  ( $c$  0.8,  $\text{CHCl}_3$ );  $^1\text{H}$  NMR (400 MHz,  $\text{CDCl}_3$ )  $\delta$  7.45–7.40 (4H, m, o,o',c,c'), 7.35–7.30 (1H, m, p), 7.30–7.20 (3H, m, a,n,n'), 7.07 (2H, d,  $J = 6.8$  Hz, b,b'), 6.49 (2H, d,  $J = 2.1$  Hz, r,r'), 6.33 (1H, t,  $J = 2.2$  Hz, t), 5.30 (1H, d,  $J = 7.5$  Hz, NH), 5.20–5.00 (1H, m, k), 3.80 (6H, s, u,u'), 3.15–3.00 (1H, m, h), 2.80–2.70 (1H, m, f), 2.70–2.55 (2H, m, i), 2.40–2.25 (1H, m, f), 2.25–2.10 (1H, m, g), 2.05–1.90 (1H, m, g), 1.34 (3H, d,  $J = 6.9$  Hz, l);  $^{13}\text{C}$  NMR (100 MHz,  $\text{CDCl}_3$ )  $\delta$

175.55 (j), 160.79 (s,s'), 147.65 (q), 143.94 (d), 143.33 (m), 128.95 (o,o'), 128.51 (n,n'), 127.16 (p), 127.07 (a), 126.85 (c,c'), 125.71 (b,b'), 105.25 (r,r'), 98.22 (t), 59.06 (e), 55.31 (u,u'), 48.83 (k), 44.70 (h), 44.54 (i), 36.98 (f), 33.41 (g), 21.81 (l); IR (neat) 3348 (N-H stretch), 2930, 1654 (C=O stretch), 1593 (C=C stretch), 1493 (N-H bend), 1451, 1427, 1203, 1149, 1059, 924. 831, 733, 697  $\text{cm}^{-1}$ ; HRMS (ESI) calcd. for  $\text{C}_{28}\text{H}_{31}\text{NaNO}_3$  (M+Na): 452.2202, found 452.2195  $m/z$ .



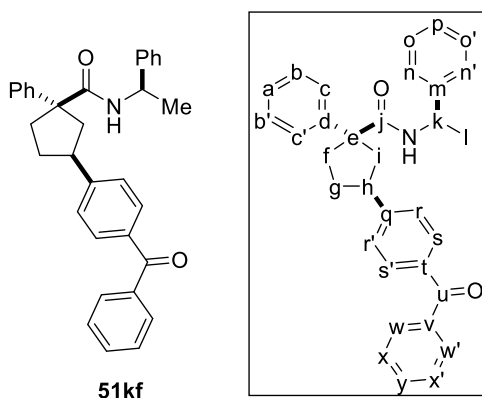
**(1R,3S)-3-([1,1'-biphenyl]-4-yl)-1-phenyl-N-((R)-1-phenylethyl)cyclopentane-1-carboxamide (51kd).** Following **GP16** with 4-bromo-1,1'-biphenyl **56** (23.3 mg, 0.1 mmol, 1.0 equiv), cross-coupling of  $\gamma$ -trifluoroborato amide **50k** (59.2 mg, 0.12 mmol, 1.2 equiv) affords, after flash chromatography on silica gel (90:10–85:15 hexanes:ethyl acetate), the title compound (31.8 mg, 71%) as a yellow oil; TLC analysis  $R_f = 0.6$  (70:30 hexanes:ethyl acetate);  $[\alpha]_D^{20} = +49^\circ$  ( $c$  1.0,  $\text{CHCl}_3$ );  $^1\text{H}$  NMR (400 MHz,  $\text{CDCl}_3$ )  $\delta$  7.61 (2H, d,  $J = 8.1$  Hz, v,v'), 7.56 (2H, d,  $J = 8.2$  Hz, s,s'), 7.50–7.40 (8H, m, b,b',c,c',r,r',w,w'), 7.40–7.30 (2H, m, n,n'), 7.30–7.20 (3H, m, o,o',x), 7.10–7.00 (2H, m, a,p), 5.34 (3H, d,  $J = 7.3$  Hz, NH), 5.15–5.05 (1H, m, k), 3.25–3.10 (1H, m, h), 2.80–2.70 (2H, m, f,i), 2.70–2.60 (1H, m, i), 2.40–2.30 (1H, m, f), 2.30–2.15 (1H, m, g), 2.10–2.00 (1H, m, g), 1.36 (3H, d,  $J = 6.9$  Hz, l);  $^{13}\text{C}$  NMR (100 MHz,  $\text{CDCl}_3$ )  $\delta$  175.68 (j), 144.38 (q), 144.12 (d), 143.36 (u), 141.12 (t), 139.08 (m), 128.98 (w,w'), 128.72 (r,r'), 128.53

(b,b'), 127.76 (v,v'), 127.19 (x), 127.15 (s,s'), 127.09 (n,n'), 127.04 (c,c'), 126.90 (p), 125.72 (p,a), 59.19 (e), 48.87 (k), 44.86 (i), 44.25 (h), 37.35 (f), 33.92 (g), 21.86 (l); IR (neat) 3334 (N-H stretch), 3026, 1651 (C=O stretch), 1598 (C=C stretch), 1486 (N-H bend), 1446, 1234, 1073, 837, 761, 732, 695  $\text{cm}^{-1}$ ; HRMS (ESI) calcd. for  $\text{C}_{32}\text{H}_{31}\text{NaNO}$  (M+Na): 468.2303, found 468.2293  $m/z$ .



**(1R,3S)-3-(6-methoxypyridin-3-yl)-1-phenyl-N-((R)-1-phenylethyl)cyclopentane-1-carboxamide (51ke).** Following **GP16** with 5-chloro-2-methoxypyridine **57** (71.8 mg, 0.5 mmol, 1.0 equiv), cross-coupling of  $\gamma$ -trifluoroborato amide **50k** (298 mg, 0.6 mmol, 1.2 equiv) affords, after flash chromatography on silica gel (85:15 hexanes:ethyl acetate), the title compound (150.2 mg, 75%) as a yellow oil; TLC analysis  $R_f = 0.25$  (80:20 hexanes:ethyl acetate);  $[\alpha]_D^{20} = +8.2^\circ$  ( $c$  0.8,  $\text{CHCl}_3$ );  $^1\text{H}$  NMR (400 MHz,  $\text{CDCl}_3$ )  $\delta$  8.00 (1H, d,  $J = 2.4$  Hz, u), 7.68 (1H, dd,  $J = 8.6$  Hz and 2.4 Hz, r), 7.45–7.40 (4H, m, c,c',o,o'), 7.40–7.30 (2H, m, n,n'), 7.30–7.20 (2H, m, b,b'), 7.10–7.00 (2H, m, a,p), 6.72 (1H, d,  $J = 8.6$  Hz, s), 5.33 (1H, d,  $J = 7.8$  Hz, NH), 5.15–5.00 (1H, m, k), 3.93 (3H, s, v), 3.15–3.05 (1H, m, h), 2.75–2.65 (2H, m, f,i), 2.60–2.50 (1H, m, i), 2.40–2.30 (1H, m, f), 2.20–2.10 (1H, m, g), 2.00–1.85 (1H, m, g), 1.34 (3H, d,  $J = 6.9$  Hz, l);  $^{13}\text{C}$  NMR (100 MHz,  $\text{CDCl}_3$ )  $\delta$  175.61 (j), 162.91 (t), 145.24 (u), 143.95 (d), 143.30 (m), 137.65 (r), 133.13 (q), 129.00 (o,o'), 128.51 (b,b'), 127.25 (n,n'), 127.09 (c,c'), 126.86 (p), 125.64

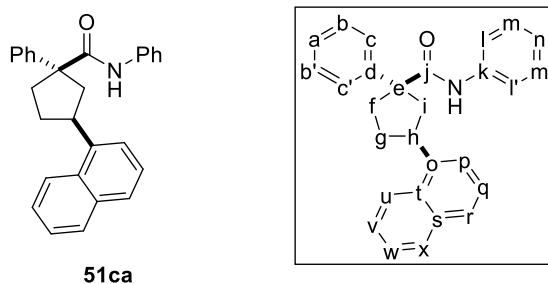
(a), 110.82 (s), 59.10 (e), 53.32 (v), 48.89 (k), 44.59 (i), 41.03 (h), 37.29 (f), 33.88 (g), 21.89 (l); IR (neat) 3323 (N-H stretch), 2942, 1645 (C=O stretch), 1604 (C=C stretch), 1491 (N-H bend), 1446, 1282, 1252, 1128, 1026, 829, 760, 697  $\text{cm}^{-1}$ ; HRMS (ESI) calcd. for  $\text{C}_{26}\text{H}_{28}\text{NaN}_2\text{O}_2$  ( $\text{M}+\text{Na}$ ): 423.2048, found 423.2033  $m/z$ .



**(1R,3S)-3-(4-benzoylphenyl)-1-phenyl-N-((R)-1-phenylethyl)cyclopentane-1-**

**carboxamide (51kf).** Using the general procedure with 4-chlorobenzophenone **58** (21.7 mg, 0.1 mmol, 1.0 equiv), cross-coupling of  $\gamma$ -trifluoroborato amide **50k** (59.2 mg, 0.12 mmol, 1.2 equiv) affords, after flash chromatography on silica gel (90:10–85:15 hexanes:ethyl acetate), the title compound (33.1 mg, 70%) as a yellow oil; TLC analysis  $R_f = 0.5$  (70:30 hexanes:ethyl acetate);  $[\alpha]_D^{20} = +63^\circ$  ( $c$  1.5,  $\text{CHCl}_3$ );  $^1\text{H}$  NMR (400 MHz,  $\text{CDCl}_3$ )  $\delta$  7.85–7.80 (2H, m, s,s'), 7.76 (2H, d,  $J = 8.2$  Hz, w,w'), 7.60 (1H, t,  $J = 7.4$  Hz, y), 7.50 (2H, t,  $J = 7.7$  Hz, b,b'), 7.45–7.40 (5H, m, c,c',o,o',p), 7.40–7.30 (2H, m, n,n'), 7.30–7.15 (4H, m, r,r',x,x'), 7.05 (1H, d,  $J = 6.8$  Hz, a), 5.36 (1H, br s, NH), 5.15–5.05 (1H, m, k), 3.30–3.15 (1H, m, h), 2.85–2.70 (2H, m, f,i), 2.65–2.55 (1H, m, i), 2.45–2.30 (1H, m, f), 2.30–2.20 (1H, m, g), 2.10–2.00 (1H, m, g), 1.35 (3H, d,  $J = 6.9$  Hz, l);  $^{13}\text{C}$  NMR (100 MHz,  $\text{CDCl}_3$ )  $\delta$  196.47 (u), 175.53 (j), 150.51 (q), 143.83 (d), 143.30 (v), 137.93 (t), 135.48 (m), 132.21 (y), 130.45 (w,w'), 130.00 (s,s'), 129.04 (o,o'), 128.53 (x,x'), 128.23 (b,b'), 127.30 (n,n'), 127.11 (c,c'), 126.88 (p), 125.68 (a), 59.22 (e), 48.94

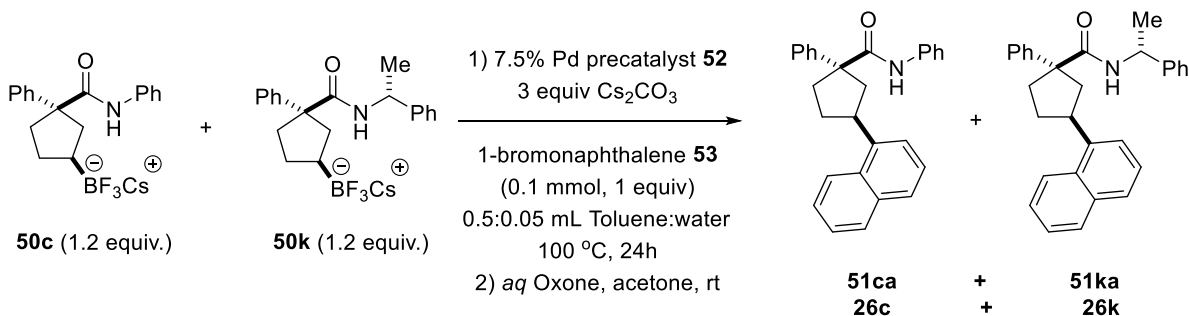
(k), 44.62 (i), 44.52 (h), 37.28 (f), 33.75 (g), 21.90 (l); IR (neat) 3346 (N-H stretch), 3054, 1651 (C=O stretch), 1598 (C=C stretch), 1493 (N-H bend), 1445, 1315, 1277, 923. 742, 696  $\text{cm}^{-1}$ ; HRMS (ESI) calcd. for  $\text{C}_{33}\text{H}_{31}\text{NaNO}_2$  (M+Na): 496.2252, found 496.2245  $m/z$ .



**(1R,3S)-3-(naphthalen-1-yl)-1-phenylcyclopentanecarboxylic acid phenyl amide (51ca).** Using the general procedure with 1-bromonaphthalene **53** (20.7 mg, 0.1 mmol, 1.0 equiv), cross-coupling of  $\gamma$ -trifluoroborato amide **50c** (55.8 mg, 0.12 mmol, 1.2 equiv) affords, after flash chromatography on silica gel (90:10 hexanes:ethyl acetate), the title compound (7.9 mg, 20%) as a yellow oil; TLC analysis  $R_f = 0.70$  (70:30 hexanes:ethyl acetate);  $[\alpha]_D^{20} = -23^\circ$  ( $c$  1.0,  $\text{CHCl}_3$ );  $^1\text{H}$  NMR (300 MHz,  $\text{CDCl}_3$ )  $\delta$  8.10–8.00 (1H, m, u), 7.95–7.85 (1H, m, x), 7.76 (1H, d,  $J = 8.2$  Hz, r), 7.70 (1H, d,  $J = 7.1$  Hz, w), 7.65–7.55 (2H, m, b,b'), 7.55–7.25 (10H, m, a,c,c',l,l',m,m',n,q,v), 7.09 (1H, tt,  $J = 7.3$  and 1.2 Hz, p), 6.83 (1H, br s, NH), 4.05–3.90 (1H, m, h), 3.00–2.80 (3H, m, i,f), 2.55–2.45 (1H, m, f), 2.45–2.35 (1H, m, g), 2.25–2.15 (1H, m, g);  $^{13}\text{C}$  NMR (75 MHz,  $\text{CDCl}_3$ )  $\delta$  174.70 (j), 143.52 (d), 140.42 (o), 137.98 (k), 133.91 (s), 132.09 (t), 129.40 (m,m'), 128.91 (x), 127.63 (n), 127.00 (b,b'), 126.72 (q), 125.83 (c,c'), 125.74 (r), 125.35 (a), 124.22 (v), 123.47 (w), 122.63 (u), 119.70 (p), 110.61 (l,l'), 59.84 (e), 43.70 (i), 39.59 (h), 37.16 (f), 32.70 (g); IR (neat) 3332 (N-H stretch), 3055, 2948, 1661 (C=O

stretch), 1596 (C=C stretch), 1515 (N-H bend), 1498, 1435, 1308, 1240, 905, 777, 751, 691  $\text{cm}^{-1}$ ; HRMS (ESI) calcd. for  $\text{C}_{28}\text{H}_{25}\text{NaNO}$  ( $\text{M}+\text{Na}$ ): 414.1834, found 414.1846  $m/z$ .

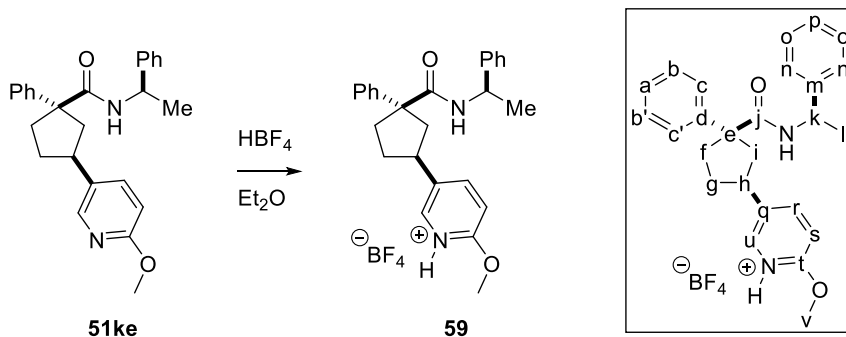
**Direct competition experiment of Suzuki-Miyaura cross-coupling.**



An 8-mL vial was charged with Pd pre-catalyst **52** (5.5 mg, 0.0075 mmol, 0.075 equiv),  $\text{Cs}_2\text{CO}_3$  (98 mg, 0.3 mmol, 3.0 equiv),  $\gamma$ -trifluoroborato amide **50k** (59.2 mg, 0.12 mmol, 1.2 equiv),  $\gamma$ -trifluoroborato amide **50c** (55.8 mg, 0.12 mmol, 1.2 equiv), 1-bromonaphthalene **53** (20.7 mg, 0.1 mmol, 1.0 equiv), toluene (0.5 mL), and water (0.05 mL). The resultant mixture was stirred at 100 °C for 24 h. After cooling to room temperature, the organic layer was separated, and water (1.0 mL) was added to the aqueous layer following by extraction with ethyl acetate (2 x 2 mL). The combined organic extracts were dried (anhyd.  $\text{Na}_2\text{SO}_4$ ) and concentrated under reduced pressure. The resulting mixture was diluted with 1.2 mL acetone and Oxone (0.6 mL of a 0.2 M solution in  $\text{H}_2\text{O}$ , 1.2 mmol, 1.2 equiv) was added in one portion. After a 0.5 h-stir, to the crude mixture was added water (1 mL) and HCl (1 mL of the 1M solution). The resultant mixture was extracted with DCM (3 x 2 mL). The combined organic extracts were dried ( $\text{Na}_2\text{SO}_4$ ), and concentrated under reduced pressure. Flash chromatography on silica gel (90:10 hexanes:ethyl acetate) affords **50c** (18.8 mg, 48%, TLC analysis  $R_f = 0.70$  (70:30 hexanes:ethyl acetate) as a yellow oil and **50k** (17.6 mg, 42%, TLC analysis  $R_f = 0.60$

(70:30 hexanes:ethyl acetate) as a yellow oil. The eluent was then switched to 85:15 DCM:EtOAc to afford a mixture of alcohols **26c** (61%) and **26k** (60%) (mass was calculated using  $^1\text{H}$  NMR ratio (1:0.98 **26c**:**26k**); total mass of **26c** and **26k** was 43.1 mg).

### Preparation of tetrafluoroborate salt **59** for x-ray crystallography



#### **2-methoxy-5-((1*S*,3*R*)-3-phenyl-3-(((*R*)-1-**

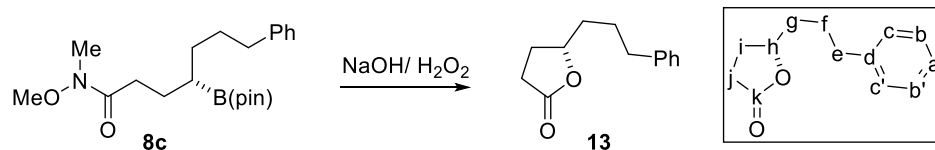
**phenylethyl)carbamoyl)cyclopentyl)pyridin-1-ium tetrafluoroborate (**59**).** A solution of (1*R*,3*S*)-pyridinyl amide **51ke** (64.9 mg, 0.162 mmol) in Et<sub>2</sub>O (4.0 mL) was treated with HBF<sub>4</sub> (54% in Et<sub>2</sub>O, 15  $\mu\text{L}$ , 1.2 equiv), which immediately produced a light yellow precipitate. The liquid was pipetted out and washed with Et<sub>2</sub>O (2 x 2 mL) and then dried under vacuum to give a white solid (69.6 mg, 88%). The salt was recrystallized (5:1 TBME/ MeOH) to give off-white single crystals (59.2 mg, 85%), and an X-ray crystal structure was obtained;  $[\alpha]_{\text{D}}^{20} = +25$  (*c* 1.2, MeOH);  $^1\text{H}$  NMR (400 MHz, CDCl<sub>3</sub>)  $\delta$  8.46 (1H, dd, *J* = 9.1 and 2.4 Hz, r), 8.24 (1H, d, *J* = 2.1 Hz, u), 7.48 (1H, d, *J* = 9.2 Hz, s), 7.45–7.35 (4H, m, b,b',o,o'), 7.30 (1H, tt, *J* = 7.0 and 1.4 Hz, p), 7.20–7.10 (3H, m, a,b,b'), 7.01 (2H, dd, *J* = 7.8 and 2.1 Hz, n,n'), 5.05–4.95 (1H, m, k), 4.21 (3H, s, v), 3.40–3.30 (1H, m, h), 2.80–2.65 (2H, m, f,i), 2.60–2.40 (2H, m, f,i), 2.40–2.25 (1H, m, g), 1.85–1.75 (1H, m, g), 1.37 (3H, d, *J* = 7.0 Hz, l);  $^{13}\text{C}$  NMR (100 MHz, CDCl<sub>3</sub>)  $\delta$

175.96 (j), 159.80 (t), 147.81 (r), 143.77 (d), 143.42 (m), 136.91 (u), 136.89 (q), 128.35 (o,o'), 127.89 (b,b'), 126.70 (p), 126.41 (a), 126.29 (c,c'), 125.44 (n,n'), 110.24 (s), 59.40 (e), 57.26 (v), 49.07 (k), 43.40 (i), 39.73 (h), 35.70 (f), 32.89 (g), 20.64 (l); IR (neat) 3378 (N-H stretch), 1646 (C=O stretch), 1597 (C=C stretch), 1555, 1529 (N-H bend), 1495, 1444, 1330, 1303, 1060, 1014, 836, 766, 703, 643  $\text{cm}^{-1}$ ; HRMS (ESI) calcd. for  $\text{C}_{26}\text{H}_{28}\text{NaN}_2\text{O}_2$  (M-HBF<sub>4</sub>+Na): 423.2048, found 423.2044  $m/z$ .



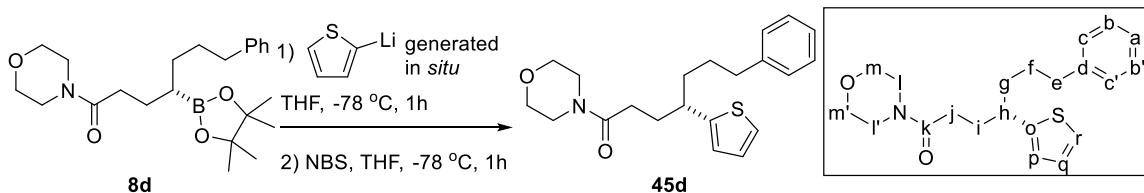
## 5.5 Other stereospecific transformations of organoboranes

### Formation of $\gamma$ -lactone via harsh oxidation of $\gamma$ -borylated Weinreb amide



**(S)-5-(3-phenylpropyl)- $\gamma$ -lactone (13).** To a solution of  $\gamma$ -borylated Weinreb amide **8c** (0.264 mmol, 99 mg) in THF (5 mL) was added aq NaOH (3M, 4 mL) and H<sub>2</sub>O<sub>2</sub> (0.5 mL of a 30% soln.). The resultant mixture was stirred for 2h at room temp. Sodium metabisulfite (Na<sub>2</sub>S<sub>2</sub>O<sub>5</sub>, 3 mL of a 10% aq soln.) was added and the resultant mixture was stirred for another 15 mins before acidifying with HCl (6M). The resulting mixture was extracted with DCM (3 x 10 mL). The combined organic extracts were dried (anhyd. Na<sub>2</sub>SO<sub>4</sub>) and concentrated under reduced pressure. Flash chromatography on silica gel (75:25 hexanes:ethyl acetate) affords the title compound (51 mg, 95%) as a yellow oil; TLC analysis *R<sub>f</sub>* 0.5 (75:25 hexanes:ethyl acetate); [ $\alpha$ ]<sub>D</sub><sup>20</sup> = -22.1° (*c* 1.04, CHCl<sub>3</sub>); literature value +21.7° (*c* 1.04, CHCl<sub>3</sub>) for the (*R*)-enantiomer;<sup>13</sup> spectroscopic data matched with literature:<sup>14</sup> <sup>1</sup>H NMR (400 MHz, CDCl<sub>3</sub>)  $\delta$  7.25–7.35 (2H, b,b'), 7.15–7.25 (2H, a,c,c'), 4.45–4.60 (1H, m, h), 2.69 (2H, t, *J* = 6.9 Hz, e), 2.54 (2H, dd, *J* = 9.4 and 7.0 Hz, j), 2.25–2.40 (1H, m, i), 1.65–1.90 (5H, m, f,g,i); <sup>13</sup>C NMR (100 MHz, CDCl<sub>3</sub>)  $\delta$  177.33 (k), 141.78 (d), 128.52 (b,b',c,c'), 126.08 (a), 80.95 (h), 35.59 (e), 35.20 (g), 28.94 (j), 28.10 (i), 27.14 (f).  $\gamma$ -lactone **23** was converting to 4-hydroxy benzyl amide **9b** following **GP1** to confirm the er.

**C(sp<sup>3</sup>)-C(sp<sup>2</sup>) coupling of boronic ester with thiophene using NBS<sup>26</sup>**

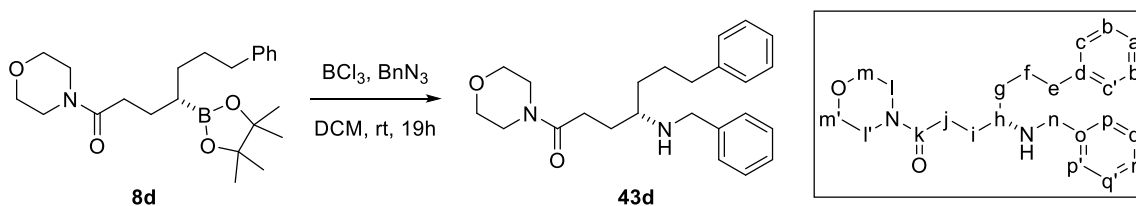


**(S)-7-phenyl-4-(thiophen-2-yl)heptanecarboxylic acid morpholino amide**

**(45d).** To a cooled (-78 °C) of thiophene (1.2 equiv, 0.3 mmol, 24  $\mu$ L) in THF (1 mL) was added *n*-BuLi (1.2 equiv, 1.6M, 0.3 mmol, 0.19 mL) dropwise. The resultant mixture was allowed to warm to room temp and stirred for 1h. The reaction mixture was cooled to -78 °C again, and a solution of  $\gamma$ -borylated morpholino amide **8d** (0.25 mmol, 100 mg) in THF (0.5 ml) was added dropwise. The resulting mixture was stirred at the same temperature for 1h and a solution of NBS (1.2 equiv, 0.3 mmol, 54 mg) in THF (1 mL) was added dropwise. After 1h at -78 °C, satd. Na<sub>2</sub>S<sub>2</sub>O<sub>3</sub> (1 mL) was added and the reaction mixture was allowed to warm to room temp. The reaction mixture was diluted with EtOAc (10 mL) and water (5 mL). The layers were separated and the aqueous layer was extracted with EtOAc (2 x 10 mL). The combined organic extracts were dried (anhyd. Na<sub>2</sub>SO<sub>4</sub>) and concentrated under reduced pressure. Flash chromatography on silica gel (95:5–80:20 DCM:ethyl acetate) affords the title compound (75 mg, 84%) as a yellow oil; TLC analysis  $R_f$  = 0.4 (80:20 DCM:ethyl acetate);  $[\alpha]_D^{20}$  = -9.1° (*c* 2.0, CHCl<sub>3</sub>); Chiral HPLC analysis (Chiralcel-OJ-H, 100% isopropanol, flow rate = 1.0 mL/min) showed peaks at 12 minutes (5.5% (*R*)) and 18 minutes (94.5% (*S*)); <sup>1</sup>H NMR (400 MHz, CDCl<sub>3</sub>)  $\delta$  7.25–7.30 (2H, m, c,c'), 7.10–7.20 (4H, m, a,b,b',r), 6.94 (1H, dd, *J* = 4.9 and 3.5 Hz, q), 6.79 (1H, d, *J* = 3.0, p), 3.55–3.70 (6H, m, l,l',m,m'), 3.25–3.35

(2H, m, l,l'), 2.90–3.00 (1H, m, h), 2.55–2.65 (2H, m, e), 2.10–2.25 (3H, m, i,j), 1.55–1.85 (5H, m, f,g,i);  $^{13}\text{C}$  NMR (100 MHz,  $\text{CDCl}_3$ )  $\delta$  171.51 (k), 149.02 (o), 142.43 (d), 128.50 (b,b'), 128.37 (c,c'), 126.65 (q), 125.79 (a), 124.28 (p), 123.18 (r), 67.02 and 66.71 (m,m'), 45.92 and 41.99 (l,l'), 40.93 (h), 37.89 (g), 35.86 (e), 33.24 (i), 30.78 (j), 29.28 (f); IR (neat) 2920, 2853, 1642 (C=O stretch), 1452, 1429, 1229, 1113, 697  $\text{cm}^{-1}$ ; HRMS (ESI) calcd. for  $\text{C}_{21}\text{H}_{27}\text{NNaO}_2\text{S}$  ( $\text{M}+\text{Na}$ ): 380.1660, found 380.1678  $m/z$ .

**General procedure for  $\text{BCl}_3$ -assisted C–B to C–N bond formation (GP17)**<sup>27</sup>

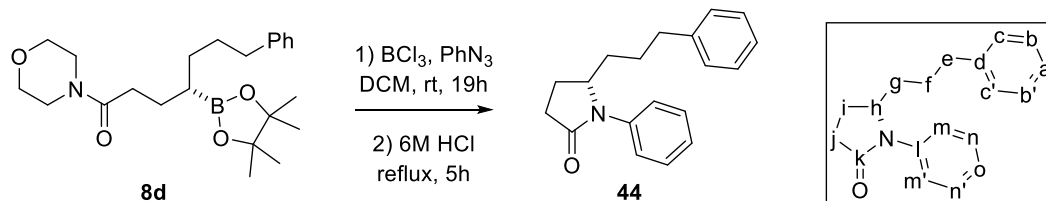


**(S)-4-(benzylamino)-7-phenylheptanecarboxylic acid morpholino amide**

**(43d).** To a solution of  $\text{BCl}_3$  (5 equiv, 1M, 0.5 mmol) in DCM was added dropwise at room temp a solution of  $\gamma$ -borylated morpholino amide **8d** (0.1 mmol, 40 mg) in DCM. After a 4h stir, the reaction mixture was carefully reduced under vacuum at room temp. It was then taken up in DCM (0.5 mL) and a solution of benzyl azide (3 equiv, 0.3 mmol, 40 mg) in DCM (0.2 mL) was added. The resultant mixture was stirred at room temp overnight and quenched with NaOH (2M). After extractions with DCM (3 x 5 mL), the combined organic extracts were dried (anhyd.  $\text{Na}_2\text{SO}_4$ ) and concentrated under reduced pressure. Flash chromatography on silica gel (20:80-0:100 hexanes:acetone) affords the title compound (24.7 mg, 65%) as a yellow oil; TLC analysis  $R_f$  0.2 (5:95 methanol:ethyl acetate);  $[\alpha]_{\text{D}}^{20} = +7.5^\circ$  ( $c$  1.5,  $\text{CHCl}_3$ ); Chiral HPLC analysis (Chiralcel-OJ-H, 90:10 hexanes:isopropanol, flow rate = 1.5 mL/min) showed peaks at 18 minutes (94.0% (*S*))

and 20 minutes (6.0% (*R*));  $^1\text{H}$  NMR (400 MHz,  $\text{CDCl}_3$ )  $\delta$  7.25–7.35 (7H, m, c,c',p,p',q,q',r), 7.15–7.25 (3H, a,b,b'), 3.70–3.80 (2H, m, n), 3.55–3.70 (6H, m, l,l',m,m'), 3.35–3.50 (2H, m, l,l'), 2.60–2.70 (3H, m, e,h), 2.36 (2H, t,  $J = 7.5$  Hz, j), 1.80–1.90 (1H, m, i), 1.60–1.80 (1H, m, f,i), 1.45–1.60 (2H, m, g);  $^{13}\text{C}$  NMR (100 MHz,  $\text{CDCl}_3$ )  $\delta$  172.10 (k), 142.40 (d), 140.76 (o), 128.55 (b,b'), 128.51 (q,q'), 128.43 (c,c'), 128.28 (p,p'), 127.06 (r), 125.89 (a), 67.04 and 66.76 (m,m'), 56.17 (h), 50.99 (n), 46.03 and 42.03 (l,l'), 36.07 (e), 33.47 (g), 29.02 (j), 28.99 (i), 27.64 (f); IR (neat) 2934, 2854, 1640 (C=O stretch), 1452, 1430, 1114, 746, 698  $\text{cm}^{-1}$ ; HRMS (ESI) calcd. for  $\text{C}_{24}\text{H}_{32}\text{N}_2\text{NaO}_2$  (M+Na): 403.2361, found 403.2363  $m/z$ .

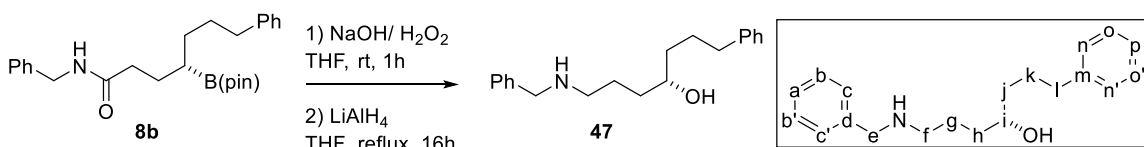
**Formation of  $\gamma$ -lactam via C–B to C–N formation followed by acidic removal of morpholino amide**



**(*S*)-*N*-phenyl-3-(phenylpropyl)- $\gamma$ -lactam (44).** Following **GP17** with phenyl azide (3 equiv, 0.3 mmol, 36 mg) affords the corresponding amine, which was then taken up in HCl (6M, 1 mL). After 6h reflux, the reaction mixture was cooled to room temp and extracted with DCM (3 x 2 mL). The combined organic extracts were dried (anhyd.  $\text{Na}_2\text{SO}_4$ ) and concentrated under reduced pressure. Flash chromatography on silica gel (80:20-40:60 hexanes:ethyl acetate) affords the title compound (19 mg, 68%) as a yellow liquid; TLC analysis  $R_f$  0.4 (40:60 hexanes:ethyl acetate);  $[\alpha]_D^{20} = +30.5^\circ$  ( $c$  0.74,  $\text{CHCl}_3$ ); Chiral HPLC analysis ((*S,S*)-WHELK-O 1, 100% isopropanol, flow rate = 1.0

mL/min) showed peaks at 9 minutes (5.5% (*R*)) and 17 minutes (94.5% (*S*));  $^1\text{H}$  NMR (400 MHz,  $\text{CDCl}_3$ )  $\delta$  7.35–7.45 (4H, m, m,m',n,n'), 7.20–7.30 (4H, m, a,b,b',o), 7.12 (2H, d,  $J = 7.2$  Hz, c,c'), 4.30–4.30 (1H, m, h), 2.50–2.70 (4H, m, e,j), 2.30–2.40 (1H, m, i), 1.80–1.90 (1H, m, i), 1.55–1.80 (3H, m, f,g), 1.40–1.50 (1H, m, g);  $^{13}\text{C}$  NMR (100 MHz,  $\text{CDCl}_3$ )  $\delta$  174.46 (k), 141.83 (d), 137.71 (l), 129.15 (n,n'), 128.50 (b,b'), 128.36 (c,c'), 126.06 (o), 126.00 (a), 124.32 (m,m'), 59.78 (h), 35.71 (e), 33.08 (g), 31.41 (j), 26.50 (f), 24.07 (i); IR (neat) 2933, 1690 (C=O stretch), 1596, 1496, 1388, 1292, 1220, 752, 693  $\text{cm}^{-1}$ ; HRMS (ESI) calcd. for  $\text{C}_{19}\text{H}_{21}\text{NNaO}$  ( $\text{M}+\text{Na}$ ): 302.1521, found 302.1534  $m/z$ .

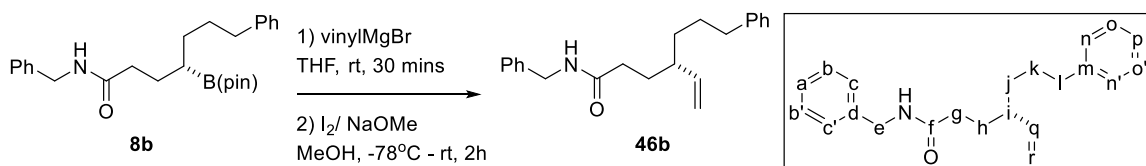
**Formation of 1,4-aminoalcohol via oxidation of C–B bond followed by amide reduction with  $\text{LiAlH}_4$**



**(*S*)-1-(benzylamino)-7-phenyl-4-heptanol (47).** To a solution of  $\gamma$ -borylated benzyl amide **8b** (0.3 mmol, 127 mg) in THF (5 mL) was added aq NaOH (3M, 6 mL) and  $\text{H}_2\text{O}_2$  (0.8 mL of a 30% soln.). The resultant mixture was stirred for 1h at room temp. After extraction with DCM and concentration under reduced pressure, without further purification, the obtained residue (crude alcohol **9b**) was taken up with THF (1.5 mL). To the cooled (0 °C) resultant mixture was added  $\text{LiAlH}_4$  (2 equiv, 0.6 mmol, 23 mg). The reaction mixture was refluxed overnight. After cooling to room temp, the resulting mixture was quenched with KOH (5M, 0.05 mL) and water (0.05 mL) followed by 30-min stir. The reaction mixture was then filtered through a pad of celite and washed with

EtOAc (3 x 2 mL). The filtrate was concentrated under reduced pressure. Flash chromatography on silica gel (50:50-0:100 hexanes:acetone) affords the title compound (84 mg, 94%) as a light yellow solid: m.p. 48.5–49.0 °C; TLC analysis  $R_f$  0.2 (5:95 methanol:ethyl acetate);  $[\alpha]_D^{20} = +20.4^\circ$  ( $c$  2.0,  $\text{CHCl}_3$ );  $^1\text{H NMR}$  (400 MHz,  $\text{CDCl}_3$ )  $\delta$  7.20–7.40 (10H, a,b,b',c,c',n,n',o,o',p), 3.80 (2H, d,  $J = 1.9$  Hz, e), 3.40–3.70 (2H, m, i,OH), 2.75–2.85 (1H, m, f), 2.67 (2H, t,  $J = 7.7$  Hz, l), 2.55–2.65 (1H, m, f), 1.65–1.90 (4H, m, h,k), 1.40–1.60 (4H, m, g,j);  $^{13}\text{C NMR}$  (100 MHz,  $\text{CDCl}_3$ )  $\delta$  142.85 (m), 139.41 (d), 128.69 (b,b'), 128.58 (o,o'), 128.45 (n,n'), 127.35 (c,c'), 127.37 (a), 125.72 (p), 71.33 (i), 53.98 (e), 49.57 (f), 37.51 (j), 37.19 (h), 36.20 (l), 27.97 (k), 27.41 (g); IR (neat) 3267 (N-H stretch, O-H stretch), 3084, 3026, 2868, 2827, 2813, 1495, 1451, 1363 (C-N stretch), 1346, 1118, 858, 734, 691  $\text{cm}^{-1}$ ; HRMS (ESI) calcd. for  $\text{C}_{20}\text{H}_{27}\text{NNaO}$  ( $\text{M}+\text{Na}$ ): 320.1990, found 320.1990  $m/z$ .

### Vinylation of boronic ester using vinylmagnesium bromide<sup>28</sup>



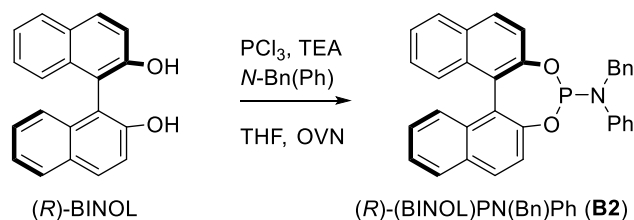
**(S)-7-phenyl-4-vinylheptanecarboxylic acid benzyl amide (46b).** To a solution of  $\gamma$ -borylated benzyl amide **8b** (0.15 mmol, 63 mg) in THF (1.5 mL) was added vinylmagnesium bromide (4 equiv, 1M, 0.6 mmol, 0.6 mL) dropwise. The resultant mixture was stirred at room temperature for 30 mins. To the above solution at  $-78^\circ\text{C}$  was added iodine (4 equiv, 0.6 mmol, 152 mg) in methanol (2.0 mL) dropwise. The reaction mixture was allowed to stir 30 mins at the same temperature followed by dropwise addition of a solution of NaOMe (8 equiv, 1.2 mmol, 65 mg) in methanol (2.5 mL). After warming to room

temp, the resultant mixture was stirred for another 1.5h. It was then diluted with pentane (20 mL) and wash sequentially with 10% aqueous soln. of Na<sub>2</sub>S<sub>2</sub>O<sub>3</sub> (5 mL) and water (5 mL). The organic layer was separated and the aqueous layer was washed with pentane (2 x 10 mL). The combined organic layers were dried (anhyd. Na<sub>2</sub>SO<sub>4</sub>) and concentrated under reduced pressure. Flash chromatography on silica gel (80:20-60:40 hexanes:ethyl acetate) affords the title compound (45 mg, 93%) as a colorless oil; TLC analysis *R<sub>f</sub>* 0.5 (50:50 hexanes:ethyl acetate);  $[\alpha]_D^{20} = -4.1^\circ$  (*c* 2.0, CHCl<sub>3</sub>); Chiral HPLC analysis (Chiralcel-OJ-H, 90:10 hexanes:isopropanol, flow rate = 1.0 mL/min) showed peaks at 18 minutes (4.0% (*R*)) and 22 minutes (96.0% (*S*)); <sup>1</sup>H NMR (400 MHz, CDCl<sub>3</sub>) δ 7.35–7.40 (2H, m, b,b'), 7.25–7.35 (5H, a, n,n',o,o'), 7.15–7.25 (3H, c,c',p), 5.76 (1H, br s, NH), 5.50 (1H, dt, *J* = 17.0 and 9.6 Hz, q), 5.02 (1H, dd, *J* = 10.1 and 1.6 Hz, r), 4.96 (1H, dd, *J* = 17.1 and 1.5 Hz, r), 4.45 (2H, dd, *J* = 5.1 and 4.0 Hz, e), 2.50–2.70 (2H, m, l), 2.20–2.30 (1H, m, g), 2.10–2.20 (1H, m, g), 1.95–2.10 (1H, m, i), 1.80–1.90 (1H, m, k), 1.50–1.75 (3H, m, h,k), 1.40–1.50 (1H, m, j), 1.30–1.40 (1H, m, j); <sup>13</sup>C NMR (100 MHz, CDCl<sub>3</sub>) δ 172.96 (f), 142.72 (q), 142.36 (m), 138.54 (d), 128.83 (o,o'), 128.53 (b,b'), 128.38 (n,n'), 127.98 (c,c') 127.63 (a), 125.76 (p), 115.58 (r), 43.96 (i), 43.71 (e), 36.03 (l), 34.77 (j), 34.59 (g), 30.69 (k), 29.13 (h); IR (neat) 3275 (N-H stretch), 3063, 3027, 2925, 2856, 1641 (C=O stretch), 1541, 1495, 1453, 911, 745, 696 cm<sup>-1</sup>; HRMS (ESI) calcd. for C<sub>22</sub>H<sub>27</sub>NNaO (M+Na): 344.1990, found 344.1996 *m/z*.

## 5.6 Preparation of chiral ligands and palladium pre-catalyst

### General precedures for preparation of effective BINOL-derived phosphoramidite

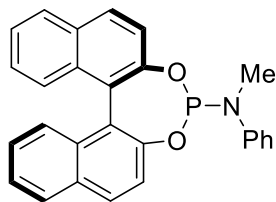
#### ligands (GP18).



**Preparation of (BINOL)PN(Bn)Ph (B2).** To a cooled (0 °C) of *N*-benzylaniline (1.41 g, 1.1 equiv, 7.7 mmol) and TEA (1.8 mL, 1.84 equiv, 12.9 mmol) in THF (50 mL) was added PCl<sub>3</sub> (0.67 mL, 1.1 equiv, 7.7 mmol) dropwise. The resultant mixture was refluxed for 6 h and slowly cooled to -78 °C. A solution of (*R*)-BINOL (2.0 g, 7.0 mmol) and TEA (3.5 mL, 3.6 equiv, 25.2 mmol) in THF (35 mL) was then added slowly to the above mixture at -78 °C. The resulting mixture was stirred at rt overnight, then filtered through a pad of celite, and washed with THF. The organic phase was concentrated under reduced pressure. Flash chromatography on silica gel (80:20–70:30 hexanes:DCM) affords the title compound (3.01 g, 86%) as a white foamy solid: mp 99.5–100.0 °C; TLC analysis  $R_f = 0.6$  (50:50 hexanes:DCM);  $[\alpha]_D^{20} = -165^\circ$  ( $c$  1.0, CHCl<sub>3</sub>); <sup>31</sup>P NMR (121 MHz, CDCl<sub>3</sub>)  $\delta$  140.95; <sup>1</sup>H NMR (300 MHz, CDCl<sub>3</sub>)  $\delta$  8.05 (1H, d,  $J = 8.8$  Hz), 8.00–7.90 (3H, m), 7.67 (1H, dd  $J = 8.8$  and 0.5 Hz), 7.50–7.40 (5H, m), 7.35–7.25 (6H, m), 7.25–7.05 (6H, m), 4.56 (1H, dd,  $J = 15.7$  and 2.1 Hz), 4.06 (1H, dd,  $J = 15.7$  and 1.6 Hz); <sup>13</sup>C NMR (75 MHz, CDCl<sub>3</sub>)  $\delta$  149.56 ( $J_{CP} = 4.9$  Hz), 149.15, 143.78, 143.47, 138.45, 132.87, 132.64, 131.58, 130.89, 130.48, 130.27, 129.09, 128.41, 128.34, 128.10, 127.84, 127.08, 126.99, 126.73, 126.24, 125.02, 124.82, 124.71, 124.55, 124.32, 124.18, 124.11, 122.69, 122.08, 121.71, 50.37; IR (neat) 3052, 1618, 1589, 1489, 1462, 1359, 1324, 1223, 1096, 1063,

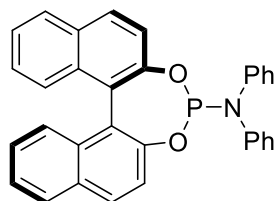


947, 819, 747, 692  $\text{cm}^{-1}$ ; HRMS (EI) calcd. for  $\text{C}_{33}\text{H}_{24}\text{NO}_2\text{P}$  (M): 497.1545, found 497.1545  $m/z$ .



(*R*)-(BINOL)PN(Me)Ph (**B1**)

**(BINOL)PN(Bn)Ph (B1)**. Following **GP18** with aniline (0.7 mL, 1.1 equiv, 7.7 mmol) affords, after flash chromatography on silica gel (75:25 hexanes:DCM), the title compound (2.42 g, 82%) as a white foamy solid; TLC analysis  $R_f$  0.6 (75:25 hexanes:DCM);  $^{31}\text{P}$  NMR (162 MHz,  $\text{CDCl}_3$ )  $\delta$  139.14;  $^1\text{H}$  NMR (400 MHz,  $\text{CDCl}_3$ )  $\delta$  8.03 (1H, d,  $J = 8.8$  Hz), 7.90–8.00 (3H, m), 7.55–7.60 (1H, m), 7.40–7.50 (4H, m), 7.41–7.25 (7H, m), 7.10–7.15 (1H, m), 2.67 (3H, d,  $J = 2.5$  Hz);  $^{13}\text{C}$  NMR (100 MHz,  $\text{CDCl}_3$ )  $\delta$  149.89, 149.18, 146.39, 146.13, 132.86, 132.64, 131.53, 130.90, 130.49, 130.24, 129.17, 128.39, 128.33, 127.02, 126.93, 126.22, 124.98, 124.79, 124.07, 123.23, 122.72, 121.83, 121.28, 121.12, 33.53 ( $J_{\text{CP}} = 4.02$  Hz).

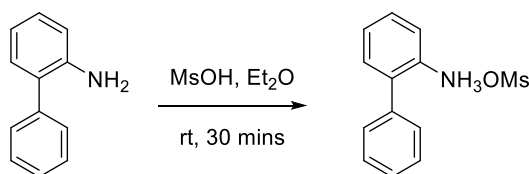


(*R*)-(BINOL)PN(Ph)Ph (**B7**)

**(BINOL)PN(Ph)Ph (B7)**. Following **GP18** with diphenyl amine (170 mg, 1.1 equiv, 1.1 mmol) affords, after flash chromatography on silica gel (75:25 hexanes:DCM), the title compound (343 mg, 71%) as a white foamy solid; TLC analysis  $R_f$  0.6 (75:25 hexanes:DCM);  $^{31}\text{P}$  NMR (162 MHz,  $\text{CDCl}_3$ )  $\delta$  143.76;  $^1\text{H}$  NMR (400 MHz,  $\text{CDCl}_3$ )  $\delta$  8.01 (1H,

d,  $J = 8.8$  Hz), 7.95 (1H, d,  $J = 8.2$  Hz), 7.81 (1H, d,  $J = 8.1$  Hz), 7.59 (1H, d,  $J = 8.8$  Hz), 7.54 (1H, d,  $J = 8.8$  Hz), 7.43 (2H, dt,  $J = 18.6$  and  $7.6$  Hz), 7.20–7.40 (6H, m), 7.05–7.20 (9H, m), 6.95–7.05 (3H, m) ;  $^{13}\text{C}$  NMR (100 MHz,  $\text{CDCl}_3$ )  $\delta$  149.97, 149.90, 148.84, 145.02, 144.92, 143.27, 133.00, 132.41, 131.65, 130.55, 129.49, 129.37, 128.87, 128.48, 128.09, 127.23, 126.86, 126.61, 126.54, 126.29, 125.91, 125.10, 124.73, 124.57, 124.50, 124.45, 122.03, 121.85, 121.14, 117.96.

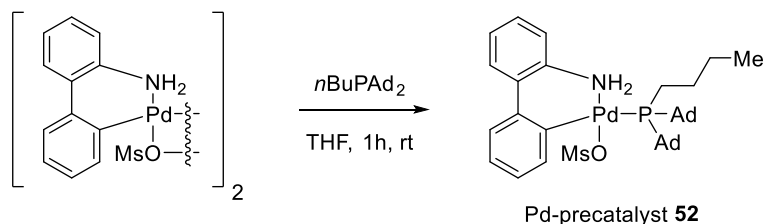
**Preparation sequence of Palladium-precatalyst 52.**<sup>29</sup>



**2-Ammoniumbiphenyl mesylate.**<sup>29</sup> To a solution of 2-aminobiphenyl (2.54 g, 15.0 mmol, 1.0 equiv) in diethyl ether (50 mL) was added a solution of methanesulfonic acid (0.97 mL, 15.0 mmol, 1.0 equiv) in diethyl ether (8 mL). After 30 min of stir, the resultant mixture was filtered and washed with diethyl ether (2 x 10 mL). The precipitate was dried under vacuum to provide the title compound (3.97 g, 99%) as a white solid: mp 152.5–153.0 °C;  $^1\text{H}$  NMR (400 MHz,  $\text{CDCl}_3$ )  $\delta$  9.17 (3H, br s,  $\text{NH}_3$ ), 7.50 (1H, dd,  $J = 7.9$  and  $0.8$  Hz), 7.45–7.35 (6H, m), 7.35–7.25 (2H, m), 2.38 (3H, s);  $^{13}\text{C}$  NMR (100 MHz,  $\text{CDCl}_3$ )  $\delta$  136.76, 136.18, 131.16, 129.42, 128.97, 128.65, 128.24, 128.19, 124.42, 38.85.



**$\mu$ -OMs dimer.**<sup>29</sup> The solution of 2-ammoniumbiphenyl mesylate (789 mg, 3.0 mmol, 1.0 equiv) and Pd(OAc)<sub>2</sub> (672 mg, 3.0 mmol, 1.0 equiv) in 12 mL anhydrous toluene was stirred at 50 °C for 1 h. After cooling to room temp, the suspension was filtered, washed with toluene (5 mL) and diethyl ether (3 x 5 mL) and dried under vacuum for 24 h to afford the title compound (1.01 g, 91%) as an off-white solid: mp 200.5–202.0 °C; <sup>1</sup>H NMR (400 MHz, CD<sub>3</sub>CN)  $\delta$  7.65–7.55 (1H, m), 7.48 (1H, dd,  $J$  = 7.5 and 1.2 Hz), 7.45–7.35 (1H, m), 7.35–7.25 (2H, m), 7.22 (1H, d,  $J$  = 7.6 Hz), 7.18 (1H, t,  $J$  = 7.4 Hz), 7.08 (1H, td,  $J$  = 7.6 and 1.4 Hz), 6.38 (2H, br s), 2.58 (3H, s); <sup>13</sup>C NMR (100 MHz, CD<sub>3</sub>CN)  $\delta$  139.19, 138.83, 136.81, 136.39, 135.55, 127.89, 127.86, 127.18, 126.28, 126.14, 125.22, 120.49, 39.10.



**Preparation of Pd-precatalyst (52).** The solution of  $\mu$ -OMs dimer (370 mg, 0.5 mmol, 0.5 equiv) and *n*BuPAd<sub>2</sub> (359 mg, 1.0 mmol, 1.0 equiv) in anhydrous THF (5 mL) was stirred at room temp for 1 h. The solvent was then concentrated under reduced pressure at room temp until ~ 0.5 mL remained. The residue was then added pentane (5 mL) to crystallize out the product. The solvent was removed by pipet and the solid was dried under vacuum to afford the title compound (671 mg, 92%) as an off-white solid: mp 219.0–220.5 °C; <sup>31</sup>P NMR (283 MHz, CDCl<sub>3</sub>)  $\delta$  47.97; <sup>1</sup>H NMR (700 MHz, CDCl<sub>3</sub>)  $\delta$

7.45–7.35 (3H, m), 7.30–7.20 (3H, m), 7.16 (1H, t,  $J = 7.4$  Hz), 7.08 (1H, t,  $J = 7.2$  Hz), 7.01 (1H, t,  $J = 7.3$  Hz), 4.18 (1H, br s), 2.83 (3H, s), 2.30–2.15 (6H, m), 2.10–2.00 (9H, m), 2.85–2.75 (9H, m), 1.65–1.55 (7H, m), 1.45–1.35 (1H, m), 1.10–1.00 (1H, m), 0.95–0.90 (1H, m), 0.60 (3H, t,  $J = 7.2$  Hz), 0.60–0.50 (1H, m), 0.40–0.20 (1H, m);  $^{13}\text{C}$  NMR (176 MHz,  $\text{CDCl}_3$ )  $\delta$  140.16, 137.58 and 137.55, 136.63 and 136.61, 128.12, 127.63, 126.91, 125.33, 125.26, 124.65, 119.83, 41.34 and 41.26, 40.55 and 40.45, 40.08, 39.87, 36.65 and 36.46, 28.84 and 28.79, 28.65 and 28.61, 27.73, 25.41 and 25.34, 17.63 and 17.51, 13.80 (observed complexity due to P-C splitting). IR (neat) 2898, 2841, 1611, 1492, 1419, 1341, 1300, 1249, 1239, 1166, 1141, 1034, 1021, 771, 754, 735, 709  $\text{cm}^{-1}$ ; HRMS (ESI) calcd. for  $\text{C}_{36}\text{H}_{49}\text{NPPd}$  (M-OMs): 632.2637, found 632.2637  $m/z$ .

## 5.7 References

- [1] Data Collection: SMART Software in APEX2 v2010.3-0 Suite. Bruker-AXS, 5465 E. Cheryl Parkway, Madison, WI 53711-5373 USA.
- [2] Data Reduction: SAINT Software in APEX2 v2010.3-0 Suite. Bruker-AXS, 5465 E. Cheryl Parkway, Madison, WI 53711-5373 USA.
- [3] International Tables for Crystallography, Vol A, 4<sup>th</sup> ed., Kluwer: Boston (1996).
- [4] Refinement: SHELXTL v2010.3-0. Bruker-AXS, 5465 E. Cheryl Parkway, Madison, WI 53711-5373 USA.
- [5] Smith, S. M.; Thacker, N. C.; Takacs, J. M., "Efficient Amide-Directed Catalytic Asymmetric Hydroboration," *J. Am. Chem. Soc.*, **2008**, *130*, 3734–3735.
- [6] Lafrance, D.; Bowles, P.; Leeman, K.; Rafka, R., "Mild Decarboxylative Activation of Malonic Acid Derivatives by 1,1'-Carbonyldiimidazole," *Org. Lett.*, **2011**, *13*, 2322–2325.
- [7] Grünanger, C. U.; Breit, B., "Remote Control of Regio- and Diastereoselectivity in the Hydroformylation of Bishomoallylic Alcohols with Catalytic Amounts of a Reversibly Bound Directing Group," *Angew. Chem., Int. Ed.*, **2010**, *49*, 967–970.
- [8] Braddock, D. C.; Cansell, G.; Hermitage, S. A., "Ortho-Substituted Iodobenzenes as Novel Organocatalysts for Bromination of Alkenes," *Chem. Commun.*, **2006**, *0*, 2483–2485.
- [9] Gaunt, M. J.; Jessiman, A. S.; Orsini, P.; Tanner, H. R.; Hook, D. F.; Ley, S. V., "Synthesis of the C-1–C-28 ABCD Unit of Spongistatin 1," *Org. Lett.*, **2003**, *5*, 4819–4822.
- [10] Yadav, J. S.; Rao, T. S.; Ravindar, K.; Reddu, B. V. S., "Total Synthesis of (+)-Aspicilin from D-Mannitol," *Synlett*, **2009**, *17*, 2828–2830.
- [11] Herrmann, A. T.; Martinez, S. R.; Zakarian, A., "A Concise Asymmetric Total Synthesis of (+)-Brevisamide," *Org. Lett.*, **2011**, *13*, 3636–3639.
- [12] Xu, G.; Yang, X.; Jiang, B.; Lei, P.; Liu, X.; Wang, Q.; Zhang, X.; Ling, Y., "Synthesis and Bioactivities of Novel Piperazine-Containing 1,5-Diphenyl-2-Penten-1-One Analogues from Natural Product Lead." *Bio. Med. Chem. Lett.*, **2016**, *26*, 1849–1853.

- [13] Crimmins, M. T.; DeBaillie, A. C., "Enantioselective Total Synthesis of Bistramide A," *J. Am. Chem. Soc.* 2006, *128*, 4936–4937.
- [14] Cao, J.; Perlmutter, P., "'One-pot' Reductive Lactone Alkylation Provides a Concise Asymmetric Synthesis of Chiral Isoprenoid Targets," *Org. Lett.*, **2013**, *15*, 4327–4329.
- [15] Musacchio, A., J.; Nguyen, L. Q.; Beard, G. H.; Knowles, R. R., "Catalytic Olefin Hydroamination with Aminium Radical Cations: A Photoredox Method for Direct C–N Bond Formation" *J. Am. Chem. Soc.*, **2014**, *136*, 12217–12220.
- [16] Deng, Z.; Wei, J.; Liao, L.; Huang, H.; Zhao, X., "Organoselenium-Catalyzed Synthesis of Oxygen- and Nitrogen-Containing Heterocycles," *Org. Lett.*, **2016**, *18*, 504–507.
- [17] Matsumoto, K.; Koyachi, K.; Shindo, M., "Asymmetric Total Syntheses of Xanthatin and 11,13-Dihydroxanthatin Using a Stereocontrolled Conjugate Allylation to  $\gamma$ -Butenolide," *Tetrahedron*, **2013**, *69*, 1043–1049.
- [18] Depres, J. P.; Greene, A. E., "Improved Selectivity in the Preparation of Some 1,1-Difunctionalized 3-Cyclopentenes. High Yield Synthesis of 3-Cyclopentenecarboxylic Acid," *J. Org. Chem.*, 1984, *49*, 928–931.
- [19] Kiyotsuka, Y.; Acharya, H. P.; Katayama, Y.; Hyodo, T.; Kobayashi, Y., "Picolinoxy Group, a New Leaving Group for anti  $S_N2'$  Selective Allylic Substitution with Aryl Anions Based on Grignard Reagents," *Org. Lett.*, **2008**, *10*, 1719–1722.
- [20] Race, N. J.; Bower, J. F., "Palladium Catalyzed Cyclizations of Oxime Esters with 1,2-Disubstituted Alkenes: Synthesis of Dihydropyrroles," *Org. Lett.*, **2013**, *15*, 4616–4619.
- [21] DeMartino, J.; Akiyama, T.; Struthers, M.; Yang, L.; Berger, J. P.; Morriello, G.; Pastemak, A.; Zhou, C.; Mills, S. G.; Butora, G.; Kothandaraman, S.; Guiadeen, D.; Tang, C.; Jiao, R.; Goble, S. D.; Moyes, C., US20060030582A1, **2006**.
- [22] Grellepois, F.; Kikelj, V.; Coia, N.; Portella, C., "1-(Trifluoromethyl)cyclopent-3-enecarboxylic Acid Derivatives: Platforms for Bifunctional Cyclic Trifluoromethyl Building Blocks," *Eur. J. Org. Chem.*, **2012**, *2012*, 509–517

- [23] Nguyen, T. B.; Sorres, J.; Tran, M. Q.; Ermolenko, L.; Al-Mourabit, A., "Boric Acid: A Highly Efficient Catalyst for Transamidation of Carboxamides with Amines," *Org. Lett.*, **2012**, *14*, 3202–3205.
- [24] Molander, G. A.; Shin, I.; Jean-Gerard, L., "Palladium-Catalyzed Suzuki–Miyaura Cross-Coupling Reactions of Enantiomerically Enriched Potassium  $\beta$ -Trifluoroboratoamides with Various Aryl- and Hetaryl Chlorides," *Org. Lett.*, **2010**, *12*, 4384–4387.
- [25] Lennox, A. J. J.; Lloyd-Jones, G. C., "Preparation of Organotrifluoroborate Salts: Precipitation-Driven Equilibrium under Non-Etching Conditions," *Angew. Chem., Int. Ed.*, **2012**, *51*, 9385–9388.
- [26] Bonet, A.; Odachowski, M.; Leonori, D.; Essafi, S.; Aggarwal, V. K., "Enantiospecific  $sp^2$ – $sp^3$  Coupling of Secondary and Tertiary Boronic Esters," *Nat. Chem.*, **2014**, *6*, 584–589.
- [27] Kubota, K.; Yamamoto, E.; Ito, H., "Regio- and Enantioselective Monoborylation of Alkenylsilanes Catalyzed by an Electron-Donating Chiral Phosphine–Copper(I) Complex," *Adv. Synth. Catal.*, **2013**, *355*, 3527–3531.
- [28] Sonawane, R. P.; Jheengut, V.; Rabalakos, C.; Larouche-Gauthier, R.; Scott, H. K.; Aggarwal, V. K., "Enantioselective Construction of Quaternary Stereogenic Centers from Tertiary Boronic Esters: Methodology and Applications," *Angew. Chem., Int. Ed.*, **2011**, *50*, 3760–3763.
- [29] N. C. Bruno, M. T. Tudge and S. L. Buchwald, "Design and Preparation of New Palladium Precatalysts for C-C and C-N Cross-Coupling Reactions," *Chem. Sci.*, **2013**, *4*, 916–920.